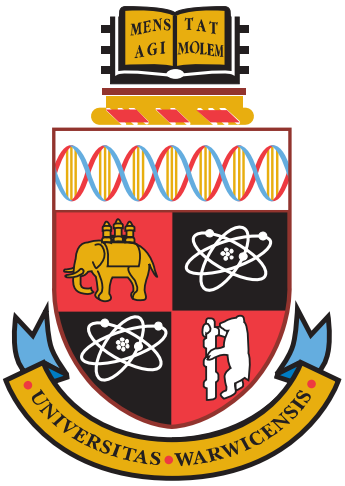

A Rat Model Study of the Spatio-temporal Effects of Progesterone Signalling on the Transcriptome of Uterine Tissues During Pregnancy and Parturition

by

Chipo Mashayamombe

Thesis

Submitted to The University of Warwick

for the degree of

Doctor of Philosophy

Systems Biology Doctoral Training Centre

September 2015

Contents

List of Figures

List of Tables

Abbreviations

$PGF_{2\alpha}$ prostaglandin $_{F2\alpha}$

PLA_2 Phospholipase A_2

Ct Threshold cycle number

15-OH-DHEA-S 15-hydroxy-dehydroepiandrosterone sulfate

16-OH-DHEA-S 16-hydroxy-dehydroepiandrosterone sulfate

Acta2 Actin α-2

Actb β-Actin

Actg2 Actin γ-2

ACTH Adrenocorticotropic hormone

AR Androgen receptor

BAM Binary alignment map

Ca^{2+} Calcium ions

Cald1 Caldesmon 1

Calm1 Calmodulin 1

Calm2 Calmodulin 2

Calm3 Calmodulin 3

cAMP Cyclic adenosine monophosphate

CAP Contraction-associated protein

CBP CREB-binding protein

cGMP Cyclic guanosine monophosphate

ChIP Chromatin immunoprecipitation

Cnn1 Calponin 1

Cnn3 Calponin 3

Cnr1 Cannabinoid receptor 1

Control-DE differentially expressed in control tissues

CREB cAMP response element binding protein

CRH Corticotropin-releasing hormone

CV Cresyl violet nuclear stain

Cx-26 Connexin-26

Cx-40 Connexin-40

Cx-45 Connexin-45

DAB Diaminobenzidine

DAG Diacyl-glycerol

DBD DNA binding domain

DE differentially expressed

DHEA Dehydroepiandrosterone

DHEA-S Dehydroepiandrosterone sulfate

E_1 Estrone

E_2 Estradiol

E_3 Estriol

E_4 Estetrol

EMG Electromyography

ER Estrogen receptor

EY Eosin yellow cytoplasmic stain

FDR False discovery rate

FP $PGF_{2\alpha}$ receptor

FSH Follicle stimulating hormone

FWER Family-wise error rate

GD19+6hrs 6hrs after gestational day 19

GD22(L) Gestational Day 22 - In Labour

GD22(NL) Gestational Day 22 - Not in Labour

Gja1 Gap junction α 1

Gja4 Gap junction α 4

Gja5 Gap junction α 5

Gja7 Gap junction α 7

Gjb2 Gap junction β 2

Gjd4 Gap junction δ 4

GLM Generalised linear model

GnRH Gonadotropin releasing hormone

GO Gene Ontology

goi Gene of interest

GPCR G protein-coupled receptor

Gpr68 G protein-coupled receptor 68

hCG human chorionic gonadotropin

Hcn4 Hyperpolarisation-activated cyclic nucleotide-gated K^+ channel 4

hPRE Human progesterone response element

Htr1D G protein-coupled 5-hydroxytryptamine (serotonin) receptor 1D

Htr2a G protein-coupled 5-hydroxytryptamine (serotonin) receptor 2A

Htr4 G protein-coupled 5-hydroxytryptamine (serotonin) receptor 4

IGV Integrative Genomics Viewer

IHC Immunohistochemical

IL-1β Interleukin-1β

IP PGI_2 receptor

IP_3 Inositol 1,4,5-trisphosphate

Kcng1 K^+ voltage-gated channel subfamily G member 1

Kcnmb1 Large conductance Ca^{2+}-activated K^+ channel subfamily M β member 1

KLF4 Krüppel-like factor 4

LBD ligand binding domain

LCM Laser capture microdissection

LH Luteinizing hormone

MAPK Mitogen-activated protein kinases

Mmp Matrix metalloproteinase

Mmp1a Matrix metallopeptidase 1

MR Mineralocorticoid receptor

MTC Multiple testing correction

Myl6b Myosin light chain 6B

Myl9 Myosin light chain 9

Mylk Myosin light chain kinase

NB Negative binomial

NCoR nuclear receptor corepressor

NCoRs nuclear receptor corepressors

NF-κB Nuclear factor -κB

NO nitric oxide

NRIP1 Nuclear receptor interacting protein 1

OCT Optimum cutting temperature embedding compound

OT oxytocin

P4-DE Differentially expressed in P4-treated tissues

PBS Phosphate buffered Saline

PBS-T Phosphate buffered Saline with Tween®20

PC Principal component

PC1 First principal component

PC2 Second principal component

PC3 Third principal component

PCA Principal Component Analysis

PG Prostaglandin

PG prostaglandin

PGE_2 prostaglandin E_2

PGF_2 prostaglandin F_2

PGI_2 prostacyclin

Pgr Progrsterone receptor gene

PIP_2 Phosphatidylinositol 4,5-bisphosphate

PKC Protein kinase C

PLC Phospholipase - C

PPROM Preterm pre-labour rupture of membranes

PR Progesterone receptor

PR^+ Progesterone Receptor-positive

PRA Progesterone receptor isoform A

PRAKO PRA knock-out

PRB Progesterone receptor isoform B

PRBKO PRB knock-out

PRE Progesterone response element

PRKO$^{-/-}$ Homozygous progesterone receptor knock-out

Ptgs1 Prostaglandin-Endoperoxide Synthase 1

Ptgs2 Prostaglandin-Endoperoxide Synthase 2

PTHrP Parathyroid hormone-related peptide

qPCR Quantitative real-time PCR

RIN RNA integrity number

RIPKO$^{-/-}$ Nuclear receptor interacting protein 1 knock-out

RNAseq RNA sequencing

RPKM Reads per Kilobase per million mapped reads

RU486 Mifepristone

RU486-DE Differentially expressed in Mifepristone-treated tissues

SAM Sequence alignment map

Slc14a11 Solute carrier family 4, sodium borate transporter, member 11

Slc17a1 Solute carrier family 17 member 1

Slc22a3 Solute carrier family 22, member 3

SMC Smooth muscle cell

SP-A surfactant protein A

SP1 Specificity protein 1

SRC steroid receptor coactivator

TAF Transactivation function

TAF-3 Transactivation function 3

TBI Traumatic Brain Injury

TF Transcription factor

Tnn Tenascin-N

TPM Transcripts per million

Tpm1 Tropomyosin 1α

Tpm2 Tropomyosin 2β

Tpm3 Tropomyosin 3

Tpm4 Tropomyosin 4

Trh Thyrotropin releasing hormone

UCSC University of California, Santa Cruz

Software Versions

7500 Fast Real-time PCR System Software version 2.0.6

BedTools version 2.19.0

BiNGO version 3.0.2

BioMart online application

Bowtie2 version 2.1.1

CruzDB version 0.5.4

Cufflinks version 2.1.1

Cytoscape version 3.1.0

DESeq2 version 1.4.5

edgeR version 3.6.7

FastQC version 0.10.1

GraphPad Prism version 6.0g

HTSeq version 0.5.4p5

Integrative Genomics Viewer version 2.3.18(20)

MemeLab online application

Pannoramic Viewer version 1.15.4

R version 3.1.0

RepeatMasker version 4.0.5

Rstudio version 0.98.943

Sailfish version 0.6.2

SAMtools version 0.1.19

seqinR version 3.0.7

TeXShop version 3.18

Tophat version 2.09

Acknowledgements

I would like to start of by thanking my examiners for taking the time to assess my work. I would also like to thank my examination advisor Dr Till Bretschneider, for being available throughout the examination process. I would like to thank my supervisors Dr Andrew Blanks and Dr Hugo van den Berg for the guidance and support they provided throughout my studies, as well as being patient with me at most times. To my advisory committee; Prof. Jan Brosens, Dr Magnus Nichols, and Dr Sascha Ott, thank you for the much needed advice. I would like to acknowledge the Systems Biology Doctoral Training Centre as well as the Biotechnology and Biological Sciences Research Council for the funding I received during my studies.

Thank you to the members of the Reproductive Health Division at Warwick Medical School for all the good times we had. A special thank you goes to my friends and relatives for their support. Dr Ben Hamilton, Dr Phil Law, and Ruban Rex thank you for consistently checking up on me and encouraging me.

To my parents, Sylvester and Tina, thank you for the encouragement and wise words. Fadzi, Kuku, Chenai, Rumbi, and Tabeth thanks for pushing me and making me want to do more. Tom, thank you for holding my hand and walking through this journey with me.

"I can do all things through Christ which strengtheneth me."

Philippians 4^{13} (*KJV*)

Kupa Rutendo

Kutanga, ndinoda kutenda avo vakaongorora basa rakanyorwa mugwaro rino. Ndinodawo kutenda Dr Till Bretschneider, vaivepo kubatsira panguva yaiwongororwa basa rangu. Ndinoda kutenda Dr Andrew Blanks uye Dr Hugo van den Berg nekutungamira uye kutsigira kwavakandiita mukudzidza kwangu, uyewo nekuva nemoyo murefu panguva zhinji. Kune komiti yaisanganisira Prof. Jan Brosens, Dr Magnus Nichols, pamwe chete naDr Sascha Ott, ndinokutendai nemazano amakandipa. Ndinoda kucherechedza Systems Biology Doctoral Training Centre pamwe nekanzuru yeBiotechnology & Biological Sciences Research nokuda kwemari dzavakandipa.

Ndinoda kupa rutendo kune nhengo dzose dzeboka reReproductive Health kuWarwick Medical School, nekuda kwomufaro watakava nawo munguva yandaiva nhengo yeboka iri. Ndinopa kutenda kunoudzamu kune hama neshamwari dzangu nokuda kworutsigiro rwavo. Dr Ben Hamilton, Dr Phil Law, naRuban Rex makaita henyu nekugara muchiongorora kuti ndaive mutano here uye nekundikurudzira.

Kune vabereki vangu, Sylvester na Tina, makaita henyu nekundikurudzira uye nekundipa mashoko anovaka. Fadzi, Kuku, Chenai, Rumbi, and Tabeth, ndinokutendai nekundipa simba rekuramba ndichida kuzvivandudza. Tom, ndinokutenda nekufamba kwaunoita neni murwendo rwehupenyu.

"Ndinogona kuita zvinhu zvose kubudikidza naiye anondipa simba."

Vafiripi 4^{13} (*BDMCS*)

Munyori akashandisa chinyorwa chinonzi warwickthesis chemhando yeLaTeX kunyora gwaro rino. LaTeX muunganidzwa wezvinyorwa zveTeX. TeX chiratidzo cheAmerican Mathematical Society.

Dedications

Salome M. Mashayamombe

*c.*1906 – 9th March, 2012

Josephine H. Takangovada

7th August, 1977 – 19th September, 2012

Priscilla R. Mapfumo-Chipuriro

13th May, 1952 – 26th March, 2013

Winnie V. Gwanzura-Mashayamombe

15th February, 1966 – 30th March, 2013

Francis Chifungo

12th October, 1947 – 12th April, 2015

"For he is not a God of the dead, but of the living: for all live unto him."

Luke 20^{38} (*KJV*)

"Haasi Mwari wavakafa, asi wavapenyu, nokuti kwaari vose vapenyu."

Ruka 20^{38} (*BDMCS*)

Declaration

This thesis is submitted to the University of Warwick in support of my application for the degree of Doctor of Philosophy. It has been composed by myself and has not been submitted in any previous application for any degree. All the experiments, including data generated and data analysis, were performed by the author except in the cases outlined below:

Prof. Robert Garfield (St. Joseph's Hospital and Medical Center – Pheonix, USA)

Conducted the animal mating experiments, progesterone, RU486 and sesame seed oil treatments, and harvested the uterine horns (***Section 5.1***).

Ms Lesley Ward & Ms Jeanette Selby (Warwick School of Life Sciences)

Prepared all sequencing libraries (***Section 5.6***).

Wellcome Trust Centre for Human Genetics – Oxford, UK

Performed the RNA-seq experiments (***Section 5.6***).

Mr Sean James (University Hospitals Coventry and Warwickshire NHS Trust)

Embedded tissue in paraffin wax, and scanned tissue slides (***Section 5.7***).

Dr Yi-wah Chan (Warwick Systems Biology Centre)

Identified predicted progesterone response elements and progesterone receptor binding sites in the rat (rn5) genome (***Section 6.5*** & ***Section 6.6***).

Dr Laura Baxter (Warwick Systems Biology Centre)

Provided the code that was used to test for the overrepresentation of enriched motifs in putative progesterone-responsive genes (***Section 6.7.3***).

Parts of this thesis have been published by the author:

Data presented in Section 8.3.1 and Section 8.3.5 were published in

Sheldon, R. E., Mashayamombe, C., Shi, S.-Q., Garfield, R. E., Shmygol, A., Blanks, A. M., & van den Berg, H. A. (2014). Alterations in gap junction connexin43/connexin45 ratio mediate a transition from quiescence to excitation in a mathematical model of the myometrium. *Journal of The Royal Society Interface*, 11

Abstract

The steroid hormone progesterone is essential for the maintenance of pregnancy in mammalian species, but its role at term and during labour is not fully understood. While the effects of progesterone be either genomic or non-genomic, this thesis focuses on the genomic effects of progesterone, and its withdrawal, on rat uterine tissues. Using laser Capture Microdissection, homogeneous cell populations from the the outer myometrium, inner myometrium, and decidua basalis were isolated from uterine horns obtained from timed-pregnant Sprague Dawley rats that were randomised to receive either progesterone, mifepristone, or vehicle treatment. These rats had a 22-day gestational period, with natural systemic withdrawal of progesterone occurring on the 19^{th} day of gestation (GD19). RNA sequencing was employed in the examination of the transcriptomes of the uterine layers, as well as gene expression profiling between GD19 and term. Analysis of the spatial expression of mRNA and proteins in the uterine tissues revealed localisation of thyrotropin-releasing hormone mRNA, as well as the Trh protein, to the decidua in late pregnancy. In addition, tenascin-n mRNA and proteins localised to the inner myometrium but not the outer myometrium during late pregnancy. Analysis of the temporal expression of mRNA transcripts showed distinct patterns of expression within each of the analysed tissues. Following the withdrawal of progesterone on GD19, changes first occur in the outer myometrium, followed by the inner myometrium, then the decidua where mRNA expression increases between GD22 before labour and GD22 during labour. In conclusion, this thesis presents a novel approach in which rat uterine tissues were studied separately. Potential tissue-specific markers for the decidua and the inner myometrium in late pregnancy were identified. The increase in gene expression prior to labour in the decidua would suggest a signal for the onset of labour. Furthermore, changes in the myometrial tissues suggest the presence of an in-built mechanism through which the myometrium knows when to prepare for labour.

Part I

Introduction

Chapter 1

Motivation

The incidence of preterm birth, defined as birth before the completion of 37 weeks of gestation (Goldenberg et al., 2008), is high in developed countries. Of the 726,572 children who were born in England and Wales in 2012, 7.3% were born preterm (Office for National Statistics, 2014). Most infant deaths are attributed to preterm birth and over 50% of neonatal illnesses are a result of being born too early (Goldenberg et al., 2008). While many of the babies that are born preterm survive, they have increased risk of impeded growth, disability, impaired neurological development, and respiratory complications (Goldenberg et al., 2008). Several risk factors are associated with preterm labour, for instance, women aged 35 and above (Astolfi & Zonta, 1999) and women younger than 18 years of age (Fraser et al., 1995) are at higher risk of delivering their babies preterm compared to other age groups. History of preterm delivery or spontaneous abortion and the weight of the mother have also been shown to increase the risk of preterm delivery (Goldenberg et al., 2008). Although there is high correlation between some risk factors and the incidence of preterm labour, the underlying molecular processes

leading to preterm labour, and labour at term, are poorly understood (Zakar & Hertelendy, 2007).

Prior to the onset of labour, the uterus is in a state of quiescence which is influenced by progesterone, a steroid hormone that is widely accepted as an essential component in the maintenance of pregnancy in mammals (Blanks & Brosens, 2012). Progesterone is essential for the maintenance of pregnancy and is used in the prevention of preterm labour in single-fetus pregnancies (Garfield et al., 2012). The onset of labour involves the transformation of the uterus into a stimulus-responsive organ, which contracts, resulting in the expulsion of the fetus(es) through a softened and dilating cervix (Smith, 2007). These uterine contractions are controlled mainly by the electrical activity of the myometrium (Laforet et al., 2011), whereby the movement of ions into and out of myometrial cells generates bursts of action potentials that have been shown to direct contractility of the uterus during labour by stimulating Ca^{2+} entry (Young, 2007; Lammers et al., 2008). Labour in some mammalian species, e.g., in rabbits, rats, and mice, is preceded by a significant drop in the levels of circulating progesterone (Hoffman et al., 2009; Vodstrcil et al., 2010). However, labour at term in humans occurs in the presence of high and sometimes increasing levels of progesterone (Snegovskikh et al., 2006), meaning that humans do not depend on the systemic withdrawal of progesterone for them to go into labour. Interestingly, the withdrawal of progesterone at any stage in human pregnancy, e.g., by the administration of the partial progesterone receptor antagonist mifepristone results in the onset of labour (Smith et al., 2007), suggesting that progesterone withdrawal may have a role in the onset of parturition in humans.

While the mechanisms involved in contractility and the role of progesterone during pregnancy have been established, the molecular mechanisms by which the uterus is activated remain poorly understood. Gaining knowledge of these mechanisms will

help in understanding the timing of birth and, more importantly, the mechanisms involved in preterm birth. This thesis, therefore, analyses the effects of progesterone on the transcriptome of the uterus during pregnancy and at term in the rat model.

1.1 Thesis Overview

This thesis consists of four parts, the first of which contains the introductory chapter which provides the motivation of the thesis and an overview of the structure of the thesis. The ensuing chapters in the first part of the thesis give a background into progesterone, its effects, and the mechanisms by which it acts, and a brief overview of the processes that are involved in the parturition process. In addition, comparisons are made between the human and rat reproductive systems. The first part of the thesis concludes by detailing the aims and objectives of the thesis.

Part II of this thesis is made up of three chapters, the first of which lists all the materials and equipment used in the study on which this thesis is based. The second chapter details the experimental protocols that were used in the study, while the third chapter provides details on the data analysis protocols that were employed.

The results of the study are presented and discussed in the third part of this thesis. In the first chapter of Part III, the transcriptomes of rat uterine tissues obtained from animals treated with sesame seed oil (the control group) are profiled. Transcripts that are expressed predominantly in the decidua, as well as those that are expressed in the myometrial tissues are identified in this chapter. As well as the identification of transcripts whose expression changes with the progression of pregnancy, between

day 19+6hrs of gestation and day 22 during labour, transcriptional differences between uterine tissues are analysed. The second chapter looks at uterine smooth muscle activation by calcium (Ca^{2+}) and the expression patterns of genes involved in uterine smooth muscle contraction in the control animal group. In the third chapter, transcriptomic profiling of rat uterine tissues from mifepristone-treated animals (accelerated progesterone withdrawal group), is conducted. Here the differential expression of transcripts with the progression of gestation and between uterine tissues is assessed. In the fourth chapter, transcripts that are differentially expressed in response to treatment with progesterone are identified. Transcripts that respond to progesterone treatment as well as those that change in response to progesterone withdrawal are analysed for the presence of common regulatory factors. The results part of the thesis concludes with a summary and discussion of the main findings, as well as suggestions for future work.

The fourth part of the thesis contains a list of references, and the thesis concludes with appendices .

Chapter 2

Progesterone

Deriving its name from the phrase "***proge****stational* ***ster****oidal ket****one***", progesterone (P4) was first discovered in mammals in 1930 (Allen, 1930, 1970). As its name suggests, P4 is a steroid hormone that is involved in the maintenance of pregnancy, as well as the preparation of uterine tissues for pregnancy, and has ketone functional groups (Dewick, 2001). More details on steroid hormones are provided in Section 2.1, while the biological actions of P4 will be discussed in Section 2.4 and Section 2.5. In addition, the chemical structure of the P4 molecule is described in Section 2.2.

2.1 Steroid Hormones

Steroid hormones are synthesised from cholesterol and have a four-ring nuclear structure consisting of 17 carbon atoms, as well as side chains that determine their specificity (Nussey & Whitehead, 2002; Rehfeld & Bundgaard, 2010). Steroid carbon atoms and rings are numbered and named following the International Union of Pure

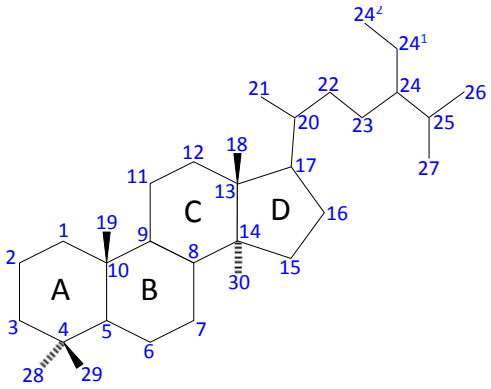

Figure 2.1: Steroid naming convention. The carbon atoms are numbered 1–30 and the rings are lettered A–D. Superscripted numbers, e.g., 24^1 and 24^2, indicate the numbering convention that is adopted for the shorter of 2 side chains that are attached to the same carbon atom. Adapted from IUPAC-IUB Joint Commission on Biochemical Nomenclature (JCBN) (1989).

and Applied Chemistry (IUPAC) recommendations (IUPAC-IUB Joint Commission on Biochemical Nomenclature (JCBN), 1989) shown in Figure 2.1.

2.1.1 Steroid Hormone Synthesis

Steroid hormones are classified into five groups; androgens, estrogens, glucocorticoids, mineralocorticoids, and progestogens (Zhang et al., 2004). The synthesis of steroid hormones from cholesterol relies upon the action of specific enzymes such as the cholesterol side chain cleavage enzyme (P450scc), and 17α-hydroxylase (P450c17) (Hall, 1985; Miller et al., 2007). Cholesterol is converted to the progestogen pregnenolone through the shortening of the cholesterol side chain, a process that is catalysed by the P450scc enzyme. Two other progestogens, P4 and 17α-hydroxypregnenolone, are synthesised from pregnenolone by 3β-hydroxysteroid dehydrogenase (3β-HSD) and P450c17, respectively. P4 is a precursor in the synthesis of the corticosteroids and mineralocorticoids through the action of 21α-hydroxylase (P450c21), 11β-hydroxylase (P450c11), and aldosterone synthase enzymes. Synthesis of both P4 and 17α-hydroxypregnenolone precedes the synthesis of the glu-

cocorticoids, androgens, and estrogens, processes that are made possible by the P450c17, 17β-hydroxysteroid dehydrogenase (17β-HSD), and aromatase enzymes (Miller et al., 2007). The synthesis of the five groups of steroid hormones from cholesterol is illustrated in Figure 2.2.

The enzyme that enables the conversion of P4 and 17α-hydroxypregnenolone to the appropriate precursors for the synthesis of androgens, estrogens, and glucocorticoids is the P450c17 enzyme, the absence of which hinders the progression of the steroid biosynthesis pathway (Hall, 1985; Miller et al., 2007). As such, during pregnancy in humans and higher primates, the synthesis of steroids from cholesterol stops with the formation of P4 because the placenta does not have the P450c17 enzyme required to convert pregnenolone to 17α-hydroxypregnenolone and P4 to 17α-hydroxyprogesterone (Mesiano, 2009). Instead, the placenta utilises the precursors dehydroepiandrosterone (DHEA) and DHEA sulfate (DHEA-S) from both the fetal and maternal circulations in the synthesis of androgens and estrogens as illustrated in Figure 2.3. The fetal hypothalamus releases corticotropin-releasing hormone (CRH), which is transported to the fetal anterior pituitary where it stimulates the release of adrenocorticotropic hormone (ACTH). ACTH stimulates the synthesis of DHEA-S by the fetal adrenal cortex, which is used in the synthesis of estrone (E_1) and estradiol (E_2). In the fetal liver, DHEA-S is converted to 15-hydroxy-dehydroepiandrosterone sulfate (15-OH-DHEA-S) and 16-hydroxy-dehydroepiandrosterone sulfate (16-OH-DHEA-S), which are subsequently converted by the placenta to estetrol (E_4) and estriol (E_3), respectively. Maternal DHEA-S and DHEA are converted to androstenedione and testosterone, which are also converted into E_1 and E_2 by the placenta. The reliance of the placenta on precursors from the fetus and the mother in the synthesis of androgens and estrogens is the foundation of the feto-placental-maternal unit (Cunningham et al., 2005; Mesiano, 2009).

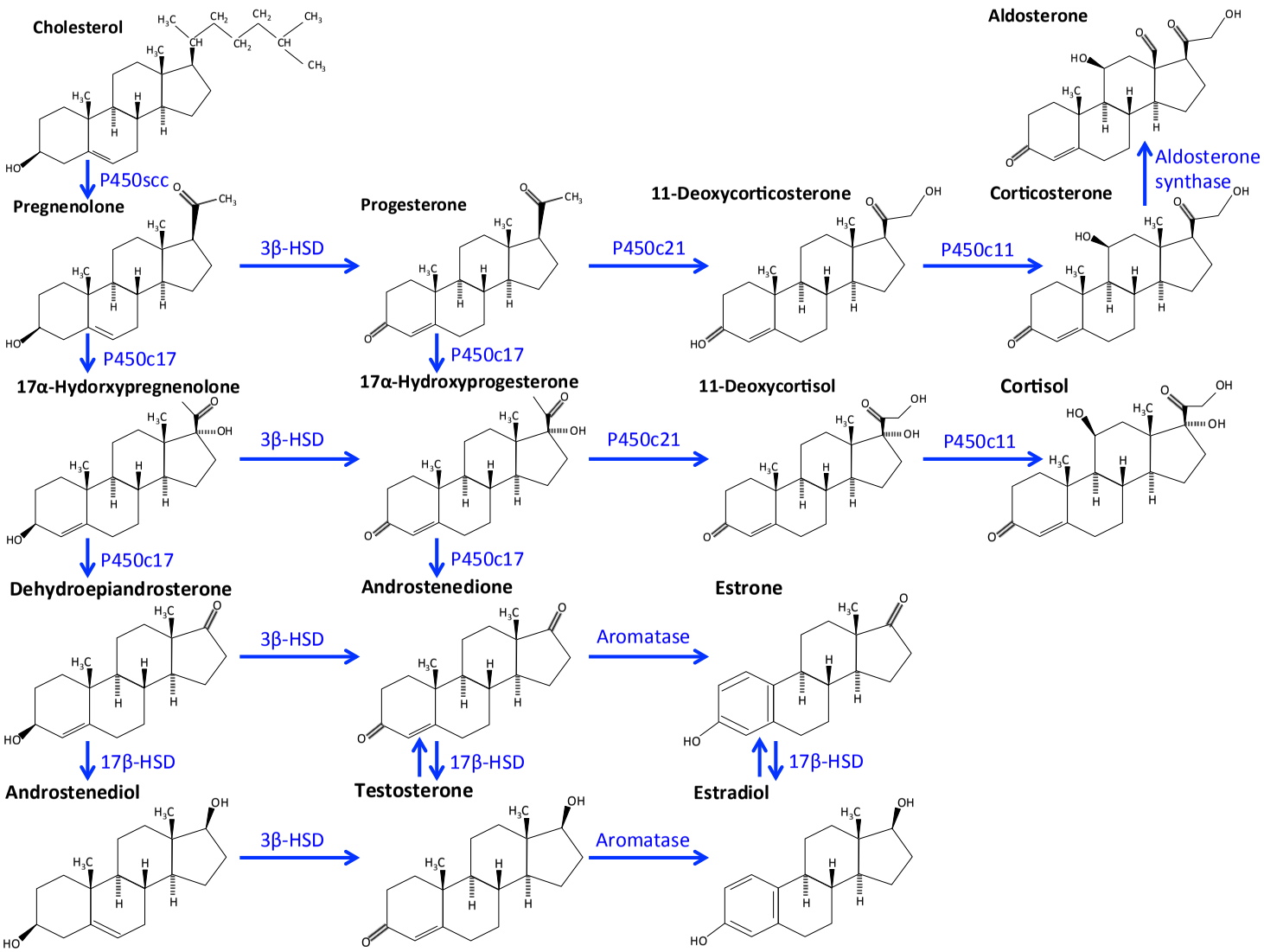

Figure 2.2: Biosynthesis of steroids. Progesterone is a precursor in the synthesis of the 21-carbon mineralocorticoids and glucocorticoids, 19-carbon androgens, and 18-carbon estrogens. Enzymes are shown in blue. The abbreviations used are: **P450scc**: cholesterol side chain cleavage enzyme; **3β-HSD**: 3β-hydroxysteroid dehydrogenase; **17β-HSD**: 17β-hydroxysteroid dehydrogenase; **P450c11**: 11β-hydroxylase; **P450c17**: 17α-hydroxylase; **P450c21**: 21α-hydroxylase. Adapted from Miller et al. (2007, p. 20)

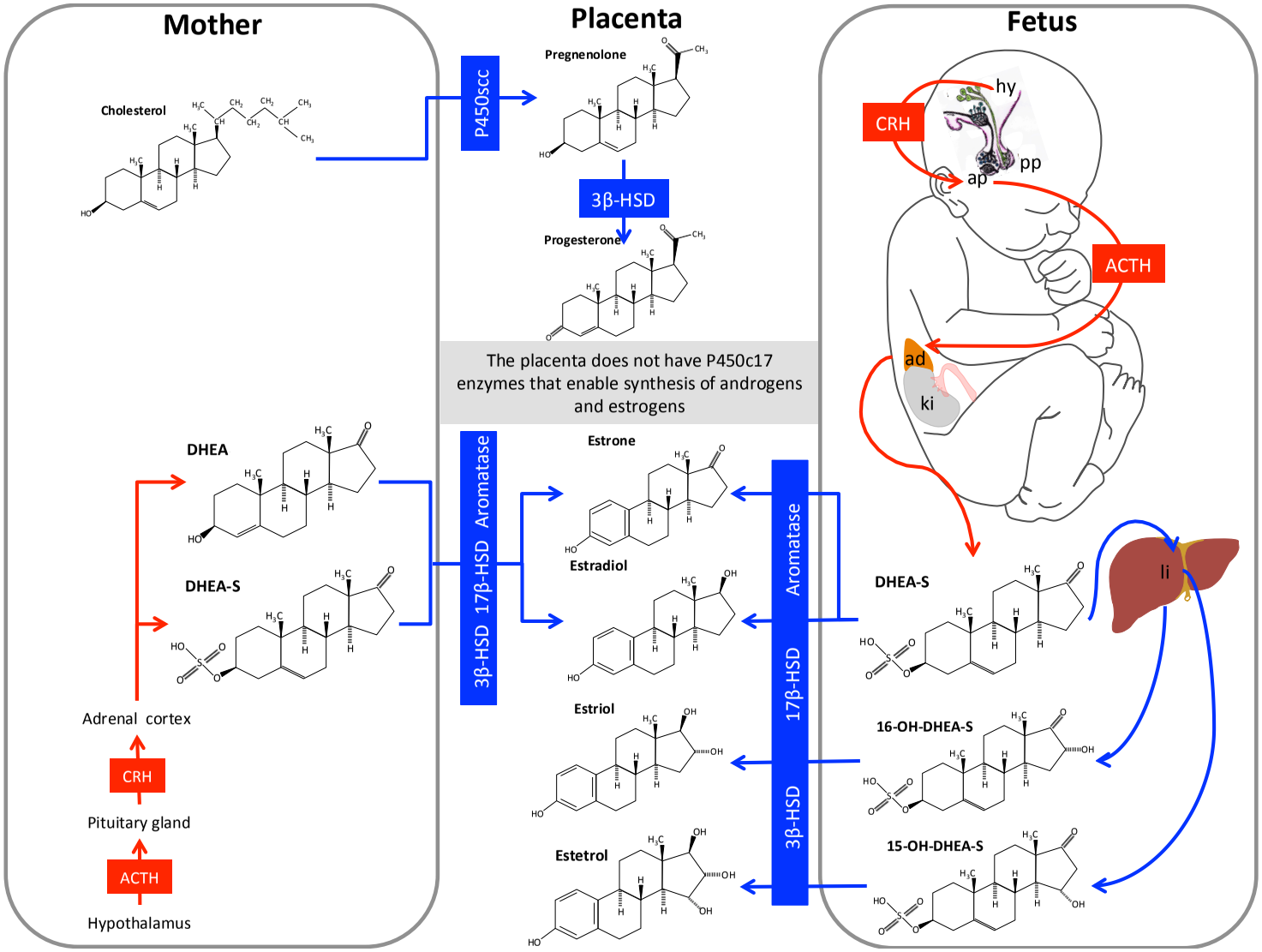

Figure 2.3: Synthesis of progesterone and estrogens by the placenta. Progesterone is synthesised predominantly from maternal cholesterol and estrogens are synthesised from the precursors DHEA-S and DHEA obtained from maternal circulation, and DHEA-S, 15-OH-DHEA-S, and 16-OH-DHEA-S from fetal circulation. Enzymes are shown in blue, and non-steroidal hormones are shown in red. The abbreviations used are: **P450scc**: cholesterol side chain cleavage enzyme; **3β-HSD**: 3β-hydroxysteroid dehydrogenase; **17β-HSD**: 17β-hydroxysteroid dehydrogenase; **DHEA**: dehydroepiandrosterone; **DHEA-S**: dehydroepiandrosterone sulfate; **15-OH-DHEA-S**: 15-hydroxy-dehydroepiandrosterone sulfate; **16-OH-DHEA-S**: 16-hydroxy-dehydroepiandrosterone sulfate; **ap**: anterior pituitary; **pp**: posterior pituitary; **hy**: hypothalamus; **ad**: adrenal gland; **ki**: kidney. Adapted from Mesiano (2009, p. 263) and Monticone et al. (2012).

2.1.2 Rapid Effects of Steroid Hormones

Steroid hormone effects are mediated by specific receptors in target tissues (Wendler et al., 2010), which include steroid cell surface receptors that mediate the rapid effects of steroid hormones. Rapid effects of steroid hormones were first observed in the 1940s (Selye, 1942), and numerous studies have since identified rapid steroid hormone effects in various tissues. Examples of the rapid effects of the five steroid groups are summarised in Table 2.1.

Table 2.1: Rapid actions of steroid hormones. Examples of rapid physiological effects of steroid hormones. Not all of these effects are mediated by cell surface receptors. In the case of rapid progestogen effects, the mechanism of action is unknown. Abbreviations: **ERK**: extracellular signal-regulated kinase; **ATPase**: adenosine triphosphatase. Adapted from Wendler et al. (2010).

Steroid type	Effect	Reference(s)
Androgens	Anti-proliferative effects on androgen-sensitive human prostate adenocarcinoma cells	Hatzoglou et al. (2005)
	Proliferative effects on human breast cancer cells	Lin et al. (2009b)
Estrogens	Activation of extracellular signal-regulated kinase (ERK) in sheep uterine endothelial cells	Chen et al. (2004)
	ERK activation & Increase in insulin synthesis	Alonso-Magdalena et al. (2008)
Glucocorticoids	Increase in ATPase activity in *Oreochromis mossambicus*	Sunny & Oommen (2001)
	Inhibition of smooth muscle contraction in guinea pig trachea	Sun et al. (2006)
Mineralocorticoids	Increase of intracellular pH in human arteries	Alzamora et al. (2000)
	Increase in phosphorylation of myosin light chain clonal vascular smooth muscle cells	Gros et al. (2007)
Progestogens	Oocyte maturation in Xenopus	Ferrell (1999)
	Acrosome reaction in human sperm	Luconi et al. (2004)

2.1.3 Genomic Effects of Steroid Hormones

In addition to cell surface receptors, steroid hormone effects are mediated by intracellular transcription factors known as nuclear steroid receptors (Bain et al., 2007).

Nuclear steroid receptors, including the androgen receptor (AR), estrogen receptor (ER), glucocorticoid receptor (GR), mineralocorticoid receptor (MR), and P4 receptor (PR), are ligand-dependent members of the superfamily of nuclear receptors whose members are classified according to the homology of their sequences as summarised in Supplementary Table A.1 (Nuclear Receptors Nomenclature Committee, 1999; Germain et al., 2006). The general structure of nuclear receptors can be subdivided into the six domains that are shown in Figure 2.4 (Beato, 1989). Domains A and B are located in the amino acid (N-) terminal region of nuclear receptors, which contains a transactivation function, TAF-1. Domain C, the DNA-binding domain (DBD), is a conserved domain among nuclear receptors which enables binding of receptors to specific DNA sequences in the promoter regions of target genes (response elements). A hinge section, domain D, separates the DBD from the ligand-binding domain (LBD), domain E, located in the carboxyl (C-) terminal region of the nuclear receptor protein. The LBD is a conserved domain which contains a transactivation function (TAF-2) to which other regulatory proteins known as coactivators bind (Kumar & Thompson, 1999; Bain et al., 2007; Pardee et al., 2011). Coactivators enhance transcription by aiding the remodelling of chromatin and the binding of other proteins (Tetel, 2009). The LBD also functions as the region where receptor dimerisation occurs (Kumar & Thompson, 1999; Bain et al., 2007; Pardee et al., 2011). A domain in the C-terminal region of nuclear receptor proteins, domain F, is present in some nuclear receptors (Pardee et al., 2011; Burris et al., 2013).

In the classic genomic mechanism of steroid nuclear receptor action, the nuclear receptor is bound to chaperone proteins in the absence of the ligand. Since steroids are small hydrophobic molecules, they can pass through the cell membrane into the cytoplasm to bind nuclear steroid receptors. Once the nuclear receptor is bound to

Figure 2.4: Organisation of the nuclear receptor domains. Shown are: **A/B**: domains A and B; **C**: domain C; **D**: domain D; **E**: domain E; **F**: domain F; **N–**: amino acid terminus; **–C**: carboxyl terminus; **DBD**: DNA-binding domain; **LBD**: ligand-binding domain; and hinge section. Adapted from Pardee et al. (2011).

a ligand, the chaperone proteins dissociate and the receptor-ligand complex translocates into the nucleus where it forms a dimer with a similar complex. The dimerised receptor-ligand complex binds to a response element in the promoter region of a target gene and recruits coregulators which enable the regulation of transcription (Beato, 1989; Chen et al., 2006).

Steroid receptor coregulators can enhance transcription (coactivators) or inhibit transcription (corepressors) (McKenna et al., 1999). Some coactivators, such as the p160 steroid receptor coactivator (SRC) family of coactivators, provide a connection between ligand-bound receptors and the basal transcriptional machinery, which is composed of general transcription factors that interact with RNA polymerase II (Carlberg & Molnár, 2014), while other coactivators, such as the cAMP response element binding protein (CREB)-binding protein (CBP) and p300 factors, contain the enzyme histone acetyltransferase, which catalyses the acetylation of the lysine residues of histones, leading to changes in chromatin structure that enable ligand-bound receptors to interact with the response elements of target genes. On the other hand, corepressors such as the nuclear receptor corepressors (NCoRs), interact with proteins that contain the enzyme histone deacetylase, which catalyses the deacetylation of the lysine residues of histones, which makes the chromatin of target genes compact and their response elements difficult to reach. NCoRs interact with NRs

that are either bound to antagonists, or unbound (McKenna et al., 1999; Leonhardt et al., 2003; Condon et al., 2003; McEwan, 2009).

Steroid hormones play an important role in regulating physiological functions, including female reproductive functions (Couse et al., 2006). This thesis focuses on the effects exerted by the steroid hormone P4 on uterine tissues, the synthesis, mechanisms of action, and biological effects of which are described in the next section.

2.2 Progesterone Structure and Synthesis

The 21-carbon steroid hormone P4 is synthesised from cholesterol in the ovaries, placenta, adrenal glands, and the central nervous system (Rone et al., 2009). Natural synthesis of P4 is achieved through the conversion of cholesterol into pregnenolone and subsequent oxidation of pregnenolone. P4 is also a precursor in the synthesis of mineralocorticoids, glucocorticoids, androgens, and estrogens as shown in Figure 2.2. In addition to the four steroid rings described in Section 2.1, the P4 molecule has methyl (CH_3) groups attached to the carbon atom at position number 10 (C_{10}) and at C_{13}, and ketone functional [$RC(=O)R'$] groups at C_3 and at C_{20} (Figure 2.5). A ketone functional group contains a double bond between carbon and oxygen atoms, the former of which is attached to two carbon containing groups as illustrated in the insert in Figure 2.5.

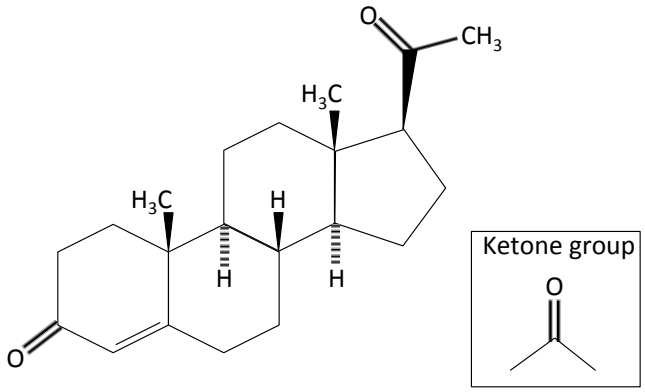

Figure 2.5: Chemical structure of progesterone and ketone functional group. Progesterone has the 4 rings typical of steroid hormones as well as methyl groups at C_{10} and C_{13}, and functional ketone groups at C_3 and C_{20}. **Insert**: Structure of a ketone functional group.

2.3 Mechanisms of Action

Like other steroid hormones, the biological effects of P4 can be transcription-dependent (genomic effects) or independent of transcription (Tan et al., 2012). Non-genomic effects of P4 tend to be rapid, and can thus be observed within a few seconds or minutes of treatment with P4. Rapid P4 effects were first described by Selye (1942) in a study that assessed the pharmacological actions of the steroids. Subsequent studies have identified rapid effects of P4 in a host of physiological processes, for example, activation of the release of enzymes from the head of human sperm, known as acrosome reaction (Luconi et al., 2004), and the promotion of *Xenopus* oocyte maturation (Ferrell, 1999). This thesis focuses on the transcription-dependent effects of P4. The rapid non-genomic effects of P4 are not discussed further in this thesis, but can be found in various reviews such as the review conducted by Gellersen et al. (2009).

Unlike the non-genomic effects of P4, genomic effects regulate gene expression, and

are typically slow, taking several hours to be observed (Steinman & Trainor, 2010). The genomic effects of P4 are mediated by the nuclear P4 receptor (PR), a ligand-activated transcription factor which is a member of the nuclear receptor super family (Wetendorf & DeMayo, 2012).

2.3.1 Nuclear Progesterone Receptor

Most of the genomic effects of P4 are mediated by two PR isoforms, P4 receptor A (PRA) and P4 receptor B (PRB), that are encoded by the same gene using two distinct transcription start sites and translated from alternating start codons (Conneely et al., 2001; Wetendorf & DeMayo, 2012). PRA and PRB have structures that are common to the members of the NR superfamily of transcription factors (Section 2.1.3). The PRA and PRB proteins are similar except for an additional sequence of 164 amino acids present in the N-terminus of the PRB protein, which contains a third transactivation function (TAF-3) as shown in Figure 2.6. PR consists of an N-terminal regulatory domain, DBD, a hinge section, a C-terminal LBD, as well as TAFs (Lydon et al., 2000; Leonhardt et al., 2003; Wetendorf & DeMayo, 2012).

The role of PR was established through gene mutation studies; Lydon et al. (1995) generated a PR knock-out ($PRKO^{-/-}$), which appeared physically normal but did not ovulate. Despite having mature follicles within their ovaries, $PRKO^{-/-}$ mice still failed to ovulate when stimulated artificially. In addition to having an anovulatory phenotype, $PRKO^{-/-}$ mice had defective implantation. Additionally, Lydon et al. (1995) observed that the development of the ducts in the mammary glands of $PRKO^{-/-}$ mice was reduced, while the lobular-alveolar structures that are essential for lactation were absent. Lydon et al. (1995) showed that that PR-mediated effects

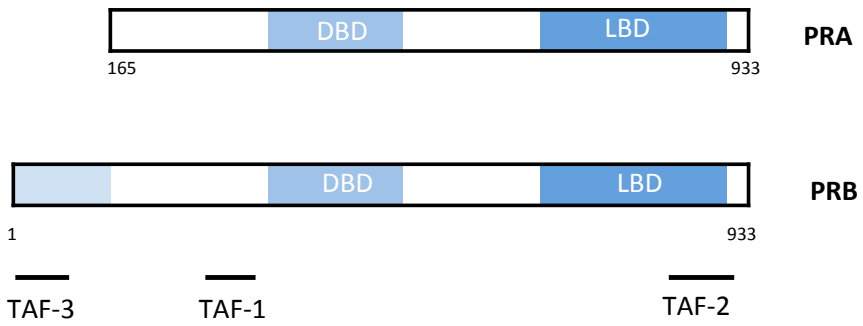

Figure 2.6: Progesterone receptor isoform domain structure. Structure of progesterone receptor isoforms showing the N-terminal domain, DNA binding domain (DBD), ligand binding domain (LBD), and transactivation functions (TAF-1, TAF-2 and TAF-3).

of P4 are essential for ovulation, successful implantation, and the development of mammary gland ducts as well as lobular-alveolar structures.

The roles of the two main PR isoforms, PRA and PRB, have also been established through gene mutation studies. In mice where PRA was selectively ablated, ($PRAKO^{-/-}$), reduced numbers of oocytes were produced in comparison to wild-type mice, despite having a large number of mature follicles within their ovaries (Mulac-Jericevic, 2000). Like in $PRKO^{-/-}$ mice, $PRAKO^{-/-}$ mice did not fall pregnant on mating with wild-type bucks. However, the effects of P4 in the mammary glands and thymus of PRAKO mice were not impeded, suggesting that PRB mediates P4 effects in the mammary glands (Conneely et al., 2001; Tan et al., 2012). In another mouse study, where PRB was selectively ablated, Mulac-Jericevic et al. (2003) demonstrated that ovulation was not affected in ($PRBKO^{-/-}$). In addition, $PRBKO^{-/-}$ mice exhibited normal mammary gland development similar to that of wild-type mice, confirming that PRB mediates P4 effects in the mammary glands.

Although PRA and PRB tend to be coexpressed in target tissues, Richer & Manning (2002) observed that PRA and PRB uniquely regulated subsets of P4-responsive genes, while nearly 25% of the P4-responsive genes studied were regulated by both

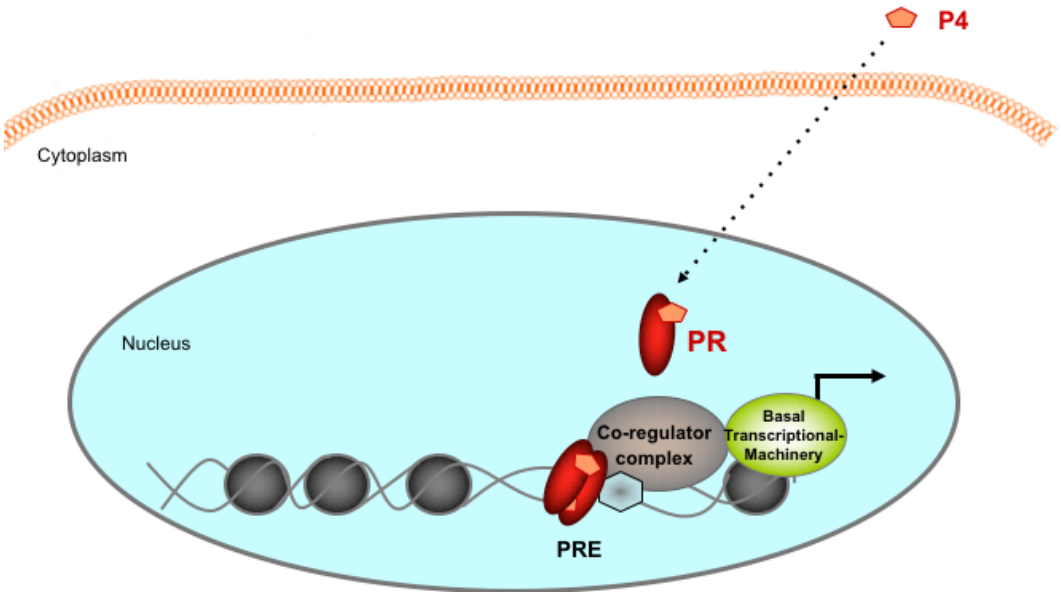

Figure 2.7: Genomic actions of progesterone. P4 diffuses into the nucleus where it binds to PR, the PR-P4 complex dimerizes and approaches the chromatin, binds to PREs on target genes, and recruits co-regulators. The co-regulators interact with general transcription factors (basal transcriptional machinery) which, in turn interact with RNA polymerase II and initiate transcription. Abbreviations: **P4**: progesterone; **PR**: progesterone receptor; **PRE**: progesterone response element;

PR isoforms in human breast cancer cells. PRB has also been shown to bind co-activators that are different from those that bind PRA, and the two isoforms respond uniquely to modulators such as the PR partial antagonist mifepristone, which inhibits the action of PRA while it acts as a weak agonist for PRB (Meyer et al., 1990; Hovland, 1998; Giangrande et al., 2000; Leo & Lin, 2008; Tung et al., 2006).

2.3.2 Genomic Mechanism of Action

While possessing distinct functions, PRA and PRB both act through the classic mechanism of nuclear receptor action which is illustrated in Figure 2.7. In the classic or genomic mechanism of P4 action, the inactive receptor is normally bound to a chaperone protein in the cytoplasm which is cleaved off following the binding of P4 to PR in the nucleus. The P4-PR complex dimerises and recruits co-regulators

that mediate changes in the chromatin structure at promoters, thereby allowing or inhibiting the PR-P4 dimer to bind to P4 response elements (PREs) in the promoter regions of target genes. Co-regulators interact with other protein complexes as well as the basal transcriptional machinery initiating the transcription of the genes as described in Section 2.1.3 (Leonhardt et al., 2003; McEwan, 2009; Wetendorf & DeMayo, 2012). Coregulators are essential for normal PR-mediated transcription as evidenced by the reduced growth and development of various tissues including the uterus and mammary glands, and resistance to progesterone in mice lacking the coactivator SRC-1. While, mice lacking the coactivator SRC-2 had delayed onset of puberty, and produced less oocytes than their wild-type counterparts (Xu et al., 1998; Tetel, 2009). In addition, (Condon et al., 2003) observed that the levels of the coregulators CPB and SRC were reduced in samples of labouring human and mouse myometrium, suggesting that the reduction in the number of PR coactivators available for recruitment may reduce PR-mediated quiescent effects of P4 at term. Nuclear receptor interacting protein 1 (NRIP1), also known as RIP140, is also a PR coregulator that affects PR action through its interaction with agonist-bound ER-α and TAF-2 on PR (Caballero et al., 2005; Nautiyal et al., 2013). While NRIP1 knock-out ($RIPKO^{-/-}$) mice exhibit an anovulatory phenotype similar to that observed in $PRKO^{-/-}$, the endocrine function of the ovaries in $RIPKO^{-/-}$ mice is normal as opposed to that of $PRKO^{-/-}$ mice (Robker et al., 2000; White et al., 2000; Leonardsson et al., 2002). Although NRIP1 is expressed in numerous reproductive tissues, Leonardsson et al. (2002) observed that the effects of NRIP1 on fertility were confined to the ovaries. In addition to its effect on ovulation, Leonardsson et al. (2002) suggested that NRIP1 may play a role in the maintenance of pregnancy as $RIPKO^{-/-}$ mice exhibited prolonged pregnancies when compared to wild-type mice.

2.3.3 Progesterone Receptor Antagonists

As well as coregulators and agonists, PR interacts with ligands, known as antagonists, that inhibit or diminish the effect of P4. While antagonists are structurally similar to P4, they tend to bind to PR with higher affinity as compared to P4. There are three main types of PR antagonists defined by their effects once bound to the receptor; Type I, Type II, and Type III (Afhüppe et al., 2010). Type I antagonists bind to the receptor and induce changes in the structure of the receptor-antagonist complex, which prevent the complex from binding to response elements on target genes. ZK-98299 (Onapristone) is an example of a Type I P4 receptor antagonist, which was developed by Schering AG (Neef et al., 1984). Onapristone is a pure PR antagonist that has been shown to possess anti-tumour characteristics. (Jonat et al., 2013; Kougioumtzi et al., 2014). Type II antagonists also induce conformational changes to the receptor-antagonist complex, but do not prevent the receptor-antagonist complex from binding to response elements on target genes. However, the receptor-antagonist complex formed with a Type II antagonist cannot initiate transcription, because its structure does not allow TAF-2 to interact with coregulators (Cadepond et al., 1997; Cabeza et al., 2015). RU486 (Mifepristone) is a Type II antagonist, which was first synthesised in 1981. Mifepristone binds to both PR and GR with high affinity (Philibert et al., 1985). Like Type II antagonists, Type III antagonists allow the receptor-antagonist complex to bind to response elements on target genes. However in contrast to Type II antagonists, the Type III receptor-antagonist complex is able to recruit and interact with corepressors, thus directly inhibiting transcription of target genes (Afhüppe et al., 2010). ZK-230211 (Lonaprisan) is a Type III antagonist that exhibits anti-proliferative characteristics and has been shown to increase the recruitment of nuclear receptor corepressor (NCoR) when bound to PR (Afhüppe et al., 2010; Jonat et al., 2013).

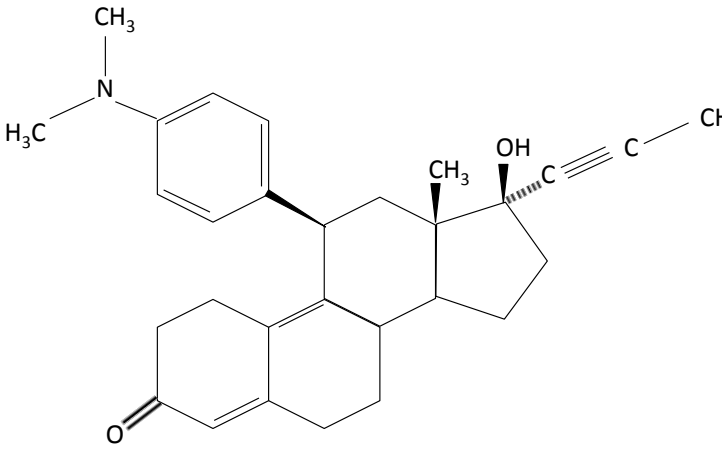

Figure 2.8: Chemical structure of mifepristone.

Mifepristone

The chemical structure of mifepristone is similar to that of progesterone as it contains four carbon rings, which allows the antagonist to bind to PR (Figure 2.8) Mifepristone has a range of clinical applications including, the prevention of pregnancy in the form of the morning-after pill and the induction of labour following intrauterine fetal death (Amer-Alshiek et al., 2015; Carp, 2015). Mifepristone cannot induce abortion during the second trimester in humans, however, treatment with mifepristone prior to the administration prostaglandins reduces the time taken for the fetus to be aborted (Thong & Baird, 1992).

Mifepristone has been used in the study of PR activation (Leonhardt et al., 2003). It has also been shown that mifepristone increases the expression gap junction proteins, which are usually suppressed by P4 (Gibb et al., 2006). Mifepristone has been shown to act as a PRB agonist in the presence of cyclic guanosine monophosphate (cGMP) and cyclic adenosine monophosphate (cAMP) (Sartorius et al., 1993; Edwards et al., 1993). In addition, Han et al. (2007) observed that mifepristone enhanced PR activity in the uterus and the mammary gland following a 3-day treat-

ment regimen with mifepristone.

In rats, mifepristone can induce abortion and preterm labour (Chwalisz, 1994). As such, mifepristone was used to induce pre-term labour in the present study.

2.4 Non-Uterine Functions of Progesterone

2.4.1 Neurological Effects

Progesterone has numerous neurological effects as it affects the neurotransmitters noradrenaline and histamine in rats (Chaudhuri et al., 1992). The neuroprotective effects of progesterone have been observed in animals with traumatic brain injury (TBI), neonatal hypoxic-ischemic encephalopathy, ischemic stroke, spinal cord injury, and multiple sclerosis (Lopez-Rodriguez et al., 2015; Peterson et al., 2015; Yousuf et al., 2014; De Nicola et al., 2013). The clinical benefits of progesterone in the treatment of TBI could, however, not be determined as the encouraging results of Phase II clinical trials could not be replicated in the Phase III trials (Lopez-Rodriguez et al., 2015). In one Phase III trial, the proportion of patients who showed signs of improvement following treatment with progesterone was similar to that of patients treated with the placebo. In addition, the proportion of patients who died while under treatment with progesterone was similar to that of patients taking the placebo (Skolnick et al., 2014).

2.4.2 Breast

Progesterone is involved in mammary gland and lobular development in the breast, where its nuclear receptors PRA and PRB are both expressed (Obr & Edwards, 2012).

While both PRA and PRB are coexpressed in normal breast tissues, their expression was seen to vary considerably in breast cancer, suggesting a role for progesterone in the development of breast cancer (Conneely et al., 2008; Mote et al., 2008). The absence of regulation of PR-mediated P4 signalling is associated with the development of cancer, not only in breast tissue, but in all tissues in which the steroid hormone P4 exerts its effects (Kougioumtzi et al., 2014). Breast cancer cells that express PR are termed PR-positive (PR^+) and have been the subject of studies involving Type I and Type II PR antagonists (Robertson et al., 1999). A Phase II randomised study was conducted in 2013 to determine whether the Type III PR antagonist Lonaprisan would be effective as a second-line therapy for PR^+ breast cancer. While Lonaprisan had not been previously associated with liver toxicity as had been observed with Onapristone, a Type I PR antagonist, patients in the study developed adverse side effects and Lonaprisan was deemed unsuitable for the treatment of breast cancer (Jonat et al., 2013). Wargon et al. (2015) postulated that the responsiveness of PR^+ breast cancer to treatment with PR antagonists is dependent upon the ratio of the PR isoforms PRA and PRB, further suggesting that tumours with a high PRA/PRB ratio could benefit from combined treatment with PR antagonists and the standard endocrine treatment with tamoxifen or progestogens.

2.4.3 Bones

The elevation of bone mass and an increase in the rate of bone formation in mice lacking the progesterone receptor as well as in wild-type mice that had been treated with mifipristone in comparison to their untreated counterparts, indicated the involvement of progesterone in bone development (Yao et al., 2010; Imai et al., 2013). Progesterone's role in bone development was further substantiated by the reduction of bone mineral density due to the use of oral contraceptives that contained proges-

terone (Yao et al., 2010).

2.5 Reproductive Functions of Progesterone

In concert with other hormones, P4 is vital to female reproductive processes, such as ovulation and the maintenance of the endometrium during pregnancy. (Conneely et al., 2003; Smith et al., 2007). In order to fully appreciate the reproductive roles of P4, the female reproductive system (Figure 2.9a) is described below.

2.5.1 Female Reproductive System

The female reproductive system consists of a set of organs that work in concert to fulfil the reproductive role of the female adult. The ovaries are the source of female gametes, all of which are produced prior to birth. As such, females are born with a finite number of immature gametes (oocytes) that mature into ova during their reproductive years (Cunningham et al., 2005). When the ovum, is released by the ovary, it is swept into the uterine tube by the fimbriae. Once in the uterine tube, the transportation of the ovum towards the uterus is facilitated by the cilia of the cells that line the wall of the uterine tube (Strauss & Lessey, 2009). It is in the uterine tube where the ovum may fuse with a sperm, the male gamete that would have travelled through the vagina, and continues the journey towards the uterine cavity where it later implants and develops into a fetus. In the absence of sperm, the ovum still travels to the uterine cavity but instead of implanting it is passed out of the body through the vagina along with the lining of the uterus as menstrual flow, a process which occurs periodically (Jabbour et al., 2006). The following sections describe the structure of the human uterus in detail, as well as the hormonal control

of the cyclical release of ova and shedding of the uterine lining.

The Human Uterus

The human uterus is a hollow muscular organ whose main body (uterine cavity) is surrounded by a wall that consists of three layers; an inner mucous layer called the endometrium, a layer of smooth muscle called the myometrium, and a thin outer layer called the serosa (Aguilar & Mitchell, 2010). The dome-shaped top of the uterus (fundus) sits above the points to which the two uterine tubes are connected, while the cylindrical-shaped bottom (cervix) is connected to the vagina (Figure 2.9a).

In the non-pregnant uterus, the endometrium consists of a functional layer and a basal layer (Figure 2.9b), the former of which contains a compact layer and a spongy layer that are both built-up and shed periodically. Unlike the functional layer, the basal layer of the endometrium does not thicken and is shed periodically (Jabbour et al., 2006; Strauss & Lessey, 2009). The changes in the endometrial layers of the uterus that are governed by P4 and other hormones, form part of the human menstrual cycle which is described in Section 2.5.2.

2.5.2 The Menstrual Cycle

During female reproductive years in humans, the uterus periodically prepares for pregnancy, a process which involves the thickening of the functional layer of the endometrium. In the absence of a fertilised ovum, implantation does not occur and the uterine lining is shed. The periodic thickening and shedding of the uterine lining and the associated ovarian changes are known as the menstrual cycle. As

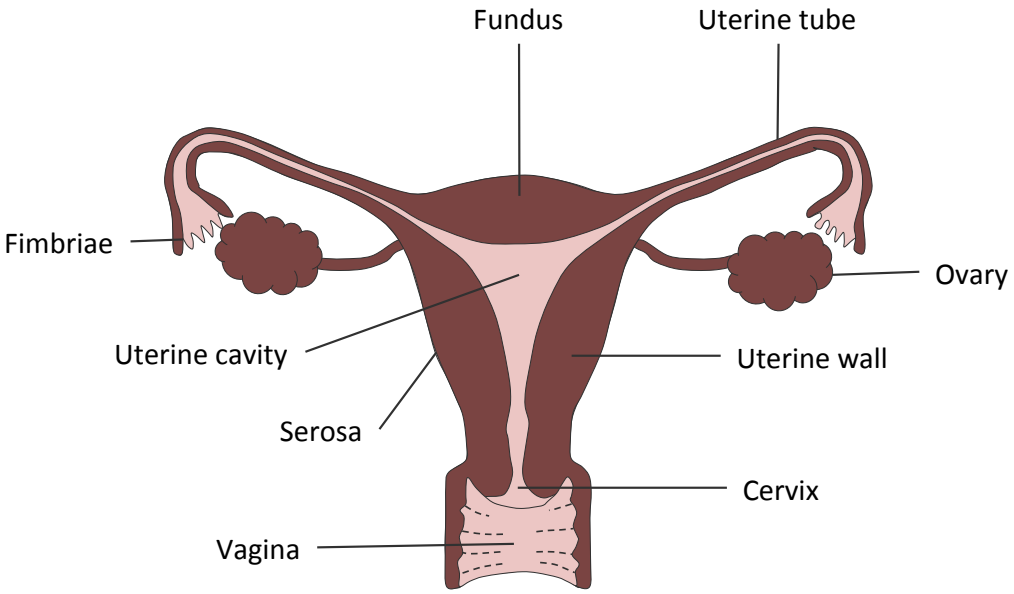

(a)

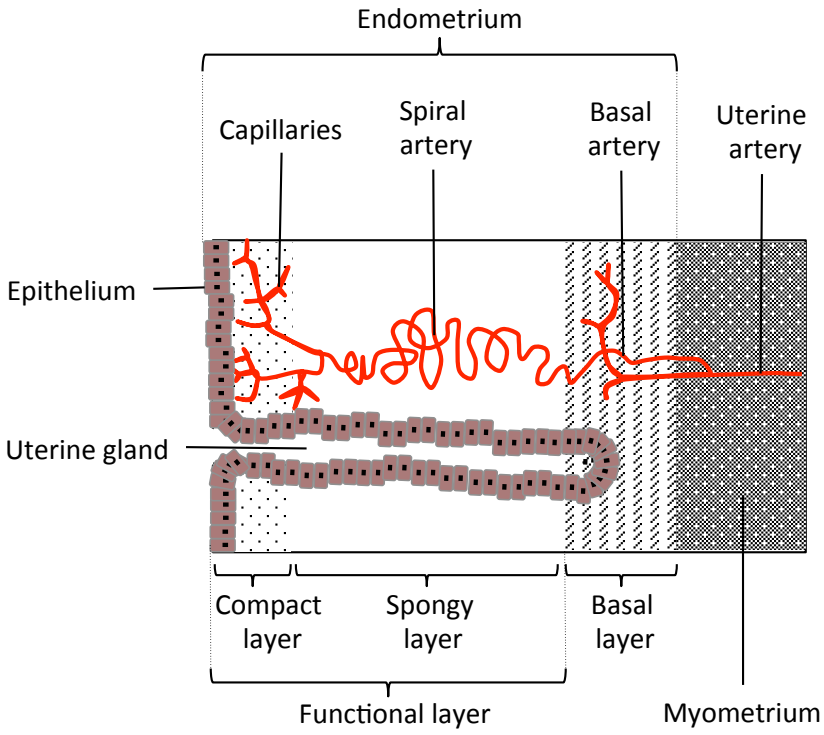

(b)

Figure 2.9: The female reproductive system. (a) Illustration of the frontal section of the female reproductive organs showing the ovaries, uterine tubes, uterus, and vagina. **(b)** Schematic of the uterine wall showing the layers of the endometrium as well as the myometrium.

such, the menstrual cycle consists of the ovarian cycle and the uterine cycle, both of which are under hormonal control. The main hormones involved in the regulation of the menstrual cycle are gonadotropin releasing hormone (GnRH) which is secreted by the hypothalamus, follicle stimulating hormone (FSH) and luteinizing hormone (LH), which are secreted by the pituitary gland, as well as E_2, inhibin, and P4, which are produced in the ovaries (Messinis, 2006; Hall, 2009).

The Ovarian Cycle

The ovarian cycle consists of two phases, one characterised by the growth and maturation of follicles (follicular phase) and another characterised by the development and degeneration of the ruptured follicle (luteal phase), that are separated by follicular rupture and release of an ovum as illustrated in Figure 2.10.

The oocytes with which females are born, are contained within follicles that are also immature. During the follicular phase of the ovarian cycle, an increase in the pulsatile secretion of GnRH stimulates the secretion of FSH, which stimulates the growth and development of the E_2-releasing immature follicles (Pansky, 1982; Marshall et al., 1993). While one of the stimulated follicles grows at a faster rate than the others and matures, E_2 stimulates the release of LH which results in a surge of LH that precipitates ovulation, the rupture of a mature follicle and release of the ovum contained therein.

In the luteal phase, the ruptured follicle is transformed into the corpus luteum which produces copious amounts of P4, as well as moderate quantities of E_2 and inhibin. Together, these hormones prevent the production and release of FSH and LH thus enabling P4 to maintain the functional layer of the endometrium in preparation for implantation. If, however, the released ovum does not fuse with a sperm cell,

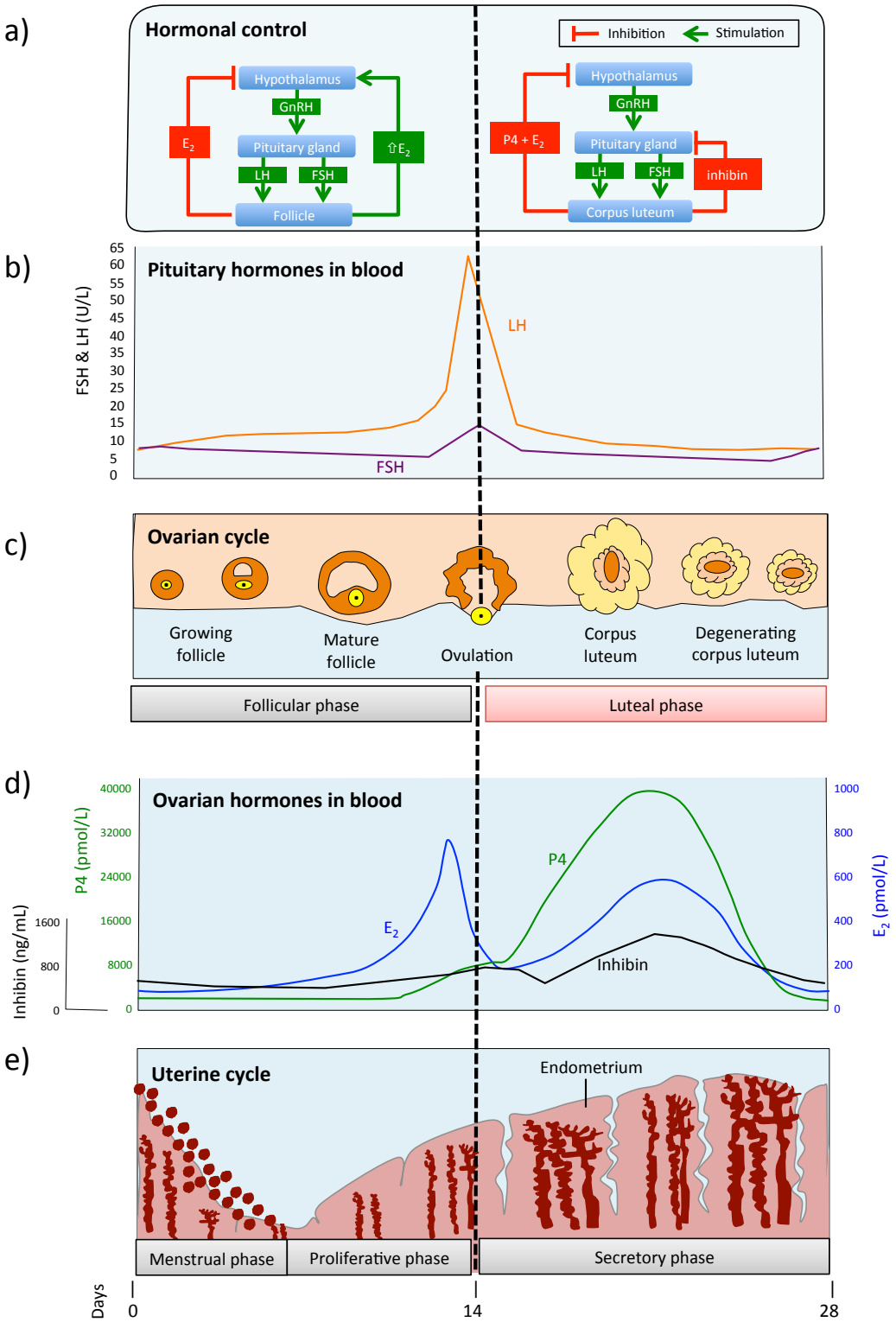

Figure 2.10: Illustration of the 28-day menstrual cycle. **(a)** Regulation of gonadotropins by ovarian hormones. Prior to ovulation, E_2 exerts both inhibitory and stimulatory effects on the synthesis of gonadotropins. During the post-ovulatory phase of the menstrual cycle, the ovarian hormones inhibit the synthesis of gonadotropins. **(b)** Changes in the concentration of gonadotropins in the blood during the menstrual cycle. The surge in LH levels, occurring after the spike in E_2 levels, precipitates ovulation. FSH levels are at their peak during ovulation. **(c)** The ovarian cycle has two phases, follicular and luteal, that are separated by ovulation. The follicular phase is characterised by follicle development while the luteal phase is characterised by the formation and degeneration of the corpus luteum. **(d)** Changes in the ovarian hormones E_2, P4, and inhibin that are associated with the menstrual cycle. A spike in E_2 levels precedes ovulation, while P4 and inhibin levels reach their peak in the middle of the luteal phase of the ovarian cycle. **(e)** Phases of the uterine cycle. Abbreviations: **E_2**: estradiol; **FSH**: follicle stimulating hormone; **GnRH**: gonadotropin releasing hormone; **LH**: luteinizing hormone; **P4**: progesterone.

implantation will not take place, and the corpus luteum degenerates as a result (Strauss & Williams, 2009).

Uterine Cycle

The uterine cycle consists of three phases as illustrated in Figure 2.10. The first is the menstrual phase, which is characterised by the break-down of the functional layer of the endometrium and its elimination from the body through the vagina. This phase lasts between 3–6 days and occurs approximately every 28 days (Hall, 2009). The second is the proliferative phase, in which the functional endometrial tissue regenerates under the influence of the E_2 secreted by the growing follicles. Both the menstrual and the proliferative phases of the uterine cycle occur prior to ovulation. The third phase of the uterine cycle, known as the secretory phase occurs after ovulation. This phase involves the growth of the spiral arteries and the uterine glands under the influence of the P4 secreted by the corpus luteum. Glandular secretions that are favourable for implantation are also produced during this phase (Gellersen et al., 2007). If fertilisation does not occur, implantation will not take place. As a result, the corpus luteum degenerates resulting in the decrease of P4 levels and the break-down of the functional endometrial layer (Strauss & Williams, 2009; Hall, 2009).

If fertilisation occurs, the fertilised ovum goes through phases of development and change for approximately 7 days, resulting in the formation of a blastocyst. A blastocyst consists of an inner cell mass which later develops into the embryo, a cavity, and an outer layer composed of trophoblast cells. Implantation of the blastocyst occurs on the 8th or 9th day following fertilisation, when the conditions in the uterus are favourable for implantation. As soon as implantation occurs, the

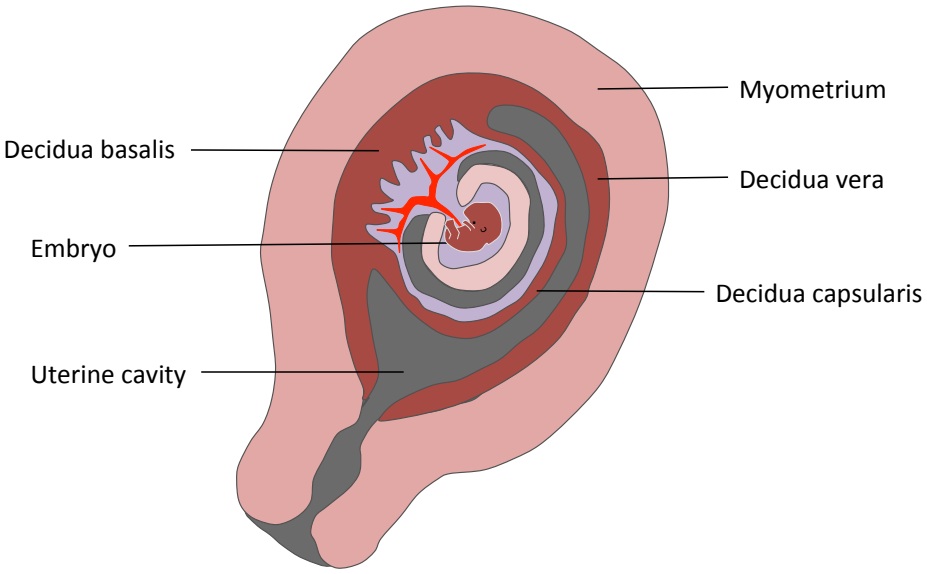

Figure 2.11: The decidua. Illustration of the location of the three decidual zones.

trophoblast cells secrete the human chorionic gonadotropin (hCG) hormone which maintains the corpus luteum. The corpus luteum, therefore, does not degenerate and continues to secrete E_2, inhibin, and P4 until about the 7th week of pregnancy when the placenta takes over the production of these hormones (Jaffe et al., 1969; Mesiano, 2009).

Under the influence of P4, the endometrial stromal cells go through morphological and functional changes known as decidualisation, a process which can occur in the absence of implantation. The process of decidualisation involves the enlargement of endometrial stromal cells, accumulation of lipids and glycogen, and transformation of the stromal cells to a secretory phenotype. While P4 is involved in the decidualisation process, endometrial stromal cells require priming by cAMP prior to P4 action (Gellersen et al., 2007). Mulac-Jericevic (2004) demonstrated that decidualisation is blocked, even when stimulated artificially, in PRAKO mice unlike in PRBKO mice, suggesting that P4 effects in the decidualisation process are mediated

by PRA. In addition, Large & DeMayo (2012) observed that during decidualisation, the expression of PRB was reduced while that of PRA was maintained in epithelial stromal cells.

During pregnancy, the decidualised endometrium, known as the decidua, has three different zones that are identified in relation to their location; the basal decidua, known as decidua basalis, is the site of implantation and is adjacent to the myometrium; decidua capsularis, the decidual layer that encloses the fetal membranes; and decidua vera, the decidua that is located on the opposite side of the uterus with respect to the implantation site (Cunningham et al., 2005), as illustrated in Figure 2.11. The decidua can be considered to be an endocrine organ as it produces prostaglandins, relaxin, and prolactin which have been implicated in the onset of parturition, and in addition it enables the exchange of nutrition, waste and other substances between fetal and maternal tissues (Riddick & Kusmik, 1977; Riddick et al., 1978; Golander et al., 1978; Bigazzi et al., 1979; Bryant-Greenwood, 1982; Kredentser et al., 1995; Hirst et al., 1998).

Once pregnancy is established, the uterus remains in a state of relevant quiescence until term, when the fetus is expelled. The next section outlines the current knowledge relating to the processes leading up to the expulsion of the fetus from the uterus.

2.6 Parturition

The uterus is quiescent prior to the onset of labour, and is transformed into a stimulus-responsive organ, which contracts, once stimulated, resulting in the expulsion of the fetus through a softening and dilating cervix, at term. The physiological

process by which the fetus is expelled from the uterus is called parturition. In many mammals, e.g., rabbits (Hoffman et al., 2009), rats, and mice, parturition is preceded by a significant reduction in the levels of P4 in the maternal system (Vodstrcil et al., 2010). In rats, a drop in the levels of circulating P4 coincides with a change in electrical activity of the uterus (de Paiva & Csapo, 1973; Garfield, 2008), suggesting an important role for P4 during labour. In humans, however, the P4 levels do not decrease at term or during labour, but the withdrawal of P4 at any stage in human pregnancy, e.g., by administering the P4 antagonist mifepristone, can initiate parturition (Chwalisz, 1994; Zakar & Hertelendy, 2007).

2.6.1 Phases of Parturition

There are four phases of parturition (Figure 2.12): Phase 0, is the prelude to parturition that is characterised by uterine quiescence; Phase 1, involves preparation of the uterus for labour by activation of the uterus from the quiescent state to a contractile state; Phase 2, which involves the softening and dilation of the cervix to allow the fetus, placenta and membranes through the birth canal; and Phase 3, which involves the restoration of the uterus to the non-pregnant state (Gibb et al., 2006).

Phase 0: Quiescence

For most of pregnancy, the uterus is relaxed and non-responsive to stimulants such as oxytocin (OT) and prostaglandins (PGs). Uterine quiescence is maintained by pro-gestational agents such as CRH, P4, prostacyclin (PGI_2), relaxin, nitric oxide (NO), and parathyroid hormone-related peptide (PTHrP).

P4 suppresses the expression of the mRNA encoding the gap junction protein

Phase	**0: Quiescence**	**1: Activation**	**2: Stimulation**	**3: Involution**
Hormones/ peptides	P4 PGI_2 Relaxin NO PTHrP CRH	E	PGE_2 OT PGF_2	OT
Uterine Changes	• Relaxation • Non-responsive to stimuli	⇧ Prostaglandin receptors ⇧ OTR ⇧ CX-43 ⇧ Ion channels ⇩ NO-system	⇧ Conductivity ⇧ Excitability ⇩ Relaxation	• Involution • Repair

Figure 2.12: Phases of parturition. A summary of the hormones involved in uterine quiescence, activation, stimulation, and involution, as well as the associated uterine changes. Abbreviations: **P4**: progesterone; **PGI2**: prostacyclin; **relaxin**: relaxin; **NO**: nitric oxide; **PTHrP**: parathyroid hormone-related peptide; **CRH**: corticotropin-releasing hormone; **E**: estrogen; **PGE_2**: prostaglandin E2; **OT**: Oxytocin; **PGF_2**: prostaglandin F2; **OTR**: oxytocin receptor; **CX-43**: connexin-43; ⇑: increases; ⇓: decreases.

connexin-43, which can be increased by the PR antagonist mifepristone (Petrocelli & Lye, 1993). In addition, (Garfield et al., 2012) showed that P4 dampens the electrical activity of the myometrium. PGI_2 is synthesised from membrane phospholipids through the action of PLA_2, COX enzymes, peroxidase activity, and PGI synthase (Michal & Schomburg, 2012, p. 310). PGI_2 is known to elevate cAMP through PGI_2 receptors (IPs) thus aiding in the relaxation of the uterus (Gibb et al., 2006). Wikland et al. (1983) observed that PGI_2 induced the relaxation of human myometrium *in-vitro*, following an initial activation. Fetalvero et al. (2008), however, showed that the activation of IP lead to an increase in the expression of CAPs in-vitro, suggesting a dual role for PGI_2 in the uterus. Relaxin, which is structurally similar to insulin, is expressed in the decidua and the placenta (Gibb et al., 2006). Relaxin stimulates the production of cAMP in the myometrium, thus suppressing uterine contractility, while regulating cervical ripening (Challis et al., 2000; Gibb et al., 2006). Endogenous NO is synthesised in the myometrium as well as in fetal membranes, and has been shown to relax smooth muscle (Gibb

et al., 2006). PTHrP, whose synthesis in the myometrium is upregulated by P4, inhibits the increase in the expression of connexin-43 at term (Gibb et al., 2006) During pregnancy, CRH stimulates the production of DHEA-S by the fetal and maternal adrenal glands, as well as the production of DHEA by the maternal adrenal glands. Both DHEA and DHEA-S are precursors in the synthesis of androgens and estrogens (Cunningham et al., 2005).

Phase 1: Activation

During this phase, the myometrium and the cervix are modified in preparation for the expulsion of the fetus from the uterus. The softening, thinning, and dilation of the cervix, collectively known as cervical ripening, is also influenced by the degradation of collagen fibres by metalloproteases, which lead to changes in the structure of the cervix. In addition, the actions of prostaglandins, i.e., prostaglandin E_2 (PGE_2) and prostaglandin F_2 (PGF_2), also influence cervical ripening (Osman et al., 2003). While the cervix is ripening, the uterus is transformed from a non-responsive organ to a contracting and powerful organ. An increase in the expression of CAPs such as gap junction proteins, ion channels, uterotonin receptors such as OT receptors (OTRs) and PG receptors (PGRs), and enzymes, is associated with the initiation of labor (Fuchs et al., 1984).

Phase 2: Labour

Labour is characterised by regular uterine contractions, cervical ripening, and cervical dilatation. Labour has three stages, the first of which is characterised by rhythmic contractions, uterine transformation, and cervical changes. During the second stage of labour, there are changes in the pelvic floor. In addition, the fetus

begins to descend. The third stage of labour is the one in which the fetal membranes and placenta are delivered (Gibb et al., 2006).

Phase 3: Involution

The last phase of parturition commences after the delivery of the placenta and fetal membranes. During this phase, myometrial contractions are maintained under the influence of OT facilitating the recovery and restoration of the uterus to its former state. The cervix also reverts to the closed and static state (Gibb et al., 2006).

While there are numerous changes that occur in the cervix in preparation for and during parturition, the following sections focus on myometrial changes that occur in Phases 1 and 2 of parturition. Cervical changes occurring at term, and pre-term, are detailed in the review conducted by Mahendroo (2012).

2.6.2 Activation of the Myometrium

The myometrium is mostly muscular and is composed of spindle-shaped cells that are tapered at both ends, known as smooth muscle cells (SMCs), as illustrated in Figure 2.13a. SMCs contain a single cylindrical nucleus which is located in the centre of the cell. The SMC cytoplasm contains an abundance of mitochondria as well as well as the sarcoplasmic reticulum, the latter of which store calcium ions (Ca^{2+}) (Jain et al., 2000). In addition, there are numerous thick, intermediate, and thin filaments that are connected to α-actin dense bodies across the cytoplasm. Thick filaments are composed of the protein myosin, while intermediate filaments are made from intermediate filament proteins such as vimentin (Tang, 2008), and the proteins actin, tropomyosin and caldesmon are the main constituents of thin

filaments in SMCs (Marston & Smith, 1985). These filaments form a "criss-cross" pattern in the cytoplasm as shown in Figure 2.13a, and are the basis of the smooth muscle contractile machinery (Smith, 2007). When contracting, the myosin filaments slide over the thin filaments causing the SMCs to become short and wide. The nucleus of the contracted SMC becomes spiral-shaped as shown in Figure 2.13b (Thiriet, 2013).

Gap Junctions

During pregnancy, adjacent SMCs are joined by small channels, as well as connective tissue, forming sheets or bundles of muscle that contract in unison. The small channels, which are formed when two connexons (Figure 2.14), each composed of six gap junction proteins (connexin proteins), are joined allowing the flow of ions, small molecules, and electrical signals between neighbouring cells (Hille, 2001; Alberts et al., 2002). There are approximately 20 different types of connexin proteins deriving their names from their molecular weights, e.g., connexin-26 (Cx-26) is a 26-kDa polypeptide, while connexin-45 (Cx-45) is a 45-kDa polypeptide (Alberts et al., 2002).

The role of gap junctions in parturition was first documented by Garfield et al. (1978), and since then, the connexin proteins Cx-26, connexin-40 (Cx-40), Cx-43, and connexin-45 (Cx-45) have been identified in the myometrium (Ou et al., 1997; Kidder & Winterhager, 2009; Sheldon et al., 2014). Cx-26 expression levels decline sharply at term prior to the onset of labour, while expression of Cx-43 in the myometrium is inhibited by P4 and upregulated by E_2 expression (Ou et al., 1997; Kidder & Winterhager, 2009; Terzidou, 2007). The importance of Cx-43 proteins in the electrical coupling of SMCs during labour was demonstrated by Döring

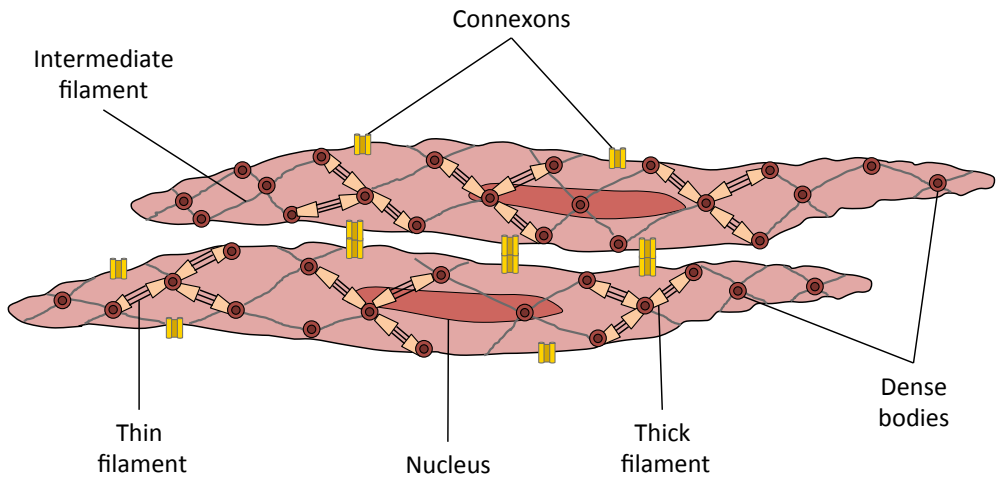

(a) Relaxed smooth muscle cells

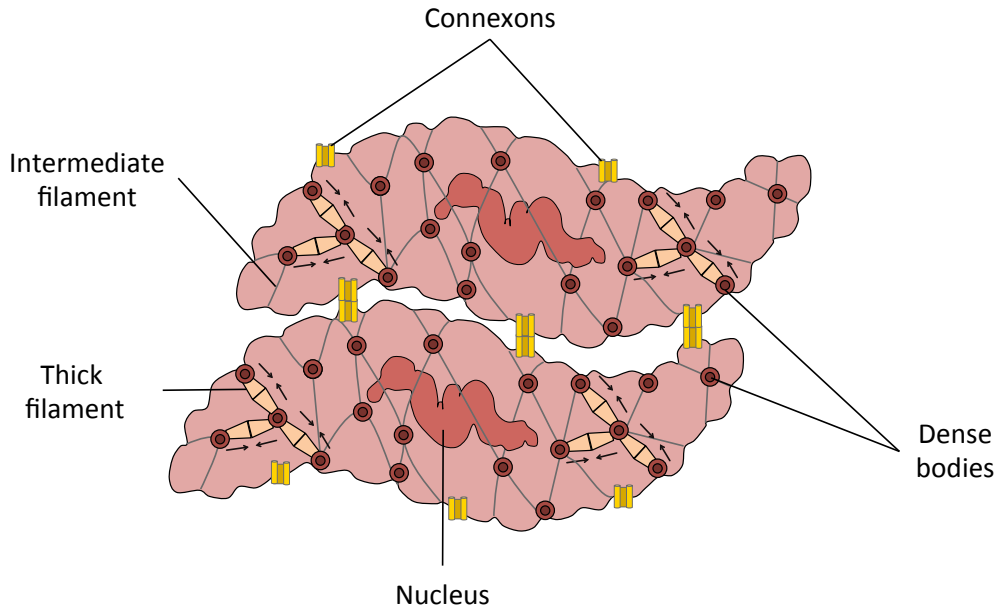

(b)

Figure 2.13: Smooth muscle cells. (a)Relaxed and (b) contracted smooth muscle cells. The contracted smooth muscle cells are thicker and shorter than relaxed smooth muscle cells. Key: →← direction of movement of thick filaments.

et al. (2006), whereby mutant mice generated through the specific deletion of the Cx-43 gene coding region in SMCs exhibited prolonged labour. Cx-43 proteins are upregulated at term and during labour, thus increasing the connectivity between SMCs, and promoting synchronised contractions (Garfield et al., 1978; Garfield &

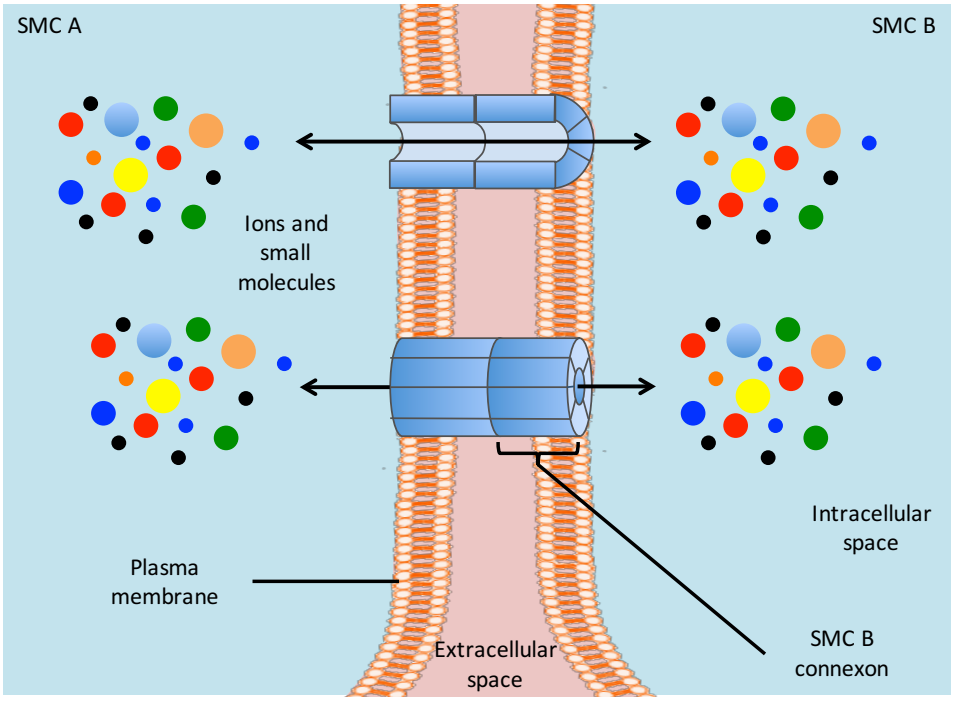

Figure 2.14: Coupling of adjacent smooth muscle cells through connexons. Each cell contributes a connexon to form a channel through which ions and small molecules are flow. Abbreviations: **SMC A**: smooth muscle cell A; **SMC B**: smooth muscle cell B.

Maner, 2007). Cx-45 proteins are expressed in both pregnant and non-pregnant myometrium, but are down-regulated prior to term (Albrecht et al., 1996). Albrecht et al. (1996) hypothesised that the expression patterns of Cx-43 and Cx-45 were important in the electrical coupling of SMCs during labour. Using a mathematical model, Sheldon et al. (2014) showed that the down-regulation of Cx-45 allows for SMC-coupling which is favourable for synchronised myometrium contractions. The role of Cx-40 during parturition is not defined, but Cx-40 proteins are expressed in the myometrium at term (Kidder & Winterhager, 2009).

2.6.3 Uterine Contractions

The protein calmodulin binds Ca^{2+} in the cytosol and induces conformational changes that enable the Ca^{2+}-calmodulin complex to activate myosin light-chain kinase enzymes. The myosin light-chain kinase enzymes phosphorylate myosin, thus activating myosin and enabling its interaction with actin, which results in SMC contractions (Vrachnis et al., 2011; Blackburn, 2014).

There are various pathways through which the entry of Ca^{2+} ions into the cytoplasm is mediated; one such pathway is through OT signalling (Michal & Schomburg, 2012, p. 292). The effects of OT are mediated by the OTR, a seven-transmembrane receptor. Like other seven-transmembrane receptors, OTR is located in the plasma membrane with both intra- and extracellular regions. The extracellular region of OTR contains the OT-binding site while its intracellular region is bound to a G-protein, which is composed of three subunits when inactive; $G\alpha_{q/11}$, $G\beta$, and $G\gamma$ (Gimpl & Fahrenholz, 2001).

When OT binds OTR, it induces conformational changes in the receptor that result in the activation of the receptor. Once the receptor is activated, the G-protein separates into its constituent subunits. The $G\alpha_{q/11}$ subunit binds to the enzyme phospholipase-C (PLC), activating the enzyme which goes on to hydrolyse a component of the cell membrane called phosphatidylinositol 4,5-bisphosphate (PIP_2). The hydrolysis of PIP_2 results in the formation of inositol 1,4,5-trisphosphate (IP_3) and diacyl-glycerol (DAG), the latter of which aids in the activation of protein kinase C (PKC) and the mitogen-activated protein kinases (MAPK) cascade leading to the synthesis of prostaglandins. IP_3, on the other hand, binds to the IP_3 receptors located on the sarcoplasmic reticulum, opening Ca^{2+} channels thus releasing Ca^{2+} ions from intracellular calcium stores. Intracellular Ca^{2+} binds calmod-

ulin resulting in smooth muscle contractions as illustrated in Figure 2.15 (Vrachnis et al., 2011).

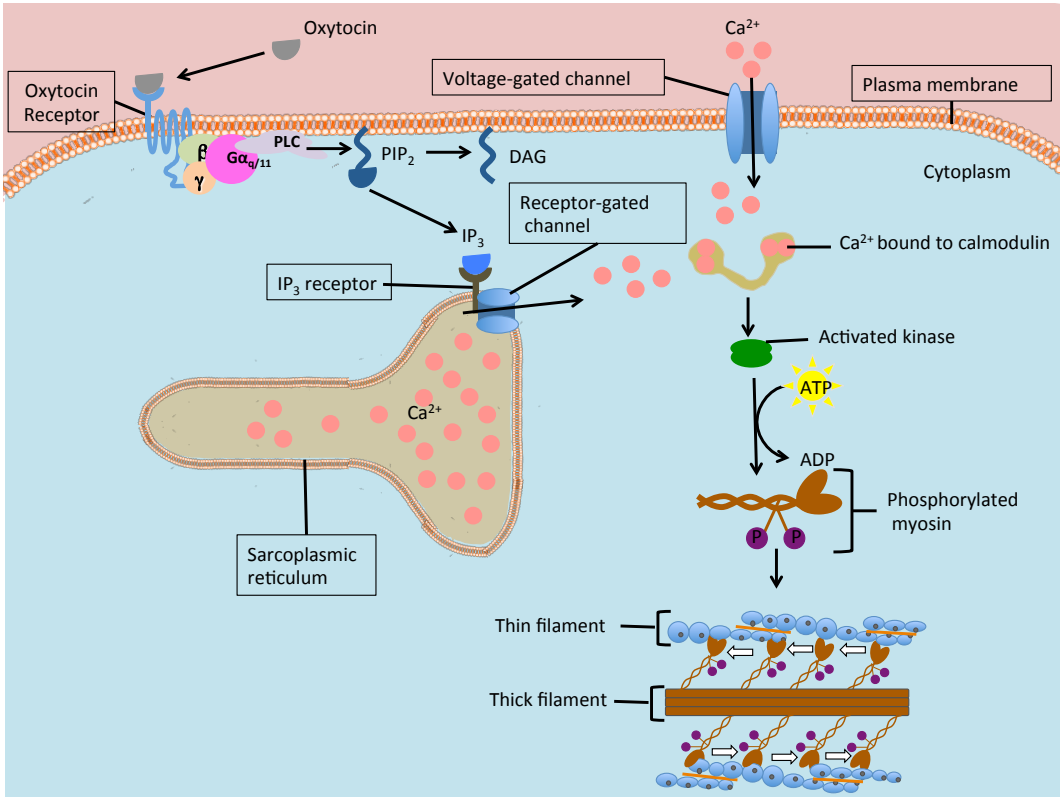

Figure 2.15: Activation of myosin by Calcium.

While OT induces the release of Ca^{2+} from intracellular stores, it also activates plasma membrane voltage-gated calcium channels, through which most of the Ca^{2+} involved in smooth muscle contraction enters the cytoplasm. The extracellular Ca^{2+} binds to calmodulin, resulting in the activation of myosin and smooth muscle contractions (Garfield & Maner, 2007). Another mechanism by which Ca^{2+} can enter the cytoplasm of SMCs is through channels that are sensitive to changes in the electrical properties of the SMCs. The depolarisation and repolarisation of the membrane through the movement of ions into and out of SMCs, generates bursts of action potentials that have been shown to influence the contractility of the uterus during labour (Laforet et al., 2011; Young, 2007; Lammers et al., 2008).

The effects of P4, and P4 withdrawal, on the mRNA transcripts encoding the proteins involved in the activation and contraction of SMCs will be analysed in Chapter 8. The next chapter in this part of the thesis gives an overview of the rat model whose study is documented in this thesis.

Chapter 3

The Female Rat

The laboratory rat (*Rattus norvegicus*) has been used in experimental studies since the early 1900s (Sengupta, 2013). A lot of knowledge has since been gained through the use of rats as model animals (Hedrich, 2000). The work presented in thesis was conducted on tissues obtained from pregnant Spague-Dawley rats. As such, in this chapter, the anatomy and characteristics of the female rat reproductive system are described, as well as compared and contrasted with the human female reproductive system. In addition, the rat uterine and ovarian cycles are also compared with those of humans. The process of parturition in the rat is subsequently described, and the chapter concludes by summarising the aims of this thesis.

3.1 The Female Rat Reproductive System

The rat reproductive system contains all the constituent organs as those of the human reproductive system, i.e., the ovary, uterine tube, uterus, cervix, and vagina. The anatomy of the female reproductive system in the rat, however, differs from

the human reproductive system in that the rat uterus is duplex, i.e., it is composed of two separate horns (Figure 3.1a). Each uterine horn is connected to an ovary, via a uterine tube, and has its own cervix. The uterine horns are joined at the vagina, forming a "Y-shape" (Komárek et al., 2000). Similar to human uterine walls, the walls of rat uterine horns consist of endometrial and serosal layers that sandwich the uterine muscle, but unlike human myometrium, the rat myometrial layer is composed of two distinct layers that are separated by a vascular layer as illustrated in Figure 3.1b. The inner layer of the myometrium, i.e., the one adjacent to the endometrium, is composed of SMC fibers that envelope the uterine horn in a circular fashion. The outer layer of the myometrium, which is sandwiched between the vascular layer and the serosa, contains SMC fibers that are arranged in "parallel" with the uterine horn (Jain et al., 2000). The inner layer is also called the circular myometrium, while the outer layer is called the longitudinal myometrium.

Unlike humans who menstruate, the uterine lining of the rat uterus is not shed and passed out of the body. Instead, the endometrial layer of the rat uterus is periodically transformed. The periodic changes in the endometrium, as well as changes that occur in the ovaries and vagina, are part of the rat estrus cycle (Westwood, 2008).

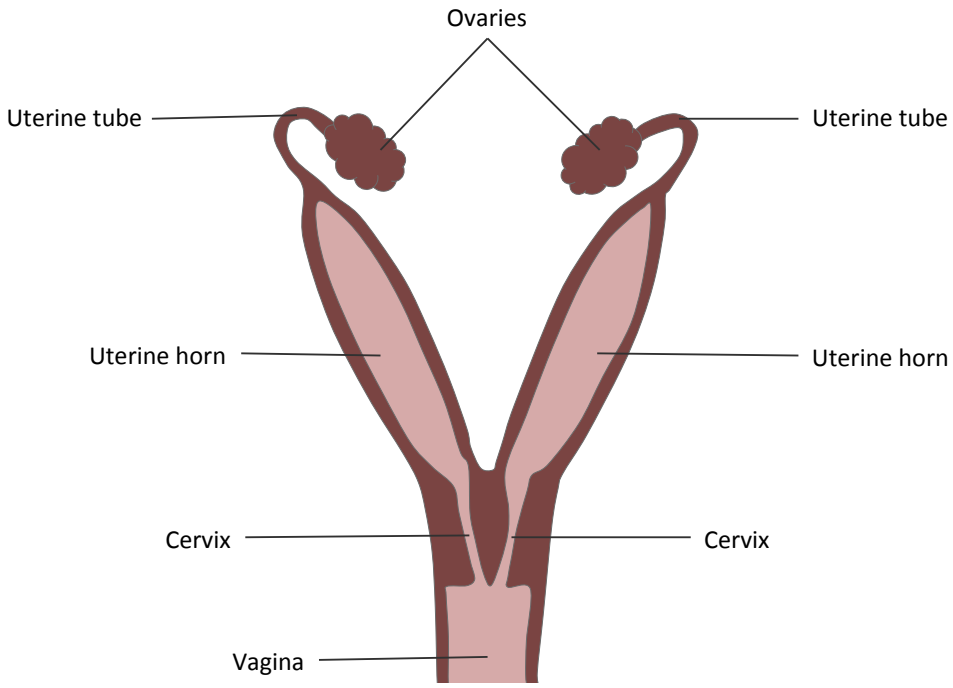

(a)

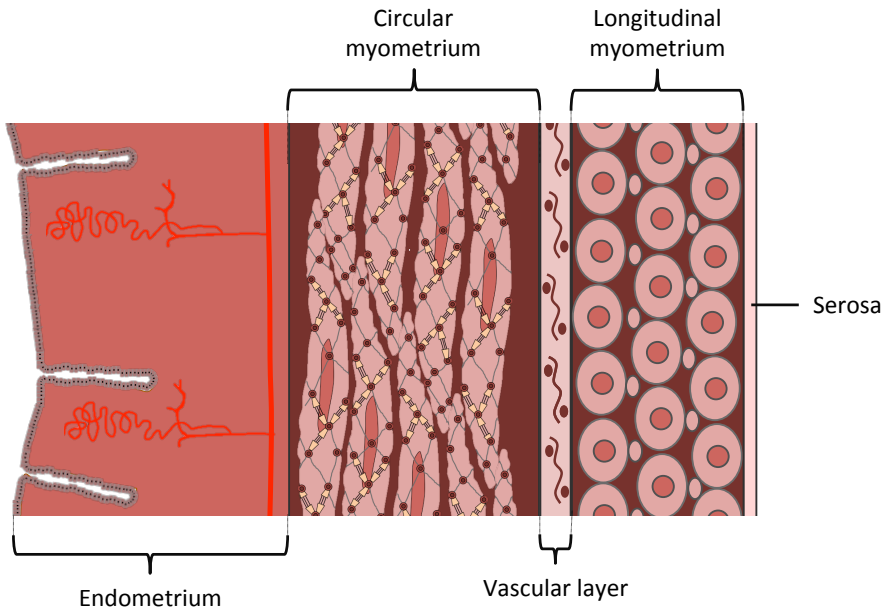

(b)

Figure 3.1: The female reproductive system in rats. (a) Illustration of the duplex uterus of the rat showing each horn with its respective ovary, uterine tube, and cervix, as well as the vagina. (b) Schematic of the walls of the uterine horns showing the distinct layers of the myometrium that are separated by a vascular layer, and sandwiched between the endometrium and serosa.

3.2 Estrus Cycle

Premature oocytes in female rats, as in humans, periodically develop and grow until ovulation after which they are transformed into corpora lutea. Puberty in the female rat is marked by the opening of the vagina 7 weeks after birth, and the ensuing regular estrus cycles (Ojeda & Skinner, 2006; Sengupta, 2013). The estrus cycle in rats, which is non-seasonal, lasts between four to five days, and can be divided into four stages; proestrus, estrus, metestrus, and diestrus (Mandl, 1951; Freeman, 2006). The main hormones that regulate the rat estrus cycle are: GnRH, which is secreted by the hypothalamus and stimulates the release of gonadotropins by the pituitary gland; the gonadotropins LH and FSH secreted by the pituitary gland; the ovarian hormones E_2, P4 and inhibin, which are synthesised in the ovaries; and prolactin, which is secreted by the pituitary gland following mating (Freeman, 2006).

3.2.1 Ovarian Cycle

During proestrus, E_2-secreting follicles grow under the influence of FSH, increasing the secretion of E_2 (Fortune, 1994; Maeda et al., 2000). The resulting surge in E_2 stimulates the release of LH by the pituitary gland, which in turn stimulates ovulation during the estrus stage of the cycle. When in estrus, rats are sexually receptive and mating can occur. Within 24-48 hours of the LH surge, ovulation occurs and the follicles are transformed into corpora lutea. The corpora lutea grow during metestrus and reach a maximum size two to four hours post-ovulation, while secreting both P4 and its analog 20α-hydroxyprogesterone, which is a non-active form of P4, as well as inhibin. In diestrus, the corpora lutea continue to secrete high quantities of P4. It is during this stage of the estrus cycle that FSH levels begin to increase in the absence of pregnancy, and stimulate the growth of a new

set of follicles, which will occur in the proestrus stage of the ensuing cycle (Freeman, 2006; Westwood, 2008). It is worth noting that while corpora lutea reduce in size in subsequent stages of the estrus cycle and become "non-functional", their functionality can be rescued in pseudopregnancy and in pregnancy (Freeman, 2006). Pseudopregnancy and pregnancy will be described in Section 3.3.1.

While there are similarities in the growth and maturation of follicles prior to ovulation between humans and rats, the number of ova that are released at ovulation, as well as the functionality of the corpora lutea differ (see Section 2.5.2). Humans normally release one ovum in each menstrual cycle, while rats, being a polytocous species, release several ova in each estrus cycle. Another difference between the ovarian cycles of these species is the method by which the released ova travel to the uterine cavity. Ova in humans are released from the ovaries and swept into the uterine tubes by the fimbriae of the uterine tubes (Section 2.5.2), while rat ova are released directly into the uterine tubes that are connected to the ovaries. Once in the tubes, the ova are directed towards the uterine horns, suspended in uterine fluid, by uterine contractions, which create waves in the fluid that move towards the uterine horns (Freeman, 2006).

3.2.2 Changes in the Uterus and Vagina

In proestrus, the surge in E_2 levels precipitates the proliferation of vaginal epithelial cells which appear rounded and nucleated in vaginal smears. At the same time, the endometrium and the uterine glands begin to grow, also under the influence of E_2 (Maeda et al., 2000; Westwood, 2008). During estrus, vaginal epithelial cells are transformed from cuboidal to stratified squamous cells without nuclei, and the uterine horns are filled with fluid, movement of which is generated by uterine

contractions and aids in the transportation of sperm and ova into the uterine horns. Meanwhile, the endometrial lining begins to degenerate and the glands begin to reduce in size. In metestrus, the lining of the endometrium continues to degenerate, while the amount of fluid in the uterine horns and the uterine contractions decrease. During this stage of the estrus cycle, vaginal smears have leukocytes as well as nucleated and non-nucleated cells. In diestrus, the endometrial layer is reduced in size, and the uterine contractions cease (Komárek et al., 2000; Freeman, 2006; Westwood, 2008).

3.3 Pregnancy and Parturition

The reproductive differences between rats and humans are not limited to the structure of their reproductive organs and cycles (see Section 3.1 and Section 3.2), but also extend to pregnancy and parturition. Rats carry multiple offspring and have short gestations of $\sim$ 22 days, while humans usually have singleton pregnancies of $\sim$ 39–40 weeks (Sengupta, 2013; Mesiano, 2009). Apart from the number of offspring, pregnancy in these two species is maintained by different endocrine organs. Pregnancy in humans is maintained by P4 synthesised in the corpus luteum during the first seven weeks of pregnancy, a role which is taken over by the placenta from week 12 to term (Mesiano, 2009). While in the rat, despite the development of several P4-secreting placentae, pregnancy is maintained by the corpora lutea, such that the removal of the ovaries results in labour and delivery of the pups (Maeda et al., 2000).

3.3.1 Pregnancy

If mating occurs at estrus, the cervix is stimulated and it signals for the release of prolactin by the pituitary gland. The secretion of prolactin inhibits the conversion of P4 to 20α-hydroxyprogesterone, thus maintaining the lining of the uterus through the secretion of high levels of P4 by the corpora lutea (Freeman, 2006). The rescuing and maintenance of luteal function in the absence of pregnancy is called pseudopregnancy, a state that usually persists for $\sim$ 11 days, before luteolysis occurs (Maeda et al., 2000; Stouffer, 2006).

If, however, the mating at estrus is fertile, fertilisation occurs and blastocysts implant $\sim$ 5 days after mating. Decidualisation in the rat is confined to the site of implantation, unlike in humans where the whole endometrium is decidualised, suggesting that the implanting embryos are involved in triggering the decidual reaction in rats (Maeda et al., 2000). While the placentae in rats secrete P4, the major source of the P4 that maintains pregnancy in rats is synthesised by the corpora lutea, which are sustained during the first half of gestation by prolactin and by placental lactogens during the latter half of gestation. In addition, E_2 is also involved in maintaining the synthesis of steroid hormones by the corpora lutea (Maeda et al., 2000).

3.3.2 Parturition

Parturition in the rat, and mouse, is preceded by a sharp decline in the levels of circulating P4, a phenomenon that is not observed in human parturition. In fact, labour in humans occurs in the presence of high, and sometimes increasing, levels of P4 (Zakar & Hertelendy, 2007). The systemic withdrawal of P4 that precedes

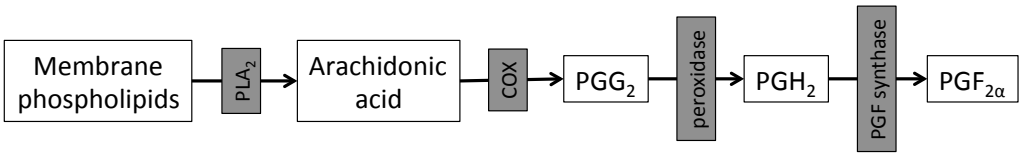

Figure 3.2: Synthesis of $PGF_{2\alpha}$. PLA_2 converts membrane phospholipids to arachidonic acid, which is in turn converted to PGG_2 by COX enzymes. Peroxide activity results in the formation of PGH_2, an unstable PG that is immediately converted to $PGF_{2\alpha}$ by PGF synthase. Abbreviations: **PLA_2**: phospholipase A_2; **COX**: cyclooxygenase; **PGH_2**: prostaglandin H_2; **PGF**: prostaglandin F; **$PGF_{2\alpha}$**: prostaglandin $F_{2\alpha}$.

labour in rats, and mice, is brought about by the luteolytic effects of prostaglandin (PG) $F_{2\alpha}$ ($PGF_{2\alpha}$). $PGF_{2\alpha}$ is synthesised from arachidonic acid, which is derived from membrane phospholipids, through the action of phospholipase A_2 (PLA_2), cyclooxygenase (COX) enzymes, peroxidase, and prostaglandin F synthase as illustrated in Figure 3.2 (Michal & Schomburg, 2012, p. 310). There are two types of COX enzymes: one which is normally expressed in various tissues of the body, COX-1; and another COX-2 whose expression can be induced (Vane et al., 1998). The effects of $PGF_{2\alpha}$ are mediated by the $PGF_{2\alpha}$ receptor (FP), a G-protein coupled receptor. Through FPs on corpora lutea, $PGF_{2\alpha}$ induces luteolysis resulting in the systemic withdrawal of P4 and the onset of labour (Ratajczak & Muglia, 2008; Sugimoto et al., 2015). $PGF_{2\alpha} - FP$ signalling has also been shown to stimulate contractility through the increase of intracellular Ca^{2+} (Funk et al., 2009).

The role of $PGF_{2\alpha}$ in the initiation of labour in mice was confirmed in studies of genetically altered mice; Sugimoto et al. (1997) demonstrated that labour could not be initiated in FP knock-out mice, $FP^{-/-}$, as luteolysis and P4 withdrawal did not occur. In addition to the maintenance of high circulating levels of P4 in $FP^{-/-}$ mice, OTR expression was not upregulated in uterine tissues as is consistent with the onset of labour. In mice lacking PLA_2, and mice lacking the constitutive COX-1 enzyme, P4 levels remained elevated and labour was delayed, suggesting that PLA_2, COX-1, $PGF_{2\alpha}$, and FP are required for luteolysis and the systemic withdrawal of P4 in mice

at term (Ratajczak & Muglia, 2008; Funk et al., 2009; Sugimoto et al., 2015).

Condon et al. (2004) proposed that the signal for the initiation of parturition at term in mice originates from the fetus through the augmented production of surfactant protein A (SP-A) from maturing pup lungs. SP-A is a component of pulmonary surfactant, which is necessary for breathing following birth as it reduces surface tension at the interface between air and water in lung alveoli (Khubchandani & Snyder, 2001). SP-A interacts with amniotic fluid macrophage Toll-like receptors culminating in their activation and migration into the uterus, thus increasing the production of interleukin-1β (IL-1β), as well as activating a nuclear factor (NF)-κB. The increase in IL-1β production and activation of NF-κB upregulates the expression of PLA_2, and induces the expression of the COX-2 enzyme leading to the increased production of $PGF_{2\alpha}$, luteolysis, and the withdrawal of progesterone. In a subsequent study, Montalbano et al. (2013) showed that SP-A-deficient, *SP-A*$^{-/-}$, mice delivered at term during their first pregnancies. In subsequent pregnancies, however, the onset of labour was delayed and was accompanied by a decrease in the expression of IL-1β as well as other pro-inflammatory markers, suggesting that initiation of the parturition cascade by fetal SP-A may not occur in first pregnancies, but in subsequent ones. Recently, using genetically altered mice, Gao et al. (2015) showed that mice lacking both SRC-1 and SRC-2, coactivators involved in regulating the transcription of the gene that encodes SP-A, had delayed parturition as a result of the inability of the pups to produce SP-A. Gao et al. (2015) further demonstrated that wild-type female mice that were mated with SRC-1/SRC-2-deficient males had delayed luteolysis and elevated levels of circulating P4 at term, suggesting that fetal signals to initiate parturition require mature lungs that can produce adequate amounts of surfactant lipoproteins such as SP-A.

3.4 Aims

The main aim of the present thesis is to identify and analyse the effects of progesterone and progesterone withdrawal on the transcriptome of the rat uterus. The work presented in this thesis follows on from the work conducted by Garfield et al. (2012) who carried out myometrial activity studies in which recordings of the electrical activity of the myometrium were made using electromyography (EMG), following treatment with P4. A catheter was implanted surgically into the myometrium of a pregnant rat, together with fine-wire electrodes that enabled the recording of single muscle activity with little cross-talk from other muscles within the body. The catheter was used to deliver P4 and carrier oils directly onto the myometrial tissue. Following treatment with P4, the electrical activity of the myometrium was dampened in comparison to vehicle-treated myometrium. The effects of P4 on the electrical properties of the uterus were observed 24 to 48 hours after administration of the hormone, a time-lag which is consistent with genomic signalling. The delay in response to treatment with P4 indicated that the effects of the hormone on the rat uterus were too slow to be non-genomic.

Laser Capture Microdissection (LCM) a technique that enables the isolation of single cells or homogeneous tissue from samples of heterogeneous tissue (Simone et al., 1998), as well as RNA Sequencing (RNAseq) will be employed in this thesis. LCM will, for the first time, enable the distinct determination of the spatio-temporal expression of genes within uterine tissues, hence the identification of tissue-specific transcriptomic changes that occur during the transition of the uterus from a quiescence to a contractile state.

Given the responsiveness of the decidua to steroid hormones, there is reason to believe that the switch may be occurring in the basal decidua. Analysis of the tran-

scriptome of the decidua may help to corroborate or disprove this hypothesis. The identification of differences in response to P4 withdrawal at the early time-point between Mifepristone-treated animals and control animals will provide information on the molecular changes that occur in pre-term labour. While comparison of natural labour and mifepristone-induced labour may provide insights into underlying differences between pre-term and term labour. In addition, the analysis of the changes in the expression of mRNA transcripts will allow a comparison of these data to data obtained from similar studies in humans.

Part II

Materials and Methods

Chapter 4

Materials

This chapter details the materials that were used in the study.

4.1 Animals

Sprague-Dawley rats (*Charles-River Laboratories, Wilmington, MA*)

4.2 Chemicals and Reagents

Ethanol (*Fisher Scientific, Loughborough, UK*)

Xylene (*Fisher Scientific, Loughborough, UK*)

Haematoxylin (*VWR International, Lutterworth, UK*)

O.C.T. Compound (*Fisher Scientific, Loughborough, UK*)

Rapid Coolant (*Leica Biosystems, Milton Keynes, UK*)

BLOXALL™ Blocking Solution (*Vector Laboratories, Peterborough, UK*)

Haematoxylin (*Vector Laboratories, Peterborough, UK*)

10% Neutral Buffered Formalin (*Genta Medical, York, UK*)

TaqMan® Gene Expression Master Mix (*Fisher Scientific, Loughborough, UK*)

4.3 Anaesthetic

Xylazine (*Burns Veterinary Supply Inc, Rockville Centre, NY*)

Ketamine Hydrochlochride (*Fort Dodge Laboratories Inc, Fort Dodge, IA*)

4.4 PR Antagonists and Agonists

Crystalline Progesterone (*Sigma Chemical Company, St. Louis, MO*)

Mifepristone (RU486) (*Sigma Chemical Company, St. Louis, MO*)

Sesame Seed Carrier Oil (*Sigma Chemical Company, St. Louis, MO*)

4.5 Kits

4.5.1 LCM Staining Kit (*Fisher Scientific, Loughborough, UK*)

Acridine Orange Stain

Cresyl Violet Stain

Slide Chambers

Dehydration Beads

RNase*Zap*® Solution

Bottles

Barrier Pen

Nuclease-free Water

4.5.2 RNAqueous®-Micro Kit (*Fisher Scientific, Loughborough, UK*)

Micro Filter Cartridge Assembly

Micro Elution Tubes

Wash Solution 1 Concentrate

Wash Solution 2/3 Concentrate

Lysis Solution

LCM Additive

DNase (2 U/µl)

10× DNase I Buffer

DNase Inactivation Reagent

Elution Solution

4.5.3 RNase-Free DNase I Set (*Omega Bio-Tek*)

OBI DNase I Digestion Buffer

RNase-free DNase I

4.5.4 Agilent RNA 6000 Pico Kit (*Agilent Technologies, Stockport, UK*)

RNA 6000 Pico Chips

Electrode Cleaners

RNA 6000 Pico Dye Concentrate

RNA 6000 Pico Marker

RNA 6000 Pico Conditioning Solution

RNA 6000 Pico Gel Matrix

RNA 6000 Pico Ladder

Spin Filters

Safe-Lock Eppendorf Tubes PCR clean (DNase/RNase free) for gel-dye mix

Syringe

4.5.5 Ovation® RNA-Seq System V2 (*NuGEN Technologies, Leek, The Netherlands*)

First Strand cDNA Reagents

First Strand Primer Mix

First Strand Buffer Mix

First Strand Enzyme Mix

Second Strand cDNA Reagents

Second Strand Buffer Mix

Second Strand Enzyme Mix

SPIA® Amplification Reagents

SPIA Primer Mix

SPIA Buffer Mix

SPIA Enzyme Mix

Nuclease-free Water

Agencourt RNAClean XP Beads

4.5.6 Ovation® Ultralow DR Multiplex Systems 1–8 (*NuGEN Technologies, The Netherlands, The Netherlands*)

End Repair Buffer Mix

End Repair Enzyme Mix

End Repair Enhancer

Ligation Buffer Mix

Ligation Adaptor Mix (×8 different sequences)

Ligation Enzyme Mix

Amplification Buffer Mix

Amplification Primer Mix

Amplification Enzyme Mix

DMSO

Nuclease-free Water

Agencourt RNAClean XP Beads

4.5.7 DAB Substrate Kit for Peroxidase (*Vector Laboratories, Peterborough, UK*)

Buffer Stock Solution

DAB Stock Solution

Hydrogen Peroxide Stock Solution

Nickel Solution

4.5.8 ImmPRESS® Reagent Kit (*Vector Laboratories, Peterborough, UK*)

ImmPRESS® Anti-Rabbit Ig Reagent

Normal Horse Serum

4.5.9 High-Capacity cDNA Reverse Transcription Kit (*Fisher Scientific, Loughborough, UK*)

10× RT Buffer

10× RT Random Buffers

25× dNTP Mix

MultiScribe™ Reverse Transcriptase

4.6 Primary Antibodies

Polyclonal Antibody to Thyrotropin-releasing Hormone (*Acris Antibodies, Herford, Germany*)

Polyclonal Antibody to Tenascin N (*Sigma Life Science, Dorset, UK*)

4.7 TaqMan® Gene Expression Assays (Fisher Scientific, Loughborough, UK)

Gene Symbol (*Assay ID*) with FAM Reporter and MGB-NFQ Quencher

Actb (*Rn00667869_m1*)

Gja1 (*Rn01433957_m1*)

Gja7 (*Rn01750705_m1*)

Oxt (*Rn00564446_g1*)

Oxtr (*Rn00563503_m1*)

Ptgs1 (*Rn00566881_m1*)

Ptgs2 (*Rn01483828_m1*)

4.8 Equipment and Accessories

Microscope Slides (*VWR International, Lutterworth, UK*)

Cryomolds (*VWR International, Lutterworth, UK*)

Dessicator (*VWR International, Lutterworth, UK*)

Desiccant (*VWR International, Lutterworth, UK*)

Disposable Microtome Blades (*Feather Safety Razor Co. Ltd*)

Membrane Slides (*Molecular Machines and Industries, Eching, Germany*)

Isolation Caps with Diffuser (*Molecular Machines and Industries, Eching, Germany*)

BioAnalyzer (*Agilent Technologies, Stockport, UK*)

LCM Workstation (*Molecular Machines and Industries, Eching, Germany*)

7500 Fast Real-Time PCR System (*Fisher Scientific, Loughborough, UK*)

Chapter 5

Experimental Methods

5.1 Animals

Twenty timed-pregnant Sprague-Dawley rats (Supplementary Table B.1), with day 1 of pregnancy being the point in time at which a sperm plug was observed, were transferred to the animal care facilities on gestational day (GD) 17, where they were housed separately under constant 12-hour light-dark cycles, with free access to food and water. The rats were treated, by subcutaneous injection, with either 4 mg progesterone (P4), 3 mg mifepristone (RU486), or the vehicle (sesame seed oil), on GD19. Control pregnant rats delivered spontaneously on GD22. The animals were allocated at random to the treatment groups as follows:

1. Three vehicle-treated (control) rats, from which tissues were collected 6 hrs post treatment, i.e., on GD19+6hrs;

2. Three mifepristone-treated rats whose tissues were harvested on GD19+6hrs;

3. Three control rats whose tissues were collected on GD20;

4. Three mifepristone-treated rats whose tissues were harvested on GD20;

5. Three control rats that had tissues collected on GD22, before going into labour;

6. Two control rats that had tissues collected on GD22, during labour, i.e, after the delivery of one pup;

7. Three rats that were treated daily with P4 from GD19 to GD22, and samples harvested on GD22. Animals in this group will not deliver even if they are left to get to the 25th day of gestation.

The animals were anaesthetised by an intra-peritoneal injection consisting of a combination of Xylazine and Ketamine hydrochloride, then whole uterine horns with the fetuses intact were flash-frozen in liquid nitrogen and then stored at $-80°$C until they were shipped to the UK on dry ice. On arrival in the UK, the samples were checked visually to make sure that they were still frozen and then stored at $-80°$C, as shown in Supplementary Figure B.1. Following visual assessment, the uterine horns were catalogued and weighed (Supplementary Table B.2).

5.2 RNA Isolation From 5 g Tissue Sections

Pieces of tissue approximately 5 g in weight were cut from each of the uterine samples using a blade that had been cleaned with 100% ethanol and RNase*Zap*®. The 5 g pieces of tissue were wrapped in RNase*Zap*®-treated foil paper and smashed with a mallet while on the bench. The pieces of foil paper were placed in liquid nitrogen to keep the tissue frozen. The smashed pieces of tissue were placed in 50 ml Falcon tubes. An aliquot of 1 ml RNA-Stat60 was added to each tube and the tubes were placed on dry ice. The samples were thawed and homogenised using a LabGen® 7

Series Homogeniser, then transferred to 1.5 ml Eppendorf tubes and placed on dry ice.

After thawing, 200 µl of chloroform was added to each of the homogenates and vortexed for 30 s. The mixtures were placed on dry ice for 20 min then thawed and centrifuged for 30 min, separating the mixtures into layers. The upper aqueous layers were transferred into clean tubes to which 200 µl of isopropanol was added. The tubes were left at room temperature ($\sim$ 20°C) for 10 min, then centrifuged for 15 min. The supernatants were removed from the tubes using a pipette. The RNA pellets were washed in 1 ml of 75% ethanol and centrifuged for 15 min. The supernatants were removed and the pellets were air dried under the flow hood for 15 min. The pellets were each dissolved in 85 µl of nuclease-free water and placed on dry ice.

DNA digestion was performed by adding 10 µl of RDD Buffer and 5 µl of DNase I, from the Qiagen® RNase-Free DNase Set, to each of the RNA samples. The Qiagen® RNeasy® Mini-Kit was used to cleanup the RNA. All centrifugation steps were performed at 4°C at 13,000 g.

RNA was eluted in nuclease-free water and RNA quantitation and quality checks were performed using the Thermo Scientific NanoDrop® 1000 Spectrophotometer and the Agilent® RNA 6000 Nano chip on The Agilent® 2100 Bioanalyzer, respectively. The quantitation and quality check results are summarised in Supplementary Table B.3 and Supplementary Figure B.2, respectively. RNA was then stored at −80°C.

5.3 Tissue Preparation for Sectioning

The uterine horns were removed from storage (−80°C) and placed on dry ice. Metal specimen stages were placed on dry ice to cool. Once cooled, Thermo Scientific® Shandon® Cryomatrix OCT embedding compound was applied to the metal specimen stages and allowed to cool but not freeze. Sections of the uterine horns containing a single pup were broken off from the main tissue samples and pressed onto individual metal specimen stages. OCT was applied onto the samples until each sample was completely covered in OCT. The samples were sprayed with Leica Microsystems® Frostbite® to freeze the OCT quickly and were stored on dry ice ready for sectioning.

5.3.1 Tissue Sectioning

The cryostat was cooled to −30°C. The microtome blade holder and anti-roll glass were cleaned with 100% ethanol each time a new sample was sectioned. The brushes for use during sectioning were washed in 100% ethanol followed by RNase*Zap*®. OCT-embedded samples were then individually removed from the dry ice and placed in the cryostat and allowed to equilibrate to the temperature of the cryostat for 10 min. A new blade was put on the microtome before sectioning each sample. Sections of 8 µm in thickness were cut and each section was adhered to a membrane slide (Molecular Machines & Industries). Staining was performed immediately after adhesion of tissue sections onto slides.

5.3.2 Staining

Staining was performed using a 7:3 ratio mix of ethanolic solutions of Cresyl Violet (CV) nuclear stain and Eosin Yellow (EY) cytoplasmic stain. The staining solutions were mixed just prior to staining as described by Clément-Ziza et al. (2008). The membrane slides with adhered tissue were placed in 95% ethanol for 30 s to fix the tissue onto the slides. Excess ethanol was drained off by tapping the slides on absorbent paper. The Ambion® Barrier® Pen was used to mark the areas around the tissue sections so as to keep the dye on the tissue. 100 µl of 7:3 CV-EY stain solution were placed on each of the tissue sections and allowed to stain for 1 min in the flow hood. Excess stain was tapped off the slides and the slides were placed in a fresh solution of 95% ethanol for 10 s to destain the tissue. The slides were transferred to another 95% ethanol solution for a further 10 s. The slides were transferred into 100% ethanol to dehydrate for 10 s. The slides were then transferred into a chamber containing xylene and were dehydrated for a further 5 min. The slides were desiccated for 5 min under vacuum. New wash and dehydration solutions were used for each sample to ensure that slides of sections from the same sample were washed and dehydrated in the same solutions. Following desiccation, laser capture microdissection (LCM) was performed immediately.

5.4 Laser Capture Microdissection

LCM was developed by the National Institutes of Health to aid the isolation and analysis of homogeneous cells from heterogeneous tumours (Simone et al., 1998). LCM involves the use of an infrared laser beam to isolate cells of interest from homogeneous tissue samples that are adhered to membrane slides. The cells that are cut

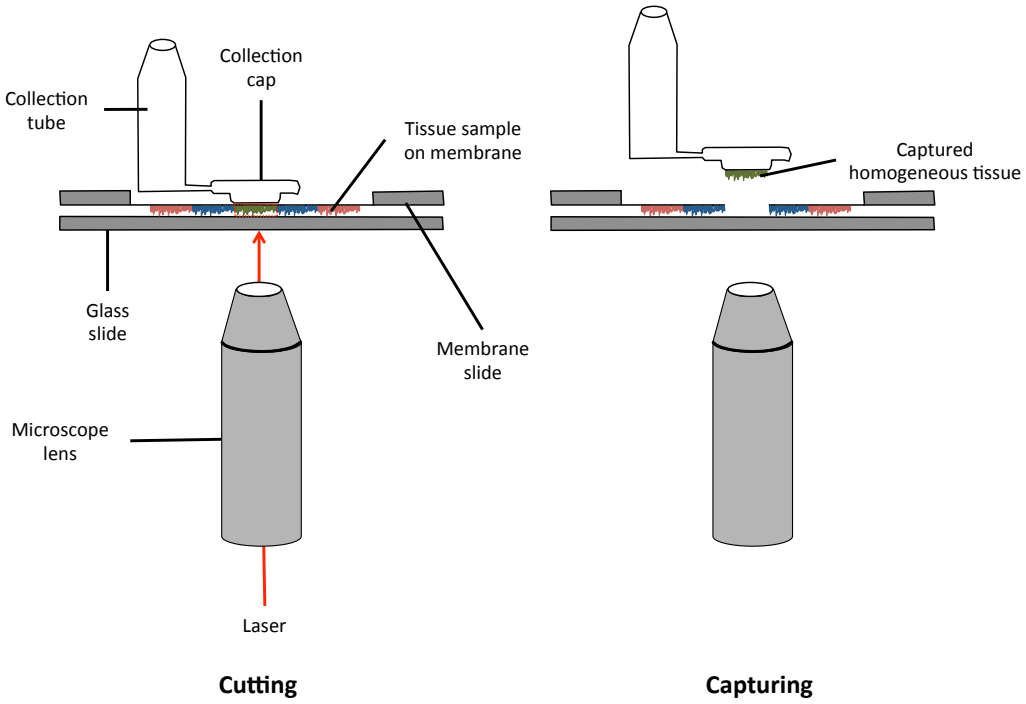

Figure 5.1: Laser-capture microdissection (LCM). Cutting: The collection tube is lowered and the surface of the adhesive cap connects with the membrane. A laser beam is used to cut the tissue of interest (shown by the red dotted lines). **Capturing**: After cutting, the collection tube is lifted together with the cut homogeneous tissue. The cap may be closed and the captured tissue can be used for analysis.

out by the laser beam are then 'captured' by the adhesive lid of a specially designed collection tube as illustrated in Figure 5.1 (Murray, 2008). The LCM components of the work presented in this thesis were performed using the mmiCellCut® laser microdissection system as described below.

A glass slide cleaned with RNase*Zap*® was placed on the flat side of each membrane slide sandwiching the tissue sections. Decidual and myometrial cells were obtained separately, while avoiding blood vessels, glands, and other tissue. Microdissected tissue sections were collected using the 500 µl mmi-Isolation® tubes with adhesive lid and diffuser. Collected tissue sections were immersed in a lysis solution and stored at $-80°$C before RNA isolation. Acquisition time was kept below 30 min so as to minimise the degradation of the RNA within the tissue.

5.5 RNA Isolation from LCM Tissue Sections

After LCM, 50 µl of extraction buffer were pipetted into the mmi-Isolation® tubes. The tubes were then inverted to ensure that the LCM tissues were completely covered by the extraction buffer. The tubes were vortexed briefly to dislodge the LCM tissues from the cap and then stored at −80°C. The lysates were thawed at room temperature, then incubated for 30 min at 42°C, followed by centrifugation at 800×g for 2 min. A 50 µl aliquot of 70% ethanol was added to each of the tubes and mixed by pipetting. Prior to transferring the ethanol-lysate mixtures onto RNA purification columns, the columns were incubated for 5 min in 250 µL of conditioning buffer and centrifuged at 16,000×g for 1 min. Once the ethanol-lysate mixtures were transferred onto the columns, the columns were centrifuged for 2 min at 100×g, to allow the RNA to bind to the column, followed immediately by centrifugation at 16,000×g for half a minute.

5.5.1 DNase Treatment

Genomic DNA was removed by pipetting a 40 µL solution, composed of 5 µL of the Qiagen DNase I stock solution and 35 µL of Buffer RDD, directly onto the membrane of each purification column. The columns were incubated at room temperature for 15 min before 40 µL of wash solution 1 (see Section 4.5) were added to each of the columns. The columns were then centrifuged at 8,000×g for 15 s.

Subsequent washes were carried out following the recommendations in the RNAqueous®-Micro Kit, and the RNA was eluted in 11 µl of elution buffer. Each RNA sample was allocated to two aliquots, one for sequencing (5 µL), and the other for quality control and validation (6 µL).

5.5.2 RNA Quantity and Quality Check

The RNA in the samples was quantitated using the Thermo Scientific NanoDrop® 1000 Spectrophotometer. To ascertain the quality of the RNA, the Agilent® RNA 6000 Pico Kit and Agilent® 2100 Bioanalyzer were used. An aliquot of 550 µl of RNA 6000 Pico gel matrix was pipetted onto a spin filter and centrifuged at 1500 g for 10 min at room temperature. The filtered gel was stored as 65 µl aliquots at −80°C. The RNA 6000 Pico dye was allowed to equilibrate to room temperature for 30 min, then vortexed and spun down. An aliquot of 1 µl of the dye was added to a thawed aliquot of filtered gel. The gel-dye mix was vortexed thoroughly and centrifuged at 13000 g for 10 min at room temperature. A new RNA 6000 Pico chip was put on the chip priming station for each batch of 11 samples. The chips were prepared and run on the Bioanalyzer following the manufacturer's recommendations. The Bioanalyzer generated a virtual gel, an electropherogram detailing visual assessment of the quality of the RNA, and an RNA integrity number (RIN) indicating the level of RNA degradation; a RIN score of 1 indicates the most degraded and a score of 10 is indicative of the most intact RNA (Mueller et al., 2004). Work previously conducted in the laboratory by Chan et al. (2014), determined that RNA samples with RIN ≥ 6 were of acceptable quality. As such, the RNA samples used in the present study had RIN scores of 6 or greater.

5.6 Library Preparation and Sequencing

RNA of acceptable quality was amplified using the Nugen Ovation RNA-Seq System V2. Amplification was initiated at the $3'$ end as well as at random throughout the whole transcriptome in the sample. The Nugen Ovation Ultralow DR Multi-

plex System (1–8) kit was used for library preparation. Double-stranded cDNA was fragmented, followed by end repair. Adapters were ligated to the cDNA fragments, and the final libraries were produced after amplification of the fragments using PCR. Libraries were validated using a DNA 1000 chip on an Agilent 2100 Bioanalyzer (Agilent Technologies, Stockport, UK) according to the manufacturer's instructions.

Libraries were sequenced on the Illumina HiSeq 2500 platform (Illumina, San Diego, CA, USA) using a 51bp paired-end indexed run. Each of the sequenced bases was assigned a Phred quality score (Ewing & Green, 1998), which expresses the probability of incorrectly identifying a nucleotide. The Phred score of a given nucleotide, Q, is defined as

$$Q = -10 \log_{10} P; \tag{5.1}$$

where P is the estimated probability of the base call being incorrect, which may be calculated from the Phred score as follows:

$$P = 10^{-Q/10}. \tag{5.2}$$

A higher Phred score is to be preferred as this is indicative of a lower error probability.

5.7 Spatial Expression of Proteins

Immunohistochemistry was performed on formalin-fixed paraffin-embedded tissues that were cut into 5 µm sections and incubated at 65°C on positively charged slides. Tissue sections were deparaffinised by washing three times Xylene for 5 min and hydrated in series-graded alcohol, then washed twice for 5 min in distilled water.

To break the protein cross-links formed by formalin fixation, slides were brought to a boil in 10 mM sodium citrate buffer (pH 6.0), and maintained at sub-boiling temperature for 2 h. Tissue slides were allowed to cool at room temperature for 30 min and then washed in distilled water before staining commenced.

To neutralise endogenous peroxidase, tissue sections were incubated in BLOXALL™ for 10 min at room temperature. The sections were then washed twice for 5 min each time in Phosphate Buffered Saline (PBS) with Tween®20 (PBS-T). A litre of PBS-T was prepared by adding 100 ml of PBS and 500 µl of Tween®20 to 900 ml of MilliQ water. To block unspecific binding sites, tissues were incubated in horse serum blocking solution for 20 min, followed by two washes in PBS-T. The slides were then placed in a humidified chamber where 100 µl of primary antibody diluted in PBS-T (1:200 dilution) was added to the tissue sections, while only PBS-T was placed on control tissue sections instead of the diluted antibody. The humidified chamber was incubated at 4°C overnight.

Following overnight incubation at 4°C, the sections were washed twice in PBS-T and incubated for 30 min in ImmPRESS® anti-rabbit reagent, then washed again in PBS-T for 5 min. While the sections were in the wash solution, a working solution of Diaminobenzidine (DAB) was prepared by adding 2 drops of buffer stock solution, 4 drops of DAB stock, and 2 drops of the hydrogen peroxide solution to 5 ml of distilled water. To detect the antibody, the tissue sections were incubated in the DAB working solution until desired staining intensity was achieved. The slides were then rinsed under a distilled water tap for 5 min, and counterstained with haematoxylin for 1 min. The counterstained slides were rinsed under a distilled water tap for 10 minutes, dehydrated, cleared, and mounted. The stained slides were then scanned using MIRAX SCAN (Carl Zeiss), and the resulting images were processed using Pannoramic Viewer software (3D Histech).

5.8 Validation of Gene Expression

Quantitative real-time PCR (qPCR) experiments were conducted to validate the gene expression patterns observed from RNAseq data.

5.8.1 Synthesis of cDNA

Reverse transcription of total RNA from LCM tissues was performed by adding 2 µl 10× RT buffer, 0.8 µl 25× dNTP mix, 2 µl 10× RT primers, 1 µl Multiscribe reverse transcriptase, and 4.2 µl of nuclease-free water to each RNA sample. The solution was incubated at 25°C for 10 min, followed by a 120 min incubation at 37°C. The reverse transcriptase was inactivated by incubating the solution at 85°C for 5 min. The cDNA was then stored at −20°C until required.

5.8.2 RT-qPCR Experimental Setup and Data Analysis

Inventoried Taqman® gene expression assays were purchased from Applied Biosystems (see Section 4.7 for full list of probes used). Each PCR reaction was made up of 100 ng of cDNA in 20 µl reaction volume containing 1 µl 20× Taqman® gene expression assay, 10 µl 2× Taqman® gene expression master mix, and 8 µl of RNAse-free water. At least 2 biological replicates per gestational time point and 3 technical replicates per biological replicate were run on the Applied Biosystems Fast 96-well platform. The RT-qPCR program was run for 10 minutes at 95°C , followed by 40 cycles of 95°C for 15 s and 60°C for 1 min.

5.8.3 Analysis of RT-qPCR Data

The threshold cycle number (Ct) for each replicate was determined by setting a horizontal threshold, unique to each gene, which cut across the exponential phase of each amplification plot. First, the mean Ct value among the technical replicates of each sample was calculated for a single gene as follows:

$$Ct_{rep-mean} = \sum_{i=1}^{n} \frac{Ct_{tech-rep(i)}}{n}, \tag{5.3}$$

where $i = \{1, \cdots, n\}$ represents the number of technical replicates. This was followed by the subtraction of the lowest $Ct_{rep-mean}$ value ($Ct_{mean-min}$) from all other $Ct_{rep-mean}$ values for that particular gene, i.e.,

$$\Delta Ct_j = Ct_{rep-mean(j)} - Ct_{mean-min}, \tag{5.4}$$

where $j = \{1, \cdots, m\}$ represents the number of samples. The efficiency of all the probes was guaranteed by the manufacturer. Accordingly, the transcript abundance was calculated as $2^{-\Delta Ct_j}$ for each sample. The abundance relative to the reference (housekeeping) gene β-Actin (Actb), was calculated through dividing the transcript abundance in a sample of the gene of interest (goi) by the transcript abundance in the same sample of Actb, thus relative abundance is

$$2^{-\Delta\Delta Ct}, \tag{5.5}$$

where $\Delta\Delta Ct = \Delta Ct_{goi} - \Delta Ct_{Actb}$. Relative transcript abundances were plotted using GraphPad Prism® and significant differences in transcript abundance between gestational time-points were tested using Kruskal-Wallis test coupled with Dunn's multiple testing correction approach with a 5% significance level.

Chapter 6

Data Quality Assessment and Analysis

The 51bp paired-end sequencing reads were presented in FASTQ format, which stores biological sequences and their corresponding Phred quality scores. The FASTQ files were inspected for low quality scores, adapter sequence contamination, and other overrepresented sequences, using FastQC (Andrews, 2012).

TopHat2 (Kim et al., 2013), a fast-splice junction mapper that aligns RNA-Seq reads to genomes, was used to align the reads against the UCSC *Rattus norvegicus* (rn5) reference transcriptome (Rat Genome Sequencing Project Consortium, 2004), obtained from the Illumina iGenomes resource. TopHat2 employs Bowtie (Langmead & Salzberg, 2012), a short read aligner, to re-align poorly mapped or previously unmapped reads. For each pair of FASTQ files, Tophat2 produced a BAM (binary alignment map) file with the reads that are aligned to the genome (accepted_hits.bam), a BAM file containing the reads that failed to align to the genome or transcriptome (unmapped.bam), a UCSC BED track of junctions (junctions.bed), and UCSC BED

tracks of insertions (insertions.bed) and deletions (deletions.bed) as output.

The accepted_hits.bam files were sorted and indexed using SAMtools (Li et al., 2009), to enable viewing of the sequences on the Integrative Genomics Viewer (IGV) (Robinson et al., 2011; Thorvaldsdóttir et al., 2012). SAMtools was also used to sort the accepted_hits.bam files by name and convert them into SAM (sequence alignment map) format, which is an uncompressed text version of the BAM format. SAM files were used as input for HTSeq (Anders et al., 2015), a piece of feature-counting software that was used to estimate transcript and gene counts.

6.1 Principal Component Analysis

Principal Component Analysis (PCA) is a technique in which variables are transformed into a set of uncorrelated variables called principal components (PCs), that are linear combinations of the original data. PCA is used to obtain insight into patterns or trends within data sets, and to identify the sources of variation within the data, which may not be discernible (Johnson & Wichern, 2002).

6.1.1 The Model

Let n be the number of gene transcripts, and p be the number of samples. Then the matrix of gene transcript expression levels can be denoted by an $n \times p$ data

matrix

$$\mathbf{X} = \begin{bmatrix} x_{11} & x_{12} & \cdots & x_{1p} \\ x_{21} & x_{22} & \cdots & x_{2p} \\ \vdots & \vdots & \ddots & \vdots \\ x_{n1} & x_{n2} & \cdots & x_{np} \end{bmatrix} \tag{6.1}$$

with mean vector $\bar{\mathbf{x}} = (\bar{x}_1, \bar{x}_2, \ldots, \bar{x}_p)$ where

$$\bar{x}_j = \frac{1}{n}\sum_{i=1}^{n} x_{ij} \tag{6.2}$$

with $j = 1, \ldots, p$, and $p \times p$ covariance matrix $\mathbf{S}$, which is symmetric, i.e., $\mathbf{S}^\top = \mathbf{S}$, as well as correlation matrix $\mathbf{R}$, which is also symmetric.

Suppose $\mathbf{S} = \mathbf{B}\boldsymbol{\Lambda}\mathbf{B}^\top$ is the spectral decomposition of $\mathbf{S}$, then $\mathbf{B}$ is an orthogonal matrix of the eigenvectors ($\boldsymbol{\beta}_j$) of $\mathbf{S}$, and Λ is the diagonal matrix of the corresponding eigenvalues (λ_j) where $j = 1, \ldots, p$ and $\lambda_1 \leq \lambda_2 \leq \cdots \leq \lambda_p$. The eigenvectors determine the p PCs, with ($p \leq n-1$). The data, $\mathbf{X}$, may be transformed into PCs, $\mathbf{Y}$, as follows:

$$\mathbf{Y} = \mathbf{B}^\top(\mathbf{X} - \bar{\mathbf{x}}), \tag{6.3}$$

where $\mathbf{Y}$ has mean $\mathbf{0}$ and variance $\boldsymbol{\Lambda}$ (Härdle & Hlávka, 2015).

The correlation matrix $\mathbf{R}$ may also be used to compute PCs; Timm (2002a) discusses the use of the correlation matrix in detail. The elements of the PCs represent the coefficients of the variables, sometimes referred to as the PC loadings, which provide a summary of the influence of the original variables on the principal components. A coefficient of large magnitude corresponds to a high loading, while a coefficient near *zero* has a low loading. A plot of the loadings gives a visual impression of the

patterns within the data (Timm, 2002a).

6.1.2 Selection of Principal Components

Let r be the number of principal components to be retained for analysis, which can be determined by considering the variance within the original data that is accounted for by each of the PCs; the k^{th} PC, $\mathbf{y}_k$, is the direction in which the data have variance λ_k. Thus the proportion of the total variance within the original data that is captured by $\mathbf{y}_k$, v_k, is calculated as

$$\mathrm{v}_k = \frac{\lambda_k}{\sum_{j=1}^{p} \lambda_j}. \tag{6.4}$$

The PCs whose cumulative variance is equal to or surpasses a predetermined threshold are retained for further analysis. Ewens & Grant (2001a) suggested a threshold of 90%, while Timm (2002a) suggested a proportion between 70% – 80%, and Jolliffe (2002a) suggested a proportion between 80% – 90%. Evidently, there is no specific threshold at which PCs are retained. As such, the individual performing the analysis may use their discretion.

Another method by which r may be determined is by plotting of the eigenvalues, λ_j, against j as illustrated in Figure 6.1. This plot, called a scree plot, is used to visually determine r by selecting the PCs whose eigenvalues are located above the point at which the variance accounted for represents a flat line (Härdle & Hlávka, 2015). The work presented in this thesis employed a minimum threshold of 85% for the cumulative variance captured by the PCs, as well as scree plots, to determine the number of PCs to retain for analysis. Jolliffe (2002b) discusses other methods that may be employed in determining r.

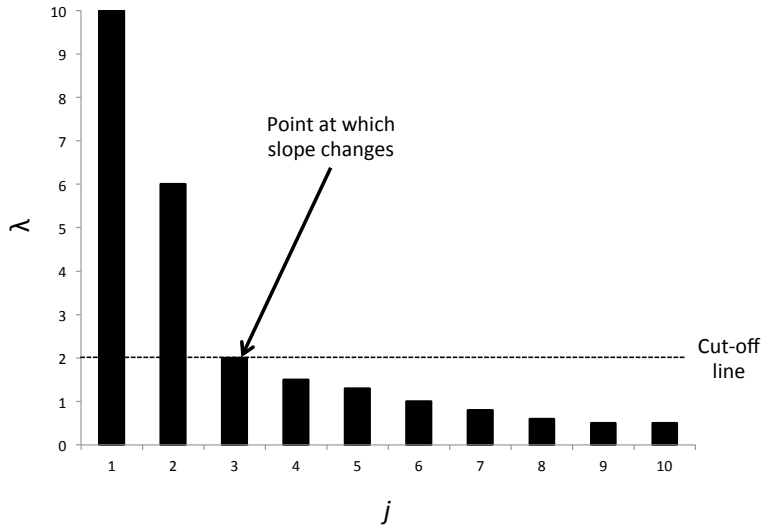

Figure 6.1: Illustration of a scree plot. The eigenvalues are plotted in descending order. The scree plot shown here indicates that the slope flattens at $i = 3$. In this case, therefore, $r = 2$. *Adapted from Timm (2002a).*

6.2 Differential Expression and Statistical Analysis

As there is no general agreement as to which differential gene expression method is the best, several comparisons have been conducted to identify the "best" method (Robles et al., 2012; Wesolowski et al., 2013; Soneson & Delorenzi, 2013). However, the methods that are currently available have differing strengths and weaknesses, which makes it difficult to select a single method.

Wesolowski et al. (2013), for example, compared the true positive rates of Cuffdiff (Trapnell et al., 2012), DESeq (Anders & Huber, 2010), baySeq (Hardcastle & Kelly, 2010), as well as an hierarchical empirical Bayes method (R-EBSeq), and noted that while DESeq identified the first half of a list of known differentially expressed transcripts from a synthetic data set, Cuffdiff and R-EBSeq were better at identifying differentially expressed transcripts. Soneson & Delorenzi (2013) compared eleven differential expression approaches, including DESeq and edgeR (Robin-

son et al., 2010), and noted that both DESeq and edgeR were the best performing methods for small sample sizes ($n = 2$), and that with an increase in sample size from 2 to 3, the false positive rate of DESeq decreased noticeably. However, Soneson & Delorenzi (2013) also observed that DESeq was more conservative than other RNA-seq differential expression analysis tools, an observation that was also made by Robles et al. (2012). Another differential expression analysis method, DESeq2 (Love et al., 2014), was described as having better specificity compared to that of Cuffdiff and its predecessor DESeq, but had poorer specificity in comparison to edgeR. Love et al. (2014) also noted that the "old DESeq" and Cuffdiff were "overly" conservative in the control of false positive results.

In order to have a balance of parametric and non-parametric approaches, strictness, sensitivity and accuracy, differential expression analysis in this thesis was performed using the following three methods:

1. **Cuffdiff**, a non-parametric method which is part of the Cufflinks package (Trapnell et al., 2012), based on a measurement of the distance between the relative abundance of transcripts in two different experimental conditions;

2. **DESeq2**, a parametric method, which models read counts as following the negative binomial distribution and utilises the Wald test (Love et al., 2014); and

3. **edgeR**, a parametric method, which also models read counts as negative binomial distributed, that utilises the exact test for pairwise comparisons, and the generalised linear model (GLM) likelihood ratio test for more complex comparisons (Robinson et al., 2010).

6.2.1 Data Normalisation

Transcript abundance estimates that are calculated from RNAseq data are susceptible to bias associated with the length of gene transcripts and the preferential alignment of reads to the reference transcriptome (Roberts et al., 2011). In addition, bias may arise due to an imbalance in the nucleotide content of the sequenced fragments (Risso et al., 2011). Normalisation minimises the influence of sequencing depth on the data, as high sequencing depths result in high numbers of reads. It also minimises the dependence on gene transcript length, which arises due to gene counts being proportional to transcript length and the mRNA expression levels (Zheng et al., 2011). By minimising bias, normalisation enables the analysis of the underlying biological variations within the data.

Cufflinks

Cufflinks uses the reads per Kilobase per million mapped reads (RPKM) normalisation method, calculated as

$$\mathrm{RPKM} = \frac{10^9 \times \mathrm{C}}{\mathrm{N} \times \mathrm{L}}, \tag{6.5}$$

where C is the number of reads mapping to a particular feature, N is the total number of mappable reads in the experiment, and L is the feature length (Mortazavi et al., 2008). RPKM reflects the concentration of a transcript in a sample by normalising for transcript length and the total number of reads. While the RPKM normalization gives an unbiased measure of feature expression, accounting for transcript length introduces a length bias (Oshlack & Wakefield, 2009).

Transcripts per Million

In light of the length bias associated with RPKM normalisation, Wagner et al. (2012) proposed an alternative normalisation approach: transcripts per million (TPM). The TPM value for a transcript represents the proportion of the transcriptome that is occupied by that transcript, while the TPM value for a gene is a sum of all the TPMs of that gene's isoforms. It is calculated as

$$\text{TPM} = \frac{r_g \times \text{rl} \times 10^6}{\text{fl}_g \times T}, \tag{6.6}$$

where r_g represents the number of reads mapping to transcript g, rl represents the mean read length, fl_g is the length of transcript g, and T represents the total number of mappable reads. While TPM and RPKM are proportional within a sample, the scaling factors of the two methods are different between samples (Wagner et al., 2012). Sailfish (Patro et al., 2014), an alignment-free algorithm, was used to estimate the TPM values presented in this thesis. Since Sailfish does not align reads to a reference transcriptome, it is faster than other abundance estimation methods. Instead, Sailfish uses counts of k-mers, sequences of length k, that are found in reads to estimate transcript abundance (Patro et al., 2014).

DESeq2

For each gene i in sample j in DESeq2, it is considered that read counts (X_{ij}) follow the negative binomial (NB) distribution with mean μ_{ij} and dispersion α_i. The mean is considered to be a product of a quantity q_{ij} that is proportional to the concentration of cDNA fragments in sample j, and a normalization factor which

accounts for differences between sample sequencing depths, s_{ij}, such that

$$\mu_{ij} = s_{ij} q_{ij}; \tag{6.7}$$

and

$$X_{ij} \sim \text{NB}(s_{ij} q_{ij}, \alpha_i). \tag{6.8}$$

The median-of-ratios method described by Anders & Huber (2010) is then used in the estimation of the normalization factors (Love et al., 2014).

EdgeR

Similar to DESeq2, for each gene i in sample j, read counts X_{ij} are modelled as NB random variables with mean μ_{ij} and dispersion α_i in edgeR. With the treatment group k to which sample j belongs, the mean is considered to be a product of the relative abundance of gene i in the treatment group k, p_{ik}, and the total number of reads in sample j, M_j, such that

$$\mu_{ij} = M_j p_{ik}; \tag{6.9}$$

and

$$X_{ij} \sim \text{NB}(M_j p_{ik}, \alpha_i). \tag{6.10}$$

Unlike in DESeq2 where the median-of-ratios method is employed, the total number of reads is used as a normalisation factor in edgeR (Robinson et al., 2010).

6.2.2 Testing for Significant Differential Expression

Under the null hypothesis (H_0) that a gene was not differentially expressed between two conditions, a test for differential expression was considered significant if the estimated probability of rejecting H_0 given that H_0 was true (p-value) was less than 0.05 using all the differential expression analysis methods.

Correcting for Multiple Testing

When there are many independent null hypotheses being tested, it is likely that some of these null hypotheses may be rejected by chance even though they are true. In such cases, multiple testing correction (MTC) methods are employed with the aim of reducing the chance rejection of true hypotheses (Ewens & Grant, 2001b). There are two main approaches for controlling false statistically significant results; the control of the family-wise error rate (FWER), and the control of the false discovery rate (FDR). The FWER is defined as the probability of the presence of at least one false significant result, whereas the FDR is a representation of the number of false significant results expressed as a proportion of all the significant results (Gyorffy et al., 2005).

There are two main types of FWER correction; single-step methods in which all p-values are adjusted by the same factor, and sequential methods in which adaptive adjustments are made to each p-value. An example of a single step method is the Bonferroni method, which rejects an hypothesis whose estimated p-value $< \alpha/m$, where α is the predefined probability of rejecting H_0 when H_0 is true, and m is the number of hypotheses being tested. Sequential or multi-step methods, on the other hand, do not adjust all p-values with the same factor. Instead, unadjusted

p-values are ordered such that $p_1 \leq p_2 \leq \ldots \leq p_m$. Each estimated p-value is then adjusted sequentially, by different factors, and only those tests whose adjusted p-value $<$ FWER are considered statistically significant. While methods that correct for the FWER reduce the chances of incorrectly rejecting a true H_0, they also reduce the chances of correctly rejecting a false H_0 (Ewens & Grant, 2001b).

When the presence of a "known negligible" proportion of false statistically significant results is acceptable, as opposed to limiting any false significant results in the case of FWER correction, FDR correction methods are employed (Rice et al., 2008). The Benjamini & Hochberg (1995) FDR , a MTC method that controls the number of false significant results, was employed in the reduction of the chance rejection of true hypotheses in this thesis. The Benjamini-Hochberg correction determines FDR-adjusted p-values known as q-values, adjusted p-values, and FDR in Cuffdiff, DESeq and edgeR, respectively. An FDR-adjusted p-value less than 0.05 was required for a gene transcript to be considered significantly differentially expressed in this thesis. Controlling for the FDR has the advantage of increasing the probability of correctly rejecting a false H_0, but also increases the chances of incorrectly rejecting a true H_0 (Mayer & Glasbey, 2005; Rice et al., 2008). In addition to employing the FDR in this thesis, therefore, gene transcripts were only considered to be significantly differentially expressed if they were identified by at least two of the differential expression methods used.

6.3 Hierarchical Clustering

An agglomerative hierarchical clustering (Timm, 2002b) method was employed to provide insights into the relationships among differentially expressed genes, tissue types, and treatments. Before clustering was performed on differentially expressed

genes, z-scores of the gene expression values (TPMs) were calculated. The z-score of the expression value of a gene at a time point or within a treatment group i, TPM_i, was calculated as follows:

$$z = \frac{TPM_i - \mu_{TPM}}{\sigma_{TPM}} \tag{6.11}$$

where μ_{TPM} represents the mean of the TPM values of a gene across all time points or treatments and σ_{TPM} represents the standard deviation of the set of expression values.

The Algorithm

The steps by which hierarchical clustering was performed are listed below.

1. Each object of interest, be it a gene, a sample, or a treatment, is defined as a group and a matrix of distances between each of the objects, **D** is computed;
2. The smallest non-zero element of the matrix **D** is then identified, and the corresponding groups combined;
3. A new matrix $\mathbf{D}^*$ which is composed of distances between the new group and the remaining groups is computed; then
4. Steps 2 and 3 are repeated until there is only group left.

The heatmap.2 function in R was used to conduct PCA as well as to produced heat maps with dendrograms that illustrated the grouping of genes, samples, or treatments.

6.4 Functional Enrichment Analysis

The analysis of Gene Ontology (GO) term enrichment is used in the annotation of the molecular function of genes, as well as the biological processes in which the genes are involved, and the location of gene products within the cell (Huntley et al., 2015). Using the entire genome of the rat as a reference gene set containing N genes, n of which have the GO term of interest, and $N - n$ of the genes do not contain the GO term. A set of m genes that are coexpressed contains both genes with the GO term and those without. The probability that the number of genes within the set of coexpressed genes that have the GO term is k can be expressed in terms of a random variable $\mathbf{X}$ that follows the hypergeometric probability, as follows:

$$P(X = k) = \frac{\binom{n}{k}\binom{N-n}{m-k}}{\binom{N}{m}}. \tag{6.12}$$

BiNGO (Maere et al., 2005) was used to test for GO term enrichment using the whole rat genome as the reference set. Overrepresentation of GO terms was established through the calculation of the number of times a GO term occurred within a set of co-expressed genes, followed by the hypergeometric test coupled with the Benjamini & Hochberg (1995) FDR correction, with a 5% level of significance.

6.5 Predicted Progesterone Response Elements

The human consensus sequence for the progesterone response element (hPRE), GNACANNNTGTNC, was identified using chromatin immunoprecipitation (ChIP) experiments on breast cancer and uterine leiomyoma cell lines by Yin et al. (2012). In order to identify the positions and base sequences for the hPRE sequence in the *Rattus norvegicus* rn5 genome, the R package called seqinR (Charif & Lobry, 2007) was

used. In addition, the positions of the complementary sequence of the hPRE, CNTGTNNNACANG, were also identified in the *Rattus norvegicus* rn5 genome.

Using CruzDB (Pedersen et al., 2013) the hPRE positions were submitted to the UCSC database to detect the first downstream and upstream genes on the same strand as the hPRE in the rn5 genome positive and negative strand, respectively. These genes were subsequently compared to lists of differentially expressed genes identified in this thesis to determine if the hPRE-associated genes in the rat were differentially expressed in rat uterine tissues during late pregnancy and parturition.

6.6 Predicted Progesterone Receptor Binding Sites

In a mouse study by Rubel et al. (2012), ChIP experiments were conducted to identify progesterone receptor (PR) binding sites in ovariectomised mice. The experiments were conducted using uterine samples from mice treated with oil (vehicle), P4, a sample where no ChIP antibody was used, and a final sample of uterus epithelium that was P4-treated.

All sample coordinates in the supplementary material (Rubel et al., 2012) were corrected for background using the ChIP background site coordinates. The background-corrected data were compared to the vehicle PR site coordinates. Each comparison step involved looking for overlaps in the coordinate sets using the mergeBed function from BedTools (Quinlan & Hall, 2010). Putative rat uterine PR-binding sites within P4-responsive genes were obtained by taking into consideration the background-corrected and vehicle-corrected P4 treated uterine PR site coordinates.

6.6.1 Genes with a PR-bound Upstream Region that Overlaps with Predicted PRE Site

To assess the uterine PR-binding sites that are associated with the PRE, the putative rat PR-binding sites were compared to predicted hPRE sites in the mouse genome. The site coordinates were merged using mergeBed, creating a list of uterine P4-responsive PR-binding sites, each associated with a varying number of predicted mouse hPREs sites. The first downstream genes on the same strand as the mouse hPREs were identified in the mm9 genome using the methods outlined in Section 6.5. This led to a unique list of mouse genes, which were associated with the uterine P4-responsive PR-binding sites. These data were subsequently compared to lists of P4-responsive genes identified in this thesis, to determine whether the hPRE-associated genes in the rat were PR-bound and differentially expressed in response to P4 treatment, and withdrawal, within uterine tissues.

6.7 Motif Analysis

A motif is a small sequence of nucleotides that may have biological function, e.g., a transcription factor binding site in the promoter region of a gene. There are two types of computational methods that are used in the analysis of motifs: algorithms that search for patterns that occur in multiple sequences within a set; and the assessment of statistical over-representation of known motifs within sequences.

6.7.1 Motif Search

To determine whether groups of differentially expressed genes were associated with the binding of common regulatory factors, regions upstream of the transcriptional start sites of genes, promoter regions, were analysed to identify common motifs. Promoter sequences with a maximum length of 500, 1000, and 2000 nucleotides, allowing for truncation if the neighbouring gene was within 2kb, were downloaded from BioMart (Kasprzyk, 2011) using the *Rattus norvegicus* (Rnor_5.0) dataset from the Ensembl Genes 75 database (Flicek et al., 2013), together with the rat genome database (RGD) gene symbols (Laulederkind et al., 2013). Repeat masking, a process by which sequences of repeated bases are hidden by replacing the repeats with Ns, was performed on the promoter sequences using RepeatMasker (Smit et al., 2010) so as to remove sequence similarities that were not representative of binding motifs. The repeat-masked sequences were used as input in MEME-LaB (Brown et al., 2013) to identify motifs that were enriched within the promoters of differentially expressed gene sets.

6.7.2 Motif Enrichment in Random Sets of Genes

To ensure that enriched motifs were unique to the treatments subjected to the uterine tissues, motif enrichment analysis was carried out on sets of genes that were selected at random from the expressed transcriptome.

Genes were selected at random, using the Uniform Distribution in R, from the expressed rat uterus transcriptome. Regions that are upstream of the selected genes were analysed for motif enrichment as described in Section 6.7.1.

6.7.3 Statistical Significance of Motif Enrichment

Using the whole rat genome as the reference set of genes, some of which contain a particular transcription factor (TF) motif within their promoter regions, the hypergeometric test was used to determine whether the overlap between the set of genes containing a motif in their promoters and another set of co-expressed genes was significantly large. Significance of TF motifs was established by employing the following steps:

1. The promoter regions of all the genes within the rat genome were inspected for the presence of all motifs. Here, three promoter lengths were considered; 500 bp, 1000 bp, and 2000 bp. Taking into account the number of times a motif was identified within the promoter as well as the number of motifs identified, a p-value was calculated for each promoter.

2. Given the p-values, a motif was considered present within the promoter regions if its p-value was below a set threshold of 0.0001

3. Hypergeometric p-values were subsequently computed for the motifs that were considered present, and a motif was considered significant if its p-value was less than 0.01.

4. JASPAR (http://jaspar.genereg.net) was used to lookup significant motifs.

Part III

Results

Chapter 7

Transcriptomic Profiling of Rat Uterine Tissues

In this chapter, the transcriptional changes that occur in rat uterine tissues following the systemic withdrawal of progesterone on the 19^{th} day of gestation are studied, in order to: document the full complement of RNA in rat uterine tissues, namely; the basal decidua, the inner circular myometrium and the outer myometrium in late pregnancy and at term; as well as to determine the patterns of gene transcript expression associated with each tissue at 4 gestational time points; GD19+6hrs, GD20, GD22(NL) and GD22(L).

7.1 Transcriptomic Landscape of the Rat Uterus in Late Pregnancy and at Term

A total of 11 Sprague-Dawley rats were injected with sesame seed oil as described in Section 5.1, and whole uterine horns were obtained at 4 time points: on GD19+6hrs; GD20; GD22(NL); and GD22(L) as illustrated in Figure 7.1. This preparation of the animal tissue was conducted by Professor Robert Garfield (St. Joseph's Hospital and Medical Center – Phoenix, USA). The uterine horns were then flash-frozen in liquid nitrogen and shipped to the UK. On arrival, the samples were checked visually to make sure that they were still frozen and then stored at $-80°C$ (Supplementary Figure B.1).

Laser-capture microdissection (LCM) was performed in order to separate the basal decidua, the inner circular myometrial layer, and the outer longitudinal myometrial layer from uterine samples following the procedure described in Section 5.4. Total

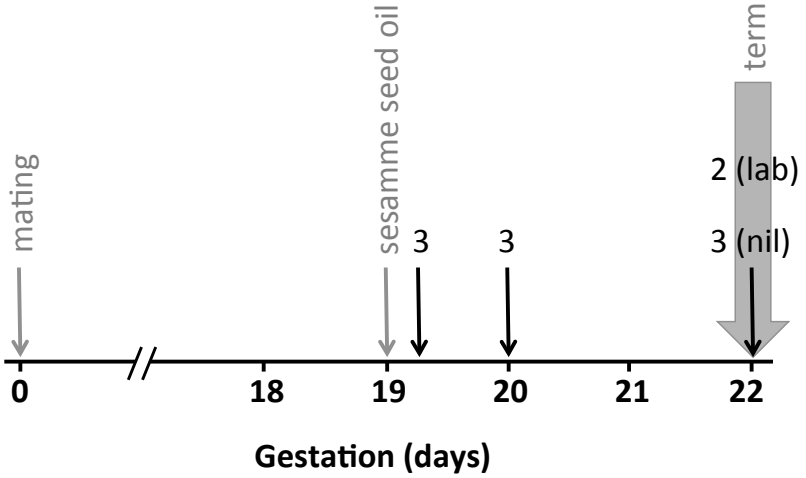

Figure 7.1: Protocol for the collection of uterine samples. The black arrows indicate the days on which animals were killed, and the numbers on top of the black arrows indicate the sample sizes. At term labouring (lab) and not-in-labour (nil) samples were collected.

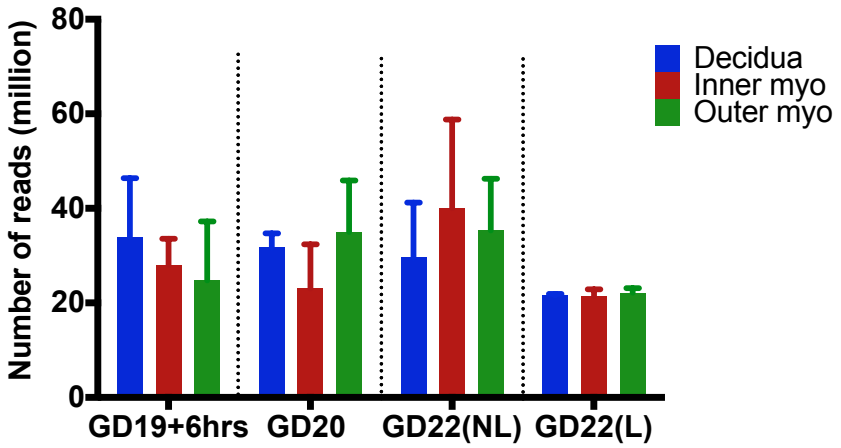

Figure 7.2: Number of reads in the sequencing files. The average number of reads generated from decidua, inner myometrium and outer myometrium samples obtained on GD19+6hrs, GD20, GD22(NL), and GD22(L). The error bars indicate the standard deviation of the number of reads within a group of biological replicates.

RNA was isolated from LCM tissues and checked for integrity using the Agilent 2100 Bioanalyzer as described in Section 5.5.2, and RNA of acceptable quality was used to prepare libraries that were sequenced on the Illumina HiSeq 2500 platform.

The transcript expression data presented here were created as described in Section 5.6. In total, 974.63 million paired-end reads, each 51 nucleotides in length, were generated across all libraries as illustrated in Figure 7.2. A full list of the number of reads per sample is provided in Table 7.1. On average, 14.77 million paired-end reads were sequenced per sample. The files with the sequencing data, in FASTQ format, for samples obtained GD19+6hrs contained between 18,172,495 and 47,412,999 reads each. Reads for GD20 samples were between 14,984,755 and 42,069,289, while those for GD22(NL) samples were between 17,906,163 and 59,347,487. Samples collected on GD22(L) had between 20,405,112 and 22,841,338 reads.

Prior to the alignment of reads to the rat transcriptome, the quality of the reads within the FastQ files was assessed using FastQC. Each quality check could return any of three results; pass, warn, or fail. Files that failed three or more of the

quality checks were discarded. Reads obtained from one GD20 decidua sample, and one GD19+6hrs decidua sample, failed several of the tests including: sequence GC content; sequence duplication; overrepresented sequences; and k-mer content. The reads generated from these samples were not trimmed at this stage. Instead new LCM tissues were isolated from the corresponding samples, from which RNA was extracted and sent for library preparation and sequencing as described in Sections 5.4–5.6. The data files were subsequently inspected using FastQC. The results of the FastQC tests conducted on sequencing data files are shown in Supplementary Table C.1.

To verify that reads were aligned correctly, sorted BAM files were loaded onto the IGV Browser to enable visual assessment of the alignments. Representative examples of alignment to the progesterone receptor gene (Pgr) of reads obtained from GD19+6hrs, GD20, GD22(NL), and GD22(L), are shown in Figures 7.3, 7.4, 7.5, and 7.6, respectively. Of the sequenced reads, 79.87% were aligned to the reference transcriptome using Tophat2, and 70.59% of the aligned reads were determined to be expressed across all gestational time points and tissues. The expressed transcriptome was covered 12.67×, 13.41×, 17.25×, and 11.88× on average in the samples obtained on GD19+6hrs, GD20, GD22(NL), and GD22(L), respectively (details in Table 7.1).

Table 7.1: Alignment of sequenced reads to the *Rattus norvegicus* transcriptome and coverage statistics of sequences. Gestation - The day during pregnancy on which the uterine sample was collected. **Tissue** - The layer of the uterus that was separated from the other tissues using laser-capture microdissection. The number illustrates the replicate number. **% Aligned** - The proportion of the sequenced reads that were aligned successfully to the *Rattus norvegicus* transcriptome using Tophat2. **% Expressed features** - The proportion of genes to which counts were assigned by HTSeq. **Expressed transcriptome (× covered)** - The number of times the expressed transcriptome was covered by the sequenced reads.

Sample					Expressed
Gestation	Tissue	Total reads	% Aligned	% Expressed features	transcriptome (× covered)
GD19+6hrs	Decidua_1	47,412,999	84.90	74.96	21.1
GD19+6hrs	Decidua_2	22,970,447	84.60	84.65	6.94
GD19+6hrs	Decidua_3	31,654,340	81.50	72.39	14.06
GD19+6hrs	Inner_Myo_1	21,711,951	80.90	66.37	6.67
GD19+6hrs	Inner_Myo_2	31,035,607	83.20	71.41	11.83
GD19+6hrs	Inner_Myo_3	31,434,913	73.60	74.13	9.05
GD19+6hrs	Outer_Myo_1	39,135,788	84.00	66.24	30.61
GD19+6hrs	Outer_Myo_2	16,941,814	76.90	69.56	5.23
GD19+6hrs	Outer_Myo_3	18,172,495	76.50	74.49	8.53
GD20	Decidua_1	30,757,580	77.70	73.98	7.89
GD20	Decidua_2	35,081,695	56.20	44.02	0.86
GD20	Decidua_3	29,305,075	79.00	61.41	19.45
GD20	Inner_Myo_1	20,758,801	76.20	57.73	15.11
GD20	Inner_Myo_2	33,340,488	83.30	76.76	9.69
GD20	Inner_Myo_3	14,984,755	71.40	61.48	7.38
GD20	Outer_Myo_1	40,458,136	79.30	74.86	23.42
GD20	Outer_Myo_2	22,414,900	80.20	73.93	13.32
GD20	Outer_Myo_3	42,069,289	86.90	75.87	23.53
GD22(NL)	Decidua_1	17,906,163	79.10	84.03	3.62
GD22(NL)	Decidua_2	29,604,137	83.90	72.27	18.46
GD22(NL)	Decidua_3	41,196,358	84.40	68.90	26.42
GD22(NL)	Inner_Myo_1	38,897,796	87.00	73.05	28.99
GD22(NL)	Inner_Myo_2	21,843,013	72.00	57.51	5.9
GD22(NL)	Inner_Myo_3	59,347,484	84.50	71.95	31.51
GD22(NL)	Outer_Myo_1	46,366,358	84.20	71.31	22.64
GD22(NL)	Outer_Myo_2	24,476,132	79.10	80.33	4.84
GD22(NL)	Outer_Myo_3	35,100,798	85.80	76.31	12.9
GD22(L)	Decidua_1	21,339,531	79.70	64.48	11.71
GD22(L)	Decidua_2	21,789,441	82.60	66.33	11.17
GD22(L)	Inner_Myo_1	22,465,983	80.00	73.05	4.29
GD22(L)	Inner_Myo_2	20,405,112	84.20	70.94	10.56
GD22(L)	Outer_Myo_1	22,841,338	82.10	72.87	15.76
GD22(L)	Outer_Myo_1	21,409,111	70.70	71.88	17.79

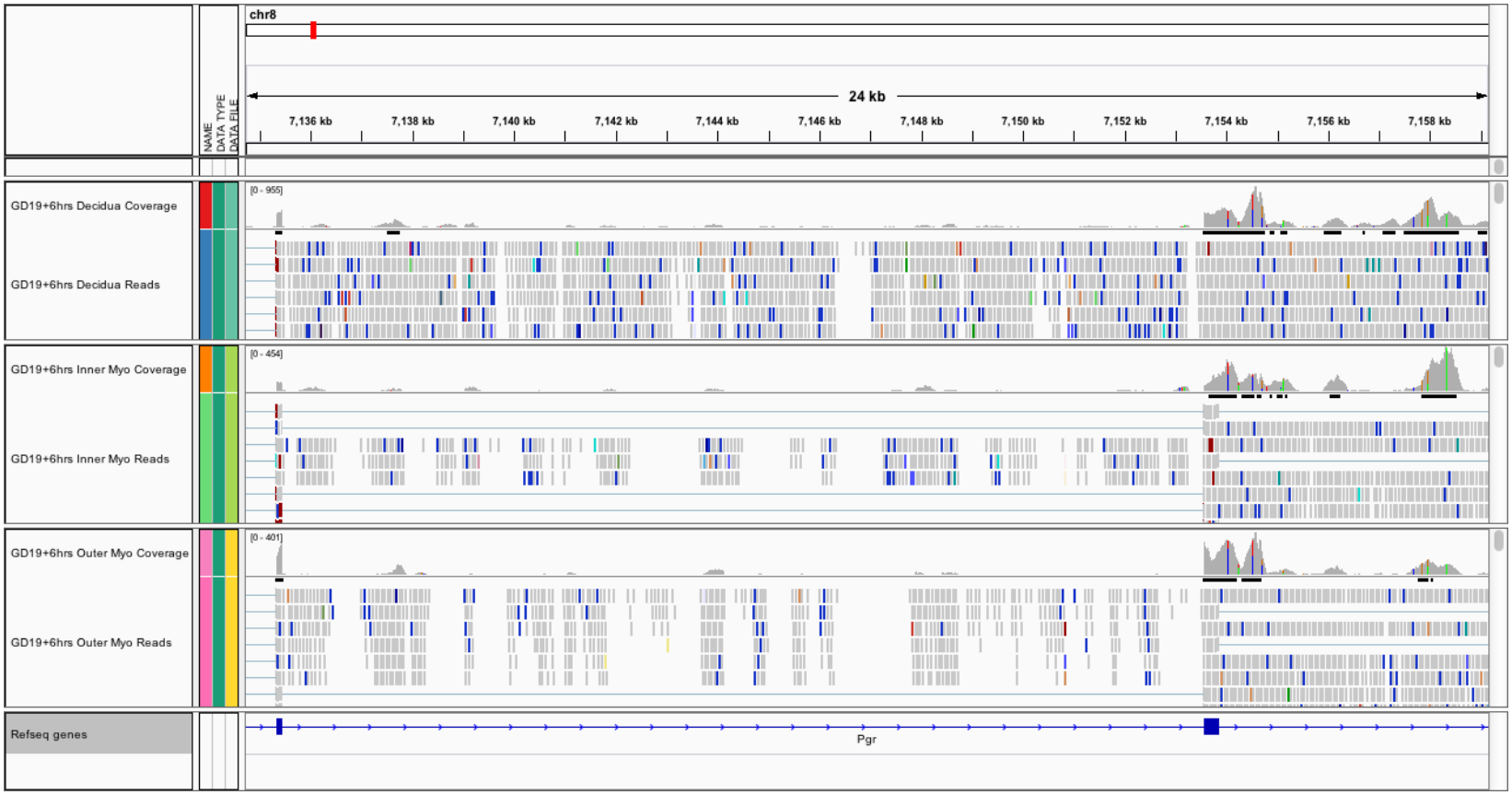

Figure 7.3: Alignment of GD19+6hrs reads to the Pgr gene. IGV browser screenshot showing reads, obtained from GD19+6hrs tissues, that aligned to a section of the Pgr gene. Reads were aligned using TopHat2, sorting and indexing of mapped reads were conducted using Samtools.

Figure 7.4: Alignment of GD20 reads to the Pgr gene. IGV browser screenshot showing reads, obtained from GD20 tissues, that aligned to a section of the Pgr gene.

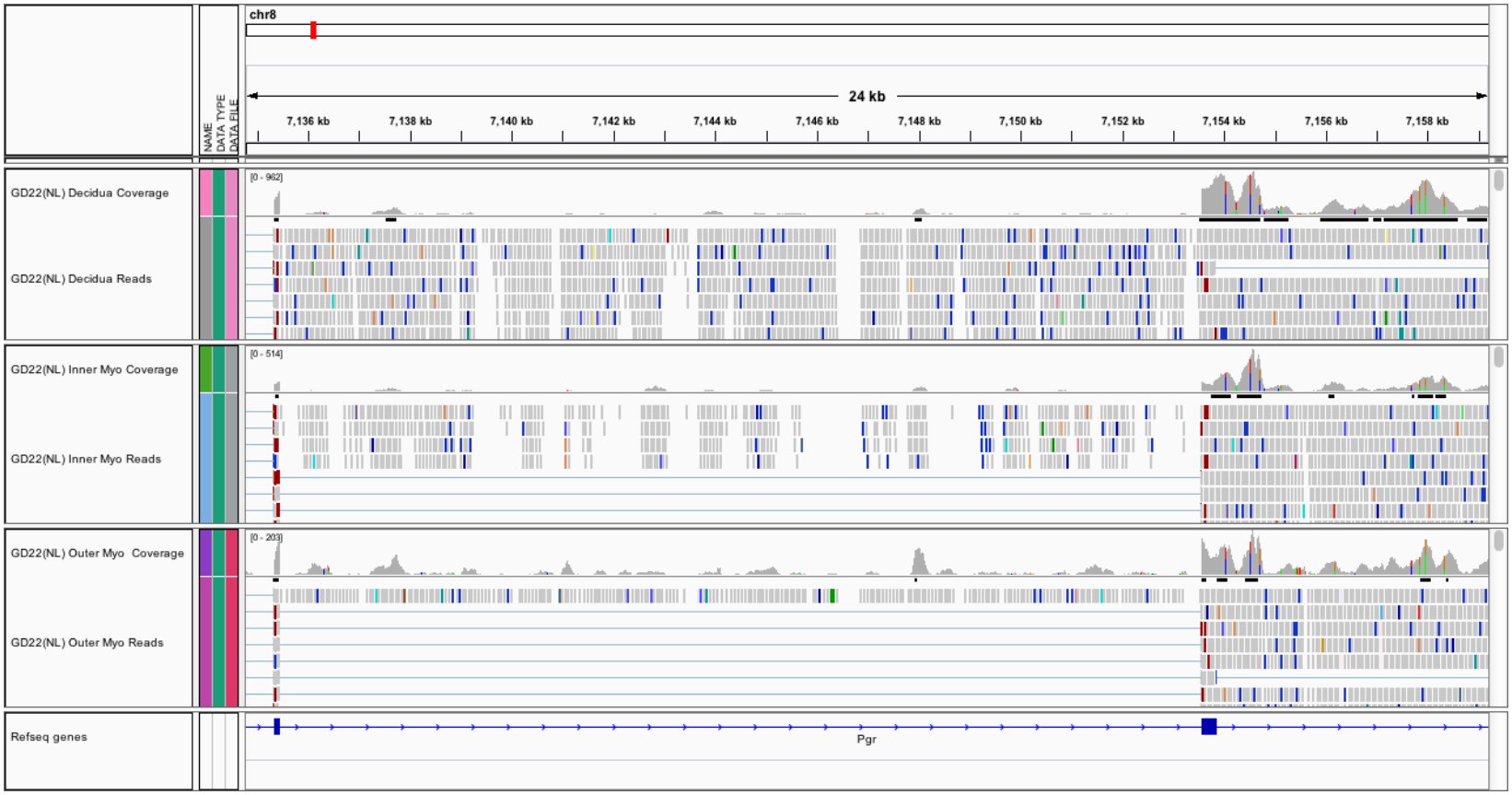

Figure 7.5: Alignment of GD22(NL) reads to the Pgr gene. IGV browser screenshot showing reads, obtained from GD22(NL) tissues, that aligned to a section of the Pgr gene.

Figure 7.6: Alignment of GD22(L) reads to the Pgr gene. IGV browser screenshot showing reads, obtained from GD22(L) tissues, that aligned to a section of the Pgr gene.

7.2 Analysis of the Expression of Tissue-Specific Gene Transcripts

The expression levels of gene transcripts within samples were estimated using three approaches, the first of which employed Sailfish to estimate transcripts per million (TPM) values, the second used Cufflinks to estimate reads per kilobase per million (RPKM), and the third used HTSeq to estimate raw gene transcript counts. To determine whether LCM had been successfully employed in the collection of pure decidual and myometrial tissues, the mean TPM expression values in the decidua were divided by the mean TPM values in the myometrium for each gestational time point. A higher ratio indicated that a gene transcript was expressed more in the decidua than in myometrial tissues.

Transcripts encoding thyrotropin releasing hormone (Trh) were, on average (mean ± SD), highly expressed in the decidua in comparison to the inner and outer layers of the myometrium (Table 7.2). Trh mRNA expression was highest in the decidua on GD19+6hrs (553.73 ± 372.47 TPM) and lowest at term (89.26 ± 89.80 TPM). On GD20 and during labour, Trh mRNA expression were 364.66 ± 583.45 TPM and 188.66±66.99 TPM, respectively. In the myometrial layers, the highest expression of Trh mRNA transcripts was observed on GD19+6hrs in the outer layer (37.31 ± 63.06 TPM). Immunohistochemical (IHC) staining for Trh was conducted on samples from all time-points to confirm the mRNA expression data. IHC studies showed that Trh was mainly localised to the decidua on GD19+6hrs (Figure 7.7). On GD20, all three layers showed Trh presence, but with the strongest staining intensity in the decidua (Figure 7.7). Staining for Trh on GD22(NL) was distinct in the decidua as well as the inner layer of the myometrium, with slightly stronger staining for Trh in the decidua (Figure 7.8). While Trh staining is present in all three uterine layers

Table 7.2: Expression of tenascin n (Tnn) and thyrotropin releasing hormone (Trh) mRNA in uterine tissues. Transcript expression values are shown in transcript per million values (mean±SD).

		Tnn		Trh	
		Mean	±SD	Mean	±SD
Decidua	GD19+6hrs	5.55	4.77	553.73	372.47
	GD20	20.17	24.33	364.66	583.45
	GD22(NL)	38.22	39.91	89.26	89.80
	GD22(L)	12.82	18.06	188.66	66.99
	Overall	19.77	25.43	309.11	366.29
Inner Myo	GD19+6hrs	86.47	39.28	1.55	2.06
	GD20	48.53	41.35	0.53	0.14
	GD22(NL)	61.51	30.36	0.17	0.27
	GD22(L)	9.89	13.41	0.92	0.23
	Overall	55.39	39.78	0.78	1.09
Outer Myo	GD19+6hrs	0.41	0.33	37.31	63.06
	GD20	5.53	3.96	0.45	0.29
	GD22(NL)	5.69	4.16	0.13	0.13
	GD22(L)	10.11	11.31	26.63	36.85
	Overall	5.01	5.58	15.18	35.18

on GD22(L), the intensity of staining is strongest in the decidua (Figure 7.8). The intensity of immunohistochemical staining in the decidua at each time-point would suggest that Trh may be used to identify the basal decidua in late pregnancy.

Tenascin-n (Tnn) mRNA expression was high the inner myometrium compared to that in the decidua, as well as in comparison to the outer layer of the myometrium (Table 7.2). Average Tnn expression across the four gestational time points was 19.77 ± 25.43 TPM in the decidua, 55.39 ± 39.78 TPM in the inner myometrium, and 5.01 ± 5.58 TPM in the outer myometrium. Immunohistochemical staining showed that Tnn was distinctly present in the decidua and the inner myometrium, but less so in the outer myometrium on GD19+6hrs and GD20 (Figure 7.9), as well as on GD22(L) (Figure 7.10). On GD22(NL), the intensity of staining for Tnn in the decidua was low, however, there was strong staining in the inner myometrium

and no staining for Tnn in the outer myometrium. Evidence suggests that Tnn expression at both the mRNA and protein level may be used to distinguish the inner layer of the myometrium from the outer layer of the myometrium.

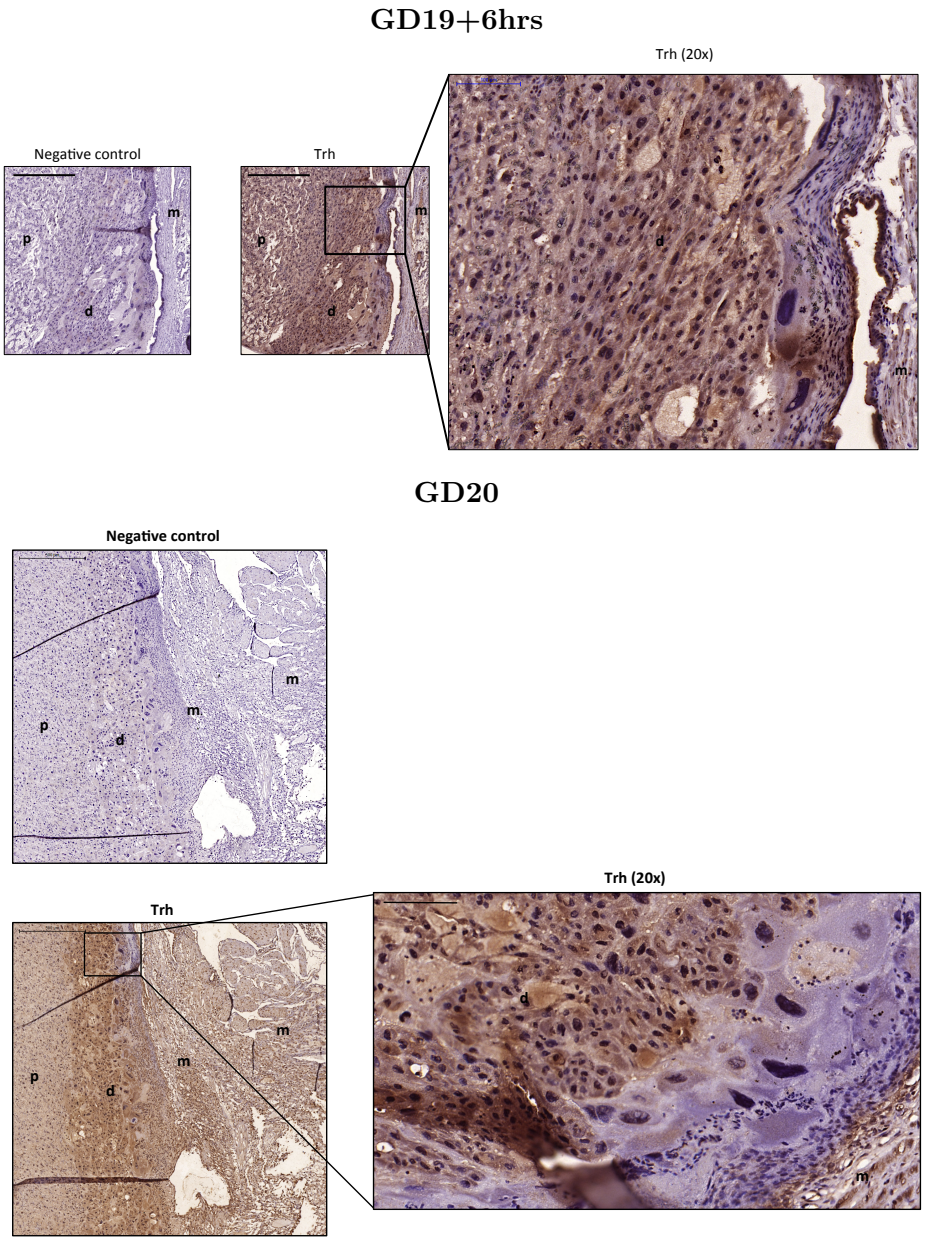

Figure 7.7: Thyrotropin-releasing hormone (Trh) is mainly localised to the decidua. Top: Expression of Trh in uterine tissues on GD19+6hrs. **Negative control**: tissues without staining. **Trh**: tissues stained for Trh. **Trh (20x)**: zoomed in image of tissues stained for Trh with 20x magnification. Bottom: Trh protein expression in the rat uterus on GD20. **Negative control**: tissues without staining. **Trh**: tissues stained for Trh. **Trh (20x)**: zoomed in image of tissues stained for Trh with 20x magnification. **p**: placenta; **d**: decidua; and **m**: myometrium. Scale bars = 500 μm [Negative control and Trh] and 100 μm [Trh (20x)].

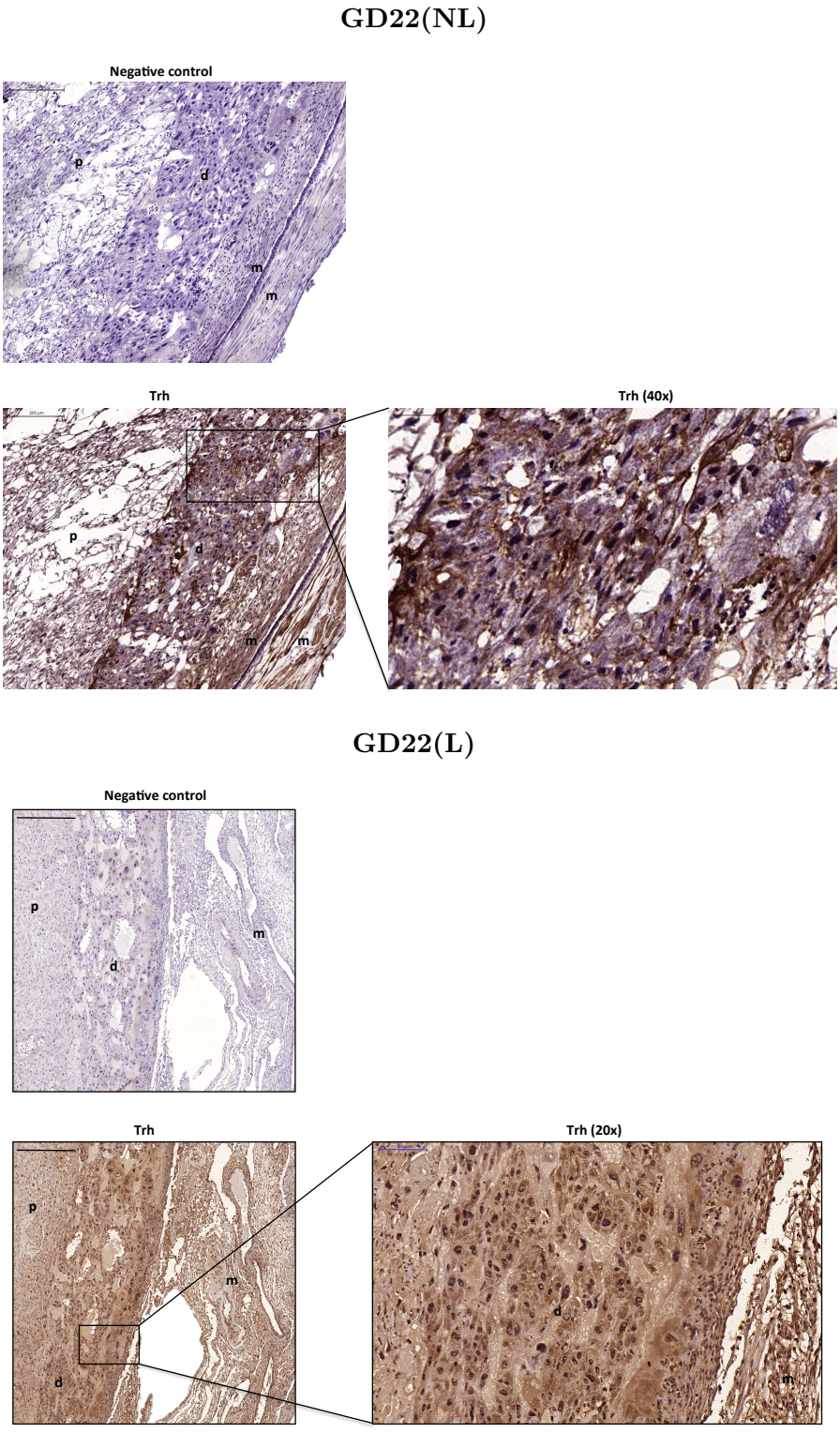

Figure 7.8: Immunohistochemical (IHC) staining for Trh in uterine tissues. Top: IHC staining for Trh in the uterus on GD22(NL). **Negative control**: tissues without staining. **Trh**: tissues stained for Trh. **Trh (40x)**: zoomed in image of tissues stained for Trh with 40x magnification. Scale bars = 200 µm [Negative control and Trh] and 50 µm [Trh (40x)]. Bottom: IHC staining for Trh on GD22(L). **Trh**: tissues stained for Trh. **Trh (20x)**: zoomed in image of tissues stained for Trh with 20x magnification. Scale bars = 500 µm [Negative control and Trh] and 100 µm [Trh (20x)]. **p**: placenta; **d**: decidua; and **m**: myometrium.

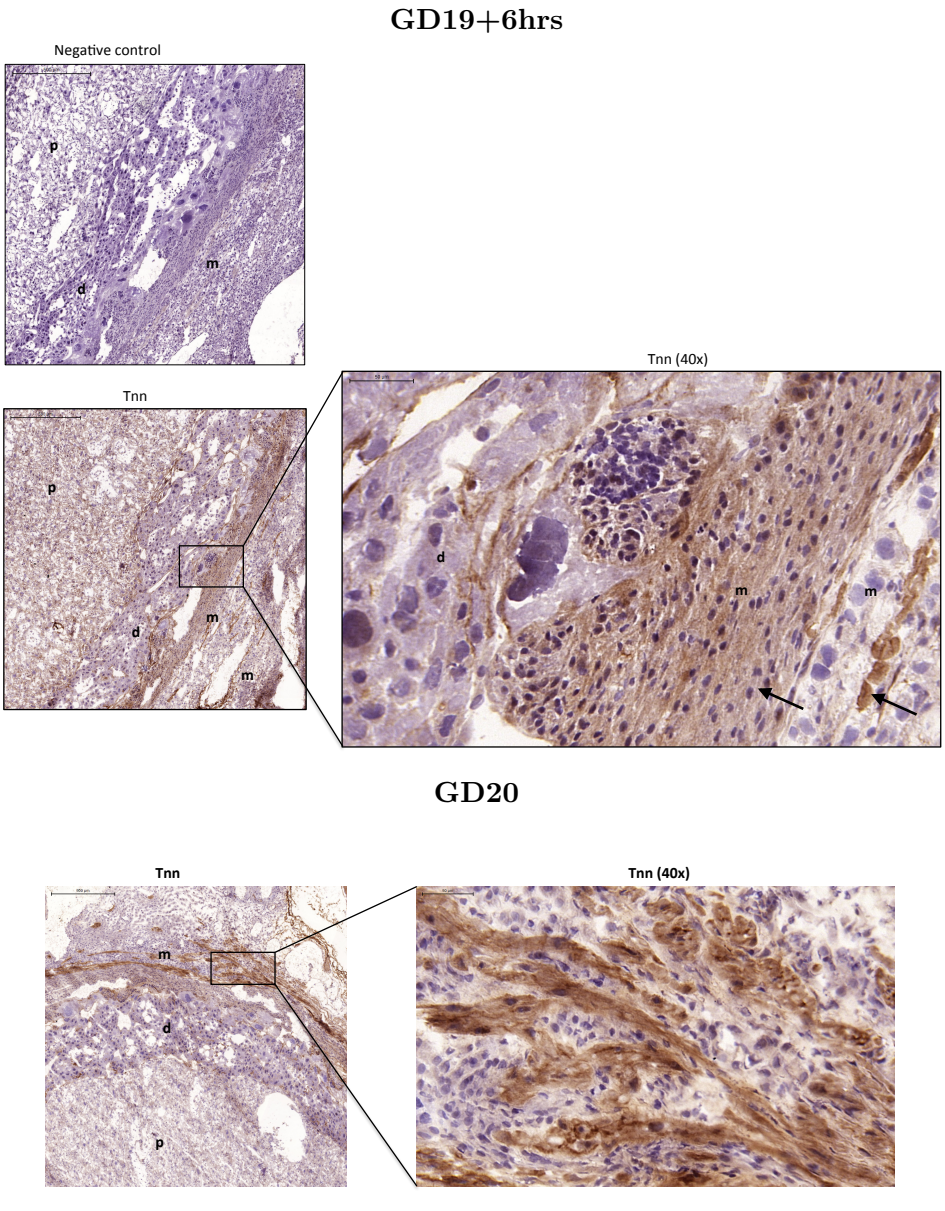

Figure 7.9: Immunohistochemical (IHC) staining for Tnn in uterine tissues. Top: **Negative control**: tissues without staining. **Tnn**: tissues stained for Tnn. **Tnn (40x)**: zoomed in image of tissues stained for Tnn with 40x magnification. Scale bars = 500 µm [Negative control and Tnn] and 50 µm [Tnn (40x)]. Bottom: IHC staining for Tnn on GD20. **Tnn**: tissues stained for Tnn. **Tnn (40x)**: zoomed in image of tissues stained for Tnn with 40x magnification. Scale bars = 200 µm [Tnn] and 50 µm [Tnn (40x)]. **p**: placenta; **d**: decidua; and **m**: myometrium.

GD22(NL)

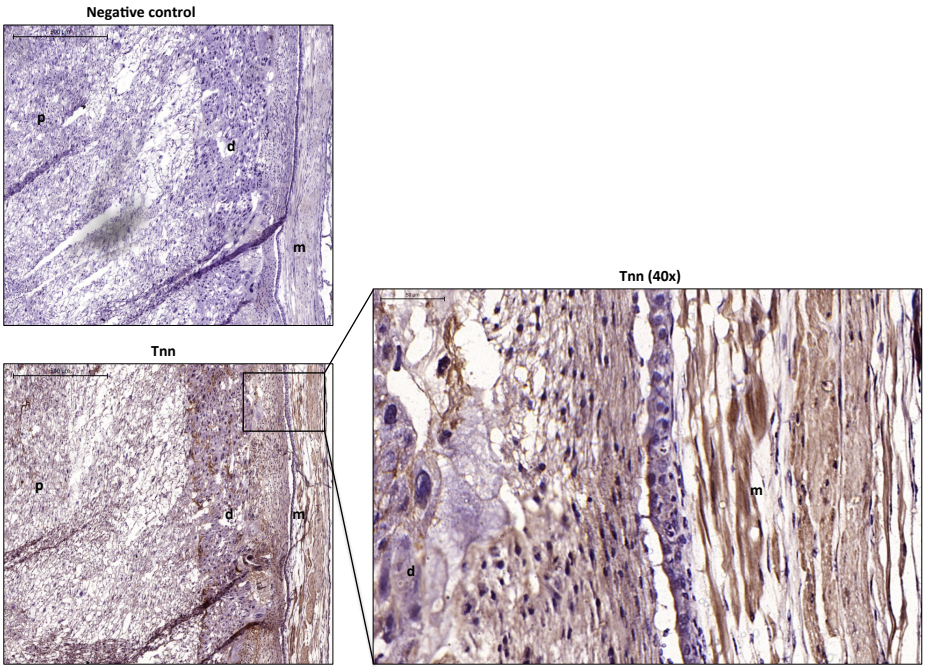

GD22(L)

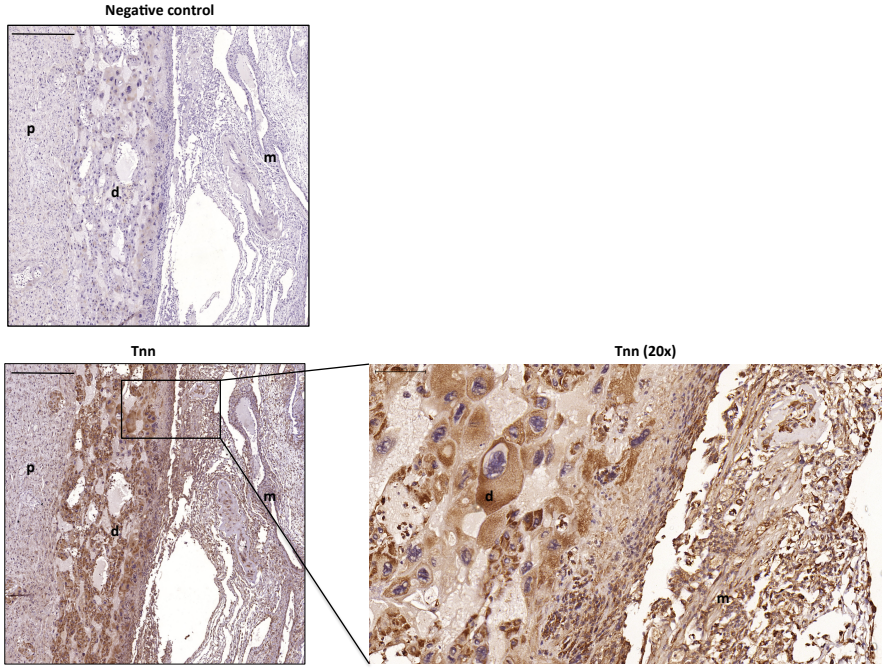

Figure 7.10: Immunohistochemical (IHC) staining for Tnn in uterine tissues. Top: **Negative control**: tissues without staining. **Tnn**: tissues stained for Tnn. **Tnn (40x)**: zoomed in image of tissues stained for Tnn with 40x magnification. Scale bars = 500 µm [Negative control and Tnn] and 50 µm [Tnn (40x)]. Bottom: **Negative control**: tissues without staining. **Tnn**: tissues stained for Tnn. **Tnn (40x)**: zoomed in image of tissues stained for Tnn with 40x magnification. Scale bars = 500 µm [Negative control and Tnn] and 100 µm [Tnn (40x)]. **p**: placenta; **d**: decidua; and **m**: myometrium.

7.3 Principal Component Analysis

Principal component analysis (PCA) of the TPM values was employed to further assess the patterns of expression of gene transcripts within the uterine tissues. To perform PCA as described in Section 6.1, the princomp function in R was used as follows:

$$\text{myPCA} = \text{princomp}(\sim .,\text{data} = \text{myData}, \text{na.action} = \text{na.exclude}, \text{cor} = \text{FALSE}),$$

where $\sim .$ indicates that all the variables (tissue samples) in the data matrix myData were used in the estimation of principal components (PCs), while na.action = na.include indicates that any gene transcripts whose expression values were denoted by NA were excluded, and cor = FALSE indicates that the covariance matrix was used in the estimation of PCs instead of the correlation matrix. The number of PCs used to assess the relationship among the data were selected using two methods; the cumulative variance captured by the PCs of 85%, and plots of the eigenvalues as described in Section 6.1.2.

7.3.1 GD19+6hrs

Following the estimation of the PCs of the mRNA transcripts expressed on GD19+6hrs in uterine tissues, both the cumulative variance captured by the PCs (Table 7.3) and a plot of the eigenvalues were used to determine the number of PCs to retain for analysis. The first PC (PC1) accounted for 66.3% of the variance in the data, while the second PC (PC2) accounted for 17.6%. Together, PC1 and PC2 accounted for 83.9% of the variance in the data. To reach the set threshold of 85% of the variance accounted for by the PCs, the third PC (PC3), which accounted for 11.4% was also retained. The plot of eigenvalues in Figure 7.11 showed that PC1 accounted for the majority of the variance, however, the next two PCs, PC2 and PC3, also accounted for a sizeable proportion of the variance. Hence three PCs were retained for analysis in this section. A three-dimensional plot of the retained PCs shows that the inner myometrium samples grouped together (Figure 7.12),

Table 7.3: Variance accounted for by principal components. Shown are the proportions of variance accounted for by principal components, as well as the cumulative proportion of variance, on GD19+6hrs, GD20, GD22(NL), and GD22(L). **PV (%)**: proportion of variance explained, expressed as a percentage; **CP (%)**: cumulative variance explained, expressed as a percentage; and **Comp.**: principal component.

	GD19+6hrs		GD20		GD22(NL)		GD22(L)	
	PV (%)	CP (%)	PV (%)	CP (%)	PV (%)	CP (%)	PV (%)	CP (%)
Comp.1	66.3%	66.3%	59.2%	59.2%	79.1%	79.1%	70.1%	70.1%
Comp.2	17.6%	83.9%	36.9%	96.1%	19.0%	98.1%	27.8%	97.9%
Comp.3	11.4%	95.3%	2.4%	98.5%	0.9%	99.0%	1.4%	99.3%
Comp.4	2.3%	97.5%	0.5%	99.0%	0.4%	99.4%	0.4%	99.7%
Comp.5	1.3%	98.8%	0.5%	99.5%	0.3%	99.7%	0.2%	99.9%
Comp.6	0.7%	99.5%	0.4%	99.8%	0.2%	99.9%	0.1%	100.0%
Comp.7	0.3%	99.8%	0.1%	99.9%	0.1%	99.9%		
Comp.8	0.2%	99.9%	0.0%	100.0%	0.0%	100.0%		
Comp.9	0.1%	100.0%	0.0%	100.0%	0.0%	100.0%		

while two of the outer myometrium samples, as well as two of the decidua samples, were separated from the other uterine samples. One outer myometrium sample and one decidua sample were not separated from the inner myometrium samples. Given that the inner myometrium is sandwiched between the decidua and the outer myometrium, it may be that some inner myometrium cells were present in the two samples that were not grouped with their respective replicates. In addition, there was clear variability among the outer myometrium samples, which may also be a result of contamination with cells from other tissues. Apart from contamination with cells from other tissues, the relationships among the mRNA expression levels in different tissues may not be linear. Thus other methods which do not consider the linear relationship between variables may need be employed.

7.3.2 GD20

Since the scree plot and cumulative variance methods used in Section 7.3.1 suggested the same number of PCs for analysis, this section as well as subsequent sections employed the cumulative variance approach to determine the number of PCs to retain for analysis. Cumulatively, PC1 and PC2 accounted for 96.1% of the variance within the mRNA expression data for GD20 samples (Table 7.3). As such, a plot of these two PCs was used to assess the

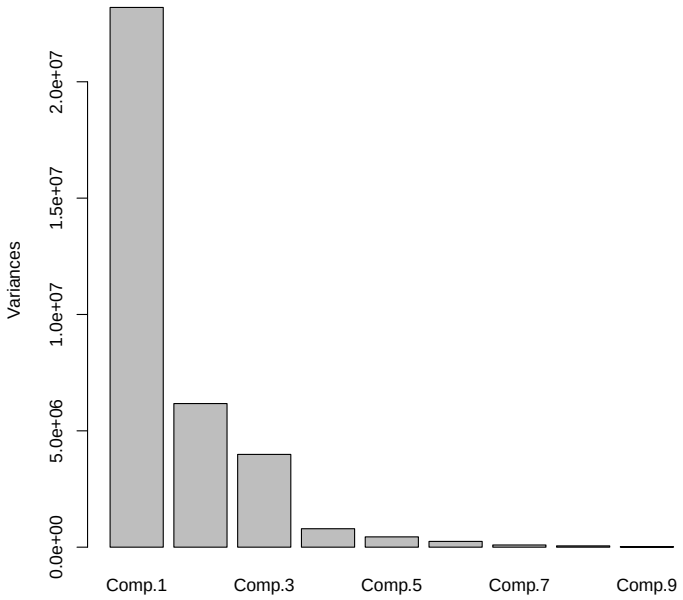

Figure 7.11: Plot of the eigenvalues of the covariance matrix of GD19+6hrs data. The low variance accounted for by principal component (Comp.) numbers 4–9 suggested that the first three PCs should be retained for analysis.

relationships among the GD20 mRNA expression data (Figure 7.13). PCA did not separate the tissues distinctly at this time-point.

7.3.3 GD22(NL) and GD22(L)

On GD22(NL) and GD22(L), 98.1% and 97.9% of the total variance was accounted for by the first two PCs, respectively. The plots of the PCs are shown in Figure 7.14. While PCA did not separate the mRNA expression levels in the uterine tissues distinctly on GD22(NL), there was distinct separation of tissues on GD22(L). However, the two inner myometrium exhibited a high degree of variability between them.

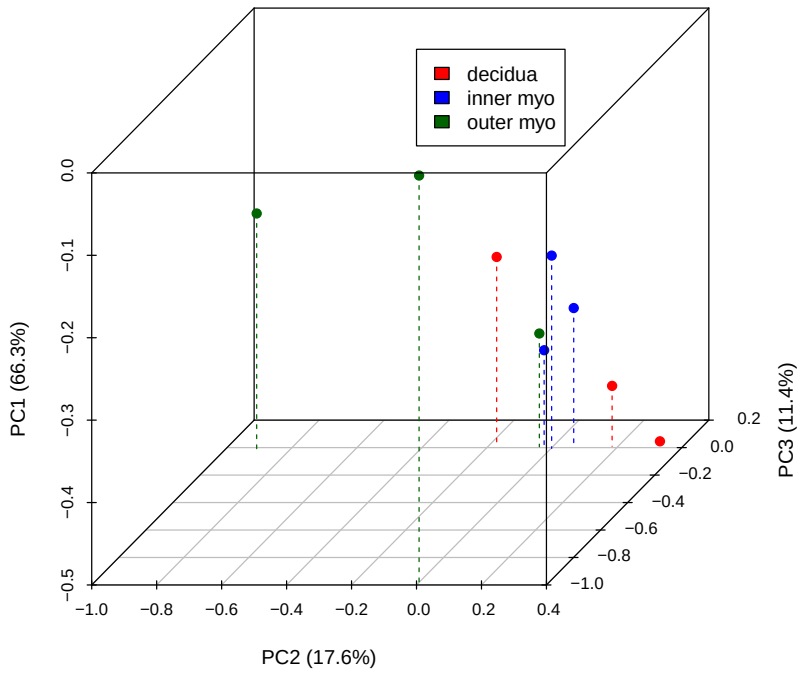

Figure 7.12: Principal component analysis (PCA) of mRNA expression on GD19+6hrs. Transcripts per million (TPM) abundances were used for PCA. The variance within the data which is accounted for by each of the first three principal components is displayed next to the corresponding principal component. **PC1**: the first principal component; **PC2**: the second principal component; **PC3**: the third principal component.

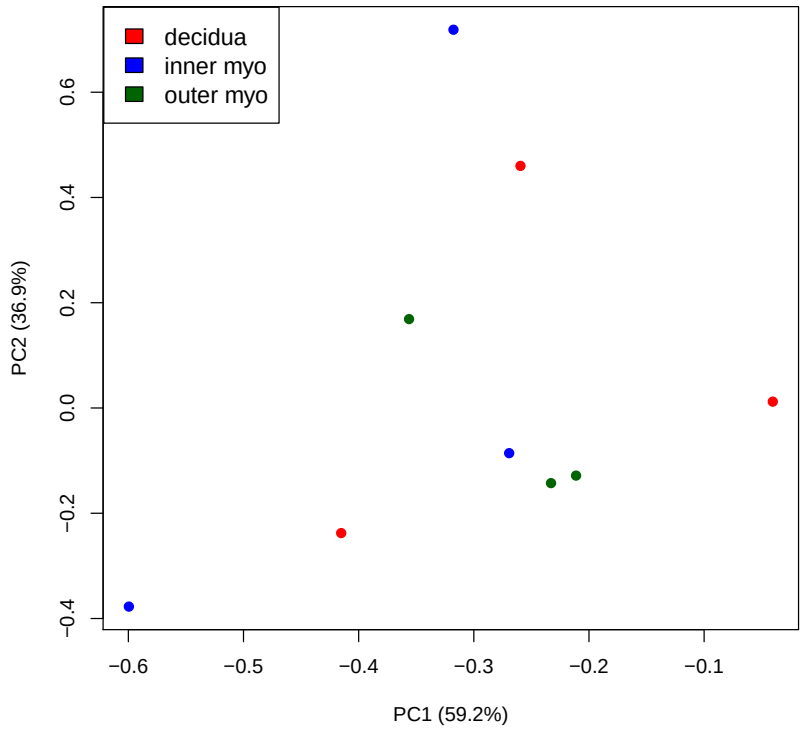

Figure 7.13: Principal component analysis (PCA) of mRNA expression on GD20. Transcripts per million (TPM) abundances were used for PCA. The variance within the data which is accounted for by each of the principal components is displayed next to the corresponding principal component. **PC1**: the first principal component; and **PC2**: the second principal component;

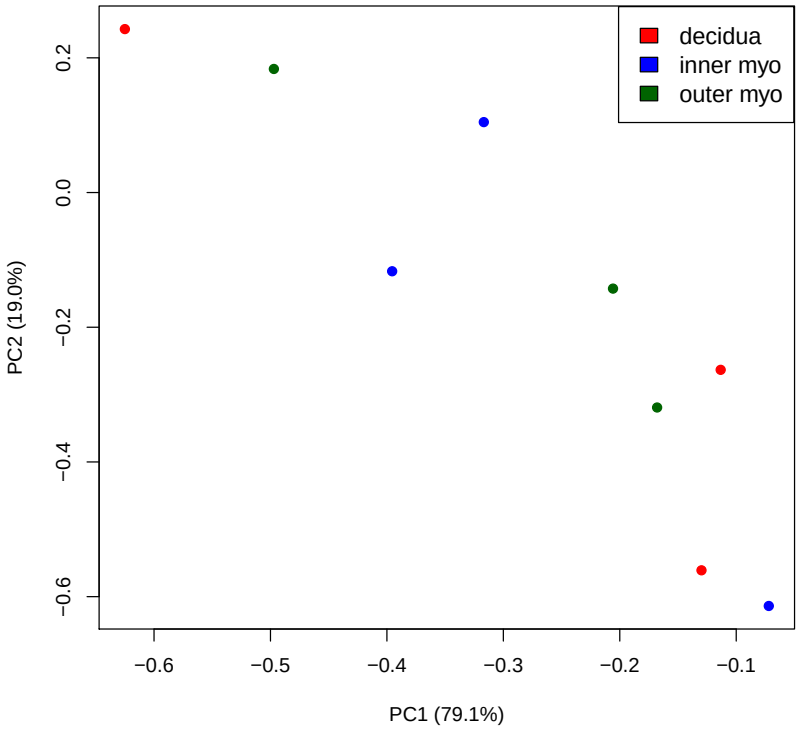

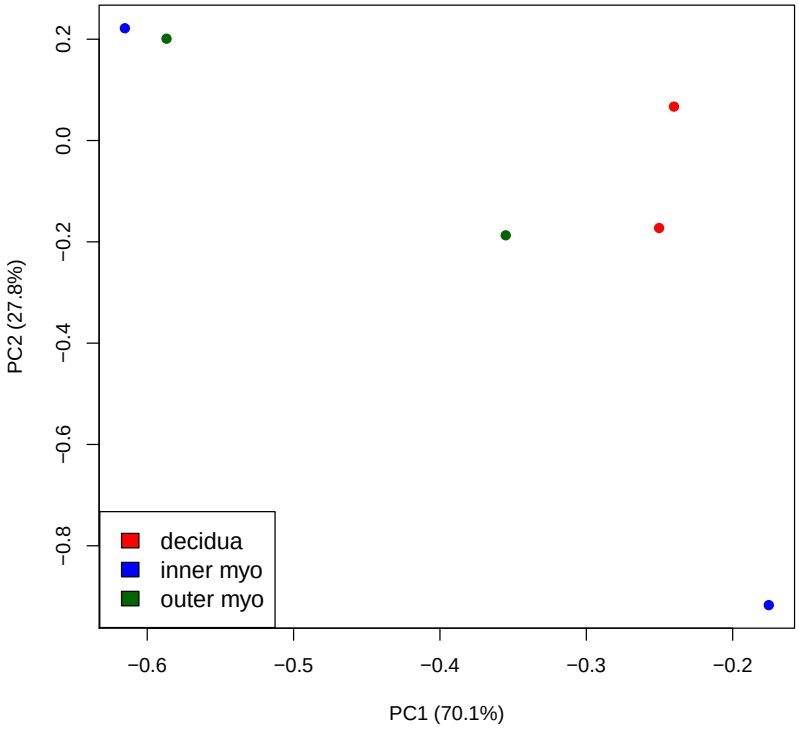

Figure 7.14: Principal component analysis (PCA) of term-pregnant rat uterine tissues. Transcripts per million (TPM) abundances were used for PCA of samples that were collected on (**Top**) GD22(NL) and (Bottom) GD22(L). The variance within the data which is accounted for by each of the first three principal components is displayed next to the corresponding principal component. **PC1**: the first principal component; **PC2**: the second principal component;

7.4 Differential Expression Analyses

To asses the patterns of gene transcript expression within the uterine samples, estimated abundances were subjected to differential expression analysis using three methods: Cuffdiff; edgeR; and DESeq2. Cuffdiff takes RPKM values estimated by Cufflinks as input, while edgeR and DESeq2 take raw gene transcript counts estimated by HTSeq as input. In each method, a gene transcript was considered differentially expressed if the associated p-value was less than a threshold of 5%. Multiple testing correction was employed in all methods and a threshold of 5% applied to the q-value in Cuffdiff, false discovery rate (FDR) in edgeR, and the adjusted p-value in DESeq2. For each pair of comparisons, a list of gene transcripts that had been identified by at least two of the three differential expression methods as differentially expressed was used for further analysis. To identify those gene transcripts whose expression patterns differed between uterine tissues, differential gene transcript expression analyses were conducted between uterine tissues at each gestational time point.

7.4.1 GD19+6hrs

A total of 361 gene transcripts were identified by Cuffdiff, 674 by edgeR, and 661 by DESeq2 as differentially expressed between the decidua and the inner myometrium, of which 480 gene transcripts were identified by at least 2 of the methods (Figure 7.15a). Of the 480 gene transcripts that were significantly differentially expressed between the decidua and the inner myometrium, 64% were upregulated in the inner layer of the myometrium (Table D.1). Between the decidua and the outer myometrium, 154 differentially expressed gene transcripts were found by Cuffdiff, 124 by edgeR and 60 by DESeq2. Sixty-nine gene transcripts were identified by at least two methods (Figure 7.15c), 74% of which were upregulated in the outer myometrium (Table D.2). The comparison between the myometrial layers yielded a set of 22 gene transcripts that were found by at least two methods from sets of 215, 30, and 15 gene transcripts that were identified as differentially expressed by Cuffdiff, edgeR and DESeq2, respectively (Figure 7.15e). Approximately 45% of the gene transcripts were upregulated in the outer myometrium (Table D.3). To further analyse the relationships among the

uterine tissues, z-scores of the TPM values were calculated and used in clustering analysis. Heat maps of the relationships shown in Figure 7.15, indicate the differences in expression patterns of gene transcripts between the tissues, particularly between the inner and outer myometrial layers.

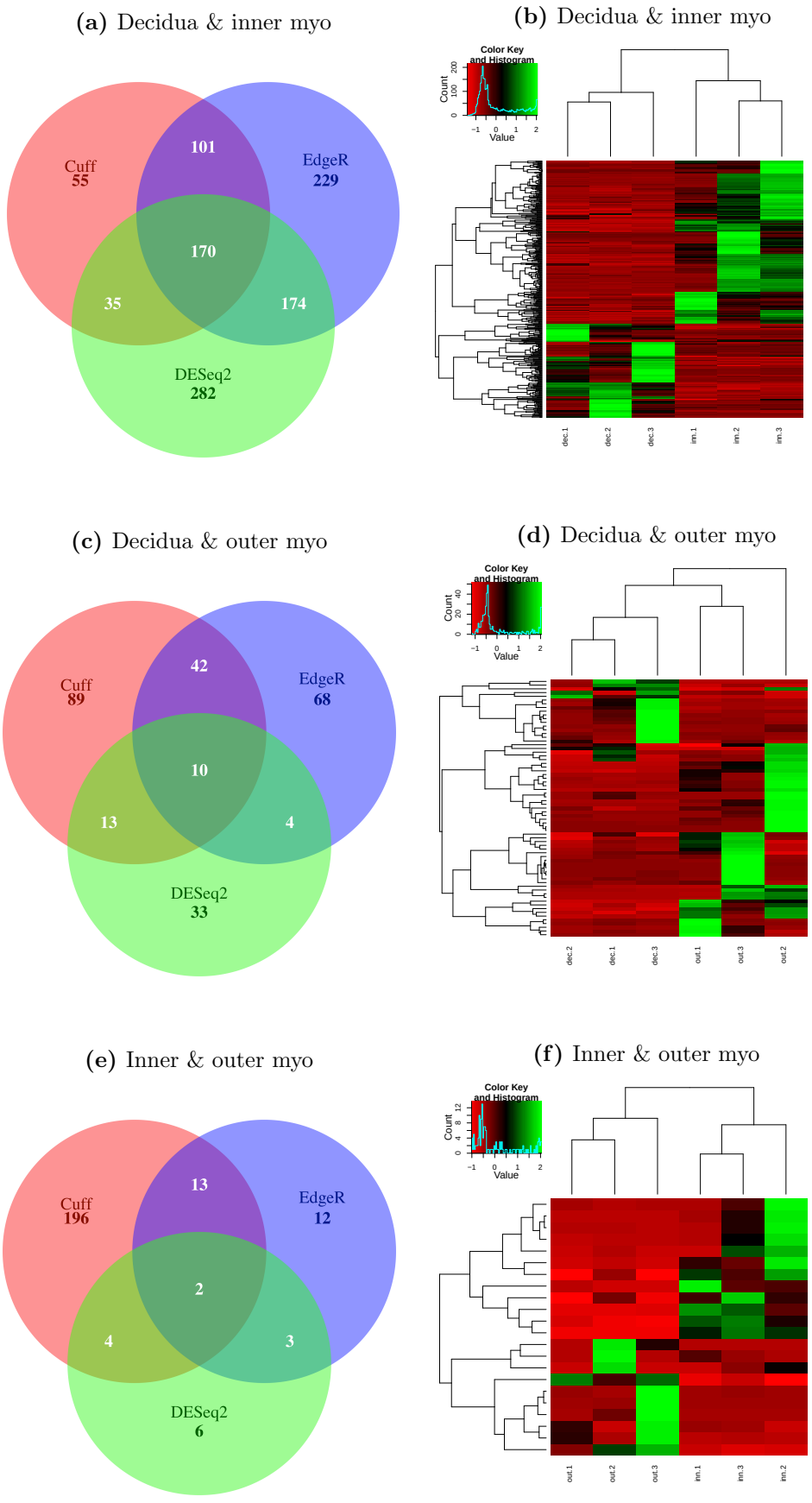

Figure 7.15: Comparisons of differentially expressed gene transcripts on GD19+6hrs. Gene transcripts were identified as differentially expressed by Cuffdiff (Cuff), edgeR, and DESeq2 between the (a – b) decidua and the inner myometrium, (c – d) decidua and the outer myometrium, and (e – f) between the inner and outer myometrial layers. Agglomerative hierarchical clustering was used to identify the relationships among the decidua (dec), inner (inn) circular myometrium (myo), and outer longitudinal myometrium (out). The tissues and gene transcripts were represented by the columns and rows, respectively.

7.4.2 GD20

On GD20, differential expression analysis using three methods identified varying numbers of gene transcripts. As regards the decidua in comparison to the inner myometrium, Cuffdiff identified 600 differentially expressed gene transcripts while edgeR and DESeq2 identified 32 and 48 differentially expressed (DE) gene transcripts, respectively. While there were no significantly DE gene transcripts in common between edgeR and DESeq2, 22 gene transcripts were found in both the Cuffdiff and DESeq2 sets of DE gene transcripts, and 12 in the Cuffdiff as well as the edgeR set of differentially expressed gene transcripts (Figure 7.16a).

Of the 34 common DE gene transcripts, approximately 68% were upregulated in the inner myometrium (Table D.4). Comparison between the decidua and the outer myometrium yielded 443 (Cuffdiff), 882 (edgeR), and 213 (DESeq2) DE gene transcripts (Figure 7.16c). A set of 232 DE gene transcripts was identified by at least two of the three methods, and 68% of them were upregulated in the outer myometrium (Table D.5). The myometrial layers had 154, 41 and 98 differentially expressed gene transcripts between them identified by Cuffdiff, edgeR and DESeq2, respectively (Figure 7.16e). Thirty-eight DE gene transcripts were identified by at least two methods, with 66% of them being upregulated in the outer myometrium as shown in Table 7.4.

Table 7.4: Genes that were differentially expressed in the outer myometrium compared to the inner myometrium on GD20. Transcript expression levels are shown in transcripts per million values (mean±SD).

		Inner		Outer	
Gene symbol	Gene name	TPM	±SD	TPM	±SD
Upregulated in outer myometrium					
Krt17	keratin 17	0.01	0.01	31.54	29.38
LOC304131	similar to C21ORF7	0.03	0.05	3.90	2.70
Cldn15	claudin 15	0.00	0.00	2.39	1.15
Mal	mal, T-cell differentiation protein	0.06	0.05	4.86	3.76
Spc25	SPC25, NDC80 kinetochore complex component	0.01	0.02	3.67	1.85
Clec1b	C-type lectin domain family 1, member B	0.41	0.72	9.81	4.12
Tbx20	T-box 20	0.01	0.01	2.76	2.15

Continued on next page

Table 7.4 – continued from previous page

		Inner		Outer	
Gene symbol	Gene name	TPM	±SD	TPM	±SD
Nrgn	neurogranin	3.56	2.74	17.36	10.33
Troap	trophinin associated protein	0.00	0.00	5.95	0.96
Msln	mesothelin	0.11	0.20	85.93	46.24
Pkhd1l1	polycystic kidney and hepatic disease 1-like 1	0.06	0.05	7.73	5.84
Clic3	chloride intracellular channel 3	0.06	0.10	36.05	28.16
Alox15	arachidonate 15-lipoxygenase	0.36	0.33	14.83	8.44
Gpr39	G protein-coupled receptor 39	0.28	0.26	9.37	10.06
F2rl2	coagulation factor II (thrombin) receptor-like 2	0.27	0.17	6.30	3.45
Sgcd	sarcoglycan, delta (dystrophin-associated glycoprotein)	0.32	0.46	16.96	10.50
Stmn4	stathmin-like 4	0.07	0.07	9.56	4.83
Bnc1	basonuclin 1	0.40	0.27	2.53	1.05
Kcng1	potassium voltage-gated channel, subfamily G, member 1	0.02	0.03	4.39	1.66
Fgf18	fibroblast growth factor 18	0.00	0.00	6.27	7.39
Krt13	keratin 13	0.00	0.00	15.56	12.22
Slc51a	solute carrier family 51, alpha subunit	0.01	0.02	5.79	3.84
G0s2	G0/G1switch 2	1.41	2.38	13.00	2.59
Vegfc	vascular endothelial growth factor C	0.00	0.01	5.24	2.71
Col14a1	collagen, type XIV, alpha 1	0.51	0.09	36.36	29.16
Down-regulated in outer myometrium					
Prl7a4	prolactin family 7, subfamily a, member 4	615.67	1059.81	0.00	0.00
Prl8a2	prolactin family 8, subfamily a, member 2	1143.72	1959.30	3.19	2.34
Prl3a1	Prolactin family 3, subfamily a, member 1	47.32	77.57	0.00	0.00
Htr1d	5-hydroxytryptamine (serotonin) receptor 1D, G protein-coupled	19.98	33.10	0.00	0.00
LOC171573	spleen protein 1 precursor	420.99	704.37	4.43	4.96
Dmrtc1c	DMRT-like family C1c	24.73	42.72	0.00	0.00
Kit	v-kit Hardy-Zuckerman 4 feline sarcoma viral oncogene homolog	22.02	17.80	2.72	1.07
Fhod1	formin homology 2 domain containing 1	47.92	38.98	10.60	5.52
Mthfd2	methylenetetrahydrofolate dehydrogenase (NADP+ dependent) 2, methenyltetrahydrofolate cyclohydrolase	40.92	35.76	7.10	0.63
Grhl2	grainyhead-like 2 (Drosophila)	19.06	14.90	2.15	1.90
Slc11a2	solute carrier family 11, member 2	58.61	48.83	11.87	3.80
Fbxl12	F-box and leucine-rich repeat protein 12	34.71	25.31	6.65	0.69
Esrrg	estrogen-related receptor gamma	17.58	16.18	0.62	0.21

Clustering analysis of the gene transcripts that were differentially expressed between the decidua and the inner myometrium (Figure 7.16b), however, did not group all the tissue replicates together. As with the case in which the decidua was compared to the inner

myometrium, clustering analysis of the gene transcripts that were differentially expressed between the decidua and the outer myometrium (Figure 7.16d) did not separate the tissues into distinct groups either. In addition, clustering analysis of the DE gene transcripts between the myometrial layers did not group the tissues appropriately (Figure 7.16f).

7.4.3 GD22(NL)

At term, gene transcripts that were differentially expressed between uterine tissues were identified using three methods as listed in Table 7.5.

Table 7.5: Genes that were differentially expressed in non-labouring samples at term. Differentially expressed genes between decidua, inner myometrium and outer myometrium were identified using Cuffdiff, edgeR and DESeq2. A significance level of 5% as well as a multiple testing correction threshold of 5% was applied in all cases.

	Differential Analysis Method			Identified by at
Comparison between:	Cuffdiff	DESeq2	edgeR	least 2 methods
decidua & inner myometrium	195	51	307	136
decidua & outer myometrium	443	213	882	434
inner myometrium & outer myometrium	301	117	393	187

When compared to the decidua, 195 (Cuffdiff), 307 (edgeR), and 51 (DESeq2) gene transcripts were differentially expressed in the inner myometrium at term in non-labouring, GD22(NL), samples. A set of 136 gene transcripts, that were identified by at least two methods, was considered to be the final set of DE gene transcripts between the decidua and the inner myometrium. Of the 136 DE gene transcripts, 53% were upregulated in the inner myometrium (Table D.6). In the outer myometrium, 434 gene transcripts were differentially expressed compared to the decidua, and of these gene transcripts 77% were upregulated (Table D.7), while 187 gene transcripts were differentially expressed compared to the inner myometrium, 93% of which were upregulated (Table D.8).

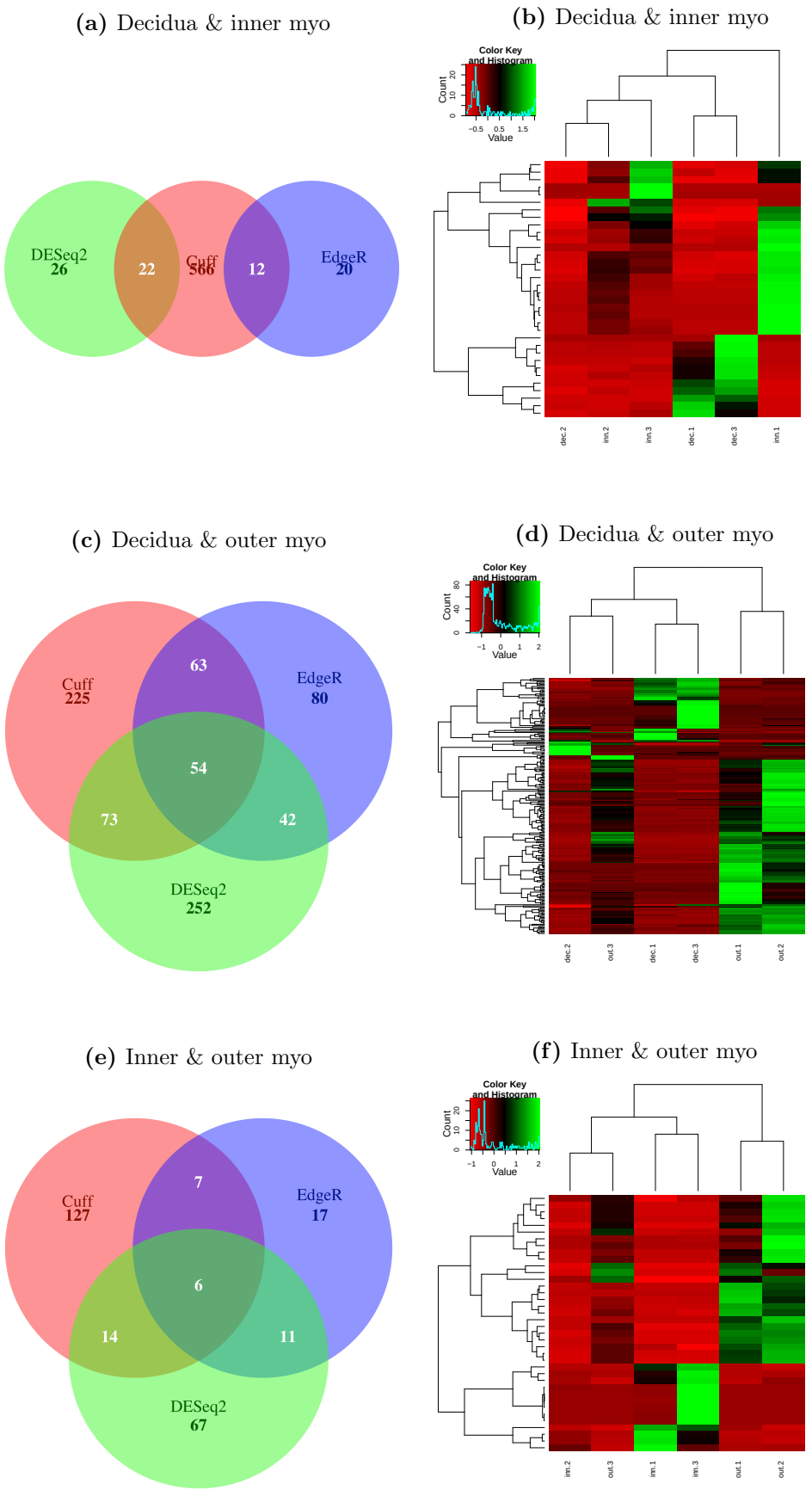

Figure 7.16: Comparisons of differentially expressed gene transcripts on GD20. Gene transcripts were identified as differentially expressed by Cuffdiff (Cuff), edgeR, and DESeq2 between the (a – b) decidua and the inner myometrium, (c – d) decidua and the outer myometrium, and (e – f) between the inner and outer myometrial layers. Agglomerative hierarchical clustering was used to identify the relationships among the decidua (dec), inner (inn) circular myometrium (myo), and outer longitudinal myometrium (out). The tissues and gene transcripts were represented by the columns and rows, respectively.

7.4.4 GD22(L)

In labouring samples, gene transcripts that were differentially expressed between uterine tissues were identified using Cuffdiff, edgeR and DESeq2. The numbers of the DE gene transcripts are listed in Table 7.6.

Table 7.6: Genes that were differentially expressed in labouring samples at term. Differentially expressed genes between decidua, inner myometrium and outer myometrium were identified using Cuffdiff, edgeR and DESeq2. A significance level of 5% as well as a multiple testing correction threshold of 5% was applied in all cases.

	Differential Analysis Method			Identified by at least 2 methods
Comparison between:	Cuffdiff	DESeq2	edgeR	
decidua & inner myometrium	260	21	67	35
decidua & outer myometrium	291	57	103	53
inner myometrium & outer myometrium	125	5	53	27

Between the decidua and the inner myometrium, 35 gene transcripts were differentially expressed, and 26% of them were upregulated in the inner myometrium (see Table D.9). Of the 53 gene transcripts that were differentially expressed in the outer myometrium in comparison to the decidua, 64% were upregulated in the outer myometrium (see Table D.10). Almost all the 27 gene transcripts that were differentially expressed by between the myometrial layers were upregulated in the outer myometrium, with only two of the genes down-regulated (see Table D.11).

7.5 Gestational Changes in Transcript Abundance

The analysis of the differential expression patterns of gene transcripts between consecutive time points in control tissues was conducted using three methods; Cuffdiff, edgeR, and DESeq2 as described in Section 6.2.2. If the associated p-value of a transcript, after multiple testing correction, was less than the predefined threshold of 5%, that transcript was classified as differentially expressed by each of the methods. A final set of transcripts com-

posed of those transcripts identified by at least two of the three methods, was considered to be the bona fide set of differentially expressed transcripts. These sets of differentially expressed transcripts were used for the analysis presented in this section. The numbers of the gene transcripts that were considered significantly different between consecutive time points within uterine tissues are shown in the graph in Figure 7.17.

7.5.1 Decidua

In the decidua, the number of transcripts that were differentially expressed between consecutive time points increased towards term. There was a 5-fold increase from the period GD19+6hrs – GD20, to the period GD20 – GD22(NL), followed by a 2.5-fold increase in the period GD22(NL) – GD22(L). Of the transcripts that were differentially expressed between GD19+6hrs and GD20, 67% were upregulated as shown in Table 7.7. Less than a third of the transcripts that were differentially expressed between GD20 and GD22(NL) were upregulated (see Table D.12), while the majority (91%) of the transcripts that were differentially

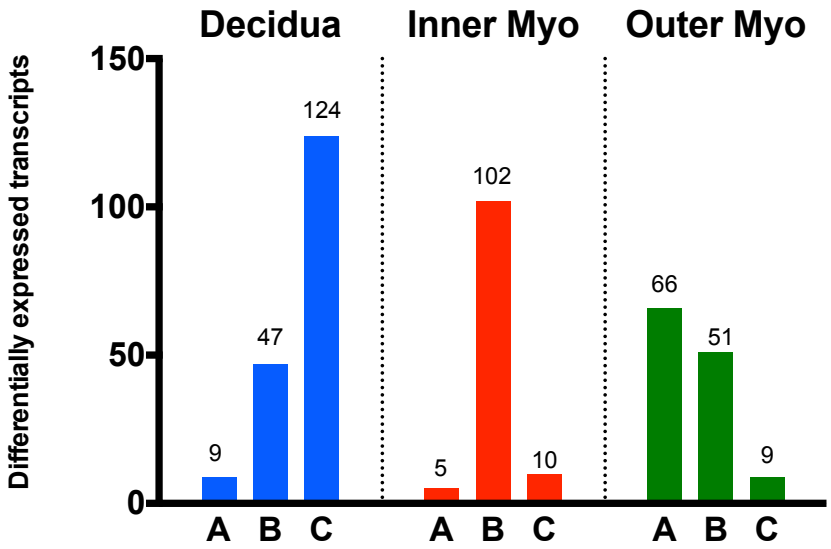

Figure 7.17: Number of genes whose transcripts were differentially expressed between consecutive time points. Number of genes differentially expressed between **A**: GD19+6hrs & GD20, **B**: GD20 & GD22(NL), and **C**: GD22(NL) & GD22(L).

expressed during labour were upregulated (see Supplementary Table D.13).

Table 7.7: Gene transcripts that were differentially expressed in the decidua, between GD19+6hrs and GD20. Transcript expression levels are shown in transcripts per million (TPM) values (mean±SD).

		GD19+6hrs		GD20	
Gene symbol	Gene name	TPM	±SD	TPM	±SD
Upregulated on GD 20					
Fhl1	four and a half LIM domains 1	16.88	13.42	237.56	380.03
Hrsp12	heat-responsive protein 12	8.70	8.48	66.77	43.98
Klk8	kallikrein related-peptidase 8	0.24	0.42	35.05	60.72
Myf6	myogenic factor 6	0.01	0.01	23.79	41.20
Serpinb12	serpin peptidase inhibitor, clade B (ovalbumin), member 12	0.00	0.00	20.63	35.71
Defa	defensin alpha	0.00	0.00	8.08	13.99
Down-regulated on GD 20					
B4galnt3	beta-1,4-N-acetyl-galactosaminyl transferase 3	9.43	5.75	0.03	0.06
Mybpc3	myosin binding protein C, cardiac	9.94	2.49	0.06	0.10
Iffo2	intermediate filament family orphan 2	11.42	4.14	0.11	0.20

7.5.2 Inner Myometrium

Instead of a pure increase or decrease, there was a bi-phasic change in the number of differentially expressed mRNA transcripts in the inner myometrium. The number of differentially expressed transcripts between consecutive time points in the inner myometrium rose between GD20 and GD22(NL), then fell between GD22(NL) and GD22(L). Of the transcripts that were differentially expressed between GD19+6hrs and GD20, three were upregulated as shown in Table 7.8. The greatest change in the expression pattern of transcripts in the inner myometrium occurred between GD20 and GD22(NL), where the number of differentially expressed transcripts rose to 102, 43% of which were upregulated (see Table D.14 for more details). Once labour commenced, the number of differentially expressed transcripts dropped to 10, with 60% of them being upregulated. Details of the gene transcripts are given in Table D.15.

Table 7.8: Gene transcripts that were differentially expressed in the inner circular myometrial layer, between GD19+6hrs and GD20. Transcript expression levels are shown in transcripts per million (TPM) values (mean±SD).

		GD19+6hrs		GD20	
Gene symbol	Gene name	TPM	±SD	TPM	±SD
Upregulated on GD 20					
Prl3a1	Prolactin family 3, subfamily a, member 1	0.08	0.15	47.32	77.57
Tmem37	transmembrane protein 37	22.56	10.44	65.21	31.84
Ascc1	activating signal cointegrator 1 complex subunit 1	5.04	1.17	36.51	23.90
Down-regulated on GD 20					
Inmt	indolethylamine N-methyltransferase	8.25	1.30	0.00	0.00
Col14a1	collagen, type XIV, alpha 1	13.78	5.92	0.51	0.09

7.5.3 Outer Myometrium

The opposite of the pattern observed in the decidua was observed in the outer myometrium, with the number of differentially expressed transcripts decreasing towards term. Between GD19+6hrs and GD20, there were 66 differentially expressed transcripts, while there were 51 and 9 transcripts differentially expressed between GD20 and GD22(NL), and between GD22(NL) and GD 20 (L), respectively. Of the transcripts that were differentially expressed between GD19+6hrs and GD20, 71% were upregulated, while 53% and 33% of the differentially expressed transcripts were upregulated on GD22(NL) and GD22(L), respectively, when compared to the preceding time point. The lists of gene transcripts whose expression patterns changed significantly in the outer layer of the myometrium with the progression of pregnancy are given in Table D.16, Table D.17, and Table 7.9, for changes occurring between GD19+6hrs and GD20, GD20 and GD22(NL), and GD22(NL) and GD22(L), respectively.

Table 7.9: Gene transcripts that were differentially expressed in the outer myometrium, between GD22(NL) and GD22(L). Transcript expression levels are shown in transcripts per million (TPM) values (mean±SD).

		GD22(NL)		GD22(L)	
Gene symbol	Gene name	TPM	±SD	TPM	±SD
Upregulated on GD22(L)					
Ano7	anoctamin 7	0.02	0.03	8.19	11.16
Prap1	proline-rich acidic protein 1	0.01	0.01	23.03	32.57
Tac1	tachykinin, precursor 1	0.00	0.00	13.35	17.54

Continued on next page

Table 7.9 – continued from previous page

Gene symbol	Gene name	GD22(NL) TPM	GD22(NL) ±SD	GD22(L) TPM	GD22(L) ±SD
Down-regulated on GD22(L)					
Np4	defensin NP-4 precursor	106.03	165.90	0.58	0.00
Mpo	myeloperoxidase	25.10	43.48	0.00	0.00
Clic3	chloride intracellular channel 3	15.03	7.96	0.00	0.00
Epx	eosinophil peroxidase	8.26	13.38	0.04	0.06
Slc22a2	solute carrier family 22 (organic cation transporter), member 2	7.63	11.10	0.06	0.03
C9	complement component 9	5.34	8.19	0.09	0.02

7.6 Summary and Discussion

Previous studies of the uterine transcriptome have provided a wealth of information on the molecular processes occurring in uterine tissues during late pregnancy and labour (Girotti & Zingg, 2003; Salomonis et al., 2005; Arthur et al., 2008; Helguera et al., 2009). Most of these studies, however, used samples that contained both endometrial and myometrial layers (Girotti & Zingg, 2003; Arthur et al., 2008), or homogenised myometrial layers (Salomonis et al., 2005; Helguera et al., 2009). In addition to indistinct tissue samples, these studies employed methods microarray or qRT-PCR in the measurement of mRNA expression. As such, to enable better understanding of uterine transcriptome within distinct layers of the myometrium, the present study employed laser-capture microdissection (LCM), a technique that enables the collection of homogeneous tissue, or individual cells, from heterogeneous tissues (Murray, 2008). While this improves the specificity with which analyses in complex tissues may be conducted, great care is required to maintain the integrity of the nucleic acids, particularly RNA, within samples (Clément-Ziza et al., 2008). To minimise the degradation of RNA during the LCM process, staining for LCM tissues was conducted using stains dissolved in ethanol. A combination of eosin yellow and cresyl violet enabled the distinction of cell types while reducing degradation of RNA during LCM. In addition

to using ethanol, tissues were stored at $-80°C$ or kept on dry ice when not in use. It is, therefore, feasible to obtain RNA of good quality from LCM tissues, provided that the tissue stains are prepared in a solvent that dehydrates the tissue, such as ethanol, and the tissue samples are maintained at suitable temperatures.

7.6.1 Why Bother with RNAseq?

In order to improve the accuracy of the measurement of mRNA transcript abundance, and to detect even those transcripts whose expression is low, a "next-generation" sequencing technique RNAseq was used to measure the expression of gene transcripts within LCM tissues in the present study. While microarray technology may be used to generate transcriptomic data, it has some weaknesses that are overcome by RNAseq. The main disadvantage of microarrays is that they require that a set of nucleotide sequences be known prior to measuring the abundance of transcripts within tissues, which is not always possible as some experiments are exploratory. Combining the known set of nucleotides with the RNA extracted from samples, a process called hybridisation, which is required when conducting microarray studies, may introduce biases that reduce the sensitivity of the technique (Baginsky et al., 2010). In addition, high numbers of biological replicates are required in order to correctly measure the variability within biological replicates and identify differentially expressed genes with microarrays (Pan et al., 2002; Churchill, 2002). While being relatively expensive in comparison to microarrays, RNAseq does not require prior knowledge of nucleotide sequences. As such, biases introduced due to hybridisation are avoided through the use of RNAseq. In addition, using RNAseq enables the concurrent exploration of an entire transcriptome and measuring of gene expression, which allows the identification of novel transcripts (Mortazavi et al., 2008). Furthermore, it is possible to identify differentially expressed genes while using low numbers of biological replicates, e.g., $n = 2$ or $n = 3$, with RNAseq (Robinson et al., 2010). A recent study by Schurch et al. (2015), however,

suggests that at least 20 biological replicates are required for RNAseq studies in order to achieve a true positive rate of 85%.

To counteract the possibility of incorrectly classifying a gene as differentially expressed, the work presented in this thesis utilised three differential expression analysis methods, and a gene was considered differentially expressed only if it had been identified as such by at least two of the methods. While this approach reduced the numbers of false positives, some gene transcripts that were differentially expressed may have been ignored.

7.6.2 Can these Data be Trusted?

While only good-quality RNA was used in the preparation of sequencing libraries, the estimated transcript abundances in transcripts per million (TPM) showed great variability among biological replicates. While differences in mRNA expression among biological replicates may be attributed to the inherent biological differences among individuals, the biological variability among similarly housed and treated animals is expected to be negligible. To obtain a better picture of the variation among individuals within the same biological group, the number of replicates could be increased as suggested by Schurch et al. (2015). However, the differential expression methods employed in this thesis take the variation among individuals into account when assessing gene transcripts (Love et al., 2014). In addition, two of the three methods employed, DESeq and edgeR, have been shown to yield credible results using low numbers of biological replicates (Robinson et al., 2010). While increasing biological replicates may improve the accuracy with which distinction may be made between treatment groups, the results presented in this thesis can be considered to be credible.

7.6.3 Tissue Specific Expression

A possible decidual marker in late pregnancy was identified in Section 7.2. The gene transcripts encoding thyrotropin releasing hormone (Trh) were predominantly expressed in the decidua across the four study time-points. Immunohistochemical staining for the Trh protein showed the localisation of Trh mainly in the decidua. Trh is known to stimulate the release of prolactin, a known decidual marker, by the pituitary (Molitch, 2009).

A gene transcript that could be used to distinguish the inner myometrium from the outer myometrium is the tenascin n (Tnn) gene transcript. Expression of Tnn was distinctly lower in the outer myometrium in comparison to the inner myometrium at both the mRNA and protein levels. Tenascin proteins are extracellular glycoproteins, which are known to be expressed in the cervix (Mahendroo, 2012), skeletal tissue (Alford & Hankenson, 2006), proliferating endometrial cells during the menstrual cycle in humans (Jabbour et al., 2006), as well as in developing tissues (Neidhardt et al., 2003; Hsia & Schwarzbauer, 2005). There are six known tenascin proteins; tenascin c, tenascin x, tenascin w, tenascin r, tenascin y, tenascin r, and Tnn. Although Kida et al. (1997) observed changes in the uterine expression of tenascin in early pregnancy, it is not clear which of the tenascin proteins was observed. Thus it is proposed in the present study that Tnn is expressed in the decidual and myometrial layers of the late-pregnant rat uterus, and that it is predominantly expressed in the inner circular layer of the myometrium.

7.6.4 Spatial Gene Expression

For the first time, the spatial expression of gene transcripts was assessed and documented in the present study. In addition, differences in the spatial expression of gene transcripts between the myometrial layers were identified at all four time-points. The data presented in Section 7.2 and Section 7.4 indicate that the transcriptional landscape of the inner my-

ometrium differs significantly from that of the outer myometrium. These observations will enrich current knowledge of the molecular processes occurring within uterine tissues.

7.6.5 Changes Occurring Towards Term

The pattern of differential expression illustrated in Figure 7.17 suggests that the uterus begins preparing for labour in the outer layer of the myometrium followed by the inner myometrium. This would suggest that the signal to prepare for labour emanates from within the uterus itself, the outer layer in particular, and travels to the inner layer of the myometrium.

The onset of labour coincides with the significant upregulation of mRNA transcript expression in the decidua. The gene transcripts upregulated in the decidua encode the following proteins among others: the voltage-dependent L type calcium channel α 1S subunit (Cacna1s), which is a component of channels through which extracellular Ca^{2+} enters the cell; gap junction proteins (Gjc2), which increase cell-to-cell coupling; glycoproteins (Psg16, Psg19, and Psg21); apolipoproteins (Apoa2, Apoh, and Apom); solute carriers (Slc1a2, Slc2a2, Scl32a1, and Slc7a9); members of the prolactin family (Prl3a1, Prl3b1, Prl3c1,Prl7a4, and Prl8a4); cyclin dependent kinase (Cdk5r2); and phosphatases (Ptn5). Gjc2 is expressed in the brain and spinal cord (Molica et al., 2014), the mutation of which is associated with Pelizaues-Merzbacher-like disease and lymphedema (Molica et al., 2014) While gap junction proteins are known to increase at term and during labour in the myometrium (Garfield & Maner, 2007), the role of Gjc2 has not been previously described in the uterus. As such, its role during parturition has not been described. Apolipoproteins are involved in transporting lipoproteins that are used in the synthesis of steroid hormones (Schreiber et al., 1985). While some of apolipoproteins are associated with the onset of labour in humans (Yuan et al., 2012), their role during labour has not been charac-

terised.

7.6.6 Extracellular Matrix Remodelling

The up-regulation of proteins involved in tissue remodelling is expected at term or during labour. Matrix metalloproteinases (Mmps) are involved in the degradation of proteins within the extracellular matrix which lead to the rupture of fetal membranes (Epstein et al., 1998). In the present study, Mmp11 and Mmp12 mRNA transcript were significantly upregulated in the inner myometrium at term, while Mmp7 and Mmp9 mRNA levels were significantly upregulated in the outer myometrium during labour. Previously, Mmp7 (Girotti & Zingg, 2003) and Mmp9 (Chan et al., 2014) expression was found to increase during labour in the myometrium. The data presented in this study, therefore, are consistent with published literature. In addition, the observations made in the current study indicate that the Mmps involved in the remodelling of the extracellular matrix during labour, are synthesised in the outer myometrium.

7.6.7 Channels and Transporters

Potassium (K^+) channels are involved in regulating the contractility of SMCs during pregnancy (Wray et al., 2014). In the present study, K^+ voltage-gated channel subfamily G member 1 (Kcng1) mRNA levels were upregulated in the outer myometrium on GD20, an observation which is in direct contrast to that of Soloff et al. (2011) who observed the upregulation of Kcng1 mRNA following treatment of human myometrial cells with P4 in culture. Also significantly upregulated in the outer myometrium on GD20 were mRNA transcripts encoding hyperpolarisation-activated cyclic nucleotide-gated K^+ channel 4 (Hcn4), which is associated with ventricular myocyte hypertrophy (Lin et al., 2009a). Pregnancy is associated with myometrial growth as a result of the hypertrophy of uterine smooth muscle

cells (SMCs) (Shynlova et al., 2010). The upregulation of Hcn4 in the outer myometrium, therefore, is in line with observations made in the heart. At term, large conductance Ca^{2+}-activated K^+ channel subfamily M β member 1 (Kcnmb1) mRNA expression was significantly down-regulated in the outer myometrium. The Ca^{2+}-activated K^+ (BK) channels, of which Kcnmb1 is a component, are expressed in myometrial SMCs where the protein and mRNA expression levels are down-regulated during labour (Song et al., 1999; Matharoo-Ball, 2002). The data presented in this chapter are in agreement with these findings.

Expression levels of mRNA transcripts encoding various solute carriers changed significantly with the progression of pregnancy. Solute carrier family 51 α subunit (Slc51a) mRNA levels were upregulated in outer myometrium on GD20 in comparison to GD19+6hrs. While that of solute carrier family 22 (organic cation transporter) member 2 (Slc22a2) mRNA decreased significantly during the same period in the outer myometrium. The genes whose transcripts encode solute carrier family 17 member 3 (Slc17a3), solute carrier family 17 member 4 (Slc17a4), solute carrier family 1 (neutral amino acid transporter), member 5 (Slc1a5),solute carrier family 4 member 1 (Slc4a1), solute carrier family 34 member 2 (Slc34a2), and solute carrier family 5 (sodium/myo-inositol co-transporter), member 3 (Slc5a3) were down-regulated in the inner myometrium at term. In contrast with observations made on GD20, Slc22a2 mRNA expression levels were significantly upregulated in the outer myometrium at term, suggesting that Slc22a2 may have a role during labour. While the level of expression of solute carrier family 2 (facilitated glucose transporter), member 4 (Slc2a4) and solute carrier family 48 (heme transporter), member 1 (Slc48a1) mRNA were reduced significantly in the outer myometrium at term. Previously, Slc1a5 has been shown to be upregulated in the myometrium during pregnancy in comparison to non-pregnant human myometrial samples (Rehman, 2003). In addition, Jeong (2005) observed the down-regulation of the gene encoding Slc1a5 in uterine tissues following P4-treatment. The down-regulation of Slc1a5 at term appears to contradict these findings.

7.6.8 G Protein-coupled Receptors

G protein-coupled receptors (GPCRs) are cell-surface receptors that mediate the effects of numerous signalling molecules such as growth factors, hormones, and neurotransmitters through G-proteins, which are composed of three subunits; $\alpha, \beta,$ and γ, that are attached to the receptors inside the cell. (Gimpl & Fahrenholz, 2001). Activation of GPCRs such as the oxytocin receptor (OTR) leads to an increase in intracellular Ca^{2+}, which is favourable for contraction of SMCs. In the present study, mRNA transcripts encoding G protein-coupled 5-hydroxytryptamine (serotonin) receptor 2A (Htr2a), and G protein-coupled 5-hydroxytryptamine (serotonin) receptor 4 (Htr4) were upregulated in the inner myometrium, while G protein-coupled 5-hydroxytryptamine (serotonin) receptor 1D (Htr1d) mRNA levels were upregulated in both the inner and outer myometrium at term. Serotonin is known to stimulate contraction of SMCs through the action of Gq-coupled 5-hydroxytryptamine receptors, the expression of which is upregulated in late pregnancy (Cohen et al., 1985; Minosyan et al., 2007). The data presented in this study are consistent with published literature. In addition, only Htr1d is upregulated in the outer myometrium at term as opposed to the inner myometrium in which Htr1d, Htr2a, and Htr4 were upregulated, indicating that the contractility of the two myometrial layers may be mediated by different receptors. Significant upregulation of serotonin receptor mRNA indicates that OTR signalling is not the only GPCR that can mediate uterine SMC contraction. In fact, Nishimori et al. (1996) observed normal labour in OTR knock-out mice. In contrast to the upregulation of mRNA encoding serotonin receptors, mRNA encoding cannabinoid receptor 1 (Cnr1) were down-regulated in the outer myometrium at term. Cnr1, which is coupled to $G\alpha_{i/o}$, inhibits adenylyl cyclase, thus increasing K^+ conductance and decreasing Ca^{2+} conductance (Childers & Deadwyler, 1996). The down-regulation of Cnr1 mRNA, therefore, leads to an increase Ca^{2+} conductance and a decrease in K^+ conductance, thus facilitating the entry of extracellular Ca^{2+} into SMCs leading to contractions.

7.6.9 Inflammatory Response

During gestation, the expression of pro-inflammatory genes is suppressed while anti-inflammatory gene expression is elevated. During labour, the tables are turned and the expression of pro-inflammatory genes is upregulated while that of anti-inflammatory genes is down-regulated (Stephen et al., 2014). The data presented in the present thesis demonstrate the down-regulation of anti-inflammatory genes; coagulation factor V (F5) and colony stimulating factor 1 (Csf1) in the inner myometrium, and Bradykinin receptor B1 (Bdkrb1) in the outer myometrium at term. The upregulation of pro-inflammatory gene transcripts; interleukin 1 receptor-like 1 in the decidua and interleukin 33 in the inner myometrium, at term was also observed.

7.7 Conclusion

This chapter set out to study the transcriptional changes occurring in rat uterine tissues following the systemic withdrawal of P4 on GD19 so as: to document the whole transcriptome of the decidua, the inner myometrium, and the outer myometrium in late pregnancy and at term; and establish the temporal expression patterns of gene transcripts across four gestational time-points. To aid the separation of homogeneous decidual, inner myometrial, and outer myometrial tissues from uterine horns, laser-capture microdissection was employed. RNA of good quality was successfully extracted from laser-captured tissue samples and used to prepare sequencing libraries. Sequencing data, consisting of reads that were 51 be in length, were assessed for bias and aligned to the reference genome. The estimated abundance of transcripts within the uterine tissues were documented and assessed for spatial and temporal differences. In addition to the identification of the spatio-temporal changes occurring in the respective myometrial tissues, a protein that may be used to distinguish the inner layer of the myometrium from the outer layer of the myometrium in late pregnancy

was identified.

The strength of the current study is in the use of two powerful techniques to interrogate the transcriptomic changes occurring in uterine tissues in late pregnancy and during labour. To the author's knowledge, this is the first time that pure decidual, inner myometrial, and outer myometrial tissues have been separated and analysed, not just for temporal changes, but also for spatial differences in the expression of gene transcripts. This study has laid the foundation for identification of other changes, such as differential splicing, in response to the systemic withdrawal of progesterone within uterine tissues. A possible drawback of the data presented here is the high variability among biological replicates. Increasing the number of biological replicates may better reflect the variability within groups of similarly treated tissues as opposed to $n = 2$ and $n = 3$. In conclusion, the onset of labour at term is characterised by numerous changes that still require investigation. The use of laser-capture microdissection and RNAseq has enabled the distinct separation of myometrial tissues and allowed the identification of genes whose transcripts change significantly in late pregnancy and during labour; including genes involved in immune/inflammatory response and excitation-contraction coupling of smooth muscle cells. The findings in this study will enrich the current knowledge of the transcriptomic changes associated with late gestation and labour. the following chapter describes the expression patterns of genes encoding proteins involved in the activation, as well as in the contraction, of smooth muscle.

Chapter 8

Uterine Smooth Muscle Contraction

The expression patterns of the genes that code for the proteins involved in the excitation and subsequent contraction of uterine smooth muscle cells are analysed in this chapter with the aim of elucidating their expression patterns in the inner myometrium and outer myometrium.

Transcript expression values that were estimated using Sailfish (TPM values), were used to assess the expression patterns of contraction-associated protein (CAP) gene transcripts. Tests for significant differences in gene transcript expression were conducted using the Kruskal-Wallis test with a significance level of 5%. Dunn's multiple testing correction approach was also employed at a 5% level of significance. Expression patterns of some of the CAP gene transcripts were validated using quantitative real-time PCR (qPCR).

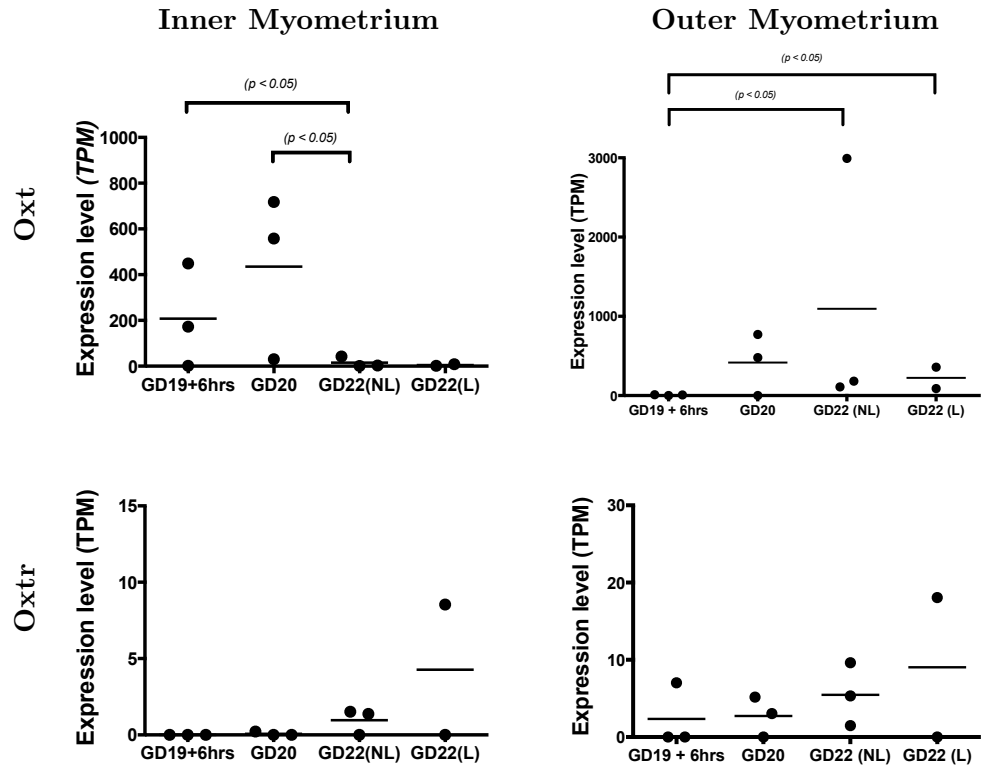

Figure 8.1: Oxytocin (Oxt) and oxytocin receptor (Oxtr) gene expression in the pregnant rat uterus. Expression levels are in transcripts per million (TPM), and the lines show the mean expression levels ±SD with n = 3 for all time points except GD22(NL) where n = 2.

8.1 Oxytocin and the Oxytocin Receptor

In the inner myometrium, the levels of Oxytocin (Oxt) increased on GD20 but dropped significantly at term and stayed low during labour as illustrated in Figure 8.1. While there was a slight decrease in Oxt expression levels during labour, Oxt expression levels were significantly higher than the Oxt levels at GD19+6hrs. In the outer myometrium, the levels of oxytocin increased significantly towards labour. Oxytocin receptor (Oxtr) levels increased gradually towards term and were at their highest during labour, in the inner myometrium (Figure 8.1). Similarly, Oxtr levels in the outer myometrium increased gradually towards term and were at their highest during labour.

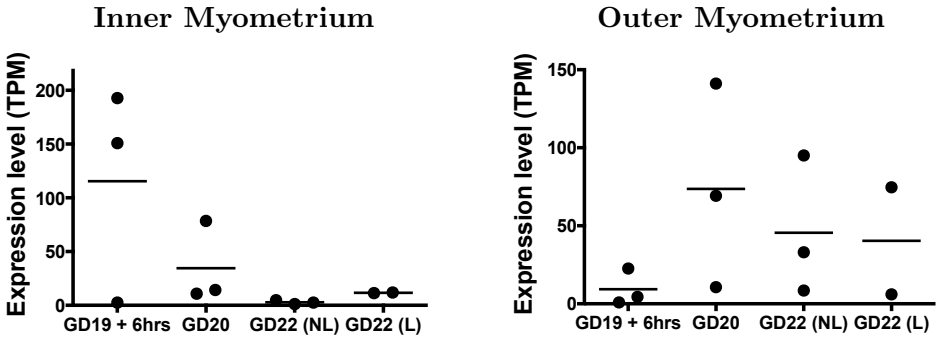

Figure 8.2: Ptgs1 mRNA transcript expression in myometrial tissues of the pregnant rat uterus. Expression levels are in transcripts per million (TPM). The horizontal bars indicate the mean expression levels. Sample size n = 3 for all time points except GD22(NL) where n = 2.

8.2 Prostaglandin-Endoperoxide Synthase mRNA Transcripts

Ptgs1 mRNA expression fell between GD19+6hrs and GD20 in the inner myometrium (Figure 8.2). There was a further drop in expression on GD22(NL) which was followed by a small increase on GD22(L). Despite the increase in expression on GD22(L), Ptgs1 expression levels were lower on GD22(L) than levels observed on GD19+6hrs. In the outer myometrium, a sharp increase in Ptgs1 mRNA levels between GD19+6hrs and GD20 preceded a slight decrease in Ptgs1 expression levels on GD22(NL), which remained unchanged on GD22(L).

Ptgs2 mRNA levels were relatively unchanged between GD19+6hrs and GD22(NL) followed by a ten-fold increase in expression on GD22(L) in the inner myometrium (Figure 8.3). The pattern of Ptgs2 expression in the outer myometrium was similar to that observed in the inner myometrium where levels of expression were relatively unchanged between GD19+6hrs and GD22(NL) followed by an increase on GD22(L).

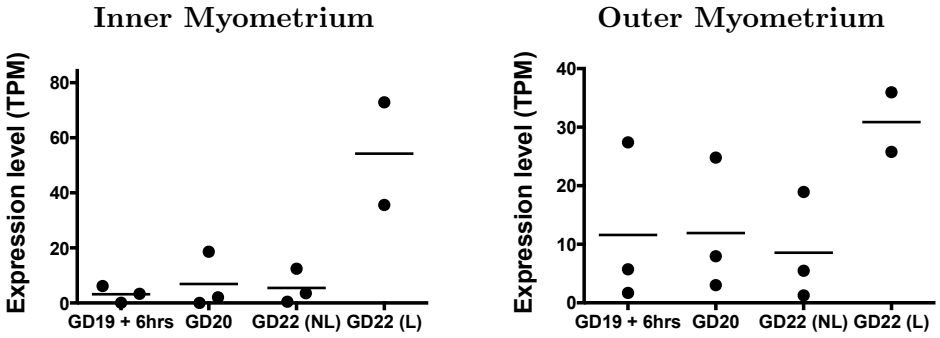

Figure 8.3: Ptgs2 mRNA transcript expression in myometrial tissues of the pregnant rat uterus. Expression levels are in transcripts per million (TPM). The horizontal bars indicate the mean expression levels. Sample size n = 3 for all time points except GD22(NL) where n = 2.

8.3 Expression of Transcripts Encoding Gap Junction Proteins

Transcripts of 17 genes that encode gap junction proteins were identified in the vehicle treated myometrial tissues. The mean (±SD) expression levels across the four gestational time points of all the mRNA transcripts encoding gap junction proteins that were expressed in myometrial tissues are summarised in Table 8.1.

Of the 17 gap junction protein-encoding genes expressed in myometrial tissues, the gene encoding Gap junction δ 4 protein (Gjd4) was only expressed in the outer myometrium at term. In both layers of the myometrium, the top five, in terms of average level of expression, expressed mRNA transcripts were for the genes encoding the proteins Gap junction α 1 (Gja1), Gap junction β 2 (Gjb2), Gap junction α 5 (Gja5), Gap junction α 4 (Gja4), and Gap junction α 7 (Gja7). The expression levels of these highly expressed transcripts are assessed further in the subsequent sections.

Table 8.1: Messenger RNA transcripts encoding gap junction proteins expressed in the inner myometrium. Transcripts are expressed in transcripts per million (TPM) values (mean±SD).

	Inner Myometrium		Outer Myometrium	
Gene	Transcripts per million	±SD	Transcripts per million	±SD
Gja1	243.16	154.99	309.86	83.71
Gjb2	230.14	186.63	198.36	124.29
Gja5	25.35	13.06	21.98	12.89
Gja4	19.64	22.70	18.76	18.20
Gja7	6.11	4.60	17.68	17.43
Gjb5	5.58	4.38	9.50	4.43
Gjb1	3.51	4.60	7.68	15.35
Gjb3	2.67	1.63	6.55	4.73
Gja3	1.75	1.29	5.75	8.67
Gjb4	1.07	0.92	4.31	4.43
Gjb6	0.71	0.45	2.28	0.40
Gja6	0.27	0.35	1.62	3.20
Gjc2	0.17	0.31	1.30	1.26
Gja10	0.10	0.16	1.31	0.88
Gjd2	0.01	0.01	0.87	0.91
Gja8	0.01	0.01	0.18	0.30
Gjd4	0.00	0.00	0.01	0.01

8.3.1 Gap junction α 1 (Gja1)

The RNAseq data indicate that there was a drop in the level of expression of Gja1, also known as connexin 43 (Cx-43), mRNA transcripts between GD19+6hrs and GD20 in the inner myometrium (Figure 8.4). This was followed by an increase at term, and a drop in transcript levels during labour. There were no significant changes in the expression of Gja1 mRNA transcripts between GD19+6hrs and GD22(L). Gja1 mRNA expression in the outer myometrium dropped slightly between GD19+6hrs and GD20, and increased at term as well as during labour. Gja1 mRNA expression levels in the outer myometrium on GD19+6hrs

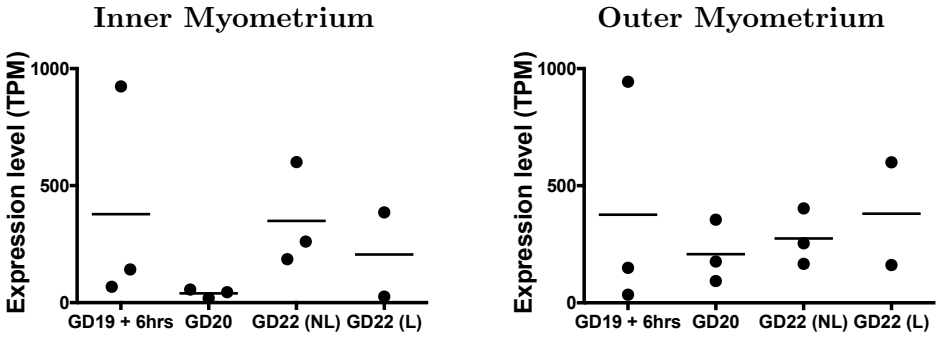

Figure 8.4: Gja1 (Cx-43) mRNA transcript expression in myometrial tissues of the pregnant rat uterus. Expression levels are in transcripts per million (TPM). The horizontal bars indicate the mean expression levels. Sample size n = 3 for all time points except GD22(NL) where n = 2.

and GD22(L) were similar, suggesting that there was negligible change in the levels of Gja1 mRNA expression between GD19+6hrs and GD22(L) as illustrated in Figure 8.4.

8.3.2 Gap junction β 2 (Gjb2)

An initial increase in Gjb2, also known as connexin 26 (Cx-26), mRNA expression between GD19+6hrs and GD20 was followed by a decrease in expression on GD22(NL) in the inner myometrium (Figure 8.5). An increase in Gjb2 mRNA during labour led to the expression levels on GD22(L) being higher than those observed on GD19+6hrs in the inner myometrium. While Gjb2 expression levels fell between GD19+6hrs and GD20 in the outer myometrium, there was no change in expression at term, but there was an increase during labour. As a result, Gjb2 mRNA levels in the outer myometrium were higher in samples obtained on GD22(L) than in samples acquired on GD19+6hrs (Figure 8.5).

8.3.3 Gap junction α 5 (Gja5)

The average expression of Gja5, also known as connexin 40 (Cx-40), in the inner myometrium was approximately a tenth of Gja1 and Gjb2 expression in the inner myometrium (Table 8.1).

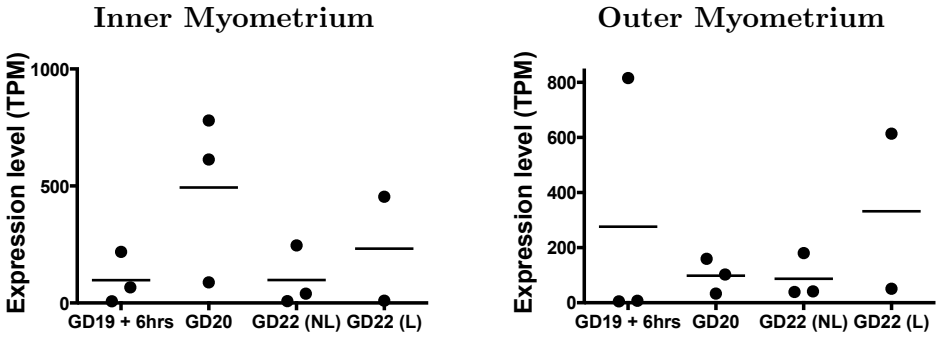

Figure 8.5: Gjb2 (Cx-26) mRNA transcript expression in myometrial tissues of the pregnant rat uterus. Expression levels are in transcripts per million (TPM). The horizontal bars indicate the mean expression levels. Sample size n = 3 for all time points except GD22(NL) where n = 2.

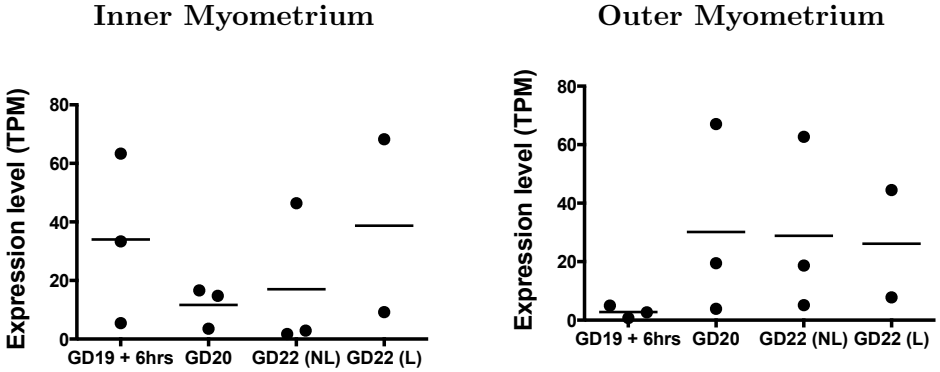

Figure 8.6: Gja5 (Cx-40) mRNA transcript expression in myometrial tissues of the pregnant rat uterus. Expression levels are in transcripts per million (TPM). The horizontal bars indicate the mean expression levels. Sample size n = 3 for all time points except GD22(NL) where n = 2.

Gja5 expression patterns in the inner myometrium were similar to those of Gja1 transcripts that were observed in the outer myometrium (see Figure 8.6 and Figure 8.4). Outer myometrium levels of Gja5 mRNA were, on average, 10% and 7% of Gjb2 and Gja1 mRNA levels in the same tissue, respectively (Table 8.1). Between GD19+6hrs and GD20 the level of Gja5 mRNA expression increased substantially and remained relatively unchanged between GD20 and GD22(L) in the outer myometrium (Figure 8.6).

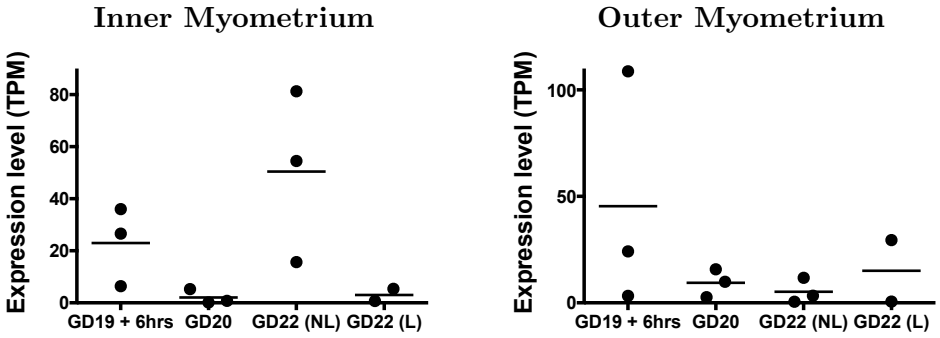

Figure 8.7: Gja4 (Cx-37) mRNA transcript expression in myometrial tissues of the pregnant rat uterus. Expression levels are in transcripts per million (TPM). The horizontal bars indicate the mean expression levels. Sample size n = 3 for all time points except GD22(NL) where n = 2.

8.3.4 Gap junction α 4 (Gja4)

Although the average level of expression of Gja4, also known as connexin-37 (Cx-37), mRNA was 8% of Gja1 mRNA expression in the inner myometrium (Table 8.1), the patterns of expression of Gja4 and Gja1 transcripts were similar as illustrated in Figure 8.7 and Figure 8.4. Gja4 mRNA levels on GD22(NL) were lower than those on GD19+6hrs. In the outer myometrium, Gja4 transcript expression fell between GD19+6hrs and GD20, and fell even further at term followed by a slight increase during labour.

8.3.5 Gap junction α 7 (Gja7)

Gja7 mRNA levels fell between GD19+6hrs and GD20, then increased on GD22(NL), and fell again on GD22(L) in the inner myometrium (Figure 8.8), a pattern of expression that was observed in the same tissue for Gja1 and Gja4 mRNA. There were more Gja7 transcripts in both the inner and outer myometrium on GD19+6hrs than on GD22(L).

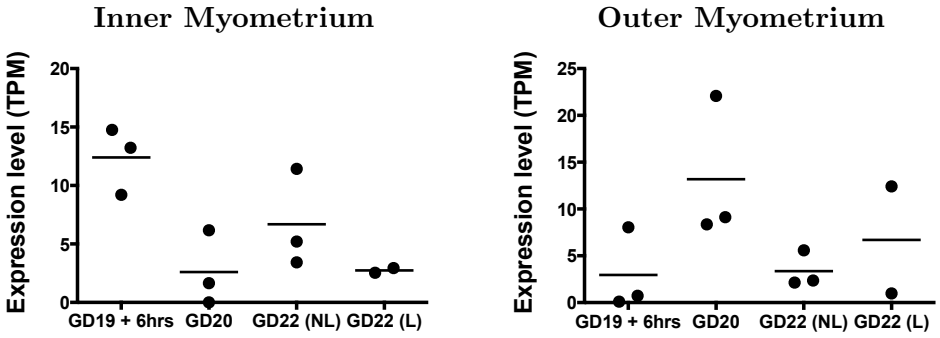

Figure 8.8: Gja7 (Cx-45) mRNA transcript expression in myometrial tissues of the pregnant rat uterus. Expression levels are in transcripts per million (TPM). The horizontal bars indicate the mean expression levels. Sample size n = 3 for all time points except GD22(NL) where n = 2.

8.3.6 Quantitative RT-PCR Experiments

Quantitative RT-PCR (qPCR) experiments were conducted for the genes encoding Oxt, Oxtr, Ptgs1, Ptgs2, Gja1, and Gja7. Data from qPCR experiments (Figure 8.9) showed an increase in relative Oxt mRNA expression throughout late gestation in the inner myometrium, while in the outer myometrium, Oxt levels decreased on GD20, then increased during labour. Validation experiments measuring expression of Oxt mRNA by qPCR showed different patterns of expression to those observed by RNAseq in the inner myometrium. In the outer myometrium however, the increase in expression detected by qPCR during labour when compared to GD19+6hrs, is consistent with RNAseq results.

The expression of Oxtr mRNA relative to Actb in the inner myometrium was undetected on GD19+6hrs and GD20, then increased remarkably at term, but dropped during labour as shown in Figure 8.10. In the outer myometrium, the relative abundance of Oxtr mRNA transcripts increased progressively in late pregnancy and reached peak levels at term. The relative expression pattern of Oxtr mRNA in the outer myometrium matched that which was observed in RNAseq experiments. In the outer myometrium, however, RNAseq and qPCR findings did not agree.

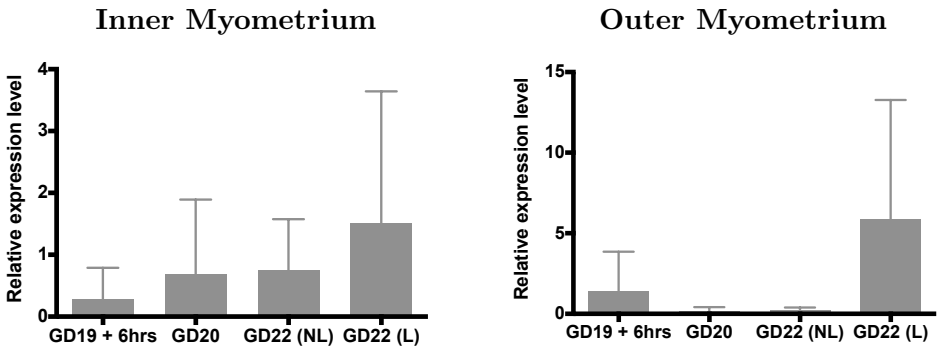

Figure 8.9: Relative abundance (mean±SD) of Oxt mRNA in myometrial tissues in the pregnant rat. Expression was normalised to the abundance of β-Actin (Actb) mRNA. Here n = 3 for all time points except GD22(NL) where n = 2.

Increases in Ptgs1 mRNA relative expression on GD20 and during labour were punctuated by a drop in expression at term (Figure 8.11). In the outer myometrium, relative expression of Ptgs1 mRNA increased throughout late pregnancy and were highest during labour. Similar to the pattern of expression observed for Ptgs1 mRNA, inner myometrial expression of Ptgs2 mRNA expression increased on GD20 then fell at term and increased during labour (Figure 8.12). During labour, Ptgs2 expression were low in comparison to Ptgs1 levels in the outer myometrium. RNAseq and qPCR results were different for both Ptgs1 and Ptgs2 in the inner and outer myometrium.

Relative expression of Gja1 mRNA peaked at term and dropped slightly during labour in the inner myometrium, while expression in the outer myometrium peaked during labour (Figure 8.13). In contrast, relative expression of Gja7 was at its lowest at term in the inner myometrium (Figure 8.14), but peaked during labour in the outer myometrium. The increase in Gja1 mRNA expression from GD20 to GD22(L), is in line with the observations that were made using RNAseq data. However, the observations in the inner myometrium for Gja1 and Gja7 mRNA, as well as for Gja7 in the outer myometrium, contradict those of RNAseq experiments.

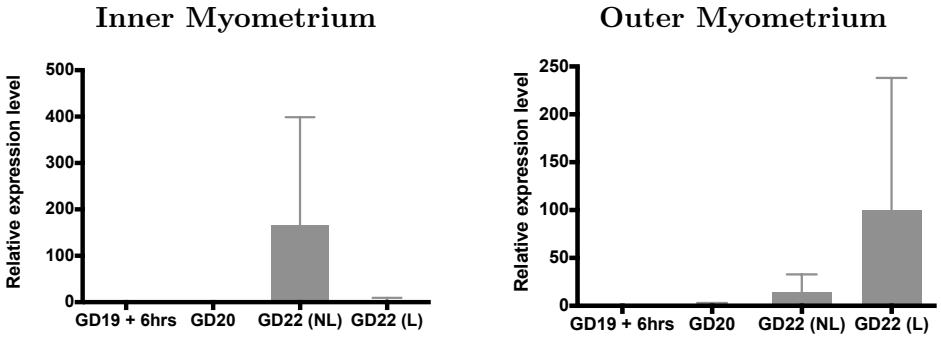

Figure 8.10: Relative abundance (mean±SD) of Oxtr mRNA in myometrial tissues in the pregnant rat. Expression was normalised to abundance of β-Actin (Actb) mRNA with n = 3 for all time points except GD22(NL) where n = 2.

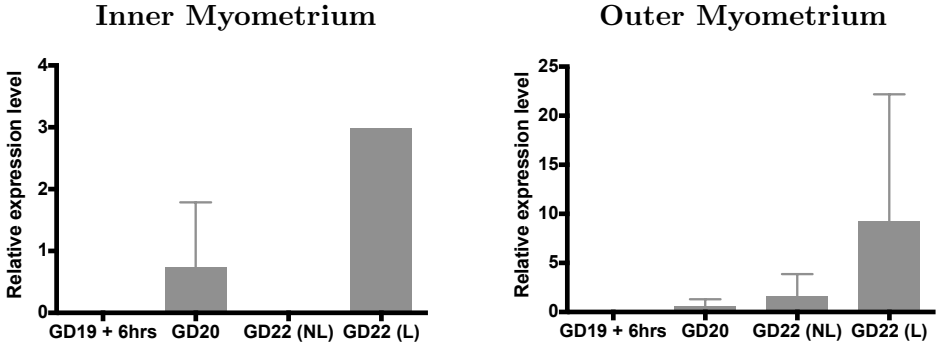

Figure 8.11: Relative abundance (mean±SD) of Ptgs1 mRNA in myometrial tissues in the pregnant rat. Expression was normalised to abundance of β-Actin (Actb) mRNA with n = 3 for all time points except GD22(NL) where n = 2.

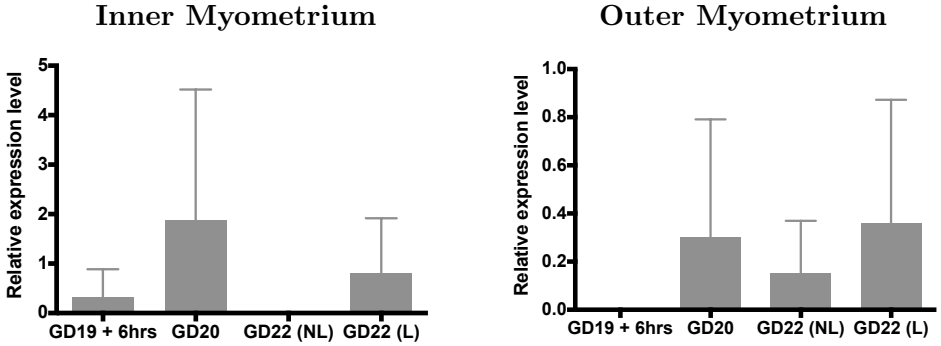

Figure 8.12: Relative abundance (mean±SD) of Ptgs2 mRNA in myometrial tissues in the pregnant rat. Expression was normalised to abundance of β-Actin (Actb) mRNA with n = 3 for all time points except GD22(NL) where n = 2.

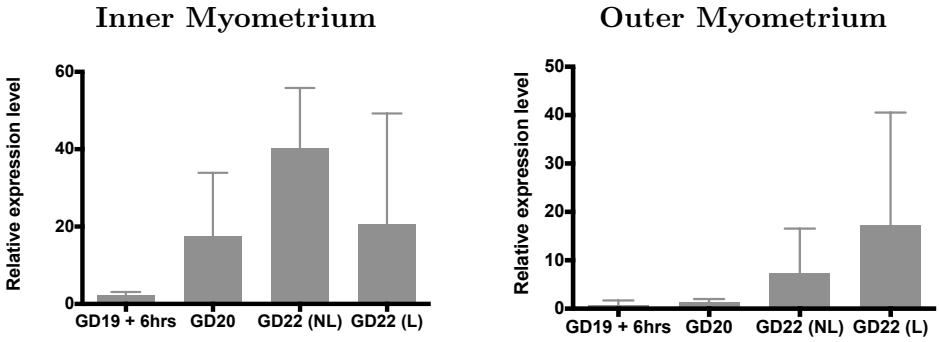

Figure 8.13: Relative abundance (mean±SD) of Gja1 mRNA in myometrial tissues in the pregnant rat. Expression was normalised to abundance of β-Actin (Actb) mRNA with n = 3 for all time points except GD22(NL) where n = 2.

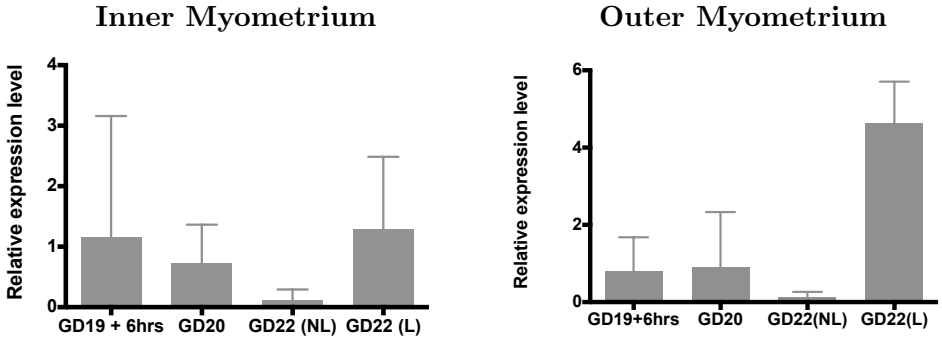

Figure 8.14: Relative abundance (mean±SD) of Gja7 mRNA in myometrial tissues in the pregnant rat. Expression was normalised to abundance of β-Actin (Actb) mRNA with n = 3 for all time points except GD22(NL) where n = 2.

8.4 Smooth Muscle Genes

The expression patterns of mRNA transcripts encoding proteins involved in the activation and contraction of smooth muscle cells, namely: Actin; Caldesmon; Calmodulin; Calponin; Myosin; Myosin light-chain kinase; and Tropomyosin were assessed in the inner and outer layers of the myometrium.

8.4.1 Actin

In the inner myometrium, actin α-2 (Acta2) mRNA expression was at its highest on GD19+6hrs then it decreased substantially on GD20 and remained relatively unchanged (Figure 8.15).

Thus, Acta2 expression levels on GD22(L) were lower than levels on GD19+6hrs in the inner myometrium. In the outer myometrium, Acta2 mRNA expression increased between GD19+6hrs and GD20. Acta2 mRNA expression levels dropped on GD22(NL) to levels that were similar to those observed on GD19+6hrs, then dropped even further on GD22(L). On GD19+6hrs, Acta2 mRNA was more abundant in the inner myometrium than the outer myometrium in contrast to the abundance observed on GD22(L).

Actin γ-2 (Actg2) mRNA levels in the inner myometrium decreased between GD19+6hrs and GD20 (Figure 8.15). This decrease was followed by a further decrease in Actg2 mRNA expression on GD22(NL) and an increase on GD22(L). The expression of Actg2 mRNA transcripts in the inner myometrium was at its peak on GD19+6hrs. In the outer myometrium, the highest level of Actg2 expression was observed on GD20 with the lowest expression level on GD22(NL). On GD19+6hrs, Actg2 mRNA expression in the inner myometrium was higher than that of the outer myometrium. On GD22(L), however, Actg2 mRNA levels were higher in the outer myometrium compared to the inner myometrium.

8.4.2 Caldesmon 1 (Cald1)

Cald1 mRNA levels in the inner myometrium decreased between GD19+6hrs and GD20 then were relatively unchanged from GD20 through to labour (Figure 8.16). In the outer myometrium, Cald1 mRNA levels increased on average (mean $\pm$ SD) from 92.93 ± 73.19 TPM to 491.70 ± 275.90 TPM between GD19+6hrs and GD20, falling to 118.00 ± 48.74 TPM at term and increasing to 227.40 ± 175.20 during labour.

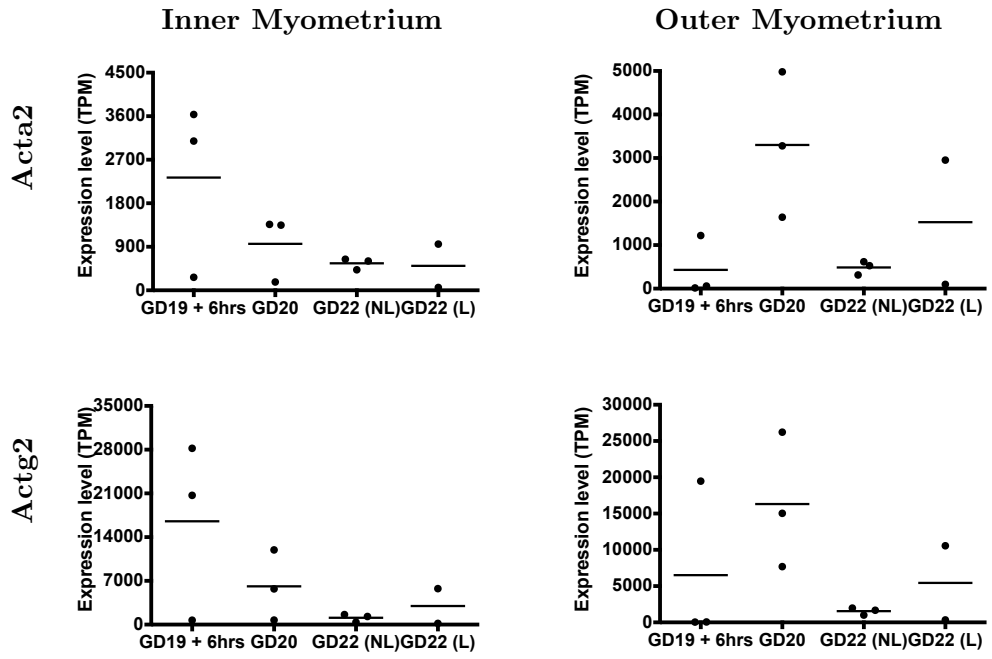

Figure 8.15: Expression of Acta2 and Actg2 mRNA transcripts in myometrial tissues of the pregnant rat uterus. Expression levels are in transcripts per million (TPM). The horizontal bars indicate the mean expression levels. Sample size n = 3 for all time points except GD22(NL) where n = 2. **Acta2**: Actin α-2; **Actg2**: Actin γ-2

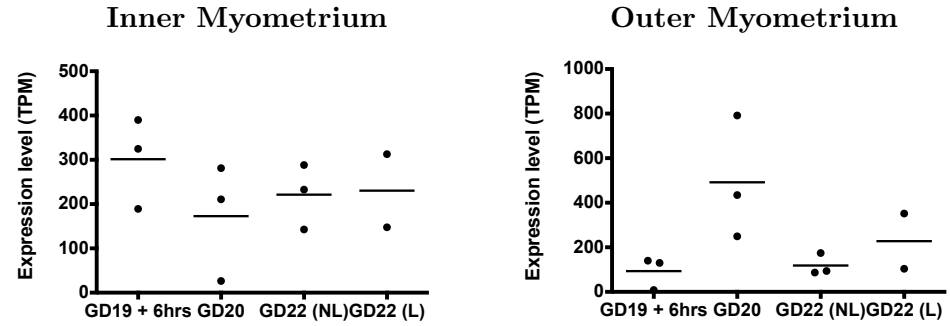

Figure 8.16: Caldesmon 1 (Cald1) mRNA transcript expression in myometrial tissues of the pregnant rat uterus. Expression levels are in transcripts per million (TPM). The horizontal bars indicate the mean expression levels. Sample size n = 3 for all time points except GD22(NL) where n = 2.

8.4.3 Calmodulin

Calmodulin 1 (Calm1) levels in the inner myometrium were relatively unchanged from GD19+6hrs through to GD22(NL), with a decrease in expression during labour (Figure 8.17).

Between GD19+6hrs and GD20, in the outer myometrium, there was an increase in Calm1 expression, followed by a drop in expression at term, and a slight increase during labour. In the inner myometrium, Calmodulin 2 (Calm2) levels decreased gradually between GD19+6hrs and GD22(NL), then remained unchanged during labour (Figure 8.17). In the outer myometrium, however, Calm2 levels decreased between GD19+6hrs and GD22(NL), but increased slightly during labour. Calmodulin 3 (Calm3) levels were relatively lower than Calm1 and Calm2 levels in the inner myometrium, with average expression values of 72.6 ± 67.87 TPM, 483.1 ± 26.48 TPM, and 119.0 ± 30.63 TPM in the inner myometrium on GD19+6hrs, respectively (Figure 8.17). Calm3 levels in the inner myometrium dropped to about 24.66 ± 18.46 TPM on GD20, remained unchanged on GD22(NL), then dropped further during labour. In the outer myometrium, Calm3 levels dropped between GD19+6hrs and GD20, increased slightly on GD22(NL), followed by a slight decrease on GD22(NL).

8.4.4 Calponin

Calponin 1 (Cnn1) mRNA expression decreased towards term in the inner myometrium, with a slight increase during labour (Figure 8.18). In the outer myometrium, however, Cnn1 expression increased significantly between GD19+6hrs and GD20 ($p < 0.05$), followed by a decrease at term and a slight increase during labour. Expression levels of mRNA transcripts encoding calponin 3 (Cnn3) remained relatively unchanged throughout late gestation and labour in the inner myometrium (Figure 8.18). Similarly, Cnn3 expression levels in the outer myometrium were relatively unchanged across the four gestational timepoints, however, Cnn3 mRNA expression was elevated in one of the biological replicates on GD19+6hrs.

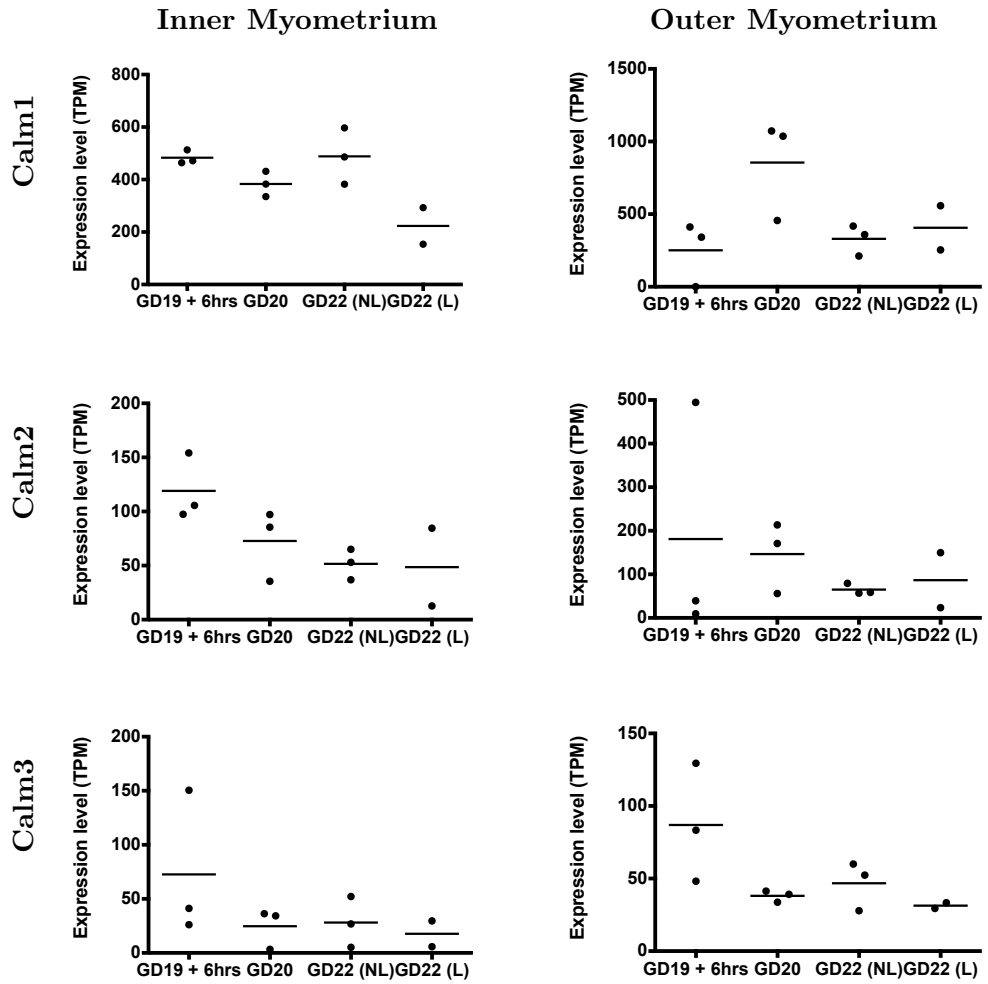

Figure 8.17: Calmodulin mRNA expression in the myometrium. Expression levels are in transcripts per million (TPM). The horizontal bars indicate the mean expression levels. Sample size n = 3 for all time points except GD22(NL) where n = 2. **Calm1**: Calmodulin 1; **Calm2**: Calmodulin 2; **Calm3**: Calmodulin 3.

8.4.5 Myosin

In the inner myometrium, myosin light chain 6B (Myl6b) transcript expression levels dropped on GD20 and GD22(NL) followed by an increase during labour (Figure 8.19). While in the outer myometrium, there was an increase in Myl6b levels on GD20 and subsequent decreases on the ensuing gestational days. Myosin light chain 9 (Myl9) gene transcript levels in the inner myometrium dropped sharply between GD19+6hrs and GD22(NL), then increased during labour (Figure 8.19). In the outer myometrium, Myl9 transcript expression increased

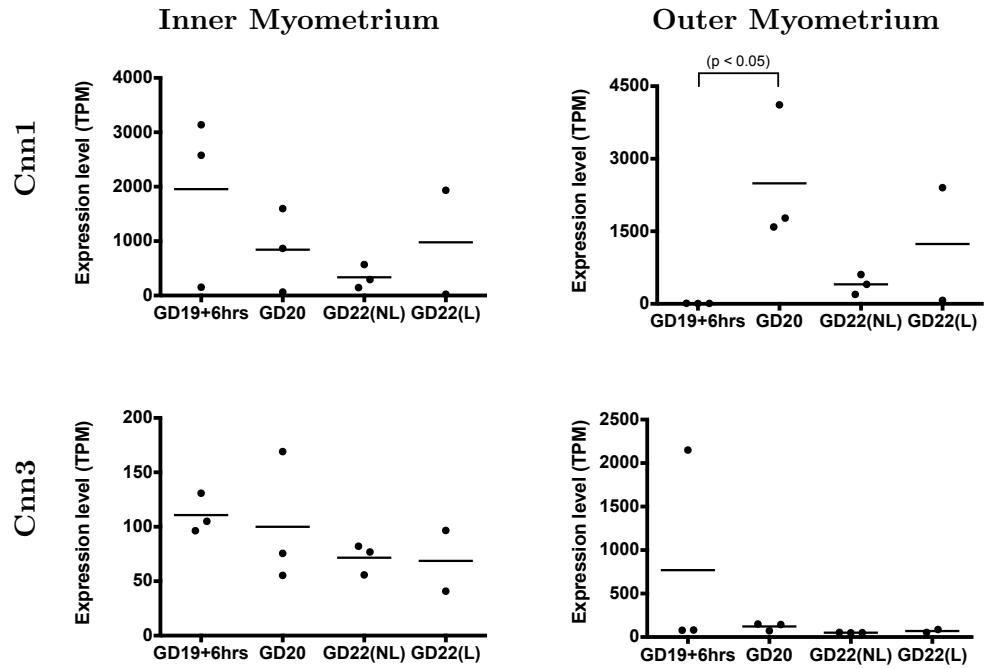

Figure 8.18: Expression of Cnn1 and Cnn3 mRNA transcripts in myometrial tissues of the pregnant rat uterus. Expression levels are in transcripts per million (TPM). The horizontal bars indicate the mean expression levels. Sample size n = 3 for all time points except GD22(NL) where n = 2. **Cnn1**: Calponin 1; **Cnn3**: Calponin 3.

significantly ($p < 0.05$) between GD19+6hrs and GD20 form an average of 41.85 ± 36.49 TPM to 4954.08 ± 3099 TPM. At term, Myl9 expression fell followed by an increase during labour. Myosin light chain kinase (Mylk) expression patterns were similar to the observed Myl9 expression patterns in both the inner and the outer myometrium (Figure 8.19). While Mylk expression increased significantly between GD19+6hrs and GD20 in the outer myometrium as did Myl9, Myl9 expression levels were five times higher than Mylk expression levels.

8.4.6 Tropomyosin

Expression of Tropomyosin 1α (Tpm1) and Tropomyosin 2β (Tpm2) mRNA transcripts was similar in the inner myometrium; there was a decrease in expression on GD20, which was followed by a further decrease at term and slight elevation during labour (Figure 8.20).

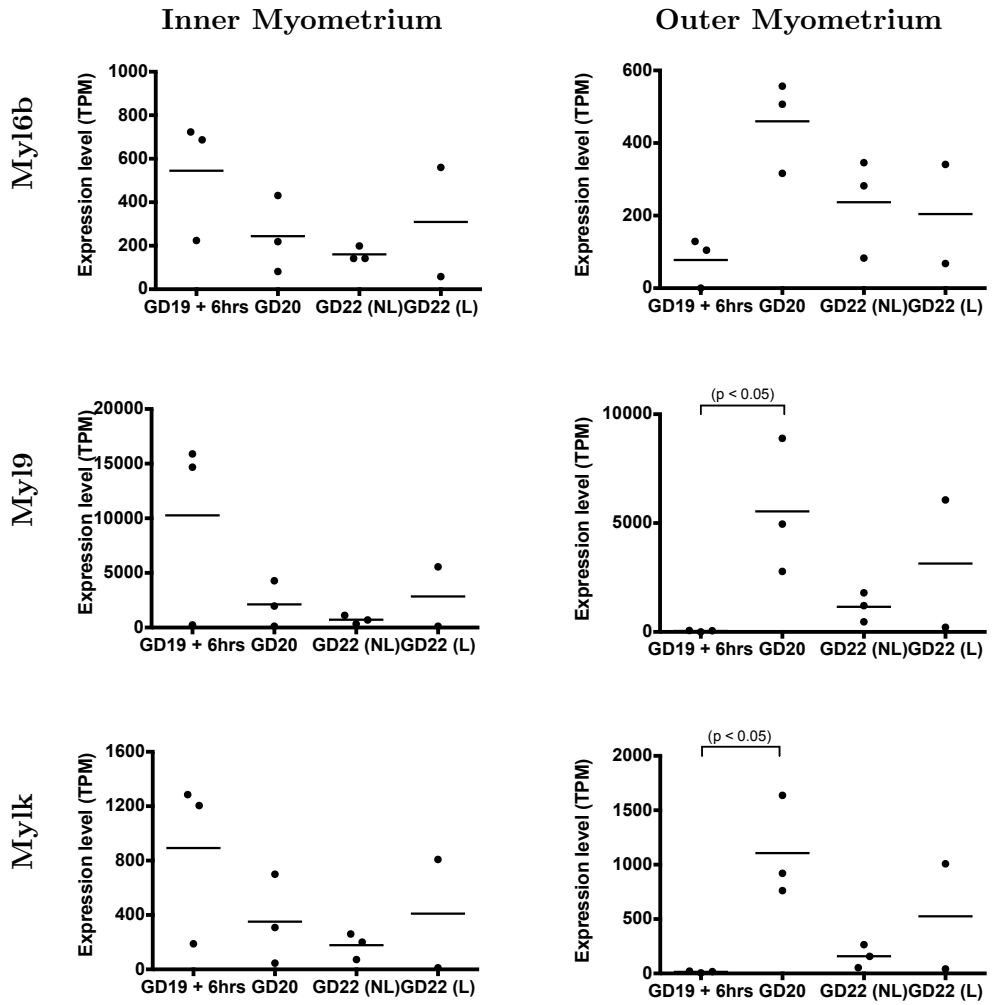

Figure 8.19: Expression of myosin and myosin kinase mRNA in myometrial tissues. Expression levels are in transcripts per million (TPM). The horizontal bars indicate the mean expression levels. Sample size n = 3 for all time points except GD22(NL) where n = 2. **Myl6b**: Myosin light chain 6B; **Myl9**: Myosin light chain 9; **Mylk**: Myosin light chain kinase.

In the outer myometrium, the expression patterns of Tpm1 and Tpm2 were also similar, with increase in expression on GD20 followed by a decrease at term and increase during labour. Tpm1 and Tpm2 are, therefore, expressed similarly within myometrial tissues, but not between the myometrial tissues. There was a slight drop in Tropomyosin 3 (Tpm3) mRNA levels between GD19+6hrs and GD20 in the inner myometrium, which was followed by an increase at term and a slight decrease in expression during labour (Figure 8.20). In the outer myometrium, Tpm3 mRNA levels were unchanged between GD19+6hrs and GD20

followed by an increase at term and a slight decrease in expression during labour. Average Tropomyosin 4 (Tpm4) mRNA expression levels were similar on GD19+6hrs and GD22(L) in the inner myometrium (Figure 8.20). Similarly, Tpm4 mRNA expression levels in the outer myometrium were similar on GD19+6hrs and GD22(L).

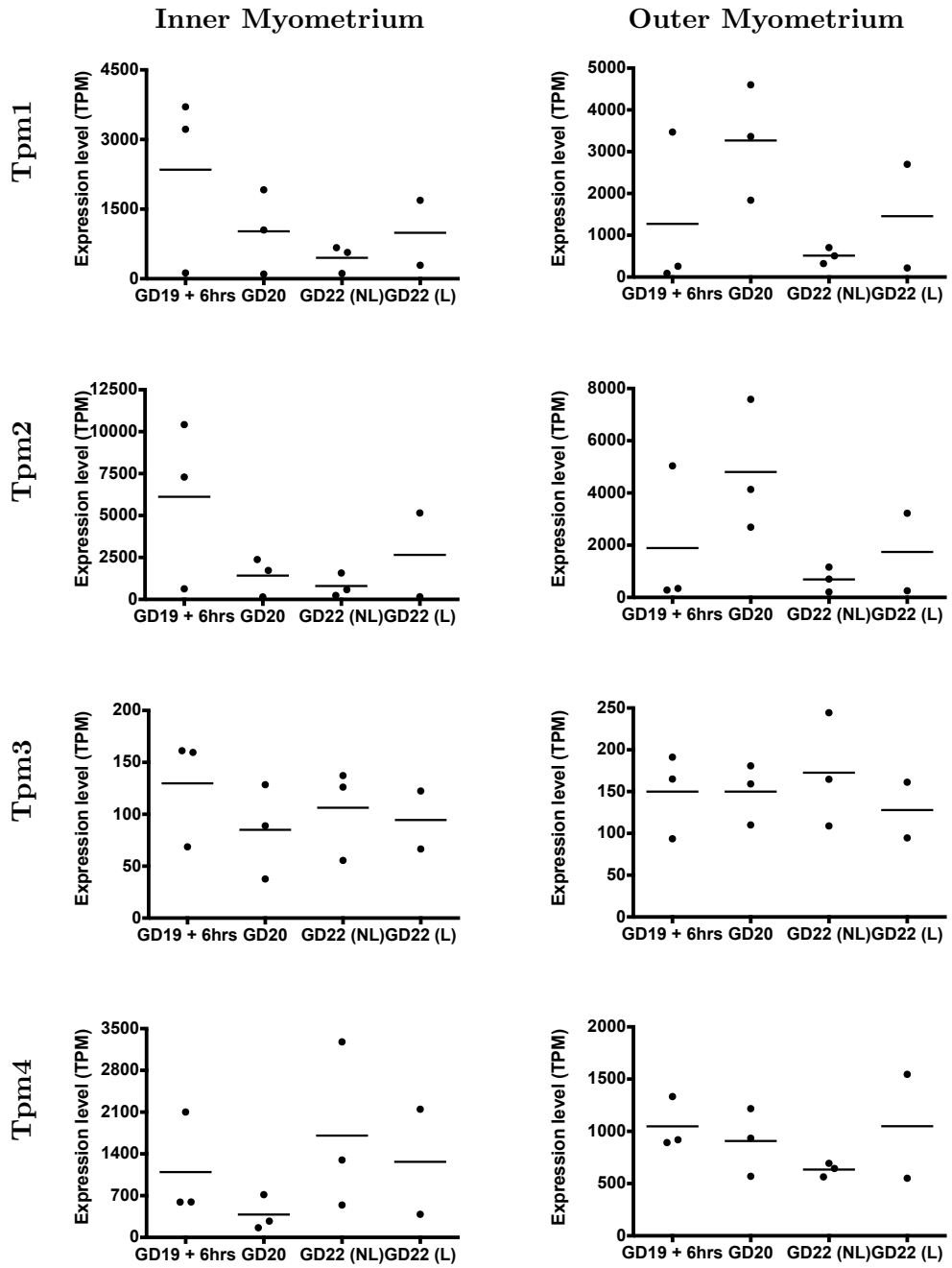

Figure 8.20: Expression of tropomyosin mRNA in myometrial tissues. Expression levels are in transcripts per million (TPM). The horizontal bars indicate the mean expression levels. Sample size n = 3 for all time points except GD22(NL) where n = 2. **Tpm1**: Tropomyosin 1α; **Tpm2**: Tropomyosin 2β; **Tpm3**: Tropomyosin 3; **Tpm4**: Tropomyosin 4.

8.5 Summary and Discussion

8.5.1 Contraction-Associated Proteins

The onset of labour is associated with an increase in the expression of CAPs within the uterus (Fuchs et al., 1984). As such, it is to be expected that the increase in protein expression is due to the upregulation of the gene transcripts that code for CAPs. In addition to assessing the temporal expression of CAP-encoding gene transcripts, the present study assessed the spatial expression of the genes encoding CAPs. For the first time, the differences, and similarities, in CAP expression between the inner myometrium and the outer myometrium have been documented. Data presented in Section 8.1 show that Oxt mRNA levels increases significantly immediately following the systemic withdrawal of P4, then drops significantly at term in the inner myometrium. Conversely, in the outer myometrium Oxt mRNA expression increases significantly between GD19+6hrs and GD22(L). In contrast to published literature, neither a significant up- (Cook et al., 2000; Helguera et al., 2009) nor down-regulation (Phaneuf et al., 2000; Mittal et al., 2010; Chan et al., 2014) of mRNA encoding the Oxtr was observed in the current study. Though not identified as significant, Oxtr mRNA levels increased throughout late gestation reaching peak expression levels during labour in both the inner and outer myometrium, which may be considered to be consistent with some of the published literature.

Labour in the rat is preceded by the systemic withdrawal of P4, which is brought about by the luteolytic effects of $PGF_{2\alpha}$, whose synthesis is dependent upon Ptgs1 and Ptgs2 enzymes (Sugimoto et al., 2015). The expression of both Ptgs1 and Ptgs2 has been previously shown to increase at term and during labour in rat myometrium (Dong et al., 1996). The data presented in Section 8.2 indicate that Ptgs1 mRNA expression in the inner myometrium decreases following the withdrawal of P4. In addition, Ptgs1 gene transcript expression in the

outer myometrium decreases following an initial increase on GD20. Ptgs2 mRNA expression is upregulated during labour in both the inner and the outer myometrium. These observations are in line with literature, which suggests that the induction of Ptgs2 is responsible for the increase in $PGF_{2\alpha}$, which leads to luteolysis and P4 withdrawal in rats (Condon et al., 2004). While the reduction in the expression of Ptgs1 mRNA in myometrial tissues may seem contradicting to the findings of Dong et al. (1996), it has been shown that the lack of Ptgs1 proteins does not inhibit labour. Instead, labour is delayed, indicating that the inducible Ptgs2 protein plays a larger role in the onset of parturition in the rat than the constitutive Ptgs1 protein (Ratajczak & Muglia, 2008; Funk et al., 2009).

8.5.2 Gap Junction Proteins

Gap junction proteins, Gja1 in particular, are known to increase in late pregnancy and during labour (Garfield & Maner, 2007). Ou et al. (1997) demonstrated that Gja1 and Gjb2 are the most abundant gap junction proteins in the myometrium, an observation that was also made in the present study. In addition to Gja1 and Gjb2, the gap junction proteins Gja5, and Gja7 have been previously identified in myometrial tissues (Albrecht et al., 1996; Garfield & Maner, 2007; Kidder & Winterhager, 2009). The spatial expression of mRNA encoding gap junction proteins however, had not been described prior to this study. There was no significant increase in Gja1 mRNA expression within either myometrial layer as was observed by Helguera et al. (2009). Since Gja1 proteins are synthesised prior to term and stored within vesicles in the cytoplasm then transported to plasma membranes at the onset of labour (Hendrix et al., 1992), the absence of a significant increase in Gja1 myometrial mRNA expression is to be expected. Instead of increasing, Gja1 mRNA levels fell in the inner myometrium. In the outer myometrium, however, a slight increase in the expression of Gja1 mRNA was observed. The differences in the pattern of Gja1 expression between myometrial tissues has also been observed in bovine myometrium (Doualla-Bell et al., 1995).

Gjb2, whose expression is induced by P4 treatment, has been shown to decrease significantly at term prior to labour (Ou et al., 1997; Kidder & Winterhager, 2009). On GD20 and during labour, Gjb2 mRNA was more abundant than Gja1 mRNA in the inner myometrium, suggesting that the Gjb2 protein may play a significant role during labour. In the outer myometrium, however, Gja1 mRNA transcripts were the most abundant among all gap junction mRNA transcripts. Also in the outer myometrium, Gjb2 mRNA expression levels dropped on GD20 and at term as has been previously described. While expression patterns of Gjb2 mRNA in the outer myometrium are consistent with the literature, the pattern of expression observed in the inner myometrium is somewhat different.

Data presented in Section 8.3.3 indicate that Gja5 mRNA expression in the inner myometrium increases towards term following an initial drop on GD20. In the outer myometrium, however, Gja5 mRNA levels increase on GD20 and remain unchanged during labour. Since Gja5 knock-out mice are fertile (Simon et al., 1998), the role of Gja5 in the uterus is unclear. Gja7 mRNA expression in the inner and outer myometrium is down-regulated between GD19+6hrs and GD22(L), observations that are consistent with those made by Albrecht et al. (1996) who suggested that the ratio of Gja1 and Gja7 proteins may be vital to the coupling of SMCs during labour. The data presented in this thesis, also indicate that other gap junction proteins apart from Gja1, Gjb2, Gja5, and Gja7 are expressed in rat myometrial tissues

8.5.3 Smooth Muscle Genes

Contraction of SMCs is brought about by the interaction of a host of proteins; calmodulin (Calm) binds Ca^{2+} and activates myosin light-chain kinase (Mylk) enzymes, which phosphorylate and activate myosin. Filaments, composed of the phosphorylated myosin, slide over thin filaments, which are composed of actin, caldesmon, and tropomyosin proteins result-

ing in the contraction of SMCs (Garfield & Maner, 2007). The expression of the proteins involved in the contraction of SMCs in the two layers of the rat myometrium have been assessed and documented in the present study, which had not been done previously.

The data presented in Section 8.4.1 indicate that Acta2 (α-actin) mRNA expression was considerably lower during labour in comparison to levels observed on GD19+6hrs in the inner myometrium. While in the outer myometrium, Acta2 mRNA levels were relatively higher than those on GD19+6hrs. These observations seem to contradict the observations made by Shynlova (2005), whereby α-actin mRNA expression remained high in the myometrium throughout gestation relative to samples obtained from non-pregnant rats. However, Shynlova (2005) observed a decrease in the relative fold change between gestation day 20 and day 23, suggesting a decrease in expression. Similar to the Acta2 mRNA expression levels in the inner myometrium, the mRNA expression levels of the Actg2 (γ-actin), in the inner myometrium were low during labour in comparison to GD19+6hrs expression levels. In the outer myometrium, however, Acta2 mRNA levels during labour were relatively similar to those observed on GD19+6hrs. Shynlova (2005), observed significant increases in the expression of γ-actin protein in the inner myometrium between the 18^{th} and the 21^{st} day of gestation in the rat, an observation which is contradicted by the findings of the present study. The only agreement between the data presented in Section 8.4.1 and the observations made by Shynlova (2005) is that γ-actin is highly expressed throughout late gestation in comparison to α-actin. Comparison of mRNA expression to protein expression is not always possible as these data demonstrate. In addition, Shynlova (2005) could not differentiate between smooth muscle γ-actin and cytoplasmic γ-actin due to the non-specific nature of the antibody that was used, hence it is not possible to refute or confirm their observations. Furthermore, Arnoldi et al. (2013) observed a significant increase in the expression of the smooth muscle γ-actin protein on the 18^{th} day of gestation in the myometrium of the rat using immunoblotting, when compared to non-pregnant rat myometrium. How-

ever, the specific layer of the myometrium in which these changes were observed was not determined.

The tissue specific expression patterns of the actin-binding proteins caldesmon and calponin have been described in the present study. The average expression levels of Cald1 mRNA in the inner and outer myometrium were relatively similar, however, the patterns of expression within the tissues were different. Cald1 mRNA levels in the inner myometrium decreased slightly then remained unchanged whilst outer myometrium levels increased initially, declined, then increased again. Expression of Cnn1 and Cnn2 mRNA levels in the inner myometrium were low during labour in comparison to GD19+6hrs levels. There was significant upregulation of Cnn1 mRNA expression on GD20. While the expression of genes encoding caldesmon and calponin has been shown to increase in differentiated cultured SMCs in comparison to dedifferentiated SMCs (Sobue et al., 1999), the tissue specific expression patterns of calmodulin and calponin mRNA transcripts have not been previously determined.

Most studies have focused on the regulation of SMC contraction by calmodulin (Walsh, 1994), the interactions between calmodulin and Ca^{2+}, as well as myosin light chain kinase (Fajmut et al., 2005), and the effect of calmodulin on the gating kinetics of gap junction channels (Peracchia et al., 2014). The spatial expression of the mRNA transcripts encoding the calmodulin isoforms, therefore, are presented in this thesis for the first time. The dynamics of tropomyosin are discussed in the review by El-Mezgueldi (2014), however, the expression patterns of the mRNA transcripts encoding various tropomyosin protein isoforms have not been described. In the present study, the spatial and temporal expression patterns of mRNA transcripts encoding four tropomyosin protein isoforms; Tpm1, Tpm2, Tpm3, and Tpm4, were described (Section 8.4.6).

8.6 Conclusion

The aim of this chapter was to analyse the pattern of expression of genes encoding proteins involved in excitation-contraction coupling in the inner myometrium and the outer myometrium. As with the previous chapter, the separation of the inner and outer myometrium enabled the identification of distinct patterns of mRNA expression between the two layers of the myometrium.

Expression patterns of contraction-associated proteins; Oxtr, Ptgs1, Ptgs2, and numerous gap junction proteins, were analysed. In addition, 17 gap junction proteins were detected in myometrial tissues, 5 of which had an average level of expression that was greater than 10 TPM in at least one of the tissues. It was also noted that mRNA transcripts encoding the gap junction protein Gjb2 are more abundant than Gja1 in the inner myometrium at some stages during late gestation. While qPCR data largely contradicted the RNAseq data, the observations made using RNAseq data were found to be consistent with published literature. The author, therefore, asserts that the RNAseq data are accurate. However, the use of more than one, or a different, housekeeping gene may yield qPCR results that are more agreeable with the RNAseq data.

In line with the aim of the chapter, the expression patterns of the "so-called" smooth muscle genes, i.e., genes encoding smooth muscle actin caldesmon, calmodulin, calponin, myosin, myosin light-chain kinase, and tropomyosin, were assessed in the inner and outer layers of the myometrium. As far as the author is aware, the spatial patterns of expression of smooth muscle gene transcripts are documented in this chapter for the first time. In conclusion, identification of the spatio-temporal expression of genes encoding proteins involved in smooth muscle excitation-contraction coupling will further enrich current knowledge into the molecular processes occurring in uterine tissues in the run-up to labour, and in preterm labour. The following chapter describes the changes in expression of mRNA transcripts

within uterine tissues that occur in response to treatment with a progesterone receptor antagonist.

Chapter 9

Transcriptomic Effects of Progesterone Receptor Antagonist-Induced Progesterone Withdrawal

In the work presented in this chapter, the partial PR antagonist Mifepristone described in Section 2.3.3 was used in the identification and analysis of transcriptomic changes that occurred in response to the withdrawal of progesterone (P4) in the rat uterus. This chapter aims to identify the gene transcripts whose expression changed in response to treatment with Mifepristone in the decidua, inner circular myometrium, and the outer longitudinal layer of the myometrium; and to further elucidate the transcriptional changes that occur during preterm labour in uterine tissues.

9.1 Transcriptomic Landscape of the Mifepristone-Treated Rat Uterus

A total of 6 pregnant Sprague-Dawley rats were treated with 3 mg of Mifepristone by subcutaneous injection on GD19. Three of the rats were sacrificed 6 hours following treatment, on GD19+6hrs, and the remaining three were sacrificed 24 hours post-treatment, on GD20. Mifepristone-treated rats delivered on GD20, however, tissues from labouring rats were not provided. Professor Robert Garfield, at St. Joseph's Hospital and Medical Centre in Phoenix (USA) treated the rats and harvested whole uterine horns which were flash-frozen in liquid nitrogen, then stored at $-80°$C until required. Laser capture microdissection (LCM), a technique for separating cells from tissues, was used to collect homogenous tissue samples containing decidua, inner myometrium, or outer myometrium cells as described in Section 5.4. RNA was isolated from each of the samples, and only RNA with a RIN score $\geq$6 (see Section 5.5.2 for checking of RNA integrity) was used for library preparation and sequencing as described in to Section 5.6.

Over 589.56 million reads were sequenced across all the libraries that were generated from Mifepristone-treated tissues, of which 50.44% were sequenced from GD19+6hrs libraries, and the remaining 49.56% from GD20 libraries as illustrated in Figure 9.1. Table 9.1 provides details on the number of reads that were generated per sample. Here, a sample represents each of the three uterine tissues; decidua, inner circular myometrium, and outer longitudinal myometrium, obtained on both GD19+6hrs and GD20, from three biological replicates. Mifepristone-treated samples from GD19+6hrs generated between 19,597,589 and 51,977,455 reads each, while those from GD20 generated between 21,584,276 and 40,005,053 reads each. On average, 32.75 million paired-end reads were sequenced per sample, 79.96% of which were aligned to the reference genome. Of the aligned reads, 71.15% were defined as expressed across the 2 gestational time points, and all the tissues. The expressed transcrip-

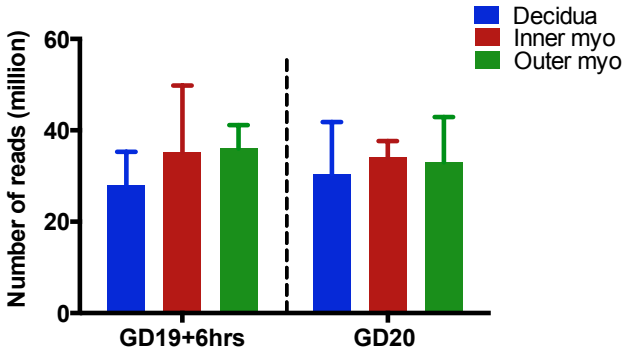

Figure 9.1: Number of reads in sequencing files generated from Mifepristone-treated tissues. The average number of reads generated from decidua, inner myometrium and outer myometrium samples obtained on GD19+6hrs, and GD20. The error bars indicate the standard deviation of the number of reads within a group of biological replicates.

tome was covered 16.09×, and 18.06× on average with respect to GD19+6hrs, and GD20 samples. Details of the sequencing coverage are provided in Table 9.1.

The abundance of transcripts was estimated using three methods: HTSeq, which was used to estimate the number of transcripts (counts); Cufflinks (Section 6.2.1), which was used to estimate abundance in the form of reads per kilobase per million (RPKM); and Sailfish (Section 6.2.1), which was used to estimate transcripts per million (TPM) values.

9.1.1 Principal Component Analysis

Principal component analysis (PCA) of the non-zero TPM values estimated using Sailfish was employed to determine the expression patterns of gene transcripts within Mifepristone-treated tissues. PCA was conducted as described in Section 6.1 using the princomp function in R as follows:

$$\mathsf{myPCA} = \mathsf{princomp}(\sim .,\mathsf{data} = \mathsf{myData},\ \mathsf{na.action} = \mathsf{na.exclude},\ \mathsf{cor} = \mathsf{FALSE}),$$

where $\sim .$ indicates that all the Mifepristone-treated tissue samples in the data matrix, represented by myData, were used in the estimation of principal components (PCs), while na.action = na.include indicates all transcripts "NA" expression values were not used in the

Table 9.1: Alignment of sequenced reads to the *Rattus norvegicus* transcriptome and coverage statistics of sequences generated from Mifepristone-treated tissues. Gestation - The day during pregnancy on which the uterine sample was collected. **Tissue** - The layer of the uterus that was separated from the other tissues using laser-capture microdissection. The number illustrates the replicate number. **% Aligned** - The proportion of the sequenced reads that were aligned successfully to the *Rattus norvegicus* transcriptome using Tophat2. **% Expressed features** - The proportion of genes to which counts were assigned by HTSeq. **Expressed transcriptome (× covered)** - The number of times the expressed transcriptome was covered by the sequenced reads.

Sample					
Gestation	Tissue	Total reads	% Aligned	% Expressed features	Expressed transcriptome (× covered)
GD19+6hrs	Decidua_1	30,347,943	74.90	64.87	17.97
GD19+6hrs	Decidua_2	19,597,589	75.90	58.14	13.30
GD19+6hrs	Decidua_3	33,752,940	76.80	86.04	9.44
GD19+6hrs	Inner_Myo_1	51,977,455	71.30	64.67	16.11
GD19+6hrs	Inner_Myo_2	25,312,372	77.50	67.38	16.64
GD19+6hrs	Inner_Myo_3	28,370,936	80.90	64.06	23.05
GD19+6hrs	Outer_Myo_1	31,354,384	78.00	79.73	7.30
GD19+6hrs	Outer_Myo_2	41,546,591	82.50	74.44	22.15
GD19+6hrs	Outer_Myo_3	35,108,356	75.30	54.29	18.86
GD20	Decidua_1	25,280,743	82.60	61.09	11.42
GD20	Decidua_2	22,500,156	80.00	70.62	12.83
GD20	Decidua_3	43,464,337	85.80	81.05	25.56
GD20	Inner_Myo_1	30,661,735	78.00	71.08	16.05
GD20	Inner_Myo_2	33,480,557	84.20	78.60	12.05
GD20	Inner_Myo_3	37,905,128	80.90	67.91	29.06
GD20	Outer_Myo_1	37,314,111	86.60	74.15	22.08
GD20	Outer_Myo_2	21,584,276	82.80	82.88	8.92
GD20	Outer_Myo_3	40,005,053	85.20	79.64	24.60

estimation of PCs, and cor = FALSE indicates that the correlation matrix was not used in the estimation of PCs. The number of PCs used to assess the relationship among the data were selected as described in Section 6.1.2.

GD19+6hrs

To determine the number of PCs to retain for analysis, the cumulative proportion of variance accounted for by the PCs was considered (Table 9.2), as well as a plot of the eigenvalues (Figure 9.2). The first two PCs, PC1 and PC2, accounted for more than 85% of the variation within the data. In addition, the plot of variances indicated that the remaining PCs, PC3–PC9, accounted for a negligible proportion of the variation within the data. As such, two

Table 9.2: Variance accounted for by principal components. Shown are the proportions of variance, as well as the cumulative proportion of variance, accounted for by principal components estimated using transcript expression values for generated from Mifepristone-treated tissue samples obtained on GD19+6hrs and GD20. **PV (%)**: proportion of variance explained, expressed as a percentage; **CP (%)**: cumulative variance explained, expressed as a percentage; and **Comp.**: principal component.

	GD19+6hrs		GD20	
	PV (%)	CP (%)	PV (%)	CP (%)
Comp.1	72.87%	72.87%	66.24%	66.24%
Comp.2	22.24%	95.11%	18.82%	85.06%
Comp.3	2.11%	97.22%	6.18%	91.24%
Comp.4	1.27%	98.49%	4.19%	95.43%
Comp.5	1.11%	99.60%	2.91%	98.34%
Comp.6	0.24%	99.84%	0.90%	99.24%
Comp.7	0.11%	99.95%	0.56%	99.80%
Comp.8	0.03%	99.98%	0.14%	99.94%
Comp.9	0.02%	100.00%	0.06%	100.00%

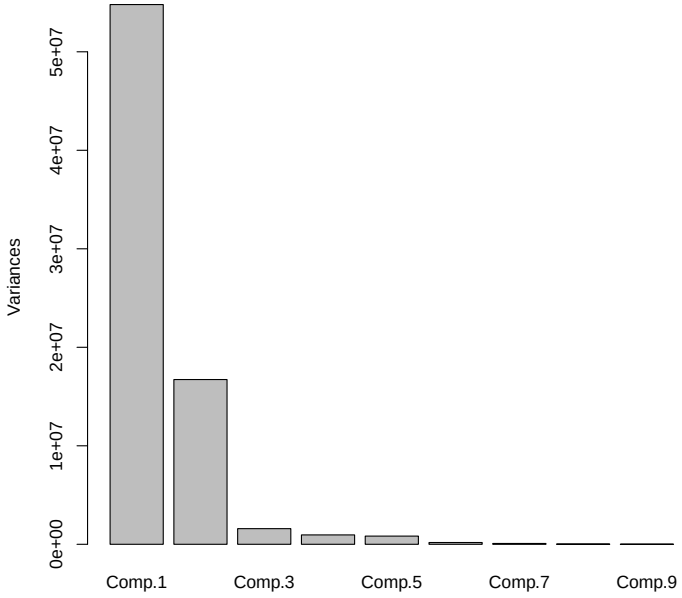

Figure 9.2: Plot of the eigenvalues of the covariance matrix of data generated from Mifepristone-treated tissue samples obtained on GD19+6hrs. The low variance accounted for by principal component (Comp.) numbers 5–9 suggests that the first two principal components should be retained for analysis.

PCs were retained for further analysis.

A plot of the retained PCs (Figure 9.3) did not show distinct separation of all the three

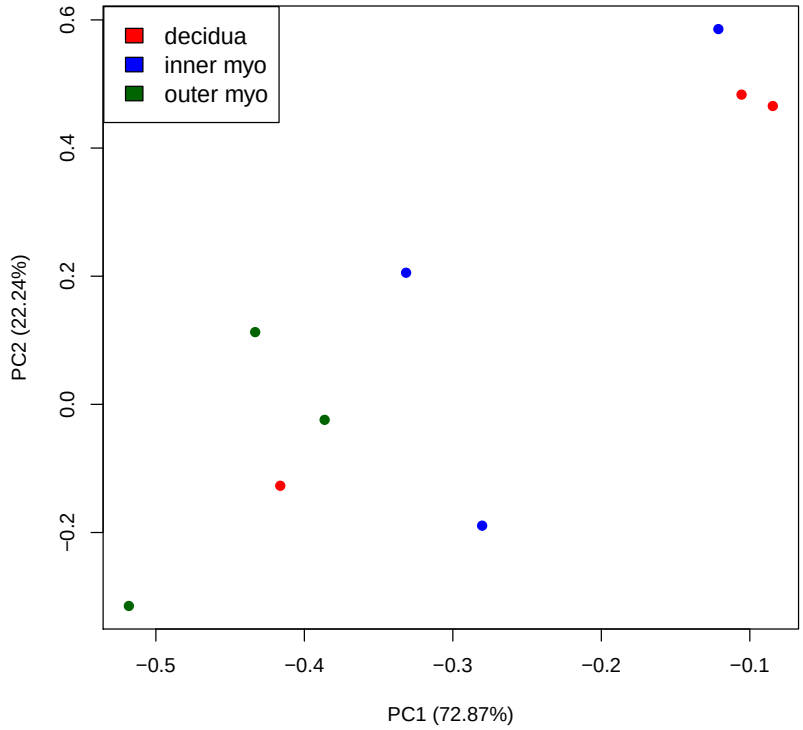

Figure 9.3: Principal component analysis (PCA) of mRNA expression in Mifepristone-treated tissue samples on GD19+6hrs. Transcripts per million (TPM) abundances were used for PCA. The variance within the data which is accounted for by each of the principal components is displayed next to the corresponding principal component. **PC1**: the first principal component; and **PC2**: the second principal component;

uterine tissues on GD19+6hrs. However, there was clear separation of two groups; one consisting of two decidual samples and one inner myometrial sample, and the other composed of all the outer myometrial tissue samples, as well as one each of decidual and inner myometrial samples. One of the decidual samples and the inner myometrial sample in the former group, were obtained from the same uterine sample, suggesting that the inner myometrial sample may have been contaminated with decidual cells. However, given the care that was taken in ensuring accurate selection of specific cell types, the similarity between these samples may indicate that this particular inner myometrial sample and the decidual sample that grouped with the rest of the samples were mislabelled. Assessment of the laser-capture and RNA isolation experiments showed that the inner myometrial sample, which was grouped together with the two decidual samples, was collected on the same day as the decidual samples, and

RNA was also extracted on the same day. In addition, the quantification or the RNA and the subsequent checks for integrity, as well as library preparation, were all conducted on the same day, further pointing to the increased likelihood of mislabelling the samples. Despite this observation, none of the samples were excluded from further analyses as it was believed that the methods employed were robust enough to "weed out" any outliers. Furthermore, there was distinct variability between one of the outer myometrial samples and the other two outer myometrial samples. Since this particular sample was neither lasered nor have RNA extracted from it on the same day as the suspected mislabelled samples, the variability was attributed to inherent biological variability.

GD20

Data generated from Mifepristone-treated tissue samples that were obtained on GD20 were subjected to PCA as previously described. PC1 and PC2 accounted for a cumulative proportion of 85.06% of the total variation within the GD20 data (Table 9.2). In addition, the scree plot of the eigenvalues (Figure 9.4) shows that the first two principal components explain the bulk of the variability within the data. Therefore, PC1 and PC2 were retained for further analysis.

The plot of the first two PCs in Figure 9.5 shows that there was more variation between tissues on GD20 in comparison to GD19+6hrs. However, not all samples within the same biological group were closely associated with their group-mates as one outer myometrial sample was closely associated with the decidua samples, indicating that mRNA transcript expression within that sample was similar to the expression within decidual samples.

9.1.2 Spatial Expression Patterns

To assess specific mRNA expression patterns within uterine tissues, the following three methods were employed: Cuffdiff, which utilises the RPKM values estimated by Cufflinks as input; edgeR; and DESeq2, both of which use the gene transcript counts estimated by

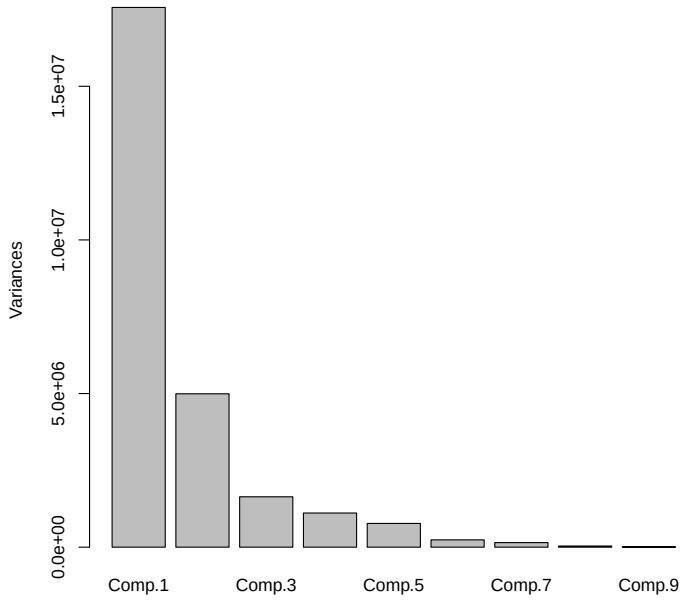

Figure 9.4: Plot of the eigenvalues of the covariance matrix of data generated from Mifepristone-treated tissue samples obtained on GD20. The low variance accounted for by principal component (Comp.) numbers 5–9 suggests that the first two principal components may be retained for analysis.

HTSeq as input. For each method, a transcript was considered differentially expressed if the associated q-value (Cuffdiff), false discovery rate (edgeR), or the adjusted p-value (DESeq2) was less than a threshold of 5%. Transcripts that were identified as differentially expressed by at least 2 of the 3 methods were used in the analyses presented in this section.

GD19+6hrs

There were 190, 30, and 36 transcripts that were identified as differentially expressed between the decidua and the inner myometrium by Cuffdiff, edgeR, and DESeq2, respectively as illustrated in Figure 9.6a. A set of 23 transcripts were identified by at least 2 methods, 78% of these were upregulated in the inner myometrium. A list of the 23 genes that were differentially expressed together with their levels of expression in the decidua and the inner myometrium are listed in Supplementary Table E.1. The heat map in Figure 9.6b pointed to a distinct separation of the decidua and the inner myometrium when agglomerative hierarchical clustering was employed. The Venn diagram in Figure 9.6c represents the overlap

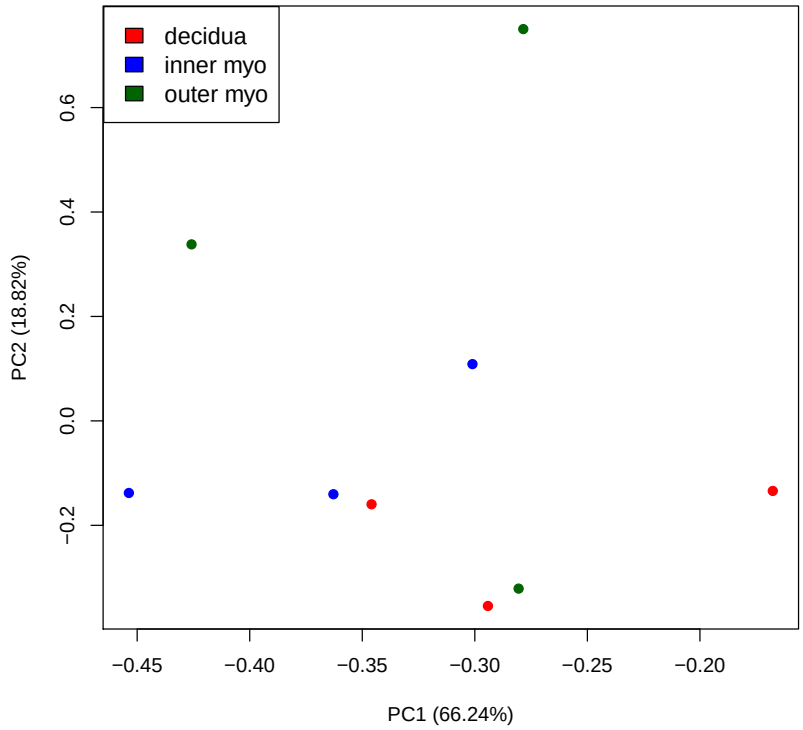

Figure 9.5: Principal component analysis (PCA) of mRNA expression in Mifepristone-treated tissue samples on GD20. Transcripts per million (TPM) abundances were used for PCA. The variance within the data which is accounted for by each of the principal components is displayed next to the corresponding principal component. **PC1**: the first principal component; and **PC2**: the second principal component;

between the number of genes identified as differentially expressed between the decidua and the outer myometrium by Cuffdiff (Cuff), edgeR and DESeq2. A total of 225 genes were identified by at least 2 methods, of which 64% were upregulated in the outer myometrium, details of which are provided in Supplementary Table E.2. Agglomerative hierarchical clustering of the differentially expressed genes separated the tissues and the differentially regulated genes into distinct clusters as illustrated in Figure 9.6d. Cuffdiff identified 123 transcripts that were differentially expressed between the inner and the outer myometrium, while edgeR identified 1, and DESeq identified 6. The genes identified by DESeq2 were not identified by any of the other methods; the gene encoding for the doublesex and mab-3 related transcription factor 2 (Dmrt2), was the only gene identified as differentially expressed by Cuffdiff and edgeR between the myometrial layers.

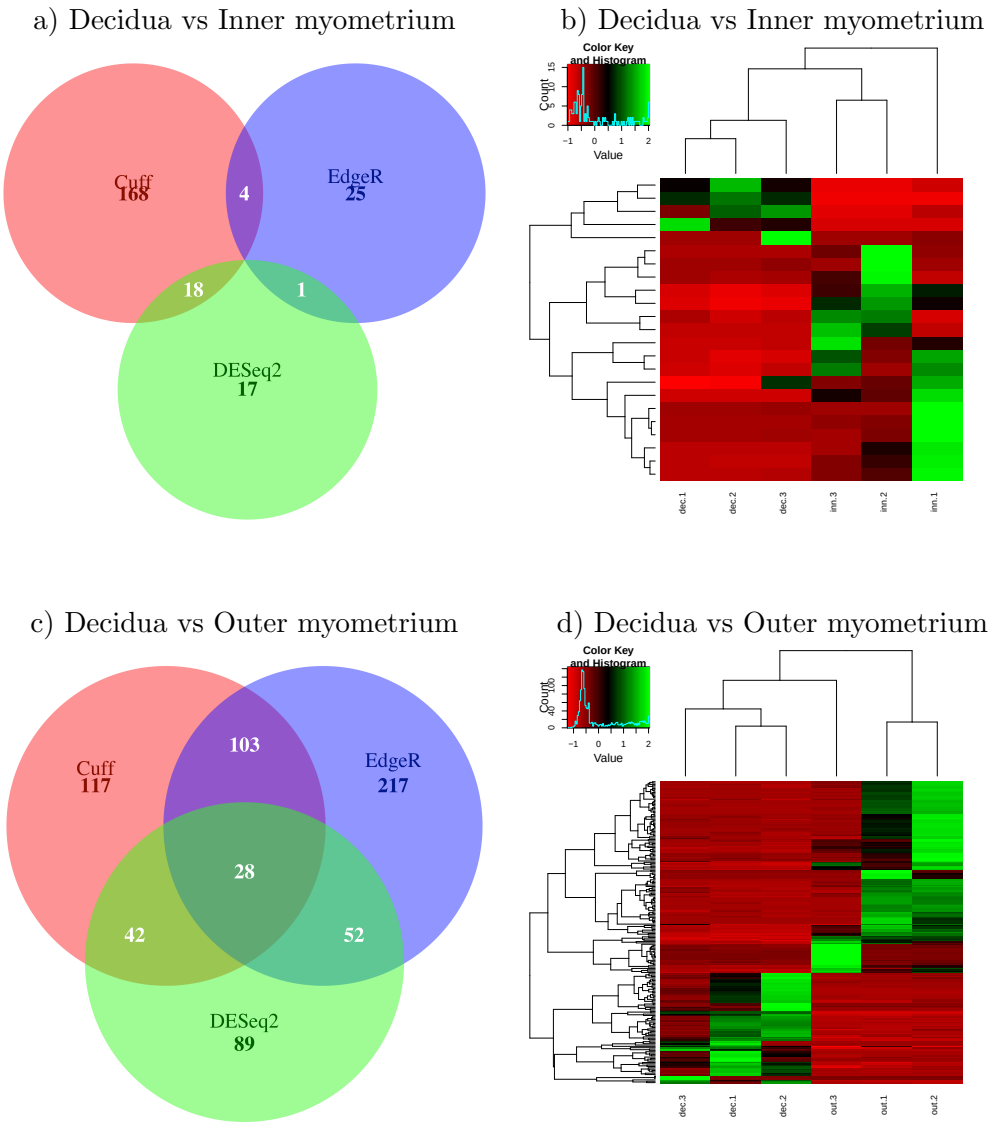

Figure 9.6: Spatial expression of gene transcripts on GD19+6hrs. Gene transcripts were identified as differentially expressed by Cuffdiff (Cuff), edgeR and DESeq2 between the (a–b) decidua and the inner myometrium, and between the (c–d) decidua and the outer myometrium. Agglomerative hierarchical clustering was used to identify the relationships among the decidua (dec), inner (inn) circular myometrium (myo), and outer longitudinal myometrium (out). The tissues and gene transcripts are represented by the columns and rows, respectively.

GD20

The decidua and inner myometrial samples on GD20 had 33 differentially expressed transcripts between them as identified by at least two of the three methods (Figure 9.7a). Clus-

tering of the 33 genes, 15% of which were upregulated in the inner myometrium, segregated the tissues and genes distinctly as illustrated by the heat map in Figure 9.7b. Figure 9.7c and Figure 9.7d show that 8 gene transcripts were differentially expressed between the decidua and the outer myometrium, and that clustering of the z-scores of the differentially expressed TPM values grouped tissues and genes into distinct sets. Between the myometrial layers, 36 transcripts were identified as differentially expressed by at least two methods (Figure 9.7e). The heat map in Figure 9.7f, shows a pattern of expression in one replicate of the inner myometrium that is different from other inner myometrium replicates. The outer myometrium replicates, however, are clustered together.

9.1.3 Temporal Expression Patterns

Analysis of the changes in expression with time in Mifepristone-treated tissues was conducted using the Cuffdiff, DESeq2, and edgeR as previously described. The largest change in transcript expression occurred in the inner myometrium where 59 transcripts were differentially expressed between GD19+6hrs and GD20, with 78% of the transcripts being upregulated on GD20 (Supplementary Table E.6). The least number of differentially expressed transcripts was observed in the outer myometrium where 14 transcripts were differentially expressed, 10 of which were upregulated on GD20 (Supplementary Table E.7). In the decidua, 30 transcripts were differentially expressed, and all but 2 of them were upregulated on GD20 (Supplementary Table E.8). Illustrations of the numbers of gene transcripts that were identified as differentially expressed between GD19+6hrs and GD20 in the decidua, inner myometrium, and outer myometrium by the 3 differential expression analysis methods are shown in Figure 9.8a, Figure 9.8c, and Figure 9.8e, respectively. Clustering of the non-zero z-scores that were derived from the TPM values of the differentially expressed genes is illustrated by the heat maps in Figure 9.8b, Figure 9.8d, and 9.8f, which show distinct separation of decidua tissues obtained on GD19+6hrs from those obtained on GD20, but not the inner myometrium or outer myometrium, respectively.

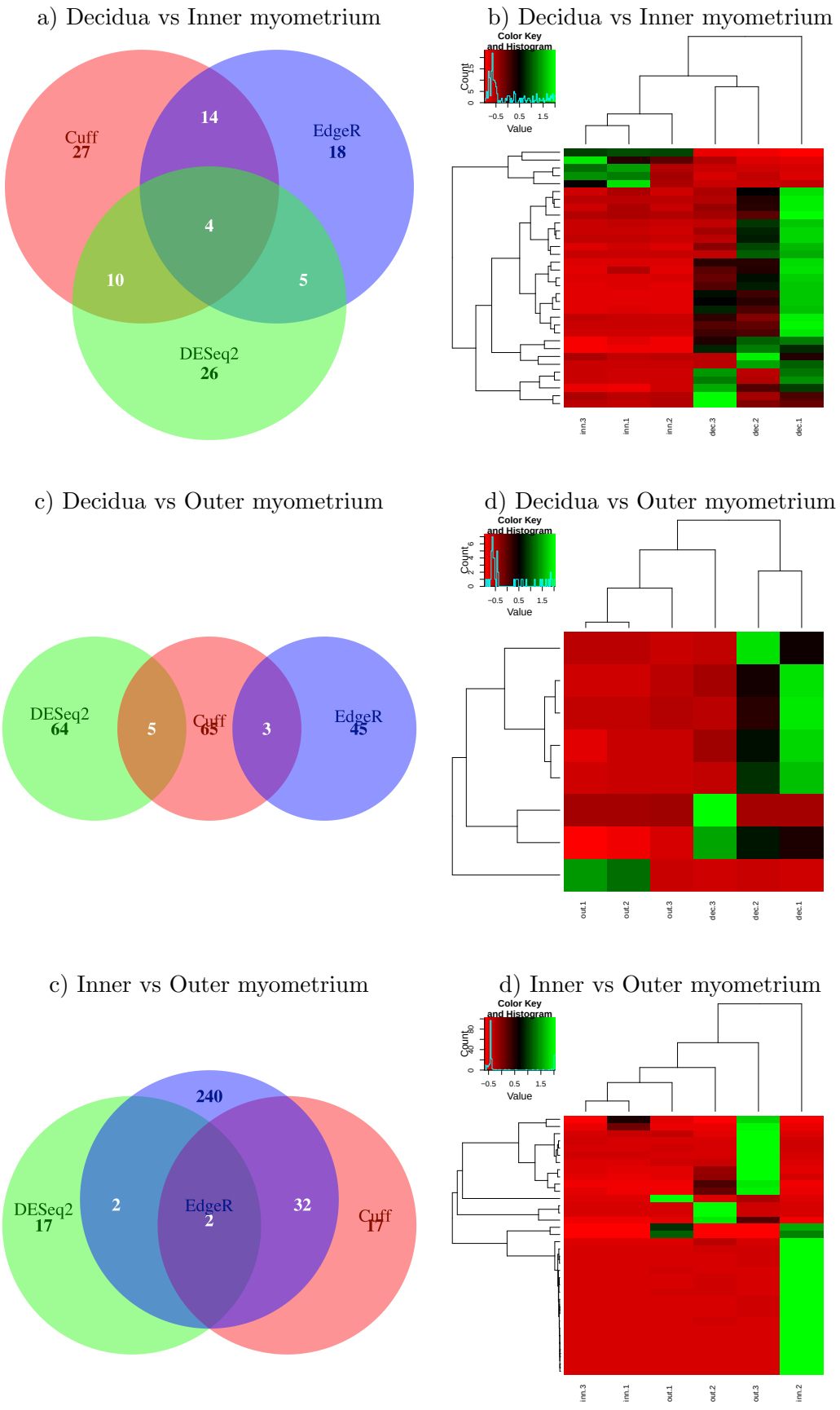

Figure 9.7: Venn diagrams and heat maps of differentially expressed gene transcripts between myometrial tissues on GD20. Gene transcripts were identified as differentially expressed by Cuffdiff (Cuff), edgeR and DESeq2 between the (a–b) decidua and the inner myometrium, (c–d) decidua and the outer myometrium, and between the (e–f) inner and outer myometrial layers. Agglomerative hierarchical clustering was used to identify the relationships among the decidua (dec), inner (inn) circular myometrium (myo), and outer longitudinal myometrium (out). The tissues and gene transcripts are represented by the columns and rows, respectively.

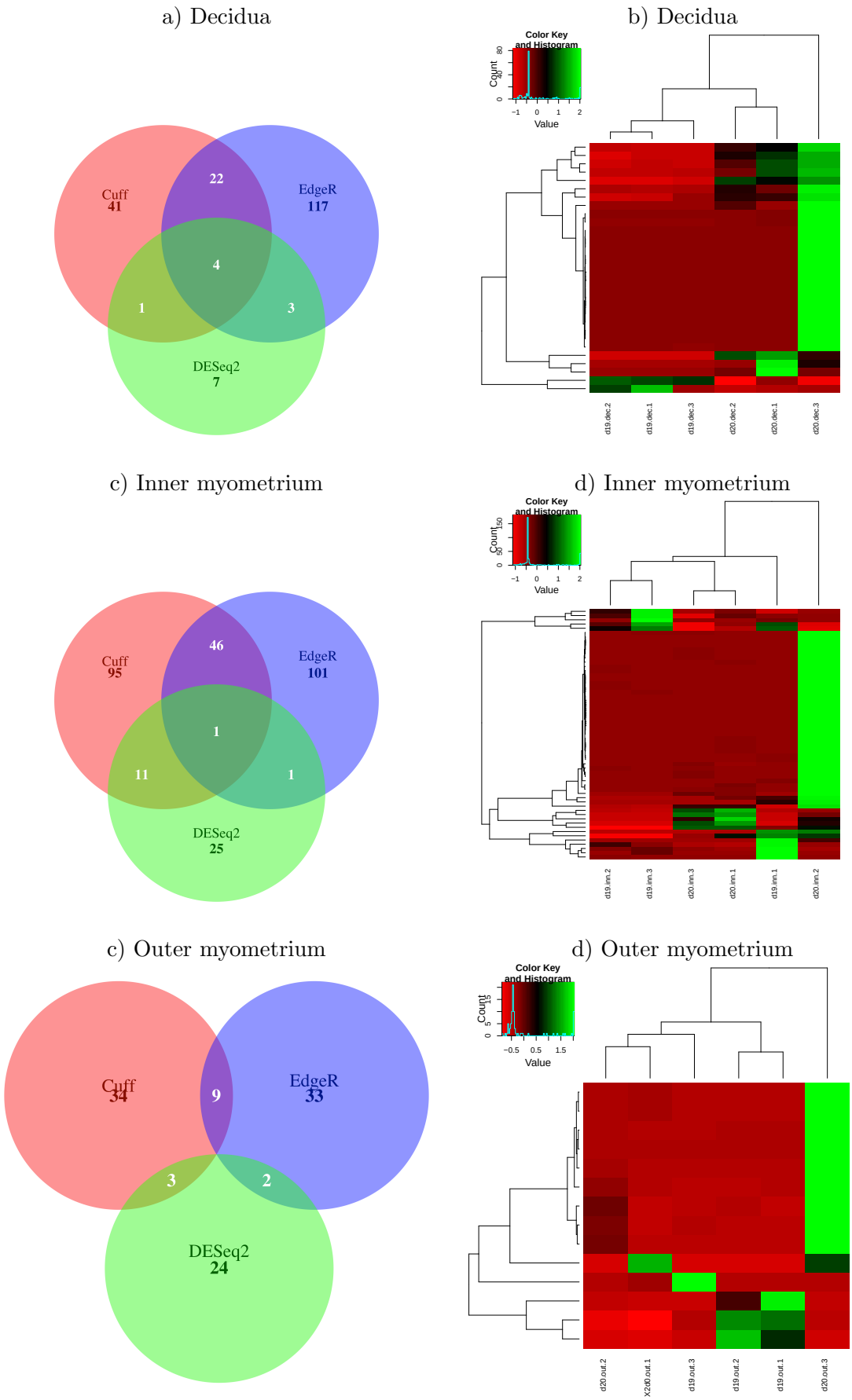

Figure 9.8: Venn diagrams and heat maps of differentially expressed gene transcripts between GD19+6hrs and GD20 in Mifepristone-treated tissues. Gene transcripts were identified as differentially expressed by Cuffdiff (Cuff), edgeR and DESeq2 in the (a–b) decidua, (c–d) inner myometrium, and the (e–f) outer myometrium. Agglomerative hierarchical clustering was used to identify the relationships among the genes and gestational time points. The tissues and gene transcripts are represented by the columns and rows, respectively.

9.2 Effects of Mifepristone

To determine the transcriptomic effects of Mifepristone on rat uterine tissues in late pregnancy, the expression of transcripts obtained from Mifepristone-treated tissues was compared with that of the control tissues that were obtained in Chapter 7. Comparisons were made between tissues obtained 6 hours after treatment (GD19+6hrs), and on the 20^{th} day of gestation (GD). To determine the transcriptional changes that occur during preterm labour in distinct uterine tissues, further comparisons were made between tissues obtained at term (GD22) before labour (NL) in control tissues with Mifepristone-treated tissues obtained on GD20. Cuffdiff, edgeR, and DESeq2 were used to identify transcripts that were differentially expressed between tissues from different treatment groups as described in Section 6.2.2.

9.2.1 GD19+6hrs

When compared to the expression in control tissues obtained on GD19+6hrs, a total of 100, 2, and 22 gene transcripts were identified as differentially expressed by at least two methods in Mifepristone-treated decidua, inner myometrium, and outer myometrium, respectively (Figure 9.9). In the outer myometrium, DESeq2 identified only one transcript as differentially expressed between control and Mifepristone-treated tissues on GD19+6hrs. This one transcript was, however, not discovered by either Cuffdiff or edgeR. A major proportion of the transcripts that were differentially expressed between control and Mifepristone-treated tissues were down-regulated with 92% down-regulated in the decidua, 1 out of 2 in the inner myometrium, and 59% in the outer myometrium. Details of the specific gene transcripts and their mean expression levels, in TPM values (±SD), are given in Supplementary Tables E.9, E.10, and E.11. Clustering of the non-zero z-scores calculated from the TPM values of the differentially expressed transcripts separated the control from the Mifepristone-treated

tissues distinctly in the decidua and inner myometrium, but failed to segregate the tissues by treatment in the outer myometrium as illustrated by the heat maps in Figure 9.9.

9.2.2 GD20

On the GD20, both of the gene transcripts that were differentially expressed between control and Mifepristone-treated decidua samples were down-regulated in response to treatment with Mifepristone (see Supplementary Table E.12). In this case, DESeq2 identified 3, edgeR 5, and Cuffdiff 148 differentially expressed transcripts as illustrated in Figure 9.11a. None of the genes identified by edgeR were identified by the other two methods. In inner myometrium tissue samples, 117 transcripts were identified as differentially expressed between control and Mifepristone-treated samples by at least 2 methods (Figure 9.11c and Supplementary Table E.13), 56% of which were down-regulated in RU486-treated tissues. Of the 54 transcripts that were identified as differentially expressed between control and Mifepristone-treated outer myometrium tissues by at least 2 methods as illustrated in Figure 9.11e, 54% were down-regulated in Mifepristone-treated samples (Supplementary Table E.14). Clustering analysis using non-zero z-scores of the expression levels of differentially expressed transcripts, in transcripts per million (TPM) values, did not separate the tissue treatments distinctly (see Figures 9.11b, 9.11d, and 9.11f for illustrations).

9.2.3 Term vs Pre-term

Pregnant rats that were treated with Mifepristone on GD19, went into labour and delivered on GD20, two days pre-term. The expression of transcripts in non-labouring GD20 Mifepristone-treated samples was compared to that of tGD22(NL) control samples to identify transcriptomic differences therein.

Differential expression analysis between term and pre-term decidua samples identified 133, 82, and 9 significantly different transcripts using Cuffdiff, edgeR, and DESeq2, respectively. As illustrated in Figure 9.11a, three transcripts were detected by all three methods, and a total of 29 gene transcripts were detected by at least two of the differential analysis methods as being significantly different between pre-term and term decidua samples, 93% of which were upregulated in pre-term decidua samples (details in Supplementary Table E.15).

In the inner myometrium, five transcripts were detected by all three differential expression analysis methods as being significantly different between pre-term and term samples. In total, 95 transcripts were detected by at least 2 methods of analysis as being differentially expressed as illustrated in Figure 9.11c. The majority of the differentially expressed transcripts (65%) were upregulated in pre-term samples.

The illustration in Figure 9.11e shows that the least number of differentially expressed transcripts were identified between the pre-term and term outer myometrium samples, where 97 transcripts were detected by Cuffdiff, 38 by edgeR, and 20 by DESeq 2 as significantly different. Only one of these transcripts was identified by all methods, and a robust set of 14 transcripts consisted of transcripts that were detected by at least 2 of the analysis methods. In contrast to the decidua and the inner myometrium, the majority of the differentially expressed transcripts in outer myometrium tissues (85%) were down-regulated in the pre-term samples. Clustering analysis of the pre-term and term non-labouring samples did not segregate the tissues.

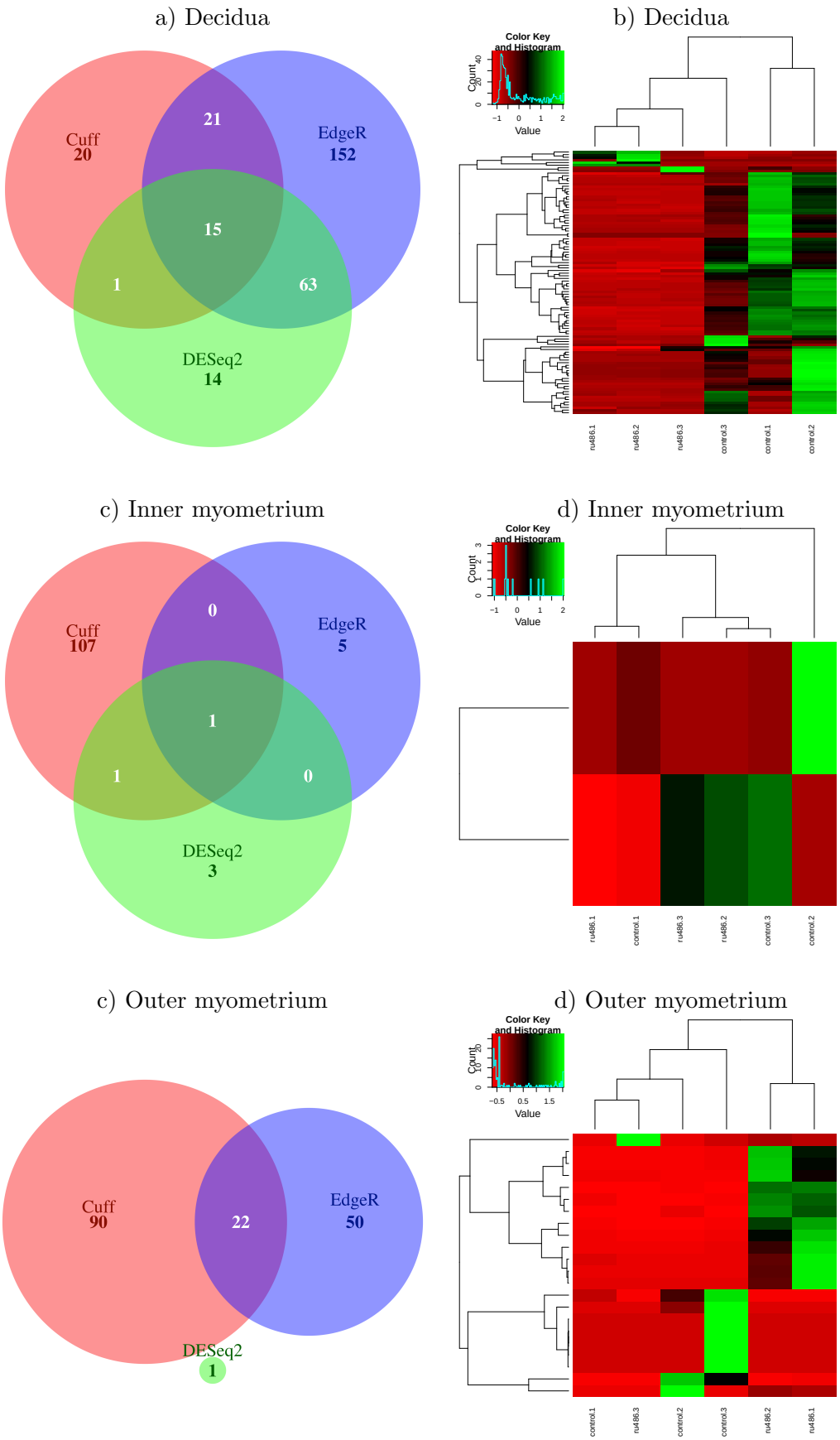

Figure 9.9: Venn diagrams and heatmaps of gene transcripts that were differentially expressed in GD19+6hrs RU486-treated tissues in comparison with GD19+6hrs control tissues. Gene transcripts were identified as differentially expressed by Cuffdiff (Cuff), edgeR and DESeq2 in the (a – b) decidua , (c – d) inner myometrium, and the (e – f) outer myometrium. Agglomerative hierarchical clustering was used to identify the relationships among the differentially expressed genes and gestational time points. The tissues and gene transcripts are represented by the columns and rows, respectively.

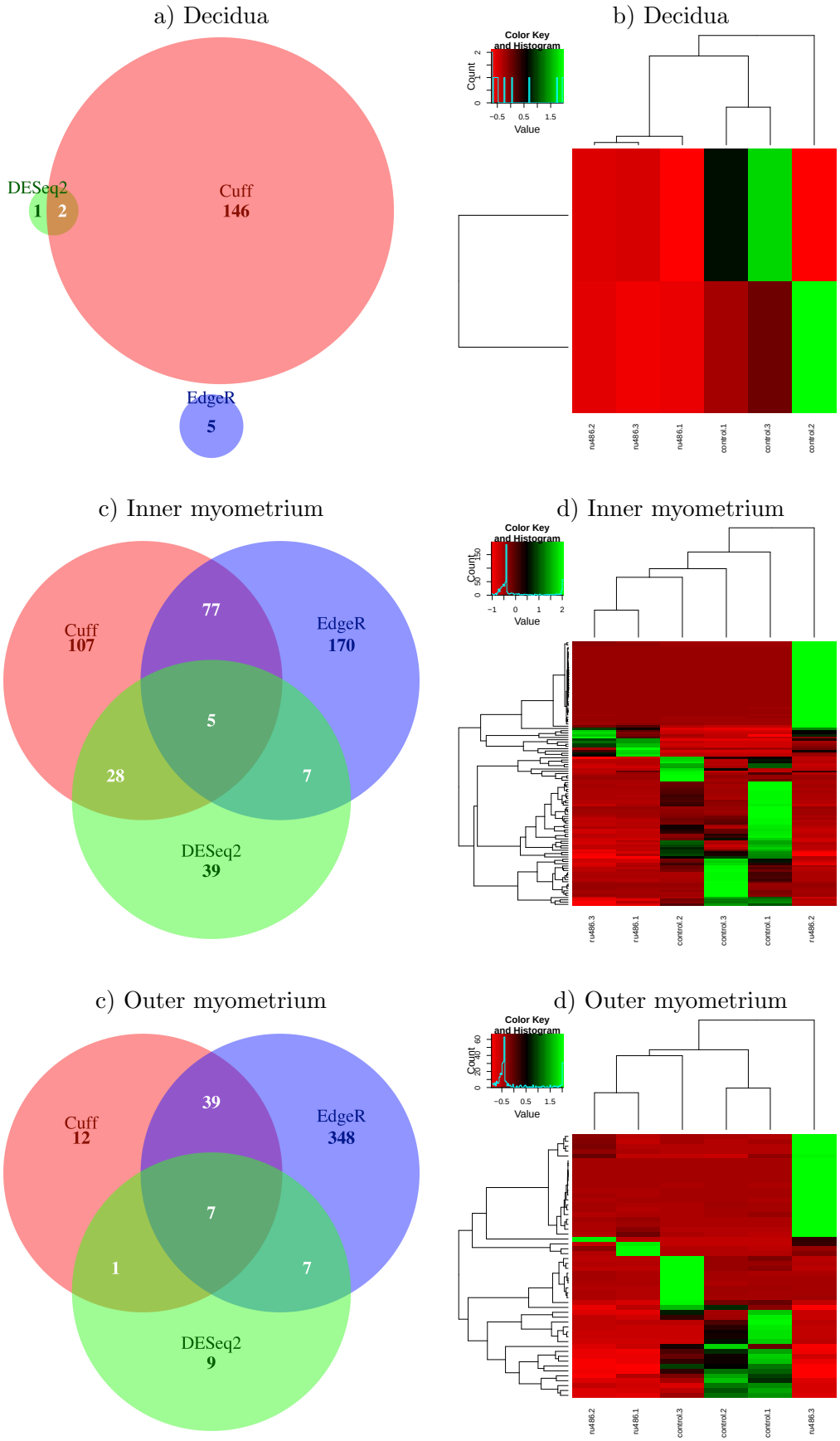

Figure 9.10: Venn diagrams and heatmaps of gene transcripts that were differentially expressed in GD20 RU486-treated tissues in comparison with GD20 control tissues. Gene transcripts were identified as differentially expressed by Cuffdiff (Cuff), edgeR and DESeq2 in the (a – b) decidua , (c – d) inner myometrium, and the (e – f) outer myometrium. Agglomerative hierarchical clustering was used to identify the relationships among the differentially expressed genes and gestational time points. The tissues and gene transcripts are represented by the columns and rows, respectively.

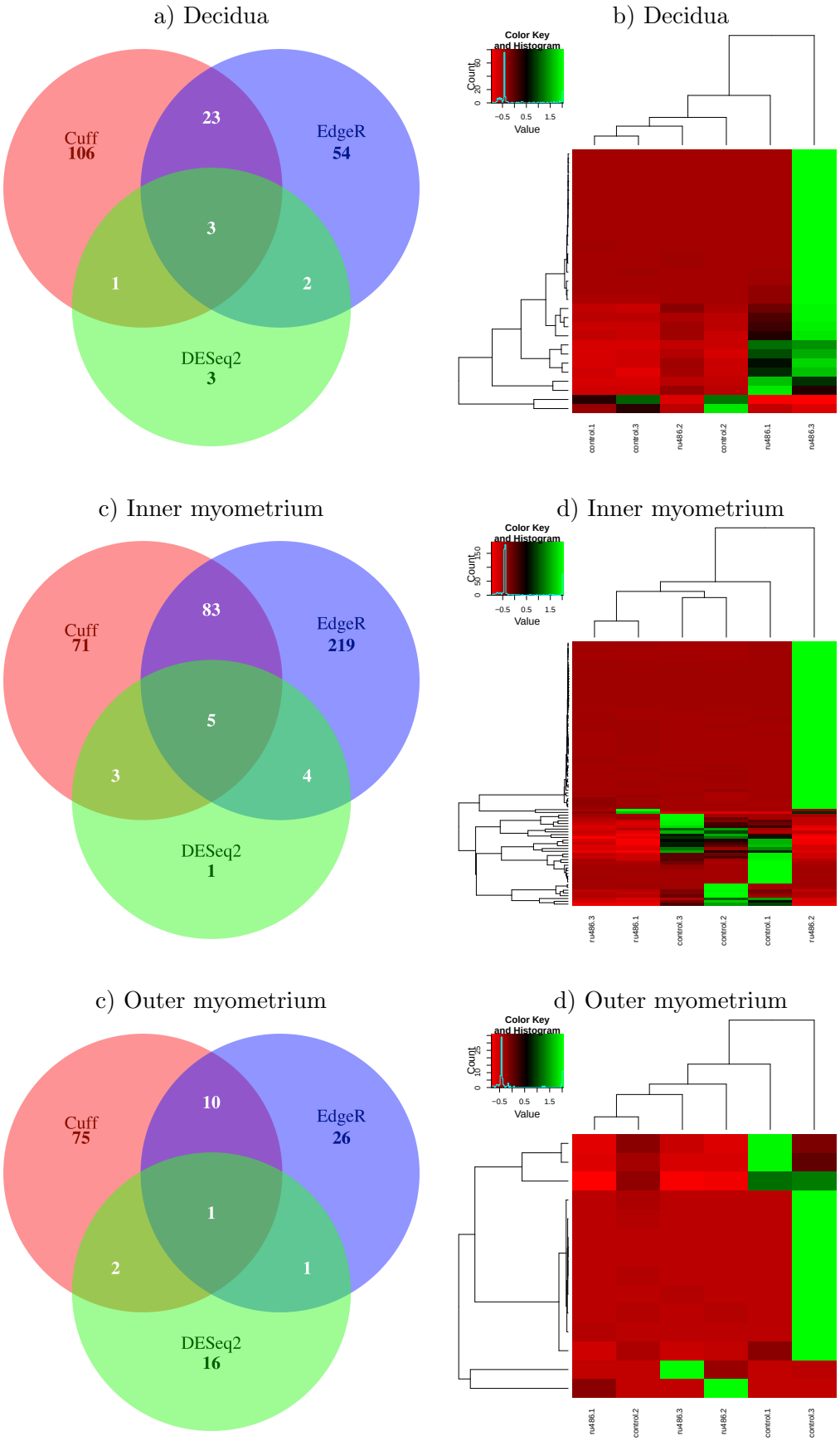

Figure 9.11: Venn diagrams and heatmaps of gene transcripts that were differentially expressed in GD20 RU486-treated tissues in comparison with non-labouring control tissues at term. Gene transcripts were identified as differentially expressed by Cuffdiff (Cuff), edgeR and DESeq2 in the (a – b) decidua , (c – d) inner myometrium, and the (e – f) outer myometrium. Agglomerative hierarchical clustering was used to identify the relationships among the differentially expressed genes and gestational time points. The tissues and gene transcripts are represented by the columns and rows, respectively.

9.3 Summary and Discussion

Preterm labour is a major cause for concern as babies born too early are faced with numerous challenges (Goldenberg et al., 2008). In this chapter, preterm labour was induced through the use of the progesterone receptor antagonist Mifepristone. The data presented in this chapter were obtained from non-labouring animals.

9.3.1 Spatial Expression

The transcripts of typical myometrium genes such as myosin light chain 9 (Myl9) and actin α 2 (Acta2) exhibited higher expression in myometrial tissues in comparison to the decidua. In addition, mRNA encoding Toll-like receptor 8 (Tlr8) were highly expressed in the inner myometrium in comparison to the outer myometrium. Toll-like receptors have been implicated in the onset of labour at term in rodents (Condon et al., 2004) and their presence in myometrial tissues may be an indication of the preparation of the uterus for labour. There were more differences in mRNA expression between the outer myometrium and the decidua, than there were between the inner myometrium and decidua, as evidenced by the numbers of differentially express mRNA transcripts. There was significantly higher expression in the outer myometrium of mRNA transcripts encoding proteins involved in smooth muscle excitation-contraction coupling such as: actin α 1 (Acta1) and Acta2 (Arnoldi et al., 2013); transgelin (Tagln), a member of the calponin family which binds actin (Assinder et al., 2009); tropomyosin 2 beta (Tpm2), basic smooth muscle calponin 1 (Cnn1), Myl9, oxytocin (Oxt), and the oxytocin receptor (Aguilar & Mitchell, 2010; Michal & Schomburg, 2012; El-Mezgueldi, 2014). Only one transcript was significantly different between the inner circular and outer longitudinal layers of the myometrium, suggesting that mRNA expression patterns in both tissues was similar. This, however, is contradicted by the differences in mRNA expression between the respective myometrial layers and the de-

cidua. If expression patterns were indeed similar, one would expect the expression of mRNA transcripts within the myometrial tissues relative to that of the decidua to be similar.

Decidua

Comparison of mRNA expression on GD19+6hrs to that on GD20 in Mifepristone-treated tissues showed an upregulation of genes encoding high density lipoproteins (Apoa1 and Apof), myometrial proteins (Acta2 and Myh11), glycoproteins (Fgb, Fgg, Psg16, and Psg19), haptoglobin (Hp), and histidine decarboxylase (Hdc) among others. The upregulation of Apoa1 in Mifepristone-treated tissues is in line with published literature; Saladin et al. (1996) demonstrated that Apoa1 mRNA is inhibited by mifepristone treatment after treatment with dexamethasone, but is elevated by treatment with Mifepristone alone in the liver. In addition, Kojima et al. (2001) observed that P4 inhibits a Apoa1 action *in-vitro*, and Apoa1 has been identified in endometrial tissues where upregulation of the protein is associated with implantation failure and endometriosis (Brosens et al., 2010). The withdrawal of P4, therefore, leads to the upregulation of Apoa1, whose role in pregnancy and during labour requires investigation. Apof regulates the metabolism of high-density lipoprotein (Paromov & Morton, 2003), but has not been previously identified in uterine tissues. It is reasonable to expect the upregulation of genes encoding Acta2 and Myh11 due to the withdrawal of P4. Their upregulation in the decidua is in line with the published literature; Oliver et al. (1999) smooth-muscle actin is present in decidual stromal cells. Additionally, Winn et al. (2007) observed that Myh11 mRNA expression was upregulated at term in biopsies of the maternal-fetal interface basal plate. The Hdc gene is regulated by P4 in mice (Khatua et al., 2006), and is expressed in uterine tissues (Wood et al., 2000). However, the specific uterine tissue in which the Hdc is expressed had not been previously identified. The data presented in this chapter not only confirms that Hdc is regulated by P4, but also demonstrates that Hdc mRNA is expressed in the decidua in rats. Berkova et al. (2001)

demonstrated that Hp levels are elevated in the decidua. As such, the data presented here support this observation. Hp protein expression has been shown to increase in response to inflammation (Wang et al., 2001). Since preterm labour is associated with inflammation (Goldenberg et al., 2008), the upregulation of Hp mRNA is consistent with an inflammatory response.

9.3.2 Myometrium

Channels and Transporters

The expression of solute carriers has been shown to decrease in response to treatment with Mifepristone in human endometrial biopsies (Catalano et al., 2007). However, non of the solute carriers identified by Catalano et al. (2007) were differentially expressed in the Mifepristone-treated tissues used in the present study. Instead, solute carrier family 13, member 3 (Slc13a3) mRNA was upregulated in preterm decidual samples, while solute carrier family 14 member 1 (Slc14a1) and solute carrier family 17 member 1 (Slc17a1) mRNA expression was upregulated in preterm inner myometrial tissues. In addition, solute carrier family 22, member 3 (Slc22a3) transcripts were upregulated, while solute carrier family 4, sodium borate transporter, member 11 (Slc14a11) transcripts were down-regulated in preterm outer myometrium.

Extracellular Matrix Remodelling

The rupture of fetal membranes prior to the completion of 37 weeks of gestation in humans, known as preterm pre-labour rupture of membranes (PPROM),is known to cause preterm labour (Vadillo-Ortega & Estrada-Gutierrez, 2005). In the present study in which a preterm labour was induced through treatment with Mifepristone, expression of Mmp11

mRNA increased in preterm inner myometrial tissues. An observation which was also made in the myometrium of control samples. In preterm outer myometrial samples, matrix metallopeptidase 1 (Mmp1a), also known as interstitial collagenase, mRNA expression was down-regulated. The down-regulation of Mmp1a contradicts observations made by Lee et al. (2012) and Chan et al. (2014) in which Mmp1 expression was upregulated by PR-knock-down and during labour at term, respectively.

G Protein-coupled Receptors and other Receptors

G protein-coupled receptor 68 (Gpr68) mRNA expression was upregulated in preterm inner myometrial tissues when compared to control tissues of a similar gestational age. Upregulation of Gpr68 mRNA has been previously observed in the human basal plate at term (Winn et al., 2007). As the preterm samples may exhibit some mRNA expression patterns similar to those of samples at term, the observations made in this study are consistent with those of Winn et al. (2007). The data presented here, therefore, indicate that Gpr68 is also expressed in myometrial tissues, specifically in the inner myometrium. Htr1d mRNA levels were upregulated in preterm outer myometrial samples when compared with control GD20 samples, an observation which is inline with observations in control tissues at term (Cohen et al., 1985; Minosyan et al., 2007), indicating that P4 inhibits the expression of Htr1d. When compared to outer myometrial samples at term, Htr2a mRNA levels in preterm inner myometrial samples were low.

Inflammation Response

Apoa1, which is upregulated in Mifepristone-treated tissues is involved in the negative regulation of cytokine secretion involved in immune response, more specifically in the negative regulation of interleukin-1 β secretion. There was upregulation of coagulation factor X

(F10), coagulation factor XI (F11), and coagulation factor XIII, B polypeptide in the inner myometrium preterm (F13b) mRNA in the inner myometrium preterm, a sign of the upregulation of anti-inflammatory molecules. In the decidua, however, coagulation factor II (F2) expression was down-regulated.

9.4 Conclusion

In this chapter, the transcriptome of laser-captured Mifepristone-treated uterine tissues are described, for the first time. Laser-capture microdissection enabled the separation of pure cell samples from heterogenous tissues, thus allowing for the extraction and sequencing of RNA from the decidua, inner circular myometrium, and outer longitudinal myometrium of Mifepristone-treated animals. Mifepristone (RU486) was administered on the 19^{th} day of gestation to induce the withdrawal of progesterone in order enable the identification of those genes whose mRNA transcripts were regulated during the withdrawal of progesterone (P4), and in the events preceding pre-term labour. The first aim of this chapter was to identify the gene transcripts whose expression changed in response to treatment with Mifepristone in the decidua, inner circular myometrium, and the outer longitudinal layer of the myometrium. Distinct spatial patterns of mRNA expression were observed between uterine tissues on GD19+6hrs, as well as on GD20. In addition, changes in transcript expression in response to treatment with Mifepristone in each of the three tissues has been documented in this chapter. The second aim of this chapter was to further elucidate the transcriptional changes that occur during preterm labour in uterine tissues. While data from animals undergoing preterm labour are not presented in this chapter, observations made using animals at the preterm time point augment current knowledge of the processes underlying the onset of pre-term tabour, and will be useful in identifying genes that are regulated by progesterone. As such, the following chapter assesses the effect of treatment with progesterone on the

transcriptomes of uterine tissues, and integrates that information with the data obtained in this chapter, together with data from Chapter 7, to identify progesterone-responsive genes.

Chapter 10

Identification of Progesterone Responsive Genes

In this chapter, the steroid hormone progesterone is used to maintain gestation in rats with the aim of identifying genes whose expression responds to treatment with progesterone. In addition, this chapter aims to identify progesterone-responsive through the integration of sets of genes that are differentially expressed in control tissues, Mifepristone-treated tissues, and P4-treated tissues, as well as regulatory features that are common among the identified P4-responsive genes.

10.1 Transcriptomic Landscape

Approximately 254 million reads were sequenced across libraries from progesterone-treated tissues (Table 10.1), of which 35.36%, 26.37%, and 38.27% were sequenced from decidua, inner myometrium, and outer myometrium libraries, respectively. An average of 14.12 million paired-end reads were sequenced per sample, 82.01% of which were aligned to the reference

Table 10.1: Alignment of sequenced reads to the *Rattus norvegicus* transcriptome and coverage statistics of sequences generated from Progesterone-treated tissues. Gestation - The day during pregnancy on which the uterine sample was collected. **Tissue** - The layer of the uterus that was separated from the other tissues using laser-capture microdissection. The number illustrates the replicate number. **% Aligned** - The proportion of the sequenced reads that were aligned successfully to the *Rattus norvegicus* transcriptome using Tophat2. **% Expressed features** - The proportion of genes to which counts were assigned by HTSeq. **Expressed transcriptome (× covered)** - The number of times the expressed transcriptome was covered by the sequenced reads.

Tissue	Total reads	% Aligned	% Expressed features	Expressed transcriptome (× covered)
Decidua_1	34,722,902	80.60	68.17	10.14
Decidua_2	35,752,903	86.80	68.89	20.26
Decidua_3	19,414,800	83.60	79.43	7.87
Inner_Myo_1	23,564,748	84.90	68.98	10.02
Inner_Myo_2	19,230,640	78.10	75.45	4.72
Inner_Myo_3	24,221,162	82.40	69.53	8.99
Outer_Myo_1	47,866,362	83.90	75.11	29.05
Outer_Myo_2	25,298,650	83.60	72.33	14.80
Outer_Myo_3	24,093,937	74.20	73.49	11.63

genome. Of the aligned reads, 72.37% were assigned a count by HTSeq, and were considered expressed. On average, the expressed transcriptome was covered 13.05× per sample.

10.2 Tissue-dependent Gene Expression

Principal component analysis (PCA) was employed to assess of the variability among P4-treated samples using non-zero mRNA transcript abundances, in transcripts per million (TPM) values as estimated by Sailfish. PCA was conducted as described in Section 6.1 using the princomp function in R. The number of PCs used to assess the relationship among the data were selected as described in Section 6.1.2. The first two PCs, whose cumulative proportion of variance exceeds 85%, were plotted to assess the relationships among the mRNA expression patterns within the decidua, inner myometrium, and outer myometrium (Figure 10.1). The myometrial tissues were separated distinctly, however, one of the decidual samples was not grouped together with the other decidual samples.

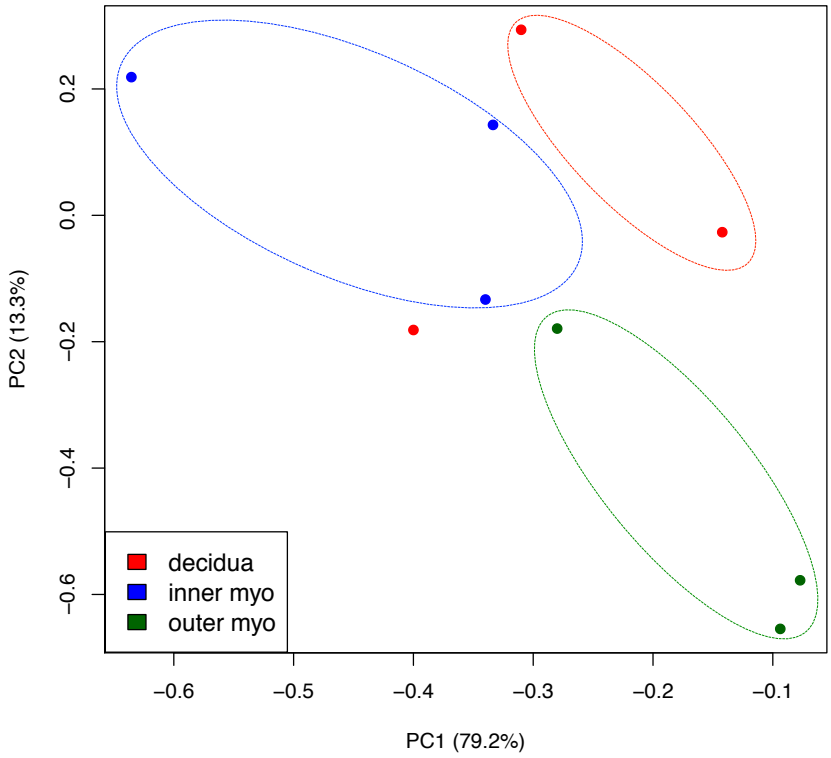

Figure 10.1: Principal component analysis (componentPCA) of P4-treated tissues. PCA was performed on P4-treated samples using transcript per million (TPM) abundances. The variance explained by each of the first three PCs is displayed next to the corresponding PC.

Further analysis was carried out on the sequencing data to determine the expression patterns of gene transcripts in uterine tissues. The Tophat-Cufflinks pipeline was used to generate transcript abundances, in the form of reads per kilo-base per million (RPKM), that were used for differential expression analysis in Cuffdiff. Two other differential expression analysis methods, edgeR and DESeq2, were used in the analysis of count data generated through the Tophat-HTSeq pipeline. To determine significant differential expression of gene transcript, a 5% significance level, a q-value of 5% (Cuffdiff), a false discovery rate (FDR) of 5% (edgeR), or an adjusted p-value of 5% (DESeq2), were used as thresholds. Compared to the decidua, 380, 323, and 258 mRNA transcripts were identified as differentially expressed in the inner myometrium by Cuffdiff, edgeR, and DESeq2, respectively (Figure 10.2). Between the de-

cidua and the outer myometrium, Cuffdiff identified 332 mRNA transcripts as differentially expressed, in comparison to 221, and 114 gene transcripts that were identified by edgeR and DESeq2, respectively. The two myometrial layers had 215, 297, and 58 genes whose transcripts were identified as differentially expressed between them by Cuffdiff, edgeR, and DESeq2, respectively. A final set of differentially expressed genes, which consisted of genes whose transcripts were identified by at least two of the differential analysis methods, are presented in Supplementary Table F.1, Supplementary Table F.2, and Supplementary Table F.3. One hundred and fifty genes were upregulated, while 101 genes were down-regulated in the inner myometrium compared to the decidua. In the outer myometrium, 148 genes were differentially expressed in comparison to the decidua, of which 121 genes were upregulated. Of the 146 genes that were differentially expressed between the myometrial tissues, 92 were upregulated in the outer layer of the myometrium compared to the inner layer.

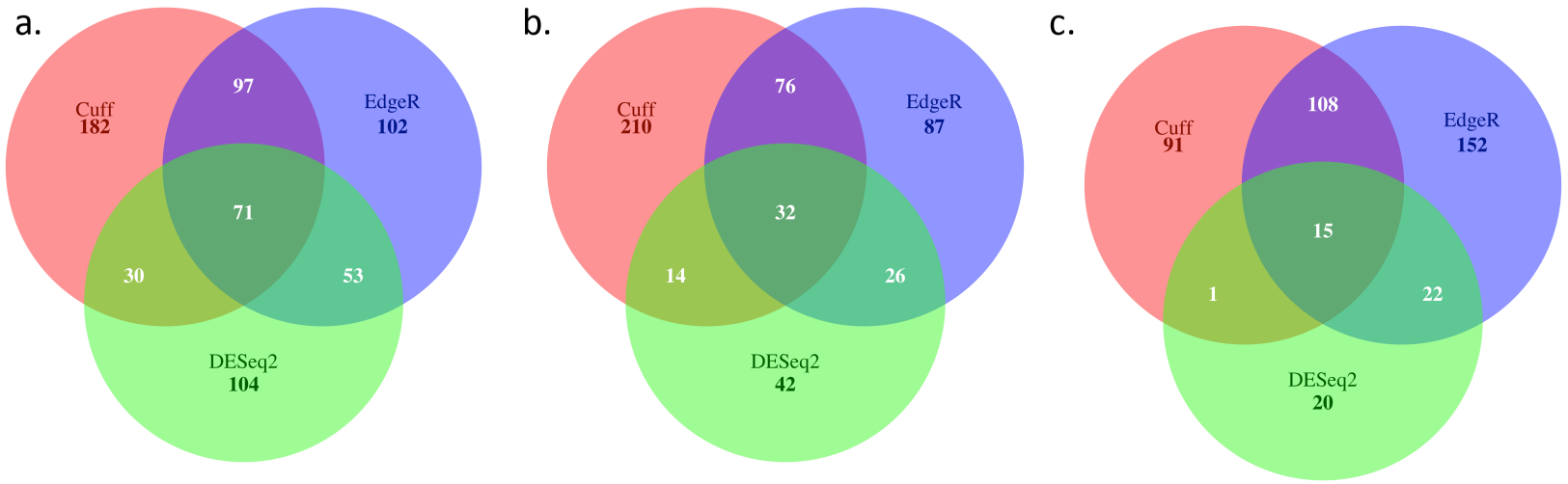

Figure 10.2: Comparison of genes that are differentially expressed between P4-treated tissues. Genes whose transcripts were differentially expressed between the a) decidua and the inner myometrium, b) decidua and the inner myometrium , and the c) inner myometrium and the outer myometrium. **Cuff**: Cuffdiff.

10.3 Early Response to Progesterone Withdrawal

Systemic withdrawal of P4 occurs naturally on GD19. At the first experimental time point, GD19+6hrs, early responses to the withdrawal of P4 may have occurred. To identify the early-response genes, as well as genes that changed due to the progression in pregnancy, but not due to the effects of P4, comparisons of expression levels of genes in control tissues, collected on GD19+6hrs, and P4-treated tissues were made. Analyses were performed using the methods described in Section 10.2. Principal component analysis of the expression values of transcripts (TPM) could not distinguish control samples obtained on GD19+6hrs from P4-treated samples (Figure 10.3), indicating that not many distinguishable changes in mRNA expression had occurred in GD19+6hrs samples even though P4 withdrawal had commenced on GD19.

Further analyses were carried out on the data to identify differential expression of gene transcripts between control samples obtained on GD19+6hrs and P4-treated samples. In the decidua, Cuffdiff, edgeR, and DESeq2 identified 76, 65, and 47 differentially expressed genes, respectively. In the inner myometrium, 115 genes were identified as differentially expressed by Cuffdiff, while edgeR and DESeq2 identified 47 and 34 genes, respectively. Cuffdiff identified the highest number of differentially expressed in the outer layer of the myometrium, 119, in comparison to the 15 genes identified by edgeR, and the 7 genes that were identified by DESeq2 (Figure 10.4).

The three methods: Cuffdiff, edgeR, and DESeq2, identified varying numbers of genes that were differentially expressed. To create sets of genes for further analysis, final sets of differentially expressed genes were created from only those genes that had been identified by at least 2 of the 3 methods (Figure 10.5). The set of genes that were differentially expressed in the decidua contained 49 genes, most of which were down-regulated in the P4-treated decidual tissues (Supplementary Table F.4). There were 62 GO terms were overrepresented

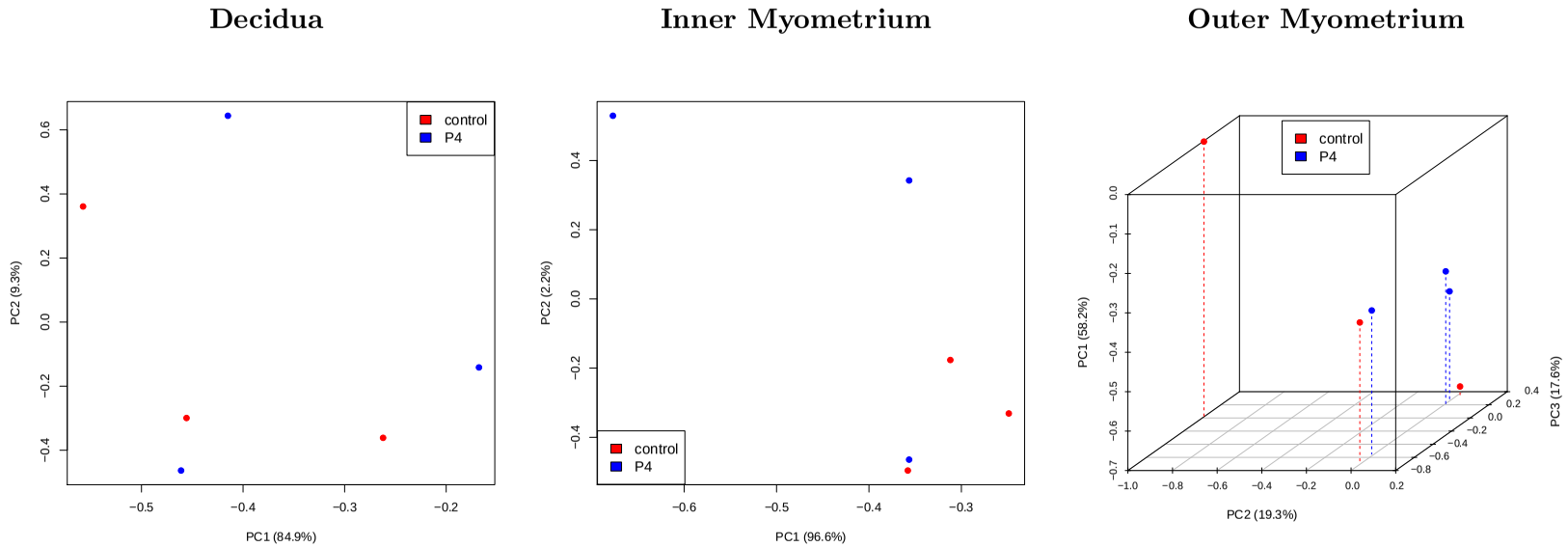

Figure 10.3: Principal component analysis (PCA) comparing control and P4-treated tissues. PCA was performed using transcript per million (TPM) abundances. The variance explained by each of the first three PCs is displayed next to the corresponding PC.

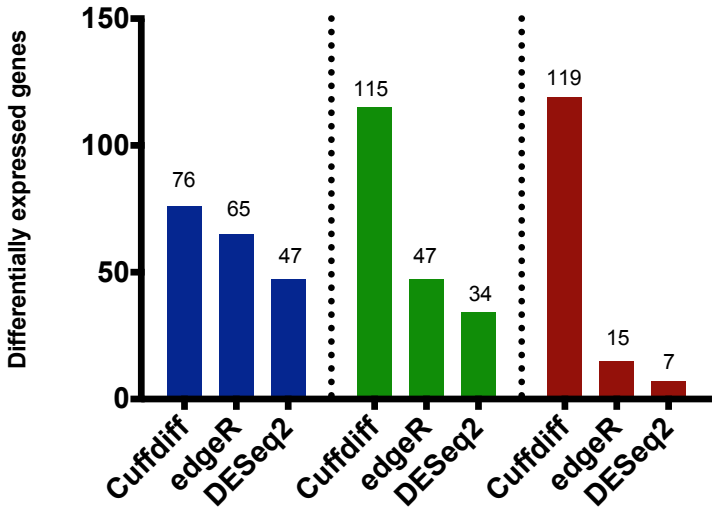

Figure 10.4: Number of differentially expressed between control (GD19+hrs) and P4-treated tissues. Genes were identified in the decidua (blue), inner myometrium (green), and outer myometrium (red) by Cuffdiff, edgeR, and DESeq2.

within the set of upregulated genes (Supplementary Table F.7). Gene ontology analysis of the down-regulated genes identified 371 overrepresented GO terms (Supplementary Table F.8). In the inner myometrium, 31 genes were common among the methods, and 5 of these genes were upregulated in P4-treated tissues (Supplementary Table F.5). GO term analysis of the upregulated genes identified 8 overrepresented GO terms (Supplementary Table F.9), while analysis of the down-regulated genes identified 89 overrepresented GO terms (Supplementary Table F.10). Ten genes were differentially expressed in the outer myometrium, of which 6 were upregulated in response to treatment with P4. GO term analysis of the up- and down-regulated genes did not yield results.

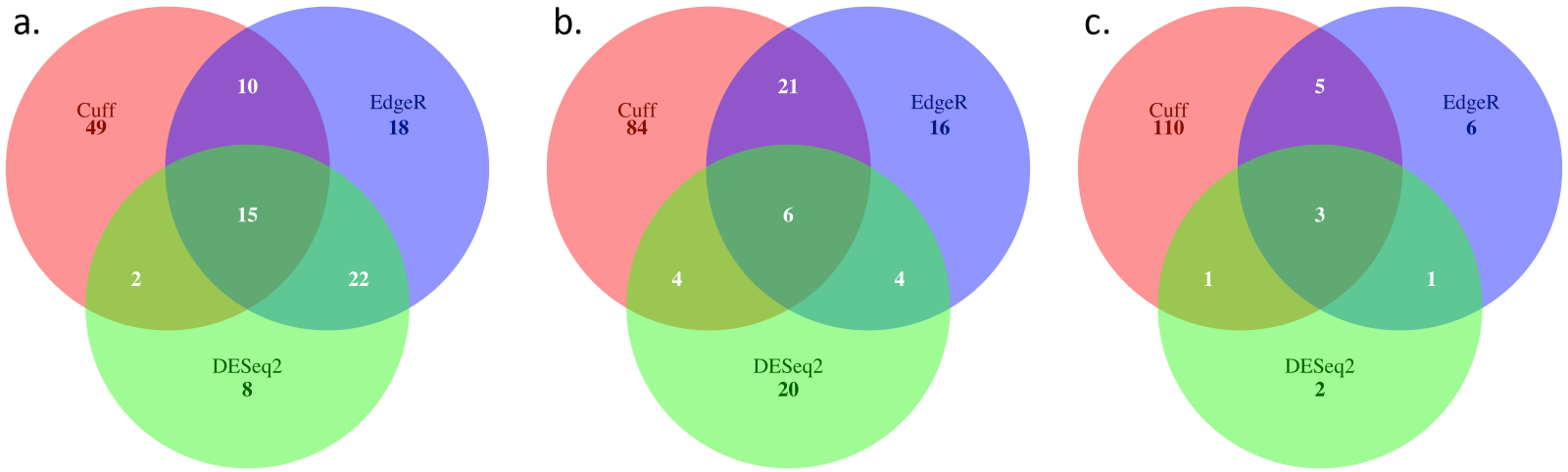

Figure 10.5: Comparison of differentially expressed genes from Cuffdiff (Cuff), edgeR, and DESeq2. Genes were differentially expressed in the a) decidua, b) inner myometrium, and c) outer myometrium between GD19+6hrs control tissues and P4-trated tissues.

10.4 Response to Treatment with Progesterone

Genes that responded to P4 treatment were identified by comparing the levels of expression of genes in control and P4-treated tissues on GD22(NL). PCA analysis was performed as described in Section 6.1 using the princomp function in R. Plots of the PC coefficients did not indicate complete separation of the control samples from the P4-treated samples in the decidua, inner myometrium, and outer myometrium (Figure 10.6).

Genes that were differentially expressed between control GD22(NL) and P4-treated tissues were identified using 3 methods as described in Section 10.2. In the decidua, 142 genes were identified as differentially expressed by Cuffdiff, whereas 149 and 15 genes were identified by edgeR and DESeq2, respectively (Figure 10.7). EdgeR also identified the highest numbers of differentially expressed genes in the inner and outer myometrial tissues of 163 and 283, respectively. Cuffdiff identified 141 differentially expressed genes in the inner myometrium and 261 genes in the outer myometrium, while DESeq2 identified 42 and 135 genes, respectively. On average, more genes were differentially expressed in the outer myometrium (226 ± 80), in comparison to the inner myometrium (115 ± 65), and the decidua (102 ± 75).

Forty-eight genes were identified as differentially expressed by at least two methods in the decidua (Figure 10.8). Of the 48 differentially expressed genes in the decidua, 75% of the genes were upregulated in P4-treated samples (Supplementary Table F.11). Gene ontology analysis of the upregulated genes identified 37 GO terms that were significantly overrepresented, including maternal process involved in female pregnancy (Supplementary Table F.14). The 12 genes that were down-regulated in P4-treated decidua tissues were involved in signalling, regulation of cell migration, and the regulation of action potentials (Supplementary Table F.15).

In the inner myometrium, 78 differentially expressed genes were identified by at least

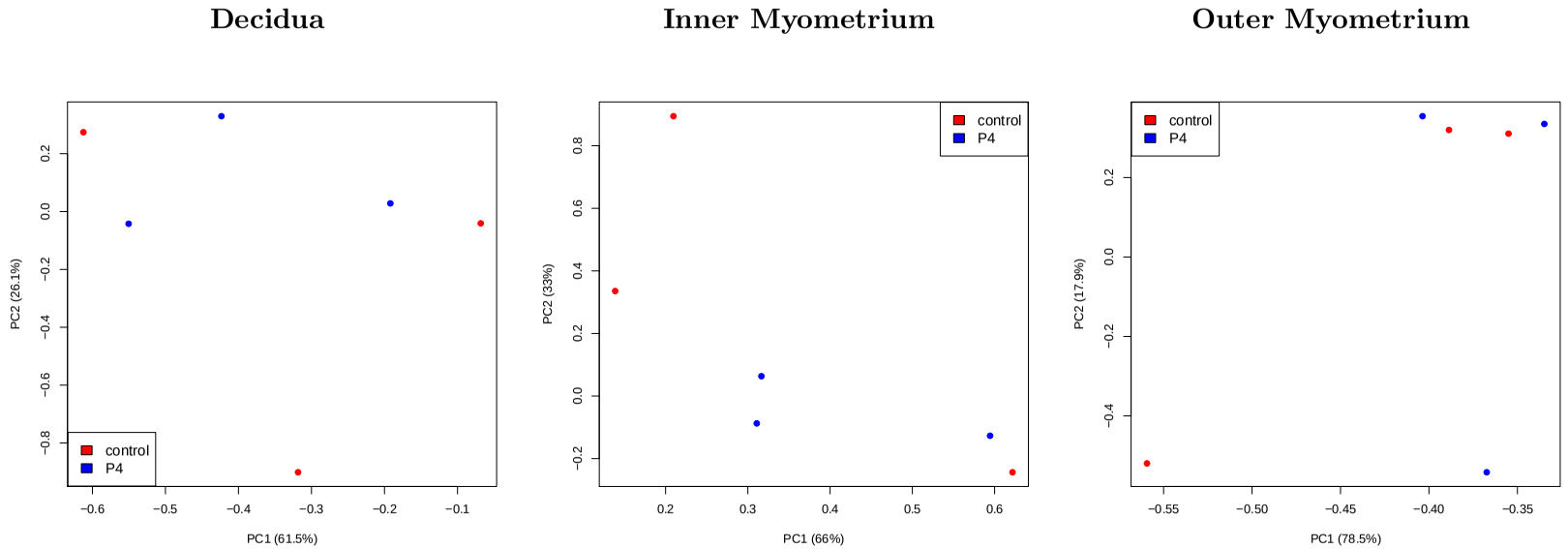

Figure 10.6: Principal component analysis (PCA) comparing control and P4-treated tissues. PCA was performed using transcript per million (TPM) abundances. The variance explained by each of the first three PCs is displayed next to the corresponding PC.

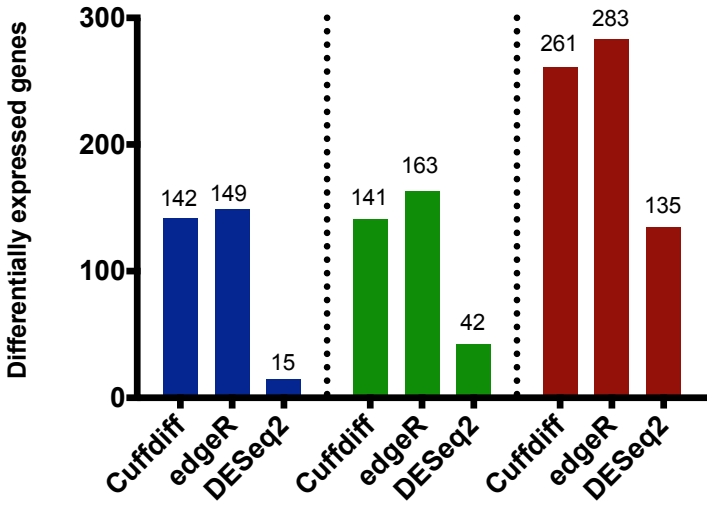

Figure 10.7: Number of genes differentially expressed in response to progesterone treatment. Genes were identified in the decidua (blue), inner myometrium (green), and outer myometrium (red) by Cuffdiff, edgeR and DESeq2.

two methods, 19 of which were upregulated in P4-treated tissues. There were no significantly overrepresented GO terms identified for the up- or down-regulated gene sets. However, the combined set of up- and down-regulated genes identified 2 overrepresented GO terms: female pregnancy (corrected p-value=0.0097), and tissue development (corrected p-value=0.0097).

In the outer myometrium, a final set of 164 genes was considered for further analysis. The set of genes consisted of 41 up- and 123 down-regulated genes (Supplementary Table F.13). The upregulated genes were involved in muscle tissue development, muscle contraction, muscle system process, and the regulation of release of sequestered calcium ions into the cytosol by the sarcoplasmic reticulum (Supplementary Table F.16). A subset of 85 down-regulated genes was used as the test set for GO analysis. Seven overrepresented GO terms were identified (Supplementary Table F.17).

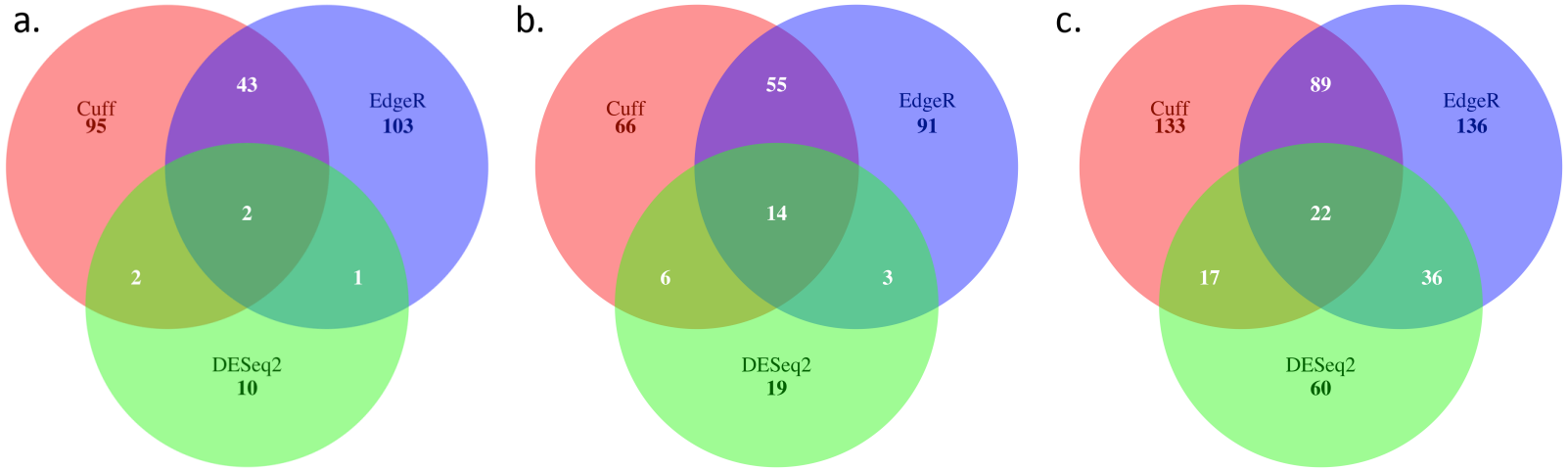

Figure 10.8: Comparison of differentially expressed genes from Cuffdiff (*Cuff*), edgeR, and DESeq2. Genes were differentially expressed in the a) decidua, b) inner myometrium, and c) outer myometrium between control and p4-treated tissues obtained on GD22(NL).

10.5 Regulation of P4 differentially Expressed Genes in Control Tissues

To identify genes that were differentially regulated in P4 and Control treatment groups, genes that were differentially expressed (DE) in P4-treated tissues (P4-DE genes) were compared to the genes that were differentially expressed in control tissues (Control-DE genes).

The number of common genes between Control-DE genes and P4-DE genes in the decidua increased with the progression of gestation in control tissues. There were no genes that were common in the decidua between P4 and GD19+6hrs-GD20 differentially expressed gene sets (Figure 10.9). Unlike the trend of common genes in the decidua, there were biphasic changes in the number of common genes in the inner myometrium, with no common genes between P4-DE genes and GD19+6hrs-GD20 Control-DE genes. Similar to the trend in the inner myometrium, the number of common genes between Control-DE genes and P4-DE genes in the outer myometrium increased between GD20 and GD22(NL), but decreased between GD22(NL) and GD22(L). These data indicate that not all changes that occur at the transcriptomic level during late pregnancy are due to steroid hormone effects.

10.5.1 Regulation Patterns of Differentially Expressed Genes

For each tissue, Control-DE genes at consecutive gestational time points were grouped by their pattern of regulation, such that there were two sets of differentially expressed genes per tissue, i.e., up- and down-regulated gene sets, at each time point. These sets of grouped genes were compared to P4-DE gene sets that were also split into groups of up- and down-regulated genes (Figure 10.10).

In the decidua, three genes were regulated differently between P4-treated samples and con-

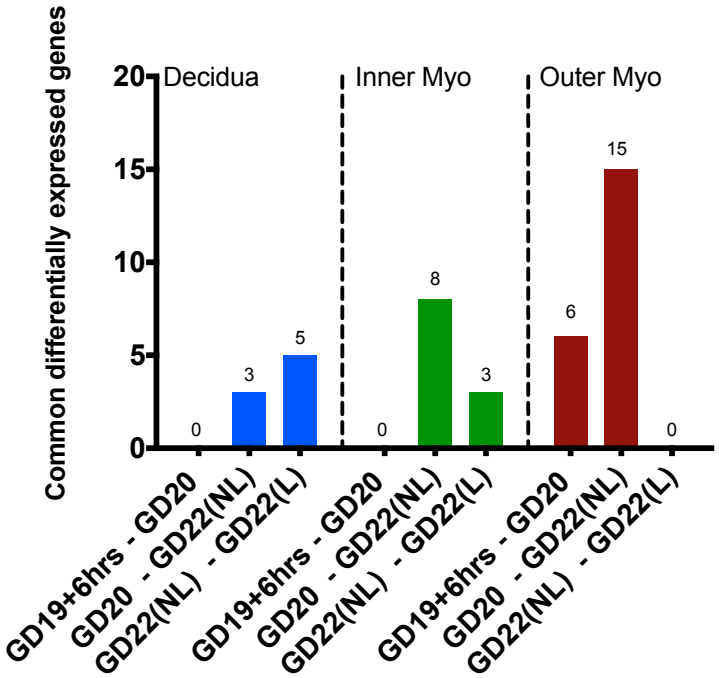

Figure 10.9: Number of differentially expressed genes that are common between P4-treated and control tissues. Comparisons were made between genes that were differentially expressed between GD22(NL) control and P4-treated tissues, and genes that were differentially expressed between consecutive time points in control tissues.

trol samples (Figure 10.10a). The three genes were down-regulated in control samples and up-regulated in P4-treated samples (Table 10.2), and are involved in the positive regulation of biological processes (Supplementary Table F.18).

Table 10.2: Differentially regulated genes in the decidua. Genes that were differentially regulated in the P4-DE gene set and the Control-DE gene set in the decidua.

Symbol	Description	P4 regulation	Control regulation
GD20-GD22(NL)			
Plagl1	pleiomorphic adenoma gene-like 1	UP	DOWN
Alb	albumin	UP	DOWN
Cdh1	cadherin 1	UP	DOWN

In the inner myometrium, 8 genes were differentially regulated in P4-treated samples compared to control samples (Figure 10.10b). The majority of the genes were up-regulated in control samples, while genes encoding cadherin 16 (Cdh16) and collagen type II alpha 1

(Col2a1) were down-regulated in control samples (Table 10.3).

Table 10.3: Differentially regulated genes in the inner myometrium. Genes that were differentially regulated in the P4-DE gene set and the Control-DE gene set in the inner layer of the myometrium.

Symbol	Description	P4 regulation	Control regulation
GD20-GD22(NL)			
LOC685544	hypothetical protein LOC685544	DOWN	UP
Oasl	2'-5'-oligoadenylate synthetase-like	DOWN	UP
Htr2a	5-hydroxytryptamine receptor 2A	DOWN	UP
Tssk6	testis-specific serine kinase 6	DOWN	UP
Cdh16	cadherin 16	UP	DOWN
Col2a1	collagen, type II, alpha 1	UP	DOWN
Cd70	Cd70 molecule	DOWN	UP
Cilp	cartilage intermediate layer protein	DOWN	UP

The highest number of genes that displayed different patterns of regulation between P4-DE genes and Control-DE genes was observed in the outer myometrium (Figure 10.10c). Three genes were down-regulated in control samples but up-regulated in P4-treated samples, while 17 genes were up-regulated in control and down-regulated in P4-treated samples (Table 10.4). The outer myometrium was the only tissue that displayed differing patterns of gene regulation between P4-DE genes and GD19+6hrs - GD20 Control-DE genes.

a. b. c.

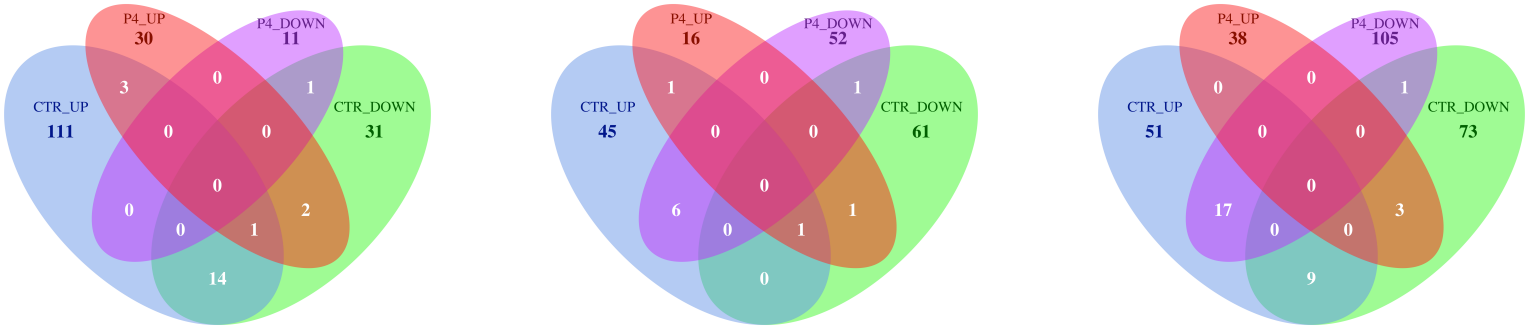

Figure 10.10: Comparison between P4-DE genes and Control-DE genes. Venn diagrams representing the numbers of differentially expressed genes in control and P4-treated samples from a) the decidua, b) the inner myometrium, and c) the outer myometrium.

Table 10.4: Differentially regulated genes in the outer myometrium. Genes that were differentially regulated in the P4-DE gene set and the Control-DE gene set in the outer layer of the myometrium.

Symbol	Description	P4 regulation	Control regulation
GD19+6hrs-GD20			
Zim1	zinc finger, imprinted 1	UP	DOWN
Alcam	activated leukocyte cell adhesion molecule	DOWN	UP
F5	coagulation factor V (proaccelerin, labile factor)	DOWN	UP
Slc10a1	solute carrier family 10 (sodium/bile acid cotransporter), member 1	DOWN	UP
Aadac	arylacetamide deacetylase	DOWN	UP
GD20-GD22(NL)			
Itm2a	integral membrane protein 2A	UP	DOWN
Sgcd	sarcoglycan, delta (dystrophin-associated glycoprotein)	UP	DOWN
Cndp1	carnosine dipeptidase 1 (metallopeptidase M20 family)	DOWN	UP
Ehhadh	enoyl-CoA, hydratase/3-hydroxyacyl CoA dehydrogenase	DOWN	UP
Lgals12	lectin, galactoside-binding, soluble, 12	DOWN	UP
LOC691352	similar to Robo-1	DOWN	UP
Mmp7	matrix metallopeptidase 7	DOWN	UP
Prl3a1	Prolactin family 3, subfamily a, member 1	DOWN	UP
RGD1309676	similar to RIKEN cDNA 5730469M10	DOWN	UP
Slc26a4	solute carrier family 26 (anion exchanger), member 4	DOWN	UP
Tcerg1l	transcription elongation regulator 1-like	DOWN	UP
Cftr	cystic fibrosis transmembrane conductance regulator	DOWN	UP
Cuzd1	CUB and zona pellucida-like domains 1	DOWN	UP
Prom1	prominin 1	DOWN	UP
Wnt7a	wingless-type MMTV integration site family, member 7A	DOWN	UP

10.6 Regulation of P4 Differentially Expressed Genes in Mifepristone-treated Tissues

To identify genes that were regulated differently in response to P4 and Mifepristone treatment, P4-DE genes were compared to genes that were differentially expressed in Mifepristone-treated (RU486-DE) samples (Figure 10.11).

In the decidua, three genes displayed different regulation patterns between P4-treated samples and Mifepristone-treated samples (Figure 10.11a. The genes were up-regulated in P4

and down-regulated in Mifepristone samples (Table 10.5). Gene ontology analysis showed that the gene cadherin 1 (Cdh1) is involved in the regulation of transcription factor import into the nucleus, while the gene erythrocyte membrane protein band 4.1-like 3 (Epb41l3) is involved in cortical actin cytoskeleton organisation, and the gene solute carrier family 4 member 1 (Slco4a1) is involved in thyroid hormone metabolic process (Supplementary Table F.21).

Table 10.5: Differentially regulated genes in the decidua. Genes that exhibited different patterns of regulation between P4-treated and Mifepristone-treated decidua samples.

Symbol	Description	P4	Mifepristone
GD19+6hrs			
Cdh1	cadherin 1	UP	DOWN
Epb41l3	erythrocyte membrane protein band 4.1-like 3	UP	DOWN
Slco4a1	solute carrier family 4(organic cation transporter), member 1	UP	DOWN

There were no genes that exhibited different patterns of regulation between P4 and Mifepristone in the inner layer of the myometrium (Figure 10.11b). In the outer layer of the myometrium, 8 genes were regulated differently in P4 and Mifepristone samples (Figure 10.11c). The genes were up-regulated in Mifepristone-treated samples and down-regulated in P4-treated samples (Table 10.6).

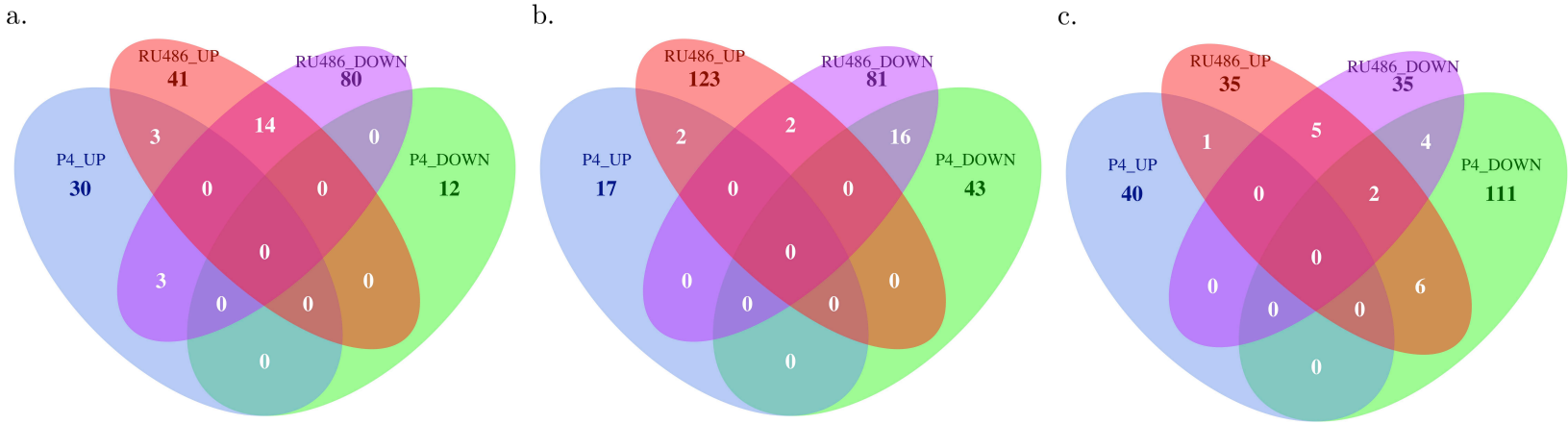

Figure 10.11: Comparison between P4-DE genes and Mifepristone-DE genes. Venn diagrams representing the numbers of differentially expressed genes in P4- and RU486-treated samples from a) the decidua, b) the inner myometrium, and c) the outer myometrium.

Table 10.6: Differentially regulated genes in the outer myometrium. Genes that exhibited different patterns of regulation between P4-treated and Mifepristone-treated samples from the outer layer of the myometrium.

Symbol	Description	P4	Mifepristone
CTR GD19+6hrs vs Mifepristone GD16+6hrs			
Kap	kidney androgen regulated protein	DOWN	UP
Lcn2	lipocalin 2	DOWN	UP
CTR GD20 vs Mifepristone GD20			
Cftr	cystic fibrosis transmembrane conductance regulator	DOWN	UP
LOC171573	spleen protein 1 precursor	DOWN	UP
Prl3a1	Prolactin family 3, subfamily a, member 1	DOWN	UP
Mifepristone GD19+6hrs vs Mifepristone GD20			
Apoa1	apolipoprotein A-I	DOWN	UP
Psg29	pregnancy-specific glycoprotein 29	DOWN	UP
Cldn4	claudin 4	DOWN	UP

10.7 Identification of Common Regulatory Features

The P4-responsive genes identified in the preceding sections were compared to the list of genes whose upstream regions were predicted to contain PR-binding sites as described in Section 6.5 and Section 6.6 to determine whether they contained predicted PR-binding sites. However, non of the P4-responsive genes identified in the present study were found to contain predicted PR-binding sites.

To determine whether common regulatory features, apart from the PR-sites, were present within the groups of P4-responsive genes, upstream regions of the genes, 500, 1000, and 2000 base pairs in length, were analysed. MEME-LaB was used to identify motifs that were enriched within the promoters of P4-responsive genes whose sequences were downloaded from Biomart and repeat masked using RepeatMasker. The repeat-masked sequences were then used as input in MEME-LaB and the results were filtered so that only those motifs that were enriched in at least 25% of the promoter sequences were displayed.

10.7.1 Motifs in 500 bp Promoters

Within the set of decidua promoter sequences, three motifs were enriched (Figure 10.12). Motifs similar to specificity protein 1 (SP1) were present in 84.3% of the regulatory regions of genes that responded to P4-treatment or P4-withdrawal, while the *Drosophila* Hunchback (hb) binding motif was associated with motifs found in 27.7% of the decidual P4-responsive gene promoter sequences. A motif without similarities to any known binding sites was also identified in 29.6% of the regulatory sequences of genes that were responsive to P4 in the decidua. In the inner myometrium, two motifs were enriched in gene promoter sequences, namely the SP1 binding motif in 57.3% of the genes, and the KLF4 binding motif in 55.9% of the genes (Figure 10.13). Two motifs were also identified in the promoter sequences of P4-responsive genes in the outer myometrium (Figure 10.14). Of the two motifs, one was present 64.9% of the regulatory sequences and was found to be similar to two known motifs, i.e., the complementary sequence of the SP1 binding motif, and the Krüppel-like factor 4 (KLF4) binding motif. The second motif was present in 54.3% of the genes, however, no known motifs with similarities to the second motif were identified.

10.7.2 Motifs in 1000 bp Promoters

In promoter sequences that were 1000 base-pairs in length, motifs similar to inhibitor of DNA-binding 1 (ID1) binding, T-box, and hb motifs were present in 55.4% of the promoter sequences of decidua P4-responsive genes (Supplementary Figure F.1). The SP1 binding site was identified in 57.8% of the decidua regulatory sequences while in 43.3% of the sequences, the same motif was present with a higher E-value, 7×10^{-18} compared to 7.7×10^{-46}, and a smaller distance score of 2.9 compared to 8.1. The KLF4 motif was also enriched in 35% of the decidua sequences (E-value = 3.4×10^{-7}). In the inner myometrium, the SP1 and KLF4 binding motifs were enriched in 97.9% of the promoter regions of P4-responsive genes

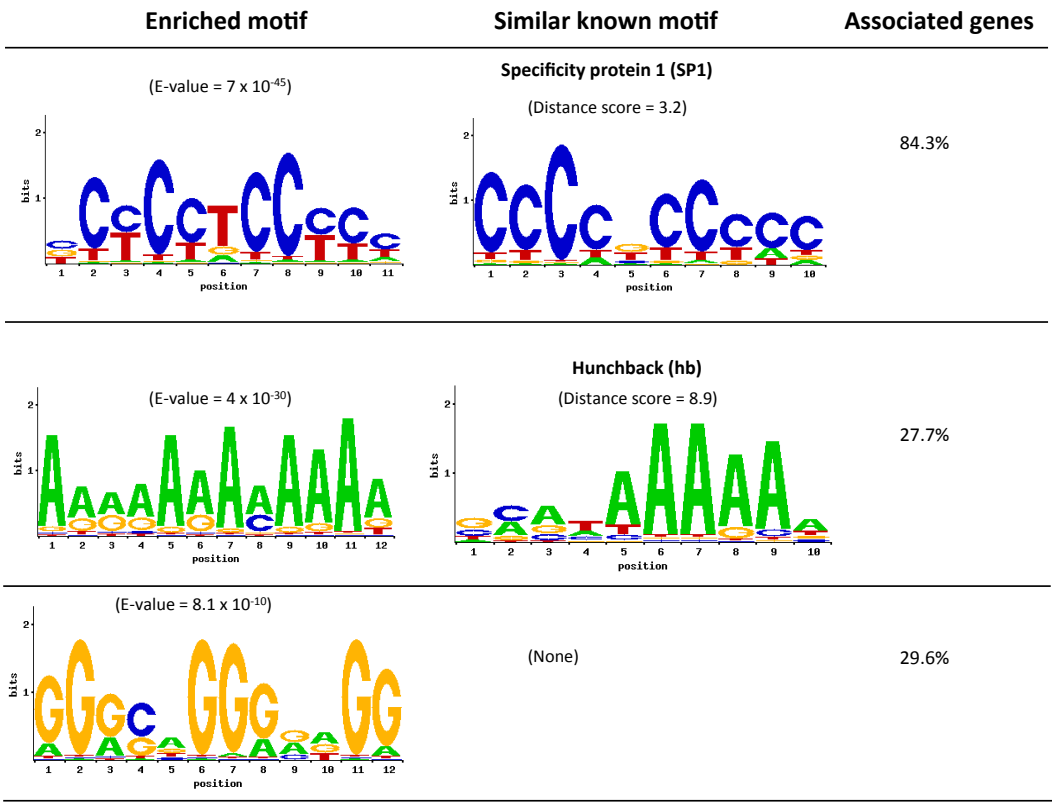

Figure 10.12: Motifs identified in genes that were responsive to progesterone in the decidua. MEME-LaB was used to identify motifs that were enriched within promoter regions of P4-responsive genes in the decidua. The promoter regions were 500 nucleotides in length.

(Supplementary Figure F.2). Motifs similar to SP1 and KLF4 were detected in regulatory sequences of P4-responsive genes in the outer myometrium, with SP1 and KLF4 motifs contained in 55.2% and 64.9% of the sequences, respectively (Supplementary Figure F.3).

10.7.3 Motifs in 2000 bp Promoters

When 2000 bp promoter regions of P4-responsive genes were assessed for motif enrichment, motifs similar to ID1, hb, SP1, and Spi-1 proto oncogene (SPI1) were identified in the promoter regions of decidual P4-responsive genes (Supplementary Figure F.4). In the set of promoter regions of inner myometrial P4-responsive genes, motifs similar to SP1 and KLF4 were identified in 52.4% of the genes with an E-value of 1.5×10^{-35} and 1.5×10^{-14}

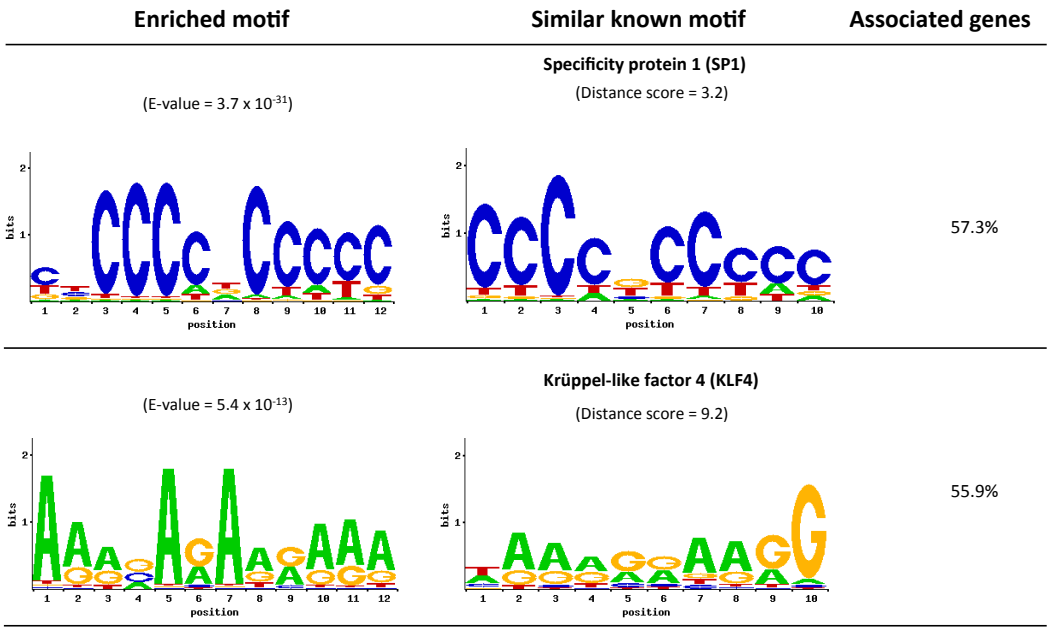

Figure 10.13: Motifs identified in genes that were P4-responsive in the inner myometrium. MEME-LaB was used to identify motifs that were enriched within promoter regions of P4-responsive genes in the inner myometrium. The promoter regions were 500 nucleotides in length.

(Supplementary Figure F.5). In the promoter regions of 97.9% of the outer myometrial P4-responsive genes, motifs similar to SP1 and KLF4 were also identified, but with an E-value of 1.3×10^{-8} (Supplementary Figure F.6).

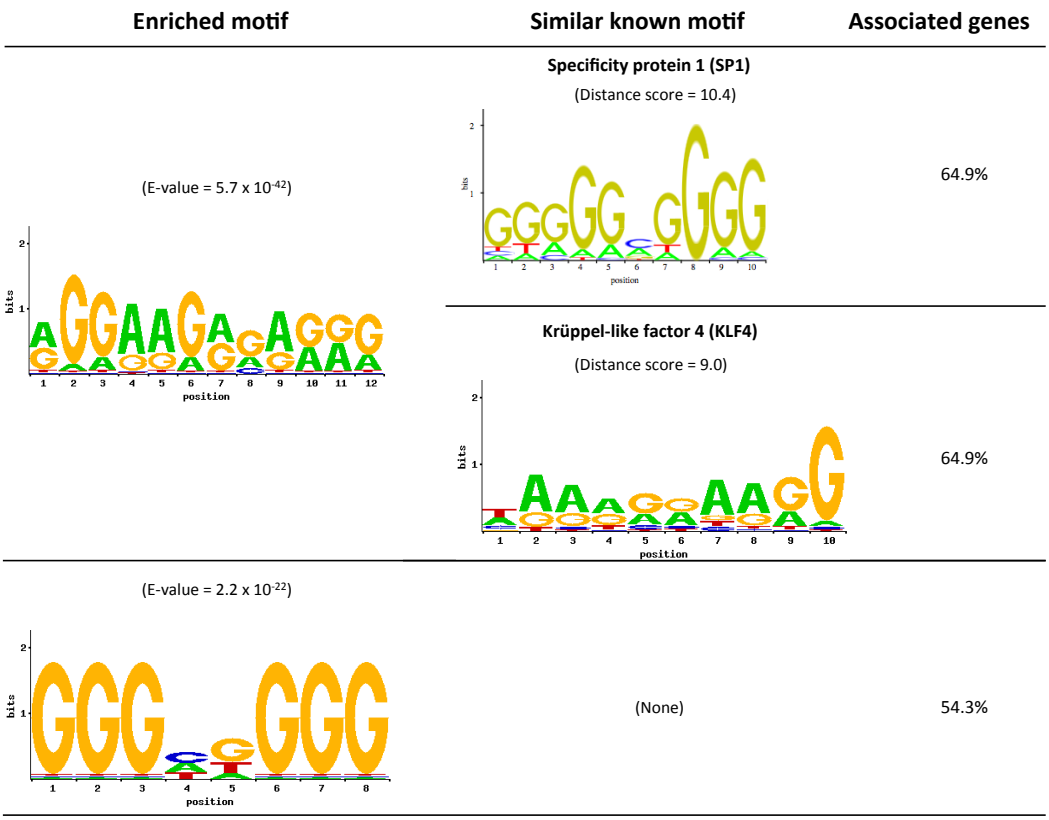

Figure 10.14: Motifs identified in genes that were responsive to progesterone in the outer myometrium. MEME-LaB was used to identify motifs that were enriched within promoter regions of P4-responsive genes in the outer myometrium. The promoter regions were 500 nucleotides in length.

10.8 Random Occurrence of Motifs in the Uterus

To check whether the enrichment of motifs was due to P4-response and not random occurrence, 10 sets of genes were selected at random and analysed for motif enrichment. A total of 125 genes per set were selected at random from the whole set of genes that were expressed in the uterine transcriptome. Sequences of the upstream regions of the selected genes were obtained and masked for repeats as described in Section 6.7.1, and analysed in MEME-LaB. Motifs that occurred in at least 25% of the genes in a set were counted. The SP1 motif was enriched in 9 of the 10 sets of genes, while the KLF4 motif was enriched in 5 and ID1 motifs were not enriched in any of the gene sets (Supplementary Figure F.7). These

findings suggest that the SP1 motif may be present in the regulatory regions of numerous genes and is, therefore, not unique in P4-responsive genes. Additionally, the presence of the KLF4 motif in half the sets of randomly selected genes may indicate that this motif is also present in numerous regulatory regions. Since ID1 was not found in any of the randomly selected gene sets, it may be a good candidate for the common regulatory factor among P4-responsive genes.

10.9 Significance Testing of Motifs

Motifs in the promoter regions of P4-responsive genes, which had been masked for repeats, were tested for significant enrichment as described in Section 6.7.3. The overrepresented motifs identified within the regulatory regions of the P-4 responsive genes are summarised in Table 10.7. Of the motifs that were identified in Section 10.7, only KLF4 was identified as statistically significant in P4-responsive decidual genes with 1000 bp- and 2000 bp-promoter regions. In addition, motifs similar to hepatocyte nuclear factor 4 alpha (Hnf4a), Nuclear Receptor Subfamily 1, Group H, Member 2: Retinoid X receptor alpha (NR1H2:RXRA), Nuclear Receptor Subfamily 2 Group F Member 1 (Nr2f1) were identified in promoter regions that were 500 bp, 1000 bp, and 2000 bp of decidual P4-responsive genes, respectively. Motifs similar to heart and neural crest derivatives-expressed protein 1: transcription factor E2A (Hand1:Tcfe2a) and peroxisome proliferator-activated receptor γ (Pparg) were identified in 500 bp- and 1000 bp-promoters of inner myometrial P4-responsive genes, respectively. While motifs similar to Hnf4a and macrophage-1 antigen (Mac1) were significant in outer myometrial regulatory regions that were 500 bp and 1000 bp long, respectively.

Table 10.7: Statistically significant motifs identified within groups of progesterone-responsive genes. The hypergeometric test was used to assess the statistical significance of motif enrichment. **myo**: myometrium.

Promoter length	Tissue	Statistically significant motif
500 bp	Decidua	Hepatocyte nuclear factor 4 alpha (Hnf4a)
	Inner myo	Heart and neural crest derivatives-expressed protein 1: transcription factor E2A (Hand1:Tcfe2a)
	Outer myo	Hepatocyte nuclear factor 4 alpha (Hnf4a)
1000 bp	Decidua	Hepatocyte nuclear factor 4 alpha (Hnf4a) Nuclear Receptor Subfamily 1, Group H, Member 2: Retinoid X receptor alpha (NR1H2:RXRA) Krüppel-like factor 4 (KLF4)
	Inner myo	Peroxisome proliferator-activated receptor γ (Pparg)
	Outer myo	Macrophage-1 antigen (Mac1)
2000 bp	Decidua	Nuclear Receptor Subfamily 2 Group F Member 1 (Nr2f1) Nuclear Receptor Subfamily 1, Group H, Member 2: Retinoid X receptor alpha (NR1H2:RXRA) Krüppel-like factor 4 (KLF4)

10.10 Summary and Discussion

P4 plays a major role in the maintenance of pregnancy in mammals (Blanks & Brosens, 2012). To help identify those gene transcripts whose expression is modulated by P4, pregnant rats were treated with P4. Pregnancy in P4-treated animals was maintained beyond term, providing further credence to the role of P4 in the maintenance of pregnancy.

10.10.1 Extracellular Matrix Remodelling

P4 has been shown to suppress matrix metalloproteinase (Mmp) activity in uterine tissues (Epstein et al., 1998), as such, the regulation of Mmps in P4-treated tissues is expected to differ from that of control tissues. In the decidua, Mmp11 mRNA levels were down-regulated in P4-treated samples. Mmp11 has not been previously associated with the onset of labour,

however, this may be due to Mmp11 levels in the decidua dropping prior to term. Analysis of earlier time-points during gestation may provide more information on the expression patterns of Mmp11 mRNA. In line with the observations made in control tissues (Girotti & Zingg, 2003; Salomonis et al., 2005), the gene encoding Mmp7 was down-regulated in P4-treated outer myometrium samples as opposed to the upregulation observed in control tissues of a similar gestational age. The expression of Mmp16 mRNA was upregulated in the outer myometrium in comparison to control tissues. While Catalano et al. (2007) observed an increase in Mmp16 expression following treatment with Mifepristone, these observations are incomparable with those made in the current study as the observations of Catalano et al. (2007) were made in endometrial samples.

10.10.2 Channels and Transporters

Potassium (K^+) channels are involved in regulating the contractility of SMCs during pregnancy (Wray et al., 2014). As such, their expression was expected to be regulated by treatment with P4. In the present study, upregulation of K^+ channel subfamily K member 2 (Kcnk2), also known as Trek-1, mRNA expression was observed in P4-treated inner myometrial tissues when compared with control tissues. Since pregnancy in P4-treated animals is maintained while the pups continue to grow, even if the pregnancy is left to persist beyond GD25, the uterine walls in these animals are subjected to immense stretch. Thus upregulation of Kcnk2 channels that were shown to be upregulated by stretch (Monaghan et al., 2011; Heyman et al., 2013) and down-regulated during labour (Buxton et al., 2010) the myometrium, is consistent with the literature. In addition, the data presented in this thesis shows that Kcnk2 channels are expressed in the inner myometrium. Conversely, K^+ intermediate/small conductance Ca^{2+}-activated channel subfamily N member 2 (Kcnn2) mRNA levels were significantly down-regulated in P4-treated myometrial tissues, indicating that Kcnn2 proteins are required for SMC contraction. This is consistent with the expres-

sion of Kcnn2 protein observed in pregnant rats by Noble et al. (2010), whereby Kcnn2 protein expression increased between GD21 and term-labouring samples.

The expression of mRNA encoding solute carrier was significantly different in P4-treated tissues in comparison to control tissues. Solute carrier family 26 (anion exchanger), member 4 (Slc26a4) mRNA expression was down-regulated in P4-treated tissues and upregulated in control tissues at term in the outer myometrium. The gene encoding solute carrier family 4 member 1 (Slc4a1), which is involved in thyroid hormone metabolic process, was upregulated in P4-treated but down-regulated in GD19+6hrs control decidual samples. In line with the observed down-regulation of aquaporin 8 (Aqp8) in the uterus at term and during labour (Helguera et al., 2009), a decrease in the expression of Aqp8 mRNA was observed in Mifepristone-treated decidual samples in comparison to control samples. In addition, Aqp8 mRNA levels decreased significantly on GD19+6hrs in control tissues when compared to P4-treated tissues. Thus Aqp8 responds early to the withdrawal of P4.

10.10.3 G Protein-coupled Receptors

Since serotonin receptors are upregulated in the myometrium of control tissues at term, It is reasonable to expect that treatment with P4 will result in a decrease in serotonin receptor mRNA expression. Htr1d and Htr2a mRNA expression levels were down-regulated in P4-treated inner myometrial samples when compared with control tissues of the same gestational age as expected.

10.10.4 P4-responsive Genes

P4-responsive genes were identified by integrating groups of genes whose transcripts were identified as differently expressed with the progression of pregnancy, in response to treat-

ment with P4, and treatment with Mifepristone. Genes that were differentially regulated between P4-treated and Mifepristone-treated tissues, as well as those genes that were differently regulated between control tissues and Mifepristone-treated tissues, were considered P4-responsive. The identified genes were involved in the regulation of transcription factor import into the nucleus, cortical actin cytoskeleton organisation, and the positive regulation of intracellular transport among others. Within the groups of P4-responsive genes, motifs similar to SP1, hb, ID1,T-box, KLF4 , and SPI1 binding motifs were found in at least 25% of P4-responsive genes in the decidua. However, of these motifs, only the KLF4 binding motif was identified as significantly enriched in decidual P4-responsive genes. It is proposed, therefore, that KLF4 mediates the action of PR in the decidua during late pregnancy. There are no agreements between motif-search results and significant overrepresentation results in either the inner or outer myometrial layers, indicating that the transcriptional changes occurring in myometrial tissues during late pregnancy are not driven entirely by P4-PR signalling.

10.11 Conclusion

This chapter set out to identify and document the effects of progesterone treatment on the transcriptome of uterine tissues during late pregnancy. Gene transcripts that tend to be upregulated in late pregnancy and at term, were down-regulated in P4-treated tissues, while the same was observed for those transcripts whose expression is down-regulated in late pregnancy and at term. In addition, this chapter brought together work that was presented in previous chapters, Chapter 7 and Chapter 9, in the identification of transcripts that were differentially regulated between P4-treated and control tissues, as well as between P4- and Mifepristone-treated tissues. These transcripts, were identified and documented, as per the second aim of this thesis. Regions that are upstream of genes whose transcripts

were differentially regulated, were assessed for common regulatory features, and a candidate was identified as regulating the signalling of progesterone in decidual tissues. The following chapter is a general discussion of this thesis.

Chapter 11

General Discussion

Preterm birth remains one of the major causes of health problems in infants, and infant death (Goldenberg et al., 2008). The steroid hormone progesterone is known to play a major role in maintenance of pregnancy in mammals. Progesterone exerts its effects through both genomic and non-genomic mechanisms. Following on from the work conducted by Garfield et al. (2012), it was hypothesised that the effect of progesterone on the uterus are genomic. As such, an analysis of the effects of progesterone, and its withdrawal, on the pregnant expression of genes in uterine tissues will augment current knowledge of the processes preceding the onset of labour at term and preterm. To investigate the effect of progesterone on the uterus, a rat model of the pregnant uterus was utilised. Animals were treated with progesterone and Mifepristone, and the changes resulting from treatments were analysed. Laser capture microdissection was used to isolate homogeneous decidual and myometrial tissues. High-throughput sequencing was used to measure the abundance of transcripts within laser-captured tissues, which were subsequently analysed for differential expression in late pregnancy, during labour, and in response to progesterone and Mifepristone treatment.

While transcriptomic studies of rat uterine tissues have been conducted in the past (Girotti & Zingg, 2003; Arthur et al., 2008; Helguera et al., 2009), the work presented in this thesis differs in that: the decidual, inner myometrial, and outer myometrial layers of the uterus were separated by laser-capture microdissection, and transcriptional changes occurring therein analysed separately; spatial assessment of transcript abundance was assessed; and a deep (high-throughput) sequencing technique was used to determine the abundance of transcripts within tissues. Sequencing of the transcriptome is one of the high-throughput sequencing methods that can be used to expand the knowledge on the underlying molecular processes of a system. The combination of high-throughput sequencing and the profiling of expressed gene transcripts was used to identify those genes whose transcription changes in response to progesterone withdrawal and treatment. The use of high-throughput sequencing technologies not only enables the understanding of the processes that underlie the onset of labour at term, or preterm, but also allows the identification of potential therapeutic targets.

Working under the hypothesis that the effects of progesterone on uterine tissues are genomic, this thesis began by assessing the transcriptional landscape of control tissues in late pregnancy in Chapter 7. Of particular interest were those changes that occurred following the natural systemic withdrawal of progesterone, hence tissues obtained after the time-point at which progesterone withdrawal commences were utilised in the study. The expressed transcriptome was covered 14-times on average, indicative of sequencing depth that is sufficient for the detection of all the mRNA transcripts within tissues. Unique transcript expression patterns within uterine tissues were identified with one particular transcript being expressed predominantly in the inner myometrium. As such, it was hypothesised that the protein coded for by this transcript, tenascin n, was inner myometrial-specific and could be used to differentiate the inner layer of the myometrium from the outer layer of the myometrium. Immunohistochemical staining for the tenascin n protein provided further evidence support-

ing this hypothesis. Another hypothesis, proposing that thyrotropin-releasing hormone is a decidual marker in late pregnancy, was put forward based on the spatial expression patterns of transcripts encoding thyrotropin-releasing hormone. While this hypothesis was supported by immunohistochemical staining for thyrotropin-releasing hormone in late pregnancy, at term and during labour, the hormone was expressed in all the three tissues under study. As such, thyrotropin hormone, which stimulates the release of the decidual marker prolactin by the pituitary (Molitch, 2009), may be considered to be a decidual marker during late pregnancy but not at term or during labour. In addition to uniquely expressed mRNA transcripts, transcripts whose expression is spatially different were identified. Furthermore, within each uterine tissue, changes in mRNA expression patterns were identified. While some of the differential expression findings were consistent with published literature, comparisons were not easy to make as this is the first study in which the uterine layers have been studied separately.

Further assessment of mRNA transcript expression was conducted in Chapter 8, whereby the expression of transcripts encoding contraction-associated proteins and myometrial proteins were delineated. Here it was also noted that mRNA transcript expression patterns in the two myometrial layers were different. While some of the patterns of expression in the myometrial layers are consistent with published literature, the fact that previous studies have tended to assess mRNA expression while treating both layers of the myometrium as a single unit makes it difficult to draw any meaningful conclusions. An attempt to validate the RNAseq data with qPCR was unsuccessful as the majority of the mRNA expression patterns observed relative to β-actin were inconsistent with RNAseq findings. This calls for further investigation and perhaps the use of more than one housekeeping gene.

The next chapter in the thesis identified and documented the transcriptional changes that occurred due to induced progesterone withdrawal. Here, a time-point at which animals went into labour preterm was used to assess the transcriptional changes preceding preterm

labour. While mRNA transcripts were differentially expressed in response to treatment with the progesterone receptor antagonist Mifepristone, these changes cannot be attributed to the withdrawal of progesterone alone as Mifepristone is also a glucocorticoid receptor antagonist. As such, the data generated in this chapter, and that from Chapter 7 were used in Chapter 10 to identify a set of "true" progesterone-responsive genes in late pregnancy and during labour.

Chapter 10 began by identifying and assessing the differences in mRNA expression between progesterone-treated and control tissues. The genes whose transcripts were differentially expressed between progesterone-treated and control samples were then compared to the sets of genes identified in Chapter 7 and Chapter 9. Those differentially expressed genes that were regulated differently in Chapter 7 and Chapter 9, in comparison to the regulation pattern of genes in progesterone-treated tissues were proposed to be the set of progesterone-responsive genes in late pregnancy. While the proposed progesterone-responsive genes were found not to contain predicted progesterone receptor binding sites within their regulatory regions, conducting chromatin immunoprecipitation experiments on the rat uterine tissues will provide a more comprehensive list of decidua-, inner myometrium-, and outer myometrium-specific genes whose regulatory regions are bound by the progesterone receptor.

The identification of genes within the progesterone-responsive gene sets in this study that are bound by the progesterone will support the hypothesis that progesterone effects in the uterus during late pregnancy are genomic. Since the progesterone receptor interacts with numerous other factors when regulating gene transcription (Leonhardt et al., 2003), the upstream regions of progesterone-responsive genes were assessed for the presence of common regulatory features. A combination of motif searching and testing for overrepresentation identified the Krüppel-like factor 4 binding site within the regulatory regions of p4-responsive genes in the decidua. Krüppel-like factor 4 has been linked to endometrial, cervical, and ovarian cancer, as well as endometriosis , and has been previously shown to mediate the

genomic effects of progesterone in human endometrial epithelial cells (Shimizu et al., 2010). It is, therefore, proposed that the effects of progesterone in the decidua are genomic and are mediated by Krüppel-like factor 4. Further investigations into the factors regulating the expression of the progesterone-responsive genes identified in this thesis such as chromatin immunoprecipitation experiments are required.

Chapter 12

Conclusions

This thesis aimed to identify and analyse the effects of progesterone withdrawal on the transcriptome of the rat uterus. This was achieved through combining the power of laser capture microdissection with that of RNAseq in the identification of the tissue-specific transcriptomic changes that occurred during the transition of the uterus from a quiescent to a contractile state. A ramping-up of stimulus in the decidua at term supports the hypothesis that the signal for the onset of labour emanates from the decidua. In addition, mRNA expression within myometrial tissues was shown to change prior to ramping-up of stimulus in the decidua, and indication that a separate signal within the uterus induces the tissues to prepare for labour. Further information on the transcriptomic changes preceding pre-term labour was obtained. In addition, differences between pre-term and term mRNA expression were identified and documented. Furthermore, comparisons of the observations made in this thesis to those made in other studies were conducted. This thesis documents observations obtained from snapshots of the transcriptomic landscape of uterine tissues at specific time-points in late pregnancy. The novelty of the work presented in this thesis is in the segregation of the decidua from the myometrial tissues, and that of the inner myometrium

from the outer myometrium, using laser capture microdissection to allow for the separate investigation of transcriptomic changes in these tissues. In conclusion, the data presented in this thesis paves the way for further inroads into identifying the underlying cause of preterm labour and labour at term.

References

Afhüppe, W., Beekman, J. M., Otto, C., Korr, D., Hoffmann, J., Fuhrmann, U., & Möller, C. (2010). In vitro characterization of ZK 230211—A type III progesterone receptor antagonist with enhanced antiproliferative properties. *The Journal of Steroid Biochemistry and Molecular Biology*, 119:pp. 45 – 55.

Aguilar, H. & Mitchell, B. (2010). Physiological pathways and molecular mechanisms regulating uterine contractility. *Human Reproduction Update*, 16:pp. 725–744.

Alberts, B., Johnson, A., Lewis, J., Raff, M., Roberts, K., & Walter, P. (2002). *Molecular Biology of The Cell*, pp. 1075–1079. New York:Garland Science, 5th edition.

Albrecht, J. L., Atal, N. S., Tadros, P. N., Orsino, A., Lye, S. J., Sadovsky, Y., & Beyer, E. C. (1996). Rat uterine myometrium contains the gap junction protein connexin45, which has a differing temporal expression pattern from connexin43. *American Journal of Obstetrics and Gynecology*, 175:pp. 853–858.

Alford, A. I. & Hankenson, K. D. (2006). Matricellular proteins: Extracellular modulators of bone development, remodeling, and regeneration. *Bone*, 38:pp. 749–757.

Allen, W. M. (1930). Physiology of the corpus luteum, V: the preparation and some chemical properties of progestin, a hormone of the corpus luteum which produces progestational proliferation. *American Journal of Physiology*, 92:pp. 174–188.

Allen, W. M. (1970). Progesterone: how did the name originate? *Southern Medical Journal*, 63:pp. 1151–1155.

Alonso-Magdalena, P., Ropero, A. B., Carrera, M. P., Cederroth, C. R., Baquie, M.,

Gauthier, B. R., Nef, S., Stefani, E., & Nadal, A. (2008). Pancreatic insulin content regulation by the estrogen receptor ERα. *PLoS ONE*, 3:p. e2069.

Alzamora, R., Michea, L., & Marusic, E. T. (2000). Role of 11β-Hydroxysteroid Dehydrogenase in Nongenomic Aldosterone Effects in Human Arteries. *Hypertension*, 35:pp. 1099 –1104.

Amer-Alshiek, J., Shiekh, O., Agmon, A., & Grisaru, D. (2015). What is the right timing for ultrasound evaluation after pregnancy termination with mifepristone? *European Journal of Obstetrics & Gynecology and Reproductive Biology*, 189:pp. 24–26.

Anders, S. & Huber, W. (2010). Differential expression analysis for sequence count data. *Genome Biology*, 11:p. R106.

Anders, S., Pyl, P. T., & Huber, W. (2015). HTSeq–a Python framework to work with high-throughput sequencing data. *Bioinformatics*, 31:pp. 166–169.

Andrews, S. (2012). FastQC A Quality Control tool for High Throughput Sequence Data. URL `http://www.bioinformatics.babraham.ac.uk/projects/fastqc/`.

Arnoldi, R., Hiltbrunner, A., Dugina, V., Tille, J.-C., & Chaponnier, C. (2013). Smooth muscle actin isoforms: A tug of war between contraction and compliance. *European Journal of Cell Biology*, 92:pp. 187–200.

Arthur, P., Taggart, M. J., Zielnik, B., Wong, S., & Mitchell, B. F. (2008). Relationship between gene expression and function of uterotonic systems in the rat during gestation, uterine activation and both term and preterm labour. *Journal of Physiology*, 586:pp. 6063–6076.

Assinder, S. J., Stanton, J.-A. L., & Prasad, P. D. (2009). Transgelin: an actin-binding protein and tumour suppressor. *The International Journal of Biochemistry & Cell Biology*, 41:pp. 482–486.

Astolfi, P. & Zonta, L. A. (1999). Risks of preterm delivery and association with maternal age, birth order, and fetal gender. *Human Reproduction*, 14:pp. 2891–2894.

Baginsky, S., Hennig, L., Zimmermann, P., & Gruissem, W. (2010). Gene Expression Analysis, Proteomics, and Network Discovery. *Plant Physiology*, 152:pp. 402–410.

Bain, D. L., Heneghan, A. F., Connaghan-Jones, K. D., & Miura, M. T. (2007). Nuclear Receptor Structure: Implications for Function. *Annual Review of Physiology*, 69:pp. 201–220.

Beato, M. (1989). Gene regulation by steroid hormones. *Cell*, 56:pp. 335–344.

Benjamini, Y. & Hochberg, Y. (1995). Controlling the false discovery rate: A Practical and powerful approach to multiple testing. *Journal of the Royal Statistical Society*, 57:pp. 289–300.

Berkova, N., Lemay, A., Dresser, D. W., Fontaine, J.-Y., Kerizit, J., & Goupil, S. (2001). Haptoglobin is present in human endometrium and shows elevated levels in the decidua during pregnancy. *Molecular Human Reproduction*, 7:pp. 747–754.

Bigazzi, M., Pollicino, G., & Nardi, E. (1979). Is Human Decidua a Specialized Endocrine Organ? *Journal of Clinical Endocrinology & Metabolism*, 49:p. 847.

Blackburn, S. T. (2014). *Maternal, Fetal & Neonatal Physiology: A Clinical Perspective*. Elsevier Saunders, 4 edition.

Blanks, A. M. & Brosens, J. J. (2012). Progesterone Action in the Myometrium and Decidua in Preterm Birth. *Facts, Views & Vision in Obstetrics and Gynaecology*, 4:pp. 188 – 194.

Brosens, J. J., Hodgetts, A., Feroze-Zaidi, F., Sherwin, J. R. A., Fusi, L., Salker, M. S., Higham, J., Rose, G. L., Kajihara, T., Young, S. L., Lessey, B. A., Henriet, P., Langford, P. R., & Fazleabas, A. T. (2010). Proteomic analysis of endometrium from fertile and infertile patients suggests a role for apolipoprotein A-I in embryo implantation failure and endometriosis. *Molecular Human Reproduction*, pp. 273–285.

Brown, P., Baxter, L., Hickman, R., Beynon, J., Moore, J. D., & Ott, S. (2013). MEME-LaB: motif analysis in clusters. *Bioinformatics*, 29:pp. 1696–1697.

Bryant-Greenwood, G. (1982). Relaxin as a new hormone. *Endocrine Reviews*, 3:p. 62.

Burris, T. P., Solt, L. A., Wang, Y., Crumbley, C., Banerjee, S., Griffett, K., Lundasen, T., Hughes, T., & Kojetin, D. J. (2013). Nuclear Receptors and Their Selective Pharmacologic Modulators. *Pharmacological Reviews*, 65:pp. 710–778.

Buxton, I. L. O., Singer, C. A., & Tichenor, J. N. (2010). Expression of Stretch-Activated Two-Pore Potassium Channels in Human Myometrium in Pregnancy and Labor. *PLOS ONE*, 5:p. e12372.

Caballero, V., Ruiz, R., Sainz, J., Cruz, M., López-Nevot, M. A., Galán, J., Real, L. M., de Castro, F., López-Villaverde, V., & Ruiz, A. (2005). Preliminary molecular genetic

analysis of the Receptor Interacting Protein 140 (RIP140) in women affected by endometriosis. *Journal of Experimental & Clinical Assisted Reproduction*, 2:pp. 11–11. URL `http://www.ncbi.nlm.nih.gov/pmc/articles/PMC1242355/`.

Cabeza, M., Heuze, Y., Sánchez, A., Garrido, M., & Bratoeff, E. (2015). Recent advances in structure of progestins and their binding to progesterone receptors. *Journal of Enzyme Inhibition and Medicinal Chemistry*, 30:pp. 152–159.

Cadepond, F., Ulmann, A., & Baulieu, E. E. (1997). RU486 (mifepristone): mechanisms of action and clinical uses. *Medicine*, 48:pp. 129–156.

Carlberg, C. & Molnár, F. (2014). The Basal Transcriptional Machinery. In *Mechanisms of Gene Regulation*, pp. 37–54. Springer, Netherlands.

Carp, H. J. A. (2015). *Progestogens in Obstetrics and Gynecology*. Springer, Switzerland, 1st edition.

Catalano, R. D., Critchley, H. O., Heikinheimo, O., Baird, D. T., Hapangama, D., Sherwin, J. R. A., Charnock-Jones, D. S., Smith, S. K., & Sharkey, A. M. (2007). Mifepristone induced progesterone withdrawal reveals novel regulatory pathways in human endometrium. *Molecular Human Reproduction*, 13:pp. 641–654.

Challis, J. R. G., Matthews, S. G., Gibb, W., & Lye, S. J. (2000). Endocrine and paracrine regulation of birth at term and preterm. *Endocrine Reviews*, 21:pp. 514–550.

Chan, Y. W., van den Berg, H. A., Moore, J. D., Quenby, S., & Blanks, A. M. (2014). Assessment of myometrial transcriptome changes associated with spontaneous human labour by high-throughput RNA-seq. *Experimental Physiology*, 99:pp. 510–524.

Charif, D. & Lobry, J. (2007). SeqinR 1.0-2: a contributed package to the R project for statistical computing devoted to biological sequences retrieval and analysis. In Bastolla, U., Porto, M., Roman, H., & Vendruscolo, M. (Editors), *Structural approaches to sequence evolution: Molecules, networks, populations*, Biological and Medical Physics, Biomedical Engineering, pp. 207–232. Springer Verlag, New York.

Chaudhuri, S. K., Chattopadhyay, R. N., Maitra, S. K., Ray, S., & Chaudhuri, S. (1992). Effects of progesterone on some brain neurotransmitters in intact rats. *Indian Journal of Physiology and Pharmacology*, 36:pp. 255–258.

Chen, D. B., Bird, I. M., Zheng, J., & Magness, R. R. (2004). Membrane estrogen receptor-dependent extracellular signal-regulated kinase pathway mediates acute activation of endothelial nitric oxide synthase by estrogen in uterine artery endothelial cells. *Endocrinology*, 145:pp. 113–125.

Chen, J., Kinyamu, H. K., & Archer, T. K. (2006). Changes in Attitude, Changes in Latitude: Nuclear Receptors Remodeling Chromatin to Regulate Transcription. *Molecular Endocrinology*, 20:pp. 1–13.

Childers, S. R. & Deadwyler, S. A. (1996). Role of cyclic AMP in the actions of cannabinoid receptors. *Biochemical Pharmacology*, 52:pp. 819–827.

Churchill, G. A. (2002). Fundamentals of experimental design for cDNA microarrays. *Nature Genetics*, 32 Suppl:pp. 490–495.

Chwalisz, K. (1994). The use of progesterone antagonists for cervical ripening and as an adjunct to labour and delivery. *Human Reproduction*, 9 Suppl 1:pp. 131–61.

Clément-Ziza, M., Munnich, A., Lyonnet, S., Jaubert, F., & Besmond, C. (2008). Stabilization of RNA during laser capture microdissection by performing experiments under argon atmosphere or using ethanol as a solvent in staining solutions. *RNA*, 14:pp. 2698–2704.

Cohen, M. L., Schenck, K. W., Colbert, W., & Wittenauer, L. (1985). Role of 5-HT2 receptors in serotonin-induced contractions of nonvascular smooth muscle. *Journal of Pharmacology and Experimental Therapeutics*, 232:pp. 770–774.

Condon, J. C., Jeyasuria, P., Faust, J. M., & Mendelson, C. R. (2004). Surfactant protein secreted by the maturing mouse fetal lung acts as a hormone that signals the initiation of parturition. *Proceedings of the National Academy of Sciences*, 101:pp. 4978–4983.

Condon, J. C., Jeyasuria, P., Faust, J. M., Wilson, J. W., & Mendelson, C. R. (2003). A decline in the levels of progesterone receptor coactivators in the pregnant uterus at term may antagonize progesterone receptor function and contribute to the initiation of parturition. *Proceedings of the National Academy of Sciences*, 100:pp. 9518–9523.

Conneely, O., Mulac-Jericevic, B., & Arnett-Mansfield, R. (2008). Progesterone Signaling in Mammary Gland Development. In Conneely, O. M. & Otto, C. (Editors), *Progestins and*

the Mammary Gland, volume 1 of *From Basic Science to Clinical Applications*, pp. 45–54. Ernst Schering Foundation Symposium Proceedings,, Springer Science & Business Media.

Conneely, O., Mulac-Jericevic, B., & Lydon, J. (2003). Progesterone-dependent regulation of female reproductive activity by two distinct progesterone receptor isoforms. *Steroids*, 68:pp. 771–778.

Conneely, O. M., Mulac-Jericevic, B., Lydon, J. P., & De Mayo, F. J. (2001). Reproductive functions of the progesterone receptor isoforms: lessons from knock-out mice. *Molecular and Cellular Endocrinology*, 179:pp. 97–103.

Cook, J. L., Zaragoza, D. B., Sung, D. H., & Olson, D. M. (2000). Expression of myometrial activation and stimulation genes in a mouse model of preterm labor: myometrial activation, stimulation, and preterm labor. *Endocrinology*, 141:pp. 1718–1728.

Couse, J. F., Hewitt, S. C., & Korach, K. S. (2006). Steroid Receptors in the Ovary and Uterus. In Neill, J. D. & Challis, J. R. G. (Editors), *Knobil and Neill's Physiology of Reproduction*, chapter 15, pp. 593–678. Gulf Professional Publishing, 3rd edition.

Cunningham, F., Leveno, K., Bloom, S., Hauth, J., Rouse, D., & Spong, C. (Editors) (2005). *Williams Obstetrics*, chapter 3: Implantation, Embryogenesis, and Placental Development. McGraw Hill, 22nd edition.

De Nicola, A. F., Coronel, F., Garay, L. I., Gargiulo-Monachelli, G., Gonzalez Deniselle, M. C., Gonzalez, S. L., Labombarda, F., Meyer, M., Guennoun, R., & Schumacher, M. (2013). Therapeutic effects of progesterone in animal models of neurological disorders. *CNS & Neurological Disorders Drug Targets*, 12:pp. 1205–1218.

de Paiva, C. E. N. & Csapo, A. I. (1973). The effect of prostaglandin on the electric activity of the pregnant uterus. *Prostaglandins*, 4:pp. 177–188.

Dewick, P. M. (2001). The Mevalonate And Deoxyxylulose Phosphate Pathways: Terpenoids And Steroids. In *Medicinal Natural Products: A Biosynthetic Approach*, volume 2nd. Wiley and Sons, West Sussex, England.

Dong, Y.-L., Gangula, P. R., Fang, L., & Yallampalli, C. (1996). Differential expression of cyclooxygenase-1 and-2 proteins in rat uterus and cervix during the estrous cycle, pregnancy, labor and in myometrial cells. *Prostaglandins*, 52:pp. 13–34.

Döring, B., Shynlova, O., Tsui, P., Eckardt, D., Janssen-Bienhold, U., Hofmann, F., Feil, S., Feil, R., Lye, S. J., & Willecke, K. (2006). Ablation of connexin43 in uterine smooth muscle cells of the mouse causes delayed parturition. *Journal of Cell Science*, 119:pp. 1715–1722.

Doualla-Bell, F., Lye, S. J., Labrie, F., & Fortier, M. A. (1995). Differential expression and regulation of connexin-43 and cell-cell coupling in myocytes from the circular and longitudinal layers of bovine myometrium. *Endocrinology*, 136:pp. 5322–5328.

Edwards, D. P., Weigel, N. L., Nordeen, S. K., & Beck, C. A. (1993). Modulators of cellular protein phosphorylation alter the trans-activation function of human progesterone receptor and the biological activity of progesterone antagonists. *Breast Cancer Research and Treatment*, 27:pp. 41–56.

El-Mezgueldi, M. (2014). Tropomyosin dynamics. *Journal of Muscle Research and Cell Motility*, 35:pp. 203 –210.

Epstein, F. H., Parry, S., & Strauss, J. F. (1998). Premature rupture of the fetal membranes. *New England Journal of Medicine*, 338:pp. 663–670.

Ewens, W. J. & Grant, G. R. (2001a). *Statistical Methods in Bioinformatics*, chapter 8: Statistics (ii): Classical Estimation Theory, pp. 275–303. Statistics for Biology and Health. Springer, 2nd edition.

Ewens, W. J. & Grant, G. R. (2001b). *Statistical Methods in Bioinformatics*, chapter 3: Statistics (i): An Introduction to Statistical Inference, pp. 111–154. Statistics for Biology and Health. Springer, 2nd edition.

Ewing, B. & Green, P. (1998). Base-calling of automated sequencer traces using phred II. Error probabilities. *Genome Research*, 8:pp. 186–194.

Fajmut, A., Brumen, M., & Schuster, S. (2005). Theoretical model of the interactions between Ca2+, calmodulin and myosin light chain kinase. *FEBS Letters*, 579:pp. 4361–4366.

Ferrell, J. E. (1999). Xenopus oocyte maturation: new lessons from a good egg. *BioEssays : News and Reviews in Molecular, Cellular and Developmental Biology*, 21:pp. 833–842.

Fetalvero, K. M., Zhang, P., Shyu, M., Young, B. T., Hwa, J., Young, R. C., & Martin, K. A. (2008). Prostacyclin primes pregnant human myometrium for an enhanced contractile response in parturition. *Journal of Clinical Investigation*, 118:pp. 3966–3979.

Flicek, P., Amode, M. R., Barrell, D., Beal, K., Billis, K., Brent, S., Carvalho-Silva, D., Clapham, P., Coates, G., Fitzgerald, S., Gil, L., Girón, C. G., Gordon, L., Hourlier, T., Hunt, S., Johnson, N., Juettemann, T., Kähäri, A. K., Keenan, S., Kulesha, E., Martin, F. J., Maurel, T., McLaren, W. M., Murphy, D. N., Nag, R., Overduin, B., Pignatelli, M., Pritchard, B., Pritchard, E., Riat, H. S., Ruffier, M., Sheppard, D., Taylor, K., Thormann, A., Trevanion, S. J., Vullo, A., Wilder, S. P., Wilson, M., Zadissa, A., Aken, B. L., Birney, E., Cunningham, F., Harrow, J., Herrero, J., Hubbard, T. J. P., Kinsella, R., Muffato, M., Parker, A., Spudich, G., Yates, A., Zerbino, D. R., & Searle, S. M. J. (2013). Ensembl 2014. *Nucleic Acids Research*, pp. 1–7.

Fortune, J. E. (1994). Ovarian follicular growth and development in mammals. *Biology of Reproduction*, 50:pp. 225–232.

Fraser, A., Brockert, J., & Ward, R. (1995). Association of young maternal age with adverse reproductive outcomes. *New England Journal of Medicine*, 332:pp. 1113–1118.

Freeman, M. E. (2006). Neuroendocrine Control of the Ovarian Cycle of the Rat. In Neill, J. D. & Challis, J. R. G. (Editors), *Knobil and Neill's Physiology of Reproduction*, chapter 43, pp. 2327 — 2388. Gulf Professional Publishing, 3rd edition.

Fuchs, A. R., Fuchs, F., Husslein, P., & Soloff, M. S. (1984). Oxytocin receptors in the human uterus during pregnancy and parturition. *American Journal of Obstetrics & Gynecology*, 150:pp. 734–741.

Funk, C. D., Song, W.-C., & FitzGerald, G. A. (2009). Prostaglandins and Other Lipid Mediators in Reproductive Medicine. In Strauss, J. E. & Barberi, R. . L. (Editors), *Yen and Jaffe's Reproductive Endocrinology: Physiology, Pathophysiology and Clinical Management*, chapter 6, pp. 121–137. Saunders: Philadelphia, 6th edition.

Gao, L., Rabbitt, E. H., Condon, J. C., Renthal, N. E., Johnston, J. M., Mitsche, M. A., Chambon, P., Xu, J., O'Malley, B. W., & Mendelson, C. R. (2015). Steroid receptor coactivators 1 and 2 mediate fetal-to-maternal signaling that initiates parturition. *Journal of Clinical Investigation*, 125:pp. 2808–2824.

Garfield, R. E. (2008). *Is knowledge of the pattern of electrical activity in the pregnant uterus helpful to our understanding of uterine function?* Focus on "Patterns of electrical propagation in the intact pregnant guinea pig uterus" by Lammers et al. *American Journal of Physiology-Regulatory, Integrative and Comparative Physiology*, 294:pp. R917–R918.

Garfield, R. E. & Maner, W. L. (2007). Physiology and electrical activity of uterine contractions. *Seminars in Cell & Developmental Biology*, 18:pp. 289–295.

Garfield, R. E., Shi, L., & Shi, S. Q. (2012). Use of progesterone and progestin analogs for inhibition of preterm birth and other uterine contractility disorders. *Facts, Views & Vision in Obstetrics and Gynaecology*, 4:pp. 237–244.

Garfield, R. E., Sims, S. M., Kannan, M. S., & Daniel, E. E. (1978). Possible role of gap junctions in activation of myometrium during parturition. *American Journal of Physiology*, 235:pp. C168–C179.

Gellersen, B., Brosens, I., & Brosens, J. (2007). Decidualization of the Human Endometrium: Mechanisms, Functions, and Clinical Perspectives. *Seminars in Reproductive Medicine*, 25:pp. 445–453.

Gellersen, B., Fernandes, M., & Brosens, J. (2009). Non-genomic progesterone actions in female reproduction. *Human Reproduction Update*, 15:pp. 119–138.

Germain, P., Staels, B., Dacquet, C., Spedding, M., & Laudet, V. (2006). Overview of Nomenclature of Nuclear Receptors. *Pharmacological Reviews*, 58:pp. 685–704.

Giangrande, P. H., Kimbrel, E. A., Edwards, D. P., & McDonnell, D. P. (2000). The opposing transcriptional activities of the two isoforms of the human progesterone receptor are due to differential cofactor binding. *Molecular and Cellular Biology*, 20:pp. 3102–3115.

Gibb, W., Lye, S. J., & Challis, J. R. G. (2006). Parturition. In Neill, J. D. & Challis, J. R. G. (Editors), *Knobil and Neill's Physiology of Reproduction*, chapter 55, pp. 2925–2974. Elsevier, Oxford, 3rd edition.

Gimpl, G. & Fahrenholz, F. (2001). The Oxytocin Receptor System: Structure, Function, and Regulation. *Physiological Reviews*, 81:pp. 629–683.

Girotti, M. & Zingg, H. (2003). Gene expression profiling of rat uterus at different stages of parturition. *Endocrinology*, 144:p. 2254.

Golander, A., Hurley, T., Barrett, J., & .. (1978). Prolactin synthesis by human chorion-decidual tissue: a possible source of prolactin in the amniotic fluid. *Science*, pp. 202–311.

Goldenberg, R. L., Culhane, J. F., Iams, J. D., & Romero, R. (2008). Epidemiology and causes of preterm birth. *The Lancet*, 371:pp. 75–84.

Gros, R., Ding, Q., Armstrong, S., O'Neil, C., Pickering, J. G., & Feldman, R. D. (2007). Rapid effects of aldosterone on clonal human vascular smooth muscle cells. *American Journal of Physiology - Cell Physiology*, 292:pp. C788–C794.

Gyorffy, B., Gyorffy, A., & Tulassay, Z. (2005). The problem of multiple testing and solutionsfor genome-wide studies. *Orvosi Hetilap*, 146:pp. 559–563.

Hall, J. E. (2009). Neuroendocrine Control of The Menstrual Cycle. In Strauss, J. E. & Barberi, R. . L. (Editors), *Yen and Jaffe's Reproductive Endocrinology: Physiology, Pathophysiology and Clinical Management*, chapter 7, pp. 139–154. Saunders: Philadelphia, 6th edition.

Hall, P. F. (1985). Role of cytochromes P-450 in the biosynthesis of steroid hormones. *Vitamins and Hormones*, 42:pp. 315–368.

Han, S. J., Tsai, S. Y., Tsai, M.-J., & O'Malley, B. W. (2007). Distinct Temporal and Spatial Activities of RU486 on Progesterone Receptor Function in Reproductive Organs of Ovariectomized Mice. *Endocrinology*, 148:pp. 2471–2486.

Hardcastle, T. & Kelly, K. (2010). BaySeq: Empirical Bayesian analysis of patterns of differential expression in count data. *BMC Bioinformatics*, 11:p. 442.

Härdle, W. K. & Hlávka, Z. (2015). *Multivariate Statistics*, chapter 11: Principle Component Analysis, pp. 183–204. Exercises and Solutions. Springer, Berlin, 2nd edition.

Hatzoglou, A., Kampa, M., Kogia, C., Charalampopoulos, I., Theodoropoulos, P. A., Anezinis, P., Dambaki, C., Papakonstanti, E. A., Stathopoulos, E. N., Stournaras, C., Gravanis, A., & E., C. (2005). Membrane androgen receptor activation induces apoptotic regression of human prostate cancer cells in vitro and in vivo. *Journal of Clinical Endocrinology and Metabolism*, 90:pp. 893–903.

Hedrich, H. J. (2000). Chapter 1 - History, Strains and Models. In Krinke, G. J. (Editor), *The Laboratory Rat*, Handbook of Experimental Animals, pp. 3–16. Academic Press, London.

Helguera, G., Eghbali, M., Sforza, D., Minosyan, T. Y., Toro, L., & Stefani, E. (2009). Changes in global gene expression in rat myometrium in transition from late pregnancy to parturition. *Physiological Genomics*, 36:pp. 89–97.

Hendrix, E. M., Mao, S. J., Everson, W., & Larsen, W. J. (1992). Myometrial connexin 43 trafficking and gap junction assembly at term and in preterm labor. *Molecular Reproduction and Development*, 33:pp. 27–38.

Heyman, N. S., Cowles, C. L., Barnett, S. D., Wu, Y. Y., Cullison, C., Singer, C. A., Leblanc, N., & Buxton, I. L. O. (2013). TREK-1 currents in smooth muscle cells from pregnant human myometrium. *AJP: Cell Physiology*, 305:pp. C632–C642.

Hille, B. (2001). *Ion Channels of Excitable Membranes*, chapter Calcium Dynamics, Epithelial Transport, and Intercellular Coupling, p. 300. Sinauer Associates, Inc, Sunderland, Massachusetts, 3rd edition.

Hirst, J., Mijovic, J., , Zakar, T., & Olson, D. M. (1998). Prostaglandin endoperoxide H synthase-1 and -2 mRNA levels and enzyme activity in human decidua at term labor. *Journal of the Society of Gynecologic Investigation*, 5:pp. 13–20.

Hoffman, K., Martínez-Alvarez, E., & Rueda-Morales, R. (2009). The inhibition of female rabbit sexual behavior by progesterone: Progesterone receptor-dependent and-independent effects. *Hormones and Behavior*, 55:pp. 84–92.

Hovland, A. R. (1998). An N-terminal Inhibitory Function, IF, Suppresses Transcription by the A-isoform but Not the B-isoform of Human Progesterone Receptors. *Journal of Biological Chemistry*, 273:pp. 5455–5460.

Hsia, H. C. & Schwarzbauer, J. E. (2005). Meet the tenascins: multifunctional and mysterious. *The Journal of Biological Chemistry*, 280:pp. 26641–26644.

Huntley, R. P., Sawford, T., Mutowo-Meullenet, P., Shypitsyna, A., Bonilla, C., Martin, M. J., & O'Donovan, C. (2015). The GOA database: Gene Ontology annotation updates for 2015. *Nucleic Acids Research*, 43:pp. D1057–D1063.

Imai, Y., Youn, M. Y., Inoue, K., Takada, I., Kouzmenko, A., & Kato, S. (2013). Nuclear Receptors in Bone Physiology and Diseases. *Physiological Reviews*, 93:pp. 481–523.

IUPAC-IUB Joint Commission on Biochemical Nomenclature (JCBN) (1989). The nomenclature of steroids. Recommendations 1989. *European Journal of Biochemistry*, 186:pp. 429–458.

Jabbour, H. N., Kelly, R. W., Fraser, H. M., & Critchley, H. O. D. (2006). Endocrine Regulation of Menstruation. *Endocrine Reviews*, 27:pp. 17–46.

Jaffe, R. B., Lee, P. A., & Midgley, A. R. (1969). Serum gonadotropins before, at the inception of, and following human pregnancy. *Journal of Clinical Endocrinology & Metabolism*, 29:p. 1281.

Jain, V., Saade, G. R., & Garfield, R. E. (2000). Structure and function of the myometrium. *Advances in Organ Biology*, 8:pp. 215–246.

Jeong, J.-W. (2005). Identification of Murine Uterine Genes Regulated in a Ligand-Dependent Manner by the Progesterone Receptor. *Endocrinology*, 146:pp. 3490–3505.

Johnson, R. A. & Wichern, D. W. (2002). *Applied Multivariate Statistical Analysis*, chapter 8: Principal Component Analysis, pp. 426–476. Prentice Hall, New Jersey, 5th edition.

Jolliffe, I. T. (2002a). *Principal Component Analysis*, chapter 1: Introduction, pp. 1–9. Springer New York, 2nd edition.

Jolliffe, I. T. (2002b). *Principal Component Analysis*, chapter 6: Choosing a Subset of Principal Components or Variables, pp. 111–149. Springer New York, 2nd edition.

Jonat, W., Bachelot, T., Ruhstaller, T., Kuss, I., Reimann, U., & Robertson, J. F. R. (2013). Randomized phase II study of lonaprisan as second-line therapy for progesterone receptor-positive breast cancer. *Annals of Oncology*, 24:pp. 2543–2548.

Kasprzyk, A. (2011). BioMart: driving a paradigm change in biological data management. *Database*, 2011:p. bar049.

Khatua, A., Wang, X., Ding, T., Zhang, Q., Reese, J., DeMayo, F. J., & Paria, B. C. (2006). Indian Hedgehog, But Not Histidine Decarboxylase or Amphiregulin, Is a Progesterone-Regulated Uterine Gene in Hamsters. *Endocrinology*, 147:pp. 4079–4092.

Khubchandani, K. R. & Snyder, J. M. (2001). Surfactant protein A (SP-A): the alveolus and beyond. *Journal of the Federation of American Societies for Experimental Biology*, 15:pp. 59–69.

Kida, H., Taga, M., Minaguchi, H., Hanazono, M., Ohashi, T., Sakakura, T., & Kusakabe, M. (1997). The change in tenascin expression in mouse uterus during early pregnancy. *Journal of Assisted Reproduction and Genetics*, 14:pp. 44–50.

Kidder, G. M. & Winterhager, E. (2009). Connexins in the Female Reproductive System. In Harris, A. & Locke, D. (Editors), *Connexins*, chapter 24, pp. 481–494. Springer Science & Business Media.

Kim, D., Pertea, G., Trapnell, C., Pimentel, H., Kelley, R., & Salzberg, S. L. (2013). TopHat2: accurate alignment of transcriptomes in the presence of insertions, deletions and gene fusions. *Genome Biology*, 14:p. R36.

Kojima, K., Abe-Dohmae, S., Arakawa, R., Murakami, I., Suzumori, K., & Yokoyama, S. (2001). Progesterone inhibits apolipoprotein-mediated cellular lipid release: a putative mechanism for the decrease of high-density lipoprotein. *Biochimica et Biophysica Acta*, 1532:pp. 173–184.

Komárek, V., Gembardt, C., Krinke, A., Mahrous, T. A., & Schaetti, P. (2000). Chapter 15 - Synopsis of the Organ Anatomy. In Krinke, G. J. (Editor), *The Laboratory Rat*, Handbook of Experimental Animals, pp. 283 – 319. Academic Press, London, 1st edition.

Kougioumtzi, A., Tsaparas, P., & Magklara, A. (2014). Deep Sequencing Reveals New Aspects of Progesterone Receptor Signaling in Breast Cancer Cells. *PLOS ONE*, 9:p. e98404.

Kredentser, J. V., Embree, J., & McCoshen, J. (1995). Prostaglandin F2 alpha output by amnion-chorion-decidua: relationship with labor and prostaglandin E2 concentration at the amniotic surface. *American Journal of Obstetrics & Gynecology*, 173:p. 199.

Kumar, R. & Thompson, E. (1999). The structure of the nuclear hormone receptors. *Steroids*, 64:pp. 310 – 319.

Laforet, J., Rabotti, C., Terrien, J., Mischi, M., & Marque, C. (2011). Towards a multiscale model of the uterine electrical activity. *Biomedical Engineering, IEEE Transactions on*, 58:pp. 3487—3490.

Lammers, W., Mirghani, H., Stephen, B., Dhanasekaran, S., Wahab, A., Sultan, M. A., & Abazer, F. (2008). Patterns of electrical propagation in the intact pregnant guinea pig uterus.

American Journal of Physiology-Regulatory, Integrative and Comparative Physiology, 294:pp. R919–R928.

Langmead, B. & Salzberg, S. (2012). Fast gapped-read alignment with Bowtie 2. *Nature Methods*, 9:pp. 357–359.

Large, M. J. & DeMayo, F. J. (2012). The regulation of embryo implantation and endometrial decidualization by progesterone receptor signaling. *Molecular and Cellular Endocrinology*, 358:pp. 155–165.

Laulederkind, S. J. F., Hayman, G. T., Wang, S.-J., Smith, J. R., Lowry, T. F., Nigam, R., Petri, V., de Pons, J., Dwinell, M. R., Shimoyama, M., Munzenmaier, D. H., Worthey, E. A., & Jacob, H. J. (2013). The Rat Genome Database 2013–data, tools and users. *Briefings in Bioinformatics*, 14:pp. 520–526.

Lee, Y., Sooranna, S. R., Terzidou, V., Christian, M., Brosens, J., Huhtinen, K., Poutanen, M., Barton, G., Johnson, M. R., & Bennett, P. R. (2012). Interactions between inflammatory signals and the progesterone receptor in regulating gene expression in pregnant human uterine myocytes. *Journal of Cellular and Molecular Medicine*, 16:pp. 2487–2503.

Leo, J. C. L. & Lin, V. C. L. (2008). The activities of progesterone receptor isoform A and B are differentially modulated by their ligands in a gene-selective manner. *International Journal of Cancer*, 122:pp. 230–243.

Leonardsson, G., Jacobs, M. A., White, R., Jeffery, R., Poulsom, R., Milligan, S., & Parker, M. (2002). Embryo transfer experiments and ovarian transplantation identify the ovary as the only site in which nuclear receptor interacting protein 1/RIP140 action is crucial for female fertility. *Endocrinology*, 143:pp. 700–707.

Leonhardt, S. A., Boonyaratanakornkit, V., & Edwards, D. P. (2003). Progesterone receptor transcription and non-transcription signaling mechanisms. *Steroids*, 68:pp. 761–770.

Li, H., Handsaker, B., Wysoker, A., Fennell, T., Ruan, J., Homer, N., Marth, G., Abecasis, G., Durbin, R., & Subgroup, . G. P. D. P. (2009). The Sequence Alignment/Map format and SAMtools. *Bioinformatics*, 25:pp. 2078–2079.

Lin, H., Xiao, J., Luo, X., Chen, G., & Wang, Z. (2009a). Transcriptional control of pacemaker

channel genes HCN2 and HCN4 by Sp1 and implications in re-expression of these genes in hypertrophied myocytes. *Cellular Physiology and Biochemistry*, 23:pp. 317–326.

Lin, H. Y., Sun, M., Lin, C., Tang, H. Y., London, D., Shih, A., Davis, F. B., & Davis, P. J. (2009b). Androgen-induced human breast cancer cell proliferation is mediated by discrete mechanisms in estrogen receptor-a-positive and -negative breast cancer cells. *Journal of Steroid Biochemistry and Molecular Biology*, 113:pp. 182–188.

Lopez-Rodriguez, A. B., Acaz-Fonseca, E., Giatti, S., Caruso, D., Viveros, M.-P., Melcangi, R. C., & Garcia-Segura, L. M. (2015). Correlation of brain levels of progesterone and dehydroepiandrosterone with neurological recovery after traumatic brain injury in female mice. *Psychoneuroendocrinology*, 56:pp. 1–11.

Love, M. I., Huber, W., & Anders, S. (2014). Moderated estimation of fold change and dispersion for RNA-seq data with DESeq2. *Genome Biology*, 15:p. 550.

Luconi, M., Francavilla, F., Porazzi, I., Macerola, B., Forti, G., & Baldi, E. (2004). Human spermatozoa as a model for studying membrane receptors mediating rapid nongenomic effects of progesterone and estrogens. *Steroids*, 69:pp. 553 – 559.

Lydon, J. P., DeMayo, F. J., Funk, C. R., Mani, S. K., Hughes, A. R., Montgomery, C. A., Shyamala, G., Conneely, O. M., & O'Malley, B. W. (1995). Mice lacking progesterone receptor exhibit pleiotropic reproductive abnormalities. *Genes & Development*, 9:pp. 2266–2278.

Lydon, J. P., Sivaraman, L., & Conneely, O. M. (2000). A reappraisal of progesterone action in the mammary gland. *Journal of Mammary Gland Biology Neoplasia*, 5:pp. 325–338.

Maeda, K.-i., Ohkura, S., & Tsukamura, H. (2000). Physiology of Reproduction. In Krinke, G. J. (Editor), *The Laboratory Rat*, Handbook of Experimental Animals, chapter 9, pp. 145 – 176. Academic Press, London, 1st edition.

Maere, S., Heymans, K., & Kuiper, M. (2005). BiNGO: a Cytoscape plugin to assess overrepresentation of Gene Ontology categories in Biological Networks. *Bioinformatics*, 21:pp. 3448–3449.

Mahendroo, M. (2012). Cervical remodeling in term and preterm birth: insights from an animal model. *Reproduction*, 143:pp. 429–438.

Mandl, A. M. (1951). The Phases of the Oestrous Cycle in the Adult White Rat. *Journal of Experimental & Biology*, 28:pp. 576–584.

Marshall, J. C., Dalkin, A. C., Haisenleder, M. L., & Kelch, R. P. (1993). GnRH pulses—the regulators of human reproduction . *Trans. Am. Clin. Climatol. Assoc.*, 104:pp. 31–46.

Marston, S. B. & Smith, C. W. (1985). The thin filaments of smooth muscles. *Journal of Muscle Research and Cell Motility*, 6:pp. 669–708.

Matharoo-Ball, B. (2002). Down-Regulation of the α- and β-Subunits of the Calcium-Activated Potassium Channel in Human Myometrium with Parturition. *Biology of Reproduction*, 68:pp. 2135–2141.

Mayer, C.-D. & Glasbey, C. (2005). Statistical Methods in Microarray Gene Expression Data Analysis. In Husmeier, D., Dybowski, R., & Roberts, S. (Editors), *Probabilistic Modeling in Bioinformatics and Medical Informatics*, Advanced Information and Knowledge Processing, chapter 7, pp. 211–238. Springer London.

McEwan, I. J. (2009). Nuclear receptors: one big family. *Methods in Molecular Biology*, 505:pp. 3–18.

McKenna, N. J., Lanz, R. B., & O'Malley, B. W. (1999). Nuclear Receptor Coregulators: Cellular and Molecular Biology. *Endocrine Reviews*, 20:pp. 321–344.

Mesiano, S. (2009). The Endocrinology of Human Pregnancy and Fetoplacental Neuroendocrine Development. In Strauss, J. E. & Barberi, R. . L. (Editors), *Yen and Jaffe's Reproductive Endocrinology: Physiology, Pathophysiology and Clinical Management*, chapter 11, pp. 249 –281. Saunders: Philadelphia, 6th edition.

Messinis, I. E. (2006). Ovarian feedback, mechanism of action and possible clinical implications. *Hum. Reprod. Update*, 12:pp. 557–571.

Meyer, M. E., Pornon, A., Ji, J. W., Bocquel, M. T., Chambon, P., & Gronemeyer, H. (1990). Agonistic and antagonistic activities of RU486 on the functions of the human progesterone receptor. *The EMBO Journal*, 9:pp. 3923–3932.

Michal, G. & Schomburg, D. (Editors) (2012). *Biochemical Pathways*, chapter Signal Transduction and Cellular Communication. An Atlas of Biochemistry and Molecular Biology. John Wiley & Sons, 2nd edition.

Miller, W. L., Geller, D. H., & Rosen, M. (2007). Ovarian and adrenal androgen biosynthesis and metabolism. In Azziz, R. (Editor), *Contemporary Endocrinology: Androgen Excess Disorders in Women: Polycystic Ovary Syndrome and Other Disorders*, pp. 19–33. Humana Press Inc., Totowa, NJ, Totowa.

Minosyan, T. Y., Lu, R., Eghbali, M., Toro, L., & Stefani, E. (2007). Increased 5-HT contractile response in late pregnant rat myometrium is associated with a higher density of 5-HT 2Areceptors. *The Journal of Physiology*, 581:pp. 91–97.

Mittal, P., Romero, R., Tarca, A. L., Gonzalez, J., Draghici, S., Xu, Y., Dong, Z., Nhan-Chang, C.-L., Chaiworapongsa, T., Lye, S., Kusanovic, J. P., Lipovich, L., Mazaki-Tovi, S., Hassan, S. S., Mesiano, S., & Kim, C. J. (2010). Characterization of the myometrial transcriptome and biological pathways of spontaneous human labor at term. *Journal of Perinatal Medicine*, 38:pp. 617–643.

Molica, F., Meens, M. J. P., Morel, S., & Kwak, B. R. (2014). Mutations in cardiovascular connexin genes. *Biology of the Cell*, 106:pp. 269–293.

Molitch, M. E. (2009). Prolactin in Human Reproduction. In Strauss, J. E. & Barberi, R. . L. (Editors), *Yen and Jaffe's Reproductive Endocrinology: Physiology, Pathophysiology and Clinical Management*, chapter 3, pp. 57 –78. Saunders: Philadelphia, 6th edition.

Monaghan, K., Baker, S. A., Dwyer, L., Hatton, W. C., Sik Park, K., Sanders, K. M., & Koh, S. D. (2011). The stretch-dependent potassium channel TREK-1 and its function in murine myometrium. *The Journal of Physiology*, 589:pp. 1221–1233.

Montalbano, A. P., Hawgood, S., & Mendelson, C. R. (2013). Mice deficient in surfactant protein A (SP-A) and SP-D or in TLR2 manifest delayed parturition and decreased expression of inflammatory and contractile genes. *Endocrinology*, 154:pp. 483–498.

Monticone, S., Auchus, R. J., & Rainey, W. E. (2012). Adrenal disorders in pregnancy. *Nature Reviews Endocrinology*, 8:pp. 668–678.

Mortazavi, A., Williams, B. A., McCue, K., Schaeffer, L., & Wold, B. (2008). Mapping and quantifying mammalian transcriptomes by RNA-Seq. *Nature Methods*, 5:pp. 621–628.

Mote, P., Graham, J., & Clarke, C. (2008). Progesterone Receptor Isoforms in Normal and Malignant Breast. In Conneely, O. M. & Otto, C. (Editors), *Progestins and the Mammary*

Gland, volume 1 of *From Basic Science to Clinical Applications*, pp. 77–107. Ernst Schering Foundation Symposium Proceedings, Springer Science & Business Media.

Mueller, O., Lightfoot, S., & Schroeder, A. (2004). RNA integrity number (RIN)–Standardization of RNA Quality Control. *Agilent Application Note, Publication*, 5989:pp. 1–8.

Mulac-Jericevic, B. (2000). Subgroup of Reproductive Functions of Progesterone Mediated by Progesterone Receptor-B Isoform. *Science*, 289:pp. 1751–1754.

Mulac-Jericevic, B. (2004). Reproductive tissue selective actions of progesterone receptors. *Reproduction*, 128:pp. 139–146.

Mulac-Jericevic, B., Lydon, J. P., DeMayo, F. J., & Conneely, O. M. (2003). Defective mammary gland morphogenesis in mice lacking the progesterone receptor B isoform. *Proceedings of the National Academy of Sciences*, 100:pp. 9744–9749.

Murray, G. I. (2008). Laser Microdissection. In Walker, J. & Rapley, R. (Editors), *Molecular Biomethods Handbook*, chapter 56, pp. 1027–1037. Humana Press, 2nd edition.

Nautiyal, J., Christian, M., & Parker, M. G. (2013). Distinct functions for RIP140 in development, inflammation, and metabolism. *TRENDS in Endocrinology and Metabolism*, 24:pp. 451–459.

Neef, G. G., Beier, S. S., Elger, W. W., Henderson, D. D., & Wiechert, R. R. (1984). New steroids with antiprogestational and antiglucocorticoid activities. *Steroids*, 44:pp. 349–372.

Neidhardt, J., Fehr, S., Kutsche, M., Löhler, J., & Schachner, M. (2003). Tenascin-N: characterization of a novel member of the tenascin family that mediates neurite repulsion from hippocampal explants. *Molecular and Cellular Neurosciences*, 23:pp. 193–209.

Nishimori, K., Young, L. J., Guo, Q., Wang, Z., Insel, T. R., & Matzuk, M. M. (1996). Oxytocin is required for nursing but is not essential for parturition or reproductive behavior. *Proceedings of the National Academy of Sciences*, 93:pp. 11699–11704.

Noble, K., Floyd, R., Shmygol, A., Shmygol, A., Mobasheri, A., & Wray, S. (2010). Distribution, expression and functional effects of small conductance Ca-activated potassium (SK) channels in rat myometrium. *Cell Calcium*, 47:pp. 47–54.

Nuclear Receptors Nomenclature Committee (1999). A Unified Nomenclature System for the Nuclear Receptor Superfamily. *Cell*, 97:pp. 161–163.

Nussey, S. S. & Whitehead, S. A. (2002). *Endocrinology: An Integrated Approach*, chapter 1, Principles of endocrinology. BIOS Scientific Publishers: Oxford. URL `http://www.ncbi.nlm.nih.gov/books/NBK20`.

Obr, A. E. & Edwards, D. P. (2012). The biology of progesterone receptor in the normal mammary gland and in breast cancer . *Molecular and Cellular Endocrinology*, 357:pp. 4–17.

Office for National Statistics (2014). Gestation-specific infant mortality, 2012. URL `http://www.ons.gov.uk/ons/publications/re-reference-tables.html?edition=tcm%3A77-349394`.

Ojeda, S. R. & Skinner, M. K. (2006). Puberty in the Rat. In Knobil, E. & Neill, J. D. (Editors), *Knobil and Neill's Physiology of Reproduction*, chapter 38, pp. 2061–2126. Gulf Professional Publishing, 3rd edition.

Oliver, C., Montes, M. J., Galindo, J. A., Ruiz, C., & Olivares, E. G. (1999). Human decidual stromal cells express alpha-smooth muscle actin and show ultrastructural similarities with myofibroblasts. *Human Reproduction*, 14:pp. 1599–1605.

Oshlack, A. & Wakefield, M. J. (2009). Transcript length bias in RNA-seq data confounds systems biology. *Biology Direct*, 4:pp. 14–14.

Osman, I., Young, A., Ledingham, M. A., Thomson, A. J., Jordan, F., Greer, I. A., & Norman, J. E. (2003). Leukocyte density and pro−inflammatory cytokine expression in human fetal membranes, decidua, cervix and myometrium before and during labour at term. *Molecular Human Reproduction*, 9:pp. 41–45.

Ou, C. W., Orsino, A., & Lye, S. J. (1997). Expression of connexin-43 and connexin-26 in the rat myometrium during pregnancy and labor is differentially regulated by mechanical and hormonal signals. *Endocrinology*, 138:pp. 5398–5407.

Pan, W., Lin, J., & Le, C. T. (2002). How many replicates of arrays are required to detect gene expression changes in microarray experiments? A mixture model approach. *Genome Biology*, 3:pp. research0022.1–0022.10.

Pansky, B. (1982). *Review of Medical Embryology*. Macmillan, New York.

Pardee, K., Necakov, A. S., & Krause, H. (2011). Nuclear Receptors: Small Molecule Sensors that Coordinate Growth, Metabolism and Reproduction . In Hughes, T. R. (Editor), *A handbook of transcription factors*, pp. 123–153. Springer, Netherlands.

Paromov, V. M. & Morton, R. E. (2003). Lipid transfer inhibitor protein defines the participation of high density lipoprotein subfractions in lipid transfer reactions mediated by cholesterol ester transfer protein (CETP). *The Journal of Biological Chemistry*, 278:pp. 40859–40866.

Patro, R., Mount, S. M., & Kingsford, C. (2014). Sailfish enables alignment-free isoform quantification from RNA-seq reads using lightweight algorithms. *Nature Biotechnology*, 32:pp. 462–464.

Pedersen, B. S., Yang, I. V., & De, S. (2013). CruzDB: software for annotation of genomic intervals with UCSC genome-browser database. *Bioinformatics*, 29:pp. 3003–3006.

Peracchia, C., Wang, X. G., & Peracchia, L. L. (2014). Slow Gating of Gap Junction Channels and Calmodulin. *The Journal of Membrane Biology*, 178:pp. 55–70.

Peterson, B. L., Won, S., Geddes, R. I., Sayeed, I., & Stein, D. G. (2015). Sex-related differences in effects of progesterone following neonatal hypoxic brain injury. *Behavioural Brain Research*, 286:pp. 152–165.

Petrocelli, T. & Lye, S. J. (1993). Regulation of transcripts encoding the myometrial gap junction protein, connexin-43, by estrogen and progesterone. *Endocrinology*, 133:pp. 284–290.

Phaneuf, S., Rodríguez-Liñares, B., TambyRaja, R. L., MacKenzie, I. Z., & López-Bernal, A. (2000). Loss of myometrial oxytocin receptors during oxytocin-induced and oxytocin-augmented labour. *Journal of Reproduction and Fertility*, 120:pp. 91–97.

Philibert, D., Moguilewsky, M., Mary, M., Lecaque, D., Tournemine, C., Secchi, J., & Deraedt, R. (1985). *Pharmacological profile of RU486 in animals*. The Antiprogestin Steroid RU486 and Human Fertility Control. Plenum Press, New York.

Quinlan, A. R. & Hall, I. M. (2010). BEDTools: a flexible suite of utilities for comparing genomic features. *Bioinformatics*, 26:pp. 841–842.

Rat Genome Sequencing Project Consortium (2004). Genome sequence of the Brown Norway rat yields insights into mammalian evolution. *Nature*, 428:pp. 493–521.

Ratajczak, C. K. & Muglia, L. J. (2008). Insights Into Parturition Biology From Genetically Altered Mice. *Pediatric Research*, 64:pp. 581–589.

Rehfeld, J. F. & Bundgaard, J. R. (Editors) (2010). *Cellular Peptide Hormone Synthesis and Secretory Pathways*, volume 50 of *Results and Problems in Cell Differentiation*. Springer-Verlag, Heidelberg.

Rehman, K. S. (2003). Human myometrial adaptation to pregnancy: cDNA microarray gene expression profiling of myometrium from non-pregnant and pregnant women. *Molecular Human Reproduction*, 9:pp. 681–700.

Rice, T. K., Schork, N. J., & Rao, D. (2008). Methods for Handling Multiple Testing. In *Genetic Dissection of Complex Traits*, volume 60 of *Advances in Genetics*, chapter 12, pp. 293 – 308. Academic Press.

Richer, J. K. & Manning, N. G. (2002). *Role of Progesterone Receptor Isoforms in Regulation of Cell Adhesion and Apoptosis*. U.S. Army Medical Research and Materiel Command, Fort Derrick, Maryland.

Riddick, D. & Kusmik, W. (1977). Decidua: a possible source of amniotic fluid prolactin. *American Journal of Obstetrics & Gynecology*, 127:pp. 187–190.

Riddick, D., Luciano, A. A., Kusmik, W., & ... (1978). De novo synthesis of prolactin by human decidua. *Life Sciences*, 23:p. 1913.

Risso, D., Schwartz, K., Sherlock, G., & Dudoit, S. (2011). GC-content normalization for RNA-Seq data. *BMC Bioinformatics*, 12:p. 480.

Roberts, A., Trapnell, C., Donaghey, J., Rinn, J. L., & Pachter, L. (2011). Improving RNA-Seq expression estimates by correcting for fragment bias. *Genome Biology*, 12:p. R22.

Robertson, J., Willsher, P., Winterbottom, L., Blamey, R., & Thorpe, S. (1999). Onapristone, a progesterone receptor antagonist, as first-line therapy in primary breast cancer. *European Journal of Cancer*, 35:pp. 214 – 218.

Robinson, J. T., Thorvaldsdóttir, H., Winckler, W., Guttman, M., Lander, E. S., Getz, G., & Mesirov, J. P. (2011). Integrative genomics viewer. *Nature*, 29:pp. 24–26.

Robinson, M. D., McCarthy, D. J., & Smyth, G. K. (2010). edgeR: a Bioconductor package for differential expression analysis of digital gene expression data. *Bioinformatics*, 26:pp. 139–140.

Robker, R., Russell, D., Espey, L., & et al (2000). Progesterone-regulated genes in the ovulation process: ADAMTS-1 and cathepsin L proteases. *Proceedings of the ...*, pp. 1–6.

Robles, J. A., Qureshi, S. E., Stephen, S. J., Wilson, S. R., Burden, C. J., & Taylor, J. M. (2012). Efficient experimental design and analysis strategies for the detection of differential expression using RNA-Sequencing. *BMC Genomics*, 13:p. 484.

Rone, M. B., Fan, J., & Papadopoulos, V. (2009). Cholesterol transport in steroid biosynthesis: Role of protein–protein interactions and implications in disease states. *Molecular and Cell Biology of Lipids*, 1791:pp. 646 – 658.

Rubel, C. A., Lanz, R. B., Kommagani, R., Franco, H. L., LYDON, J. P., & DeMayo, F. J. (2012). Research resource: Genome-wide profiling of progesterone receptor binding in the mouse uterus. *Molecular Endocrinology*, 26:pp. 1428–1442.

Saladin, R., Vu-Dac, N., Fruchart, J. C., Auwerx, J., & Staels, B. (1996). Transcriptional induction of rat liver apolipoprotein A-I gene expression by glucocorticoids requires the glucocorticoid receptor and a labile cell-specific protein. *European Journal of Biochemistry*, 239:pp. 451–459.

Salomonis, N., Cotte, N., Zambon, A. C., Pollard, K. S., Vranizan, K., Doniger, S. W., Dolganov, G., & Conklin, B. R. (2005). Identifying genetic networks underlying myometrial transition to labor. *Genome Biology*, 6:p. R12.

Sartorius, C. A., Tung, L., Takimoto, G. S., & Horwitz, K. B. (1993). Antagonist-occupied human progesterone receptors bound to DNA are functionally switched to transcriptional agonists by cAMP. *Journal of Biological Chemistry*, 268:pp. 9262–9266.

Schreiber, J. R., Edelstein, C., & Scanu, A. M. (1985). Effect of high-density lipoproteins with varying ratios of apolipoprotein A-I to apolipoprotein A-II on steroidogenesis by cultured rat ovary granulosa cells. *Biochimica et Biophysica Acta*, 835:pp. 169–175.

Schurch, N. J., Schofield, P., Gierliński, M., Cole, C., Sherstnev, A., Singh, V., Wrobel, N., Gharbi, K., Simpson, G. G., Owen-Hughes, T., Blaxter, M., & Barton, G. J.

(2015). Evaluation of tools for differential gene expression analysis by RNA-seq on a 48 biological replicate experiment. *ArXiv e-prints*. 1505.02017.

Selye, H. (1942). Correlations between the chemical structure and the pharmacological actions of the steroids. *Endocrinology*, 30:pp. 437–453.

Sengupta, P. (2013). The Laboratory Rat: Relating Its Age With Human's. *International Journal of Preventive Medicine*, 4:pp. 624—630.

Sheldon, R. E., Mashayamombe, C., Shi, S.-Q., Garfield, R. E., Shmygol, A., Blanks, A. M., & van den Berg, H. A. (2014). Alterations in gap junction connexin43/connexin45 ratio mediate a transition from quiescence to excitation in a mathematical model of the myometrium. *Journal of The Royal Society Interface*, 11.

Shimizu, Y., Takeuchi, T., Mita, S., Notsu, T., Mizuguchi, K., & Kyo, S. (2010). Krüppel-like factor 4 mediates anti-proliferative effects of progesterone with G0/G1 arrest in human endometrial epithelial cells. *Journal of Endocrinological Investigation*, 33:pp. 745–750.

Shynlova, O. (2005). Expression and Localization of Alpha-Smooth Muscle and Gamma-Actins in the Pregnant Rat Myometrium. *Biology of Reproduction*, 73:pp. 773–780.

Shynlova, O., Kwong, R., & Lye, S. J. (2010). Mechanical stretch regulates hypertrophic phenotype of the myometrium during pregnancy. *Reproduction*, 139:pp. 247–253.

Simon, A. M., Goodenough, D. A., & Paul, D. L. (1998). Mice lacking connexin40 have cardiac conduction abnormalities characteristic of atrioventricular block and bundle branch block. *Current Biology*, 8:pp. 295–298.

Simone, N., Bonner, R., Gillespie, J., Emmert-Buck, M., & Liotta, L. (1998). Laser-capture microdissection: opening the microscopic frontier to molecular analysis. *Trends in Genetics*, 14:pp. 272–276.

Skolnick, B. E., Maas, A. I., Narayan, R. K., van der Hoop, R. G., MacAllister, T., Ward, J. D., Nelson, N. R., Stocchetti, N., & SYNAPSE Trial Investigators (2014). A clinical trial of progesterone for severe traumatic brain injury. *New England Journal of Medicine*, 371:pp. 2467–2476.

Smit, A. F. A., Hubley, R., & Green, P. (2010). RepeatMasker version open-4.0.5. URL `http://www.repeatmasker.org`.

Smith, R. (2007). Parturition. *New England Journal of Medicine*, 356:pp. 271–83.

Smith, R., McClure, M., Smith, M., Abel, P., & Bradley, M. (2007). The role of voltage-gated potassium channels in the regulation of mouse uterine contractility. *Reproductive Biology and Endocrinology*, 5:p. 41.

Snegovskikh, V., Park, J. S., & Norwitz, E. R. (2006). Endocrinology of Parturition. *Endocrinolology and Metabolism Clinics of North America*, 35:pp. 173–191.

Sobue, K., Hayashi, K., & Nishida, W. (1999). Expressional regulation of smooth muscle cell-specific genes in association with phenotypic modulation. *Molecular and Cellular Biochemistry*, 190:pp. 105–118.

Soloff, M. S., Jeng, Y.-J., Izban, M. G., Sinha, M., Luxon, B. A., Stamnes, S. J., & England, S. K. (2011). Effects of progesterone treatment on expression of genes involved in uterine quiescence. *Reproductive Sciences*, 18:pp. 781–797.

Soneson, C. & Delorenzi, M. (2013). A comparison of methods for differential expression analysis of RNA-seq data. *BMC Bioinformatics*, 14:p. 91.

Song, M., Zhu, N., Olcese, R., Barila, B., Toro, L., & Stefani, E. (1999). Hormonal control of protein expression and mRNA levels of the MaxiK channel alpha subunit in myometrium. *FEBS Letters*, 460:pp. 427–432.

Steinman, M. Q. & Trainor, B. C. (2010). Rapid Effects of Steroid Hormones on Animal Behavior. *Nature Education Knowledge*, 1:p. 1.

Stephen, G. L., Lui, S., Hamilton, S. A., Tower, C. L., Harris, L. K., Stevens, A., & Jones, R. L. (2014). Transcriptomic Profiling of Human Choriodecidua During Term Labor: Inflammation as a Key Driver of Labor. *American Journal of Reproductive Immunology*, 73:pp. 36–55.

Stouffer, R. L. (2006). Structure, Function, and Regulation of the Corpus Luteum. In Neill, J. D. & Challis, J. R. G. (Editors), *Knobil and Neill's Physiology of Reproduction*, chapter 12, pp. 475—526. Gulf Professional Publishing, 3rd edition.

Strauss, J. E. & Lessey, B. A. (2009). The Structure, Function, and Evaluation of the Female Reproductive Tract. In Strauss, J. E. & Barberi, R. . L. (Editors), *Yen and Jaffe's Reproduc-*

tive Endocrinology: Physiology, Pathophysiology and Clinical Management, chapter 9. Saunders: Philadelphia, 6th edition.

Strauss, J. E. & Williams, C. J. (2009). The Ovarian Life Cycle. In Strauss, J. E. & Barberi, R. . L. (Editors), *Yen and Jaffe's Reproductive Endocrinology: Physiology, Pathophysiology and Clinical Management*, chapter 8, pp. 155–190. Saunders: Philadelphia, 6th edition.

Sugimoto, Y., Inazumi, T., & Tsuchiya, S. (2015). Roles of prostaglandin receptors in female reproduction. *Journal of Biochemistry*, 157:pp. 73–80.

Sugimoto, Y., Yamasaki, A., Segi, E., Tsuboi, K., Aze, Y., Nishimura, T., Oida, H., Yoshida, N., Tanaka, T., Katsuyama, M., Hasumoto, K.-y., Murata, T., Hirata, M., Ushikubi, F., Negishi, M., Ichikawa, A., & Narumiya, S. (1997). Failure of Parturition in Mice Lacking the Prostaglandin F Receptor. *Science*, 277:pp. 681–683.

Sun, H.-W., Miao, C.-Y., Liu, L., Zhou, J., Su, D.-F., Wang, Y.-X., & Jiang, C.-L. (2006). Rapid inhibitory effect of glucocorticoids on airway smooth muscle contractions in guinea pigs. *Steroids*, 71:pp. 154 – 159.

Sunny, F. & Oommen, O. V. (2001). Rapid action of glucocorticoids on branchial {ATPase} activity in Oreochromis mossambicus: an in vivo and in vitro study. *Comparative Biochemistry and Physiology Part B: Biochemistry and Molecular Biology*, 130:pp. 323 – 330.

Tan, H., Yi, L., Rote, N. S., Hurd, W. W., & Mesiano, S. (2012). Progesterone Receptor-A and -B Have Opposite Effects on Proinflammatory Gene Expression in Human Myometrial Cells: Implications for Progesterone Actions in Human Pregnancy and Parturition. *Journal of Clinical Endocrinology & Metabolism*, 97:pp. E719–E730.

Tang, D. D. (2008). Intermediate Filaments In Smooth Muscle. *American Journal of Physiology-Cell Physiology*, 294:pp. C869–C878.

Terzidou, V. (2007). Biochemical and endocrinological preparation for parturition. *Best Practice & Research Clinical Obstetrics and Gynaecology*, 21:pp. 729–756.

Tetel, M. J. (2009). Nuclear Receptor Coactivators: Essential Players for Steroid Hormone Action in the Brain and in Behaviour. *Journal of Neuroendocrinology*, 21:pp. 229–237.

Thiriet, M. (2013). Smooth Myocytes. In *Tissue Functioning and Remodeling in the Circulatory and Ventilatory Systems*, volume 5, chapter 8, pp. 381–452. Springer New York.

Thong, K. & Baird, D. (1992). A study of gemeprost alone, dilapan or mifepristone in combination with gemeprost for the termination of second trimester pregnancy. *Contraception*, 46:pp. 11 – 17.

Thorvaldsdóttir, H., Robinson, J. T., & Mesirov, J. P. (2012). Integrative Genomics Viewer (IGV): high-performance genomics data visualization and exploration. *Briefings in Bioinformatics*, pp. 178–192.

Timm, N. H. (2002a). *Applied Multivariate Analysis*, chapter 8: Principal Component, Canonical Correlation, and Exploratory Factor Analysis, pp. 445–514. Springer New York.

Timm, N. H. (2002b). *Applied Multivariate Analysis*, chapter 9: Cluster Analysis and Multidimensional Scaling, pp. 515–556. Springer New York.

Trapnell, C., Roberts, A., Goff, L., Pertea, G., andD. R. Kelley, D. K., Pimentel, H., Salzberg, S. L., Rinn, J. L., & Pachter, L. (2012). Differential gene and transcript expression analysis of RNA-seq experiments with TopHat and Cufflinks. *Nature Protocols*, 7:pp. 562–578.

Tung, L., Abdel-Hafiz, H., Shen, T., Harvell, D., Nitao, L., Richer, J., Sartorius, C., Takimoto, G., & Horwitz, K. (2006). Progesterone receptors (PR)-B and-A regulate transcription by different mechanisms: AF-3 exerts regulatory control over coactivator binding to PR-B. *Molecular Endocrinology*, 20:pp. 2656–2670.

Vadillo-Ortega, F. & Estrada-Gutierrez, G. (2005). Role of matrix metalloproteinases in preterm labour. *BJOG: An International Journal of Obstetrics & Gynaecology*, 112 Suppl 1:pp. 19–22.

Vane, J. R., Bakhle, Y. S., & Botting, R. M. (1998). Cyclooxygenases 1 and 2. *Annual Review of Pharmacology and Toxicology*, 38:pp. 97–120.

Vodstrcil, L. A., Shynlova, O., Westcott, K., Laker, R., Simpson, E., Wlodek, M. E., & Parry, L. J. (2010). Progesterone withdrawal, and not increased circulating relaxin, mediates the decrease in myometrial relaxin receptor (RXFP1) expression in late gestation in rats. *Biology of Reproduction*, 83:pp. 825–32.

Vrachnis, N., Malamas, F. M., Sifakis, S., Deligeoroglou, E., & Iliodromiti, Z. (2011). The Oxytocin-Oxytocin Receptor System and Its Antagonists as Tocolytic Agents. *International Journal of Endocrinology*. URL `http://dx.doi.org/10.1155/2011/350546`.

Wagner, G., Kin, K., & Lynch, V. (2012). Measurement of mRNA abundance using RNA-seq data: RPKM measure is inconsistent among samples. *Theory in Biosciences*, 131:pp. 281–285.

Walsh, M. P. (1994). Calmodulin and the regulation of smooth muscle contraction. *Molecular and Cellular Biochemistry*, 135:pp. 21–41.

Wang, Y., Kinzie, E., Berger, F., Lim, S.-K., & Baumann, H. (2001). Haptoglobin, an inflammation-inducible plasma protein. *Redox Report*, 6:pp. 379–385.

Wargon, V., Riggio, M., Giulianelli, S., Sequeira, G. R., Rojas, P., May, M., Polo, M. L., Gorostiaga, M. A., Jacobsen, B., Molinolo, A., Novaro, V., & Lanari, C. (2015). Progestin and antiprogestin responsiveness in breast cancer is driven by the PRA/PRB ratio via AIB1 or SMRT recruitment to the CCND1 and MYC promoters. *International Journal of Cancer*, 136:pp. 2680–2692.

Wendler, A., Baldi, E., Harvey, B. J., Nadal, A., Norman, A., & Wehling, M. (2010). Rapid responses to steroids: current status and future prospects. *European Journal of Endocrinology*, 162:pp. 825–830.

Wesolowski, S., Birtwistle, M., & Rempala, G. (2013). A Comparison of Methods for RNA-Seq Differential Expression Analysis and a New Empirical Bayes Approach. *Biosensors*, 3:pp. 238–258.

Westwood, F. R. (2008). The Female Rat Reproductive Cycle: A Practical Histological Guide to Staging. *Toxicologic Pathology*, 36:pp. 375–384.

Wetendorf, M. & DeMayo, F. J. (2012). The progesterone receptor regulates implantation, decidualization, and glandular development via a complex paracrine signaling network. *Molecular and Cellular Endocrinology*, 357:pp. 108–118.

White, R., Leonardsson, G., Rosewell, I., Ann Jacobs, M., Milligan, S., & Parker, M. (2000). The nuclear receptor co-repressor nrip1 (RIP140) is essential for female fertility. *Nature Medicine*, 6:pp. 1368–1374.

Wikland, M., Lindblom, B., Hammarström, S., & Wiqvist, N. (1983). The effect of prostaglandin I on the contractility of the term pregnant human myometrium. *Prostaglandins*, 26:pp. 905–916.

Winn, V. D., Haimov-Kochman, R., Paquet, A. C., Yang, Y. J., Madhusudhan, M. S., Gormley, M., Feng, K.-T. V., Bernlohr, D. A., McDonagh, S., Pereira, L., Sali, A., & Fisher, S. J. (2007). Gene Expression Profiling of the Human Maternal-Fetal Interface Reveals Dramatic Changes between Midgestation and Term. *Endocrinology*, 148:pp. 1059–1079.

Wood, G. W., Hausmann, E. H., Choudhuri, R., & Dileepan, K. N. (2000). Expression and regulation of histidine decarboxylase mRNA expression in the uterus during pregnancy in the mouse. *Cytokine*, 12:pp. 622–629.

Wray, S., Burdyga, T., Noble, D., Noble, K., Borysova, L., & Arrowsmith, S. (2014). Progress in understanding electro-mechanical signalling in the myometrium. *Acta Physiologica*, 213:pp. 417–431.

Xu, J., Qiu, Y., Demayo, F., Tsai, S., Tsai, M., & O'Malley, B. (1998). Partial hormone resistance in mice with disruption of the steroid receptor coactivator-1 (SRC-1) gene. *Science*, 279:pp. 1922–1925.

Yao, W., Dai, W., Shahnazari, M., Pham, A., Chen, Z., Chen, H., Guan, M., & Lane, N. (2010). Inhibition of the progesterone nuclear receptor during the bone linear growth phase increases peak bone mass in female mice. *PLoS One*, 5:p. e11410.

Yin, P., Roqueiro, D., Huang, L., Owen, J. K., Xie, A., Navarro, A., Monsivais, D., Coon, J. S., V, Kim, J. J., Dai, Y., & Bulun, S. E. (2012). Genome-Wide Progesterone Receptor Binding: Cell Type-Specific and Shared Mechanisms in T47D Breast Cancer Cells and Primary Leiomyoma Cells. *PLOS ONE*, 7:p. e29021.

Young, R. C. (2007). Myocytes, Myometrium, and Uterine Contractions. *Annals of the New York Academy of Sciences*, 1101:pp. 72–84.

Yousuf, S., Atif, F., Sayeed, I., Tang, H., & Stein, D. G. (2014). Progesterone in transient ischemic stroke: a dose–response study. *Psychopharmacology*, 231:pp. 3313–3323.

Yuan, W., Heesom, K., Phillips, R., Chen, L., Trinder, J., & Lopez Bernal, A. (2012). Low abundance plasma proteins in labour. *Reproduction*, 144:pp. 505–518.

Zakar, T. & Hertelendy, F. (2007). Progesterone withdrawal: key to parturition. *American Journal of Obstetrics & Gynecology*, 196:pp. 289–296.

Zhang, Z., Burch, P. E., Cooney, A. J., Lanz, R. B., Pereira, F. A., Wu, J., Gibbs, R. A., Weinstock, G., & Wheeler, D. A. (2004). Genomic analysis of the nuclear receptor family: new insights into structure, regulation, and evolution from the rat genome. *Genome Research*, 14:pp. 580–590.

Zheng, W., Chung, L. M., & Zhao, H. (2011). Bias detection and correction in RNA-Sequencing data. *BMC Bioinformatics*, 12:p. 290.

Part IV

Appendix

Appendix A

Nuclear Receptor Nomenclature

Table A.1: Proposed Nomenclature for Nuclear Receptors.

Subfamily and Group	NR/Gene	Trivial Names	Accession Number
Group 1			
1A	NR1A1	TRα, c-erbA-1, THRA	M24748
	NR1A2	TRβ, c-erbA-2, THRB	X04707
1B	NR1B1	RARα	X06538
	NR1B2	RARβ, HAP	Y00291
	NR1B3	RAR?, RARD	M57707
1C	NR1C1	PPARα	L02932
	NR1C2	PPARβ, NUC1, PPAR?, FAAR	L07592
	NR1C3	PPAR?	L40904
1D	NR1D1	REVERBα, EAR1, EAR1A	M24898
	NR1D2	REVERBβ, EAR1β, BD73, RVR, HZF2	L31785
	NR1D3	E75	X51548
1E	NR1E1	E78, DR-78	U01087
1F	NR1F1	RORα, RZRα	U04897
	NR1F2	RORβ, RZRβ	Y08639
	NR1F3	ROR, TOR	U16997
	NR1F4	HR3, DHR3, MHR3, GHR3, CNR3, CHR3	M90806 U13075
1G	NR1G1	CNR14	U13074
1H	NR1H1	ECR	M74078
	NR1H2	UR, OR-1, NER1, RIP15, LXRβ	U07132
	NR1H3	RLD1, LXR, LXRα	U22662
	NR1H4	FXR, RIP14, HRR1	U09416
1I	NR1I1	VDR	J03258
	NR1I2	ONR1, PXR, SXR, BXR	X75163
	NR1I3	MB67, CAR1, CARα	Z30425
	NR1I4	CAR2, CARβ	AF00932
1J	NR1J1	DHR96	U36792
1K	NR1K1	NHR1	U19360
Group 2			

Continued on next page

Table A.1 – continued from previous page

Subfamily and Group	NR/Gene	Trivial Names	Accession Number
2A	NR2A1	HNF4	X76930
	NR2A2	HNF4G	Z49826
	NR2A3	HNF4B	Z49827
	NR2A4	DHNF4, HNF4D	U70874
2B	NR2B1	RXRA	X52773
	NR2B2	RXRB, H-2RIIBP, RCoR-1	M84820
	NR2B3	RXRG	X66225
	NR2B4	USP, Ultraspiracle, 2C1, CF1	X52591
2C	NR2C1	TR2, TR2-11	M29960
	NR2C2	TR4, TAK1	L27586
2D	NR2D1	DHR78	U36791
2E	NR2E1	TLL, TLX, XTLL	S72373
	NR2E2	TLL, Tailless	M34639
2F	NR2F1	COUP-TFI, COUPTFA, EAR3, SVP44	X12795
	NR2F2	COUP-TFII, COUPTFB, ARP1, SVP40	M64497
	NR2F3	SVP, COUP-TF	M28863
	NR2F4	COUP-TFIII, COUPTFG	X63092
	NR2F5	SVP46	X70300
	NR2F6	EAR2	X12794
Group 3			
3A	NR3A1	ERα	X03635
	NR3A2	ERβ	U57439
3B	NR3B1	ERR1, ERRα	X51416
	NR3B2	ERR2, ERRβ	X51417
3C	NR3C1	GR	X03225
	NR3C2	MR	M16801
	NR3C3	PR	M15716
	NR3C4	AR	M20132
Group 4			
4A	NR4A1	NGFIB, TR3, N10, NUR77, NAK1	L13740
	NR4A2	NURR1, NOT, RNR1, HZF-3, TINOR	X75918
	NR4A3	NOR1, MINOR	D38530
	NR4A4	DHR38, NGFIB	U36762
		CNR8, C48D5	U13076
Group 5			
5A	NR5A1	SF1, ELP, FTZ-F1, AD4BP	D88155
	NR5A2	LRH1, xFF1rA, xFF1rB, FFLR, PHR, FTF	U93553
	NR5A3	FTZ-F1	M63711
5B	NR5B1	DHR39, FTZF1B	L06423
Group 6			
6A	NR6A1	GCNF1, RTR	U14666
Group 0			
0A	NR0A1	KNI, Knirps	X13331
	NR0A2	KNRL, Knirps related	X14153
	NR0A3	EGON, Embryonic gonad, EAGLE	X16631
	NR0A4	ODR7	U16708
	NR0A5	Trithorax	M31617
0B	NR0B1	DAX1, AHCH	S74720
	NR0B2	SHP	L76571

Appendix B

Animals Used in the Study

Table B.1: Animals used in the study. GD indicates the gestational day.

Treatment	Collection Day	Number of Animals
Control	GD19+6hrs	3
RU486	GD19+6hrs	3
Control	GD20	3
RU486	GD20	3
Control	GD22	2
Control	GD22 (NL)	3
P4	GD22	3

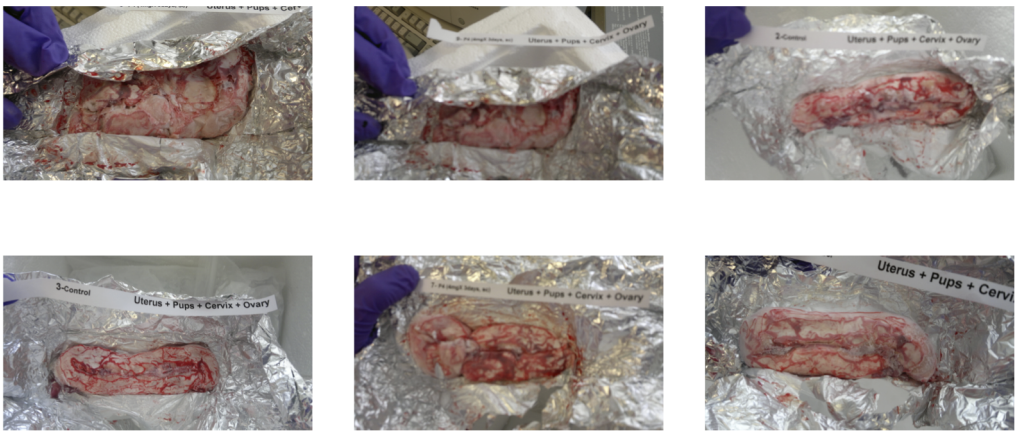

Figure B.1: Visual checking of samples. Six frozen whole uterus samples being checked visually to make sure they are still frozen.

Table B.2: Whole uterine samples for the research. The samples were catalogued and weighed after 24h of receipt.

Sample ID	Treatment	Day of Sacrifice	Weight (in g)
1	Vehicle	GD22	40.4
2	Vehicle	GD22	64.7
3	Vehicle	GD22	43.7
7	P4 (×3 days, 4mg)	GD22	61.1
8	P4 (×3 days, 4mg)	GD22	62.5
9	P4 (×3 days, 4mg)	GD22	65.3
R1	Vehicle	GD19 + 6h	25.9
R2	Vehicle	GD19 + 6h	29.9
R3	Vehicle	GD19 + 6h	26.6
R4	Vehicle	GD20	30.6
R5	Vehicle	GD20	23.4
R6	Vehicle	GD20	32.8
R7	RU486 (3mg)	GD19 + 6h	14.4
R8	RU486 (3mg)	GD19 + 6h	22.2
R9	RU486 (3mg)	GD19 + 6h	31.5
R10	RU486 (3mg)	GD20 + 6h	33.6
R11	RU486 (3mg)	GD20 + 6h	33.6
R12	RU486 (3mg)	GD20 + 6h	39.9
A-CTR	Vehicle	GD22	4
B-CTR	Vehicle	GD22	38.9
C-CTR	Vehicle	GD22	49.1

Table B.3: Quantitation of total RNA using the NanoDrop®.

Sample ID	Concentration (ng/µl)	260/280	260/230
1	2651.165	2.04	2.16
2	676.415	2.15	1.4
3	1464.56	2.08	1.76
7	775.615	2.16	1.22
8	1407.735	2.14	1.86
9	803.595	2.28	1.24
R1	3832.835	1.83	1.92
R2	2735.875	1.86	1.93
R3	3375.49	1.95	2.06
R4	2024.57	2.05	1.78
R5	2739.56	2.01	2.19
R6	2583.53	1.94	2.22
R7	3779.27	1.85	1.98
R8	3311.345	1.97	2.08
R9	4069.135	1.67	1.78
R10	2958.995	1.93	2.14
R11	3966.2	1.78	1.78
R12	3585.295	1.73	1.84
A-CTR	3442.875	1.92	2.09
B-CTR	3985.61	1.77	1.87
C-CTR	2503.64	1.97	2.15

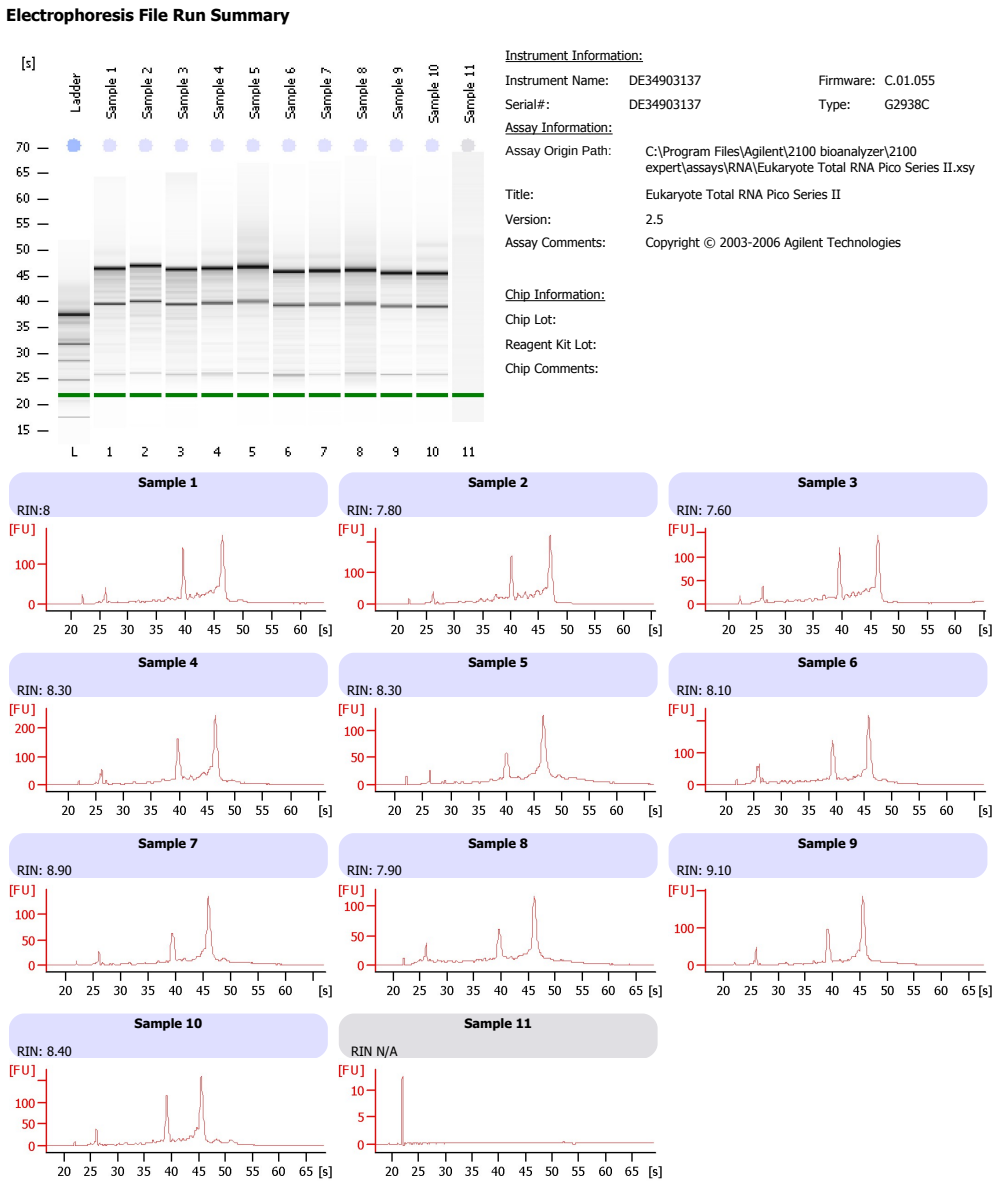

Figure B.2: Bioanalyzer traces. The RIN indicates the integrity of the RNA, where 10 is the most intact and 1 is the most degraded. **RIN**: RNA integrity number.

Appendix C

Inspection for Bias

Table C.1: Inspection of FASTQ files. FASTQ files were inspected for contamination and sequencing errors. A pass (green) indicated that a file passed a test, while a warning (orange) was issued if the test result result was borderline, and a fail (red) indicated that the file had not passed the test. **GD19q**: 6 hours after the 19^{th} day of gestation; **GD20**: 20^{th} day of gestation; **GD22**: 22^{nd} day of gestation - not in labour; **GD22L)**: 22^{nd} day of gestation - in labour; **CTR**: control; **RU486**: mifepristone-treated; **P4**: progesterone treated; **DEC**: decidua; **INN**: inner myometrium; **OUT**: outer myometrium.

File	Basic Stats	Seq Quality	Quality Scores	Seq Content	Base GC Content	Seq GC Content	N Content	Seq Length	Seq Duplicates	Overrepresented Seqs	Kmer Content
GD19q-CTR-DEC-r1a	PASS	PASS	PASS	WARN	PASS	FAIL	PASS	PASS	FAIL	FAIL	FAIL
GD19q-CTR-DEC-r1a	PASS	PASS	PASS	WARN	PASS	FAIL	PASS	PASS	FAIL	FAIL	FAIL
GD19q-CTR-DEC-r2a	PASS	PASS	PASS	WARN	PASS	PASS	PASS	PASS	WARN	WARN	FAIL
GD19q-CTR-DEC-r2a	PASS	PASS	PASS	WARN	PASS	PASS	PASS	PASS	WARN	WARN	FAIL
GD19q-CTR-DEC-r3a	PASS	PASS	PASS	WARN	PASS	PASS	PASS	PASS	FAIL	WARN	WARN
GD19q-CTR-DEC-r3a	PASS	PASS	PASS	WARN	PASS	PASS	PASS	PASS	FAIL	WARN	WARN
GD19q-CTR-INN-r1b	PASS	PASS	PASS	WARN	PASS	PASS	PASS	PASS	FAIL	WARN	FAIL
GD19q-CTR-INN-r1b	PASS	PASS	PASS	WARN	PASS	PASS	PASS	PASS	FAIL	WARN	FAIL
GD19q-CTR-INN-r2b	PASS	PASS	PASS	PASS	PASS	PASS	PASS	PASS	WARN	WARN	WARN
GD19q-CTR-INN-r2b	PASS	PASS	PASS	PASS	PASS	PASS	PASS	PASS	WARN	WARN	WARN
GD19q-CTR-INN-r3b	PASS	PASS	PASS	PASS	PASS	PASS	PASS	PASS	WARN	WARN	WARN
GD19q-CTR-INN-r3b	PASS	PASS	PASS	PASS	PASS	PASS	PASS	PASS	WARN	WARN	WARN
GD19q-CTR-OUT-r1c	PASS	PASS	PASS	PASS	PASS	PASS	PASS	PASS	FAIL	PASS	WARN
GD19q-CTR-OUT-r1c	PASS	PASS	PASS	PASS	PASS	PASS	PASS	PASS	FAIL	PASS	WARN
GD19q-CTR-OUT-r2c	PASS	PASS	PASS	WARN	PASS	PASS	PASS	PASS	WARN	WARN	FAIL
GD19q-CTR-OUT-r2c	PASS	PASS	PASS	WARN	PASS	PASS	PASS	PASS	WARN	WARN	FAIL
GD19q-CTR-OUT-r3c	PASS	PASS	PASS	WARN	PASS	WARN	PASS	PASS	FAIL	WARN	WARN
GD19q-CTR-OUT-r3c	PASS	PASS	PASS	WARN	PASS	WARN	PASS	PASS	FAIL	WARN	FAIL
GD19q-RU486-DEC-r7a	PASS	PASS	PASS	WARN	WARN	PASS	PASS	PASS	FAIL	WARN	WARN
GD19q-RU486-DEC-r7a	PASS	PASS	PASS	WARN	WARN	PASS	PASS	PASS	FAIL	WARN	WARN
GD19q-RU486-DEC-r8a	PASS	PASS	PASS	WARN	WARN	WARN	PASS	PASS	FAIL	PASS	WARN
GD19q-RU486-DEC-r8a	PASS	PASS	PASS	PASS	WARN	WARN	PASS	PASS	FAIL	WARN	WARN
GD19q-RU486-INN-r8b	PASS	PASS	PASS	PASS	WARN	PASS	PASS	PASS	FAIL	PASS	WARN
GD19q-RU486-INN-r8b	PASS	PASS	PASS	PASS	WARN	PASS	PASS	PASS	FAIL	WARN	WARN
GD19q-RU486-INN-r9b	PASS	PASS	PASS	PASS	PASS	PASS	PASS	PASS	FAIL	WARN	FAIL
GD19q-RU486-INN-r9b	PASS	PASS	PASS	PASS	PASS	PASS	PASS	PASS	FAIL	WARN	FAIL
GD19q-RU486-OUT-r7c	PASS	PASS	PASS	WARN	WARN	PASS	PASS	PASS	WARN	WARN	FAIL
GD19q-RU486-OUT-r7c	PASS	PASS	PASS	WARN	PASS	PASS	PASS	PASS	WARN	WARN	FAIL
GD19q-RU486-OUT-r8c	PASS	PASS	PASS	PASS	PASS	PASS	PASS	PASS	FAIL	WARN	WARN
GD19q-RU486-OUT-r8c	PASS	PASS	PASS	PASS	PASS	PASS	PASS	PASS	FAIL	WARN	WARN

Continued on next page

Table C.1 – continued from previous page

File	Basic Stats	Seq Quality	Quality Scores	Seq Content	Base GC Content	Seq GC Content	N Content	Seq Length	Seq Duplicates	Overrepresented Seqs	Kmer Content
GD19q-RU486-OUT-r9c	PASS	PASS	PASS	WARN	PASS	WARN	PASS	PASS	FAIL	WARN	FAIL
GD19q-RU486-OUT-r9c	PASS	PASS	PASS	WARN	PASS	WARN	PASS	PASS	FAIL	WARN	FAIL
GD20-CTR-DEC-r4a	PASS	PASS	PASS	WARN	PASS	PASS	PASS	PASS	WARN	WARN	WARN
GD20-CTR-DEC-r4a	PASS	PASS	PASS	WARN	PASS	PASS	PASS	PASS	WARN	WARN	WARN
GD20-CTR-DEC-r5a	PASS	PASS	PASS	FAIL	WARN	FAIL	PASS	PASS	FAIL	FAIL	FAIL
GD20-CTR-DEC-r5a	PASS	PASS	PASS	FAIL	WARN	FAIL	PASS	PASS	FAIL	FAIL	FAIL
GD20-CTR-DEC-r6a	PASS	PASS	PASS	PASS	PASS	PASS	PASS	PASS	FAIL	WARN	FAIL
GD20-CTR-DEC-r6a	PASS	PASS	PASS	PASS	PASS	PASS	PASS	PASS	FAIL	WARN	FAIL
GD20-CTR-INN-r4b	PASS	PASS	PASS	PASS	WARN	PASS	PASS	PASS	FAIL	WARN	FAIL
GD20-CTR-INN-r4b	PASS	PASS	PASS	PASS	PASS	PASS	PASS	PASS	FAIL	WARN	FAIL
GD20-CTR-INN-r5b	PASS	PASS	PASS	WARN	PASS	PASS	PASS	PASS	WARN	WARN	WARN
GD20-CTR-INN-r5b	PASS	PASS	PASS	WARN	PASS	PASS	PASS	PASS	WARN	WARN	WARN
GD20-CTR-INN-r6b	PASS	PASS	PASS	WARN	WARN	WARN	PASS	PASS	FAIL	WARN	FAIL
GD20-CTR-INN-r6b	PASS	PASS	PASS	WARN	WARN	WARN	PASS	PASS	FAIL	WARN	FAIL
GD20-CTR-INN-r6b	PASS	PASS	PASS	WARN	WARN	WARN	PASS	PASS	FAIL	WARN	FAIL
GD20-CTR-INN-r6b	PASS	PASS	PASS	WARN	WARN	WARN	PASS	PASS	FAIL	WARN	FAIL
GD20-CTR-INN-r6b	PASS	PASS	PASS	WARN	WARN	WARN	PASS	PASS	FAIL	WARN	FAIL
GD20-CTR-OUT-r4c	PASS	PASS	PASS	WARN	PASS	PASS	PASS	PASS	FAIL	WARN	WARN
GD20-CTR-OUT-r4c	PASS	PASS	PASS	WARN	PASS	PASS	PASS	PASS	FAIL	WARN	WARN
GD20-CTR-OUT-r5c	PASS	PASS	PASS	WARN	PASS	PASS	PASS	PASS	FAIL	WARN	WARN
GD20-CTR-OUT-r5c	PASS	PASS	PASS	PASS	PASS	PASS	PASS	PASS	FAIL	WARN	WARN
GD20-CTR-OUT-r6c	PASS	PASS	PASS	PASS	PASS	PASS	PASS	PASS	FAIL	WARN	WARN
GD20-CTR-OUT-r6c	PASS	PASS	PASS	PASS	PASS	PASS	PASS	PASS	FAIL	WARN	WARN
GD20-RU486-DEC-r10a	PASS	PASS	PASS	PASS	PASS	PASS	PASS	PASS	FAIL	WARN	WARN
GD20-RU486-DEC-r10a	PASS	PASS	PASS	PASS	PASS	PASS	PASS	PASS	FAIL	WARN	FAIL
GD20-RU486-DEC-r11a	PASS	PASS	PASS	WARN	PASS	WARN	PASS	PASS	FAIL	WARN	FAIL
GD20-RU486-DEC-r11a	PASS	PASS	PASS	WARN	PASS	WARN	PASS	PASS	FAIL	WARN	FAIL
GD20-RU486-DEC-r12a	PASS	PASS	PASS	PASS	PASS	PASS	PASS	PASS	FAIL	WARN	WARN
GD20-RU486-DEC-r12a	PASS	PASS	PASS	PASS	PASS	PASS	PASS	PASS	FAIL	PASS	WARN
GD20-RU486-INN-r10b	PASS	PASS	PASS	WARN	PASS	PASS	PASS	PASS	FAIL	WARN	FAIL
GD20-RU486-INN-r10b	PASS	PASS	PASS	WARN	PASS	PASS	PASS	PASS	FAIL	WARN	FAIL
GD20-RU486-INN-r11b	PASS	PASS	PASS	WARN	PASS	PASS	PASS	PASS	FAIL	PASS	WARN
GD20-RU486-INN-r11b	PASS	PASS	PASS	WARN	PASS	PASS	PASS	PASS	FAIL	PASS	WARN
GD20-RU486-INN-r11b	PASS	PASS	PASS	PASS	PASS	PASS	PASS	PASS	FAIL	PASS	WARN
GD20-RU486-INN-r11b	PASS	PASS	PASS	PASS	PASS	PASS	PASS	PASS	FAIL	PASS	WARN
GD20-RU486-INN-r12b	PASS	PASS	PASS	PASS	PASS	PASS	PASS	PASS	FAIL	WARN	FAIL
GD20-RU486-INN-r12b	PASS	PASS	PASS	PASS	PASS	PASS	PASS	PASS	FAIL	WARN	FAIL
GD20-RU486-OUT-r10c	PASS	PASS	PASS	WARN	PASS	PASS	PASS	PASS	FAIL	PASS	WARN
GD20-RU486-OUT-r10c	PASS	PASS	PASS	WARN	PASS	PASS	PASS	PASS	FAIL	PASS	WARN
GD20-RU486-OUT-r11c	PASS	PASS	PASS	WARN	PASS	PASS	PASS	PASS	WARN	WARN	WARN
GD20-RU486-OUT-r11c	PASS	PASS	PASS	WARN	PASS	PASS	PASS	PASS	WARN	WARN	WARN
GD20-RU486-OUT-r12c	PASS	PASS	PASS	PASS	PASS	PASS	PASS	PASS	FAIL	PASS	WARN
GD20-RU486-OUT-r12c	PASS	PASS	PASS	PASS	PASS	PASS	PASS	PASS	FAIL	PASS	WARN
GD22-CTR-DEC-1a	PASS	PASS	PASS	WARN	PASS	PASS	PASS	PASS	WARN	WARN	WARN
GD22-CTR-DEC-1a	PASS	PASS	PASS	WARN	PASS	PASS	PASS	PASS	WARN	WARN	FAIL
GD22-CTR-DEC-2a	PASS	PASS	PASS	PASS	PASS	PASS	PASS	PASS	FAIL	WARN	FAIL
GD22-CTR-DEC-2a	PASS	PASS	PASS	PASS	PASS	PASS	PASS	PASS	FAIL	WARN	FAIL
GD22-CTR-DEC-3a	PASS	PASS	PASS	PASS	PASS	PASS	PASS	PASS	FAIL	WARN	WARN
GD22-CTR-DEC-3a	PASS	PASS	PASS	PASS	PASS	PASS	PASS	PASS	FAIL	WARN	WARN
GD22-CTR-INN-1b	PASS	PASS	PASS	PASS	PASS	PASS	PASS	PASS	FAIL	WARN	WARN
GD22-CTR-INN-1b	PASS	PASS	PASS	PASS	PASS	PASS	PASS	PASS	FAIL	WARN	WARN
GD22-CTR-INN-2b	PASS	PASS	PASS	WARN	PASS	WARN	PASS	PASS	FAIL	WARN	FAIL
GD22-CTR-INN-2b	PASS	PASS	PASS	WARN	PASS	WARN	PASS	PASS	FAIL	WARN	FAIL
GD22-CTR-INN-3b	PASS	PASS	PASS	PASS	PASS	PASS	PASS	PASS	FAIL	WARN	WARN
GD22-CTR-INN-3b	PASS	PASS	PASS	PASS	PASS	PASS	PASS	PASS	FAIL	WARN	WARN
GD22L-CTR-DEC-b-ctr-a	PASS	PASS	PASS	PASS	PASS	PASS	PASS	PASS	FAIL	WARN	WARN
GD22L-CTR-DEC-b-ctr-a	PASS	PASS	PASS	PASS	PASS	WARN	PASS	PASS	FAIL	WARN	WARN
GD22L-CTR-DEC-c	PASS	PASS	PASS	PASS	PASS	PASS	PASS	PASS	FAIL	PASS	WARN
GD22L-CTR-DEC-c	PASS	PASS	PASS	PASS	PASS	PASS	PASS	PASS	FAIL	PASS	WARN
GD22L-CTR-INN-b-ctr-b	PASS	PASS	PASS	WARN	PASS	PASS	PASS	PASS	WARN	WARN	WARN
GD22L-CTR-INN-b-ctr-b	PASS	PASS	PASS	WARN	PASS	PASS	PASS	PASS	WARN	WARN	WARN
GD22L-CTR-INN-c	PASS	PASS	PASS	PASS	PASS	PASS	PASS	PASS	FAIL	WARN	WARN
GD22L-CTR-INN-c	PASS	PASS	PASS	PASS	PASS	PASS	PASS	PASS	FAIL	WARN	WARN
GD22L-CTR-OUT-b	PASS	PASS	PASS	PASS	PASS	PASS	PASS	PASS	FAIL	WARN	WARN
GD22L-CTR-OUT-b	PASS	PASS	PASS	PASS	PASS	PASS	PASS	PASS	FAIL	WARN	WARN
GD22L-CTR-OUT-c-ctr-c	PASS	PASS	PASS	WARN	WARN	WARN	PASS	PASS	FAIL	WARN	WARN
GD22L-CTR-OUT-c-ctr-c	PASS	PASS	PASS	WARN	WARN	WARN	PASS	PASS	FAIL	WARN	WARN
GD22-CTR-OUT-1c	PASS	PASS	PASS	PASS	PASS	PASS	PASS	PASS	FAIL	WARN	WARN

Continued on next page

Table C.1 – continued from previous page

File	Basic Stats	Seq Quality	Quality Scores	Seq Content	Base GC Content	Seq GC Content	N Content	Seq Length	Seq Duplicates	Overrepresented Seqs	Kmer Content
GD22-CTR-OUT-1c	PASS	PASS	PASS	PASS	PASS	PASS	PASS	PASS	FAIL	WARN	WARN
GD22-CTR-OUT-3c	PASS	PASS	PASS	WARN	PASS	PASS	PASS	PASS	WARN	WARN	WARN
GD22-CTR-OUT-3c	PASS	PASS	PASS	PASS	PASS	PASS	PASS	PASS	WARN	WARN	WARN
GD22-CTR-PP-DEC	PASS	PASS	PASS	WARN	WARN	PASS	PASS	PASS	WARN	PASS	FAIL
GD22-CTR-PP-DEC	PASS	PASS	PASS	WARN	PASS	PASS	PASS	PASS	WARN	PASS	FAIL
GD22-CTR-PP-INN	PASS	PASS	PASS	PASS	PASS	WARN	PASS	PASS	FAIL	PASS	WARN
GD22-CTR-PP-INN	PASS	PASS	PASS	PASS	PASS	PASS	PASS	PASS	FAIL	PASS	WARN
GD22-CTR-PP-OUT	PASS	PASS	PASS	PASS	PASS	PASS	PASS	PASS	FAIL	PASS	WARN
GD22-CTR-PP-OUT	PASS	PASS	PASS	PASS	PASS	PASS	PASS	PASS	FAIL	PASS	WARN
GD22-P4-DEC-7a	PASS	PASS	PASS	WARN	PASS	PASS	PASS	PASS	WARN	PASS	WARN
GD22-P4-DEC-7a	PASS	PASS	PASS	PASS	PASS	PASS	PASS	PASS	FAIL	WARN	WARN
GD22-P4-DEC-7a	PASS	PASS	PASS	WARN	PASS	PASS	PASS	PASS	WARN	PASS	WARN
GD22-P4-DEC-7a	PASS	PASS	PASS	PASS	PASS	PASS	PASS	PASS	FAIL	WARN	WARN
GD22-P4-DEC-9a	PASS	PASS	PASS	WARN	PASS	PASS	PASS	PASS	WARN	WARN	WARN
GD22-P4-DEC-9a	PASS	PASS	PASS	WARN	PASS	PASS	PASS	PASS	WARN	WARN	WARN
GD22-P4-INN-7b	PASS	PASS	PASS	WARN	PASS	PASS	PASS	PASS	FAIL	WARN	WARN
GD22-P4-INN-7b	PASS	PASS	PASS	PASS	PASS	PASS	PASS	PASS	FAIL	WARN	WARN
GD22-P4-INN-8b	PASS	PASS	PASS	WARN	PASS	PASS	PASS	PASS	WARN	WARN	WARN
GD22-P4-INN-8b	PASS	PASS	PASS	WARN	PASS	PASS	PASS	PASS	WARN	WARN	WARN
GD22-P4-INN-9b	PASS	PASS	PASS	WARN	PASS	PASS	PASS	PASS	FAIL	WARN	WARN
GD22-P4-INN-9b	PASS	PASS	PASS	WARN	PASS	PASS	PASS	PASS	FAIL	WARN	WARN
GD22-P4-OUT-8c	PASS	PASS	PASS	PASS	PASS	PASS	PASS	PASS	FAIL	PASS	WARN
GD22-P4-OUT-8c	PASS	PASS	PASS	PASS	PASS	PASS	PASS	PASS	FAIL	PASS	WARN

Appendix D

Transcriptomic Landscape of the Rat Uterus in Late Pregnancy and at Term

D.1 GD19 + 6 hours

Table D.1: Genes that were differentially expressed in the inner myometrium compared to the decidua on GD19+6hrs. Transcript expression levels are shown in transcripts per million values (mean±SD).

		Decidua		Inner myometrium	
Gene symbol	Gene name	TPM	±SD	TPM	±SD
Upregulated genes					
Akap12	A kinase (PRKA) anchor protein 12	4.53	1.80	58.94	46.29
Lrrc4b	leucine rich repeat containing 4B	1.99	0.25	27.59	40.52
Mrvi1	murine retrovirus integration site 1 homolog	3.15	0.48	70.63	52.25
Sult1a1	sulfotransferase family, cytosolic, 1A, phenol-preferring, member 1	2.26	1.32	69.09	58.78
Olr303	olfactory receptor 303	0.06	0.11	39.59	68.26
Aoc3	amine oxidase, copper containing 3	2.92	0.80	148.63	120.24
Meox1	mesenchyme homeobox 1	0.19	0.06	4.77	5.32
Popdc2	popeye domain containing 2	2.77	1.94	40.97	33.48
Lmod1	leiomodin 1 (smooth muscle)	4.36	2.72	91.61	82.28
Dpt	dermatopontin	1.44	0.80	67.59	55.44
Crp	C-reactive protein, pentraxin-related	0.01	0.01	5.87	9.78
Ppp1r12b	protein phosphatase 1, regulatory subunit 12B	28.84	19.70	104.21	72.45
Sorcs2	sortilin-related VPS10 domain containing receptor 2	1.11	0.36	50.80	41.11
C1qtnf9	C1q and tumor necrosis factor related protein 9	0.01	0.01	4.08	6.08

Continued on next page

Table D.1 – continued from previous page

Gene symbol	Gene name	Decidua TPM	Decidua ±SD	Inner myometrium TPM	Inner myometrium ±SD
Isyna1	inositol-3-phosphate synthase 1	17.38	14.26	718.80	625.89
Pdlim3	PDZ and LIM domain 3	18.64	17.83	226.33	206.87
Acta1	actin, alpha 1, skeletal muscle	10.77	1.79	2208.48	2003.48
Vtcn1	V-set domain containing T cell activation inhibitor 1	1.51	0.42	54.06	59.22
Cpa3	carboxypeptidase A3, mast cell	0.00	0.00	3.19	5.52
Glrb	glycine receptor, beta	0.01	0.02	2.50	1.93
Lrat	lecithin-retinol acyltransferase (phosphatidylcholine-retinol-O-acyltransferase)	2.88	2.35	120.84	118.41
Csf1	colony stimulating factor 1 (macrophage)	5.88	8.46	159.80	202.04
Ptgs1	prostaglandin-endoperoxide synthase 1	7.53	6.51	115.41	100.00
Slc24a3	solute carrier family 24 (sodium/potassium/calcium exchanger), member 3	2.35	1.27	44.63	33.68
Slc4a11	solute carrier family 4, sodium borate transporter, member 11	3.24	3.60	125.33	110.33
Bpi	bactericidal/permeability-increasing protein	0.02	0.03	2.91	4.27
Cxcl12	chemokine (C-X-C motif) ligand 12	1.69	0.51	69.61	59.34
Abcb1b	ATP-binding cassette, subfamily B (MDR/TAP), member 1B	6.74	3.23	129.18	118.61
Ptn	pleiotrophin	33.07	52.75	191.90	204.81
Crhr2	corticotropin releasing hormone receptor 2	0.02	0.03	7.59	12.90
Kif12	kinesin family member 12	0.96	1.66	5.78	8.34
Guca2b	guanylate cyclase activator 2B	15.16	25.37	1329.53	1960.71
C1qc	complement component 1, q subcomponent, C chain	4.13	2.94	196.15	166.18
Mchr1	melanin-concentrating hormone receptor 1	0.07	0.11	17.12	19.70
Olr894	olfactory receptor 894	0.07	0.11	78.02	135.13
Krt83	keratin 83	0.67	0.79	10.00	8.98
Cnn1	calponin 1, basic, smooth muscle	16.49	18.28	1955.91	1586.11
Crabp1	cellular retinoic acid binding protein 1	0.00	0.00	35.65	60.11
Abcg4	ATP-binding cassette, subfamily G (WHITE), member 4	1.09	0.44	134.92	115.13
Tagln	transgelin	47.17	10.26	2038.89	1613.39
RGD1562136	similar to D1Ertd622e protein	10.11	7.63	48.96	40.45
Mrgprf	MAS-related GPR, member F	0.78	0.30	44.82	37.99
Bcam	basal cell adhesion molecule (Lutheran blood group)	9.18	1.83	89.57	73.51
Bcl3	B-cell CLL/lymphoma 3	3.14	1.99	70.42	112.00
Ltbp4	latent transforming growth factor beta binding protein 4	0.58	0.20	29.47	30.97
Fut2	fucosyltransferase 2 (secretor status included)	3.39	2.21	39.70	35.35
Pgm5	phosphoglucomutase 5	2.74	3.92	143.59	119.34
Clec10a	C-type lectin domain family 10, member A	29.21	32.75	209.17	111.03
Lpo	lactoperoxidase	2.41	0.46	31.16	34.21
Itfg3	integrin alpha FG-GAP repeat containing 3	18.11	17.34	161.02	143.13
Myocd	myocardin	5.34	2.67	35.81	34.08
Slc5a3	solute carrier family 5 (sodium/myo-inositol cotransporter), member 3	3.32	2.27	38.84	38.06
Eln	elastin	2.07	0.67	35.00	31.86
Mrc1	mannose receptor, C type 1	2.40	1.61	20.31	19.23
Egr1	early growth response 1	13.37	5.89	126.07	120.74
Rasd2	RASD family, member 2	16.34	20.72	40.12	39.71
Hmgcs2	3-hydroxy-3-methylglutaryl-CoA synthase 2 (mitochondrial)	10.72	14.27	78.42	71.42
Thbs4	thrombospondin 4	35.78	36.75	701.39	634.49
Mecom	MDS1 and EVI1 complex locus	0.81	0.34	10.08	7.72
Rxfp1	relaxin/insulin-like family peptide receptor 1	10.62	10.57	44.82	43.30
Oxt	oxytocin/neurophysin 1 prepropeptide	17.92	11.92	207.67	226.00
Pax8	paired box 8	3.44	5.00	68.56	65.21
Myl9	myosin, light chain 9, regulatory	132.69	126.93	10272.75	8708.75
Atp6v0a4	ATPase, H+ transporting, lysosomal V0 subunit A4	0.74	0.53	25.42	21.81
Fam13a	family with sequence similarity 13, member A	2.05	0.39	20.96	23.16
Kap	kidney androgen regulated protein	23.68	12.26	682.17	1078.09
Mgp	matrix Gla protein	68.27	49.59	545.96	646.80
Fgr	feline Gardner-Rasheed sarcoma viral oncogene	2.00	1.43	27.50	41.65
Prkaa2	protein kinase, AMP-activated, alpha 2 catalytic subunit	5.31	6.67	20.40	17.33
C1qa	complement component 1, q subcomponent, A chain	3.39	1.92	213.84	178.11
Igfbp6	insulin-like growth factor binding protein 6	79.47	124.30	810.09	660.39
Mmp3	matrix metallopeptidase 3	5.81	9.25	113.39	138.29
Slc9a9	solute carrier family 9, subfamily A (NHE9, cation proton antiporter 9), member 9	2.21	2.02	10.22	10.51
C3	complement component 3	8.75	2.09	120.89	163.61
Figf	c-fos induced growth factor	7.53	11.98	151.41	121.46
Igfbp4	insulin-like growth factor binding protein 4	42.20	12.56	92.64	30.17
Adamts1	ADAM metallopeptidase with thrombospondin type 1 motif, 1	13.49	8.63	58.99	11.88
Hip1	huntingtin interacting protein 1	33.66	37.12	47.47	8.72
Sgcb	sarcoglycan, beta (dystrophin-associated glycoprotein)	2.44	3.55	22.68	11.99
Lix1l	Lix1 homolog (mouse)-like	14.69	16.13	95.56	21.84
Pygb	phosphorylase, glycogen; brain	12.73	5.24	60.87	40.33
Nod1	nucleotide-binding oligomerization domain containing 1	3.60	2.15	23.77	12.48

Continued on next page

Table D.1 – continued from previous page

Gene symbol	Gene name	Decidua TPM	Decidua ±SD	Inner myometrium TPM	Inner myometrium ±SD
Suclg2	succinate-CoA ligase, GDP-forming, beta subunit	13.21	7.11	63.55	15.30
Ston1	stonin 1	19.30	3.24	76.90	22.71
Apol9a	apolipoprotein L 9a	17.47	5.61	81.51	42.62
Tmem47	transmembrane protein 47	15.18	9.90	71.33	37.53
Mill1	MHC I like leukocyte 1	2.89	0.52	36.28	8.50
Spon1	spondin 1, extracellular matrix protein	13.08	20.67	160.06	65.31
Ifitm1	interferon induced transmembrane protein 1	8.48	5.25	90.42	5.05
Ptprcap	protein tyrosine phosphatase, receptor type, C-associated protein	0.55	0.80	9.70	10.13
Synm	synemin, intermediate filament protein	7.34	5.43	56.14	39.38
Bgn	biglycan	76.41	33.31	1370.81	886.27
Ifitm2	interferon induced transmembrane protein 2	28.97	15.72	461.16	188.59
Slit3	slit homolog 3 (Drosophila)	14.88	8.84	108.08	39.54
Col1a1	collagen, type I, alpha 1	29.68	19.91	858.18	406.81
Serpinf1	serpin peptidase inhibitor, clade F , member 1	87.68	64.69	634.33	287.77
Mx1	myxovirus (influenza virus) resistance 1	3.64	0.67	53.07	30.97
Atp2b4	ATPase, Ca++ transporting, plasma membrane 4	3.07	2.12	49.80	36.69
Fmod	fibromodulin	5.12	4.67	76.89	70.56
Tnn	tenascin N	5.55	4.77	86.47	39.28
Spp1	secreted phosphoprotein 1	19.31	16.55	607.02	435.91
Phf11	PHD finger protein 11	9.08	11.60	42.93	32.24
Rbpms	RNA binding protein with multiple splicing	10.35	5.03	229.42	58.03
Pdlim7	PDZ and LIM domain 7	122.62	17.09	568.90	71.58
Svil	supervillin	10.82	6.95	85.24	55.33
Cd74	Cd74 molecule, major histocompatibility complex, class II invariant chain	4.70	2.97	160.00	113.58
Nfix	nuclear factor I/X (CCAAT-binding transcription factor)	12.03	8.93	200.84	27.11
Fam198b	family with sequence similarity 198, member B	0.70	0.21	26.12	14.38
Col11a1	collagen, type XI, alpha 1	0.97	1.02	23.94	13.60
F3	coagulation factor III (thromboplastin, tissue factor)	23.81	1.81	308.08	246.32
Gbp2	guanylate binding protein 2, interferon-inducible	7.28	4.79	72.47	59.84
Vcan	versican	3.14	1.66	41.59	23.76
Ptgfrn	prostaglandin F2 receptor inhibitor	11.60	9.03	166.59	102.79
Gpr88	G-protein coupled receptor 88	2.90	1.90	51.02	45.46
Ier3	immediate early response 3	24.97	16.91	241.00	101.82
Cfb	complement factor B	3.86	1.44	77.92	53.61
Lcn2	lipocalin 2	2.43	2.87	221.06	177.26
Frzb	frizzled-related protein	3.14	1.40	105.08	52.79
Ptgis	prostaglandin I2 (prostacyclin) synthase	2.03	2.23	140.19	82.43
Cav1	caveolin 1, caveolae protein	15.58	2.29	269.86	198.87
Tmem176a	transmembrane protein 176A	24.45	20.53	849.07	590.52
C1r	complement component 1, r subcomponent	13.08	7.26	153.14	50.13
Cacna2d1	calcium channel, voltage-dependent, alpha2/delta subunit 1	1.21	0.98	51.60	39.60
Tmem176b	transmembrane protein 176B	23.31	8.30	261.90	39.39
Inmt	indolethylamine N-methyltransferase	0.00	0.00	8.25	1.30
Antxr1	anthrax toxin receptor 1	25.45	16.64	277.48	223.08
C1s	complement component 1, s subcomponent	5.54	2.80	141.14	61.93
Abcc9	ATP-binding cassette, subfamily C (CFTR/MRP), member 9	1.51	1.26	22.91	15.25
Sdc3	syndecan 3	9.88	13.29	46.60	30.19
Bnc2	basonuclin 2	1.96	0.38	28.46	9.45
C1qb	complement component 1, q subcomponent, B chain	3.33	1.74	108.99	78.62
Vwa1	von Willebrand factor A domain containing 1	3.53	2.10	78.35	47.33
Slc8a1	solute carrier family 8 (sodium/calcium exchanger), member 1	4.44	4.59	20.42	14.41
Fbln5	fibulin 5	4.08	3.01	67.25	43.40
Igf1	insulin-like growth factor 1	4.16	4.20	73.30	30.07
Col14a1	collagen, type XIV, alpha 1	0.70	0.51	13.78	5.92
Ly6e	lymphocyte antigen 6 complex, locus E	35.02	3.22	530.44	339.82
Col3a1	collagen, type III, alpha 1	50.32	26.71	1091.52	272.63
Bok	BCL2-related ovarian killer	8.16	3.62	188.81	103.11
Igfbp5	insulin-like growth factor binding protein 5	7.33	6.61	135.79	124.66
Fhl1	four and a half LIM domains 1	16.88	13.42	858.68	631.95
Enpp3	ectonucleotide pyrophosphatase/phosphodiesterase 3	6.80	3.10	60.66	61.32
Ssc5d	scavenger receptor cysteine rich domain containing (5 domains)	8.02	10.06	33.16	14.08
Dact3	dishevelled-binding antagonist of beta-catenin 3	3.64	3.66	58.36	42.05
Rgma	repulsive guidance molecule family member A	3.06	1.93	64.25	30.48
Pde3b	phosphodiesterase 3B, cGMP-inhibited	3.30	2.25	17.84	10.09
Tgfb1i1	transforming growth factor beta 1 induced transcript 1	29.18	21.16	227.16	139.43
Mpeg1	macrophage expressed 1	4.64	4.32	61.03	39.44
Ehd2	EH-domain containing 2	17.98	13.99	123.83	90.57
Ifitm3	interferon induced transmembrane protein 3	245.64	245.12	3474.50	648.65

Continued on next page

Table D.1 – continued from previous page

Gene symbol	Gene name	Decidua TPM	Decidua ±SD	Inner myometrium TPM	Inner myometrium ±SD
Irf7	interferon regulatory factor 7	23.36	14.11	156.06	70.44
Gda	guanine deaminase	26.48	20.26	146.59	75.49
Acta2	actin, alpha 2, smooth muscle, aorta	51.44	43.99	2331.00	1806.03
Ifi47	interferon gamma inducible protein 47	13.38	11.35	90.95	63.47
Anxa6	annexin A6	19.42	6.78	107.82	47.27
Lpp	LIM domain containing preferred translocation partner in lipoma	21.48	9.23	166.83	130.05
Pla1a	phospholipase A1 member A	4.32	0.87	39.01	28.88
Mylk	myosin light chain kinase	16.67	5.04	892.90	611.27
Oasl2	2'-5' oligoadenylate synthetase-like 2	8.05	6.78	57.24	39.14
Rgs5	regulator of G-protein signaling 5	7.25	8.97	100.30	34.49
Bcl2	B-cell CLL/lymphoma 2	4.10	2.28	48.67	52.83
Prelp	proline/arginine-rich end leucine-rich repeat protein	85.16	135.79	1433.10	1165.88
Fcer1g	Fc fragment of IgE, high affinity I, receptor for; gamma polypeptide	19.97	23.06	185.60	146.71
Ifi204	myeloid cell nuclear differentiation antigen	6.35	4.76	52.10	25.21
Hsd11b1	hydroxysteroid 11-beta dehydrogenase 1	29.57	23.65	215.59	27.39
Aebp1	AE binding protein 1	20.34	15.02	150.44	42.82
Pcdh7	protocadherin 7	0.39	0.40	25.81	11.50
Smtn	smoothelin	25.44	15.60	174.71	45.11
Wnt5a	wingless-type MMTV integration site family, member 5A	1.18	0.33	20.46	22.13
Tlr3	toll-like receptor 3	5.55	2.32	33.82	12.19
Zfp521	zinc finger protein 521	0.83	0.19	10.72	4.54
Dclk1	doublecortin-like kinase 1	3.97	1.33	35.06	24.70
Kcnd3	potassium voltage-gated channel, Shal-related subfamily, member 3	0.19	0.19	7.97	5.11
Adh1	alcohol dehydrogenase 1 (class I)	10.83	12.42	79.74	51.54
Lmo4	LIM domain only 4	12.75	12.09	79.74	46.57
Col6a2	collagen, type VI, alpha 2	57.77	41.62	466.26	316.67
Susd2	sushi domain containing 2	24.94	12.09	143.79	64.68
Aif1	allograft inflammatory factor 1	4.11	2.65	83.32	66.60
Thbs1	thrombospondin 1	7.50	1.13	40.28	12.68
Rassf2	Ras association (RalGDS/AF-6) domain family member 2	6.39	8.05	27.38	12.95
Prkag2	protein kinase, AMP-activated, gamma 2 non-catalytic subunit	9.16	4.67	53.85	23.61
Dbf4	DBF4 homolog (S. cerevisiae)	1.24	0.43	24.77	26.86
Tnfrsf1a	tumor necrosis factor receptor superfamily, member 1a	16.56	6.17	80.10	29.81
Steap4	STEAP family member 4	4.40	0.94	29.13	14.23
Cnr1	cannabinoid receptor 1 (brain)	8.94	9.45	28.93	10.99
Nfia	nuclear factor I/A	3.70	1.08	32.54	20.08
Flrt2	fibronectin leucine rich transmembrane protein 2	2.47	2.09	32.72	16.29
Pld4	phospholipase D family, member 4	18.78	28.08	66.28	53.73
Csf2rb	colony stimulating factor 2 receptor, beta, low-affinity (granulocyte-macrophage)	3.69	1.71	40.11	19.75
Slc2a13	solute carrier family 2 (facilitated glucose transporter), member 13	3.19	3.85	9.61	7.83
Mcam	melanoma cell adhesion molecule	16.18	2.30	135.38	103.87
Plod2	procollagen lysine, 2-oxoglutarate 5-dioxygenase 2	22.64	14.20	162.90	69.38
Rexo2	RNA exonuclease 2	37.22	26.05	273.82	163.92
Cd276	Cd276 molecule	16.91	9.03	88.55	35.72
Filip1	filamin A interacting protein 1	2.64	1.59	17.20	7.58
Gls	glutaminase	13.78	6.61	93.60	60.74
Klf7	Kruppel-like factor 7 (ubiquitous)	42.97	31.40	137.39	39.30
Sp110	SP110 nuclear body protein	10.34	5.31	48.98	37.83
Ar	androgen receptor	2.79	2.72	24.83	16.68
Kcnmb1	potassium large conductance calcium-activated channel, subfamily M, beta member 1	0.80	0.65	174.59	134.24
Rprm	reprimo, TP53 dependent G2 arrest mediator candidate	2.83	4.07	40.31	24.32
Car12	carbonic anyhydrase 12	1.27	0.46	58.75	38.73
Mmp17	matrix metallopeptidase 17	0.53	0.10	19.98	6.66
Penk	proenkephalin	0.66	0.72	33.28	41.82
C4a	complement component 4A (Rodgers blood group)	2.95	2.23	87.49	71.46
Pla2g2d	phospholipase A2, group IID	0.90	0.87	17.97	14.26
Wbscr17	Williams-Beuren syndrome chromosome region 17	1.20	0.79	36.68	23.62
RT1-Da	RT1 class II, locus Da	1.33	1.19	36.72	23.40
RT1-Ba	RT1 class II, locus Ba	1.56	0.97	21.30	14.27
RT1-Db1	RT1 class II, locus Db1	0.71	0.48	17.45	7.15
Cacna1c	calcium channel, voltage-dependent, L type, alpha 1C subunit	0.62	0.62	14.89	3.84
Acy3	aspartoacylase (aminocyclase) 3	0.45	0.50	27.76	22.74
Tlr8	toll-like receptor 8	0.30	0.22	9.23	8.77
LOC100910940	ecotropic viral integration site 2B	1.81	0.65	26.77	7.49
Tlr2	toll-like receptor 2	0.32	0.32	9.77	1.71
Dio3	deiodinase, iodothyronine, type III	1.78	1.15	32.23	19.05
Klrk1	killer cell lectin-like receptor subfamily K, member 1	0.43	0.63	14.29	12.88
Cx3cr1	chemokine (C-X3-C motif) receptor 1	1.28	0.87	33.14	18.50

Continued on next page

Table D.1 – continued from previous page

Gene symbol	Gene name	Decidua TPM	Decidua ±SD	Inner myometrium TPM	Inner myometrium ±SD
Tm4sf1	transmembrane 4 L six family member 1	0.35	0.25	10.29	3.99
Six4	SIX homeobox 4	3.15	2.08	9.47	2.80
Hoxb7	homeo box B7	0.98	0.09	20.87	16.09
Cd180	CD180 molecule	1.73	1.55	22.91	18.96
Cyp4b1	cytochrome P450, family 4, subfamily b, polypeptide 1	0.48	0.16	10.65	10.64
Fas	Fas cell surface death receptor	0.34	0.24	10.02	7.51
Osr2	odd-skipped related transciption factor 2	3.43	4.55	59.53	47.50
Lmo2	LIM domain only 2	1.93	1.72	25.23	13.96
Ociad2	OCIA domain containing 2	7.95	11.02	22.71	14.80
Gpm6b	glycoprotein m6b	0.73	0.57	15.83	12.48
Tmem252	transmembrane protein 252	1.70	0.47	20.62	14.85
Nptx2	neuronal pentraxin II	0.09	0.15	11.63	4.47
Gstt1	glutathione S-transferase theta 1	17.53	21.55	187.75	195.71
Cd37	CD37 molecule	0.60	0.68	19.19	17.79
Astn1	astrotactin 1	0.20	0.18	3.74	1.59
Gpc4	glypican 4	2.59	1.08	22.77	5.31
Kctd15	potassium channel tetramerization domain containing 15	3.84	1.80	35.17	5.62
Arsj	arylsulfatase family, member J	0.40	0.34	10.72	8.61
Tpm2	tropomyosin 2, beta	338.24	143.17	6114.96	4999.49
Sema4a	sema domain, (semaphorin) 4A	2.48	1.86	34.62	21.47
Cacna1g	calcium channel, voltage-dependent, T type, alpha 1G subunit	0.41	0.39	6.98	3.28
Unc93b1	unc-93 homolog B1 (C. elegans)	4.87	3.25	43.94	18.23
Oasl	2'-5'-oligoadenylate synthetase-like	2.47	1.80	25.90	16.40
Fjx1	four jointed box 1 (Drosophila)	0.72	0.48	20.16	8.24
Tifa	TRAF-interacting protein with forkhead-associated domain	1.31	0.47	17.94	9.38
Oas1a	2'-5' oligoadenylate synthetase 1A	2.15	2.63	34.01	9.52
Cyp7b1	cytochrome P450, family 7, subfamily b, polypeptide 1	0.32	0.32	7.13	5.37
C1qtnf7	C1q and tumor necrosis factor related protein 7	1.93	1.64	27.81	18.03
Arhgef25	Rho guanine nucleotide exchange factor (GEF) 25	1.87	0.45	26.84	22.18
Vcam1	vascular cell adhesion molecule 1	0.67	0.47	7.59	4.55
Gja5	gap junction protein, alpha 5	13.57	17.96	34.03	28.97
Has2	hyaluronan synthase 2	0.36	0.48	2.79	2.25
Tnfaip8l2	tumor necrosis factor, alpha-induced protein 8-like 2	1.31	1.50	20.16	9.11
Foxs1	forkhead box S1	2.66	2.29	40.14	39.21
Fam20c	family with sequence similarity 20, member C	4.45	2.69	37.39	23.92
Pltp	phospholipid transfer protein	71.18	67.34	598.66	551.87
Gem	GTP binding protein overexpressed in skeletal muscle	2.13	1.75	23.18	12.83
Cndp1	carnosine dipeptidase 1 (metallopeptidase M20 family)	1.01	0.72	12.24	12.83
Xk	X-linked Kx blood group (McLeod syndrome)	0.28	0.25	3.48	2.44
Il13ra1	interleukin 13 receptor, alpha 1	2.46	2.35	25.44	5.25
Limd2	LIM domain containing 2	13.24	19.61	32.50	26.90
Sulf1	sulfatase 1	1.24	1.35	12.92	13.42
MGC108823	similar to interferon-inducible GTPase	13.47	14.09	78.38	70.41
Ltbp1	latent transforming growth factor beta binding protein 1	18.25	11.25	165.89	164.13
Atp1b2	ATPase, Na+/K+ transporting, beta 2 polypeptide	1.63	1.38	14.68	3.16
Meis1	Meis homeobox 1	5.15	0.97	29.28	7.13
Folr2	folate receptor 2 (fetal)	1.62	1.60	28.14	31.02
Cnrip1	cannabinoid receptor interacting protein 1	0.93	0.14	13.07	6.84
Tnfaip6	tumor necrosis factor alpha induced protein 6	6.22	5.15	43.39	42.05
Ism1	isthmin 1, angiogenesis inhibitor	4.58	7.75	62.25	17.77
Igfbp2	insulin-like growth factor binding protein 2	174.41	187.05	1386.43	515.28
Cd24	CD24 molecule	105.48	19.18	789.11	703.67
Ddx52	DEAD (Asp-Glu-Ala-Asp) box polypeptide 52	5.40	1.00	33.44	14.53
Tnfrsf26	tumor necrosis factor receptor superfamily, member 26	4.18	0.86	17.92	3.43
Clic2	chloride intracellular channel 2	3.74	3.18	29.09	12.24
Flna	filamin A, alpha	112.68	80.13	997.33	645.61
Rxfp2	relaxin/insulin-like family peptide receptor 2	3.08	3.26	11.57	5.86
Pde7b	phosphodiesterase 7B	2.00	2.61	8.73	2.37
Ccl6	chemokine (C-C motif) ligand 6	0.59	0.90	14.99	10.06
Tmem119	transmembrane protein 119	5.34	3.15	38.34	21.66
Ror2	receptor tyrosine kinase-like orphan receptor 2	0.71	0.39	13.38	6.48
RT1-S3	RT1 class Ib, locus S3	11.35	10.02	64.22	31.23
Tmem200a	transmembrane protein 200A	0.14	0.07	0.92	0.56
Car14	carbonic anhydrase 14	1.83	1.06	56.26	50.21
Ppp1r36	protein phosphatase 1, regulatory subunit 36	7.90	9.23	20.92	7.22
Tmem45b	transmembrane protein 45b	1.96	0.40	8.40	5.22
Acp5	acid phosphatase 5, tartrate resistant	2.14	1.04	20.44	4.81
Clec4a1	C-type lectin domain family 4, member A1	26.68	26.57	64.50	54.32

Continued on next page

Table D.1 – continued from previous page

Gene symbol	Gene name	Decidua TPM	Decidua ±SD	Inner myometrium TPM	Inner myometrium ±SD
Krt75	keratin 75	2.24	3.03	19.69	15.79
Itgb8	integrin, beta 8	0.42	0.49	3.97	1.17
RT1-T24-3	RT1 class I, locus T24, gene 3	5.36	1.79	39.41	9.71
Gal3st4	galactose-3-O-sulfotransferase 4	0.80	0.67	10.09	11.65
Zbed3	zinc finger, BED-type containing 3	5.37	1.11	34.66	6.09
Casq2	calsequestrin 2 (cardiac muscle)	0.42	0.18	4.05	2.94
Rab38	RAB38, member RAS oncogene family	0.19	0.00	4.16	1.08
Synpo2	synaptopodin 2	55.74	59.63	418.19	355.70
S1pr3	sphingosine-1-phosphate receptor 3	7.93	12.45	8.55	5.53
Lysmd2	LysM, putative peptidoglycan-binding, domain containing 2	2.81	3.13	27.02	17.51
Tlr1	toll-like receptor 1	0.42	0.27	6.13	4.09
Plac8	placenta-specific 8	26.44	20.79	163.90	86.49
Plac9	placenta-specific 9	15.78	24.55	16.02	8.80
Apol3	apolipoprotein L, 3	2.76	1.21	19.65	4.95
Pik3r1	phosphoinositide-3-kinase, regulatory subunit 1 (alpha)	18.63	14.34	49.89	32.35
Dennd1c	DENN/MADD domain containing 1C	1.16	0.38	10.12	6.60
Ogfrl1	opioid growth factor receptor-like 1	5.54	2.85	30.56	24.18
Slc44a1	solute carrier family 44 (choline transporter), member 1	30.78	28.66	204.19	124.35
Irf2bpl	interferon regulatory factor 2 binding protein-like	4.69	2.81	41.85	20.75
Map4k1	mitogen activated protein kinase kinase kinase kinase 1	0.46	0.28	9.42	5.83
Grid2	glutamate receptor, ionotropic, delta 2	0.13	0.12	1.54	0.66
Downregulated genes					
Psg16	pregnancy specific glycoprotein 16	198.37	219.18	2.57	3.19
Psg29	pregnancy-specific glycoprotein 29	389.64	390.73	5.07	8.19
Tex36	testis expressed 36	5.20	9.01	0.00	0.00
Sparcl1	SPARC-like 1 (hevin)	324.73	557.73	159.00	126.33
Sftpc	surfactant protein C	0.16	0.15	0.02	0.04
Atp4b	ATPase, H+/K+ exchanging, beta polypeptide	3.82	5.47	0.00	0.00
Prl3a1	Prolactin family 3, subfamily a, member 1	110.97	136.74	0.08	0.15
Prl3d4	prolactin family 3, subfamily d, member 4	854.67	1382.74	7.83	9.29
Trib3	tribbles pseudokinase 3	5.31	5.99	0.02	0.04
Snhg11	small nucleolar RNA host gene 11 (non-protein coding)	15.74	20.19	4.71	2.64
Reln	reelin	32.68	51.74	2.68	1.25
Slc46a2	solute carrier family 46, member 2	0.47	0.80	0.00	0.00
Serpina12	serpin peptidase inhibitor, clade A , member 12	0.60	0.64	0.00	0.00
Slc38a4	solute carrier family 38, member 4	125.54	192.17	7.97	6.11
Ucn2	urocortin 2	2.66	2.75	0.19	0.08
Gpbar1	G protein-coupled bile acid receptor 1	14.60	15.29	0.00	0.00
Mreg	melanoregulin	6.81	9.10	0.00	0.00
Alpi	alkaline phosphatase, intestinal	2.96	2.75	0.01	0.02
Rrm1	ribonucleotide reductase M1	129.70	207.42	23.32	1.21
Nsg2	neuron specific gene family member 2	44.26	55.60	0.78	0.87
Cldn4	claudin 4	65.29	77.05	1.48	1.08
Fga	fibrinogen alpha chain	78.63	39.83	13.85	21.64
Apom	apolipoprotein M	87.18	33.70	10.27	15.16
Mmp9	matrix metallopeptidase 9	1.99	2.83	0.04	0.03
Pgf	placental growth factor	445.84	758.60	22.05	13.19
Sema3b	sema domain, (semaphorin) 3B	104.43	169.48	13.83	5.81
Utf1	undifferentiated embryonic cell transcription factor 1	7.59	2.39	0.00	0.00
Tcp11l2	t-complex 11, testis-specific-like 2	70.19	26.42	17.62	7.50
Mllt4	myeloid/lymphoid or mixed-lineage leukemia translocated to, 4	37.28	23.79	11.07	1.87
Tjp2	tight junction protein 2	31.15	12.84	9.39	1.22
F11r	F11 receptor	161.64	79.66	51.47	7.94
Cd55	Cd55 molecule	114.51	37.56	44.26	22.20
Lamc2	laminin, gamma 2	157.00	157.65	13.91	8.07
Irs2	insulin receptor substrate 2	45.93	34.10	25.19	7.74
Socs6	suppressor of cytokine signaling 6	44.04	51.76	18.56	2.14
Phf17	jade family PHD finger 1	51.38	50.73	29.32	14.66
Prdm1	PR domain containing 1, with ZNF domain	41.67	34.78	11.34	3.93
Procr	protein C receptor, endothelial	53.45	46.12	14.77	6.28
Emp1	epithelial membrane protein 1	122.02	93.43	38.30	10.50
Slc6a6	solute carrier family 6 (neurotransmitter transporter), member 6	74.57	104.90	22.21	8.83
Lbh	limb bud and heart development	68.68	77.72	28.54	6.21
Kif3c	kinesin family member 3C	65.60	77.76	19.93	13.33
Rps6ka5	ribosomal protein S6 kinase, polypeptide 5	9.40	8.77	3.09	0.47
Uaca	uveal autoantigen with coiled-coil domains and ankyrin repeats	51.69	1.35	13.04	1.93

Continued on next page

Table D.1 – continued from previous page

Gene symbol	Gene name	Decidua TPM	Decidua ±SD	Inner myometrium TPM	Inner myometrium ±SD
Lama1	laminin, alpha 1	5.89	6.47	1.67	0.60
Slc40a1	solute carrier family 40 (iron-regulated transporter), member 1	62.84	77.00	4.98	3.79
Ptprm	protein tyrosine phosphatase, receptor type, M	13.79	9.67	3.70	1.19
Bcor	BCL6 co-repressor	45.68	9.93	16.15	3.07
RGD1564534	similar to CHCHD4 protein	20.58	26.35	6.81	3.40
Efnb1	ephrin B1	42.77	5.54	12.61	4.91
Plagl1	pleiomorphic adenoma gene-like 1	20.40	20.57	4.08	2.22
Sbsn	suprabasin	547.12	821.99	24.58	17.84
Rtn4rl1	reticulon 4 receptor-like 1	61.54	91.74	6.23	0.94
Pla2g10	phospholipase A2, group X	3.62	2.67	0.00	0.01
Slc22a5	solute carrier family 22 (organic cation/carnitine transporter), member 5	31.07	47.36	3.55	0.94
Gap43	growth associated protein 43	5.02	2.30	3.44	1.79
Tfrc	transferrin receptor	146.78	58.21	15.35	7.60
Tmem37	transmembrane protein 37	174.04	45.70	22.56	10.44
Pkp1	plakophilin 1	28.19	33.75	3.98	4.17
Tgfb2	transforming growth factor, beta 2	211.97	173.93	31.23	10.87
Hopx	HOP homeobox	643.48	925.76	93.71	72.66
Prom1	prominin 1	22.79	30.13	3.68	1.37
Anxa3	annexin A3	100.05	91.01	11.82	1.63
Kit	v-kit Hardy-Zuckerman 4 feline sarcoma viral oncogene homolog	22.82	23.71	3.49	3.34
Cpe	carboxypeptidase E	221.20	191.35	26.01	14.03
Ctsr	cathepsin R	955.05	500.72	83.06	86.91
Ctsq	cathepsin Q	206.52	82.99	11.77	15.51
Ctsj	cathepsin J	660.36	372.10	53.08	59.67
Prl8a2	prolactin family 8, subfamily a, member 2	787.71	816.32	29.84	35.98
Prl3b1	Prolactin family 3, subfamily b, member 1	938.94	1457.12	77.21	96.93
Cdh3	cadherin 3	151.40	144.60	11.94	2.94
Fa2h	fatty acid 2-hydroxylase	3.44	1.88	0.03	0.04
Lpar3	lysophosphatidic acid receptor 3	6.34	1.63	0.22	0.26
Usp53	ubiquitin specific peptidase 53	85.04	96.12	9.28	4.18
Aif1l	allograft inflammatory factor 1-like	245.86	176.45	32.09	14.64
Rnf128	ring finger protein 128, E3 ubiquitin protein ligase	68.91	76.56	9.21	7.18
Slc6a13	solute carrier family 6 (neurotransmitter transporter), member 13	194.59	331.90	0.06	0.10
Slc6a12	solute carrier family 6 (neurotransmitter transporter), member 12	492.76	783.27	11.46	4.59
Acer2	alkaline ceramidase 2	255.36	295.41	27.52	13.16
Aqp7	aquaporin 7	2.46	1.37	0.00	0.00
Ehd3	EH-domain containing 3	696.47	821.12	18.94	14.74
Slc5a6	solute carrier family 5 (sodium/multivitamin and iodide cotransporter), member 6	98.95	133.93	13.22	8.26
Flvcr2	feline leukemia virus subgroup C cellular receptor family, member 2	33.92	33.82	15.09	13.65
Mfsd12	major facilitator superfamily domain containing 12	125.81	136.81	10.79	2.33
Fndc3c1	fibronectin type III domain containing 3C1	63.47	44.76	7.83	7.87
Itm2a	integral membrane protein 2A	22.48	29.82	5.60	3.24
Arhgef6	Rac/Cdc42 guanine nucleotide exchange factor (GEF) 6	49.62	27.71	5.47	3.62
Vnn1	vanin 1	17.52	3.75	1.32	1.02
Wdr62	WD repeat domain 62	19.01	6.73	3.33	1.47
Cdhr5	cadherin-related family member 5	74.25	99.68	6.42	7.34
Car4	carbonic anhydrase 4	72.54	35.73	13.91	10.90
Dlx3	distal-less homeobox 3	35.93	24.35	0.80	0.15
Tmem204	transmembrane protein 204	101.81	92.12	20.45	5.19
Tlr5	toll-like receptor 5	52.00	54.27	9.47	6.56
Ctsql2	cathepsin Q-like 2	996.54	599.53	67.21	73.38
Wfdc1	WAP four-disulfide core domain 1	242.67	277.12	28.42	0.84
Cdc14a	cell division cycle 14A	46.50	32.52	7.99	4.43
Hyal4	hyaluronoglucosaminidase 4	3.13	2.89	0.27	0.07
Slc13a4	solute carrier family 13 (sodium/sulfate symporter), member 4	33.43	16.92	3.19	2.97
Cyp26b1	cytochrome P450, family 26, subfamily b, polypeptide 1	52.02	23.82	7.37	10.90
Rp1	retinitis pigmentosa 1 (human)	7.12	10.96	0.83	0.67
Tgfb3	transforming growth factor, beta 3	865.90	904.04	74.01	60.51
Ston2	stonin 2	23.23	2.01	3.63	2.87
RGD1310507	similar to RIKEN cDNA 1300017J02	25.76	23.50	4.56	3.09
Efhc2	EF-hand domain (C-terminal) containing 2	1.34	0.35	0.02	0.03
Dlg3	discs, large homolog 3 (Drosophila)	18.54	9.42	1.79	0.74
MGC114529	similar to melanoma antigen family A, 10	36.14	18.27	2.73	3.53
Trh	thyrotropin releasing hormone	553.73	372.47	1.55	2.06
Dsc3	desmocollin 3	9.79	8.39	0.03	0.05
Alpk3	alpha-kinase 3	19.37	15.48	0.39	0.45
Anxa8	annexin A8	146.94	141.90	4.17	4.15
Cst6	cystatin E/M	29.93	22.72	0.31	0.51

Continued on next page

Table D.1 – continued from previous page

Gene symbol	Gene name	Decidua TPM	Decidua ±SD	Inner myometrium TPM	Inner myometrium ±SD
Tns4	tensin 4	29.34	16.37	1.05	1.27
Snap91	synaptosomal-associated protein 91	7.04	6.22	0.33	0.26
MGC114246	similar to cathepsin R	33.80	20.69	1.28	0.68
Nkd2	naked cuticle homolog 2 (Drosophila)	22.42	9.54	1.57	0.84
Slc9b2	solute carrier family 9, subfamily B (NHA2, cation proton antiporter 2), member 2	6.70	4.29	0.23	0.24
Scara3	scavenger receptor class A, member 3	17.87	30.03	17.05	8.30
Irx4	iroquois homeobox 4	10.44	5.92	0.24	0.09
Ins2	insulin 2	27.87	35.55	3.19	4.94
B4galnt3	beta-1,4-N-acetyl-galactosaminyl transferase 3	9.43	5.75	0.12	0.16
Slc30a2	solute carrier family 30 (zinc transporter), member 2	1.61	1.64	0.14	0.03
Plg	plasminogen	2.54	2.01	0.14	0.21
Csrp3	cysteine and glycine-rich protein 3 (cardiac LIM protein)	10.24	6.67	0.08	0.15
Fgb	fibrinogen beta chain	33.96	11.46	3.40	4.54
Klhl40	kelch-like family member 40	21.37	27.20	1.40	1.92
Prl2b1	Prolactin family 2, subfamily b, member 1	1070.25	1736.94	4.69	6.28
Exoc3l4	exocyst complex component 3-like 4	5.36	2.08	0.05	0.09
Afm	afamin	5.95	5.10	0.26	0.46
Fmo1	flavin containing monooxygenase 1	16.56	6.65	1.47	2.12
Aadat	aminoadipate aminotransferase	20.54	12.08	1.90	2.39
Fhod3	formin homology 2 domain containing 3	3.29	0.82	0.23	0.24
Cryab	crystallin, alpha B	4544.38	2993.44	469.59	192.83
Otud3	OTU domain containing 3	19.45	27.48	2.54	2.48
Mrgprg	MAS-related GPR, member G	8.83	6.81	0.23	0.38
Gpc3	glypican 3	25.97	15.46	3.54	4.50
Serpinb9d	serine (or cysteine) peptidase inhibitor, clade B, member 9d	15.17	10.20	0.19	0.33
Adora1	adenosine A1 receptor	7.21	5.25	0.03	0.05
Arid3a	AT rich interactive domain 3A (Bright like)	29.50	2.52	5.49	2.51
Tceanc	transcription elongation factor A (SII) N-terminal and central domain containing	9.92	3.12	0.47	0.39
Ces4a	carboxylesterase 4A	2.50	1.51	0.03	0.04
Pc	pyruvate carboxylase	48.04	36.51	6.35	4.38
Elovl4	ELOVL fatty acid elongase 4	27.64	23.55	3.01	2.26
Ghrl	ghrelin/obestatin prepropeptide	28.12	20.63	1.06	0.99
Rassf8	Ras association (RalGDS/AF-6) domain family (N-terminal) member 8	21.88	11.70	4.32	1.74
Gata4	GATA binding protein 4	3.42	0.84	0.05	0.05
Pax1	paired box 1	7.38	7.86	0.05	0.09
Tmeff1	transmembrane protein with EGF-like and two follistatin-like domains 1	7.09	8.46	0.35	0.40
Mettl7b	methyltransferase like 7B	18.00	16.05	1.68	1.52
Slc6a3	solute carrier family 6 (neurotransmitter transporter), member 3	1.48	1.33	0.00	0.00
LOC691083	hypothetical protein LOC691083	9.83	9.94	0.61	0.55
Shisa7	shisa family member 7	0.98	0.88	0.06	0.07
Tm4sf20	transmembrane 4 L six family member 20	6.12	3.31	0.31	0.07
Phlda2	pleckstrin homology-like domain, family A, member 2	15.88	18.86	1.79	1.01
Rgcc	regulator of cell cycle	38.12	33.62	5.12	3.96
Duoxa1	dual oxidase maturation factor 1	4.15	2.73	0.11	0.01
Ccnjl	cyclin J-like	9.82	4.06	4.89	3.59
Rasgrf2	RAS protein-specific guanine nucleotide-releasing factor 2	10.17	14.61	0.88	0.79
Smim1	small integral membrane protein 1	11.88	15.19	2.31	0.88
Kng2	kininogen 2	5.80	1.70	0.50	0.71
Gata3	GATA binding protein 3	55.02	8.58	6.18	3.62
Angpt2	angiopoietin 2	14.72	14.29	1.81	0.40
Rps6ka6	ribosomal protein S6 kinase polypeptide 6	9.10	3.19	1.04	1.20
Adhfe1	alcohol dehydrogenase, iron containing, 1	2.52	1.52	0.07	0.13
Shisa3	shisa family member 3	0.72	0.36	0.00	0.00
Pard6b	par-6 family cell polarity regulator beta	11.96	13.69	4.33	2.56
Afap1l1	actin filament associated protein 1-like 1	10.31	3.97	0.85	0.80
Espn	espin	1.66	0.40	0.17	0.10
Mical1	microtubule associated monooxygenase, calponin and LIM domain containing 1	27.15	11.64	4.99	2.51
Sptb	spectrin, beta, erythrocytic	26.14	42.30	0.09	0.08
RGD1562726	similar to Putative protein C21orf62 homolog	5.02	7.92	0.72	0.53
Osbp2	oxysterol binding protein 2	8.90	8.86	0.36	0.06
Pvrl4	poliovirus receptor-related 4	27.22	16.82	4.24	2.56

Table D.2: Genes that were differentially expressed in the outer myometrium compared to the decidua on GD19+6hrs. Transcript expression levels are shown in transcripts per million values (mean±SD).

		Decidua		Outer myometrium	
Gene symbol	Gene name	TPM	±SD	TPM	±SD
Upregulated genes					
Myod1	myogenic differentiation 1	1.32	1.05	13.91	12.33
Myh8	myosin, heavy chain 8, skeletal muscle, perinatal	1.33	1.66	27.64	47.77
Aoc3	amine oxidase, copper containing 3	2.92	0.80	6.80	4.23
Meox1	mesenchyme homeobox 1	0.19	0.06	19.54	26.93
Myog	myogenin	0.05	0.02	13.35	11.65
Dpt	dermatopontin	1.44	0.80	11.18	15.76
Sparcl1	SPARC-like 1 (hevin)	324.73	557.73	1713.69	2941.03
Cabs1	calcium-binding protein, spermatid-specific 1	0.10	0.06	0.15	0.15
Acta1	actin, alpha 1, skeletal muscle	10.77	1.79	249.16	212.72
Tmem176a	transmembrane protein 176A	24.45	20.53	654.65	1001.41
Cxcl12	chemokine (C-X-C motif) ligand 12	1.69	0.51	7.56	7.13
Ptn	pleiotrophin	33.07	52.75	73.28	75.41
Abcc9	ATP-binding cassette, subfamily C (CFTR/MRP), member 9	1.51	1.26	18.58	26.10
Slc46a2	solute carrier family 46, member 2	0.47	0.80	2.92	5.05
C1qc	complement component 1, q subcomponent, C chain	4.13	2.94	32.07	16.50
Col14a1	collagen, type XIV, alpha 1	0.70	0.51	5.15	8.42
Cntn1	contactin 1	0.03	0.02	1.07	1.01
Crabp1	cellular retinoic acid binding protein 1	0.00	0.00	13.04	22.57
Abcg4	ATP-binding cassette, subfamily G (WHITE), member 4	1.09	0.44	81.12	139.98
Actc1	actin, alpha, cardiac muscle 1	1.53	1.27	87.83	146.54
Aebp1	AE binding protein 1	20.34	15.02	216.48	331.30
C1qb	complement component 1, q subcomponent, B chain	3.33	1.74	70.54	94.04
Cd163	CD163 molecule	0.47	0.30	30.26	50.99
Figf	c-fos induced growth factor	7.53	11.98	123.46	199.82
Ltbp4	latent transforming growth factor beta binding protein 4	0.58	0.20	17.94	19.81
Mrgprf	MAS-related GPR, member F	0.78	0.30	4.10	5.84
Myh3	myosin, heavy chain 3, skeletal muscle, embryonic	2.71	4.39	76.52	132.23
Pla2g2a	phospholipase A2, group IIA (platelets, synovial fluid)	1.02	0.85	17.13	17.42
Ptgis	prostaglandin I2 (prostacyclin) synthase	2.03	2.23	65.89	72.52
Zfhx4	zinc finger homeobox 4	0.41	0.14	5.07	8.35
Sema5a	sema domain, (semaphorin) 5A	2.60	2.25	7.67	3.83
Dclk1	doublecortin-like kinase 1	3.97	1.33	18.26	21.12
Vcan	versican	3.14	1.66	22.72	20.93
Ly6e	lymphocyte antigen 6 complex, locus E	35.02	3.22	177.18	225.33
Col5a1	collagen, type V, alpha 1	16.29	4.43	34.30	37.89
Fbln5	fibulin 5	4.08	3.01	34.22	17.63
Fkbp10	FK506 binding protein 10	5.33	0.67	49.87	35.17
Gpc4	glypican 4	2.59	1.08	48.14	46.75
Hip1	huntingtin interacting protein 1	33.66	37.12	47.29	42.59
Nfix	nuclear factor I/X (CCAAT-binding transcription factor)	12.03	8.93	56.45	34.93
Tgfbi	transforming growth factor, beta induced	5.17	1.49	35.05	21.70
Thbs2	thrombospondin 2	1.14	0.73	14.04	5.72
Zfp521	zinc finger protein 521	0.83	0.19	11.92	7.34
Col11a1	collagen, type XI, alpha 1	0.97	1.02	32.09	37.99
Dpp4	dipeptidylpeptidase 4	0.69	0.08	17.13	16.75
Acp5	acid phosphatase 5, tartrate resistant	2.14	1.04	39.62	19.99
Fam198b	family with sequence similarity 198, member B	0.70	0.21	9.64	6.57
Pcdh7	protocadherin 7	0.39	0.40	8.22	4.44
Scara5	scavenger receptor class A, member 5 (putative)	0.39	0.16	12.59	13.02
Col3a1	collagen, type III, alpha 1	50.32	26.71	215.00	196.84
Scara3	scavenger receptor class A, member 3	17.87	30.03	33.15	37.61
Downregulated genes					
Nox4	NADPH oxidase 4	55.68	73.79	3.47	3.04
Rtn4rl1	reticulon 4 receptor-like 1	61.54	91.74	12.03	9.48
Slc44a5	solute carrier family 44, member 5	2.79	2.48	2.54	4.40
Trh	thyrotropin releasing hormone	553.73	372.47	37.31	63.06
Zc2hc1c	zinc finger, C2HC-type containing 1C	6.87	7.80	0.00	0.00
Grem1	gremlin 1	31.14	48.11	5.16	6.05
Mfap5	microfibrillar associated protein 5	77.49	65.13	51.57	80.47
Nov	nephroblastoma overexpressed	62.93	75.26	7.11	6.01

Continued on next page

Table D.2 – continued from previous page

Gene symbol	Gene name	Decidua TPM	Decidua ±SD	Outer myometrium TPM	Outer myometrium ±SD
Nsg2	neuron specific gene family member 2	44.26	55.60	3.54	2.98
Scg5	secretogranin V (7B2 protein)	41.58	67.69	2.37	2.32
Slpi	secretory leukocyte peptidase inhibitor	14.06	12.06	3.07	2.53
Trpc4	transient receptor potential cation channel, subfamily C, member 4	21.69	31.29	1.81	1.52
Kcnj16	potassium inwardly-rectifying channel, subfamily J, member 16	1.42	0.78	0.06	0.06
Lbh	limb bud and heart development	68.68	77.72	10.94	12.54
Hopx	HOP homeobox	643.48	925.76	60.32	37.46
Cpe	carboxypeptidase E	221.20	191.35	20.09	11.80
Ppp1r14c	protein phosphatase 1, regulatory (inhibitor) subunit 14c	30.45	24.46	1.06	0.54
Gnat2	guanine nucleotide binding protein (G protein), alpha transducing activity polypeptide 2	14.18	13.88	0.85	0.79

Table D.3: Genes that were differentially expressed in the outer myometrium compared to the inner myometrium on GD19+6hrs. Transcript expression levels are shown in transcripts per million values (mean±SD).

Gene symbol	Gene name	Inner myometrium TPM	Inner myometrium ±SD	Outer myometrium TPM	Outer myometrium ±SD
Upregulated genes					
Ibsp	integrin-binding sialoprotein	0.71	0.43	52.10	73.90
LOC641520	popeye domain containing 3	0.00	0.00	1.49	1.67
Fam26e	family with sequence similarity 26, member E	6.16	6.43	19.36	33.53
Atg9b	autophagy related 9B	16.12	18.50	26.36	45.65
Grhl3	grainyhead-like 3 (Drosophila)	0.01	0.01	1.26	1.38
Itm2a	integral membrane protein 2A	5.60	3.24	125.71	207.64
Cldn4	claudin 4	1.48	1.08	87.02	144.75
Efnb1	ephrin B1	12.61	4.91	45.01	43.14
Tmem37	transmembrane protein 37	22.56	10.44	133.19	41.23
Vnn1	vanin 1	1.32	1.02	24.26	14.46
Down-regulated genes					
Cldn10	claudin 10	28.56	25.43	1.01	1.41
Slc17a3	solute carrier family 17 (organic anion transporter), member 3	4.32	5.38	0.20	0.16
Vtcn1	V-set domain containing T cell activation inhibitor 1	54.06	59.22	0.65	0.38
Lrat	lecithin-retinol acyltransferase (phosphatidylcholine-retinol-O-acyltransferase)	120.84	118.41	1.56	1.26
Lcn2	lipocalin 2	221.06	177.26	9.09	12.62
Hcn4	hyperpolarization activated cyclic nucleotide-gated potassium channel 4	15.05	15.60	0.00	0.00
Inmt	indolethylamine N-methyltransferase	8.25	1.30	0.01	0.01
Mill1	MHC I like leukocyte 1	36.28	8.50	4.03	1.77
Csf2rb	colony stimulating factor 2 receptor, beta, low-affinity (granulocyte-macrophage)	40.11	19.75	8.78	10.10
Tnn	tenascin N	86.47	39.28	0.41	0.33
Hoxb7	homeo box B7	20.87	16.09	0.65	0.79
Nptx2	neuronal pentraxin II	11.63	4.47	1.36	2.24

D.2 GD20

Table D.4: Genes that were differentially expressed in the inner myometrium compared to the decidua on GD20. Transcript expression levels are shown in transcripts per million values (mean±SD).

Gene symbol	Gene name	Decidua TPM	Decidua ±SD	Inner myometrium TPM	Inner myometrium ±SD
Upregulated genes					
Fut2	fucosyltransferase 2 (secretor status included)	1.09	1.14	175.95	215.98

Continued on next page

Table D.4 – continued from previous page

Gene symbol	Gene name	Decidua TPM	Decidua ±SD	Inner myometrium TPM	Inner myometrium ±SD
Gngt2	guanine nucleotide binding protein (G protein), gamma transducing activity polypeptide 2	0.00	0.00	12.34	16.81
Gabrp	gamma-aminobutyric acid (GABA-A) receptor, pi	0.31	0.53	128.25	141.85
Slc4a11	solute carrier family 4, sodium borate transporter, member 11	0.14	0.13	392.42	478.35
Abcb1b	ATP-binding cassette, subfamily B (MDR/TAP), member 1B	0.36	0.32	448.31	578.32
Hpgds	hematopoietic prostaglandin D synthase	0.03	0.03	31.75	42.30
B4galnt3	beta-1,4-N-acetyl-galactosaminyl transferase 3	0.03	0.06	19.00	32.72
Kif12	kinesin family member 12	0.03	0.03	46.13	55.08
Smc1b	structural maintenance of chromosomes 1B	0.18	0.31	8.44	14.55
Prtg	protogenin	0.64	0.52	75.81	109.07
Cldn7	claudin 7	7.21	7.49	165.01	94.28
Slc5a3	solute carrier family 5 (sodium/myo-inositol cotransporter), member 3	2.11	2.99	57.11	54.54
Slc7a7	solute carrier family 7 (amino acid transporter light chain, y+L system), member 7	4.49	1.55	55.91	12.50
Cdh1	cadherin 1	8.88	4.99	126.93	45.69
Emb	embigin	0.99	1.01	60.60	42.02
Mab21l3	mab-21-like 3 (C. elegans)	2.21	2.41	38.50	33.49
Fjx1	four jointed box 1 (Drosophila)	0.00	0.00	21.16	20.38
Slco4a1	solute carrier organic anion transporter family, member 4a1	8.95	13.28	277.95	180.45
Epcam	epithelial cell adhesion molecule	26.28	11.66	434.22	324.52
Wdr72	WD repeat domain 72	0.00	0.01	4.19	2.15
Ehf	ets homologous factor	0.26	0.14	45.68	35.58
Igfbp2	insulin-like growth factor binding protein 2	92.67	80.49	1481.23	943.51
Fkbp11	FK506 binding protein 11	2.61	3.38	41.52	27.93
Downregulated genes					
LOC171161	common salivary protein 1	30.39	37.35	0.00	0.00
Matn1	matrilin 1, cartilage matrix protein	48.13	83.36	0.02	0.03
Tmem204	transmembrane protein 204	80.44	69.90	5.41	4.05
Pkp1	plakophilin 1	56.99	75.54	0.32	0.38
Anxa3	annexin A3	86.79	89.23	9.26	4.62
Mamdc4	MAM domain containing 4	2.24	2.41	0.05	0.06
Slc6a12	solute carrier family 6 (neurotransmitter transporter), member 12	591.70	520.75	4.51	4.45
Slc6a6	solute carrier family 6 (neurotransmitter transporter), member 6	71.23	72.75	8.48	6.05
Ehd3	EH-domain containing 3	389.61	348.12	11.80	10.06
Tgfb3	transforming growth factor, beta 3	375.47	353.65	13.03	18.12
RGD1307554	similar to CG16812-PA	32.43	34.23	2.95	1.35

Table D.5: Genes that were differentially expressed in the outer myometrium compared to the decidua on GD20. Transcript expression levels are shown in transcripts per million values (mean±SD).

Gene symbol	Gene name	Decidua TPM	Decidua ±SD	Outer myometrium TPM	Outer myometrium ±SD
Upregulated genes					
Cox6b2	cytochrome c oxidase subunit VIb polypeptide 2	0.00	0.00	6.96	7.43
Nmb	neuromedin B	0.00	0.00	10.73	13.90
Trim58	tripartite motif-containing 58	0.03	0.02	5.51	8.68
Hoxb7	homeo box B7	0.05	0.08	16.99	16.46
Csf3	colony stimulating factor 3 (granulocyte)	0.00	0.00	11.61	14.94
Alox15b	arachidonate 15-lipoxygenase, type B	0.02	0.03	7.92	11.60
Lmod1	leiomodin 1 (smooth muscle)	2.58	3.19	196.29	111.88
Crp	C-reactive protein, pentraxin-related	0.00	0.00	10.39	15.09
Btc	betacellulin	0.00	0.00	23.60	24.84
Isyna1	inositol-3-phosphate synthase 1	7.80	7.03	1052.83	1069.36
Defb1	defensin beta 1	0.00	0.00	36.69	36.60
Ppp2r2b	protein phosphatase 2, regulatory subunit B, beta	0.29	0.40	2.70	2.83
Marveld3	MARVEL domain containing 3	0.00	0.00	14.12	12.05
Tmem171	transmembrane protein 171	0.02	0.03	7.55	11.06
Gzmk	granzyme K	0.05	0.08	5.55	6.55
Lypd6b	LY6/PLAUR domain containing 6B	0.15	0.14	4.46	5.49
Foxa2	forkhead box A2	0.04	0.04	4.25	4.94
Gfi1b	growth factor independent 1B transcription repressor	0.01	0.01	9.06	11.09
RGD1564114	similar to FLJ46082 protein	0.25	0.22	3.11	4.92

Continued on next page

Table D.5 – continued from previous page

Gene symbol	Gene name	Decidua TPM	Decidua ±SD	Outer myometrium TPM	Outer myometrium ±SD
Slc4a11	solute carrier family 4, sodium borate transporter, member 11	0.14	0.13	268.24	284.96
Cd8a	CD8a molecule	0.00	0.00	4.26	4.21
Abcb1b	ATP-binding cassette, subfamily B (MDR/TAP), member 1B	0.36	0.32	271.55	265.10
Hpgds	hematopoietic prostaglandin D synthase	0.03	0.03	28.67	36.58
Ttc22	tetratricopeptide repeat domain 22	0.01	0.02	7.97	7.89
Nr0b2	nuclear receptor subfamily 0, group B, member 2	0.00	0.00	9.14	8.06
Fhl5	four and a half LIM domains 5	0.02	0.03	5.18	4.55
Kif12	kinesin family member 12	0.03	0.03	9.89	13.86
Sostdc1	sclerostin domain containing 1	0.00	0.00	21.60	19.70
Krtcap3	keratinocyte associated protein 3	0.40	0.44	7.59	8.57
Tac2	tachykinin 2	0.03	0.06	9.01	11.67
Zfpm2	zinc finger protein, multitype 2	3.61	6.10	3.68	3.98
Arc	activity-regulated cytoskeleton-associated protein	0.20	0.11	4.45	3.96
Wdr72	WD repeat domain 72	0.00	0.01	4.52	5.94
Epor	erythropoietin receptor	0.01	0.02	10.83	15.08
Faim2	Fas apoptotic inhibitory molecule 2	0.02	0.04	12.28	12.70
Ctxn1	cortexin 1	0.81	0.84	355.51	189.63
Akap12	A kinase (PRKA) anchor protein 12	4.54	4.46	111.25	63.31
Rgma	repulsive guidance molecule family member A	2.24	2.63	110.40	74.97
Slc35g1	solute carrier family 35, member G1	0.02	0.04	5.81	5.84
Hpn	hepsin	0.02	0.03	12.21	4.51
Synm	synemin, intermediate filament protein	4.07	3.11	125.90	55.14
P2ry6	pyrimidinergic receptor P2Y, G-protein coupled, 6	0.46	0.41	4.13	3.68
Rasl11a	RAS-like family 11 member A	0.04	0.07	11.02	6.25
Chi3l1	chitinase 3-like 1 (cartilage glycoprotein-39)	0.02	0.04	2.91	0.91
Cd84	CD84 molecule	0.01	0.01	3.67	0.56
Hsd11b1	hydroxysteroid 11-beta dehydrogenase 1	10.93	9.47	495.45	406.14
Ldb2	LIM domain binding 2	3.97	2.75	38.86	10.07
Pdlim2	PDZ and LIM domain 2	0.15	0.16	12.87	10.92
Pdlim3	PDZ and LIM domain 3	14.51	12.99	187.43	105.57
Zdhhc2	zinc finger, DHHC-type containing 2	0.04	0.04	9.89	3.39
Fgf2	fibroblast growth factor 2	0.00	0.00	8.27	3.06
Dusp15	dual specificity phosphatase 15	0.31	0.38	4.79	2.80
Napepld	N-acyl phosphatidylethanolamine phospholipase D	0.01	0.02	7.08	6.67
Gp9	glycoprotein IX (platelet)	0.00	0.00	4.70	1.54
Clec4a	C-type lectin domain family 4, member A	0.00	0.01	4.49	3.14
C1r	complement component 1, r subcomponent	12.05	11.96	188.05	90.13
Ptn	pleiotrophin	19.10	15.89	362.30	217.46
Kcnj8	potassium inwardly-rectifying channel, subfamily J, member 8	3.48	4.14	116.24	87.86
Sh3d21	SH3 domain containing 21	1.92	1.70	5.45	1.77
Arhgap5	Rho GTPase activating protein 5	11.34	9.68	97.15	49.22
Slc8a1	solute carrier family 8 (sodium/calcium exchanger), member 1	0.86	1.27	31.14	17.33
Igfbp6	insulin-like growth factor binding protein 6	16.21	17.29	1256.56	759.01
Slc25a23	solute carrier family 25 (mitochondrial carrier; phosphate carrier), member 23	0.05	0.06	9.50	1.09
Pdcl3	phosducin-like 3	5.88	6.21	72.75	38.97
Figf	c-fos induced growth factor	4.36	2.54	148.41	97.87
Gnaq	guanine nucleotide binding protein (G protein), q polypeptide	5.06	8.06	170.63	87.88
Serpinb9	serpin peptidase inhibitor, clade B (ovalbumin), member 9	10.03	6.38	72.38	21.66
Svil	supervillin	6.34	5.93	82.99	50.62
Sqrdl	sulfide quinone reductase-like (yeast)	4.97	4.96	72.45	51.51
Fam83d	family with sequence similarity 83, member D	0.01	0.02	2.32	0.23
Prkag2	protein kinase, AMP-activated, gamma 2 non-catalytic subunit	2.07	2.66	39.28	16.66
Tes	testis derived transcript	25.83	6.38	102.47	35.95
Prkaa2	protein kinase, AMP-activated, alpha 2 catalytic subunit	1.40	0.63	35.48	25.78
Ppp1r12a	protein phosphatase 1, regulatory subunit 12A	11.22	9.81	205.11	111.00
RGD1562136	similar to D1Ertd622e protein	6.74	5.99	56.64	30.27
Il13ra1	interleukin 13 receptor, alpha 1	1.62	1.40	26.43	8.26
Lilrb3	leukocyte immunoglobulin-like receptor, subfamily B (with TM and ITIM domains), member 3	0.09	0.12	2.54	1.75
Slc8a2	solute carrier family 8 (sodium/calcium exchanger), member 2	0.04	0.05	6.32	3.01
Cyp2f4	cytochrome P450, family 2, subfamily f, polypeptide 4	0.03	0.05	7.13	2.41
Ppp1r14a	protein phosphatase 1, regulatory (inhibitor) subunit 14A	0.03	0.04	10.88	6.76
Sh3gl3	SH3-domain GRB2-like 3	0.01	0.01	3.71	1.65
Tppp	tubulin polymerization promoting protein	0.00	0.00	9.55	8.09
Scn1b	sodium channel, voltage-gated, type I, beta subunit	0.16	0.14	20.86	13.18
Siglec5	sialic acid binding Ig-like lectin 5	0.07	0.13	3.48	3.32
Folr2	folate receptor 2 (fetal)	0.14	0.25	23.53	11.68
Gria1	glutamate receptor, ionotropic, AMPA 1	0.07	0.12	4.09	2.06

Continued on next page

Table D.5 – continued from previous page

Gene symbol	Gene name	Decidua TPM	Decidua ±SD	Outer myometrium TPM	Outer myometrium ±SD
Gngt2	guanine nucleotide binding protein (G protein), gamma transducing activity polypeptide 2 gamma transducing activity polypeptide 2	0.00	0.00	14.25	13.53
Aoc3	amine oxidase, copper containing 3	3.94	2.62	199.44	120.89
Fn3k	fructosamine 3 kinase	0.02	0.03	5.95	0.81
Alox15	arachidonate 15-lipoxygenase	0.00	0.00	14.83	8.44
Ccl6	chemokine (C-C motif) ligand 6	0.00	0.00	13.80	4.85
Krt13	keratin 13	2.51	4.35	15.56	12.22
Chaf1b	chromatin assembly factor 1, subunit B (p60)	0.02	0.03	3.26	2.31
Selplg	selectin P ligand	0.00	0.00	25.76	8.23
Faim3	Fas apoptotic inhibitory molecule 3	0.08	0.08	16.74	18.87
Sult1d1	sulfotransferase family 1D, member 1	0.01	0.01	7.68	5.09
Gata4	GATA binding protein 4	0.02	0.04	8.10	6.50
Efnb2	ephrin B2	0.02	0.02	4.64	3.20
Adrb2	adrenoceptor beta 2, surface	5.12	6.96	13.51	8.89
Slc14a1	solute carrier family 14 (urea transporter), member 1	0.00	0.00	5.43	4.05
Lyl1	lymphoblastic leukemia derived sequence 1	0.00	0.00	17.90	6.75
Prss12	protease, serine, 12 neurotrypsin (motopsin)	0.01	0.01	5.27	2.37
Fcrls	Fc receptor-like S, scavenger receptor	0.00	0.00	7.17	1.74
Ptger3	prostaglandin E receptor 3 (subtype EP3)	0.00	0.00	7.08	3.90
Gstt1	glutathione S-transferase theta 1	1.97	3.25	17.88	4.01
Tspyl4	TSPY-like 4	0.09	0.08	2.65	1.22
Slc24a3	solute carrier family 24 (sodium/potassium/calcium exchanger), member 3	4.89	4.28	93.47	89.76
Fjx1	four jointed box 1 (Drosophila)	0.00	0.00	12.43	4.65
C1rl	complement component 1, r subcomponent-like	0.00	0.00	5.04	2.59
Fam180a	family with sequence similarity 180, member A	1.14	1.33	9.01	7.35
Alox5	arachidonate 5-lipoxygenase	0.00	0.01	5.39	3.97
Iffo2	intermediate filament family orphan 2	0.11	0.20	6.57	3.84
Pigv	phosphatidylinositol glycan anchor biosynthesis, class V	2.71	2.30	6.82	1.80
Mdga2	MAM domain containing glycosylphosphatidylinositol anchor 2	0.03	0.03	1.82	0.82
Itgb8	integrin, beta 8	0.00	0.00	6.19	2.33
Mchr1	melanin-concentrating hormone receptor 1	0.00	0.00	15.32	11.55
Mfng	MFNG O-fucosylpeptide 3-beta-N-acetylglucosaminyltransferase	0.00	0.00	6.51	4.35
Pdgfb	platelet-derived growth factor beta polypeptide	0.44	0.32	9.23	4.38
Hyal3	hyaluronoglucosaminidase 3	0.10	0.17	34.77	20.21
Abcg4	ATP-binding cassette, subfamily G (WHITE), member 4	1.14	1.58	124.24	46.42
Il1rl2	interleukin 1 receptor-like 2	0.19	0.24	3.65	2.20
Adam23	ADAM metallopeptidase domain 23	0.01	0.02	5.76	3.49
Lepr	leptin receptor	1.78	2.10	64.87	28.80
Begain	brain-enriched guanylate kinase-associated	0.02	0.04	4.47	3.21
Nmur2	neuromedin U receptor 2	0.38	0.51	18.42	11.50
RT1-Ba	RT1 class II, locus Ba	0.04	0.04	59.90	47.52
RT1-Db1	RT1 class II, locus Db1	0.06	0.04	25.53	20.53
Tpd52l1	tumor protein D52-like 1	0.02	0.02	29.50	9.18
Ppp1r36	protein phosphatase 1, regulatory subunit 36	0.00	0.01	19.73	11.09
Fez1	fasciculation and elongation protein zeta 1 (zygin I)	0.13	0.21	30.69	15.80
Lgals5	lectin, galactose binding, soluble 5	0.26	0.35	59.63	32.23
Rgs1	regulator of G-protein signaling 1	0.00	0.00	20.40	13.84
Tenm2	teneurin transmembrane protein 2	0.08	0.09	11.44	5.65
Bnc1	basonuclin 1	0.18	0.23	2.53	1.05
Mgll	monoglyceride lipase	0.03	0.03	16.73	17.45
Gimap4	GTPase, IMAP family member 4	0.79	0.44	17.02	10.49
Lilrb3l	leukocyte immunoglobulin-like receptor, subfamily B (with TM and ITIM domains), member 3-like	0.22	0.17	16.10	8.89
Id4	inhibitor of DNA binding 4	0.47	0.50	35.05	32.05
Dmbt1	deleted in malignant brain tumors 1	0.13	0.03	13.26	5.17
Ociad2	OCIA domain containing 2	0.33	0.38	34.19	1.17
Bves	blood vessel epicardial substance	0.21	0.24	34.28	12.26
Kcnb1	potassium voltage gated channel, Shab-related subfamily, member 1	0.03	0.05	9.57	6.62
Mst1r	macrophage stimulating 1 receptor (c-met-related tyrosine kinase)	0.01	0.02	7.14	2.94
Astn1	astrotactin 1	0.02	0.04	5.09	2.52
Hyal1	hyaluronoglucosaminidase 1	0.10	0.09	13.10	10.16
Slc2a13	solute carrier family 2 (facilitated glucose transporter), member 13	0.14	0.16	12.41	3.78
Slc6a9	solute carrier family 6 (neurotransmitter transporter, glycine), member 9	7.15	12.20	11.37	5.25
Gata6	GATA binding protein 6	0.46	0.55	25.10	14.52
Cdca7	cell division cycle associated 7	0.06	0.06	5.43	2.45
Wnt5a	wingless-type MMTV integration site family, member 5A	0.27	0.07	17.42	14.74
Cnp	2',3'-cyclic nucleotide 3' phosphodiesterase	0.43	0.16	25.99	8.56

Continued on next page

Table D.5 – continued from previous page

Gene symbol	Gene name	Decidua TPM	Decidua ±SD	Outer myometrium TPM	Outer myometrium ±SD
Emb	embigin	0.99	1.01	65.08	69.41
Nrxn2	neurexin 2	13.28	16.18	25.61	7.95
Pla2g2d	phospholipase A2, group IID	0.62	0.77	12.61	6.91
Rad51	RAD51 recombinase	0.10	0.09	10.50	1.95
Arhgap26	Rho GTPase activating protein 26	0.21	0.14	7.64	5.36
Nek11	NIMA-related kinase 11	0.08	0.13	1.98	0.91
Ogn	osteoglycin	22.79	38.12	235.09	159.09
Downregulated genes					
Klk8	kallikrein related-peptidase 8	35.05	60.72	0.00	0.00
Dmrt2	doublesex and mab-3 related transcription factor 2	9.39	16.09	0.21	0.07
Lrtomt	O-methyltransferase domain containing	13.00	22.52	0.02	0.03
LOC171161	common salivary protein 1	30.39	37.35	0.00	0.00
Myh3	myosin, heavy chain 3, skeletal muscle, embryonic	219.70	380.48	2.17	2.16
Tprg1	tumor protein p63 regulated 1	7.50	12.97	0.15	0.09
Enam	enamelin	1.92	3.32	0.00	0.00
Mcpt2	mast cell protease 2	6.76	9.86	1.23	2.13
Prl8a2	prolactin family 8, subfamily a, member 2	354.83	439.23	3.19	2.34
Olr1667	olfactory receptor 1667	75.53	130.83	0.00	0.00
Ces4a	carboxylesterase 4A	2.57	4.45	0.01	0.02
Vgll2	vestigial like 2 (Drosophila)	6.94	12.02	0.00	0.00
Trim10	tripartite motif-containing 10	5.77	4.68	3.81	4.29
Cst5	cystatin D	4.00	6.93	0.00	0.00
Bpifa2	BPI fold containing family A, member 2	16.21	27.86	0.01	0.01
Bpifa2f	BPI fold containing family A, member 2F	27.98	48.46	0.00	0.00
Pck1	phosphoenolpyruvate carboxykinase 1 (soluble)	15.88	22.33	1.54	1.24
Pbp2	phosphatidylethanolamine binding protein 2	6.34	10.49	0.00	0.00
Htr1d	5-hydroxytryptamine (serotonin) receptor 1D, G protein-coupled	9.84	8.53	0.00	0.00
LOC682102	hypothetical protein LOC682102	4.07	6.90	0.20	0.05
RGD1305627	hypothetical LOC314467	27.17	32.06	0.00	0.00
Smgc	submandibular gland protein C	18.50	32.01	0.00	0.00
Myf6	myogenic factor 6	23.79	41.20	0.00	0.00
Gldn	gliomedin	5.03	8.69	0.00	0.00
Dmrtc1c	DMRT-like family C1c	13.50	20.83	0.00	0.00
Rhox4g	reproductive homeobox 4G	8.16	12.75	0.00	0.00
Krt10	keratin 10	264.25	457.37	2.02	1.70
Ceacam11	carcinoembryonic antigen-related cell adhesion molecule 11	2156.53	2749.06	7.53	8.09
Dkk1	dickkopf WNT signaling pathway inhibitor 1	7.13	6.37	0.60	0.29
Zfp39	zinc finger protein 39	9.17	6.51	4.71	0.17
Pkp1	plakophilin 1	56.99	75.54	4.78	5.71
Limch1	LIM and calponin homology domains 1	31.83	35.76	3.44	2.22
Slc10a2	solute carrier family 10 (sodium/bile acid cotransporter), member 2	36.80	49.68	12.43	4.33
Tpbpa	trophoblast specific protein alpha	1358.04	1781.76	5.35	5.44
Prl3b1	Prolactin family 3, subfamily b, member 1	144.12	132.01	19.98	33.39
Inhba	inhibin beta-A	165.88	160.51	14.43	9.31
LOC682105	receptor accessory protein 2	83.10	72.74	26.19	10.36
Wfdc1	WAP four-disulfide core domain 1	193.06	215.95	36.20	11.50
Aif1l	allograft inflammatory factor 1-like	165.43	128.55	35.79	21.68
Tfpi	tissue factor pathway inhibitor (lipoprotein-associated coagulation inhibitor)	487.67	411.14	48.33	14.87
Slc6a12	solute carrier family 6 (neurotransmitter transporter), member 12	591.70	520.75	6.15	7.59
Slc6a6	solute carrier family 6 (neurotransmitter transporter), member 6	71.23	72.75	12.36	5.55
Smim1	small integral membrane protein 1	32.07	30.11	8.94	4.94
Ehd3	EH-domain containing 3	389.61	348.12	80.84	27.36
Slc5a6	solute carrier family 5 (sodium/multivitamin and iodide cotransporter), member 6	129.12	22.80	14.70	2.44
Tgfb3	transforming growth factor, beta 3	375.47	353.65	39.59	17.73
Cpm	carboxypeptidase M	28.44	32.14	12.37	2.41
Slc38a4	solute carrier family 38, member 4	70.46	78.45	5.69	2.11
Ncam1	neural cell adhesion molecule 1	10.27	10.55	5.33	3.39
Ptk7	protein tyrosine kinase 7	44.15	42.11	7.01	4.56
Slc29a1	solute carrier family 29 (equilibrative nucleoside transporter), member 1	58.98	51.11	6.02	2.08
Fndc3c1	fibronectin type III domain containing 3C1	54.74	74.41	1.07	1.62
Tmem204	transmembrane protein 204	80.44	69.90	20.57	11.69
Serpine1	serpin peptidase inhibitor, clade E (nexin, plasminogen activator inhibitor type 1), member 1	838.81	856.95	36.01	19.61
Prom1	prominin 1	22.65	20.02	4.60	4.59
Kdm1b	lysine (K)-specific demethylase 1B	22.27	33.35	3.71	2.12
Gadd45g	growth arrest and DNA-damage-inducible, gamma	166.58	144.85	84.32	2.27

Continued on next page

Table D.5 – continued from previous page

Gene symbol	Gene name	Decidua TPM	Decidua ±SD	Outer myometrium TPM	Outer myometrium ±SD
S100a4	S100 calcium-binding protein A4	274.82	394.40	65.11	4.28
Traf3	Tnf receptor-associated factor 3	40.80	18.50	15.63	4.51
Cmtm7	CKLF-like MARVEL transmembrane domain containing 7	54.57	47.24	31.32	8.93
Pttg1	pituitary tumor-transforming 1	10.34	17.92	10.31	4.25
Prl7a4	prolactin family 7, subfamily a, member 4	121.86	177.85	0.00	0.00
Prl8a5	prolactin family 8, subfamily a, member 5	2011.73	742.77	6.02	8.05
Prl8a7	prolactin family 8, subfamily a, member 7	8949.40	8357.04	4.74	5.05
Prl8a4	prolactin family 8, subfamily a, member 4	967.13	784.32	3.57	3.17
Ticam2	toll-like receptor adaptor molecule 2	91.23	138.75	4.47	0.24
Ceacam3	carcinoembryonic antigen-related cell adhesion molecule 3	36.70	39.13	0.13	0.08
Psg16	pregnancy specific glycoprotein 16	50.94	45.68	0.10	0.11
Cgm4	carcinoembryonic antigen gene family 4	220.61	181.00	0.50	0.38
Psgb1	pregnancy-specific beta 1-glycoprotein	1513.64	2597.60	0.05	0.08
Pik3r5	phosphoinositide-3-kinase, regulatory subunit 5	15.76	27.07	4.14	1.09
Phf11	PHD finger protein 11	2238.65	3875.68	20.10	4.08
Psg29	pregnancy-specific glycoprotein 29	115.70	140.20	0.11	0.04
Srpx	sushi-repeat-containing protein, X-linked	457.14	787.56	88.71	61.11

D.3 GD22(NL)

Table D.6: Genes that were differentially expressed in the inner myometrium compared to the decidua on GD22(NL). Transcript expression levels are shown in transcripts per million values (mean±SD).

Gene symbol	Gene name	Decidua TPM	Decidua ±SD	Inner myometrium TPM	Inner myometrium ±SD
Upregulated genes					
Abcc9	ATP-binding cassette, subfamily C (CFTR/MRP), member 9	8.03	8.57	18.88	28.39
Adcyap1r1	adenylate cyclase activating polypeptide 1 receptor 1	2.09	1.91	30.49	47.47
Aoc3	amine oxidase, copper containing 3	5.62	3.61	32.63	27.88
Apbb1ip	amyloid beta (A4) precursor protein-binding, family B, member 1 interacting protein	3.74	2.74	60.28	69.49
Asgr1	asialoglycoprotein receptor 1	0.14	0.13	6.06	4.98
Ass1	argininosuccinate synthase 1	5.55	4.61	56.19	84.75
B3gnt7	UDP-GlcNAc:betaGal beta-1,3-N-acetylglucosaminyltransferase 7	1.62	0.28	28.18	39.84
Cd53	Cd53 molecule	3.59	3.25	26.31	22.03
Cdh1	cadherin 1	2.09	1.21	21.35	36.08
Cdkn1c	cyclin-dependent kinase inhibitor 1C	54.14	35.49	462.85	190.55
Cenpf	centromere protein F	0.65	0.47	8.55	2.89
Cldn4	claudin 4	5.35	5.09	248.75	405.09
Cldn7	claudin 7	2.53	2.67	56.65	97.63
Cmbl	carboxymethylenebutenolidase homolog (Pseudomonas)	2.44	1.76	45.50	38.94
Creb3l1	cAMP responsive element binding protein 3-like 1	29.59	14.62	215.34	89.87
Ctsm	cathepsin M	4.68	5.20	224.42	353.44
Ctxn1	cortexin 1	6.35	4.54	71.27	31.12
Cxcl13	chemokine (C-X-C motif) ligand 13	3.90	2.63	47.32	50.10
Dhrs3	dehydrogenase/reductase (SDR family) member 3	19.50	6.55	110.95	100.97
Dlx3	distal-less homeobox 3	0.81	0.38	26.97	46.14
Ebf3	early B-cell factor 3	0.86	0.80	18.63	21.52
Ednrb	endothelin receptor type B	48.74	20.61	346.91	137.08
Enpp3	ectonucleotide pyrophosphatase/phosphodiesterase 3	5.42	4.00	60.16	53.61
Epcam	epithelial cell adhesion molecule	5.48	5.31	42.27	70.02
Eps8l2	EPS8-like 2	5.21	2.40	37.79	61.61
Fam110c	family with sequence similarity 110, member C	21.32	32.11	21.58	26.48
Fbln1	fibulin 1	26.41	17.99	62.05	107.47
Fmod	fibromodulin	3.07	1.01	50.99	81.26
Folr1	folate receptor 1 (adult)	2.35	1.50	41.98	70.89
Gfpt2	glutamine-fructose-6-phosphate transaminase 2	3.73	0.61	31.56	33.54
Gpm6a	glycoprotein m6a	1.14	0.76	22.82	38.91
Gprc5b	G protein-coupled receptor, family C, group 5, member B	3.24	2.15	42.10	70.08

Continued on next page

Table D.6 – continued from previous page

Gene symbol	Gene name	Decidua TPM	Decidua ±SD	Inner myometrium TPM	Inner myometrium ±SD
Hgd	homogentisate 1, 2-dioxygenase	2.06	2.19	65.02	96.01
Hmgcs2	3-hydroxy-3-methylglutaryl-CoA synthase 2 (mitochondrial)	2.87	3.79	27.14	36.72
Htr2a	5-hydroxytryptamine (serotonin) receptor 2A, G protein-coupled	1.63	0.18	86.91	148.90
Ifi204	myeloid cell nuclear differentiation antigen	8.18	9.36	151.67	157.03
Itm2a	integral membrane protein 2A	1.77	0.47	27.31	44.56
Kcnmb1	potassium large conductance calcium-activated channel, subfamily M, beta member 1	3.83	2.68	69.93	74.90
Kctd15	potassium channel tetramerization domain containing 15	11.78	9.19	167.92	261.06
Lcn2	lipocalin 2	8.24	3.36	160.85	170.17
LOC498662	testis development related protein	0.98	0.37	16.31	24.61
Lrrc63	leucine rich repeat containing 63	0.67	0.44	12.33	20.81
Mgst1	microsomal glutathione S-transferase 1	32.50	19.07	185.45	187.57
Mpeg1	macrophage expressed 1	9.54	7.41	117.83	96.74
Mx1	myxovirus (influenza virus) resistance 1	13.22	10.17	116.26	117.87
Npl	N-acetylneuraminate pyruvate lyase	4.35	2.45	50.87	59.27
Oasl	2'-5'-oligoadenylate synthetase-like	9.29	8.88	131.13	159.32
Olr1590	olfactory receptor 1590	0.00	0.00	9.87	17.10
Pcdh7	protocadherin 7	3.82	1.72	38.60	47.61
Pde4a	phosphodiesterase 4A, cAMP-specific	3.25	2.03	50.95	80.06
Pdpn	podoplanin	13.45	11.62	114.37	67.08
Perp	PERP, TP53 apoptosis effector	1.29	1.77	33.53	29.26
Pla1a	phospholipase A1 member A	9.61	6.37	85.68	70.17
Pnoc	prepronociceptin	0.01	0.02	9.91	16.24
Podxl	podocalyxin-like	4.13	1.33	27.00	26.85
Ppp1r12b	protein phosphatase 1, regulatory subunit 12B	29.13	27.84	70.35	75.76
Prl3a1	Prolactin family 3, subfamily a, member 1	0.00	0.00	12.10	15.73
Psg16	pregnancy specific glycoprotein 16	3.63	2.07	754.24	1242.57
Psg29	pregnancy-specific glycoprotein 29	3.08	2.60	662.38	1056.85
Ptch2	patched homolog 2 (Drosophila)	0.14	0.15	5.76	4.42
Ptprc	protein tyrosine phosphatase, receptor type, C	6.65	7.50	24.65	23.22
Rfx5	regulatory factor X, 5 (influences HLA class II expression)	3.27	1.66	27.97	39.93
Rhox12	reproductive homeobox 12	0.06	0.03	1.85	2.77
Rsad2	radical S-adenosyl methionine domain containing 2	9.52	7.00	50.42	21.61
Sdc1	syndecan 1	12.47	9.29	75.09	40.71
Sgce	sarcoglycan, epsilon	8.75	5.76	119.44	79.72
Slco4a1	solute carrier organic anion transporter family, member 4a1	2.74	2.31	23.45	39.85
Ssc5d	scavenger receptor cysteine rich domain containing (5 domains)	5.45	4.38	64.46	91.68
St3gal5	ST3 beta-galactoside alpha-2,3-sialyltransferase 5	5.49	1.68	47.33	57.02
Tlr7	toll-like receptor 7	1.41	1.35	18.00	16.68
Tpx2	TPX2, microtubule-associated	2.29	0.69	18.00	22.08
Vav3	vav 3 guanine nucleotide exchange factor	1.94	1.52	12.17	8.20
Downregulated genes					
Abp1	amiloride binding protein 1 (amine oxidase copper-containing)	13476.76	10528.29	482.48	348.16
Acer2	alkaline ceramidase 2	230.07	184.92	22.06	13.17
Ampd3	adenosine monophosphate deaminase 3	182.62	141.49	23.00	16.60
Angpt2	angiopoietin 2	14.94	11.93	0.80	0.49
Arsg	arylsulfatase G	65.63	52.38	2.95	0.66
Bmp6	bone morphogenetic protein 6	181.20	146.39	11.10	13.15
Cdhr5	cadherin-related family member 5	275.61	307.44	6.77	9.62
Cdon	cell adhesion associated, oncogene regulated	28.39	22.57	2.46	0.46
Ceacam9	carcinoembryonic antigen-related cell adhesion molecule 9	514.25	886.25	12.94	7.58
Clic5	chloride intracellular channel 5	674.00	544.53	56.52	26.64
Cmah	cytidine monophospho-N-acetylneuraminic acid hydroxylase	84.99	111.17	1.83	2.81
Cryab	crystallin, alpha B	3593.53	2550.04	182.84	163.06
Cspg4	chondroitin sulfate proteoglycan 4	117.16	95.35	7.53	3.13
Csrp3	cysteine and glycine-rich protein 3 (cardiac LIM protein)	3.82	4.10	0.00	0.00
Ctgf	connective tissue growth factor	1562.03	1121.93	126.87	83.31
Cyp26b1	cytochrome P450, family 26, subfamily b, polypeptide 1	228.05	216.17	13.11	4.48
Doxl2	diamine oxidase-like protein 2	3.62	3.84	0.04	0.05
Dync1i1	dynein cytoplasmic 1 intermediate chain 1	11.42	8.95	0.54	0.56
Ehd3	EH-domain containing 3	335.34	257.89	22.93	23.33
Enpp1	ectonucleotide pyrophosphatase/phosphodiesterase 1	114.74	91.63	8.97	6.01
Gatm	glycine amidinotransferase (L-arginine:glycine amidinotransferase)	479.19	443.48	23.16	18.54
Gnat2	guanine nucleotide binding protein (G protein), alpha transducing activity polypeptide 2	115.07	94.43	4.69	7.88
Hopx	HOP homeobox	415.16	372.91	32.65	17.32
Hspb7	heat shock protein family, member 7 (cardiovascular)	71.83	69.41	4.71	5.10
Hyal4	hyaluronoglucosaminidase 4	4.27	3.09	0.13	0.09

Continued on next page

Table D.6 – continued from previous page

Gene symbol	Gene name	Decidua TPM	Decidua ±SD	Inner myometrium TPM	Inner myometrium ±SD
Il1rl1	interleukin 1 receptor-like 1	21.84	30.81	1.60	0.67
Itgbl1	integrin, beta-like 1	286.33	219.40	28.82	16.44
Kcna1	potassium voltage-gated channel, shaker-related subfamily, member 1	2.13	3.46	0.06	0.03
LOC691083	hypothetical protein LOC691083	9.65	7.32	0.12	0.08
Mboat2	membrane bound O-acyltransferase domain containing 2	25.06	22.58	2.07	1.95
Mdfic	MyoD family inhibitor domain containing	42.72	28.55	9.39	2.66
Mfsd12	major facilitator superfamily domain containing 12	256.78	221.05	13.65	17.23
Mogat1	monoacylglycerol O-acyltransferase 1	2.04	0.26	0.09	0.16
Nalcn	sodium leak channel, non-selective	9.11	6.55	0.33	0.11
Nsg2	neuron specific gene family member 2	53.53	45.75	4.82	3.69
Pgf	placental growth factor	752.54	615.73	19.21	7.28
Phactr3	phosphatase and actin regulator 3	5.60	6.44	0.00	0.00
Pkp1	plakophilin 1	59.31	49.85	3.46	3.96
Plcxd2	phosphatidylinositol-specific phospholipase C, X domain containing 2	7.76	6.74	0.66	0.26
Prdm1	PR domain containing 1, with ZNF domain	66.53	50.45	6.68	2.43
Prom1	prominin 1	32.99	33.17	3.62	3.47
Prss35	protease, serine, 35	26.84	27.76	0.47	0.19
Ptprn2	protein tyrosine phosphatase, receptor type, N polypeptide 2	7.84	6.14	0.27	0.11
Ptprr	protein tyrosine phosphatase, receptor type, R	2.65	1.84	0.11	0.03
Ramp3	receptor (G protein-coupled) activity modifying protein 3	624.16	692.21	58.80	31.50
Reln	reelin	42.64	35.74	3.00	2.26
Rrm2	ribonucleotide reductase M2	141.53	185.22	13.40	4.06
S100a4	S100 calcium-binding protein A4	624.60	421.62	41.13	31.11
Scg5	secretogranin V (7B2 protein)	58.11	52.30	2.25	1.96
Sema3b	(semaphorin) 3B	206.03	188.52	9.99	10.27
Slc6a12	solute carrier family 6 (neurotransmitter transporter), member 12	824.03	675.56	20.29	30.55
Slc6a6	solute carrier family 6 (neurotransmitter transporter), member 6	139.81	93.01	16.32	8.16
Sostdc1	sclerostin domain containing 1	1.71	2.95	0.00	0.00
Syt4	synaptotagmin IV	0.79	1.19	0.05	0.02
Tgfa	transforming growth factor alpha	28.15	25.42	3.25	2.91
Tgfb2	transforming growth factor, beta 2	171.44	142.67	19.19	11.63
Tmeff1	transmembrane protein with EGF-like and two follistatin-like domains 1	11.41	10.34	0.26	0.16
Tmem204	transmembrane protein 204	200.68	162.41	8.95	10.82
Uck2	uridine-cytidine kinase 2	201.50	164.04	6.50	5.87
Usp53	ubiquitin specific peptidase 53	57.82	47.14	4.88	0.71
Vldlr	very low density lipoprotein receptor	123.50	110.20	14.10	9.93
Vom2r34	vomeronasal 2 receptor, 34	130.98	203.13	8.51	1.50
Wfdc1	WAP four-disulfide core domain 1	577.72	535.36	22.16	21.11
Zc2hc1c	zinc finger, C2HC-type containing 1C	5.20	4.47	0.01	0.02

Table D.7: Genes that were differentially expressed in the outer myometrium compared to the decidua on GD22(NL). Transcript expression levels are shown in transcripts per million values (mean±SD).

Gene symbol	Gene name	Decidua TPM	Decidua ±SD	Outer myometrium TPM	Outer myometrium ±SD
Upregulated genes					
A1i3	alpha-1-inhibitor 3	0.38	0.06	39.68	68.23
Aadac	arylacetamide deacetylase	0.04	0.06	8.90	15.32
Aadat	aminoadipate aminotransferase	2.05	1.67	41.93	42.22
Abcc8	ATP-binding cassette, subfamily C (CFTR/MRP), member 8	0.02	0.04	8.44	7.39
Abcg2	ATP-binding cassette, subfamily G (WHITE), member 2	0.60	0.66	15.93	11.24
Acot12	acyl-CoA thioesterase 12	0.08	0.13	7.75	12.35
Acsl1	acyl-CoA synthetase long-chain family member 1	3.22	1.41	49.13	67.79
Adra1b	adrenoceptor alpha 1B	0.00	0.00	3.37	5.29
Adtrp	androgen-dependent TFPI-regulating protein	0.41	0.12	26.74	20.75
Afm	afamin	0.06	0.11	11.40	18.78
Afp	alpha-fetoprotein	1.87	2.01	3683.71	2943.42
Agxt2	alanine-glyoxylate aminotransferase 2	0.06	0.10	21.84	37.20
Ahr	aryl hydrocarbon receptor	0.83	1.00	10.27	5.58
Akr1c14	aldo-keto reductase family 1, member C14	23.80	22.00	465.31	410.16
Alas1	aminolevulinate, delta-, synthase 1	15.45	6.64	206.45	197.01
Alas2	aminolevulinate, delta-, synthase 2	2.36	0.44	28.53	41.56
Aldh1b1	aldehyde dehydrogenase 1 family, member B1	0.00	0.00	3.85	6.59

Continued on next page

Table D.7 – continued from previous page

Gene symbol	Gene name	Decidua TPM	Decidua ±SD	Outer myometrium TPM	Outer myometrium ±SD
Alox15b	arachidonate 15-lipoxygenase, type B	0.05	0.08	6.34	8.35
Alpl	alkaline phosphatase, liver/bone/kidney	3.22	0.62	34.71	48.23
Amdhd1	amidohydrolase domain containing 1	0.00	0.00	11.24	19.04
Amy1a	amylase, alpha 1A (salivary)	0.01	0.03	6.14	10.62
Ankrd22	ankyrin repeat domain 22	0.02	0.03	2.63	2.26
Apcs	amyloid P component, serum	0.00	0.01	28.50	49.18
Apoa2	apolipoprotein A-II	0.00	0.00	104.68	178.40
Apof	apolipoprotein F	0.12	0.22	5.50	8.93
Apol3	apolipoprotein L, 3	1.91	0.58	30.76	24.35
Apon	apolipoprotein N	0.44	0.09	9.62	11.96
Arl5c	ADP-ribosylation factor-like 5C	0.00	0.01	2.34	4.04
Arsb	arylsulfatase B	15.57	8.84	181.41	222.54
As3mt	arsenic (+3 oxidation state) methyltransferase	5.61	4.13	40.56	54.29
Asgr1	asialoglycoprotein receptor 1	0.14	0.13	42.89	59.49
Aspm	asp (abnormal spindle) homolog, microcephaly associated (Drosophila)	0.50	0.16	5.86	5.27
Ass1	argininosuccinate synthase 1	5.55	4.61	223.08	184.38
Atp7b	ATPase, Cu++ transporting, beta polypeptide	0.09	0.08	13.36	17.33
Azgp1	alpha-2-glycoprotein 1, zinc-binding	0.06	0.11	59.58	103.10
B3gnt7	UDP-GlcNAc:betaGal beta-1,3-N-acetylglucosaminyltransferase 7	1.62	0.28	42.13	61.50
Baiap2l1	BAI1-associated protein 2-like 1	1.39	0.99	26.26	31.70
Bcam	basal cell adhesion molecule (Lutheran blood group)	4.22	4.08	44.66	36.97
Brca1	breast cancer 1, early onset	0.40	0.30	3.48	2.18
Bub1	BUB1 mitotic checkpoint serine/threonine kinase	1.26	0.37	8.13	6.38
Bucs1	acyl-CoA synthetase medium-chain family member 1	0.01	0.01	35.57	61.34
C3	complement component 3	11.31	17.57	1199.02	1226.91
C4bpa	complement component 4 binding protein, alpha	0.01	0.03	13.12	22.58
C4bpb	complement component 4 binding protein, beta	0.09	0.10	52.51	90.75
Camp	cathelicidin antimicrobial peptide	0.11	0.18	37.38	64.73
Car1	carbonic anhydrase I	0.00	0.00	7.42	12.84
Ccdc64b	coiled-coil domain containing 64B	0.00	0.00	3.01	3.04
Ccl21	chemokine (C-C motif) ligand 21	0.13	0.13	19.05	22.06
Ccna2	cyclin A2	1.96	0.64	22.59	15.09
Ccnb2	cyclin B2	1.30	0.40	16.63	13.60
Cd4	Cd4 molecule	1.00	0.62	16.06	17.75
Cd79b	Cd79b molecule, immunoglobulin-associated beta	0.01	0.01	4.80	8.20
Cdh1	cadherin 1	2.09	1.21	179.51	198.89
Ceacam1	carcinoembryonic antigen-related cell adhesion molecule 1 (biliary glycoprotein)	12.81	17.33	55.77	36.10
Cenpf	centromere protein F	0.65	0.47	23.52	18.14
Cfb	complement factor B	2.73	3.71	157.75	97.41
Cfh	complement factor H	1.24	0.90	37.81	42.05
Cfhr1	complement factor H-related 1	0.02	0.04	5.63	9.20
Cfi	complement factor I	4.05	2.86	48.20	53.03
Cftr	cystic fibrosis transmembrane conductance regulator	0.82	0.59	22.54	29.22
Cideb	cell death-inducing DFFA-like effector b	7.17	9.12	47.99	34.09
Cit	citron (rho-interacting, serine/threonine kinase 21)	0.47	0.38	8.30	5.80
Ckmt1b	creatine kinase, mitochondrial 1B	0.44	0.32	19.76	13.85
Cldn1	claudin 1	0.64	0.57	20.50	25.59
Cldn2	claudin 2	1.65	2.71	135.04	114.17
Cldn4	claudin 4	5.35	5.09	367.31	529.47
Cldn7	claudin 7	2.53	2.67	72.57	79.21
Cldn8	claudin 8	0.00	0.01	4.29	5.87
Clmn	calmin	0.62	0.56	23.05	26.47
Cndp1	carnosine dipeptidase 1 (metallopeptidase M20 family)	0.83	0.53	35.15	22.93
Col2a1	collagen, type II, alpha 1	0.10	0.05	8.56	14.79
Coro2a	coronin, actin binding protein 2A	0.16	0.19	6.53	6.43
Cpn1	carboxypeptidase N, polypeptide 1	0.02	0.04	10.15	10.54
Cpn2	carboxypeptidase N, polypeptide 2	0.01	0.02	10.27	16.58
Creb3l1	cAMP responsive element binding protein 3-like 1	29.59	14.62	165.27	175.08
Creb3l3	cAMP responsive element binding protein 3-like 3	0.62	0.34	33.39	41.91
Crip1	cysteine-rich protein 1 (intestinal)	14.15	9.71	171.22	132.17
Csf1r	colony stimulating factor 1 receptor	14.57	5.08	100.47	85.43
Ctsg	cathepsin G	0.00	0.00	4.11	6.75
Ctsm	cathepsin M	4.68	5.20	107.27	182.78
Ctxn1	cortexin 1	6.35	4.54	75.65	19.18
Cubn	cubilin (intrinsic factor-cobalamin receptor)	0.14	0.03	25.73	21.78
Cuzd1	CUB and zona pellucida-like domains 1	10.68	17.89	492.78	409.84
Cx3cl1	chemokine (C-X3-C motif) ligand 1	0.71	0.66	17.66	18.54
Cxcl16	chemokine (C-X-C motif) ligand 16	8.86	6.79	68.94	68.02

Continued on next page

Table D.7 – continued from previous page

Gene symbol	Gene name	Decidua TPM	Decidua ±SD	Outer myometrium TPM	Outer myometrium ±SD
Cyp2c22	cytochrome P450, family 2, subfamily c, polypeptide 22	0.00	0.01	6.25	10.51
Cyp2d1	cytochrome P450, family 2, subfamily d, polypeptide 1	0.52	0.91	5.86	6.24
Cyp3a62	cytochrome P450, family 3, subfamily a, polypeptide 62	0.00	0.01	2.27	3.11
Cyp4a2	cytochrome P450, family 4, subfamily a, polypeptide 2	0.02	0.03	5.48	9.19
Dcdc2	doublecortin domain containing 2	2.48	3.19	18.15	13.93
Defa	defensin alpha	0.07	0.12	76.90	132.33
Dhrs11	dehydrogenase/reductase (SDR family) member 11	2.57	0.65	18.39	10.30
Dhtkd1	dehydrogenase E1 and transketolase domain containing 1	1.81	1.20	11.63	14.38
Dmbt1	deleted in malignant brain tumors 1	0.65	0.45	18.86	13.45
Dpp4	dipeptidylpeptidase 4	0.15	0.01	4.48	3.25
Dsc2	desmocollin 2	1.96	0.75	42.35	53.92
Ehf	ets homologous factor	1.06	1.23	29.02	34.55
Ehhadh	enoyl-CoA, hydratase/3-hydroxyacyl CoA dehydrogenase	1.89	1.28	21.25	16.87
Elf3	E74-like factor 3	1.75	2.37	70.44	73.54
Emb	embigin	2.99	3.75	32.47	27.92
Entpd2	ectonucleoside triphosphate diphosphohydrolase 2	16.36	6.45	151.88	111.70
Epb41l3	erythrocyte membrane protein band 4.1-like 3	0.66	0.13	17.60	11.00
Epcam	epithelial cell adhesion molecule	5.48	5.31	352.04	262.99
Epha2	Eph receptor A2	1.44	0.30	14.75	9.18
Eps8l1	EPS8-like 1	0.12	0.02	5.83	3.71
Eps8l2	EPS8-like 2	5.21	2.40	73.65	82.21
Epsti1	epithelial stromal interaction 1 (breast)	2.25	0.63	24.95	26.49
Epx	eosinophil peroxidase	0.03	0.04	8.26	13.38
Ercc6l	excision repair cross-complementing rodent repair deficiency complementation group 6 - like	0.28	0.16	3.25	2.19
Exoc6	exocyst complex component 6	1.12	0.43	19.85	16.30
Eya2	eyes absent homolog 2 (Drosophila)	1.02	1.45	37.63	37.38
F11	coagulation factor XI	0.02	0.02	5.03	6.70
F2rl1	coagulation factor II (thrombin) receptor-like 1	7.48	3.58	39.54	16.00
F5	coagulation factor V (proaccelerin, labile factor)	0.82	0.67	39.50	32.53
Fabp1	fatty acid binding protein 1, liver	0.00	0.00	91.57	158.60
Faim3	Fas apoptotic inhibitory molecule 3	0.60	0.45	13.33	7.74
Fam167a	family with sequence similarity 167, member A	1.49	1.10	15.38	11.67
Fam84a	family with sequence similarity 84, member A	0.05	0.05	3.90	2.47
Fcgbp	Fc fragment of IgG binding protein	0.52	0.59	20.48	25.88
Fgd4	FYVE, RhoGEF and PH domain containing 4	0.78	0.48	5.08	3.78
Fhdc1	FH2 domain containing 1	1.32	0.72	9.59	5.01
Fhl1	four and a half LIM domains 1	46.77	43.41	291.70	108.06
Fmod	fibromodulin	3.07	1.01	21.12	6.88
Folr1	folate receptor 1 (adult)	2.35	1.50	162.60	159.02
Fxyd4	FXYD domain-containing ion transport regulator 4	0.22	0.14	9.49	5.19
Gabrp	gamma-aminobutyric acid (GABA-A) receptor, pi	0.00	0.00	3.76	4.09
Gatsl2	GATS protein-like 2	21.24	6.98	71.36	34.62
Gca	grancalcin	0.59	0.30	12.74	8.91
Gckr	glucokinase (hexokinase 4) regulator	0.00	0.00	6.79	11.66
Gcnt1	glucosaminyl (N-acetyl) transferase 1, core 2	2.15	0.32	12.87	7.82
Ghrl	ghrelin/obestatin prepropeptide	0.09	0.08	14.37	19.54
Gnmt	glycine N-methyltransferase	0.01	0.02	107.74	186.61
Gpa33	glycoprotein A33 (transmembrane)	0.40	0.36	24.22	28.58
Gpc3	glypican 3	0.82	0.62	44.34	31.72
Gpx2	glutathione peroxidase 2	5.29	6.55	160.81	81.14
Gramd1b	GRAM domain containing 1B	3.13	0.57	26.96	20.74
Grik2	glutamate receptor, ionotropic, kainate 2	0.29	0.26	6.42	2.72
Gsta3	glutathione S-transferase alpha 3	7.75	1.03	71.62	93.58
Haao	3-hydroxyanthranilate 3,4-dioxygenase	0.01	0.01	17.24	29.68
Hao1	hydroxyacid oxidase (glycolate oxidase) 1	0.05	0.08	10.21	17.58
Hemgn	hemogen	1.05	0.93	55.11	91.97
Hgfac	HGF activator	0.29	0.48	23.55	23.19
Hjurp	Holliday junction recognition protein	0.30	0.21	4.92	3.13
Hmgcs2	3-hydroxy-3-methylglutaryl-CoA synthase 2 (mitochondrial)	2.87	3.79	100.87	169.45
Hnf1b	HNF1 homeobox B	0.34	0.35	10.65	12.63
Hnf4a	hepatocyte nuclear factor 4, alpha	0.02	0.03	36.88	22.69
Hook1	hook microtubule-tethering protein 1	0.23	0.11	3.14	2.13
Hoxb8	homeo box B8	1.83	0.60	18.48	28.79
Hp	haptoglobin	2.65	0.74	511.81	885.89
Hpd	4-hydroxyphenylpyruvate dioxygenase	0.02	0.03	69.38	119.72
Hpx	hemopexin	1.12	0.52	82.09	136.29
Ifitm1	interferon induced transmembrane protein 1	27.54	18.87	236.37	143.09

Continued on next page

Table D.7 – continued from previous page

Gene symbol	Gene name	Decidua TPM	Decidua ±SD	Outer myometrium TPM	Outer myometrium ±SD
Igfals	insulin-like growth factor binding protein, acid labile subunit	0.00	0.00	4.22	5.21
Igsf5	immunoglobulin superfamily, member 5	0.03	0.05	8.04	7.70
Il1a	interleukin 1 alpha	0.16	0.20	9.88	10.42
Ildr1	immunoglobulin-like domain containing receptor 1	0.11	0.09	4.74	3.34
Irf6	interferon regulatory factor 6	0.47	0.41	20.26	14.60
Itga6	integrin, alpha 6	2.19	1.54	23.89	18.92
Itgb4	integrin, beta 4	1.81	1.77	31.49	25.12
Itih1	inter-alpha trypsin inhibitor, heavy chain 1	0.02	0.03	44.95	77.65
Itpr2	inositol 1,4,5-trisphosphate receptor, type 2	2.28	0.68	10.99	7.00
Kap	kidney androgen regulated protein	17.01	28.41	1514.85	999.61
Kazn	kazrin, periplakin interacting protein	4.02	1.89	21.73	21.97
Kcnj16	potassium inwardly-rectifying channel, subfamily J, member 16	0.10	0.03	6.87	6.70
Keg1	glycine-N-acyltransferase-like 2	0.04	0.01	7.44	12.04
Kif11	kinesin family member 11	1.11	0.79	9.36	6.68
Kif23	kinesin family member 23	1.32	1.16	26.13	22.56
Krt19	keratin 19	33.21	26.87	396.19	327.46
Lad1	ladinin 1	1.25	0.43	149.58	221.93
Lamb3	laminin, beta 3	0.29	0.38	22.91	17.10
Lcn2	lipocalin 2	8.24	3.36	126.31	66.72
Lcn5	lipocalin 5	0.06	0.11	7.34	12.71
Lgals2	lectin, galactoside-binding, soluble, 2	0.02	0.02	30.51	23.52
Lgr4	leucine-rich repeat-containing G protein-coupled receptor 4	2.08	1.00	13.51	10.12
Llgl2	lethal giant larvae homolog 2 (Drosophila)	1.04	0.64	15.11	11.65
LOC360228	WDNM1 homolog	0.04	0.04	27.85	15.10
LOC498222	similar to specifically androgen-regulated protein	0.24	0.07	3.18	1.89
LOC498368	similar to RIKEN cDNA 0610040J01	0.30	0.16	6.81	5.47
LOC500797	mitotic spindle positioning	0.49	0.24	24.58	20.86
LOC641520	popeye domain containing 3	0.00	0.00	2.45	2.66
LOC684112	SIK family kinase 3	9.48	5.23	27.45	12.17
LOC689064	beta-globin	39.69	29.70	1489.39	2365.58
Lpcat4	lysophosphatidylcholine acyltransferase 4	4.60	2.60	67.64	67.55
Lpo	lactoperoxidase	3.18	5.50	99.94	125.95
Lrp2	low density lipoprotein receptor-related protein 2	0.28	0.26	17.89	15.16
Lrrc66	leucine rich repeat containing 66	0.06	0.05	2.23	0.85
Lsr	lipolysis stimulated lipoprotein receptor	3.48	1.82	82.74	68.07
Lurap1l	leucine rich adaptor protein 1-like	0.14	0.22	9.97	3.17
Lypd3	Ly6/Plaur domain containing 3	0.21	0.28	6.86	0.81
Macc1	metastasis associated in colon cancer 1	0.20	0.34	4.52	3.27
Mal2	mal, T-cell differentiation protein 2	0.38	0.41	32.51	32.69
Manba	mannosidase, beta A, lysosomal	7.45	1.87	26.17	10.74
Map7	microtubule-associated protein 7	1.12	0.36	11.82	10.71
Mat1a	methionine adenosyltransferase I, alpha	1.35	1.18	38.17	64.94
Mecom	MDS1 and EVI1 complex locus	1.42	0.79	13.64	12.88
Met	met proto-oncogene	0.73	0.65	12.53	7.83
Mgst1	microsomal glutathione S-transferase 1	32.50	19.07	181.62	249.08
Mki67	marker of proliferation Ki-67	1.85	1.26	36.01	32.97
Mlxipl	MLX interacting protein-like	1.74	2.18	17.63	23.88
Mmp17	matrix metallopeptidase 17	2.18	2.30	16.35	1.74
Mmp7	matrix metallopeptidase 7	9.86	17.00	131.36	56.43
Mpzl2	myelin protein zero-like 2	5.47	4.65	47.52	40.78
Mrc1	mannose receptor, C type 1	0.73	0.62	6.95	8.45
Ms4a8a	membrane-spanning 4-domains, subfamily A, member 8A	0.00	0.00	3.12	4.14
Msx1	msh homeobox 1	0.53	0.37	20.51	21.33
Myh14	myosin, heavy chain 14, non-muscle	1.31	1.40	40.59	36.09
Napsa	napsin A aspartic peptidase	1.06	0.82	42.31	33.89
Ngp	neutrophilic granule protein	0.00	0.00	24.71	41.14
Npl	N-acetylneuraminate pyruvate lyase	4.35	2.45	62.26	58.25
Nr1i2	nuclear receptor subfamily 1, group I, member 2	0.01	0.03	6.49	11.16
Nt5e	5' nucleotidase, ecto	1.61	0.65	16.60	11.38
Nusap1	nucleolar and spindle associated protein 1	1.39	0.59	11.88	8.84
P2ry4	pyrimidinergic receptor P2Y, G-protein coupled, 4	0.00	0.00	2.09	1.93
Pah	phenylalanine hydroxylase	0.01	0.01	27.06	46.80
Paqr9	progestin and adipoQ receptor family member IX	0.42	0.73	18.69	31.80
Parm1	prostate androgen-regulated mucin-like protein 1	12.75	7.34	112.71	107.20
Pax8	paired box 8	1.23	0.92	33.09	38.30
Pbld1	phenazine biosynthesis-like protein domain containing 1	0.06	0.05	7.87	11.31
Pced1b	PC-esterase domain containing 1B	5.63	2.35	64.02	83.06
Pdpn	podoplanin	13.45	11.62	335.56	393.33

Continued on next page

Table D.7 – continued from previous page

Gene symbol	Gene name	Decidua TPM	Decidua ±SD	Outer myometrium TPM	Outer myometrium ±SD
Perp	PERP, TP53 apoptosis effector	1.29	1.77	98.98	97.77
Phlda1	pleckstrin homology-like domain, family A, member 1	7.74	1.76	54.13	54.73
Pigr	polymeric immunoglobulin receptor	1.26	1.04	55.40	69.41
Pip5k1b	phosphatidylinositol-4-phosphate 5-kinase, type I, beta	0.26	0.19	5.70	3.97
Pklr	pyruvate kinase, liver and RBC	2.23	0.65	27.71	27.58
Pkp2	plakophilin 2	4.27	3.71	44.33	42.76
Plcb1	phospholipase C, beta 1 (phosphoinositide-specific)	0.63	0.27	6.10	6.28
Plekhd1	pleckstrin homology domain containing, family D (with coiled-coil domains) member 1	0.85	0.22	18.19	13.33
Plekhh1	pleckstrin homology domain containing, family H (with MyTH4 domain) member 1	4.43	0.60	53.21	49.26
Plk5	polo-like kinase 5	0.04	0.06	6.15	9.11
Plvap	plasmalemma vesicle associated protein	8.69	4.43	46.28	47.64
Plxnb2	plexin B2	13.91	10.76	69.59	50.50
Pnoc	prepronociceptin	0.01	0.02	120.54	147.72
Podxl	podocalyxin-like	4.13	1.33	53.81	49.43
Ppp1r12b	protein phosphatase 1, regulatory subunit 12B	29.13	27.84	60.32	23.04
Prc1	protein regulator of cytokinesis 1	3.51	0.98	36.80	31.76
Prkaa2	protein kinase, AMP-activated, alpha 2 catalytic subunit	0.97	0.71	10.40	8.88
Prkcb	protein kinase C, beta	0.17	0.12	5.27	5.05
Prkcz	protein kinase C, zeta	0.38	0.36	7.52	6.61
Prl3a1	Prolactin family 3, subfamily a, member 1	0.00	0.00	16.33	5.06
Prl3d4	prolactin family 3, subfamily d, member 4	16.49	23.55	826.10	1424.54
Prodh2	proline dehydrogenase (oxidase) 2	0.00	0.01	21.12	36.49
Prrt1	proline-rich transmembrane protein 1	1.15	0.35	12.05	12.18
Prss30	protease, serine, 30	0.00	0.00	2.31	3.00
Psat1	phosphoserine aminotransferase 1	1.54	1.77	21.17	18.95
Psg16	pregnancy specific glycoprotein 16	3.63	2.07	716.10	1237.31
Psg29	pregnancy-specific glycoprotein 29	3.08	2.60	648.04	1117.62
Ptgs1	prostaglandin-endoperoxide synthase 1	2.31	1.14	45.52	44.58
Ptprf	protein tyrosine phosphatase, receptor type, F	4.36	2.69	23.40	17.48
Ptprh	protein tyrosine phosphatase, receptor type, H	0.98	1.06	49.37	42.47
Rab11fip1	RAB11 family interacting protein 1 (class I)	6.06	4.10	47.84	41.67
Rab17	RAB17, member RAS oncogene family	0.27	0.47	17.60	13.99
Rarres1	retinoic acid receptor responder (tazarotene induced) 1	5.94	2.27	46.29	45.43
Rbp4	retinol binding protein 4, plasma	1.96	1.58	593.30	896.31
RGD1309313	transmembrane protein 180	7.14	6.94	53.18	40.76
RGD1309821	similar to KIAA1161 protein	1.93	0.27	18.70	13.63
RGD1310507	similar to RIKEN cDNA 1300017J02	1.90	1.50	133.95	103.79
RGD1310587	similar to hypothetical protein FLJ14146	2.98	3.55	28.51	18.14
RGD1563547	small integral membrane protein 22	0.32	0.14	28.31	20.33
RGD1564614	similar to complement factor H-related protein	0.01	0.02	6.67	11.20
RGD1564894	similar to glycine-N-acyltransferase isoform a	0.00	0.00	17.76	30.66
Rgs20	regulator of G-protein signaling 20	0.04	0.05	6.40	9.52
Rhox12	reproductive homeobox 12	0.06	0.03	4.18	3.34
Rnf208	ring finger protein 208	0.00	0.00	6.23	5.14
Rtp3	receptor (chemosensory) transporter protein 3	2.00	0.38	21.09	20.82
Sdc3	syndecan 3	3.46	3.67	22.41	16.45
Sema4a	(semaphorin) 4A	1.30	0.93	30.26	33.24
Sema4g	(semaphorin) 4G	0.30	0.30	17.71	18.35
Sepp1	selenoprotein P, plasma, 1	45.60	23.88	865.70	728.25
Sgce	sarcoglycan, epsilon	8.75	5.76	92.76	117.09
Sgms1	sphingomyelin synthase 1	1.42	0.65	25.90	24.57
Sgms2	sphingomyelin synthase 2	1.12	1.09	13.94	13.37
Sipa1l3	signal-induced proliferation-associated 1 like 3	7.84	4.21	51.75	50.62
Slc16a14	solute carrier family 16, member 14	1.14	0.91	28.20	33.75
Slc1a1	solute carrier family 1 (neuronal/epithelial high affinity glutamate transporter, system Xag), member 1	0.07	0.03	8.19	7.64
Slc22a23	solute carrier family 22, member 23	3.98	1.69	33.68	24.39
Slc25a37	solute carrier family 25 (mitochondrial iron transporter), member 37	2.62	1.97	27.89	31.46
Slc26a4	solute carrier family 26 (anion exchanger), member 4	1.26	2.07	69.38	68.87
Slc27a5	solute carrier family 27 (fatty acid transporter), member 5	0.00	0.00	9.51	16.01
Slc28a2	solute carrier family 28 (sodium-coupled nucleoside transporter), member 2	5.56	0.33	36.76	11.80
Slc2a2	solute carrier family 2 (facilitated glucose transporter), member 2	0.03	0.01	22.17	22.06
Slc34a2	solute carrier family 34 (type II sodium/phosphate contransporter), member 2	1.46	2.13	24.89	23.72
Slc38a4	solute carrier family 38, member 4	14.54	13.24	202.40	309.79
Slc39a8	solute carrier family 39 (zinc transporter), member 8	4.88	1.32	28.25	13.92
Slc44a4	solute carrier family 44, member 4	0.91	0.59	38.47	42.57
Slc45a3	solute carrier family 45, member 3	0.59	0.50	8.03	7.58
Slc4a1	solute carrier family 4 (anion exchanger), member 1	1.73	0.66	92.03	153.87

Continued on next page

Table D.7 – continued from previous page

Gene symbol	Gene name	Decidua TPM	Decidua ±SD	Outer myometrium TPM	Outer myometrium ±SD
Slc5a3	solute carrier family 5 (sodium/myo-inositol cotransporter), member 3	1.85	0.80	16.42	14.05
Slc6a14	solute carrier family 6 (amino acid transporter), member 14	0.09	0.15	5.53	4.79
Slc7a9	solute carrier family 7 (amino acid transporter light chain, bo,+ system), member 9	0.00	0.00	10.30	8.64
Slc9a3r1	solute carrier family 9, subfamily A (NHE3, cation proton antiporter 3), member 3 regulator 1	45.15	12.76	311.36	201.25
Slco1a1	solute carrier organic anion transporter family, member 1a1	0.01	0.01	2.91	4.91
Slco4c1	solute carrier organic anion transporter family, member 4C1	0.03	0.05	4.11	2.71
Smlr1	small leucine-rich protein 1	0.00	0.00	9.12	12.15
Snhg11	small nucleolar RNA host gene 11 (non-protein coding)	2.34	1.16	7.20	6.89
Sort1	sortilin 1	3.15	2.13	23.31	16.87
Spint1	serine peptidase inhibitor, Kunitz type 1	0.97	0.46	45.26	38.51
Spint2	serine peptidase inhibitor, Kunitz type, 2	36.22	24.98	203.59	229.62
Spns2	spinster homolog 2	2.94	2.31	14.41	9.66
Spp1	secreted phosphoprotein 1	22.43	21.05	177.65	144.31
Sprr1a	small proline-rich protein 1A	0.04	0.07	32.13	49.80
St14	suppression of tumorigenicity 14 (colon carcinoma)	1.64	2.21	59.10	42.80
St8sia3	ST8 alpha-N-acetyl-neuraminide alpha-2,8-sialyltransferase 3	0.00	0.00	5.65	9.16
Stard4	StAR-related lipid transfer (START) domain containing 4	3.00	2.99	12.40	4.39
Stat5b	signal transducer and activator of transcription 5B	1.87	1.18	22.59	20.44
Stfa3	stefin A3	0.98	0.32	19.76	29.44
Sult1b1	sulfotransferase family, cytosolic, 1B, member 1	0.00	0.00	6.82	9.63
Taok3	TAO kinase 3	6.36	3.50	31.35	2.88
Tcf7l1	transcription factor 7-like 1 (T-cell specific, HMG-box)	7.21	4.00	54.92	50.46
Tf	transferrin	1.63	0.72	1446.88	1856.73
Timd2	T-cell immunoglobulin and mucin domain containing 2	3.93	1.52	56.86	42.93
Tmc4	transmembrane channel-like 4	0.87	0.97	62.03	69.32
Tmem171	transmembrane protein 171	0.65	0.48	12.98	11.29
Tmem246	transmembrane protein 246	0.13	0.05	3.91	1.51
Tmem252	transmembrane protein 252	2.33	1.90	25.70	13.93
Tmem30b	transmembrane protein 30B	0.08	0.10	14.20	15.23
Tnfaip6	tumor necrosis factor alpha induced protein 6	14.57	13.29	101.61	108.15
Tonsl	tonsoku-like, DNA repair protein	1.05	0.40	8.62	9.51
Top2a	topoisomerase (DNA) II alpha	1.50	1.10	24.51	19.83
Tpx2	TPX2, microtubule-associated	2.29	0.69	19.68	15.15
Trpv6	transient receptor potential cation channel, subfamily V, member 6	0.29	0.13	16.66	18.45
Tspan1	tetraspanin 1	1.60	2.18	67.06	39.29
Tspan13	tetraspanin 13	4.23	1.48	36.33	22.37
Ttc22	tetratricopeptide repeat domain 22	0.01	0.01	2.79	4.08
Ugt1a1	UDP glucuronosyltransferase 1 family, polypeptide A1	0.02	0.03	7.75	9.17
Ugt1a5	UDP glucuronosyltransferase 1 family, polypeptide A5	0.60	0.50	23.36	39.08
Ugt1a7c	UDP glucuronosyltransferase 1 family, polypeptide A7C	2.68	1.60	49.66	42.40
Uhrf1	ubiquitin-like with PHD and ring finger domains 1	0.50	0.38	5.92	2.46
Unc5cl	unc-5 homolog C (C. elegans)-like	0.13	0.18	17.36	9.72
Upb1	ureidopropionase, beta	0.02	0.04	16.36	28.14
Upk1b	uroplakin 1B	0.24	0.14	26.98	14.78
Vax2	ventral anterior homeobox 2	0.00	0.00	5.06	8.30
Vtcn1	V-set domain containing T cell activation inhibitor 1	0.65	0.09	14.37	16.06
Vtn	vitronectin	1.75	1.28	196.99	333.38
Wnt7a	wingless-type MMTV integration site family, member 7A	0.20	0.14	11.54	9.93
Zmynd12	zinc finger, MYND-type containing 12	0.04	0.07	5.37	5.94
Downregulated genes					
Acer2	alkaline ceramidase 2	230.07	184.92	20.19	7.40
Adamts12	ADAM metallopeptidase with thrombospondin type 1 motif, 12	40.54	32.29	3.41	3.78
Ampd3	adenosine monophosphate deaminase 3	182.62	141.49	14.90	7.90
Atg4al1	autophagy related 4A, cysteine peptidase-like 1	198.54	149.16	17.08	9.57
Bdnf	brain-derived neurotrophic factor	8.64	8.34	1.54	0.33
Bmp6	bone morphogenetic protein 6	181.20	146.39	13.61	12.44
Btbd3	BTB (POZ) domain containing 3	197.51	148.67	28.89	9.33
Camk2a	calcium/calmodulin-dependent protein kinase II alpha	5.91	5.77	0.14	0.15
Cdh3	cadherin 3	173.14	134.14	15.36	16.24
Cdhr5	cadherin-related family member 5	275.61	307.44	17.67	14.49
Ceacam9	carcinoembryonic antigen-related cell adhesion molecule 9	514.25	886.25	40.76	22.98
Chodl	chondrolectin	57.86	49.01	0.81	1.17
Clic5	chloride intracellular channel 5	674.00	544.53	28.98	13.51
Cmah	cytidine monophospho-N-acetylneuraminic acid hydroxylase	84.99	111.17	1.36	1.17
Cpe	carboxypeptidase E	794.87	666.43	26.39	20.83

Continued on next page

Table D.7 – continued from previous page

Gene symbol	Gene name	Decidua TPM	Decidua ±SD	Outer myometrium TPM	Outer myometrium ±SD
Crim1	cysteine rich transmembrane BMP regulator 1 (chordin like)	245.45	201.55	34.23	3.97
Cryab	crystallin, alpha B	3593.53	2550.04	133.57	92.52
Cryl1	crystallin, lambda 1	52.98	44.63	7.19	2.32
Ctgf	connective tissue growth factor	1562.03	1121.93	68.87	32.78
Cyp26b1	cytochrome P450, family 26, subfamily b, polypeptide 1	228.05	216.17	7.11	2.18
Ehd3	EH-domain containing 3	335.34	257.89	35.29	28.12
Enpp1	ectonucleotide pyrophosphatase/phosphodiesterase 1	114.74	91.63	6.59	1.51
Epdr1	ependymin related 1	78.10	53.63	10.73	8.34
Fam134b	family with sequence similarity 134, member B	219.76	184.81	17.42	4.41
Fam25a	family with sequence similarity 25, member A	210.52	129.46	6.87	4.86
Gadd45g	growth arrest and DNA-damage-inducible, gamma	915.00	747.80	111.74	65.34
Gatm	glycine amidinotransferase (L-arginine:glycine amidinotransferase)	479.19	443.48	15.04	1.72
Gnat2	guanine nucleotide binding protein (G protein), alpha transducing activity polypeptide 2	115.07	94.43	0.38	0.29
Grem1	gremlin 1	103.82	84.95	4.44	2.83
Hopx	HOP homeobox	415.16	372.91	33.35	20.48
Inhba	inhibin beta-A	1234.68	972.39	37.05	24.34
Irx4	iroquois homeobox 4	35.59	38.50	0.14	0.10
Itgb5	integrin, beta 5	566.31	459.64	53.43	20.75
Itgbl1	integrin, beta-like 1	286.33	219.40	14.49	21.29
Kcnmb4	potassium large conductance calcium-activated channel, subfamily M, beta member 4	3.77	1.19	0.00	0.00
Krt23	keratin 23 (histone deacetylase inducible)	46.49	56.70	3.78	3.91
Larp6	La ribonucleoprotein domain family, member 6	49.58	37.18	3.57	1.68
LOC680549	PBX/knotted 1 homeobox 2	55.93	41.23	6.10	4.93
LOC682105	receptor accessory protein 2	85.90	69.12	8.27	1.31
Map1a	microtubule-associated protein 1A	105.65	83.02	10.71	6.47
Mfap5	microfibrillar associated protein 5	92.69	69.59	9.37	8.18
Mfsd12	major facilitator superfamily domain containing 12	256.78	221.05	19.71	4.57
Mgp	matrix Gla protein	508.86	346.75	89.38	73.40
Mrgprg	MAS-related GPR, member G	79.26	93.25	0.20	0.34
Mustn1	musculoskeletal, embryonic nuclear protein 1	618.94	531.20	45.31	32.81
Nbl1	neuroblastoma 1, DAN family BMP antagonist	1771.85	1383.23	116.24	57.97
Nkd2	naked cuticle homolog 2 (Drosophila)	66.57	72.34	4.64	6.11
Nox4	NADPH oxidase 4	67.01	59.69	5.38	1.18
Npr2	natriuretic peptide receptor B/guanylate cyclase B (atrionatriuretic peptide receptor B)	34.07	23.58	4.51	1.13
Olig1	oligodendrocyte transcription factor 1	4.03	3.18	0.12	0.09
Pde4dip	phosphodiesterase 4D interacting protein	101.42	82.96	13.21	3.40
Pea15	phosphoprotein enriched in astrocytes 15	571.28	443.95	65.53	6.03
Pgf	placental growth factor	752.54	615.73	9.08	3.96
Pkp1	plakophilin 1	59.31	49.85	1.17	0.91
Pla2g16	phospholipase A2, group XVI	247.85	177.76	36.28	28.46
Plk2	polo-like kinase 2	347.65	246.92	49.71	12.24
Ppp1r14c	protein phosphatase 1, regulatory (inhibitor) subunit 14c	31.69	28.48	3.16	1.96
Pqlc3	PQ loop repeat containing 3	73.78	52.78	12.09	8.39
Praf2	PRA1 domain family, member 2	214.85	136.42	31.82	9.12
Prdm1	PR domain containing 1, with ZNF domain	66.53	50.45	8.04	4.38
Prl7d1	prolactin family 7, subfamily d, member 1	39.70	63.54	2.37	1.48
Procr	protein C receptor, endothelial	85.61	75.90	7.46	1.86
Pros1	protein S (alpha)	103.77	79.71	13.46	7.53
Prss35	protease, serine, 35	26.84	27.76	0.76	0.27
Ramp3	receptor (G protein-coupled) activity modifying protein 3	624.16	692.21	35.15	30.65
Rasd1	RAS, dexamethasone-induced 1	216.96	206.58	19.31	10.70
RGD1563441	similar to RIKEN cDNA A030009H04	4.70	3.29	0.04	0.07
Rtn4rl1	reticulon 4 receptor-like 1	41.76	49.66	2.59	0.76
S100a4	S100 calcium-binding protein A4	624.60	421.62	33.96	17.13
Scg5	secretogranin V (7B2 protein)	58.11	52.30	1.79	1.81
Sema3b	(semaphorin) 3B	206.03	188.52	4.77	1.72
Sema3e	(semaphorin) 3E	23.59	18.12	3.20	1.50
Sipa1l2	signal-induced proliferation-associated 1 like 2	68.27	40.93	11.78	5.50
Slc29a1	solute carrier family 29 (equilibrative nucleoside transporter), member 1	154.98	129.23	7.42	3.43
Slc5a6	solute carrier family 5 (sodium/multivitamin and iodide cotransporter), member 6	103.83	80.92	10.30	4.20
Slc6a12	solute carrier family 6 (neurotransmitter transporter), member 12	824.03	675.56	6.65	4.52
Slc6a6	solute carrier family 6 (neurotransmitter transporter), member 6	139.81	93.01	17.11	8.51
Smoc2	SPARC related modular calcium binding 2	56.00	76.77	4.85	2.62
St8sia2	ST8 alpha-N-acetyl-neuraminide alpha-2,8-sialyltransferase 2	2.77	4.80	0.00	0.00
Stmn4	stathmin-like 4	57.94	54.63	5.33	3.77
Tac1	tachykinin, precursor 1	9.63	8.51	0.00	0.00
Tgfb2	transforming growth factor, beta 2	171.44	142.67	12.88	12.22
Tgfb3	transforming growth factor, beta 3	1372.94	1188.02	40.26	6.08

Continued on next page

Table D.7 – continued from previous page

Gene symbol	Gene name	Decidua TPM	Decidua ±SD	Outer myometrium TPM	Outer myometrium ±SD
Tmeff1	transmembrane protein with EGF-like and two follistatin-like domains 1	11.41	10.34	0.04	0.05
Tmem204	transmembrane protein 204	200.68	162.41	7.27	3.44
Tnfaip2	tumor necrosis factor, alpha-induced protein 2	83.77	67.43	8.83	4.41
Tnfaip8	tumor necrosis factor, alpha-induced protein 8	47.03	24.75	9.66	2.32
Tnfrsf11b	tumor necrosis factor receptor superfamily, member 11b	130.76	102.38	15.86	9.11
Trpc4	transient receptor potential cation channel, subfamily C, member 4	25.84	19.51	1.19	0.80
Tshz3	teashirt zinc finger homeobox 3	19.48	14.80	2.40	0.77
Tspan5	tetraspanin 5	95.74	67.25	15.71	7.08
Uap1	UDP-N-acteylglucosamine pyrophosphorylase 1	62.65	41.35	12.85	2.85
Uck2	uridine-cytidine kinase 2	201.50	164.04	8.40	2.43
Usp53	ubiquitin specific peptidase 53	57.82	47.14	7.09	5.15
Vamp5	vesicle-associated membrane protein 5	19.01	13.90	0.36	0.53
Vldlr	very low density lipoprotein receptor	123.50	110.20	9.57	2.77
Wfdc1	WAP four-disulfide core domain 1	577.72	535.36	11.82	10.67
Wt1	Wilms tumor 1	61.54	46.12	7.09	2.80

Table D.8: Genes that were differentially expressed in the outer myometrium compared to the inner myometrium on GD22(NL). Transcript expression levels are shown in transcripts per million values (mean±SD).

Gene symbol	Gene name	Inner myometrium TPM	Inner myometrium ±SD	Outer myometrium TPM	Outer myometrium ±SD
Upregulated genes					
Aass	aminoadipate-semialdehyde synthase	0.00	0.00	3.50	4.38
Acadm	acyl-CoA dehydrogenase, C-4 to C-12 straight chain	10.04	5.15	82.00	62.41
Acot4	acyl-CoA thioesterase 4	4.64	6.51	21.26	23.04
Acsl1	acyl-CoA synthetase long-chain family member 1	3.98	1.18	49.13	67.79
Acsm5	acyl-CoA synthetase medium-chain family member 5	0.00	0.00	2.70	4.68
Ahsg	alpha-2-HS-glycoprotein	2.99	4.87	1290.62	2231.35
Aldh1a1	aldehyde dehydrogenase 1 family, member A1	0.00	0.00	13.84	11.51
Aldh1a7	aldehyde dehydrogenase family 1, subfamily A7	0.02	0.04	9.44	9.53
Aldh2	aldehyde dehydrogenase 2 family (mitochondrial)	24.87	8.28	99.32	47.79
Alox15b	arachidonate 15-lipoxygenase, type B	0.00	0.00	6.34	8.35
Als2cr12	amyotrophic lateral sclerosis 2 (juvenile) chromosome region, candidate 12	0.00	0.00	4.59	6.03
Amdhd1	amidohydrolase domain containing 1	0.01	0.02	11.24	19.04
Amy1a	amylase, alpha 1A (salivary)	0.00	0.00	6.14	10.62
Apcs	amyloid P component, serum	0.00	0.00	28.50	49.18
Apoa1	apolipoprotein A-I	2.43	3.93	1327.79	1142.31
Apoa4	apolipoprotein A-IV	7.88	13.51	432.20	376.34
Aspdh	aspartate dehydrogenase domain containing	0.00	0.00	30.44	52.32
Bhmt	betaine-homocysteine S-methyltransferase	1.04	1.40	236.57	407.41
Bspry	B-box and SPRY domain containing	0.21	0.29	15.94	16.72
C3	complement component 3	11.78	14.87	1199.02	1226.91
C9	complement component 9	0.07	0.03	5.34	8.19
Camp	cathelicidin antimicrobial peptide	0.00	0.00	37.38	64.73
Ceacam1	carcinoembryonic antigen-related cell adhesion molecule 1 (biliary glycoprotein)	4.95	2.69	55.77	36.10
Cfhr1	complement factor H-related 1	0.00	0.00	5.63	9.20
Cfi	complement factor I	2.19	1.94	48.20	53.03
Ckmt1b	creatine kinase, mitochondrial 1B	0.34	0.51	19.76	13.85
Clca4	chloride channel accessory 4	0.20	0.10	7.93	6.15
Cldn1	claudin 1	1.31	1.20	20.50	25.59
Cldn8	claudin 8	0.00	0.00	4.29	5.87
Col2a1	collagen, type II, alpha 1	0.05	0.05	8.56	14.79
Cpamd8	C3 and PZP-like, alpha-2-macroglobulin domain containing 8	0.00	0.00	11.58	19.93
Crp	C-reactive protein, pentraxin-related	0.00	0.00	23.28	40.33
Cubn	cubilin (intrinsic factor-cobalamin receptor)	0.76	0.87	25.73	21.78
Cyp2b1	cytochrome P450, family 2, subfamily b, polypeptide 1	0.00	0.00	4.99	5.35
Cyp2b2	cytochrome P450, family 2, subfamily b, polypeptide 2	0.00	0.00	3.90	3.83
Cyp2b3	cytochrome P450, family 2, subfamily b, polypeptide 3	0.02	0.01	2.68	4.16
Cyp2c12	cytochrome P450, family 2, subfamily c, polypeptide 12	0.00	0.00	5.90	9.84
Cyp4a8	cytochrome P450, family 4, subfamily a, polypeptide 8	8.34	6.93	85.73	103.28
Cyp7a1	cytochrome P450, family 7, subfamily a, polypeptide 1	0.13	0.00	12.58	21.00
Cyp8b1	cytochrome P450, family 8, subfamily b, polypeptide 1	0.00	0.00	35.09	60.67
Dcdc2	doublecortin domain containing 2	1.28	0.86	18.15	13.93

Continued on next page

Table D.8 – continued from previous page

Gene symbol	Gene name	Inner myometrium TPM	Inner myometrium ±SD	Outer myometrium TPM	Outer myometrium ±SD
Defa	defensin alpha	0.00	0.00	76.90	132.33
Dhcr24	24-dehydrocholesterol reductase	1.00	1.02	42.97	56.93
Dpy19l3	dpy-19-like 3 (C. elegans)	2.92	2.02	13.84	8.78
Ehf	ets homologous factor	0.03	0.06	29.02	34.55
Ehhadh	enoyl-CoA, hydratase/3-hydroxyacyl CoA dehydrogenase	1.31	1.46	21.25	16.87
Elf3	E74-like factor 3	2.65	3.07	70.44	73.54
Emp1	epithelial membrane protein 1	21.37	5.48	191.08	170.45
Etnk2	ethanolamine kinase 2	0.01	0.01	4.38	7.04
Eya2	eyes absent homolog 2 (Drosophila)	0.15	0.20	37.63	37.38
Fam84a	family with sequence similarity 84, member A	0.04	0.05	3.90	2.47
Fcer2	Fc fragment of IgE, low affinity II, receptor for (CD23)	0.77	1.07	3.65	5.74
Fgb	fibrinogen beta chain	1.40	2.16	651.41	993.37
Fgg	fibrinogen gamma chain	1.81	2.45	797.41	1172.83
Fgl1	fibrinogen-like 1	0.00	0.00	18.93	32.71
Glrx	glutaredoxin (thioltransferase)	14.09	7.43	135.84	123.07
Gpc3	glypican 3	2.87	3.95	44.34	31.72
Gpr151	G protein-coupled receptor 151	0.00	0.00	2.57	4.35
Gpx2	glutathione peroxidase 2	6.70	11.45	160.81	81.14
Grik2	glutamate receptor, ionotropic, kainate 2	0.02	0.04	6.42	2.72
Gucy2c	guanylate cyclase 2C	0.47	0.46	11.04	8.82
H6pd	hexose-6-phosphate dehydrogenase (glucose 1-dehydrogenase)	8.63	3.03	40.43	29.93
Haao	3-hydroxyanthranilate 3,4-dioxygenase	0.00	0.00	17.24	29.68
Hao1	hydroxyacid oxidase (glycolate oxidase) 1	0.00	0.00	10.21	17.58
Hdc	histidine decarboxylase	0.70	0.71	212.31	366.46
Hemgn	hemogen	1.12	1.68	55.11	91.97
Hgfac	HGF activator	0.07	0.12	23.55	23.19
Hnf4a	hepatocyte nuclear factor 4, alpha	0.27	0.44	36.88	22.69
Hp	haptoglobin	9.33	11.73	511.81	885.89
Igfals	insulin-like growth factor binding protein, acid labile subunit	0.00	0.00	4.22	5.21
Il24	interleukin 24	0.00	0.00	2.37	2.59
Itih4	inter-alpha-trypsin inhibitor heavy chain family, member 4	1.13	0.81	55.77	96.37
Kap	kidney androgen regulated protein	18.99	31.19	1514.85	999.61
Kif23	kinesin family member 23	1.61	1.23	26.13	22.56
Klkb1	kallikrein B, plasma 1	0.00	0.00	16.45	28.23
Kntc1	kinetochore associated 1	0.74	0.47	5.68	3.53
Lad1	ladinin 1	9.33	15.34	149.58	221.93
Lamb3	laminin, beta 3	0.08	0.08	22.91	17.10
Lcn12	lipocalin 12	0.00	0.01	3.97	6.62
Lgals12	lectin, galactoside-binding, soluble, 12	0.08	0.02	4.37	4.30
Lgr5	leucine rich repeat containing G protein coupled receptor 5	0.02	0.02	4.06	4.83
LOC500797	mitotic spindle positioning	0.15	0.07	24.58	20.86
Lpcat4	lysophosphatidylcholine acyltransferase 4	9.85	4.31	67.64	67.55
Lpo	lactoperoxidase	1.03	0.85	99.94	125.95
Lrp2	low density lipoprotein receptor-related protein 2	1.06	0.62	17.89	15.16
Lypd6b	LY6/PLAUR domain containing 6B	0.23	0.15	5.67	4.55
Macc1	metastasis associated in colon cancer 1	0.02	0.02	4.52	3.27
Mfi2	antigen p97 (melanoma associated) identified by monoclonal antibodies 133.2 and 96.5	0.14	0.06	29.61	25.59
Mug2	murinoglobulin 2	0.02	0.03	4.06	7.02
Myh14	myosin, heavy chain 14, non-muscle	0.59	0.33	40.59	36.09
Mylk2	myosin light chain kinase 2	0.00	0.00	3.16	5.46
Npbwr1	neuropeptides B/W receptor 1	0.02	0.03	21.42	27.19
Nr1i2	nuclear receptor subfamily 1, group I, member 2	0.00	0.00	6.49	11.16
Olr1662	olfactory receptor 1662	0.11	0.12	81.48	140.60
Olr1748	olfactory receptor 1748	0.00	0.00	0.00	0.00
Olr299	olfactory receptor 299	0.00	0.00	45.82	79.37
Oxt	oxytocin/neurophysin 1 prepropeptide	15.25	23.58	1094.37	1644.29
Pah	phenylalanine hydroxylase	0.00	0.00	27.06	46.80
Pla2g4c	phospholipase A2, group IVC	0.00	0.00	4.57	4.58
Plg	plasminogen	1.14	1.10	202.16	329.93
Ppl	periplakin	4.80	6.72	46.99	34.96
Prodh2	proline dehydrogenase (oxidase) 2	0.00	0.00	21.12	36.49
Prom1	prominin 1	3.62	3.47	105.22	100.68
Prox1	prospero homeobox 1	1.83	1.36	26.74	41.19
Ptgs1	prostaglandin-endoperoxide synthase 1	2.84	1.79	45.52	44.58
Pzp	pregnancy-zone protein	0.93	0.35	127.17	219.61
Rab11fip4	RAB11 family interacting protein 4 (class II)	0.12	0.05	6.95	3.63
Rbp4	retinol binding protein 4, plasma	1.62	1.80	593.30	896.31
RGD1309313	transmembrane protein 180	4.68	3.44	53.18	40.76

Continued on next page

Table D.8 – continued from previous page

Gene symbol	Gene name	Inner myometrium TPM	Inner myometrium ±SD	Outer myometrium TPM	Outer myometrium ±SD
RGD1310507	similar to RIKEN cDNA 1300017J02	5.20	5.95	133.95	103.79
RGD1559600	RGD1559600	0.00	0.00	10.97	18.78
RGD1564614	similar to complement factor H-related protein	0.06	0.07	6.67	11.20
Rtp3	receptor (chemosensory) transporter protein 3	0.72	0.57	21.09	20.82
S100a9	S100 calcium binding protein A9	5.41	4.32	157.30	267.66
Scnn1a	sodium channel, nonvoltage-gated 1 alpha	4.93	6.80	63.50	75.41
Serpina1	serpin peptidase inhibitor, clade A (alpha-1 antiproteinase, antitrypsin), member 1	2.88	4.83	1295.37	2065.82
Serpina3k	serine (or cysteine) peptidase inhibitor clade A member 3K	0.00	0.00	169.13	292.60
Serpinb11	serpin peptidase inhibitor, clade B (ovalbumin), member 11	0.00	0.00	1.51	1.20
Slc16a14	solute carrier family 16, member 14	0.71	0.40	28.20	33.75
Slc17a1	solute carrier family 17 (organic anion transporter), member 1	0.00	0.00	3.70	6.08
Slc17a3	solute carrier family 17 (organic anion transporter), member 3	0.04	0.04	1.74	2.21
Slc26a3	solute carrier family 26 (anion exchanger), member 3	0.00	0.00	3.36	2.23
Slc30a10	solute carrier family 30, member 10	0.00	0.00	6.05	10.27
Slc34a2	solute carrier family 34 (type II sodium/phosphate contransporter), member 2	0.96	1.30	24.89	23.72
Slc36a2	solute carrier family 36 (proton/amino acid symporter), member 2	0.05	0.06	3.36	5.66
Slc4a1	solute carrier family 4 (anion exchanger), member 1	3.65	4.40	92.03	153.87
Slc5a1	solute carrier family 5 (sodium/glucose cotransporter), member 1	0.00	0.00	2.26	3.41
Slc6a14	solute carrier family 6 (amino acid transporter), member 14	0.02	0.03	5.53	4.79
Slco1a1	solute carrier organic anion transporter family, member 1a1	0.00	0.00	2.91	4.91
Spp2	secreted phosphoprotein 2	2.27	3.53	166.71	195.06
Stard4	StAR-related lipid transfer (START) domain containing 4	1.68	1.06	12.40	4.39
Sult1b1	sulfotransferase family, cytosolic, 1B, member 1	0.00	0.00	6.82	9.63
Tfcp2l1	transcription factor CP2-like 1	1.87	0.43	8.81	1.55
Tmc4	transmembrane channel-like 4	5.07	7.67	62.03	69.32
Tmem171	transmembrane protein 171	0.03	0.04	12.98	11.29
Tppp3	tubulin polymerization-promoting protein family member 3	8.12	8.38	193.38	163.72
Tspan1	tetraspanin 1	0.20	0.34	67.06	39.29
Ttpa	tocopherol (alpha) transfer protein	0.00	0.00	8.13	10.52
Ugt1a1	UDP glucuronosyltransferase 1 family, polypeptide A1	0.06	0.08	7.75	9.17
Ugt1a5	UDP glucuronosyltransferase 1 family, polypeptide A5	0.06	0.07	23.36	39.08
Ugt1a7c	UDP glucuronosyltransferase 1 family, polypeptide A7C	1.80	2.36	49.66	42.40
Ugt2b1	UDP glucuronosyltransferase 2 family, polypeptide B1	0.00	0.00	3.36	5.80
Ugt8	UDP glycosyltransferase 8	0.00	0.00	2.18	2.87
Upk1b	uroplakin 1B	1.75	0.90	26.98	14.78
Ush1c	Usher syndrome 1C	0.00	0.00	4.20	6.12
Usp43_predicted	ubiquitin specific peptidase 43	0.04	0.07	9.24	9.55
Vnn3	vanin 3	0.00	0.00	1.97	3.32
Vom2r34	vomeronasal 2 receptor, 34	8.51	1.50	221.27	337.86
Vtn	vitronectin	2.20	1.63	196.99	333.38
Wnt7a	wingless-type MMTV integration site family, member 7A	0.24	0.15	11.54	9.93
Zfhx4	zinc finger homeobox 4	0.16	0.03	1.56	1.11
Dmbt1	deleted in malignant brain tumors 1	0.64	0.51	18.86	13.45
Cuzd1	CUB and zona pellucida-like domains 1	3.16	4.53	492.78	409.84
Gabrp	gamma-aminobutyric acid (GABA-A) receptor, pi	0.00	0.00	3.76	4.09
Alcam	activated leukocyte cell adhesion molecule	5.57	2.35	86.39	83.80
Pigr	polymeric immunoglobulin receptor	0.22	0.22	55.40	69.41
F5	coagulation factor V (proaccelerin, labile factor)	1.34	0.48	39.50	32.53
Lrrc66	leucine rich repeat containing 66	0.00	0.00	2.23	0.85
Adcy1	adenylate cyclase 1 (brain)	0.17	0.20	2.88	2.72
Fignl1	fidgetin-like 1	0.01	0.02	1.26	0.73
Thrb	thyroid hormone receptor beta	3.04	1.85	18.52	11.57
Adam28	ADAM metallopeptidase domain 28	0.00	0.00	2.68	2.07
Cndp1	carnosine dipeptidase 1 (metallopeptidase M20 family)	1.35	0.80	35.15	22.93
Cdh16	cadherin 16	0.00	0.00	12.25	12.69
Fa2h	fatty acid 2-hydroxylase	0.01	0.02	3.28	1.53
Galnt5	UDP-N-acetyl-alpha-D-galactosamine:polypeptide N-acetylgalactosaminyltransferase 5 (GalNAc-T5)	0.00	0.00	1.76	1.06
Myo3b	myosin IIIB	0.10	0.13	1.99	1.89
Cldn2	claudin 2	3.34	5.26	135.04	114.17
Cftr	cystic fibrosis transmembrane conductance regulator	0.14	0.17	22.54	29.22
Tmem88b	transmembrane protein 88B	0.84	0.36	4.62	1.99
Slc26a4	solute carrier family 26 (anion exchanger), member 4	0.73	0.80	69.38	68.87
Gnat1	guanine nucleotide binding protein (G protein), alpha transducing activity polypeptide 1	0.00	0.00	4.64	0.69
Rab17	RAB17, member RAS oncogene family	0.04	0.04	17.60	13.99

Continued on next page

Table D.8 – continued from previous page

Gene symbol	Gene name	Inner myometrium TPM	Inner myometrium ±SD	Outer myometrium TPM	Outer myometrium ±SD
Mal2	mal, T-cell differentiation protein 2	0.55	0.79	32.51	32.69
Down-regulated genes					
Ccdc82	coiled-coil domain containing 82	17.74	21.28	1.95	0.68
Ebf3	early B-cell factor 3	18.63	21.52	1.02	0.79
Htr2a	5-hydroxytryptamine (serotonin) receptor 2A, G protein-coupled	86.91	148.90	3.04	1.75
Kctd15	potassium channel tetramerization domain containing 15	167.92	261.06	9.16	7.71
LOC685544	hypothetical protein LOC685544	106.53	184.51	0.17	0.16
LOC686999	M phase phosphoprotein 6	78.19	90.38	10.76	2.21
Lrrc63	leucine rich repeat containing 63	12.33	20.81	0.02	0.02
Nudt18	nudix (nucleoside diphosphate linked moiety X)-type motif 18	54.02	74.12	4.11	1.79
Syt13	synaptotagmin XIII	8.71	14.99	0.03	0.02
Tatdn3	TatD DNase domain containing 3	61.33	66.95	6.76	4.98
Tnn	tenascin N	61.51	30.36	5.69	4.16
Tssk6	testis-specific serine kinase 6	42.14	72.99	0.02	0.03
Prl7a3	prolactin family 7, subfamily a, member 3	153.98	51.71	20.37	21.81

D.4 GD22(L)

Table D.9: Gene transcripts that were differentially expressed in the inner myometrium compared to the decidua on GD22(L). Transcript expression levels are shown in transcripts per million (TPM) values (mean±SD).

Gene symbol	Gene name	Decidua TPM	Decidua ±SD	Inner myometrium TPM	Inner myometrium ±SD
Upregulated in inner myometrium					
Upk1b	uroplakin 1B	0.00	0.00	84.52	119.01
Msr1	macrophage scavenger receptor 1	0.00	0.00	15.22	0.72
C3ar1	complement component 3a receptor 1	0.00	0.00	11.69	10.15
LOC300308	similar to hypothetical protein 4930509O22	0.00	0.00	4.67	2.87
Tmem182	transmembrane protein 182	0.03	0.04	0.12	0.03
Lrguk	leucine-rich repeats and guanylate kinase domain containing	0.04	0.06	9.29	11.01
Ctse	cathepsin E	0.06	0.02	10.10	0.95
Pla2g2a	phospholipase A2, group IIA (platelets, synovial fluid)	0.13	0.18	51.29	27.03
Trpc3	transient receptor potential cation channel, subfamily C, member 3	1.20	0.33	30.75	40.68
Down-regulated in inner myometrium					
Khdrbs2	KH domain containing, RNA binding, signal transduction associated 2	16.46	22.61	0.71	0.03
St8sia3	ST8 alpha-N-acetyl-neuraminide alpha-2,8-sialyltransferase 3	17.21	24.34	0.00	0.00
Plin1	perilipin 1	21.91	30.52	0.33	0.23
Sfrp2	secreted frizzled-related protein 2	23.45	9.83	1.92	0.36
Fabp7	fatty acid binding protein 7, brain	26.75	36.60	0.06	0.08
B3gat1	beta-1,3-glucuronyltransferase 1 (glucuronosyltransferase P)	27.82	39.35	0.00	0.00
Scg3	secretogranin III	31.24	44.18	0.00	0.00
S100a3	S100 calcium binding protein A3	31.47	12.25	0.15	0.21
Fezf2	Fez family zinc finger 2	31.53	44.59	0.05	0.04
Map2	microtubule-associated protein 2	31.80	35.73	0.35	0.28
Ankrd34a	ankyrin repeat domain 34A	39.62	49.23	6.76	7.28
Cpa3	carboxypeptidase A3, mast cell	45.50	64.34	0.01	0.01
Vamp5	vesicle-associated membrane protein 5	49.68	56.04	1.11	0.51
Cma1	chymase 1, mast cell	51.79	73.24	0.04	0.05
Sec1	secretory blood group 1	52.51	74.26	0.00	0.00
Nrsn2	neurensin 2	52.59	74.37	0.01	0.01
Gng3	guanine nucleotide binding protein (G protein), gamma 3	69.26	82.49	0.28	0.21
Rln1	relaxin 1	78.52	111.05	0.01	0.01
Stfa3	stefin A3	81.53	113.02	2.95	0.49
Crmp1	collapsin response mediator protein 1	90.47	127.49	0.03	0.04

Continued on next page

Table D.9 – continued from previous page

Gene symbol	Gene name	Decidua TPM	Decidua ±SD	Inner myometrium TPM	Inner myometrium ±SD
Stmn2	stathmin-like 2	93.83	132.69	0.00	0.00
Alb	albumin	121.74	60.53	1.51	0.87
Aqp5	aquaporin 5	121.83	172.20	0.00	0.00
Trh	thyrotropin releasing hormone	188.66	66.99	0.92	0.23
Gatm	glycine amidinotransferase (L-arginine:glycine amidinotransferase)	313.84	258.39	11.70	6.30
S100a4	S100 calcium-binding protein A4	525.50	638.03	13.55	9.65

Table D.10: Gene transcripts that were differentially expressed in the outer myometrium compared to the decidua on GD22(L). Transcript expression levels are shown in transcripts per million (TPM) values (mean±SD)

Gene symbol	Gene name	Decidua TPM	Decidua ±SD	Outer myometrium TPM	Outer myometrium ±SD
Upregulated in outer myometrium					
Cuzd1	CUB and zona pellucida-like domains 1	1.83	2.28	483.46	526.98
Mmp7	matrix metallopeptidase 7	0.05	0.07	121.68	79.93
Slc26a4	solute carrier family 26 (anion exchanger), member 4	0.05	0.08	119.61	138.16
Cxcl17	chemokine (C-X-C motif) ligand 17	0.00	0.00	96.32	126.04
Pck1	phosphoenolpyruvate carboxykinase 1 (soluble)	1.24	0.46	42.93	31.50
Myh14	myosin, heavy chain 14, non-muscle	2.64	0.24	40.26	30.07
Slc44a4	solute carrier family 44, member 4	0.06	0.08	34.99	2.65
Trpc3	transient receptor potential cation channel, subfamily C, member 3	1.20	0.33	28.15	33.60
Slc16a14	solute carrier family 16, member 14	0.43	0.16	26.79	33.08
RGD1563547	small integral membrane protein 22	0.12	0.11	23.40	11.27
Akr1cl	aldo-keto reductase family 1, member C-like	0.00	0.00	22.86	29.97
B3gnt3	UDP-GlcNAc:betaGal beta-1,3-N-acetylglucosaminyltransferase 3	0.14	0.20	22.62	23.60
Wisp2	WNT1 inducible signaling pathway protein 2	0.00	0.00	22.22	29.01
Mep1a	meprin 1 alpha	0.00	0.00	21.09	29.83
Rgn	regucalcin	0.03	0.04	20.58	25.92
Chi3l1	chitinase 3-like 1 (cartilage glycoprotein-39)	0.00	0.00	20.57	25.35
Slc26a3	solute carrier family 26 (anion exchanger), member 3	0.00	0.00	19.92	25.56
G6pc	glucose-6-phosphatase, catalytic subunit	0.00	0.00	19.04	19.56
Cyp2c23	cytochrome P450, family 2, subfamily c, polypeptide 23	0.02	0.03	17.61	20.70
Upk1b	uroplakin 1B	0.00	0.00	17.54	24.20
Ehf	ets homologous factor	0.05	0.07	17.40	19.87
Bhmt2	betaine-homocysteine S-methyltransferase 2	0.00	0.00	17.18	23.55
Ccdc65	coiled-coil domain containing 65	0.00	0.00	16.02	22.56
Cbs	cystathionine beta synthase	0.00	0.00	15.36	20.26
Them6	thioesterase superfamily member 6	0.10	0.01	15.18	1.01
P2ry6	pyrimidinergic receptor P2Y, G-protein coupled, 6	0.13	0.03	15.11	19.07
Cacna1c	calcium channel, voltage-dependent, L type, alpha 1C subunit	0.11	0.03	14.66	14.40
Tmprss4	transmembrane protease, serine 4	0.03	0.04	14.21	0.87
Igsf5	immunoglobulin superfamily, member 5	0.01	0.02	13.83	12.27
Klkb1	kallikrein B, plasma 1	0.02	0.03	13.56	6.60
Cyp4b1	cytochrome P450, family 4, subfamily b, polypeptide 1	0.00	0.00	13.38	17.11
Itih4	inter-alpha-trypsin inhibitor heavy chain family, member 4	0.00	0.00	12.66	11.04
Clec7a	C-type lectin domain family 7, member A	0.51	0.20	12.22	12.86
Lingo4	leucine rich repeat and Ig domain containing 4	0.29	0.08	9.56	11.84
Down-regulated in outer myometrium					
Atp2a3	ATPase, Ca++ transporting, ubiquitous	0.00	0.00	7.94	0.01
C8b	complement component 8, beta polypeptide	0.00	0.00	7.80	3.55
Emr1	EGF-like module containing, mucin-like, hormone receptor-like 1	0.00	0.00	6.81	7.74
Khdrbs2	KH domain containing, RNA binding, signal transduction associated 2	16.46	22.61	0.51	0.18
Nefl	neurofilament, light polypeptide	75.27	106.36	0.30	0.24
Map2	microtubule-associated protein 2	31.80	35.73	0.23	0.24
Nell2	NEL-like 2 (chicken)	31.91	42.68	0.11	0.01
Tmem182	transmembrane protein 182	0.03	0.04	0.10	0.03
Actn3	actinin alpha 3	36.52	51.06	0.09	0.12
Sln	sarcolipin	98.09	138.64	0.05	0.02
Ebf2	early B-cell factor 2	12.64	17.83	0.05	0.01
Nrsn2	neurensin 2	52.59	74.37	0.05	0.07
Sec1	secretory blood group 1	52.51	74.26	0.00	0.00
Rln1	relaxin 1	78.52	111.05	0.00	0.00

Continued on next page

Table D.10 – continued from previous page

Gene symbol	Gene name	Decidua TPM	Decidua ±SD	Outer myometrium TPM	Outer myometrium ±SD
Myog	myogenin	110.43	156.11	0.00	0.00
Adprhl1	ADP-ribosylhydrolase like 1	23.25	32.87	0.00	0.00
B3gat1	beta-1,3-glucuronyltransferase 1 (glucuronosyltransferase P)	27.82	39.35	0.00	0.00
Trpc5	transient receptor potential cation channel, subfamily C, member 5	12.93	18.28	0.00	0.00
S100a3	S100 calcium binding protein A3	31.47	12.25	0.00	0.00

Table D.11: Gene transcripts that were differentially expressed in the outer myometrium compared to the inner myometrium on GD22 (L). Transcript expression levels are shown in transcripts per million (TPM) values (mean±SD).

Gene symbol	Gene name	Inner TPM	Inner ±SD	Outer TPM	Outer ±SD
Upregulated in outer myometrium					
Alb	albumin	1.51	0.87	1558.24	1728.57
Cuzd1	CUB and zona pellucida-like domains 1	6.24	8.65	483.46	526.98
Ahsg	alpha-2-HS-glycoprotein	0.69	0.42	346.92	343.38
Mmp7	matrix metallopeptidase 7	1.29	1.23	121.68	79.93
Serpina3k	serine (or cysteine) peptidase inhibitor, clade A, member 3K	0.00	0.00	61.88	80.69
Fabp1	fatty acid binding protein 1, liver	0.22	0.11	36.87	38.24
Hdc	histidine decarboxylase	0.00	0.00	36.33	28.05
Lgals4	lectin, galactoside-binding, soluble, 4	0.00	0.00	26.44	37.39
Prap1	proline-rich acidic protein 1	0.01	0.01	23.03	32.57
B3gnt3	UDP-GlcNAc:betaGal beta-1,3-N-acetylglucosaminyltransferase 3	0.07	0.10	22.62	23.60
Hpd	4-hydroxyphenylpyruvate dioxygenase	0.00	0.00	18.19	13.90
LOC299282	Serine protease inhibitor	0.12	0.02	17.42	23.54
Bhmt2	betaine-homocysteine S-methyltransferase 2	0.00	0.01	17.18	23.55
Apoc4	apolipoprotein C-IV	0.03	0.05	16.12	7.00
Fgl1	fibrinogen-like 1	0.01	0.01	16.02	22.66
Anxa13	annexin A13	0.00	0.00	15.44	21.83
Serpina3n	serine (or cysteine) peptidase inhibitor, clade A, member 3N	0.03	0.04	14.99	17.37
Klkb1	kallikrein B, plasma 1	0.01	0.02	13.56	6.60
Cpb2	carboxypeptidase B2 (plasma)	0.15	0.01	13.49	9.25
Tfr2	transferrin receptor 2	0.02	0.03	12.58	12.92
Azgp1	alpha-2-glycoprotein 1, zinc-binding	0.00	0.00	12.53	16.27
Aqp9	aquaporin 9	2.10	0.08	11.67	5.24
Itih1	inter-alpha trypsin inhibitor, heavy chain 1	0.00	0.00	11.65	16.08
Clca1	chloride channel accessory 1	0.01	0.01	11.52	16.29
Pah	phenylalanine hydroxylase	0.00	0.00	10.31	12.29
Cytl1	cytokine like 1	0.01	0.01	9.25	13.09
C8b	complement component 8, beta polypeptide	0.00	0.00	7.80	3.55
Bucs1	acyl-CoA synthetase medium-chain family member 1	0.02	0.02	7.43	9.98
Down-regulated in outer myometrium					
Acan	aggrecan	26.33	37.11	0.07	0.01
Hapln1	hyaluronan and proteoglycan link protein 1	51.51	72.68	0.02	0.02

D.5 Temporal Expression of Transcripts in Control Tissues

Table D.12: Gene transcripts that were differentially expressed in the decidua, between GD20 and GD22(NL). Transcript expression levels are shown in transcripts per million (TPM) values (mean±SD).

Gene symbol	Gene name	GD20 TPM	GD20 ±SD	GD22(NL) TPM	GD22(NL) ±SD

Continued on next page

Table D.12 – continued from previous page

Gene symbol	Gene name	GD20 TPM	GD20 ±SD	GD22 (NL) TPM	GD22 (NL) ±SD
Upregulated on GD22 (NL)					
Chac1	ChaC, cation transport regulator homolog 1 (E. coli)	0.05	0.09	7.16	3.18
Cilp	cartilage intermediate layer protein, nucleotide pyrophosphohydrolase	1.43	1.13	30.73	6.24
Cpe	carboxypeptidase E	46.27	38.46	794.87	666.43
Gadd45a	growth arrest and DNA-damage-inducible, alpha	21.27	15.72	245.03	73.24
Gngt2	guanine nucleotide binding protein (G protein), gamma transducing activity polypeptide 2	0.00	0.00	7.14	4.48
Ifit1	interferon-induced protein with tetratricopeptide repeats 1	8.42	8.23	107.34	93.98
Il1rl1	interleukin 1 receptor-like 1	0.66	1.05	21.84	30.81
Pigv	phosphatidylinositol glycan anchor biosynthesis, class V	2.71	2.30	5.56	0.65
Plk2	polo-like kinase 2	12.99	16.54	347.65	246.92
Ramp3	receptor (G protein-coupled) activity modifying protein 3	7.65	11.15	624.16	692.21
Slc7a7	solute carrier family 7 (amino acid transporter light chain, y+L system), member 7	4.49	1.55	50.55	34.04
Sox4	SRY (sex determining region Y)-box 4	9.61	8.67	83.89	50.35
Down-regulated on GD22 (NL)					
Afp	alpha-fetoprotein	1324.86	1254.26	1.87	2.01
Alb	albumin	2322.68	4019.70	0.98	0.19
Apoa1	apolipoprotein A-I	216.98	146.74	0.71	0.59
Apoa2	apolipoprotein A-II	22.33	31.31	0.00	0.00
Apob	apolipoprotein B	826.54	986.55	0.69	0.69
Apoc2	apolipoprotein C-II	33.14	29.69	0.14	0.14
Apoh	apolipoprotein H (beta-2-glycoprotein I)	46.38	68.47	0.05	0.07
Ass1	argininosuccinate synthase 1	19.93	20.56	5.55	4.61
Car1	carbonic anhydrase I	57.50	99.53	0.00	0.00
Cdh1	cadherin 1	8.88	4.99	2.09	1.21
Cgm4	carcinoembryonic antigen gene family 4	220.61	181.00	12.45	12.42
Clec3a	C-type lectin domain family 3, member A	7.19	12.31	0.00	0.00
Creb3l3	cAMP responsive element binding protein 3-like 3	4.57	4.03	0.62	0.34
Creg1	cellular repressor of E1A-stimulated genes 1	324.75	268.19	36.21	43.63
Cubn	cubilin (intrinsic factor-cobalamin receptor)	4.19	4.59	0.14	0.03
Cyp2c22	cytochrome P450, family 2, subfamily c, polypeptide 22	25.48	44.13	0.00	0.01
Defb4	defensin beta 4	4.93	8.47	0.00	0.00
Doc2b	double C2-like domains, beta	36.26	61.37	0.01	0.01
Fabp1	fatty acid binding protein 1, liver	6.86	11.72	0.00	0.00
Fga	fibrinogen alpha chain	391.13	608.42	0.21	0.06
Hmgcs1	3-hydroxy-3-methylglutaryl-CoA synthase 1 (soluble)	35.25	42.91	12.76	7.71
Hnf4a	hepatocyte nuclear factor 4, alpha	6.38	7.17	0.02	0.03
Hrsp12	heat-responsive protein 12	66.77	43.98	22.11	10.74
Klk8	kallikrein related-peptidase 8	35.05	60.72	0.00	0.01
Lypd5	Ly6/Plaur domain containing 5	31.88	55.22	0.00	0.00
Mki67	marker of proliferation Ki-67	18.94	30.58	1.85	1.26
Myf6	myogenic factor 6	23.79	41.20	0.01	0.01
Plagl1	pleiomorphic adenoma gene-like 1	22.01	31.38	2.10	2.32
Prl3b1	Prolactin family 3, subfamily b, member 1	144.12	132.01	34.85	12.31
Prl8a4	prolactin family 8, subfamily a, member 4	967.13	784.32	38.99	16.72
Psg16	pregnancy specific glycoprotein 16	50.94	45.68	3.63	2.07
Sepp1	selenoprotein P, plasma, 1	161.72	179.46	45.60	23.88
Sftpb	surfactant protein B	14.24	24.45	0.00	0.00
Stfa3	stefin A3	38.29	64.79	0.98	0.32
Ttr	transthyretin	165.81	155.62	0.59	0.54

Table D.13: Gene transcripts that were differentially expressed in the decidua, between GD22(NL) and GD22(L). Transcript expression levels are shown in transcripts per million (TPM) values (mean±SD).

Gene symbol	Gene name	GD22(NL) TPM	GD22(NL) ±SD	GD22(L) TPM	GD22(L) ±SD
Upregulated on GD22 (L)					
Aard	alanine and arginine rich domain containing protein	0.10	0.02	13.55	18.75
Abi3	ABI family, member 3	4.39	0.85	222.75	308.93
Adrb3	adrenoceptor beta 3	0.01	0.02	6.62	9.36
Alb	albumin	0.98	0.19	121.74	60.53

Continued on next page

Table D.13 – continued from previous page

Gene symbol	Gene name	GD22 (NL) TPM	GD22 (NL) ±SD	GD22 (L) TPM	GD22 (L) ±SD
Angptl1	angiopoietin-like 1	0.47	0.34	32.36	45.00
Apoa2	apolipoprotein A-II	0.00	0.00	8.38	11.85
Apobec2	apolipoprotein B mRNA editing enzyme, catalytic polypeptide-like 2	0.02	0.04	82.50	116.67
Apoh	apolipoprotein H (beta-2-glycoprotein I)	0.05	0.07	22.35	28.48
Apom	apolipoprotein M	0.18	0.14	133.79	188.19
Asgr1	asialoglycoprotein receptor 1	0.14	0.13	10.20	14.35
Ass1	argininisuccinate synthase 1	5.55	4.61	94.88	112.79
Cacna1s	calcium channel, voltage-dependent, L type, alpha 1S subunit	0.05	0.08	6.60	9.33
Calb1	calbindin 1	0.01	0.02	6.93	9.81
Casq1	calsequestrin 1 (fast-twitch, skeletal muscle)	3.47	0.40	132.31	184.84
Cdk5r2	cyclin-dependent kinase 5, regulatory subunit 2 (p39)	0.00	0.00	15.68	22.18
Cdo1	cysteine dioxygenase type 1	1.73	0.34	100.33	125.59
Ceacam1	carcinoembryonic antigen-related cell adhesion molecule 1 (biliary glycoprotein)	12.81	17.33	225.82	306.33
Cgm4	carcinoembryonic antigen gene family 4	12.45	12.42	736.55	925.96
Chrnd	cholinergic receptor, nicotinic, delta (muscle)	0.00	0.00	5.28	7.46
Ckmt2	creatine kinase, mitochondrial 2, sarcomeric	0.00	0.01	89.98	127.25
Cldn6	claudin 6	2.26	0.14	51.10	69.03
Clec3a	C-type lectin domain family 3, member A	0.00	0.00	8.54	12.07
Clstn3	calsyntenin 3	0.08	0.14	13.42	18.97
Cma1	chymase 1, mast cell	0.41	0.71	51.79	73.24
Col2a1	collagen, type II, alpha 1	0.10	0.05	34.55	48.43
Cox8b	cytochrome c oxidase, subunit VIIIb	0.25	0.29	25.91	32.94
Cpn1	carboxypeptidase N, polypeptide 1	0.02	0.04	6.84	9.67
Defa	defensin alpha	0.07	0.12	18.08	25.57
Dpp6	dipeptidylpeptidase 6	0.04	0.08	10.10	14.29
Dpysl5	dihydropyrimidinase-like 5	1.58	1.75	59.90	83.74
Eno3	enolase 3, beta, muscle	2.66	1.55	188.24	248.17
Epb42	erythrocyte membrane protein band 4.2	2.09	0.85	7.66	7.79
Eps8l2	EPS8-like 2	5.21	2.40	61.62	59.16
Espl1	extra spindle pole bodies homolog 1 (S. cerevisiae)	0.68	0.36	18.66	21.48
Fam5c/Brinp3	bone morphogenetic protein/retinoic acid inducible neural-specific 3	0.06	0.01	6.66	9.36
Fezf2	Fez family zinc finger 2	0.01	0.01	31.53	44.59
Fga	fibrinogen alpha chain	0.21	0.06	115.82	150.55
Fgb	fibrinogen beta chain	0.22	0.13	12.38	1.72
Fitm1	fat storage-inducing transmembrane protein 1	0.00	0.00	23.47	33.19
Fxyd3	FXYD domain-containing ion transport regulator 3	0.26	0.16	12.57	13.92
Gabrp	gamma-aminobutyric acid (GABA-A) receptor, pi	0.00	0.00	17.14	23.83
Ggt6	gamma-glutamyl transferase 6	0.17	0.30	15.06	21.10
Gjc2	gap junction protein, gamma 2	0.01	0.02	7.95	11.25
Gng3	guanine nucleotide binding protein (G protein), gamma 3	2.14	1.31	69.26	82.49
Grxcr2	glutaredoxin, cysteine rich 2	0.01	0.01	8.31	11.75
Hand1	heart and neural crest derivatives expressed 1	4.73	1.60	137.03	150.83
Hoxb5	homeo box B5	1.04	0.71	83.47	116.62
Hspb3	heat shock protein B3	0.01	0.01	6.09	8.61
Ifnk	interferon kappa	22.55	9.57	310.55	372.27
Itgb1bp2	integrin beta 1 binding protein 2	0.59	0.67	28.49	36.78
Khdrbs2	KH domain containing, RNA binding, signal transduction associated 2	0.50	0.12	16.46	22.61
Krt14	keratin 14	0.04	0.07	42.70	60.39
Krt15	keratin 15	0.01	0.01	20.35	28.77
Krt17	keratin 17	0.06	0.10	36.85	51.77
Lamp5	lysosomal-associated membrane protein family, member 5	0.00	0.01	14.90	21.07
Letm2	leucine zipper-EF-hand containing transmembrane protein 2	1.78	1.61	43.45	50.54
LOC641520/Popdc3	popeye domain containing 3	0.00	0.00	5.73	8.10
LOC685612/Col26a1	collagen, type XXVI, alpha 1	0.00	0.01	19.99	28.26
Map2	microtubule-associated protein 2	0.68	0.56	31.80	35.73
Mest	mesoderm specific transcript	2.78	1.99	200.32	274.18
Mybph	myosin binding protein H	0.60	0.31	43.09	54.71
Myf6	myogenic factor 6	0.01	0.01	6.47	9.14
Myl3	myosin, light chain 3, alkali; ventricular, skeletal, slow	0.04	0.03	187.19	264.73
Myl4	myosin, light chain 4	2.53	0.86	160.44	219.46
Myog	myogenin	0.02	0.03	110.43	156.11
Nefl	neurofilament, light polypeptide	0.47	0.76	75.27	106.36
Neurod1	neuronal differentiation 1	0.03	0.03	8.60	12.16
Nrsn2	neurensin 2	0.02	0.03	52.59	74.37
P2ry4	pyrimidinergic receptor P2Y, G-protein coupled, 4	0.00	0.00	12.03	16.82
Panx3	pannexin 3	0.02	0.03	9.82	10.13
Plekhd1	pleckstrin homology domain containing, family D (with coiled-coil domains) member 1	0.85	0.22	4.68	5.29
Plekhh1	pleckstrin homology domain containing, family H	4.43	0.60	41.68	48.95

Continued on next page

Table D.13 – continued from previous page

Gene symbol	Gene name	GD22 (NL) TPM	GD22 (NL) ±SD	GD22 (L) TPM	GD22 (L) ±SD
	(with MyTH4 domain) member 1				
Pnoc	prepronociceptin	0.01	0.02	10.34	14.62
Pou3f4	POU class 3 homeobox 4	0.01	0.02	7.35	10.40
Prl3a1	Prolactin family 3, subfamily a, member 1	0.00	0.00	35.52	50.23
Prl3b1	Prolactin family 3, subfamily b, member 1	34.85	12.31	888.44	1110.55
Prl3c1	Prolactin family 3, subfamily c, member 1	0.04	0.07	13.80	19.26
Prl7a4	prolactin family 7, subfamily a, member 4	9.01	13.53	114.39	112.85
Prl8a4	prolactin family 8, subfamily a, member 4	38.99	16.72	2989.87	3569.19
Prox1	prospero homeobox 1	1.09	1.09	19.76	27.11
Psg16	pregnancy specific glycoprotein 16	3.63	2.07	138.63	173.62
Psg19	pregnancy specific glycoprotein 19	27.38	18.58	645.27	621.10
Psg29	pregnancy-specific glycoprotein 29	3.08	2.60	243.08	335.75
Ptpn5	protein tyrosine phosphatase, non-receptor type 5	0.01	0.01	16.67	23.58
Rbfox1	RNA binding protein, fox-1 homolog (C. elegans) 1	2.89	1.05	13.15	13.60
Rln1	relaxin 1	0.00	0.00	78.52	111.05
Rnase13	ribonuclease, RNase A family, 13 (non-active)	0.00	0.00	4.18	5.91
Rnf144a	ring finger protein 144A	2.77	0.43	64.54	76.77
Rnf208	ring finger protein 208	0.00	0.00	46.24	65.40
Rxrg	retinoid X receptor gamma	0.00	0.01	12.31	17.40
Sec1	secretory blood group 1	0.00	0.01	52.51	74.26
Siah3	siah E3 ubiquitin protein ligase family member 3	0.00	0.00	21.45	30.34
Slc1a2	solute carrier family 1 (glial high affinity glutamate transporter), member 2	0.01	0.02	9.61	13.41
Slc2a2	solute carrier family 2 (facilitated glucose transporter), member 2	0.03	0.01	19.57	26.73
Slc32a1	solute carrier family 32 (GABA vesicular transporter), member 1	0.24	0.21	6.95	9.38
Slc7a9	solute carrier family 7 (amino acid transporter light chain, bo,+ system), member 9	0.00	0.00	6.21	8.79
Sln	sarcolipin	0.36	0.41	98.09	138.64
Smpx	small muscle protein, X-linked	0.00	0.00	43.94	62.14
Snhg11	small nucleolar RNA host gene 11 (non-protein coding)	2.34	1.16	7.76	7.58
Spns2	spinster homolog 2	2.94	2.31	70.62	94.74
Sptb	spectrin, beta, erythrocytic	0.12	0.12	19.97	20.98
Sst	somatostatin	0.05	0.02	14.12	19.94
St8sia3	ST8 alpha-N-acetyl-neuraminide alpha-2,8-sialyltransferase 3	0.00	0.00	17.21	24.34
Stfa3	stefin A3	0.98	0.32	81.53	113.02
Stmn3	stathmin-like 3	0.07	0.06	16.13	22.81
Tf	transferrin	1.63	0.72	230.61	309.81
Tmem151b	transmembrane protein 151B	0.00	0.00	35.60	50.34
Tnnt1	troponin T type 1 (skeletal, slow)	0.17	0.08	257.97	361.74
Tppp3	tubulin polymerization-promoting protein family member 3	1.83	1.32	71.21	92.79
Trim3	tripartite motif-containing 3	20.37	13.67	154.24	96.95
Tspyl4	TSPY-like 4	0.24	0.05	12.21	11.41
Vgll2	vestigial-like family member 2	0.00	0.01	30.08	42.54
Zfp575	zinc finger protein 575	0.01	0.02	14.47	20.47
Down-regulated on GD22 (L)					
Car13	carbonic anhydrase 13	2.33	2.24	0.00	0.00
Ccdc65	coiled-coil domain containing 65	2.61	1.97	0.00	0.00
Cyp4b1	cytochrome P450, family 4, subfamily b, polypeptide 1	4.47	5.30	0.00	0.00
Ercc2	excision repair cross-complementation group 2	5.42	2.82	0.00	0.00
Ifit1	interferon-induced protein with tetratricopeptide repeats 1	107.34	93.98	2.69	1.10
Nppa	natriuretic peptide A	22.21	7.17	0.47	0.67
Nppb	natriuretic peptide B	890.97	937.67	31.66	26.48
Nupr1l	nuclear protein, transcriptional regulator, 1-like	3.36	0.99	0.03	0.03
Rnase1l1	ribonuclease, RNase A family, 1-like 1 (pancreatic)	11.86	11.55	0.00	0.00
Rnf113a1	ring finger protein 113A1	4.53	2.43	0.00	0.00
Tmem26	Tmem26	7.04	4.49	0.23	0.01

Table D.14: Gene transcripts that were differentially expressed in the inner myometrium, between GD20 and GD22 (NL). Transcript expression levels are shown in transcripts per million (TPM) values (mean±SD).

Gene symbol	Gene name	GD20 TPM	GD20 ±SD	GD22 (NL) TPM	GD22 (NL) ±SD
Upregulated on GD22 (NL)					
LOC685544	hypothetical protein LOC685544	0.00	0.01	106.53	184.51

Continued on next page

Table D.14 – continued from previous page

Gene symbol	Gene name	GD20 TPM	GD20 ±SD	GD22 (NL) TPM	GD22 (NL) ±SD
Angptl4	angiopoietin-like 4	5.08	8.46	148.90	145.71
Apbb1ip	amyloid beta (A4) precursor protein-binding, family B, member 1 interacting protein	3.47	3.34	60.28	69.49
Apod	apolipoprotein D	0.20	0.25	17.56	17.10
Ccrl2	chemokine (C-C motif) receptor-like 2	0.01	0.03	6.63	8.93
Cd70	Cd70 molecule	0.00	0.01	16.60	27.92
Cilp	cartilage intermediate layer protein, nucleotide pyrophosphohydrolase	0.19	0.33	46.49	28.93
Cp	ceruloplasmin (ferroxidase)	15.71	7.09	182.13	147.67
Csgalnact1	chondroitin sulfate N-acetylgalactosaminyltransferase 1	2.00	1.41	42.79	34.06
Cst7	cystatin F (leukocystatin)	0.02	0.03	4.97	8.48
Fbln5	fibulin 5	9.18	9.11	111.98	71.43
Fcrl6	Fc receptor-like 6	4.99	4.47	105.72	104.53
G0s2	G0/G1switch 2	1.41	2.38	5.48	2.38
Htr2a	5-hydroxytryptamine (serotonin) receptor 2A, G protein-coupled	3.21	3.85	86.91	148.90
Ifi204	interferon activated gene 204	11.37	2.46	151.67	157.03
Ifit3	interferon-induced protein with tetratricopeptide repeats 3	15.27	19.75	184.38	151.78
Igfbp4	insulin-like growth factor binding protein 4	16.16	22.00	191.54	123.83
Igsf10	immunoglobulin superfamily, member 10	1.10	1.18	100.94	90.15
Il33	interleukin 33	2.15	1.93	53.08	81.72
Klhl10	kelch-like family member 10	0.00	0.01	5.36	8.95
LOC686539	hypothetical protein LOC686539	11.98	12.18	175.95	115.20
Lrrc63	leucine rich repeat containing 63	0.00	0.01	12.33	20.81
Mgp	matrix Gla protein	20.07	18.84	231.75	194.45
Mmp11	matrix metallopeptidase 11	58.99	63.71	2574.78	1613.84
Mmp12	matrix metallopeptidase 12	4.03	2.63	66.61	28.87
Nav3	neuron navigator 3	1.24	1.13	16.45	11.66
Ncam1	neural cell adhesion molecule 1	4.34	2.93	60.56	54.77
Neu2	sialidase 2	1.82	2.60	120.24	72.79
Nov	nephroblastoma overexpressed	0.83	0.88	28.92	19.13
Nppb	natriuretic peptide B	16.44	25.42	1134.81	598.98
Oasl	2'-5'-oligoadenylate synthetase-like	7.14	6.36	131.13	159.32
Pla1a	phospholipase A1 member A	4.00	4.32	85.68	70.17
Prl2c1	Prolactin family 2, subfamily c, member 1	2.79	3.18	805.52	591.09
Prl5a1	prolactin family 5, subfamily a, member 1	9.59	13.49	1092.25	866.74
Prl5a2	prolactin family 5, subfamily a, member 2	31.40	32.14	1024.67	644.50
Prl7b1	prolactin family 7, subfamily b, member 1	100.18	168.57	7866.18	3998.27
RGD1562284	glutaminyl-peptide cyclotransferase	9.65	15.60	95.85	106.99
Rnase1	ribonuclease, RNase A family, 1 (pancreatic)	4.73	4.61	277.71	449.07
Sema6d	sema domain, transmembrane domain (TM), and cytoplasmic domain, (semaphorin) 6D	15.60	10.65	342.72	385.81
Sox4	SRY (sex determining region Y)-box 4	7.56	3.47	91.46	66.89
Thbs1	thrombospondin 1	8.68	9.40	129.58	94.92
Tssk6	testis-specific serine kinase 6	0.00	0.00	42.14	72.99
Vcan	versican	3.19	3.61	70.64	57.12
Zc3h10	zinc finger CCCH type containing 10	0.65	0.61	48.80	61.47
	Down-regulated on GD22 (NL)				
Abcb1b	ATP-binding cassette, subfamily B (MDR/TAP), member 1B	448.31	578.32	7.46	9.93
Abcc4	ATP-binding cassette, subfamily C (CFTR/MRP), member 4	12.98	10.12	1.28	0.43
Adcy1	adenylate cyclase 1 (brain)	33.29	32.47	0.17	0.20
Alcam	activated leukocyte cell adhesion molecule	117.22	128.91	5.57	2.35
Aldh2	aldehyde dehydrogenase 2 family (mitochondrial)	97.80	12.61	24.87	8.28
Apoa1	apolipoprotein A-I	270.94	466.59	2.43	3.93
Atp7b	ATPase, Cu++ transporting, beta polypeptide	28.06	24.15	0.06	0.10
C3	complement component 3	529.32	659.41	11.78	14.87
Cdh16	cadherin 16	21.19	35.86	0.00	0.00
Cfb	complement factor B	437.51	470.37	23.60	29.95
Chdh	choline dehydrogenase	90.27	132.12	4.58	5.37
Cldn8	claudin 8	8.70	8.89	0.00	0.00
Col2a1	collagen, type II, alpha 1	20.34	34.51	0.05	0.05
Csf1	colony stimulating factor 1 (macrophage)	346.31	424.63	4.21	3.77
Csf3	colony stimulating factor 3 (granulocyte)	14.54	11.15	0.00	0.00
Cubn	cubilin (intrinsic factor-cobalamin receptor)	12.35	19.70	0.76	0.87
Cyb561	cytochrome b-561	67.28	100.58	2.28	1.33
Defb1	defensin beta 1	12.55	12.39	0.00	0.00
Dio3	deiodinase, iodothyronine, type III	356.99	417.12	9.75	16.62
Ehf	ets homologous factor	45.68	35.58	0.03	0.06
Emb	embigin	60.60	42.02	2.35	2.21
Enpp1	ectonucleotide pyrophosphatase/phosphodiesterase 1	57.85	13.55	8.97	6.01
Eya2	eyes absent homolog 2 (Drosophila)	36.18	4.77	0.15	0.20

Continued on next page

Table D.14 – continued from previous page

Gene symbol	Gene name	GD20 TPM	GD20 ±SD	GD22 (NL) TPM	GD22 (NL) ±SD
F5	coagulation factor V (proaccelerin, labile factor)	13.39	8.88	1.34	0.48
Gabrp	gamma-aminobutyric acid (GABA-A) receptor, pi	128.25	141.85	0.00	0.00
Gpx2	glutathione peroxidase 2	160.83	111.13	6.70	11.45
Htr4	5-hydroxytryptamine (serotonin) receptor 4, G protein-coupled	13.82	23.25	0.00	0.00
Iapp	islet amyloid polypeptide	37.67	55.80	0.00	0.00
Isyna1	inositol-3-phosphate synthase 1	1489.69	1669.42	18.66	6.69
Itfg3	integrin alpha FG-GAP repeat containing 3	581.32	748.48	15.04	3.41
Kif12	kinesin family member 12	46.13	55.08	0.00	0.00
Lifr	leukemia inhibitory factor receptor alpha	127.37	84.77	21.74	11.02
LOC688553	hypothetical protein LOC688553	20.63	15.17	0.21	0.36
Lpo	lactoperoxidase	98.90	75.56	1.03	0.85
Lrat	lecithin-retinol acyltransferase (phosphatidylcholine-retinol-O-acyltransferase)	308.27	357.79	2.25	1.90
Lrp2	low density lipoprotein receptor-related protein 2	69.42	63.47	1.06	0.62
Nr0b2	nuclear receptor subfamily 0, group B, member 2	10.58	13.18	0.00	0.00
Oxt	oxytocin/neurophysin 1 prepropeptide	435.40	359.58	15.25	23.58
Pax8	paired box 8	161.20	170.81	10.21	16.38
Pinlyp	phospholipase A2 inhibitor and LY6/PLAUR domain containing	151.15	123.87	5.71	8.38
Ppl	periplakin	63.45	32.27	4.80	6.72
Psph	phosphoserine phosphatase	85.84	117.51	3.62	2.15
Rbp4	retinol binding protein 4, plasma	93.46	159.64	1.62	1.80
RGD1559493	similar to Hypothetical protein MGC58608	9.61	16.64	0.00	0.00
RGD1562136	similar to D1Ertd622e protein	43.70	17.64	6.59	0.98
Sctr	secretin receptor	39.67	23.41	0.38	0.52
Sema4a	sema domain, immunoglobulin domain (Ig), transmembrane domain (TM) and short cytoplasmic domain, (semaphorin) 4A	112.00	130.43	2.09	2.61
Slc17a3	solute carrier family 17 (organic anion transporter), member 3	14.03	12.11	0.04	0.04
Slc17a4	solute carrier family 17, member 4	19.05	29.87	0.00	0.00
Slc1a5	solute carrier family 1 (neutral amino acid transporter), member 5	65.52	53.64	2.81	0.66
Slc34a2	solute carrier family 34 (type II sodium/phosphate contransporter), member 2	81.71	78.36	0.96	1.30
Slc4a1	solute carrier family 4 (anion exchanger), member 1	60.90	69.47	3.65	4.40
Slc5a3	solute carrier family 5 (sodium/myo-inositol cotransporter), member 3	57.11	54.54	2.62	2.43
Tf	transferrin	138.84	193.37	10.31	6.22
Thbs4	thrombospondin 4	289.73	348.89	4.53	3.79
Tshr	thyroid stimulating hormone receptor	15.08	15.69	0.22	0.10
Vtcn1	V-set domain containing T cell activation inhibitor 1	34.64	25.88	1.32	0.91
Wfs1	Wolfram syndrome 1 (wolframin)	142.57	163.66	13.54	6.05

Table D.15: Gene transcripts that were differentially expressed in the inner myometrium, between GD22 (NL) and GD22 (L). Transcript expression levels are shown in transcripts per million (TPM) values (mean±SD).

Gene symbol	Gene name	GD22 (NL) TPM	GD22 (NL) ±SD	GD22 (L) TPM	GD22 (L) ±SD
Upregulated on GD22 (L)					
Acan	aggrecan	0.20	0.30	26.33	37.11
Col11a2	collagen, type XI, alpha 2	0.00	0.00	18.89	26.42
Col2a1	collagen, type II, alpha 1	0.05	0.05	264.17	373.25
Col9a1	collagen, type IX, alpha 1	0.00	0.00	18.12	25.47
Myh7	myosin, heavy chain 7, cardiac muscle, beta	0.08	0.09	9.95	12.56
Vom2r34	vomeronasal 2 receptor, 34	8.51	1.50	391.32	499.84
Down-regulated on GD22 (L)					
A2m	alpha-2-macroglobulin	1284.66	917.60	453.92	574.31
Fam150b	family with sequence similarity 150, member B	21.86	36.95	0.00	0.00
Ifit1	interferon-induced protein with tetratricopeptide repeats 1	191.56	144.00	5.88	4.59
Serpina3n	serine (or cysteine) peptidase inhibitor, clade A, member 3N	21.11	33.92	0.03	0.04

Continued on next page

Table D.16 – continued from previous page

Gene symbol	Gene name	GD19+6hrs TPM	GD19+6hrs ±SD	GD20 TPM	GD20 ±SD

Table D.16: Gene transcripts that were differentially expressed in the outer myometrium, between GD19+6hrs and GD20. Transcript expression levels are shown in transcripts per million (TPM) values (mean±SD).

Gene symbol	Gene name	GD19+6hrs TPM	GD19+6hrs ±SD	GD20 TPM	GD20 ±SD
Upregulated on GD 20					
Isyna1	inositol-3-phosphate synthase 1	25.10	12.58	1052.83	1069.36
Hsd11b1	hydroxysteroid 11-beta dehydrogenase 1	43.36	51.25	495.45	406.14
Lyz2	lysozyme 2	64.28	60.28	499.34	307.16
Lrat	lecithin-retinol acyltransferase (phosphatidylcholine-retinol-O-acyltransferase)	1.56	1.26	220.09	219.89
Itfg3	integrin alpha FG-GAP repeat containing 3	14.39	6.71	223.82	245.87
Alcam	activated leukocyte cell adhesion molecule	5.28	3.99	112.37	106.09
Aldob	aldolase B, fructose-bisphosphate	1.09	1.23	105.04	166.77
Igfbp1	insulin-like growth factor binding protein 1	4.04	5.77	94.70	69.66
Ptgs1	prostaglandin-endoperoxide synthase 1	9.32	11.66	73.66	65.33
Slc5a3	solute carrier family 5 (sodium/myo-inositol cotransporter), member 3	3.20	1.12	52.64	58.26
Defb1	defensin beta 1	0.00	0.00	36.69	36.60
Art3	ADP-ribosyltransferase 3	2.60	3.00	37.89	18.94
Cfi	complement factor I	1.22	0.96	34.83	24.27
Upk3bl	uroplakin 3B-like	0.00	0.00	31.40	28.63
Pon3	paraoxonase 3	0.38	0.56	31.69	16.67
Cldn10	claudin 10	1.01	1.41	29.12	35.23
Ly6c	Ly6-C antigen	1.89	1.08	28.22	15.11
Csf2rb	colony stimulating factor 2 receptor, beta, low-affinity (granulocyte-macrophage)	8.78	10.10	34.86	10.68
C4bpb	complement component 4 binding protein, beta	0.00	0.00	22.68	38.19
F5	coagulation factor V (proaccelerin, labile factor)	12.06	20.69	32.97	18.54
Alox15	arachidonate 15-lipoxygenase	0.02	0.03	14.83	8.44
Marveld3	MARVEL domain containing 3	0.00	0.00	14.12	12.05
Tnfaip8l2	tumor necrosis factor, alpha-induced protein 8-like 2	1.36	0.59	14.69	7.25
Faim2	Fas apoptotic inhibitory molecule 2	1.04	1.81	12.28	12.70
Krt83	keratin 83	0.16	0.20	10.80	7.10
Slc17a4	solute carrier family 17, member 4	0.06	0.10	9.88	12.47
Nptx2	neuronal pentraxin II	1.36	2.24	10.94	6.45
Paqr9	progestin and adipoQ receptor family member IX	0.35	0.61	9.72	7.63
Fam5b/Brinp2	bone morphogenetic protein/retinoic acid inducible neural-specific 2	0.26	0.14	7.97	7.79
Clec1b	C-type lectin domain family 1, member B	2.74	4.50	9.81	4.12
Inmt	indolethylamine N-methyltransferase	0.01	0.01	6.04	8.52
Slc10a1	solute carrier family 10 (sodium/bile acid cotransporter), member 1	1.39	2.38	7.29	6.82
Klkb1	kallikrein B, plasma 1	0.00	0.00	5.67	9.70
Gp9	glycoprotein IX (platelet)	0.14	0.24	4.70	1.54
Kcng1	potassium voltage-gated channel, subfamily G, member 1	0.00	0.00	4.39	1.66
Aadac	arylacetamide deacetylase	0.00	0.00	4.06	5.90
Bucs1	acyl-CoA synthetase medium-chain family member 1	8.65	14.96	12.49	21.49
Nmb	neuromedin B	6.89	11.94	10.73	13.90
Itih1	inter-alpha trypsin inhibitor, heavy chain 1	4.09	7.09	7.47	12.87
LOC308990	hypothetical protein LOC308990	0.00	0.00	2.37	1.50
Plekhg4	pleckstrin homology domain containing, family G (with RhoGef domain) member 4	0.25	0.44	1.95	1.57
Nccrp1	non-specific cytotoxic cell receptor protein 1 homolog (zebrafish)	13.37	23.15	14.52	16.16
F11	coagulation factor XI	3.96	6.83	4.98	2.84
C3	complement component 3	6.39	1.02	510.34	168.32
Hcn4	hyperpolarization activated cyclic nucleotide-gated potassium channel 4	0.00	0.00	6.11	4.02
Scn2b	sodium channel, voltage-gated, type II, beta	2.39	4.15	4.29	1.82
Slc17a3	solute carrier family 17 (organic anion transporter), member 3	0.20	0.16	16.58	16.57
Down-regulated on GD 20					
LOC171573	spleen protein 1 precursor	1612.19	2779.47	4.43	4.96
Prl8a9	prolactin family 8, subfamily a, member 9	1217.52	2033.12	5.07	6.08
S100a8	S100 calcium binding protein A8	482.62	835.31	14.45	4.90
Prl8a2	prolactin family 8, subfamily a, member 2	370.32	587.96	3.19	2.34
Dusp9	dual specificity phosphatase 9	254.03	262.39	8.21	6.96
Cited1	Cbp/p300-interacting transactivator with Glu/Asp-rich carboxy-terminal domain 1	231.66	296.75	40.05	23.43
Sbsn	suprabasin	174.88	220.49	7.90	1.60
Col4a3	collagen, type IV, alpha 3	152.17	263.41	3.42	1.25
Prl7a4	prolactin family 7, subfamily a, member 4	139.64	208.43	0.00	0.00
Pparg	peroxisome proliferator-activated receptor gamma	51.39	43.27	3.01	1.11

Continued on next page

Table D.16 – continued from previous page

Gene symbol	Gene name	GD19+6hrs TPM	GD19+6hrs ±SD	GD20 TPM	GD20 ±SD
Hic2	hypermethylated in cancer 2	50.49	42.29	6.92	0.34
Ncam1	neural cell adhesion molecule 1	42.05	38.32	5.33	3.39
Idi1	isopentenyl-diphosphate delta isomerase 1	34.92	56.39	34.15	26.13
Atg9b	autophagy related 9B	26.36	45.65	8.64	7.98
Lpar2	lysophosphatidic acid receptor 2	26.19	24.53	7.81	0.71
Zim1	zinc finger, imprinted 1	25.92	16.42	2.57	0.94
Sh3gl3	SH3-domain GRB2-like 3	21.96	37.89	3.71	1.65
Htr1d	5-hydroxytryptamine (serotonin) receptor 1D, G protein-coupled	21.69	30.92	0.00	0.00
Tmem132e	transmembrane protein 132E	20.32	17.38	1.92	0.87
Dmrtc1c	DMRT-like family C1c1	19.87	34.26	0.00	0.00
Fam26e	family with sequence similarity 26, member E	19.36	33.53	2.99	2.22
Otc	ornithine carbamoyltransferase	18.62	32.26	11.05	18.86
Cd79b	Cd79b molecule, immunoglobulin-associated beta	17.40	30.14	2.97	0.58
Mybph	myosin binding protein H	10.01	12.77	0.00	0.00
Cd244	Cd244 molecule, natural killer cell receptor 2B4	6.39	11.05	2.60	0.85
Ggt1	gamma-glutamyltransferase 1	6.10	10.29	5.83	2.09
Rimbp2	RIMS binding protein 2	5.56	1.23	0.58	0.14
Mmp9	matrix metallopeptidase 9	3.20	5.24	0.00	0.00
Myh6	myosin, heavy chain 6, cardiac muscle, alpha	1.04	0.89	0.02	0.03

Table D.17: Gene transcripts that were differentially expressed in the outer myometrium, between GD20 and GD22 (NL). Transcript expression levels are shown in transcripts per million (TPM) values (mean±SD).

Gene symbol	Gene name	GD20 TPM	GD20 ±SD	GD22 (NL) TPM	GD22 (NL) ±SD
Upregulated on GD22 (NL)					
Prl8a2	prolactin family 8, subfamily a, member 2	3.19	2.34	676.30	1155.28
Cuzd1	CUB and zona pellucida-like domains 1	4.68	7.25	492.78	409.84
Serpine1	serpin peptidase inhibitor, clade E (nexin, plasminogen activator inhibitor type 1), member 1	36.01	19.61	297.03	107.48
RGD1309676	family with sequence similarity 213, member A	34.40	26.96	178.41	127.27
Cited1	Cbp/p300-interacting transactivator with Glu/Asp-rich carboxy-terminal domain 1	40.05	23.43	156.19	51.56
Mmp7	matrix metallopeptidase 7	0.22	0.31	131.36	56.43
Taf7l	TAF7-like RNA polymerase II, TATA box binding protein (TBP)-associated factor	0.61	0.77	112.99	113.12
Prl7a4	prolactin family 7, subfamily a, member 4	0.00	0.00	106.52	174.73
Prom1	prominin 1	4.60	4.59	105.22	100.68
Fndc3c1	fibronectin type III domain containing 3C1	1.07	1.62	96.35	148.44
Slc26a4	solute carrier family 26 (anion exchanger), member 4	2.87	2.80	69.38	68.87
Cndp1	carnosine dipeptidase 1 (metallopeptidase M20 family)	8.94	6.27	35.15	22.93
Sfmbt2	Scm-like with four mbt domains 2	4.54	2.69	32.45	32.63
Apobr	apolipoprotein B receptor	4.62	2.62	28.31	14.70
Htr1d	5-hydroxytryptamine (serotonin) receptor 1D, G protein-coupled	0.00	0.00	25.53	41.90
Igsf9	immunoglobulin superfamily, member 9	2.51	1.39	23.02	8.12
Cftr	cystic fibrosis transmembrane conductance regulator	0.42	0.49	22.54	29.22
Ehhadh	enoyl-CoA, hydratase/3-hydroxyacyl CoA dehydrogenase	2.67	0.62	21.25	16.87
Prl3a1	Prolactin family 3, subfamily a, member 1	0.00	0.00	16.33	5.06
Wnt7a	wingless-type MMTV integration site family, member 7A	0.12	0.03	11.54	9.93
Dmrtc1c	DMRT-like family C1c1	0.00	0.00	9.79	15.09
Slc22a2	solute carrier family 22 (organic cation transporter), member 2	0.06	0.01	7.63	11.10
Mmp9	matrix metallopeptidase 9	0.00	0.00	7.42	11.32
Tcerg1l	transcription elongation regulator 1-like	0.00	0.00	7.00	11.83
LOC691352	similar to Robo-1	0.51	0.14	6.84	5.45
Lgals12	lectin, galactoside-binding, soluble, 12	0.09	0.04	4.37	4.30
Myo3b	myosin IIIB	0.00	0.00	1.99	1.89
Down-regulated on GD22 (NL)					
Endou	endonuclease, poly(U)-specific	4.99	4.47	0.00	0.00
Bdkrb1	bradykinin receptor B1	2.12	2.71	0.02	0.04
Gp9	glycoprotein IX (platelet)	4.70	1.54	0.04	0.07
Rprml	reprimo-like	15.31	4.91	0.07	0.12
Mfrp	membrane frizzled-related protein	3.55	1.93	0.07	0.08
Tacr2	tachykinin receptor 2	3.10	2.32	0.17	0.13

Continued on next page

Table D.17 – continued from previous page

Gene symbol	Gene name	GD20		GD22 (NL)	
		TPM	±SD	TPM	±SD
Slc2a4	solute carrier family 2 (facilitated glucose transporter), member 4	6.73	3.29	0.22	0.01
Fam5b/Brinp2	bone morphogenetic protein/retinoic acid inducible neural-specific 2	7.97	7.79	0.22	0.19
Vamp5	vesicle-associated membrane protein 5	6.76	3.56	0.36	0.53
Tenm2	teneurin transmembrane protein 2	11.44	5.65	0.60	0.36
Il13ra2	interleukin 13 receptor, alpha 2	47.43	37.17	1.02	0.87
Galnt18	UDP-N-acetyl-alpha-D-galactosamine:polypeptide 18 N-acetylgalactosaminyltransferase	51.82	38.88	1.71	1.20
Sgcd	sarcoglycan, delta (dystrophin-associated glycoprotein)	16.96	10.50	2.11	2.52
Sema3e	sema domain, immunoglobulin domain (Ig), short basic domain, secreted, (semaphorin) 3E	28.78	18.94	3.20	1.50
Srpx	sushi-repeat-containing protein, X-linked	88.71	61.11	3.23	3.97
C1qtnf2	C1q and tumor necrosis factor related protein 2	18.83	7.20	3.29	1.16
Pkia	protein kinase (cAMP-dependent, catalytic) inhibitor alpha	30.81	15.68	3.31	1.13
Bves	blood vessel epicardial substance	34.28	12.26	3.83	2.44
Abcb1b	ATP-binding cassette, subfamily B (MDR/TAP), member 1B	271.55	265.10	3.84	2.13
Lepr	leptin receptor	64.87	28.80	5.37	2.84
Car12	carbonic anyhydrase 12	87.79	38.69	5.40	1.46
Enpp1	ectonucleotide pyrophosphatase/phosphodiesterase 1	62.78	43.28	6.59	1.51
Abcg4	ATP-binding cassette, subfamily G (WHITE), member 4	124.24	46.42	8.10	4.12
Adam15	ADAM metallopeptidase domain 15	77.74	16.13	8.72	4.70
Thbs4	thrombospondin 4	261.53	327.27	9.47	4.85
Itm2a	integral membrane protein 2A	117.15	133.34	9.51	6.30
Dact3	dishevelled-binding antagonist of beta-catenin 3	70.03	28.97	9.60	0.74
Sorcs2	sortilin-related VPS10 domain containing receptor 2	69.58	34.16	10.24	2.41
Cnr1	cannabinoid receptor 1 (brain)	25.19	12.26	10.47	12.48
Pdlim3	PDZ and LIM domain 3	187.43	105.57	11.58	10.89
Akap12	A kinase (PRKA) anchor protein 12	111.25	63.31	11.78	7.34
Svil	supervillin	82.99	50.62	11.98	9.34
Cxcl13	chemokine (C-X-C motif) ligand 13	115.60	61.69	13.35	5.26
Atp2b4	ATPase, Ca++ transporting, plasma membrane 4	84.20	50.52	13.84	9.43
Tsc22d3	TSC22 domain family, member 3	84.81	36.62	14.59	5.40
Cercam	cerebral endothelial cell adhesion molecule	83.11	51.82	14.83	5.25
Synm	synemin, intermediate filament protein	125.90	55.14	15.06	7.14
Rgma	repulsive guidance molecule family member A	110.40	74.97	15.17	10.20
Slc48a1	solute carrier family 48 (heme transporter), member 1	90.88	47.10	16.46	3.92
Aoc3	amine oxidase, copper containing 3	199.44	120.89	24.84	9.72
Ehd2	EH-domain containing 2	266.01	157.37	35.35	17.11
Isyna1	inositol-3-phosphate synthase 1	1052.83	1069.36	35.48	20.29
Lims2	LIM and senescent cell antigen like domains 2	235.85	120.37	38.53	11.27
Kcnmb1	potassium large conductance calcium-activated channel, subfamily M, beta member 1	219.14	110.71	40.07	17.77
Ptn	pleiotrophin	362.30	217.46	47.91	25.16
Acta1	actin, alpha 1, skeletal muscle	1253.59	735.94	87.43	35.62
Prkcdbp	protein kinase C, delta binding protein	376.06	76.79	92.45	90.97
Hspb1	heat shock protein 1	752.54	365.52	126.15	47.87
Igfbp6	insulin-like growth factor binding protein 6	1256.56	759.01	131.92	42.01
Prelp	proline/arginine-rich end leucine-rich repeat protein	1401.54	973.40	155.55	66.39
Actg2	actin, gamma 2, smooth muscle, enteric	16313.36	9336.30	1552.40	497.02

Appendix E

RU486-treated Tissues

Table E.1: Gene transcripts that were differentially expressed following treatment with RU486 in the inner myometrium compared to the decidua on GD19+6hrs. Transcript expression levels are shown in transcripts per million (TPM) values (mean±SD).

		Decidua		Inner myometrium	
Gene symbol	Gene name	TPM	±SD	TPM	±SD
Upregulated in inner myometrium					
Acta2	actin, alpha 2, smooth muscle, aorta	6.78	5.26	416.51	411.72
Apob	apolipoprotein B	0.97	0.24	19.99	24.51
Atp2b4	ATPase, Ca++ transporting, plasma membrane 4	1.07	1.13	48.68	44.27
C1qb	complement component 1, q subcomponent, B chain	0.15	0.20	44.23	60.93
Cdh1	cadherin 1	1.45	0.80	70.46	55.53
Csf1	colony stimulating factor 1 (macrophage)	1.22	0.45	28.60	28.95
Gpr56	G protein-coupled receptor 56	0.50	0.16	17.76	11.65
Itsn1	intersectin 1 (SH3 domain protein)	4.01	3.04	58.05	32.49
Kcnb1	potassium voltage gated channel, Shab-related subfamily, member 1	0.03	0.04	7.47	6.86
Mtss1l	metastasis suppressor 1-like	1.62	1.37	46.40	13.36
Myl9	myosin, light chain 9, regulatory	29.60	44.99	2389.83	3530.97
Pde3a	phosphodiesterase 3A, cGMP inhibited	2.86	0.58	17.37	20.39
Plat	plasminogen activator, tissue	8.72	4.57	67.37	57.58
Ppp1r12b	protein phosphatase 1, regulatory subunit 12B	21.91	29.33	44.85	28.65
Rgma	repulsive guidance molecule family member A	1.84	0.92	26.83	11.25
Rgs1	regulator of G-protein signaling 1	0.01	0.02	0.37	0.64
Tlr8	toll-like receptor 8	0.01	0.01	2.69	4.66
Tns3	tensin 3	3.72	1.48	35.96	22.30
Down-regulated in inner myometrium					
Ephb1	Eph receptor B1	2.47	0.88	0.30	0.11
Gpr1	G protein-coupled receptor 1	5.50	3.40	0.00	0.00
Hapln1	hyaluronan and proteoglycan link protein 1	29.42	50.95	1.50	2.60
Pdyn	prodynorphin	2.12	1.14	0.10	0.17
Tsx	testis specific X-linked gene	4.01	0.58	0.00	0.00

Table E.2: Gene transcripts that were differentially expressed following treatment with RU486 in the outer myometrium compared to the decidua on GD19+6hrs. Transcript expression levels are shown in transcripts per million (TPM) values (mean±SD).

		Decidua		Outer myometrium	
Gene symbol	Gene name	TPM	±SD	TPM	±SD
Upregulated in outer myometrium					
Abcb1b	ATP-binding cassette, subfamily B (MDR/TAP), member 1B	0.49	0.30	101.85	88.70
Acta1	actin, alpha 1, skeletal muscle	18.96	27.53	699.89	747.97
Acta2	actin, alpha 2, smooth muscle, aorta	6.78	5.26	1036.93	1086.75
Adcy1	adenylate cyclase 1 (brain)	0.01	0.02	11.40	10.33
Aebp1	AE binding protein 1	15.32	12.63	127.34	57.56
Alcam	activated leukocyte cell adhesion molecule	2.34	1.65	40.54	38.02
Ankh	ANKH inorganic pyrophosphate transport regulator	3.99	2.94	17.83	16.96
Anxa6	annexin A6	7.21	6.46	80.90	67.09
Aoc3	amine oxidase, copper containing 3	3.01	2.18	77.20	68.19
Apob	apolipoprotein B	0.97	0.24	22.12	19.74
Ar	androgen receptor	0.29	0.33	8.33	5.68
Asb2	ankyrin repeat and SOCS box-containing 2	0.00	0.00	7.09	10.08
Atp2b4	ATPase, Ca++ transporting, plasma membrane 4	1.07	1.13	39.37	28.60
Bgn	biglycan	60.10	78.77	677.18	554.77
Bok	BCL2-related ovarian killer	4.64	2.70	149.61	98.68
C1r	complement component 1, r subcomponent	7.13	3.53	71.14	59.95
C1s	complement component 1, s subcomponent	1.89	1.79	53.46	45.99
C3	complement component 3	4.91	2.58	328.78	314.39
C4a	complement component 4A (Rodgers blood group)	2.03	1.95	83.13	53.95
C4b	complement component 4B (Chido blood group)	0.76	0.92	21.97	8.25
Ca2	carbonic anhydrase 2	1.23	0.71	23.69	2.45
Cacna1c	calcium channel, voltage-dependent, L type, alpha 1C subunit	0.47	0.20	13.06	12.91
Car12	carbonic anyhydrase 12	0.21	0.26	20.90	13.02
Cav1	caveolin 1, caveolae protein	1.75	1.74	158.10	147.13
Ccl21	chemokine (C-C motif) ligand 21	0.00	0.00	30.34	29.68
Cd24	CD24 molecule	110.82	53.44	1292.54	89.57
Cdh1	cadherin 1	1.45	0.80	49.99	35.37
Cdh16	cadherin 16	0.00	0.00	8.02	7.33
Cfb	complement factor B	2.87	3.09	162.21	140.33
Chchd10	coiled-coil-helix-coiled-coil-helix domain containing 10	3.42	1.49	35.99	24.56
Cnn1	calponin 1, basic, smooth muscle	5.21	3.93	1291.98	1106.88
Col3a1	collagen, type III, alpha 1	14.42	15.69	632.82	499.55
Col6a2	collagen, type VI, alpha 2	31.09	26.72	416.47	317.12
Crip1	cysteine-rich protein 1 (intestinal)	1.14	1.58	27.22	14.30
Csf1	colony stimulating factor 1 (macrophage)	1.22	0.45	109.08	130.17
Ctsc	cathepsin C	1.27	1.07	34.60	29.15
Cxcl12	chemokine (C-X-C motif) ligand 12	0.66	0.78	25.24	24.24
Defb1	defensin beta 1	0.03	0.05	31.84	38.48
Dhrs11	dehydrogenase/reductase (SDR family) member 11	1.04	0.57	28.04	42.13
Dpep1	dipeptidase 1 (renal)	0.11	0.19	22.53	18.48
Ehd2	EH-domain containing 2	4.48	3.63	73.18	70.97
Emb	embigin	0.87	0.96	35.79	27.40
Epb41l3	erythrocyte membrane protein band 4.1-like 3	0.44	0.33	12.86	11.00
Fam20c	family with sequence similarity 20, member C	1.12	0.46	27.78	23.59
Fam46b	family with sequence similarity 46, member B	0.00	0.00	7.12	8.50
Fcrl6	Fc receptor-like 6	2.43	1.88	255.78	441.53
Fhl1	four and a half LIM domains 1	6.51	5.59	573.19	572.86
Fhl3	four and a half LIM domains 3	2.84	2.40	88.97	106.18
Fut2	fucosyltransferase 2 (secretor status included)	2.78	2.55	51.18	43.44
Gabbr1	gamma-aminobutyric acid (GABA) B receptor 1	4.26	3.49	51.81	72.74
Gls	glutaminase	5.95	3.62	101.89	89.84
Gpr56	G protein-coupled receptor 56	0.50	0.16	15.51	7.59
Gpt	glutamic-pyruvate transaminase (alanine aminotransferase)	0.20	0.34	21.34	11.24
Gpx1	glutathione peroxidase 1	54.59	42.37	642.55	278.44
Gpx2	glutathione peroxidase 2	9.49	13.86	370.37	356.33
Hsd11b1	hydroxysteroid 11-beta dehydrogenase 1	6.54	6.51	262.11	169.49
Iapp	islet amyloid polypeptide	0.00	0.00	22.93	36.23

Continued on next page

Table E.2 – continued from previous page

Gene symbol	Gene name	Decidua		Outer myometrium	
		TPM	±SD	TPM	±SD
Ifi204	myeloid cell nuclear differentiation antigen	3.17	3.75	14.85	15.01
Igfbp5	insulin-like growth factor binding protein 5	8.00	8.60	110.71	109.05
Igfbp6	insulin-like growth factor binding protein 6	8.59	6.65	612.72	621.51
Isyna1	inositol-3-phosphate synthase 1	18.03	9.01	684.90	600.84
Itfg3	integrin alpha FG-GAP repeat containing 3	10.04	6.17	139.06	127.15
Jrk	jerky homolog (mouse)	1.49	1.32	34.78	52.09
Kap	kidney androgen regulated protein	11.57	16.48	713.32	665.47
Kb23	type II keratin 23	0.01	0.01	5.84	5.59
Kcnf1	potassium voltage-gated channel, subfamily F, member 1	0.00	0.00	7.64	6.81
Kcnmb1	potassium large conductance calcium-activated channel, subfamily M, beta member 1	1.06	0.94	79.84	58.57
Lamb3	laminin, beta 3	0.16	0.29	10.94	2.99
Lcn2	lipocalin 2	8.33	11.49	366.02	435.02
Lpo	lactoperoxidase	1.10	1.10	63.04	54.71
Lrat	lecithin-retinol acyltransferase (phosphatidylcholine-retinol-O-acyltransferase)	1.42	1.18	101.55	97.13
Lrp2	low density lipoprotein receptor-related protein 2	0.57	0.14	25.45	27.31
Ltbp4	latent transforming growth factor beta binding protein 4	0.39	0.34	21.06	12.94
Lurap1l	leucine rich adaptor protein 1-like	0.01	0.02	11.50	10.39
Lyz2	lysozyme 2	23.38	32.13	402.51	528.49
MGC114464	similar to expressed sequence AI836003	1.42	2.07	25.12	41.41
Mmp17	matrix metallopeptidase 17	0.28	0.17	15.97	13.41
Mmp1a	matrix metallopeptidase 1a (interstitial collagenase)	0.83	0.53	95.74	165.74
Mtss1l	metastasis suppressor 1-like	1.62	1.37	31.53	24.60
Myh11	myosin, heavy chain 11, smooth muscle	4.39	3.36	847.62	784.51
Myh3	myosin, heavy chain 3, skeletal muscle, embryonic	0.35	0.16	14.24	24.47
Myl9	myosin, light chain 9, regulatory	29.60	44.99	3006.63	2580.67
Mylk	myosin light chain kinase	7.63	6.28	456.88	468.29
Net1	neuroepithelial cell transforming 1	12.31	6.76	102.90	19.48
Neu2	sialidase 2	1.77	0.53	62.56	106.60
Nnat	neuronatin	2.65	2.96	61.26	100.89
Nsmf	NMDA receptor synaptonuclear signaling and neuronal migration factor	2.01	2.55	61.45	91.04
Ociad2	OCIA domain containing 2	0.52	0.82	17.43	11.38
Odz4	teneurin transmembrane protein 4	0.45	0.36	8.84	4.62
Oxt	oxytocin/neurophysin 1 prepropeptide	40.50	68.42	399.04	345.77
Oxtr	oxytocin receptor	0.00	0.00	8.19	8.45
Pcdh7	protocadherin 7	0.12	0.17	24.82	11.72
Pcsk7	proprotein convertase subtilisin/kexin type 7	10.47	1.40	74.61	54.10
Pdzk1ip1	PDZK1 interacting protein 1	0.06	0.06	33.68	27.09
Phlda3	pleckstrin homology-like domain, family A, member 3	0.60	0.55	24.93	15.05
Plxnb2	plexin B2	5.82	4.68	35.51	23.02
Ppl	periplakin	6.07	3.62	81.34	60.80
Ppp1r12b	protein phosphatase 1, regulatory subunit 12B	21.91	29.33	62.80	53.78
Prelp	proline/arginine-rich end leucine-rich repeat protein	24.26	27.08	518.67	559.42
Prkag2	protein kinase, AMP-activated, gamma 2 non-catalytic subunit	5.80	0.24	39.63	22.67
Prl2c1	Prolactin family 2, subfamily c, member 1	6.16	6.61	131.43	219.04
Psmb8	proteasome (prosome, macropain) subunit, beta type, 8	0.33	0.50	16.38	11.97
Ptch2	patched homolog 2 (Drosophila)	0.00	0.00	4.48	6.65
Ptn	pleiotrophin	3.81	3.93	121.50	134.86
Rexo2	RNA exonuclease 2	29.79	7.67	199.55	106.97
RGD1563547	small integral membrane protein 22	0.41	0.24	9.94	3.65
RGD1564664	similar to LOC387763 protein	3.17	2.62	160.81	131.96
Rgma	repulsive guidance molecule family member A	1.84	0.92	33.18	39.49
Rgs1	regulator of G-protein signaling 1	0.01	0.02	6.64	7.68
S100a16	S100 calcium binding protein A16	1.27	1.71	28.28	23.49
Sepp1	selenoprotein P, plasma, 1	8.85	9.59	296.52	215.44
Serpina1	serpin peptidase inhibitor, clade A (alpha-1 antiproteinase, antitrypsin), member 1	4.31	2.68	78.15	100.04
Sgk1	serum/glucocorticoid regulated kinase 1	28.86	17.25	219.14	149.87
Slc34a2	solute carrier family 34, member 2 (type II sodium/phosphate contransporter)	0.68	0.57	69.45	60.39
Slc6a14	solute carrier family 6, member 14	0.05	0.09	5.31	4.94

Continued on next page

Table E.2 – continued from previous page

Gene symbol	Gene name	Decidua TPM	Decidua ±SD	Outer myometrium TPM	Outer myometrium ±SD
	(amino acid transporter)				
Slc8a1	solute carrier family 8, member 1 (sodium/calcium exchanger)	1.05	1.13	14.13	13.03
Slco2b1	solute carrier organic anion transporter family, member 2b1	0.13	0.22	5.53	3.00
Socs2	suppressor of cytokine signaling 2	3.59	3.67	28.30	24.25
Sparcl1	SPARC-like 1 (hevin)	0.90	0.82	105.00	93.02
Spns2	spinster homolog 2	1.47	1.01	16.90	3.15
Spp1	secreted phosphoprotein 1	16.17	13.05	889.53	771.63
Srpx	sushi-repeat-containing protein, X-linked	0.18	0.10	25.26	27.81
Stbd1	starch binding domain 1	1.15	0.39	16.46	6.95
Svil	supervillin	2.75	1.05	34.19	20.63
Synm	synemin, intermediate filament protein	1.20	1.02	46.93	40.43
Synpo2	synaptopodin 2	14.23	11.79	234.22	205.03
Tagln	transgelin	11.26	12.61	1410.37	1261.54
Taok3	TAO kinase 3	3.85	4.68	60.38	86.65
Thbs2	thrombospondin 2	2.08	2.00	21.80	18.70
Tlr8	toll-like receptor 8	0.01	0.01	4.51	4.27
Tmem176a	transmembrane protein 176A	3.35	5.64	114.05	63.59
Tmem229b	transmembrane protein 229B	0.62	0.91	17.77	9.01
Tnfsf13	tumor necrosis factor (ligand) superfamily, member 13	0.61	0.47	24.07	12.35
Tnnt2	troponin T type 2 (cardiac)	0.95	1.22	36.41	25.81
Tns3	tensin 3	3.72	1.48	30.35	26.29
Top1mt	topoisomerase (DNA) I, mitochondrial	1.86	1.46	32.89	51.00
Tpm2	tropomyosin 2, beta	234.29	208.77	2765.58	2225.69
Trem2	triggering receptor expressed on myeloid cells 2	0.04	0.07	8.39	7.78
Tshr	thyroid stimulating hormone receptor	0.51	0.17	2.14	1.79
Tubb2a	tubulin, beta 2A class IIa	9.90	7.54	86.98	56.56
Ugt1a1	UDP glucuronosyltransferase 1 family, polypeptide A1	0.27	0.41	25.69	25.98
Upk3bl	uroplakin 3B-like	0.00	0.00	22.32	26.61
Usp43_predicted	ubiquitin specific peptidase 43	0.00	0.00	11.98	17.25
Down-regulated in outer myometrium					
Acad11	acyl-CoA dehydrogenase family, member 11	20.13	8.55	3.36	2.28
Arhgef6	Rac/Cdc42 guanine nucleotide exchange factor (GEF) 6	59.50	44.85	3.97	3.78
Atp4b	ATPase, H+/K+ exchanging, beta polypeptide	13.93	19.94	0.00	0.00
Bcor	BCL6 co-repressor	115.37	101.57	5.18	2.45
Brd3	bromodomain containing 3	111.80	94.38	11.52	3.31
Ccin	calicin	1.43	1.43	0.06	0.04
Cdc14a	cell division cycle 14A	45.54	13.87	3.72	1.90
Cdh3	cadherin 3	115.25	13.91	2.52	1.80
Chrna3	cholinergic receptor, nicotinic, alpha 3 (neuronal)	1.84	2.19	0.00	0.00
Cilp2	cartilage intermediate layer protein 2	4.42	3.47	0.02	0.04
Cldn4	claudin 4	472.76	531.31	2.68	2.35
Cln8	ceroid-lipofuscinosis, neuronal 8 (epilepsy, progressive with mental retardation)	59.51	38.33	5.99	1.48
Col2a1	collagen, type II, alpha 1	85.93	148.44	1.27	0.93
Comp	cartilage oligomeric matrix protein	12.91	22.31	0.08	0.03
Creg1	cellular repressor of E1A-stimulated genes 1	2259.82	1605.20	78.17	20.36
Creld2	cysteine-rich with EGF-like domains 2	70.81	42.18	8.33	5.15
Cyp11a1	cytochrome P450, family 11, subfamily a, polypeptide 1	76.73	79.78	0.06	0.10
Defb36	defensin beta 36	17.48	30.28	0.02	0.04
Dmrtc1c	DMRT-like family C1c	21.97	17.61	0.04	0.07
Ednrb	endothelin receptor type B	516.74	507.39	10.85	9.38
Ehd3	EH-domain containing 3	171.34	158.14	6.69	3.47
Eva1a	eva-1 homolog A	27.63	22.13	2.05	1.16
Fam46a	family with sequence similarity 46, member A	80.48	50.59	9.07	6.09
Flvcr2	feline leukemia virus subgroup C cellular receptor family, member 2	40.77	9.82	11.03	13.67
Fndc3c1	fibronectin type III domain containing 3C1	334.61	283.17	4.27	5.95
Fosl1	fos-like antigen 1	122.48	105.33	3.17	2.78
Gadd45b	growth arrest and DNA-damage-inducible, beta	62.71	27.29	6.81	1.75
Gata3	GATA binding protein 3	55.22	42.65	0.23	0.17
Gstm7	glutathione S-transferase, mu 7	1.73	0.99	0.17	0.04
Hap1	huntingtin-associated protein 1	3.11	2.73	0.17	0.25
Hdac5	histone deacetylase 5	51.48	39.33	3.17	4.37
Hs3st6	heparan sulfate (glucosamine) 3-O-sulfotransferase 6	50.63	52.92	0.00	0.00

Continued on next page

Table E.2 – continued from previous page

Gene symbol	Gene name	Decidua TPM	Decidua ±SD	Outer myometrium TPM	Outer myometrium ±SD
Hsd17b3	hydroxysteroid (17-beta) dehydrogenase 3	13.06	11.37	0.07	0.11
Il17f	interleukin 17F	28.40	22.11	0.01	0.01
Il2rg	interleukin 2 receptor, gamma	143.59	102.85	7.46	3.01
Inhba	inhibin beta-A	364.85	331.45	19.58	13.86
Kcnh6	potassium voltage-gated channel, subfamily H (eag-related), member 6	6.49	8.92	0.00	0.00
Lamc2	laminin, gamma 2	62.78	23.21	9.20	7.10
Limk2	LIM domain kinase 2	85.59	22.40	8.30	4.86
LOC171573	spleen protein 1 precursor	8126.30	5720.53	11.65	16.42
LOC690326	hypothetical protein LOC690326	32.78	31.45	0.29	0.34
Lpcat1	lysophosphatidylcholine acyltransferase 1	26.31	11.26	3.67	1.08
Matn1	matrilin 1, cartilage matrix protein	10.55	18.27	0.03	0.02
Mmd	monocyte to macrophage differentiation-associated	43.19	14.97	7.46	5.59
Mycbpap	Mycbp associated protein	25.23	20.91	0.58	0.55
Nhs	Nance-Horan syndrome (congenital cataracts and dental anomalies)	20.20	14.59	1.24	0.55
Prl3b1	Prolactin family 3, subfamily b, member 1	1101.88	1204.17	8.37	7.25
Prl3d2	Prolactin family 3, subfamily d, member 2	159.94	10.16	0.01	0.01
Prl3d4	prolactin family 3, subfamily d, member 4	3699.29	2139.84	2.97	3.25
Prl7a3	prolactin family 7, subfamily a, member 3	1082.68	833.63	8.12	11.71
Prl8a2	prolactin family 8, subfamily a, member 2	2395.37	1633.06	9.43	14.20
Prl8a5	prolactin family 8, subfamily a, member 5	14633.75	9552.24	33.75	47.10
Prl8a7	prolactin family 8, subfamily a, member 7	32217.60	12642.42	75.88	92.91
Prl8a9	prolactin family 8, subfamily a, member 9	12359.02	5600.73	130.85	214.95
RGD1563945	jade family PHD finger 3	29.69	19.24	2.65	0.80
RGD1564534	similar to CHCHD4 protein	42.37	29.80	1.02	1.12
Rilpl1	Rab interacting lysosomal protein-like 1	70.36	40.96	9.34	6.72
Rnf128	ring finger protein 128, E3 ubiquitin protein ligase	218.27	152.89	5.15	5.61
Sdf2l1	stromal cell-derived factor 2-like 1	83.98	28.92	12.36	5.93
Sfmbt2	Scm-like with four mbt domains 2	166.02	166.99	8.09	12.08
Sftpa1	surfactant protein A1	52.11	34.85	0.08	0.09
Sgce	sarcoglycan, epsilon	167.09	141.12	11.00	12.27
Sipa1l2	signal-induced proliferation-associated 1 like 2	62.47	38.98	5.78	2.87
Slc25a25	solute carrier family 25, member 25 (mitochondrial carrier, phosphate carrier)	26.37	15.61	4.76	0.85
Slc29a1	solute carrier family 29, member 1 (equilibrative nucleoside transporter)	52.80	25.15	3.28	2.13
Slc38a4	solute carrier family 38, member 4	874.15	742.95	7.88	8.64
Slc6a2	solute carrier family 6 (neurotransmitter transporter), member 2	28.18	10.80	0.83	0.71
Slco5a1	solute carrier organic anion transporter family, member 5A1	36.21	29.99	3.16	1.49
Syn3	synapsin III	11.33	8.29	0.05	0.05
Tbc1d2	TBC1 domain family, member 2	69.99	58.57	7.81	3.59
Tgfb3	transforming growth factor, beta 3	237.04	127.64	19.51	3.51
Thrsp	thyroid hormone responsive	8.09	6.06	0.24	0.19
Tmem37	transmembrane protein 37	277.58	197.93	4.03	2.88
Trh	thyrotropin releasing hormone	412.51	442.62	1.49	1.31
Unc5b	unc-5 homolog B (C. elegans)	97.07	85.26	6.70	1.38
Utf1	undifferentiated embryonic cell transcription factor 1	21.73	21.43	0.00	0.00
Vmo1	vitelline membrane outer layer 1 homolog (chicken)	12.23	8.87	0.00	0.00
Wdr62	WD repeat domain 62	38.11	30.64	2.43	1.16
Wdr7	WD repeat domain 7	16.83	15.34	1.65	1.66
Wfdc6a	WAP four-disulfide core domain 6A	3.74	3.27	0.01	0.01
Zbtb44	zinc finger and BTB domain containing 44	35.77	20.54	6.53	5.18
Zp1	zona pellucida glycoprotein 1 (sperm receptor)	9.93	10.00	0.01	0.01

Table E.3: Gene transcripts that were differentially expressed following treatment with RU486 in the inner myometrium compared to the decidua on GD20. Transcript expression levels are shown in transcripts per million (TPM) values (mean±SD).

Gene symbol	Gene name	Decidua TPM	Decidua ±SD	Inner myometrium TPM	Inner myometrium ±SD
Upregulated in inner myometrium					
Chchd10	coiled-coil-helix-coiled-coil-helix domain containing 10	20.13	15.73	171.59	107.61
Fbln5	fibulin 5	10.56	4.41	102.02	66.08

Continued on next page

Table E.3 – continued from previous page

Gene symbol	Gene name	Decidua TPM	Decidua ±SD	Inner myometrium TPM	Inner myometrium ±SD
Figf	c-fos induced growth factor	5.36	3.56	182.25	167.75
Igsf10	immunoglobulin superfamily, member 10	0.66	0.55	16.41	0.43
Stox2	storkhead box 2	1.92	0.84	28.39	20.14
Down-regulated in inner myometrium					
Aif1l	allograft inflammatory factor 1-like	343.61	170.50	14.89	4.75
Anxa3	annexin A3	122.77	109.38	8.75	8.55
Anxa8	annexin A8	125.08	87.82	3.90	0.40
Ccl27	chemokine (C-C motif) ligand 27	282.50	125.39	5.10	2.79
Cdh3	cadherin 3	192.41	170.29	15.35	15.77
Cyp26b1	cytochrome P450, family 26, subfamily b, polypeptide 1	218.71	204.89	4.51	3.02
Doxl2	diamine oxidase-like protein 2	5.07	6.52	0.01	0.02
Efhd1	EF-hand domain family, member D1	55.55	33.46	0.29	0.16
Gata2	GATA binding protein 2	143.69	85.93	18.73	15.00
Gnat2	guanine nucleotide binding protein (G protein), alpha transducing activity polypeptide 2	70.65	58.68	0.01	0.02
Hyal4	hyaluronoglucosaminidase 4	2.69	2.82	0.17	0.13
Irx4	iroquois homeobox 4	29.28	4.52	0.14	0.15
Lamc2	laminin, gamma 2	59.38	15.58	3.45	1.86
Mfap5	microfibrillar associated protein 5	119.62	95.81	3.43	2.21
Mrgprg	MAS-related GPR, member G	37.67	21.48	0.12	0.07
Nsg2	neuron specific gene family member 2	85.79	71.77	1.77	0.85
Pgf	placental growth factor	439.87	469.80	6.77	6.70
Prl3d4	prolactin family 3, subfamily d, member 4	1118.79	879.35	13.28	12.32
Prl7a3	prolactin family 7, subfamily a, member 3	566.61	496.56	4.53	4.00
Prl8a2	prolactin family 8, subfamily a, member 2	1046.66	498.79	13.20	6.32
Prl8a7	prolactin family 8, subfamily a, member 7	4599.90	3495.08	69.14	79.56
Procr	protein C receptor, endothelial	104.44	64.93	4.17	3.19
Psg16	pregnancy specific glycoprotein 16	267.78	315.01	6.37	7.44
Rnf128	ring finger protein 128, E3 ubiquitin protein ligase	84.23	35.20	8.31	5.60
Sbsn	suprabasin	670.74	589.50	15.18	16.93
Slc38a4	solute carrier family 38, member 4	203.93	212.16	11.89	7.50
Slc6a12	solute carrier family 6, member 12 (neurotransmitter transporter)	840.73	752.38	10.61	6.46
Tfpi	tissue factor pathway inhibitor (lipoprotein-associated coagulation inhibitor)	987.46	452.11	45.64	14.11

Table E.4: Gene transcripts that were differentially expressed following treatment with RU486 in the outer myometrium compared to the decidua on GD20. Transcript expression levels are shown in transcripts per million (TPM) values (mean±SD).

Gene symbol	Gene name	Decidua TPM	Decidua ±SD	Outer myometrium TPM	Outer myometrium ±SD
Upregulated in outer myometrium					
Irx1	iroquois homeobox 1	0.02	0.03	8.54	7.36
Down-regulated in outer myometrium					
Irx1	iroquois homeobox 1	0.02	0.03	8.54	7.36
Pzp	pregnancy-zone protein	79.83	137.85	0.55	0.63
Mmp10	matrix metallopeptidase 10 (stromelysin 2)	97.79	101.48	2.97	2.46
Rrm1	ribonucleotide reductase M1	159.00	117.95	11.08	9.76
Mt1a	metallothionein 1a	979.42	285.58	142.14	60.40
Slc6a12	solute carrier family 6, member 12 (neurotransmitter transporter)	840.73	752.38	10.60	15.12
Pgf	placental growth factor	439.87	469.80	12.00	17.81
Ehd3	EH-domain containing 3	496.17	437.17	32.14	24.67

Table E.5: Gene transcripts that were differentially expressed following treatment with RU486 in the outer myometrium compared to the inner myometrium on GD20. Transcript expression levels are shown in transcripts per million (TPM) values (mean±SD).

		Inner myometrium		Outer myometrium	
Gene symbol	Gene name	TPM	±SD	TPM	±SD
Upregulated in outer myometrium					
Prl8a2	prolactin family 8, subfamily a, member 2	221.96	355.86	814.23	1407.10
Psgb1	pregnancy-specific beta 1-glycoprotein	9.42	6.60	247.71	426.97
Ctsq	cathepsin Q	2.51	2.18	238.80	412.27
Prl7a3	prolactin family 7, subfamily a, member 3	91.12	146.43	193.09	301.74
Taf7l	TAF7-like RNA polymerase II, TATA box binding protein (TBP)-associated factor	9.59	6.48	99.41	154.73
Ctsm	cathepsin M	2.68	2.47	69.34	116.76
Ins2	insulin 2	0.41	0.71	62.95	87.82
Sftpc	surfactant protein C	0.19	0.32	57.37	98.75
Serpinb9d	serine (or cysteine) peptidase inhibitor, clade B, member 9d	0.16	0.17	46.61	69.33
Lrp2	low density lipoprotein receptor-related protein 2	0.80	0.94	22.66	30.41
Sftpb	surfactant protein B	0.00	0.00	20.10	33.75
Cubn	cubilin (intrinsic factor-cobalamin receptor)	0.20	0.11	14.61	16.24
Glp1r	glucagon-like peptide 1 receptor	0.15	0.12	3.84	4.62
Tbx5	T-box 5	0.00	0.00	3.57	3.86
Aloxe3	arachidonate lipoxygenase 3	0.00	0.00	3.33	5.26
Down-regulated in outer myometrium					
Apcs	amyloid P component, serum	7.95	13.76	0.00	0.00
Clec4f	C-type lectin domain family 4, member F	2.29	3.96	0.00	0.00
Crp	C-reactive protein, pentraxin-related	24.65	42.70	0.00	0.00
Ctsg	cathepsin G	7.02	12.15	0.00	0.00
Agr2	anterior gradient 2	11.75	20.35	0.01	0.02
Aspdh	aspartate dehydrogenase domain containing	6.25	10.82	0.10	0.17
Dpys	dihydropyrimidinase	4.24	7.26	0.10	0.08
Nefl	neurofilament, light polypeptide	2.69	4.54	0.31	0.32
Pzp	pregnancy-zone protein	209.84	362.79	0.55	0.63
Cldn1	claudin 1	30.78	53.05	1.06	0.53
Hpx	hemopexin	161.40	277.84	1.59	1.63
Vtn	vitronectin	255.66	439.88	2.00	0.74
Plg	plasminogen	216.20	373.49	3.20	3.04
Hdc	histidine decarboxylase	315.63	545.31	3.35	2.09
Igfbp1	insulin-like growth factor binding protein 1	152.42	263.60	3.41	4.54
Slc36a2	solute carrier family 36, member 2 (proton/amino acid symporter)	4.68	7.93	4.36	7.31
Fetub	fetuin B	278.59	481.09	4.83	5.94
Aldob	aldolase B, fructose-bisphosphate	338.37	584.28	4.84	5.44
Gc	group specific component	142.65	246.56	5.34	4.60
Hist1h1b	histone cluster 1, H1b	341.16	572.03	23.50	4.44
Serpinf2	serpin peptidase inhibitor, clade F (alpha-2 antiplasmin, pigment epithelium derived factor), member 2	105.75	182.30	77.12	129.15

E.1 Temporal Expression Patterns

Table E.6: Gene transcripts that were differentially expressed in RU486-treated decidua between GD19+6hrs and GD20. Transcript expression levels are shown in transcripts per million (TPM) values (mean±SD).

		GD19+6hrs		GD20	
Gene symbol	Gene name	TPM	±SD	TPM	±SD
Upregulated on GD20					
Apoa1	apolipoprotein A-I	2.04	1.26	767.55	1319.41

Continued on next page

Table E.6 – continued from previous page

Gene symbol	Gene name	GD19+6hrs TPM	GD19+6hrs ±SD	GD20 TPM	GD20 ±SD
Actg2	actin, gamma 2, smooth muscle, enteric	25.57	15.60	758.45	368.90
Fgg	fibrinogen gamma chain	2.23	1.56	608.78	1054.08
Fgb	fibrinogen beta chain	1.86	0.80	515.52	891.80
Myl9	myosin, light chain 9, regulatory	29.60	44.99	382.53	246.39
Acta2	actin, alpha 2, smooth muscle, aorta	6.78	5.26	264.47	146.50
Aldob	aldolase B, fructose-bisphosphate	1.24	0.72	239.98	414.93
Rbp4	retinol binding protein 4, plasma	2.35	1.03	238.32	409.14
Ambp	alpha-1-microglobulin/bikunin precursor	1.09	0.87	223.74	387.53
Hdc	histidine decarboxylase	1.01	0.27	163.80	283.27
Hp	haptoglobin	3.03	3.64	143.68	240.74
Cnn1	calponin 1, basic, smooth muscle	5.21	3.93	116.59	26.05
Cps1	carbamoyl-phosphate synthetase 1	0.50	0.13	97.69	169.17
Hamp	hepcidin antimicrobial peptide	0.01	0.01	91.15	157.88
Myh11	myosin, heavy chain 11, smooth muscle	4.39	3.36	84.29	29.92
Ins2	insulin 2	0.00	0.00	61.79	102.12
Phlda3	pleckstrin homology-like domain, family A, member 3	0.60	0.55	45.70	28.78
Hpd	4-hydroxyphenylpyruvate dioxygenase	0.08	0.08	27.47	47.35
Vnn1	vanin 1	0.94	0.30	27.31	23.43
Kirrel	kin of IRRE like (Drosophila)	0.43	0.21	24.60	9.39
Cpn1	carboxypeptidase N, polypeptide 1	0.00	0.00	12.50	21.66
Gnmt	glycine N-methyltransferase	0.04	0.07	11.88	20.57
Slc13a3	solute carrier family 13, member 3 (sodium-dependent dicarboxylate transporter)	0.09	0.10	10.58	18.15
Rassf6	Ras association (RalGDS/AF-6) domain family member 6	0.23	0.02	9.32	14.80
Lurap1l	leucine rich adaptor protein 1-like	0.01	0.02	6.82	7.39
Pllp	plasmolipin	0.02	0.04	6.05	8.26
Ggt5	gamma-glutamyltransferase 5	0.00	0.00	5.22	6.88
G6pc	glucose-6-phosphatase, catalytic subunit	0.01	0.01	4.33	7.49
Down-regulated on GD20					
Il2rg	interleukin 2 receptor, gamma	143.59	102.85	20.06	8.57
Prl3d2	Prolactin family 3, subfamily d, member 2	159.94	10.16	21.62	29.80

Table E.7: Gene transcripts that were differentially expressed in RU486-treated inner myometrium between GD19+6hrs and GD20. Transcript expression levels are shown in transcripts per million (TPM) values (mean±SD).

Gene symbol	Gene name	GD19+6hrs TPM	GD19+6hrs ±SD	GD20 TPM	GD20 ±SD
Upregulated on GD20					
Aass	aminoadipate-semialdehyde synthase	0.00	0.00	2.43	4.19
Aldob	aldolase B, fructose-bisphosphate	1.29	0.57	338.12	584.50
Ambp	alpha-1-microglobulin/bikunin precursor	2.12	1.84	296.30	512.15
Amdhd1	amidohydrolase domain containing 1	0.05	0.09	7.38	12.64
Apcs	amyloid P component, serum	0.00	0.00	7.95	13.76
Bhmt2	betaine-homocysteine S-methyltransferase 2	0.00	0.00	11.39	19.67
C8b	complement component 8, beta polypeptide	0.00	0.00	23.04	39.90
Camp	cathelicidin antimicrobial peptide	0.00	0.00	9.35	16.13
Cpn2	carboxypeptidase N, polypeptide 2	0.03	0.06	8.75	15.16
Cps1	carbamoyl-phosphate synthetase 1	0.50	0.44	109.00	188.21
Crp	C-reactive protein, pentraxin-related	0.05	0.09	24.69	42.67
Ctsg	cathepsin G	0.02	0.04	7.02	12.15
Cyp2d2	cytochrome P450, family 2, subfamily d, polypeptide 2	0.00	0.00	8.95	15.43
Dpys	dihydropyrimidinase	0.07	0.12	4.23	7.27
F10	coagulation factor X	0.00	0.00	15.93	25.69
F11	coagulation factor XI	0.15	0.05	6.50	11.16
F13b	coagulation factor XIII, B polypeptide	0.00	0.00	8.62	14.92
Fetub	fetuin B	1.90	1.90	278.67	481.02
Fgb	fibrinogen beta chain	2.21	2.01	415.60	716.50
Gc	group specific component	1.14	0.95	142.71	246.51
Grem2	gremlin 2	0.00	0.00	2.81	4.48
Hdc	histidine decarboxylase	1.99	0.37	315.80	545.16

Continued on next page

Table E.7 – continued from previous page

Gene symbol	Gene name	GD19+6hrs TPM	GD19+6hrs ±SD	GD20 TPM	GD20 ±SD
Hpd	4-hydroxyphenylpyruvate dioxygenase	0.00	0.00	32.67	56.41
Ly6c	Ly6-C antigen	0.09	0.10	16.81	9.79
Mep1a	meprin 1 alpha	0.00	0.00	4.11	6.80
Mmp11	matrix metallopeptidase 11	35.32	29.27	1023.38	759.76
Onecut1	one cut homeobox 1	0.22	0.19	7.84	12.86
Pah	phenylalanine hydroxylase	0.00	0.00	5.38	9.27
Pbld1	phenazine biosynthesis-like protein domain containing 1	3.77	6.53	3.77	5.90
Pon1	paraoxonase 1	1.49	2.58	5.03	8.72
Ppargc1a	peroxisome proliferator-activated receptor gamma, coactivator 1 alpha	1.32	2.29	6.20	8.70
Prodh2	proline dehydrogenase (oxidase) 2	0.00	0.00	12.38	21.44
Samd10	sterile alpha motif domain containing 10	0.06	0.05	6.83	3.95
Sbk1	SH3 domain binding kinase 1	0.68	1.18	5.25	0.68
Scg2	secretogranin II	1.26	2.18	2.24	1.10
Serpinb10	serpin peptidase inhibitor, clade B (ovalbumin), member 10	0.00	0.00	8.50	13.94
Sgpp2	sphingosine-1-phosphate phosphatase 2	0.28	0.49	6.58	11.39
Slamf7	SLAM family member 7	0.00	0.00	4.70	1.56
Slc14a1	solute carrier family 14 (urea transporter), member 1	0.01	0.02	10.74	14.41
Slc17a1	solute carrier family 17 (organic anion transporter), member 1	0.00	0.00	8.96	15.52
St8sia3	ST8 alpha-N-acetyl-neuraminide alpha-2,8-sialyltransferase 3	0.00	0.00	7.53	13.05
Tfr2	transferrin receptor 2	0.00	0.00	19.04	32.89
Tnni1	troponin I type 1 (skeletal, slow)	0.00	0.00	13.73	23.55
Trim10	tripartite motif-containing 10	0.81	0.22	14.08	22.17
Trim58	tripartite motif-containing 58	0.00	0.00	10.91	18.90
Tsx	testis specific X-linked gene	0.00	0.00	8.25	13.90
Ttpa	tocopherol (alpha) transfer protein	0.00	0.01	8.46	14.34
Vcam1	vascular cell adhesion molecule 1	1.39	0.81	18.21	11.76
Vtn	vitronectin	2.18	0.58	256.49	439.16
Down-regulated on GD20					
Cbln1	cerebellin 1 precursor	4.06	5.90	0.01	0.02
Ctsq	cathepsin Q	254.32	395.88	2.75	1.78
Gjb2	gap junction protein, beta 2	400.71	88.75	37.84	43.46
Kank1	KN motif and ankyrin repeat domains 1	29.77	29.80	10.81	2.73
Lgals4	lectin, galactoside-binding, soluble, 4	83.96	145.32	18.88	32.70
Lrp2	low density lipoprotein receptor-related protein 2	12.97	13.22	0.80	0.93
Mcam	melanoma cell adhesion molecule	158.70	180.92	22.11	9.28
Ndufaf3	NADH dehydrogenase (ubiquinone) complex I, assembly factor 3	57.34	23.72	11.93	8.86
Ppl	periplakin	22.63	17.84	7.96	5.48
Sgcg	sarcoglycan, gamma (dystrophin-associated glycoprotein)	8.93	15.28	0.00	0.00

Table E.8: Gene transcripts that were differentially expressed in RU486-treated outer myometrium between GD19+6hrs and GD20. Transcript expression levels are shown in transcripts per million (TPM) values (mean±SD).

Gene symbol	Gene name	GD19+6hrs TPM	GD19+6hrs ±SD	GD20 TPM	GD20 ±SD
Upregulated on GD20					
Apoa1	apolipoprotein A-I	17.43	19.35	699.44	937.94
Psg29	pregnancy-specific glycoprotein 29	1.34	1.13	466.71	801.10
Cldn4	claudin 4	2.68	2.35	268.77	456.88
Ins2	insulin 2	0.02	0.04	62.95	87.82
Cldn6	claudin 6	3.96	1.77	50.61	68.38
Ptges	prostaglandin E synthase	0.00	0.00	25.58	42.75
Utf1	undifferentiated embryonic cell transcription factor 1	0.00	0.00	20.30	32.88
Pax1	paired box 1	0.06	0.10	12.16	10.94

Continued on next page

Table E.8 – continued from previous page

Gene symbol	Gene name	GD19+6hrs TPM	GD19+6hrs ±SD	GD20 TPM	GD20 ±SD
Slc22a3	solute carrier family 22, member 3 (organic cation transporter)	0.00	0.00	4.33	7.10
Grip2	glutamate receptor interacting protein 2	0.05	0.08	3.98	5.98
Down-regulated on GD20					
Slc4a11	solute carrier family 4, sodium borate transporter, member 11	119.21	102.23	3.18	3.33
Lcn2	lipocalin 2	366.02	435.02	4.25	3.63
Mmp1a	matrix metallopeptidase 1 (interstitial collagenase)	95.74	165.74	4.55	6.69
Pcsk6	proprotein convertase subtilisin/kexin type 6	57.97	36.35	6.98	7.57

E.2 Comparison with Control Tissues

Table E.9: Gene transcripts that were differentially expressed in response to treatment with RU486 in the decidua. Comparisons were made between transcript expression in control tissues obtained on GD19+6hrs and transcript expression in RU486-treated tissues obtained on GD19+6hrs. Transcript expression levels are shown in transcripts per million (TPM) values (mean±SD).

Gene symbol	Gene name	GD19+6hrs Control TPM	GD19+6hrs Control ±SD	GD19+6hrs RU486 TPM	GD19+6hrs RU486 ±SD
Upregulated in RU486-treated tissue					
Creg1	cellular repressor of E1A-stimulated genes 1	167.41	159.25	2259.82	1605.20
Fkbp11	FK506 binding protein 11	15.34	7.43	78.75	60.49
Slit1	slit homolog 1 (Drosophila)	3.67	3.13	37.60	36.10
Alb	albumin	1.74	1.62	29.41	22.63
Defb36	defensin beta 36	0.00	0.00	17.48	30.28
Matn1	matrilin 1, cartilage matrix protein	0.11	0.20	10.55	18.27
Zp1	zona pellucida glycoprotein 1 (sperm receptor)	0.02	0.04	9.93	10.00
Lect1	leukocyte cell derived chemotaxin 1	1.26	2.03	6.31	10.94
Down-regulated in RU486-treated tissue					
Clrn3	clarin 3	4.33	1.81	0.00	0.00
Ins2	insulin 2	27.87	35.55	0.00	0.00
Asic3	acid-sensing (proton-gated) ion channel 3	5.60	4.48	0.01	0.01
Bend7	BEN domain containing 7	1.83	1.17	0.01	0.02
Rgs1	regulator of G-protein signaling 1	2.50	3.48	0.01	0.02
Abcc8	ATP-binding cassette, subfamily C (CFTR/MRP), member 8	5.67	4.81	0.02	0.03
Pllp	plasmolipin	2.60	2.50	0.02	0.04
Tnni1	troponin I type 1 (skeletal, slow)	7.08	4.18	0.03	0.03
Hgd	homogentisate 1, 2-dioxygenase	0.85	0.76	0.03	0.04
Ace2	angiotensin I converting enzyme 2	8.28	3.87	0.06	0.10
Pdzk1ip1	PDZK1 interacting protein 1	25.36	22.95	0.06	0.06
Mybpc3	myosin binding protein C, cardiac	9.94	2.49	0.07	0.13
Slc22a3	solute carrier family 22 (organic cation transporter), member 3	2.36	3.10	0.09	0.08
Tm4sf20	transmembrane 4 L six family member 20	6.12	3.31	0.09	0.06
Slc13a3	solute carrier family 13 (sodium-dependent dicarboxylate transporter), member 3	5.07	6.80	0.09	0.10
RGD1305807	hypothetical LOC298077	2.14	2.08	0.09	0.16
Gcm1	glial cells missing homolog 1 (Drosophila)	8.82	6.00	0.09	0.09
Wnk3	WNK lysine deficient protein kinase 3	5.15	1.00	0.12	0.12
Ephx1	epoxide hydrolase 1, microsomal (xenobiotic)	5.28	1.37	0.13	0.06
Apoc2	apolipoprotein C-II	73.03	57.13	0.13	0.03
Hnf4a	hepatocyte nuclear factor 4, alpha	5.87	1.83	0.15	0.14
Heph	hephaestin	1.47	1.38	0.17	0.19
Psat1	phosphoserine aminotransferase 1	3.73	3.25	0.17	0.15
Slc2a2	solute carrier family 2 (facilitated glucose transporter), member 2	5.37	3.33	0.19	0.04
Kitlg	KIT ligand	21.69	19.14	0.20	0.19
Apoa2	apolipoprotein A-II	255.70	230.37	0.21	0.36
Proc	protein C	279.51	466.82	0.22	0.20

Continued on next page

Table E.9 – continued from previous page

Gene symbol	Gene name	GD19+6hrs Control		GD19+6hrs RU486	
		TPM	±SD	TPM	±SD
Rbp1	retinol binding protein 1, cellular	13.18	11.46	0.22	0.17
Rassf6	Ras association (RalGDS/AF-6) domain family member 6	4.58	2.98	0.23	0.02
Fmo1	flavin containing monooxygenase 1	16.56	6.65	0.25	0.16
Aqp8	aquaporin 8	15.88	8.58	0.26	0.19
Adtrp	androgen-dependent TFPI-regulating protein	12.39	4.12	0.29	0.27
F2	coagulation factor II	38.52	19.11	0.30	0.12
Rps6ka6	ribosomal protein S6 kinase polypeptide 6	9.10	3.19	0.30	0.25
Slc22a23	solute carrier family 22, member 23	7.98	7.51	0.32	0.33
Fxyd2	FXYD domain-containing ion transport regulator 2	23.85	15.48	0.33	0.58
B4galnt3	beta-1,4-N-acetyl-galactosaminyl transferase 3	9.43	5.75	0.37	0.21
Gcgr	glucagon receptor	15.08	6.49	0.37	0.27
RGD1309313	similar to RIKEN cDNA 4930538D17	14.46	8.70	0.39	0.60
Gucy2c	guanylate cyclase 2C	3.11	0.95	0.41	0.10
Slco4a1	solute carrier organic anion transporter family, member 4a1	18.89	16.96	0.41	0.30
RGD1563547	RGD1563547	1.98	1.38	0.41	0.24
Kirrel	kin of IRRE like (Drosophila)	5.45	4.75	0.43	0.21
Epb41l3	erythrocyte membrane protein band 4.1-like 3	8.87	4.67	0.44	0.33
RGD1305347	similar to RIKEN cDNA 2610528J11	14.43	14.65	0.46	0.42
Apon	apolipoprotein N	4.06	3.19	0.49	0.10
Cubn	cubilin (intrinsic factor-cobalamin receptor)	34.90	17.01	0.50	0.53
Ervfrd.1	endogenous retrovirus group FRD, member 1	13.85	8.64	0.54	0.44
Tns4	tensin 4	29.34	16.37	0.56	0.53
Lrp2	low density lipoprotein receptor-related protein 2	31.12	15.16	0.57	0.14
Apom	apolipoprotein M	87.18	33.70	0.58	0.45
Spp2	secreted phosphoprotein 2	100.64	96.49	0.59	0.11
Phlda3	pleckstrin homology-like domain, family A, member 3	23.65	11.12	0.60	0.55
Afap1l1	actin filament associated protein 1-like 1	10.31	3.97	0.60	0.40
Gc	group specific component	10.20	5.38	0.61	0.24
Phlda2	pleckstrin homology-like domain, family A, member 2	15.88	18.86	0.62	0.54
Akr1e2	aldo-keto reductase family 1, member E2	9.77	2.96	0.65	0.74
Slc13a4	solute carrier family 13 (sodium/sulfate symporter), member 4	33.43	16.92	0.80	1.02
Tst	thiosulfate sulfurtransferase	28.25	10.97	0.84	0.25
Aadat	aminoadipate aminotransferase	20.54	12.08	0.89	1.03
Vnn1	vanin 1	17.52	3.75	0.94	0.30
Apob	apolipoprotein B	535.64	256.06	0.97	0.24
Crip1	cysteine-rich protein 1 (intestinal)	38.08	22.05	1.14	1.58
Stbd1	starch binding domain 1	12.37	8.98	1.15	0.39
S100a16	S100 calcium binding protein A16	12.97	3.04	1.27	1.71
Ctsc	cathepsin C	39.64	19.99	1.27	1.07
Cdh1	cadherin 1	60.65	26.14	1.45	0.80
Depdc7	DEP domain containing 7	13.42	3.79	1.52	0.99
S100g	S100 calcium binding protein G	71.45	76.21	1.52	1.50
Pdpn	podoplanin	31.84	19.37	1.68	1.68
Mlxipl	MLX interacting protein-like	7.69	3.92	1.79	2.11
Cspg5	chondroitin sulfate proteoglycan 5 (neuroglycan C)	3.59	2.27	1.80	1.59
Fgb	fibrinogen beta chain	33.96	11.46	1.86	0.80
Apoa1	apolipoprotein A-I	651.04	422.62	2.04	1.26
Ttr	transthyretin	660.29	525.55	2.20	1.29
MGC114246	similar to cathepsin R	33.80	20.69	2.23	1.00
Fgg	fibrinogen gamma chain	42.01	21.19	2.23	1.56
Rbp4	retinol binding protein 4, plasma	126.35	153.08	2.35	1.03
Car4	carbonic anhydrase 4	72.54	35.73	2.38	1.81
Padi3	peptidyl arginine deiminase, type III	285.62	494.62	2.75	2.25
Fga	fibrinogen alpha chain	78.63	39.83	2.86	1.92
Klf5	Kruppel-like factor 5	35.75	25.56	3.15	2.01
Npl	N-acetylneuraminate pyruvate lyase	30.75	19.15	3.27	1.87
Tns3	tensin 3	29.83	11.50	3.72	1.48
F2rl1	coagulation factor II (thrombin) receptor-like 1	15.96	3.91	5.06	6.17
Hsd17b2	hydroxysteroid (17-beta) dehydrogenase 2	104.89	142.55	7.97	8.11
Sepp1	selenoprotein P, plasma, 1	119.39	108.66	8.85	9.59
Afp	alpha-fetoprotein	2331.59	1656.67	15.58	10.49
Ctsql2	cathepsin Q-like 2	996.54	599.53	16.86	16.46
Ctsq	cathepsin Q	206.52	82.99	19.77	14.49
Apoa4	apolipoprotein A-IV	213.84	113.78	23.92	2.78
Ctsr	cathepsin R	955.05	500.72	28.19	18.16

Table E.10: Gene transcripts that were differentially expressed in response to treatment with RU486 in the inner myometrium. Comparisons were made between transcript expression in control tissues obtained on GD19+6hrs and transcript expression in RU486-treated tissues obtained on GD19+6hrs. Transcript expression levels are shown in transcripts per million (TPM) values (mean±SD).

		GD19+6hrs Control		GD19+6hrs RU486	
Gene symbol	Gene name	TPM	±SD	TPM	±SD
Upregulated in RU486-treated tissue					
Lcn2	lipocalin 2	2.43	2.87	3.12	2.73
Down-regulated in RU486-treated tissue					
Fam71f2	family with sequence similarity 71, member F2	2.05	2.88	0.00	0.00

Table E.11: Gene transcripts that were differentially expressed in response to treatment with RU486 in the outer myometrium. Comparisons were made between transcript expression in control tissues obtained on GD19+6hrs and transcript expression in RU486-treated tissues obtained on GD19+6hrs. Transcript expression levels are shown in transcripts per million (TPM) values (mean±SD).

		GD19+6hrs Control		GD19+6hrs RU486	
Gene symbol	Gene name	TPM	±SD	TPM	±SD
Upregulated in RU486-treated tissue					
Spp1	secreted phosphoprotein 1	27.88	22.27	889.53	771.63
Kap	kidney androgen regulated protein	9.83	12.09	713.32	665.47
Isyna1	inositol-3-phosphate synthase 1	25.10	12.58	684.90	600.84
Guca2b	guanylate cyclase activator 2B	6.77	11.55	631.78	688.46
Lcn2	lipocalin 2	9.09	12.62	366.02	435.02
C3	complement component 3	6.39	1.02	328.78	314.39
Lrat	lecithin-retinol acyltransferase (phosphatidylcholine-retinol-O-acyltransferase)	1.56	1.26	101.55	97.13
Slc4a11	solute carrier family 4, member 11 (sodium borate transporter)	1.86	2.84	33.47	42.01
Defb1	defensin beta 1	0.00	0.00	31.84	38.48
Cldn10	claudin 10	1.01	1.41	27.51	23.67
Upk3bl	uroplakin 3B-like	0.00	0.00	22.32	26.61
Kif12	kinesin family member 12	0.09	0.16	13.03	11.29
Slc17a3	solute carrier family 17, member 3 (organic anion transporter)	0.20	0.16	7.16	6.87
Down-regulated in RU486-treated tissue					
Hs3st6	heparan sulfate (glucosamine) 3-O-sulfotransferase 6	18.57	31.97	0.00	0.00
Ptges	prostaglandin E synthase	43.71	39.21	0.00	0.00
Slc22a3	solute carrier family 2, member 3 (organic cation transporter)	6.20	10.70	0.00	0.00
Ebf2	early B-cell factor 2	5.93	5.73	0.04	0.04
Pax1	paired box 1	14.59	19.58	0.06	0.10
Psg16	pregnancy specific glycoprotein 16	198.30	340.80	1.16	1.52
Psg29	pregnancy-specific glycoprotein 29	406.70	686.64	1.34	1.13
Dlk1	delta-like 1 homolog (Drosophila)	512.71	887.85	2.13	1.55
Atg9b	autophagy related 9B	26.36	45.65	7.77	6.84

Table E.12: Gene transcripts that were differentially expressed in response to treatment with RU486 in the decidua. Comparisons were made between transcript expression in control tissues obtained on GD20 and transcript expression in RU486-treated tissues obtained on GD20. Transcript expression levels are shown in transcripts per million (TPM) values (mean±SD).

		GD20 Control		GD20 RU486	
Gene symbol	Gene name	TPM	±SD	TPM	±SD
Down-regulated in RU486-treated tissue					

Continued on next page

Table E.12 – continued from previous page

Gene symbol	Gene name	GD20 Control TPM	GD20 Control ±SD	GD20 RU486 TPM	GD20 RU486 ±SD
Hsd11b2	hydroxysteroid 11-beta dehydrogenase 2	309.05	301.48	12.11	5.17
Ogdhl	oxoglutarate dehydrogenase-like	17.81	16.91	2.13	1.77

Table E.13: Gene transcripts that were differentially expressed in response to treatment with RU486 in the inner myometrium. Comparisons were made between transcript expression in control tissues obtained on GD20 and transcript expression in RU486-treated tissues obtained on GD20. Transcript expression levels are shown in transcripts per million (TPM) values (mean±SD).

Gene symbol	Gene name	GD20 Control TPM	GD20 Control ±SD	GD20 RU486 TPM	GD20 RU486 ±SD
Upregulated in RU486-treated tissue					
Rnase1	ribonuclease, RNase A family, 1 (pancreatic)	4.73	4.61	402.21	586.18
Hdc	histidine decarboxylase	0.97	0.32	315.80	545.16
Plg	plasminogen	2.31	1.84	216.14	373.54
Pzp	pregnancy-zone protein	0.66	0.29	209.88	362.76
Myh10	myosin, heavy chain 10, non-muscle	14.11	3.34	171.38	104.30
Serpinc1	serpin peptidase inhibitor, clade C (antithrombin), member 1	1.37	1.60	156.53	270.42
Fgl2	fibrinogen-like 2	3.16	3.78	154.06	138.88
Cps1	carbamoyl-phosphate synthetase 1	0.81	0.63	109.00	188.21
Itih4	inter-alpha-trypsin inhibitor heavy chain family, member 4	1.03	1.51	98.25	169.94
Bhmt	betaine-homocysteine S-methyltransferase 2	1.38	1.69	93.58	161.30
Cpox	coproporphyrinogen oxidase	2.54	0.41	88.22	140.65
Hamp	hepcidin antimicrobial peptide	0.00	0.00	41.80	72.09
Ikzf1	IKAROS family zinc finger 1	0.93	1.44	39.49	38.11
Stox2	storkhead box 2	1.26	0.76	28.39	20.14
Lgals4	lectin, galactoside-binding, soluble, 4	0.01	0.01	18.88	32.70
Tmem178a	transmembrane protein 178A	0.01	0.01	17.81	12.34
Nrgn	neurogranin	3.56	2.74	17.33	8.89
Krt20	keratin 20	0.00	0.00	17.28	29.92
A1cf	APOBEC1 complementation factor	0.00	0.00	14.00	24.25
Upb1	ureidopropionase, beta	0.00	0.00	13.87	24.02
Troap	trophinin associated protein	0.00	0.00	13.55	22.76
Ptgfr	prostaglandin F receptor	0.17	0.26	12.89	9.77
Prodh2	proline dehydrogenase (oxidase) 2	0.00	0.00	12.38	21.44
Gstm7	glutathione S-transferase, mu 7	0.18	0.23	12.18	20.42
Agr2	anterior gradient 2	0.00	0.00	11.77	20.33
Spc25	SPC25, NDC80 kinetochore complex component	0.01	0.02	10.21	15.94
Ccrl2	chemokine (C-C motif) receptor-like 2	0.01	0.03	10.15	10.49
RGD1559600	RGD1559600	0.02	0.04	10.11	17.52
C9	complement component 9	0.14	0.14	9.98	17.12
Camp	cathelicidin antimicrobial peptide	0.00	0.00	9.35	16.13
Msi1	musashi RNA-binding protein 1	0.01	0.02	9.13	6.95
Nags	N-acetylglutamate synthase	0.00	0.01	8.38	14.52
Apcs	amyloid P component, serum	0.00	0.00	7.95	13.76
Fabp7	fatty acid binding protein 7, brain	0.00	0.00	7.59	13.14
St8sia3	ST8 alpha-N-acetyl-neuraminide alpha-2,8-sialyltransferase 3	0.00	0.00	7.53	13.05
Zfp428	zinc finger protein 428	0.15	0.22	7.53	1.99
RGD1564614	similar to complement factor H-related protein	0.01	0.01	7.46	12.88
Amdhd1	amidohydrolase domain containing 1	0.00	0.00	7.38	12.64
Anxa13	annexin A13	0.00	0.00	7.26	12.57
Mamdc4	MAM domain containing 4	0.05	0.06	7.22	11.10
Ctsg	cathepsin G	0.00	0.00	7.02	12.15
Sgpp2	sphingosine-1-phosphate phosphatase 2	0.00	0.00	6.58	11.39
Prkg2	protein kinase, cGMP-dependent, type II	0.00	0.01	6.03	10.38
Pah	phenylalanine hydroxylase	0.00	0.00	5.38	9.27
Slamf7	SLAM family member 7	0.00	0.00	4.70	1.56
Nr1i2	nuclear receptor subfamily 1, group I, member 2	0.00	0.00	4.50	7.79
Cst7	cystatin F (leukocystatin)	0.02	0.03	4.49	2.62
Shisa3	shisa family member 3	0.00	0.00	4.31	7.47

Continued on next page

Table E.13 – continued from previous page

Gene symbol	Gene name	GD20 Control TPM	GD20 Control ±SD	GD20 RU486 TPM	GD20 RU486 ±SD
Dpys	dihydropyrimidinase	0.10	0.10	4.23	7.27
Igsf1	immunoglobulin superfamily, member 1	0.01	0.01	3.74	6.21
Gpr68	G protein-coupled receptor 68	0.00	0.00	2.50	1.44
Down-regulated in RU486-treated tissue					
Agtr1b	angiotensin II receptor, type 1b	1.90	3.27	0.00	0.00
Iapp	islet amyloid polypeptide	37.67	55.80	0.00	0.00
Ica1l	islet cell autoantigen 1-like	10.85	18.66	0.00	0.00
Nr0b2	nuclear receptor subfamily 0, group B, member 2	10.58	13.18	0.00	0.00
RGD1559493	similar to Hypothetical protein MGC58608	9.61	16.64	0.00	0.00
Sgcg	sarcoglycan, gamma (dystrophin-associated glycoprotein)	3.48	3.55	0.00	0.00
Syt6	synaptotagmin VI	9.02	15.04	0.00	0.00
Wfdc11	WAP four-disulfide core domain 11	8.88	9.60	0.00	0.00
Cbln1	cerebellin 1 precursor	3.21	5.55	0.01	0.02
Defb1	defensin beta 1	12.55	12.39	0.01	0.02
Col4a4	collagen, type IV, alpha 4	6.67	10.62	0.09	0.09
LOC688553	hypothetical protein LOC688553	20.63	15.17	0.26	0.24
Cubn	cubilin (intrinsic factor-cobalamin receptor)	12.35	19.70	0.31	0.11
Abcb1a	ATP-binding cassette, sub-family B (MDR/TAP), member 1A	22.81	23.92	0.65	0.44
Tshr	thyroid stimulating hormone receptor	15.08	15.69	0.70	0.17
Scel	sciellin	58.57	79.90	0.80	0.55
Lrp2	low density lipoprotein receptor-related protein 2	69.42	63.47	0.80	0.93
Abcb1b	ATP-binding cassette, subfamily B (MDR/TAP), member 1B	448.31	578.32	1.00	0.72
Ccdc64	coiled-coil domain containing 64	71.18	68.46	1.16	1.00
Tmprss4	transmembrane protease, serine 4	87.55	119.72	1.24	1.08
Pax8	paired box 8	161.20	170.81	1.29	0.16
Ehf	ets homologous factor	45.68	35.58	1.56	1.15
Cyb561	cytochrome b-561	67.28	100.58	1.66	1.66
Jag1	jagged 1	4.04	7.00	2.10	1.91
Pkib	protein kinase (cAMP-dependent, catalytic) inhibitor beta	41.81	55.26	2.49	1.05
Mab21l3	mab-21-like 3 (C. elegans)	38.50	33.49	2.49	0.92
Folr1	folate receptor 1 (adult)	87.37	83.78	2.52	0.79
Slc34a2	solute carrier family 34, member 2 (type II sodium/phosphate contransporter)	81.71	78.36	2.55	2.17
Ctsm	cathepsin M	167.78	254.19	2.68	2.46
Ctsq	cathepsin Q	307.15	382.03	2.75	1.78
Sgms2	sphingomyelin synthase 2	35.69	35.97	3.19	3.02
Lamc2	laminin, gamma 2	41.50	43.65	3.45	1.86
Slc5a3	solute carrier family 5, member 3 (sodium/myo-inositol cotransporter)	57.11	54.54	3.46	3.21
Kazn	kazrin, periplakin interacting protein	44.47	26.70	3.55	0.47
Chmp4c	charged multivesicular body protein 4C	32.78	30.89	3.84	1.97
Taf7l	TAF7-like RNA polymerase II, TATA box binding protein (TBP)-associated factor	132.46	211.15	3.97	3.45
Fut2	fucosyltransferase 2 (secretor status included)	175.95	215.98	4.11	5.59
Arhgef6	Rac/Cdc42 guanine nucleotide exchange factor 6	76.26	85.24	4.16	1.84
Slco4a1	solute carrier organic anion transporter family, member 4a1	277.95	180.45	4.17	1.51
Psgb1	pregnancy-specific beta 1-glycoprotein	368.01	616.85	4.18	4.30
Dysf	dysferlin	25.19	11.95	4.77	2.88
Tppp3	tubulin polymerization-promoting protein family member 3	77.74	70.19	5.36	1.05
Napsa	napsin A aspartic peptidase	88.74	90.18	5.70	2.39
Lpo	lactoperoxidase	98.90	75.56	5.70	9.33
Prss8	protease, serine, 8	90.32	62.40	6.19	5.28
Slc4a11	solute carrier family 4, sodium borate transporter, member 11	392.42	478.35	6.45	2.86
Lrat	lecithin-retinol acyltransferase (phosphatidylcholine-retinol-O-acyltransferase)	308.27	357.79	6.58	1.55
St14	suppression of tumorigenicity 14 (colon carcinoma)	69.06	27.33	7.65	7.94
Ppl	periplakin	63.45	32.27	7.96	5.48
RGD1562136	similar to D1Ertd622e protein	43.70	17.64	8.09	4.43
Pdzk1ip1	PDZK1 interacting protein 1	79.22	16.02	8.18	10.73

Continued on next page

Table E.13 – continued from previous page

Gene symbol	Gene name	GD20 Control TPM	GD20 Control ±SD	GD20 RU486 TPM	GD20 RU486 ±SD
Csf1	colony stimulating factor 1 (macrophage)	346.31	424.63	8.22	1.42
Guca2b	guanylate cyclase activator 2B	451.06	334.58	8.91	13.84
Oxt	oxytocin/neurophysin 1 prepropeptide	435.40	359.58	8.93	12.40
Enpp1	ectonucleotide pyrophosphatase/ phosphodiesterase 1	57.85	13.55	11.39	7.16
Wfs1	Wolfram syndrome 1 (wolframin)	142.57	163.66	12.07	5.56
Perp	PERP, TP53 apoptosis effector	156.75	78.00	12.19	17.34
Thbs4	thrombospondin 4	289.73	348.89	12.22	17.80
Abhd2	abhydrolase domain containing 2	77.61	17.56	14.00	4.43
Ctsr	cathepsin R	1663.16	2083.44	14.44	12.38
Prl3b1	Prolactin family 3, subfamily b, member 1	626.45	830.23	16.55	14.30
Ctsj	cathepsin J	1622.67	2078.93	17.47	14.20
Crip2	cysteine-rich protein 2	127.22	107.48	22.67	12.13
Lcn2	lipocalin 2	329.97	238.57	28.72	26.02
Gjb2	gap junction protein, beta 2	493.48	360.92	37.84	43.46
Rexo2	RNA exonuclease 2	226.13	101.76	68.23	16.11

Table E.14: Gene transcripts that were differentially expressed in response to treatment with RU486 in the outer myometrium. Comparisons were made between transcript expression in control tissues obtained on GD20 and transcript expression in RU486-treated tissues obtained on GD20. Transcript expression levels are shown in transcripts per million (TPM) values (mean±SD).

Gene symbol	Gene name	GD20 Control TPM	GD20 Control ±SD	GD20 RU486 TPM	GD20 RU486 ±SD
Upregulated in RU486-treated tissue					
LOC171573	spleen protein 1 precursor	4.43	4.96	1303.85	2246.62
Prl8a2	prolactin family 8, subfamily a, member 2	3.19	2.34	814.23	1407.10
Serpine1	serpin peptidase inhibitor, clade E, member 1 (nexin, plasminogen activator inhibitor type 1)	36.01	19.61	430.89	633.87
Sbsn	suprabasin	7.90	1.60	321.53	551.52
Slc38a4	solute carrier family 38, member 4	5.69	2.11	287.91	497.03
Dusp9	dual specificity phosphatase 9	8.21	6.96	161.84	214.60
Prl7a4	prolactin family 7, subfamily a, member 4	0.00	0.00	158.89	240.88
Fndc3c1	fibronectin type III domain containing 3C1	1.07	1.62	146.04	249.96
Prl3a1	Prolactin family 3, subfamily a, member 1	0.00	0.00	87.00	100.72
Slc13a4	solute carrier family 13, member 4 (sodium/sulfate symporter)	4.01	3.76	81.70	136.01
Pla2g10	phospholipase A2, group X	0.00	0.00	71.27	107.43
Sfmbt2	Scm-like with four mbt domains 2	4.54	2.69	62.35	101.24
RGD1564534	similar to CHCHD4 protein	3.30	1.98	47.16	78.82
Htr1d	5-hydroxytryptamine (serotonin) receptor 1D, G protein-coupled	0.00	0.00	41.73	72.12
Kit	v-kit Hardy-Zuckerman 4 feline sarcoma viral oncogene homolog	2.72	1.07	23.64	33.60
Dmrtc1c	DMRT-like family C1c1	0.00	0.00	22.44	38.74
Rimbp2	RIMS binding protein 2	0.58	0.14	15.27	19.89
Il17f	interleukin 17F	0.00	0.00	6.81	11.75
LOC367830	similar to FAM48A protein	0.00	0.00	4.68	7.68
Grip2	glutamate receptor interacting protein 2	0.00	0.00	3.98	5.98
Tbx5	T-box 5	0.00	0.00	3.57	3.86
Tmem59l	transmembrane protein 59-like	0.00	0.00	3.32	4.88
Atp4a	ATPase, H+/K+ exchanging, alpha polypeptide	0.35	0.23	3.32	5.67
Cftr	cystic fibrosis transmembrane conductance regulator	0.42	0.49	2.87	3.56
Gdap1l1	ganglioside-induced differentiation-associated protein 1-like 1	0.00	0.00	2.84	4.38
Down-regulated in RU486-treated tissue					
Crp	C-reactive protein, pentraxin-related	10.39	15.09	0.00	0.00
Dpys	dihydropyrimidinase	3.18	5.36	0.10	0.08
Pzp	pregnancy-zone protein	45.48	78.08	0.55	0.63
Ect2	epithelial cell transforming 2	6.23	2.58	0.64	0.14
Cldn1	claudin 1	35.46	14.62	1.06	0.53
Tenm2	teneurin transmembrane protein 2	11.44	5.65	1.38	1.59

Continued on next page

Table E.14 – continued from previous page

Gene symbol	Gene name	GD20 Control TPM	GD20 Control ±SD	GD20 RU486 TPM	GD20 RU486 ±SD
Atp6v0a4	ATPase, H+ transporting, lysosomal V0 subunit A4	47.10	52.05	1.61	1.18
Vtn	vitronectin	71.06	87.40	2.00	0.74
F5	coagulation factor V (proaccelerin, labile factor)	32.97	18.54	2.91	1.81
Fst	follistatin	33.92	23.08	2.93	0.69
Fam111a	family with sequence similarity 111, member A	61.38	58.35	3.11	2.13
Slc4a11	solute carrier family 4, sodium borate transporter, member 11	268.24	284.96	3.18	3.33
Plg	plasminogen	69.47	109.37	3.20	3.04
Sult1a1	sulfotransferase family, cytosolic, 1A, phenol-preferring, member 1	68.95	19.12	3.20	1.68
Igfbp1	insulin-like growth factor binding protein 1	94.70	69.66	3.41	4.54
Lcn2	lipocalin 2	162.92	103.93	4.25	3.63
Ahsg	alpha-2-HS-glycoprotein	527.33	911.90	4.45	7.58
Col11a1	collagen, type XI, alpha 1	48.21	28.64	4.63	4.50
Fetub	fetuin B	117.16	173.61	4.83	5.94
Aldob	aldolase B, fructose-bisphosphate	105.04	166.77	4.84	5.44
Gc	group specific component	121.95	116.89	5.34	4.60
Uchl1	ubiquitin carboxyl-terminal esterase L1 (ubiquitin thiolesterase)	105.05	76.27	6.65	1.60
Hmgcs2	3-hydroxy-3-methylglutaryl-CoA synthase 2 (mitochondrial)	61.29	34.41	8.00	7.37
Abcb1b	ATP-binding cassette, subfamily B (MDR/TAP), member 1B	271.55	265.10	9.05	12.49
Gatm	glycine amidinotransferase (L-arginine:glycine amidinotransferase)	183.23	227.90	12.50	0.81
Tspan8	tetraspanin 8	334.97	393.33	12.61	2.91
Nnat	neuronatin	177.76	149.85	13.33	7.06
Isyna1	inositol-3-phosphate synthase 1	1052.83	1069.36	23.59	16.69
Mt2A	metallothionein 2A	1034.18	166.76	153.67	5.28

Table E.15: Gene transcripts that were differentially expressed in response to treatment with RU486 in the decidua. Comparisons were made between transcript expression in control tissues obtained on GD22 (NL) and transcript expression in RU486-treated tissues obtained on GD20. Transcript expression levels are shown in transcripts per million (TPM) values (mean±SD).

Gene symbol	Gene name	GD22 (NL) Control TPM	GD22 (NL) Control ±SD	GD20 RU486 TPM	GD20 RU486 ±SD
Upregulated in RU486-treated tissue					
Prl8a9	prolactin family 8, subfamily a, member 9	272.97	371.84	6801.82	5576.89
Prl3d4	prolactin family 3, subfamily d, member 4	16.49	23.55	1118.79	879.35
Psg19	pregnancy specific glycoprotein 19	27.38	18.58	1049.76	828.40
Creg1	cellular repressor of E1A-stimulated genes 1	36.21	43.63	811.68	708.11
Timp3	TIMP metallopeptidase inhibitor 3	40.32	26.12	466.68	333.89
Psg16	pregnancy specific glycoprotein 16	3.63	2.07	267.78	315.01
Slc38a4	solute carrier family 38, member 4	14.54	13.24	203.93	212.16
Psg29	pregnancy-specific glycoprotein 29	3.08	2.60	202.80	311.83
Hp	haptoglobin	2.65	0.74	143.68	240.74
Slc4a1	solute carrier family 4, member 1 (anion exchanger)	1.73	0.66	136.97	234.07
Vtn	vitronectin	1.75	1.28	84.33	136.99
Folr1	folate receptor 1 (adult)	2.35	1.50	70.90	118.51
Perp	PERP, TP53 apoptosis effector	1.29	1.77	55.48	56.28
Apoa2	apolipoprotein A-II	0.00	0.00	50.15	86.86
Car1	carbonic anhydrase I	0.00	0.00	31.83	55.13
Hpd	4-hydroxyphenylpyruvate dioxygenase	0.02	0.03	27.47	47.35
Ocm	hypothetical protein LOC498662	0.43	0.36	22.83	21.12
LOC498662	testis development related protein	0.98	0.37	22.51	16.46
Fabp1	fatty acid binding protein 1, liver	0.00	0.00	21.05	36.46
Slc2a2	solute carrier family 2, member 2 (facilitated glucose transporter)	0.03	0.01	16.84	29.17
Asgr1	asialoglycoprotein receptor 1	0.14	0.13	14.26	24.13
Cpn1	carboxypeptidase N, polypeptide 1	0.02	0.04	12.50	21.66
Cubn	cubilin (intrinsic factor-cobalamin receptor)	0.14	0.03	12.15	19.31
Gnmt	glycine N-methyltransferase	0.01	0.02	11.88	20.57

Continued on next page

Table E.15 – continued from previous page

Gene symbol	Gene name	GD22 (NL) Control TPM	±SD	GD20 RU486 TPM	±SD
RGD1564894	similar to glycine-N-acyltransferase isoform a	0.00	0.00	10.56	18.29
Apof	apolipoprotein F	0.12	0.22	9.17	15.88
Amdhd1	amidohydrolase domain containing 1	0.00	0.00	8.31	14.39
Down-regulated in RU486-treated tissue					
Slc4a7	solute carrier family 4, sodium bicarbonate cotransporter, member 7	26.01	19.54	5.25	1.57
Hsd11b2	hydroxysteroid 11-beta dehydrogenase 2	100.16	24.95	12.11	5.17

Table E.16: Gene transcripts that were differentially expressed in response to treatment with RU486 in the inner myometrium. Comparisons were made between transcript expression in control tissues obtained on GD22 (NL) and transcript expression in RU486-treated tissues obtained on GD20. Transcript expression levels are shown in transcripts per million (TPM) values (mean±SD).

Gene symbol	Gene name	GD22 (NL) Control TPM	±SD	GD20 RU486 TPM	±SD
Upregulated in RU486-treated tissue					
Fgg	fibrinogen gamma chain	1.81	2.45	902.25	1559.17
Apoa1	apolipoprotein A-I	2.43	3.93	549.55	936.67
Hemgn	hemogen	1.12	1.68	442.61	763.44
Fgb	fibrinogen beta chain	1.40	2.16	415.60	716.50
Hist1h1b	histone cluster 1, H1b	6.43	7.06	339.82	573.19
Hdc	histidine decarboxylase	0.70	0.71	315.80	545.16
Rbp4	retinol binding protein 4, plasma	1.62	1.80	300.26	510.30
Vtn	vitronectin	2.20	1.63	256.49	439.16
Plg	plasminogen	1.14	1.10	216.14	373.54
Pzp	pregnancy-zone protein	0.93	0.35	209.88	362.76
Itih4	inter-alpha-trypsin inhibitor heavy chain family, member 4	1.13	0.81	98.25	169.94
Cfi	complement factor I	2.19	1.94	94.25	162.29
Slc25a37	solute carrier family 25, member 37 (mitochondrial iron transporter)	2.14	1.18	86.27	133.28
Sptb	spectrin, beta, erythrocytic	0.56	0.91	74.45	126.84
Pklr	pyruvate kinase, liver and RBC	3.18	3.61	72.34	121.72
Ube2c	ubiquitin-conjugating enzyme E2C	1.85	1.31	69.56	118.03
Defa	defensin alpha-like	0.00	0.00	57.84	97.77
Psat1	phosphoserine aminotransferase 1	1.97	2.87	55.74	88.72
Spta1	spectrin, alpha, erythrocytic 1 (elliptocytosis 2)	0.33	0.24	54.07	93.02
Cldn1	claudin 1	1.31	1.20	32.06	51.98
F5	coagulation factor V (proaccelerin, labile factor)	1.34	0.48	25.34	42.04
Crp	C-reactive protein, pentraxin-related	0.00	0.00	24.69	42.67
Lgals4	lectin, galactoside-binding, soluble, 4	0.00	0.00	18.88	32.70
Krt20	keratin 20	0.00	0.00	17.28	29.92
Dmbt1	deleted in malignant brain tumors 1	0.64	0.51	15.28	9.87
Klkb1	kallikrein B, plasma 1	0.00	0.00	14.22	24.62
Prodh2	proline dehydrogenase (oxidase) 2	0.00	0.00	12.38	21.44
Haao	3-hydroxyanthranilate 3,4-dioxygenase	0.00	0.00	11.99	20.67
Agr2	anterior gradient 2	0.00	0.00	11.77	20.33
Alpi	alkaline phosphatase, intestinal	0.01	0.02	10.55	18.28
RGD1559600	RGD1559600	0.00	0.00	10.11	17.52
C9	complement component 9	0.07	0.03	9.98	17.12
Camp	cathelicidin antimicrobial peptide	0.00	0.00	9.35	16.13
Slc17a1	solute carrier family 17, member 1 (organic anion transporter)	0.00	0.00	8.96	15.52
Ttpa	tocopherol (alpha) transfer protein	0.00	0.00	8.46	14.34
Slc30a10	solute carrier family 30, member 10	0.00	0.00	8.38	14.52
Apcs	amyloid P component, serum	0.00	0.00	7.95	13.76
Hnf4g	hepatocyte nuclear factor 4, gamma	0.00	0.00	7.82	13.55
RGD1564614	similar to complement factor H-related protein	0.06	0.07	7.46	12.88
Amdhd1	amidohydrolase domain containing 1	0.01	0.02	7.38	12.64
Anxa13	annexin A13	0.01	0.01	7.26	12.57

Continued on next page

Table E.16 – continued from previous page

Gene symbol	Gene name	GD22 (NL) Control TPM	±SD	GD20 RU486 TPM	±SD
Mamdc4	MAM domain containing 4	0.00	0.00	7.22	11.10
Guca2a	guanylate cyclase activator 2a (guanylin)	0.00	0.00	6.46	11.19
Aspdh	aspartate dehydrogenase domain containing	0.00	0.00	6.25	10.82
Gcg	glucagon	0.00	0.00	5.47	9.47
Pah	phenylalanine hydroxylase	0.00	0.00	5.38	9.27
Gp5	glycoprotein V (platelet)	0.00	0.00	4.96	8.39
Slc17a3	solute carrier family 17, member 3 (organic anion transporter)	0.04	0.04	4.89	8.26
Slc26a3	solute carrier family 26, member 3 (anion exchanger)	0.00	0.00	4.71	8.07
Slc36a2	solute carrier family 36, member 2 (proton/amino acid symporter)	0.05	0.06	4.68	7.93
Nr1i2	nuclear receptor subfamily 1, group I, member 2	0.00	0.00	4.50	7.79
Aldh1a1	aldehyde dehydrogenase 1 family, member A1	0.00	0.00	4.01	6.93
Stmn2	stathmin-like 2	0.00	0.00	3.46	6.00
Tmem229a	transmembrane protein 229A	0.25	0.06	3.40	4.85
Clec12b	C-type lectin domain family 12, member B	0.00	0.00	3.38	5.46
Hepacam2	HEPACAM family member 2	0.00	0.00	2.93	5.08
Cpamd8	C3 and PZP-like, alpha-2-macroglobulin domain containing 8	0.00	0.00	2.44	4.10
Aass	aminoadipate-semialdehyde synthase	0.00	0.00	2.43	4.19
Slc5a1	solute carrier family 5, member 1 (sodium/glucose cotransporter)	0.00	0.00	2.33	3.94
Hhip	Hedgehog-interacting protein	0.06	0.07	2.10	3.59
Cyp7a1	cytochrome P450, family 7, subfamily a, polypeptide 1	0.13	0.00	2.09	3.09
Slitrk4	SLIT and NTRK-like family, member 4	0.00	0.00	1.21	2.09
Down-regulated in RU486-treated tissue					
LOC685544	hypothetical protein LOC685544	106.53	184.51	0.00	0.00
Olr1218	olfactory receptor 1218	7.21	9.02	0.00	0.00
Gnat2	guanine nucleotide binding protein (G protein), alpha transducing activity polypeptide 2	4.69	7.88	0.01	0.02
Krt17	keratin 17	7.67	13.28	0.02	0.03
Sftpc	surfactant protein C	2.95	5.11	0.02	0.04
Drp2	dystrophin related protein 2	8.78	5.76	0.09	0.09
LOC690326	hypothetical protein LOC690326	28.36	25.68	0.63	0.66
Apod	apolipoprotein D	17.56	17.10	0.74	0.56
Nppa	natriuretic peptide A	58.89	63.00	1.47	1.19
Ebf3	early B-cell factor 3	18.63	21.52	1.48	1.03
Htr2a	5-hydroxytryptamine (serotonin) receptor 2A, G protein-coupled	86.91	148.90	2.22	2.15
Prl7a4	prolactin family 7, subfamily a, member 4	267.85	446.91	2.32	2.86
Folr1	folate receptor 1 (adult)	41.98	70.89	2.52	0.79
PCOLCE2	procollagen C-endopeptidase enhancer 2	60.75	37.17	2.55	2.36
Rhox9	reproductive homeobox 9	59.41	43.55	2.58	3.50
Ctsm	cathepsin M	224.42	353.44	2.68	2.46
Ctsq	cathepsin Q	124.52	215.09	2.75	1.78
Hpgd	hepatocyte nuclear factor 4, gamma	35.26	17.77	3.43	1.22
Dmkn	dermokine	59.60	64.61	3.44	3.59
Fndc3c1	fibronectin type III domain containing 3C1	169.74	138.42	3.63	3.37
Taf7l	TAF7-like RNA polymerase II, TATA box binding protein (TBP)-associated factor	321.55	209.52	3.97	3.45
Psgb1	pregnancy-specific beta 1-glycoprotein	318.33	547.14	4.18	4.30
Prl7a3	prolactin family 7, subfamily a, member 3	153.98	51.71	4.53	4.00
Cilp	cartilage intermediate layer protein, nucleotide pyrophosphohydrolase	46.49	28.93	5.54	5.38
Prima1	proline rich membrane anchor 1	25.88	27.79	5.75	2.78
Adamts9	ADAM metallopeptidase with thrombospondin type 1 motif, 9	36.93	4.63	6.99	2.15
Foxo4	forkhead box O4	132.66	49.22	10.48	8.63
Prl8a2	prolactin family 8, subfamily a, member 2	508.14	727.51	13.20	6.32
Ednrb	endothelin receptor type B	346.91	137.08	13.54	3.49
Cited1	Cbp/p300-interacting transactivator with Glu/Asp-rich carboxy-terminal domain 1	483.54	198.23	33.07	41.19
Prl2c1	Prolactin family 2, subfamily c, member 1	805.52	591.09	69.94	61.57
Prl5a1	prolactin family 5, subfamily a, member 1	1092.25	866.74	82.30	72.80
Prl2a1	Prolactin family 2, subfamily a, member 1	4322.65	1652.99	226.20	258.79

Table E.17: Gene transcripts that were differentially expressed in response to treatment with RU486 in the outer myometrium. Comparisons were made between transcript expression in control tissues obtained on GD22 (NL) and transcript expression in RU486-treated tissues obtained on GD20. Transcript expression levels are shown in transcripts per million (TPM) values (mean±SD).

		GD22 (NL) Control		GD20 RU486	
Gene symbol	Gene name	TPM	±SD	TPM	±SD
Upregulated in RU486-treated tissue					
Car4	carbonic anhydrase 4	2.78	1.02	61.52	89.52
Tac1	tachykinin, precursor 1	0.00	0.00	11.13	15.99
Down-regulated in RU486-treated tissue					
Apcs	amyloid P component, serum	28.50	49.18	0.00	0.00
Crp	C-reactive protein, pentraxin-related	23.28	40.33	0.00	0.00
Cyp2c12	cytochrome P450, family 2, subfamily c, polypeptide 12	5.90	9.84	0.02	0.04
Dpys	dihydropyrimidinase	6.69	11.25	0.10	0.08
Fabp7	fatty acid binding protein 7, brain	126.13	217.96	0.14	0.24
Aldh1a7	aldehyde dehydrogenase family 1, subfamily A7	9.44	9.53	0.18	0.13
Pzp	pregnancy-zone protein	127.17	219.61	0.55	0.63
Cldn1	claudin 1	20.50	25.59	1.06	0.53
Vtn	vitronectin	196.99	333.38	2.00	0.74
Lcn2	lipocalin 2	126.31	66.72	4.25	3.63
Hp	haptoglobin	511.81	885.89	7.18	8.93
Glrx	glutaredoxin (thioltransferase)	135.84	123.07	15.83	9.86

Appendix F

Identification of Progesterone Responsive Genes

F.1 Tissue dependent Gene Expression

Table F.1: Transcripts that were significantly differentially expressed between the decidua and the inner myometrium in P4-treated samples. Transcript expression levels are shown in transcripts per million (TPM) (mean±SD).

		Decidua		Inner Myometrium	
Gene symbol	Gene name	TPM	±SD	TPM	±SD
Upregulated genes					
Prl2a1	Prolactin family 2 subfamily a member 1	1667.40	1446.93	9530.79	15251.66
Prl5a2	prolactin family 5 subfamily a member 2	13.26	6.55	3804.28	6382.97
Actg2	actin gamma 2 smooth muscle enteric	283.80	447.52	3496.57	3891.67
Prl7b1	prolactin family 7 subfamily b member 1	109.32	68.41	2862.78	2440.30
Postn	periostin osteoblast specific factor	44.06	57.45	2349.30	2212.21
Lum	lumican	31.89	49.35	2318.22	2911.58
Myl9	myosin light chain 9 regulatory	257.24	356.90	2047.32	1974.55
Serpine2	serpin peptidase inhibitor clade E (nexin plasminogen activator inhibitor type 1) member 2	312.44	272.19	1710.00	1035.12
Mmp11	matrix metallopeptidase 11	10.30	14.50	1039.57	940.36
Gpnmb	glycoprotein (transmembrane) nmb	204.66	93.34	1037.34	839.09
Sparcl1	SPARC-like 1 (hevin)	787.53	1327.26	838.87	1283.81
Plau	plasminogen activator urokinase	11.44	13.25	792.04	736.94
Apoe	apolipoprotein E	119.13	126.39	753.72	423.99
Igfbp2	insulin-like growth factor binding protein 2	56.88	50.68	628.57	701.20
Pltp	phospholipid transfer protein	125.22	123.67	623.06	593.47
Cnn1	calponin 1 basic smooth muscle	25.90	27.46	620.15	723.62
Prl5a1	prolactin family 5 subfamily a member 1	168.44	238.01	609.38	165.58
Ifi27l2b	interferon alpha-inducible protein 27 like 2B	124.71	147.14	457.83	155.50
Tmem176a	transmembrane protein 176A	79.84	95.21	408.66	385.85

Continued on next page

Table F.1 – continued from previous page

		decidua		Inner Myometrium	
Gene symbol	Gene name	TPM	±SD	TPM	±SD
Gadd45a	growth arrest and DNA-damage-inducible alpha	46.69	23.65	370.73	289.30
Mmp3	matrix metallopeptidase 3	1.35	1.18	353.47	344.19
Aebp1	AE binding protein 1	25.26	11.27	309.58	267.99
Sema6d	semaphorin 6D	9.17	8.54	308.28	368.53
Serpinf1	serpin peptidase inhibitor clade F (alpha-2 antiplasmin pigment epithelium derived factor) member 1	122.14	88.04	303.11	109.50
Igfbp6	insulin-like growth factor binding protein 6	8.92	13.16	292.33	377.57
Mylk	myosin light chain kinase	15.42	13.21	291.49	367.94
Tmem176b	transmembrane protein 176B	29.06	13.08	274.36	233.29
Prl2c1	Prolactin family 2 subfamily c member 1	10.78	15.34	272.41	344.78
Fhl1	four and a half LIM domains 1	39.31	32.94	261.58	285.63
Acta1	actin alpha 1 skeletal muscle	25.89	39.57	252.92	300.23
Ifitm2	interferon induced transmembrane protein 2	76.12	66.97	236.71	233.97
Ltbp1	latent transforming growth factor beta binding protein 1	10.94	7.06	202.69	174.93
Igfbp5	insulin-like growth factor binding protein 5	6.55	4.21	173.73	183.88
LOC100361444	rCG31799-like	3.48	2.69	161.64	138.36
Mmp12	matrix metallopeptidase 12	7.33	9.10	155.87	197.91
Antxr1	anthrax toxin receptor 1	40.00	37.90	148.87	115.38
Chchd10	coiled-coil-helix-coiled-coil-helix domain containing 10	8.41	6.09	141.60	196.53
Ly6e	lymphocyte antigen 6 complex locus E	41.68	21.47	141.32	106.38
Figf	c-fos induced growth factor	1.82	1.78	130.14	145.18
Fgl2	fibrinogen-like 2	14.71	16.48	126.26	140.89
Rnase4	ribonuclease RNase A family 4	21.61	18.95	124.89	111.54
Sod2	superoxide dismutase 2 mitochondrial	60.84	68.03	122.03	46.13
Plac8	placenta-specific 8	14.54	16.56	117.36	106.56
Csdc2	cold shock domain containing C2 RNA binding	24.85	18.27	107.86	67.91
Mgp	matrix Gla protein	21.76	11.39	106.51	104.31
Tnn	tenascin N	0.56	0.60	98.26	118.24
Gda	guanine deaminase	21.57	9.39	94.86	67.63
Penk	proenkephalin	7.58	7.81	85.69	73.73
F3	coagulation factor III (thromboplastin tissue factor)	25.71	10.10	81.13	52.80
C1s	complement component 1 s subcomponent	6.71	6.21	80.16	74.87
Klf7	Kruppel-like factor 7 (ubiquitous)	30.90	19.82	78.39	31.41
C1r	complement component 1 r subcomponent	14.92	8.84	71.68	57.92
Hsd11b1	hydroxysteroid 11-beta dehydrogenase 1	27.02	15.90	71.29	64.49
Ednra	endothelin receptor type A	11.59	2.87	68.53	55.36
Fbln5	fibulin 5	9.00	14.07	67.90	61.82
Mmp19	matrix metallopeptidase 19	13.49	6.32	67.88	66.65
Spon1	spondin 1 extracellular matrix protein	8.32	7.94	64.28	62.90
Neu2	sialidase 2	1.62	2.49	61.43	95.09
Rnf8	ring finger protein 8 E3 ubiquitin protein ligase	34.18	46.94	61.01	42.46
Pygb	phosphorylase glycogen brain	9.58	2.77	58.98	45.71
Derl3	derlin 3	4.30	2.88	58.22	67.66
Mgst1	microsomal glutathione S-transferase 1	5.78	3.06	57.21	74.64
Cp	ceruloplasmin (ferroxidase)	5.48	5.21	57.00	47.61
Plxdc2	plexin domain containing 2	8.93	6.16	56.68	64.79
Vwa1	von Willebrand factor A domain containing 1	5.45	5.58	55.67	73.12
Slc28a2	solute carrier family 28 (sodium-coupled nucleoside transporter) member 2	2.41	2.17	54.63	52.42
Ddr2	discoidin domain receptor tyrosine kinase 2	18.59	5.84	53.70	49.52
Pla1a	phospholipase A1 member A	9.92	10.49	49.29	46.61
Rasd2	RASD family member 2	42.28	71.52	49.14	65.64
Krt75	keratin 75	0.76	1.03	47.78	41.48
Ifitm1	interferon induced transmembrane protein 1	13.25	10.73	47.19	38.89
Gpr88	G-protein coupled receptor 88	2.70	3.28	46.53	49.41
Gbp2	guanylate binding protein 2 interferon-inducible	4.77	4.54	44.60	35.47
Cxcl10	chemokine (C-X-C motif) ligand 10	1.22	1.88	44.15	39.93
Dclk1	doublecortin-like kinase 1	7.96	3.23	43.50	41.31
Kcnk2	potassium channel subfamily K member 2	1.72	2.32	42.86	36.78
Sh3kbp1	SH3-domain kinase binding protein 1	15.52	3.87	41.97	20.07
Adh1	alcohol dehydrogenase 1 (class I)	10.25	8.21	41.66	33.55
Plxdc1	plexin domain containing 1	3.99	5.35	40.43	35.28
Ctxn1	cortexin 1	1.57	2.42	40.01	35.29
Dram	damage-regulated autophagy modulator	13.34	3.22	39.83	25.40
Npas2	neuronal PAS domain protein 2	4.72	3.10	39.57	29.91
Igf1	insulin-like growth factor 1	10.41	12.48	33.37	28.92
Ctsc	cathepsin C	4.94	4.55	32.67	27.04
Lpcat2	lysophosphatidylcholine acyltransferase 2	5.81	2.71	31.85	24.62
Abcg4	ATP-binding cassette subfamily G (WHITE) member 4	1.57	1.64	30.86	31.07

Continued on next page

Table F.1 – continued from previous page

		decidua		Inner Myometrium	
Gene symbol	Gene name	TPM	±SD	TPM	±SD
Pgm5	phosphoglucomutase 5	3.78	3.65	29.15	23.41
Nrp1	neuropilin 1	3.46	1.29	29.02	29.64
Aoc3	amine oxidase copper containing 3	5.19	4.26	26.75	23.56
Limd2	LIM domain containing 2	10.88	13.00	26.12	5.49
Slc26a2	solute carrier family 26 (sulfate transporter) member 2	4.85	4.77	25.11	22.66
Gem	GTP binding protein overexpressed in skeletal muscle	1.36	0.79	24.54	21.55
Mafb	v-maf musculoaponeurotic fibrosarcoma oncogene homolog B (avian)	1.69	1.99	23.91	29.77
Kcnmb1	potassium large conductance calcium-activated channel subfamily M beta member 1	3.25	3.67	23.63	29.56
Cnr1	cannabinoid receptor 1 (brain)	11.39	14.20	21.92	16.24
Fam198b	family with sequence similarity 198 member B	3.05	1.46	21.46	17.40
Ifi204	myeloid cell nuclear differentiation antigen	7.45	3.78	21.29	16.47
Fgf7	fibroblast growth factor 7	0.27	0.36	21.26	22.78
Enpp3	ectonucleotide pyrophosphatase/phosphodiesterase 3	3.90	4.16	21.17	17.93
Pla2g2a	phospholipase A2 group IIA (platelets synovial fluid)	6.76	9.52	20.44	17.73
Acsbg1	acyl-CoA synthetase bubblegum family member 1	1.10	1.57	19.78	21.28
Osr2	odd-skipped related 2 (Drosophila)	1.90	2.47	18.94	17.99
Kcnj8	potassium inwardly-rectifying channel subfamily J member 8	1.72	1.23	18.68	23.40
C4b	complement component 4B (Chido blood group)	0.64	0.79	18.53	18.80
Car12	carbonic anyhydrase 12	1.03	0.90	18.48	14.70
Stox2	storkhead box 2	1.29	0.91	17.65	18.26
Hpse	heparanase	6.35	6.68	17.29	4.79
Asb5	ankyrin repeat and SOCS box-containing 5	3.58	3.28	16.86	12.54
Rprm	reprimo TP53 dependent G2 arrest mediator candidate	2.95	5.10	16.65	6.80
C1qtnf7	C1q and tumor necrosis factor related protein 7	1.16	1.61	16.42	16.60
Cxcl16	chemokine (C-X-C motif) ligand 16	4.98	3.33	16.04	13.49
RGD1304595	similar to RIKEN cDNA 6330416G13 gene	2.90	1.27	14.62	12.90
Myo7b	myosin VIIb	1.83	0.39	14.10	14.43
Frzb	frizzled-related protein	1.71	1.22	13.93	12.96
Nkg7	natural killer cell group 7 sequence	2.56	4.35	13.85	12.03
Qprt	quinolinate phosphoribosyltransferase	4.32	6.61	13.80	8.93
Ptprn	protein tyrosine phosphatase receptor type N	5.98	9.60	13.05	3.61
Thbs2	thrombospondin 2	1.39	0.92	12.97	10.96
Rassf2	Ras association (RalGDS/AF-6) domain family member 2	4.10	6.30	11.91	2.26
Adcy2	adenylate cyclase 2 (brain)	2.31	0.48	11.54	11.96
Sall2	sal-like 2 (Drosophila)	5.89	9.11	11.39	6.79
Col11a1	collagen type XI alpha 1	0.77	0.97	11.32	9.88
Ube2ql1	ubiquitin-conjugating enzyme E2Q family-like 1	0.35	0.58	9.46	12.63
Cmtm5	CKLF-like MARVEL transmembrane domain containing 5	0.76	0.61	9.33	11.67
Fam163b	family with sequence similarity 163 member B	0.00	0.00	8.75	15.15
Igsf10	immunoglobulin superfamily member 10	0.81	0.91	7.96	6.84
Rab27a	RAB27A member RAS oncogene family	2.34	1.25	7.75	6.34
Atp1b2	ATPase Na /K transporting beta 2 polypeptide	1.00	0.56	7.69	7.02
Cacna1c	calcium channel voltage-dependent L type alpha 1C subunit	0.43	0.27	7.36	6.72
Sash3	SAM and SH3 domain containing 3	4.08	6.61	7.24	3.99
Nptx2	neuronal pentraxin II	0.10	0.18	6.51	11.27
Prf1	perforin 1 (pore forming protein)	3.17	2.96	6.37	5.72
Ccl6	chemokine (C-C motif) ligand 6	0.28	0.41	6.06	8.33
Ptgfr	prostaglandin F receptor	1.55	0.68	5.90	4.72
Rxfp2	relaxin/insulin-like family peptide receptor 2	1.05	1.27	5.12	5.25
Trpv4	transient receptor potential cation channel subfamily V member 4	0.12	0.16	5.06	7.55
Fez1	fasciculation and elongation protein zeta 1 (zygin I)	0.15	0.21	4.95	6.49
Rgs1	regulator of G-protein signaling 1	0.08	0.15	4.60	4.59
Arhgef28	Rho guanine nucleotide exchange factor (GEF) 28	0.50	0.34	4.41	4.72
Syk	spleen tyrosine kinase	0.30	0.09	4.05	4.05
Aldh1a3	aldehyde dehydrogenase 1 family member A3	0.01	0.02	3.53	4.87
Egr2	early growth response 2	2.44	2.35	3.33	4.03
Cdca3	cell division cycle associated 3	0.10	0.10	2.96	3.11
Slamf8	SLAM family member 8	0.09	0.09	2.91	3.72
Ccl5	chemokine (C-C motif) ligand 5	0.11	0.16	2.68	3.01
Tdo2	tryptophan 23-dioxygenase	0.14	0.14	2.54	3.54
Ccl12	chemokine (C-C motif) ligand 12	0.03	0.02	2.42	3.35
Hey1	hairy/enhancer-of-split related with YRPW motif 1	0.18	0.28	1.97	1.55
Rnase1l1	ribonuclease RNase A family 1-like 1 (pancreatic)	0.00	0.00	0.83	0.87
Lrrn3	leucine rich repeat neuronal 3	0.00	0.00	0.06	0.11
down-regulated genes					
Acsm5	acyl-CoA synthetase medium-chain family member 5	2.84	4.82	0.00	0.00

Continued on next page

Table F.1 – continued from previous page

		decidua		Inner Myometrium	
Gene symbol	Gene name	TPM	±SD	TPM	±SD
Asic3	acid-sensing (proton-gated) ion channel 3	17.22	29.74	0.00	0.00
Hpd	4-hydroxyphenylpyruvate dioxygenase	5.10	8.57	0.00	0.00
Mir431	microRNA 431	128.54	222.64	0.00	0.00
Snx22	sorting nexin 22	38.94	66.27	0.00	0.00
Trim52	tripartite motif-containing 52	35.67	61.78	0.00	0.00
Triml2	tripartite motif family-like 2	26.51	45.83	0.00	0.01
Hcn2	hyperpolarization activated cyclic nucleotide-gated potassium channel 2	25.25	43.31	0.01	0.01
Got1l1	glutamic-oxaloacetic transaminase 1-like 1	4.97	8.60	0.01	0.01
Slc22a3	solute carrier family 22 (extraneuronal monoamine transporter) member 3	4.84	8.29	0.01	0.02
RGD1562871	similar to BMI1-like protein	6.62	11.43	0.02	0.02
Hmx3	H6 family homeobox 3	17.14	29.63	0.02	0.04
Camk1g	calcium/calmodulin-dependent protein kinase IG	25.55	43.34	0.02	0.03
LOC680590	hypothetical protein LOC680590	21.86	37.48	0.03	0.06
Gbx2	gastrulation brain homeobox 2	13.32	22.92	0.04	0.05
Elf5	E74-like factor 5	4.21	6.71	0.04	0.03
Irx3	iroquois homeobox 3	12.48	20.35	0.04	0.04
MGC114246	similar to cathepsin R	16.97	28.97	0.08	0.10
Alox15	arachidonate 15-lipoxygenase	19.98	34.45	0.08	0.09
Ambp	alpha-1-microglobulin/bikunin precursor	7.67	12.93	0.10	0.18
B4galnt3	beta-14-N-acetyl-galactosaminyl transferase 3	101.88	176.12	0.11	0.15
Cyp1a1	cytochrome P450 family 1 subfamily a polypeptide 1	5.11	8.65	0.11	0.04
Pnma5	paraneoplastic Ma antigen family member 5	7.03	11.87	0.12	0.21
Utf1	undifferentiated embryonic cell transcription factor 1	70.65	119.81	0.15	0.14
LOC498222	similar to specifically androgen-regulated protein	11.11	16.91	0.16	0.21
Syna	syncytin a	166.53	287.80	0.17	0.11
Tns4	tensin 4	149.62	258.41	0.18	0.31
Grip2	glutamate receptor interacting protein 2	9.40	15.44	0.20	0.20
Tspyl4	TSPY-like 4	2.67	3.73	0.20	0.26
Sall3	sal-like 3 (Drosophila)	2.67	3.57	0.26	0.19
Insc	inscuteable homolog (Drosophila)	7.84	13.01	0.31	0.37
Dlk1	delta-like 1 homolog (Drosophila)	237.27	408.86	0.43	0.23
Dlx3	distal-less homeobox 3	132.75	228.07	0.55	0.30
Foxc1	forkhead box C1	1.72	1.89	0.55	0.16
Plagl1	pleiomorphic adenoma gene-like 1	98.87	169.04	0.61	0.41
Hand1	heart and neural crest derivatives expressed 1	72.19	106.52	0.72	0.51
Aloxe3	arachidonate lipoxygenase 3	25.08	41.00	0.81	1.39
Kit	v-kit Hardy-Zuckerman 4 feline sarcoma viral oncogene homolog	34.39	41.47	1.05	0.94
Hoxc4	homeo box C4	7.47	11.16	1.09	1.22
Epn3	epsin 3	52.58	84.46	1.15	1.07
Map7	microtubule-associated protein 7	10.27	14.82	1.25	0.47
Itm2a	integral membrane protein 2A	193.05	333.78	1.53	2.60
Zim1	zinc finger imprinted 1	38.14	62.72	1.91	1.67
Cdh1	cadherin 1	108.55	173.41	1.91	1.27
Shroom4	shroom family member 4	57.82	94.12	2.14	1.31
Cyp11a1	cytochrome P450 family 11 subfamily a polypeptide 1	39.02	34.77	2.19	3.71
Eps8l2	EPS8-like 2	131.61	219.35	2.38	1.70
Epb4.1l5	erythrocyte protein band 4.1-like 5	37.25	54.83	3.10	2.42
Mrgpre	MAS-related GPR member E	182.94	301.89	3.26	4.64
Pak6	p21 protein (Cdc42/Rac)-activated kinase 6	35.20	51.11	3.40	5.90
Slc38a4	solute carrier family 38 member 4	144.73	223.60	3.67	3.67
Lgalsl	lectin galactoside-binding-like	28.16	39.50	3.76	2.01
Kif13b	kinesin family member 13B	19.92	18.67	3.97	1.86
Arhgef6	Rac/Cdc42 guanine nucleotide exchange factor (GEF) 6	137.60	226.71	4.08	0.78
RGD1564534	similar to CHCHD4 protein	148.16	249.98	4.10	4.09
Ccnjl	cyclin J-like	38.49	59.68	4.18	5.12
Wwc2	WW and C2 domain containing 2	12.03	9.46	4.24	3.71
Fbxl19	F-box and leucine-rich repeat protein 19	67.63	107.77	4.80	4.70
Oxsr1	oxidative-stress responsive 1	23.77	29.28	4.80	2.57
Ctsj	cathepsin J	1071.79	1841.32	4.90	5.97
Sbsn	suprabasin	137.67	119.05	5.20	6.91
Zfpm1	zinc finger protein multitype 1	76.07	118.92	5.32	3.32
Cmtm4	CKLF-like MARVEL transmembrane domain containing 4	70.30	111.40	5.32	3.91
Ctsr	cathepsin R	900.80	1551.03	5.52	4.58
Prl3d4	prolactin family 3 subfamily d member 4	73.60	115.96	6.02	7.34
Nrm	nurim (nuclear envelope membrane protein)	47.53	62.39	6.30	4.18
Lad1	ladinin 1	137.41	216.00	6.60	10.45
Ccdc92	coiled-coil domain containing 92	87.59	136.76	7.00	2.42
Ctsql2	cathepsin Q-like 2	1698.26	2928.99	7.35	6.25

Continued on next page

Table F.1 – continued from previous page

		decidua		Inner Myometrium	
Gene symbol	Gene name	TPM	±SD	TPM	±SD
Ihh	Indian hedgehog	15.32	13.19	7.47	12.90
Adora1	adenosine A1 receptor	8.89	15.01	8.74	15.14
Stra6	stimulated by retinoic acid 6	183.44	306.82	9.20	5.85
Stard8	StAR-related lipid transfer (START) domain containing 8	103.26	146.79	9.77	13.73
Rnf128	ring finger protein 128 E3 ubiquitin protein ligase	36.18	28.10	10.10	10.78
Slc16a3	solute carrier family 16 member 3 (monocarboxylic acid transporter 4)	120.68	194.36	10.12	10.57
Flt1	FMS-related tyrosine kinase 1	40.16	34.57	11.92	13.67
Fndc3c1	fibronectin type III domain containing 3C1	68.30	74.04	12.14	10.67
Prl2b1	Prolactin family 2 subfamily b member 1	72.72	94.83	12.50	21.66
Ppl	periplakin	39.90	18.67	14.02	10.68
Flvcr2	feline leukemia virus subgroup C cellular receptor family member 2	38.13	39.67	14.21	15.37
Uaca	uveal autoantigen with coiled-coil domains and ankyrin repeats	80.98	90.40	15.30	16.65
Tjp2	tight junction protein 2	36.59	8.27	15.90	17.90
Nrk	Nik related kinase	71.61	61.75	18.80	14.63
Cldn4	claudin 4	47.15	17.50	21.50	34.07
Pdlim5	PDZ and LIM domain 5	125.27	84.33	24.94	7.54
Prl7a3	prolactin family 7 subfamily a member 3	179.30	274.49	25.51	5.23
Dysf	dysferlin	42.05	29.62	26.40	28.75
Psgb1	pregnancy-specific beta 1-glycoprotein	29.38	46.37	27.64	47.81
Dscr6	ripply transcriptional repressor 3	50.59	46.44	31.03	42.55
Abhd2	abhydrolase domain containing 2	100.65	42.17	41.43	50.86
Creg1	cellular repressor of E1A-stimulated genes 1	87.02	36.84	42.64	56.25
Psg19	pregnancy specific glycoprotein 19	99.10	61.06	47.74	51.82
Cgm4	carcinoembryonic antigen gene family 4	110.49	150.82	98.11	160.21
Psg29	pregnancy-specific glycoprotein 29	103.43	172.57	102.36	173.48
Timp3	TIMP metallopeptidase inhibitor 3	310.24	110.24	124.74	92.11
Tfpi	tissue factor pathway inhibitor (lipoprotein-associated coagulation inhibitor)	497.90	400.24	146.49	174.07
Prl8a4	prolactin family 8 subfamily a member 4	462.84	534.50	149.60	132.52
LOC171573	spleen protein 1 precursor	772.77	695.57	292.37	481.57
Lamc2	laminin gamma 2	355.81	570.33	340.99	582.94
Prl8a9	prolactin family 8 subfamily a member 9	882.21	758.51	504.46	817.09
Prl8a5	prolactin family 8 subfamily a member 5	829.21	779.64	591.67	854.40

Table F.2: Transcripts that were significantly differentially expressed between the decidua and the outer myometrium in P4-treated samples. Transcript expression levels are shown in transcripts per million (TPM) (mean±SD).

		Decidua		Outer Myometrium	
Gene symbol	Gene name	TPM	±SD	TPM	±SD
Upregulated genes					
Postn	periostin osteoblast specific factor	44.06	57.45	2361.32	1367.00
Lum	lumican	31.89	49.35	2344.62	2677.06
Acta1	actin alpha 1 skeletal muscle	25.89	39.57	1499.72	2277.22
Mmp11	matrix metallopeptidase 11	10.30	14.50	1098.70	905.78
Hapln1	hyaluronan and proteoglycan link protein 1	0.17	0.22	889.75	1540.59
Lect1	leukocyte cell derived chemotaxin 1	0.38	0.64	642.71	1112.33
Fhl1	four and a half LIM domains 1	39.31	32.94	537.32	117.61
Plau	plasminogen activator urokinase	11.44	13.25	519.64	651.28
Cnn1	calponin 1 basic smooth muscle	25.90	27.46	456.50	365.57
Mgp	matrix Gla protein	21.76	11.39	415.97	235.86
Tnnt3	troponin T type 3 (skeletal fast)	1.49	1.91	362.45	619.87
Matn3	matrilin 3	0.06	0.06	349.20	604.72
Actc1	actin alpha cardiac muscle 1	1.95	0.78	341.45	582.30
Aebp1	AE binding protein 1	25.26	11.27	327.55	160.36
Sema6d	semaphorin 6D	9.17	8.54	307.30	359.10
RGD1311447	LOC363276	12.20	20.62	279.86	472.26
Igfbp5	insulin-like growth factor binding protein 5	6.55	4.21	275.08	167.71
Tmem176b	transmembrane protein 176B	29.06	13.08	265.98	148.80
Leprel4	leprecan-like 4	30.59	20.35	255.44	374.95
Mfap2	microfibrillar-associated protein 2	5.39	8.85	248.02	375.19
Smoc2	SPARC related modular calcium binding 2	4.05	4.53	232.65	367.52
Capn6	calpain 6	0.30	0.26	225.78	382.74
Ltbp1	latent transforming growth factor beta binding protein 1	10.94	7.06	181.18	178.19
Ccl21	chemokine (C-C motif) ligand 21	0.08	0.13	179.26	306.59

Continued on next page

Table F.2 – continued from previous page

		Decidua		Outer Myometrium	
Gene symbol	Gene name	TPM	±SD	TPM	±SD
Fkbp10	FK506 binding protein 10	10.31	6.50	175.52	232.59
Figf	c-fos induced growth factor	1.82	1.78	155.91	118.34
C1s	complement component 1 s subcomponent	6.71	6.21	146.38	107.16
C1r	complement component 1 r subcomponent	14.92	8.84	144.77	88.32
Frzb	frizzled-related protein	1.71	1.22	135.53	155.67
Epyc	epiphycan	0.01	0.01	112.12	194.21
Flrt2	fibronectin leucine rich transmembrane protein 2	9.03	13.68	111.39	36.96
Penk	proenkephalin	7.58	7.81	106.51	44.86
Matn1	matrilin 1 cartilage matrix protein	0.04	0.07	105.89	183.32
Scrg1	stimulator of chondrogenesis 1	94.74	164.10	100.38	173.87
Mmp3	matrix metallopeptidase 3	1.35	1.18	94.88	97.50
Egr1	early growth response 1	4.91	2.71	93.67	75.82
Ednra	endothelin receptor type A	11.59	2.87	89.84	59.17
Dpt	dermatopontin	2.65	2.71	84.78	31.34
Olfml2b	olfactomedin-like 2B	8.12	7.07	84.60	30.65
Nfia	nuclear factor I/A	4.98	5.23	83.31	75.20
Mia	melanoma inhibitory activity	0.04	0.07	78.53	135.58
Klf7	Kruppel-like factor 7 (ubiquitous)	30.90	19.82	76.46	22.22
Ctxn1	cortexin 1	1.57	2.42	75.14	44.09
Mafb	v-maf musculoaponeurotic fibrosarcoma oncogene homolog B (avian)	1.69	1.99	69.86	46.83
Spon1	spondin 1 extracellular matrix protein	8.32	7.94	62.34	18.52
Slc28a2	solute carrier family 28 (sodium-coupled nucleoside transporter) member 2	2.41	2.17	59.05	70.50
Aoc3	amine oxidase copper containing 3	5.19	4.26	58.42	28.70
Thbs2	thrombospondin 2	1.39	0.92	57.71	50.31
Ifi204	myeloid cell nuclear differentiation antigen	7.45	3.78	57.20	49.64
C4b	complement component 4B (Chido blood group)	0.64	0.79	54.42	38.23
Clec11a	C-type lectin domain family 11 member A	1.32	0.75	53.01	84.84
Zfp521	zinc finger protein 521	1.67	2.25	52.79	58.33
Cxcl12	chemokine (C-X-C motif) ligand 12	2.64	2.89	49.55	14.38
Prf1	perforin 1 (pore forming protein)	3.17	2.96	48.15	28.78
Pafah1b3	platelet-activating factor acetylhydrolase 1b catalytic subunit 3	21.48	31.57	47.91	30.20
Serpina3n	serine (or cysteine) peptidase inhibitor clade A member 3N	1.50	1.93	47.46	56.32
Tnmd	tenomodulin	0.01	0.02	43.15	74.74
Igsf10	immunoglobulin superfamily member 10	0.81	0.91	42.05	36.90
Crabp1	cellular retinoic acid binding protein 1	0.69	1.06	41.48	27.44
Fam101a	family with sequence similarity 101 member A	0.00	0.00	40.90	67.63
Mmp16	matrix metallopeptidase 16	1.12	0.93	39.48	61.01
Fxyd2	FXYD domain-containing ion transport regulator 2	0.66	0.60	37.96	41.73
Nrp1	neuropilin 1	3.46	1.29	37.80	23.18
Cpz	carboxypeptidase Z	1.68	2.33	36.61	11.30
Zfp354c	zinc finger protein 354C	1.53	0.68	35.79	41.55
Ppp1r1b	protein phosphatase 1 regulatory (inhibitor) subunit 1B	0.03	0.02	34.53	59.80
Tnn	tenascin N	0.56	0.60	33.66	21.36
Adcy2	adenylate cyclase 2 (brain)	2.31	0.48	31.47	18.31
Pgm5	phosphoglucomutase 5	3.78	3.65	29.91	12.70
Gem	GTP binding protein overexpressed in skeletal muscle	1.36	0.79	27.18	18.13
Trpv4	transient receptor potential cation channel subfamily V member 4	0.12	0.16	26.41	39.51
Atp1b4	ATPase (Na)/K transporting beta 4 polypeptide	0.49	0.28	25.70	43.63
Ptprs	protein tyrosine phosphatase	4.13	2.04	24.89	17.00
Cd300le-ps1	Cd300 molecule-like family member E	0.44	0.45	22.56	18.15
Id4	inhibitor of DNA binding 4	7.03	9.07	20.93	9.79
Tac2	tachykinin 2	0.05	0.03	17.66	27.55
Cldn5	claudin 5	0.04	0.06	17.35	20.31
Tnxa-ps1	tenascin XA	0.15	0.19	16.19	5.70
Myoz1	myozenin 1	0.03	0.05	15.55	25.20
Rprm	reprimo TP53 dependent G2 arrest mediator candidate	2.95	5.10	15.09	4.74
B4galt2	UDP-Gal:betaGlcNAc beta 14- galactosyltransferase polypeptide 2	0.19	0.03	14.39	16.15
Myh2	myosin heavy chain 2 skeletal muscle adult	0.01	0.02	14.23	24.56
Rassf2	Ras association (RalGDS/AF-6) domain family member 2	4.10	6.30	13.66	6.34
Tpsb2	tryptase beta 2	0.11	0.04	13.13	5.20
Cacna1c	calcium channel voltage-dependent L type alpha 1C subunit	0.43	0.27	12.42	6.97
Fap	fibroblast activation protein alpha	0.04	0.04	12.35	9.40
Ngfr	nerve growth factor receptor	1.03	1.23	12.32	4.38
Msi1	musashi RNA-binding protein 1	0.12	0.18	11.91	14.36
Gpr77	complement component 5a receptor 2	0.08	0.11	11.88	10.05
Krt75	keratin 75	0.76	1.03	11.75	10.69
G0s2	G0/G1switch 2	4.35	3.72	11.74	5.26
Cacng1	calcium channel voltage-dependent gamma subunit 1	0.00	0.00	11.55	19.45

Continued on next page

Table F.2 – continued from previous page

		Decidua		Outer Myometrium	
Gene symbol	Gene name	TPM	±SD	TPM	±SD
Rtn2	reticulon 2	0.12	0.02	10.82	7.78
Bves	blood vessel epicardial substance	0.33	0.57	10.41	2.93
Tceal7	transcription elongation factor A (SII)-like 7	0.06	0.10	10.17	13.19
Cpxm2	carboxypeptidase X (M14 family) member 2	1.59	1.14	10.10	14.38
Sgca	sarcoglycan alpha (dystrophin-associated glycoprotein)	0.04	0.06	10.01	11.46
Lhfpl2	lipoma HMGIC fusion partner-like 2	0.16	0.14	9.95	8.02
Klf14	Kruppel-like factor 14	4.08	6.86	9.46	6.61
Rnase1l1	ribonuclease RNase A family 1-like 1 (pancreatic)	0.00	0.00	8.25	13.48
Ccl19	chemokine (C-C motif) ligand 19	0.00	0.00	8.08	12.25
Arhgef28	Rho guanine nucleotide exchange factor (GEF) 28	0.50	0.34	7.64	4.61
Kazald1	Kazal-type serine peptidase inhibitor domain 1	2.70	4.64	7.13	10.29
Egr2	early growth response 2	2.44	2.35	7.09	2.03
Hey1	hairy/enhancer-of-split related with YRPW motif 1	0.18	0.28	6.83	4.63
Rasgrp4	RAS guanyl releasing protein 4	1.39	2.20	6.54	7.76
Slamf8	SLAM family member 8	0.09	0.09	5.69	4.28
Cib2	calcium and integrin binding family member 2	1.19	0.75	5.56	6.49
Tpsab1	tryptase alpha/beta 1	0.01	0.02	5.05	4.12
Lsamp	limbic system-associated membrane protein	1.42	1.07	5.03	3.91
Tcf21	transcription factor 21	0.13	0.16	4.65	6.52
Nsg1	neuron specific gene family member 1	0.09	0.11	4.23	2.34
Fam19a5	family with sequence similarity 19 (chemokine (C-C motif)-like) member A5	0.01	0.02	4.09	3.35
Kcnn4	potassium intermediate/small conductance calcium-activated channel subfamily N member 4	0.08	0.15	3.63	1.72
Bcl11a	B-cell CLL/lymphoma 11A (zinc finger protein)	1.92	0.76	3.44	1.22
Vstm2b	V-set and transmembrane domain containing 2B	0.07	0.02	3.36	4.30
Lrrn3	leucine rich repeat neuronal 3	0.00	0.00	3.36	5.52
Aldh1a3	aldehyde dehydrogenase 1 family member A3	0.01	0.02	2.84	1.64
Ccbp2	chemokine binding protein 2	0.09	0.06	2.54	1.22
Klhl4	kelch-like family member 4	0.05	0.07	2.04	3.30
Myh1	myosin heavy chain 1 skeletal muscle adult	0.01	0.01	1.23	1.95
Down-regulated genes					
Ces4a	carboxylesterase 4A	1.73	1.43	0.00	0.00
Hmx3	H6 family homeobox 3	17.14	29.63	0.00	0.00
LOC680590	hypothetical protein LOC680590	21.86	37.48	0.00	0.00
Lpo	lactoperoxidase	32.58	56.31	0.00	0.00
Phactr3	phosphatase and actin regulator 3	2.75	2.42	0.00	0.00
Acsm5	acyl-CoA synthetase medium-chain family member 5	2.84	4.82	0.02	0.04
Hyal4	hyaluronoglucosaminidase 4	3.51	2.10	0.16	0.05
Psg16	pregnancy specific glycoprotein 16	30.32	37.21	1.57	1.50
Ppp1r3a	protein phosphatase 1 regulatory subunit 3A	5.18	8.18	2.04	2.97
Cgm4	carcinoembryonic antigen gene family 4	110.49	150.82	2.84	2.60
LOC171573	spleen protein 1 precursor	772.77	695.57	3.33	3.87
Lamc2	laminin gamma 2	355.81	570.33	3.40	2.37
Gnai1	guanine nucleotide binding protein (G protein) alpha inhibiting activity polypeptide 1	22.19	18.58	3.45	2.08
Prdm1	PR domain containing 1 with ZNF domain	37.93	30.17	3.49	1.41
Slc22a5	solute carrier family 22 (organic cation/carnitine transporter) member 5	15.35	13.22	4.24	1.98
Itpripl1	inositol 145-trisphosphate receptor interacting protein-like 1	22.01	38.00	5.66	2.75
Slc6a12	solute carrier family 6 (neurotransmitter transporter betaine/GABA) member 12	209.04	359.00	6.00	5.15
Usp53	ubiquitin specific peptidase 53	70.43	61.14	6.65	1.90
Cdh3	cadherin 3	189.71	153.30	10.16	6.84
Kif3c	kinesin family member 3C	26.96	21.34	12.37	3.16
Creg1	cellular repressor of E1A-stimulated genes 1	87.02	36.84	14.25	6.36
Tmem204	transmembrane protein 204	134.18	71.70	17.61	7.66
Psg19	pregnancy specific glycoprotein 19	99.10	61.06	17.90	11.02
Pgf	placental growth factor	446.64	771.11	20.81	15.20
Prl8a9	prolactin family 8 subfamily a member 9	882.21	758.51	25.59	33.78
Tgfb2	transforming growth factor beta 2	239.98	170.11	31.57	17.84
Hopx	HOP homeobox	211.07	272.70	38.26	11.78

Table F.3: Transcripts that were significantly differentially expressed between the inner myometrium and the outer myometrium in P4-treated samples. Transcript expression levels are shown in transcripts per million (TPM) (mean±SD).

		inner Myometrium		Outer Myometrium	
Gene symbol	Gene name	TPM	±SD	TPM	±SD
Upregulated genes					
Igf2	insulin-like growth factor 2	1198.03	2013.74	3180.07	3014.82
Dlk1	delta-like 1 homolog (Drosophila)	237.27	408.86	2564.29	3955.38
LOC689064	beta-globin	429.62	676.80	2150.31	3410.46
Ctsr	cathepsin R	900.80	1551.03	2055.89	3437.70
Ucma	upper zone of growth plate and cartilage matrix associated	0.98	1.61	1172.11	2027.06
Itm2a	integral membrane protein 2A	193.05	333.78	1111.71	1574.43
Alb	albumin	115.79	174.01	559.77	919.82
C1qtnf3	C1q and tumor necrosis factor related protein 3	0.60	0.63	453.63	771.85
Plagl1	pleiomorphic adenoma gene-like 1	98.87	169.04	408.40	455.53
Mest	mesoderm specific transcript	80.99	137.85	323.67	380.50
Myh8	myosin heavy chain 8 skeletal muscle perinatal	0.14	0.19	269.58	458.13
Hist2h3c2	histone cluster 2 H3c2	79.55	102.95	264.37	254.04
Mfap2	microfibrillar-associated protein 2	5.39	8.85	248.02	375.19
Capn6	calpain 6	0.30	0.26	225.78	382.74
Synpo	synaptopodin	20.13	9.12	144.76	201.46
Col14a1	collagen type XIV alpha 1	2.25	2.86	135.26	166.79
Eln	elastin	60.82	102.71	130.55	97.67
Zim1	zinc finger imprinted 1	38.14	62.72	130.36	183.00
Scrg1	stimulator of chondrogenesis 1	94.74	164.10	100.38	173.87
MGC114246	similar to cathepsin R	16.97	28.97	89.72	150.53
Serpina1	serpin peptidase inhibitor clade A (alpha-1 antiproteinase antitrypsin) member 1	37.50	51.32	87.73	136.99
Dpt	dermatopontin	2.65	2.71	84.78	31.34
Gpc3	glypican 3	26.58	44.16	84.62	64.79
Col27a1	collagen type XXVII alpha 1	2.65	2.27	61.86	102.86
Alas2	aminolevulinate delta-synthase 2	26.68	44.86	56.22	83.53
Cytl1	cytokine like 1	1.84	3.11	49.51	78.52
Ccnd2	cyclin D2	8.19	11.03	44.36	43.46
Ltbp4	latent transforming growth factor beta binding protein 4	9.08	14.26	43.56	34.79
Flvcr2	feline leukemia virus subgroup C cellular receptor family member 2	38.13	39.67	38.24	43.00
Ppp1r1b	protein phosphatase 1 regulatory (inhibitor) subunit 1B	0.03	0.02	34.53	59.80
Myl3	myosin light chain 3 alkali ventricular skeletal slow	0.28	0.35	33.63	55.40
Sim2	single-minded homolog 2 (Drosophila)	0.31	0.19	33.32	57.63
Stxbp6	syntaxin binding protein 6 (amisyn)	10.58	12.20	31.92	25.96
Lrp5	low density lipoprotein receptor-related protein 5	19.19	23.20	29.43	20.55
Leprel1	leprecan-like 1	21.51	32.58	28.72	23.42
Podxl	podocalyxin-like	25.31	34.96	28.19	28.21
Ambp	alpha-1-microglobulin/bikunin precursor	7.67	12.93	26.20	43.91
Atp1b4	ATPase (Na)/K transporting beta 4 polypeptide	0.49	0.28	25.70	43.63
Sh2d3c	SH2 domain containing 3C	12.33	18.86	24.73	8.31
Etv5	ets variant 5	13.00	14.68	24.69	19.35
Ninj2	ninjurin 2	1.99	3.31	23.37	35.05
Kitlg	KIT ligand	20.01	15.33	23.29	32.46
Egfl6	EGF-like-domain multiple 6	1.02	1.12	19.96	29.69
Slc1a3	solute carrier family 1 (glial high affinity glutamate transporter) member 3	0.33	0.41	19.18	29.02
Zfp385b	zinc finger protein 385B	1.20	1.89	18.82	31.56
Cdo1	cysteine dioxygenase type 1	2.95	1.80	18.75	14.11
Kif23	kinesin family member 23	11.16	10.38	18.00	17.70
Lpar4	lysophosphatidic acid receptor 4	3.74	1.34	17.37	14.51
Cma1	chymase 1 mast cell	0.24	0.39	16.08	16.78
Foxc1	forkhead box C1	1.72	1.89	14.99	23.82
Fgf18	fibroblast growth factor 18	0.13	0.19	14.76	23.66
Nlgn3	neuroligin 3	2.40	1.98	14.74	23.56
Myom1	myomesin 1	1.88	2.29	14.01	21.90
Fry	furry homolog (Drosophila)	2.09	0.66	13.13	13.27
Fzd9	frizzled family receptor 9	0.77	1.23	11.57	20.03
Cacng1	calcium channel voltage-dependent gamma subunit 1	0.00	0.00	11.55	19.45
Gucy1a3	guanylate cyclase 1 soluble alpha 3	0.98	1.11	11.45	9.03
Csn2	casein beta	0.51	0.81	10.87	18.80
Pth1r	parathyroid hormone 1 receptor	1.83	3.01	10.86	12.88
Hoxc4	homeo box C4	7.47	11.16	10.54	14.12
Six2	SIX homeobox 2	0.22	0.18	10.48	10.61

Continued on next page

Table F.3 – continued from previous page

		Inner Myometrium		Outer Myometrium	
Gene symbol	Gene name	TPM	±SD	TPM	±SD
Galnt16	UDP-N-acetyl-alpha-D-galactosamine:polypeptide N-acetylgalactosaminyltransferase 16	1.53	2.28	10.46	2.68
Kif18b	kinesin family member 18B	3.36	3.94	10.30	7.98
Tceal7	transcription elongation factor A (SII)-like 7	0.06	0.10	10.17	13.19
Cpxm2	carboxypeptidase X (M14 family) member 2	1.59	1.14	10.10	14.38
Ggnbp1	gametogenetin-binding protein 1	2.29	2.45	8.82	7.92
Kera	keratocan	0.02	0.02	7.63	13.06
Cav3	caveolin 3	0.00	0.00	7.43	12.79
Mcf2l	MCF.2 cell line derived transforming sequence-like	3.72	3.72	7.27	3.64
Sox8	SRY (sex determining region Y)-box 8	2.21	0.89	6.94	4.28
RGD1561795	similar to RIKEN cDNA 1700012B09	3.20	5.47	6.31	8.87
Slc25a23	solute carrier family 25 (mitochondrial carrier; phosphate carrier)	2.58	3.03	6.19	5.02
Hoxa2	homeo box A2	0.88	1.49	6.17	9.35
Zic3	Zic family member 3	4.04	3.52	6.02	8.23
LOC688276	transmembrane channel-like 8	3.06	3.32	5.99	2.00
Zfpm2	zinc finger protein multitype 2	0.90	1.46	5.91	6.20
Cacna1s	calcium channel voltage-dependent L type alpha 1S subunit	0.05	0.06	5.65	9.25
Gcgr	glucagon receptor	3.47	5.43	5.46	8.35
Hpd	4-hydroxyphenylpyruvate dioxygenase	5.10	8.57	5.46	6.41
Asb4	ankyrin repeat and SOCS box-containing 4	1.17	1.49	5.39	6.41
Tpsab1	tryptase alpha/beta 1	0.01	0.02	5.05	4.12
LOC361016	similar to RIKEN cDNA 4933406L09	4.08	5.49	4.66	6.25
Trdn	triadin	0.13	0.09	4.19	7.15
Pgc	progastricsin (pepsinogen C)	0.75	0.65	4.18	4.78
Bmper	BMP-binding endothelial regulator	1.89	2.97	3.99	3.70
Epha3	Eph receptor A3	0.29	0.28	3.56	5.09
Tspyl4	TSPY-like 4	2.67	3.73	3.33	3.35
Megf6	multiple EGF-like-domains 6	0.35	0.56	3.30	4.59
Cntn2	contactin 2 (axonal)	0.35	0.57	3.20	5.22
Lrrn1	leucine rich repeat neuronal 1	0.15	0.15	2.37	2.59
Slco4c1	solute carrier organic anion transporter family member 4C1	0.81	0.68	2.33	3.10
Kcna6	potassium voltage gated channel shaker related subfamily member 6	0.33	0.30	1.76	2.59
Down-regulated genes					
Lpo	lactoperoxidase	32.58	56.31	0.00	0.00
Olr773	olfactory receptor 773	5.08	8.78	0.00	0.00
Fancd2os	FANCD2 opposite strand	0.44	0.49	0.15	0.02
Chrm2	cholinergic receptor muscarinic 2	1.94	1.78	1.14	0.97
Rorb	RAR-related orphan receptor B	9.31	10.73	1.20	0.66
Ppp1r3a	protein phosphatase 1 regulatory subunit 3A	5.18	8.18	2.04	2.97
Prdm1	PR domain containing 1 with ZNF domain	37.93	30.17	3.49	1.41
Pnma5	paraneoplastic Ma antigen family member 5	7.03	11.87	3.61	6.25
Insc	inscuteable homolog (Drosophila)	7.84	13.01	3.80	3.56
Elf5	E74-like factor 5	4.21	6.71	4.17	6.88
Slc22a3	solute carrier family 22 (extraneuronal monoamine transporter) member 3	4.84	8.29	4.53	7.18
Grip2	glutamate receptor interacting protein 2	9.40	15.44	5.55	9.13
Slc6a12	solute carrier family 6 (neurotransmitter transporter betaine/GABA) member 12	209.04	359.00	6.00	5.15
Alox15	arachidonate 15-lipoxygenase	19.98	34.45	6.10	9.73
LOC498222	similar to specifically androgen-regulated protein	11.11	16.91	6.24	8.82
Smtnl1	smoothelin-like 1	9.02	15.53	6.93	11.83
Pak6	p21 protein (Cdc42/Rac)-activated kinase 6	35.20	51.11	8.46	9.57
Irx3	iroquois homeobox 3	12.48	20.35	8.92	13.05
Cdkn3	cyclin-dependent kinase inhibitor 3	0.22	0.25	9.45	6.30
Prl2b1	Prolactin family 2 subfamily b member 1	72.72	94.83	11.82	20.47
RGD1309139	similar to CG5435-PA	55.45	71.41	13.20	5.76
Baiap2l1	BAI1-associated protein 2-like 1	15.34	20.61	13.98	9.80
Zfp423	zinc finger protein 423	1.80	0.29	16.19	7.60
Sgcd	sarcoglycan, delta (dystrophin-associated glycoprotein)	0.64	0.55	17.89	15.44
Caskin2	cask-interacting protein 2	23.62	34.63	18.20	17.94
Hmgcs2	3-hydroxy-3-methylglutaryl-CoA synthase 2 (mitochondrial)	32.95	49.45	19.55	7.89
Pgf	placental growth factor	446.64	771.11	20.81	15.20
Utf1	undifferentiated embryonic cell transcription factor 1	70.65	119.81	22.91	34.34
B4galnt3	beta-14-N-acetyl-galactosaminyl transferase 3	101.88	176.12	22.92	25.32
Dock8	dedicator of cytokinesis 8	3.07	0.72	25.88	15.89
Vwf	von Willebrand factor	1.61	1.66	25.89	24.95
Stard10	StAR-related lipid transfer (START) domain containing 10	38.84	66.06	30.28	12.21
Ptp4a3	protein tyrosine phosphatase type IVA member 3	44.38	56.70	33.19	11.85

Continued on next page

Table F.3 – continued from previous page

		Inner Myometrium		Outer Myometrium	
Gene symbol	Gene name	TPM	±SD	TPM	±SD
Sort1	sortilin 1	2.65	0.65	36.02	19.03
Dlc1	deleted in liver cancer 1	4.21	1.22	36.19	14.22
Glis2	GLIS family zinc finger 2	3.22	2.40	38.66	36.18
Lgalsl	lectin, galactoside-binding-like	3.43	1.91	38.89	29.93
St14	suppression of tumorigenicity 14 (colon carcinoma)	48.79	38.29	41.47	64.00
Sema4d	semaphorin 4D	2.20	1.06	43.94	46.50
Shroom4	shroom family member 4	57.82	94.12	45.02	58.27
Dlx3	distal-less homeobox 3	132.75	228.07	47.80	76.50
Stard8	StAR-related lipid transfer (START) domain containing 8	103.26	146.79	58.84	75.41
Hand1	heart and neural crest derivatives expressed 1	72.19	106.52	65.12	109.39
Tns3	tensin 3	10.29	0.74	67.51	48.28
Cdh1	cadherin 1	108.55	173.41	72.03	107.33
Slc38a4	solute carrier family 38 member 4	144.73	223.60	75.16	107.29
Csgalnact1	chondroitin sulfate N-acetylgalactosaminyltransferase 1	7.81	5.46	79.87	79.72
Eps8l2	EPS8-like 2	131.61	219.35	83.50	98.29
Tns4	tensin 4	149.62	258.41	86.50	130.57
Slc16a3	solute carrier family 16 member 3 (monocarboxylic acid transporter 4)	120.68	194.36	87.70	48.37
Fbn1	fibrillin 1	7.71	2.29	87.95	30.19
Nrk	Nik related kinase	12.39	8.16	124.60	86.77
Nrep	neuronal regeneration related protein	3.49	2.50	159.63	176.43
Slc7a5	solute carrier family 7 (amino acid transporter light chain L system) member 5	499.07	857.67	237.93	338.10

F.2 Early Response to Progesterone Withdrawal

Table F.4: Genes that change significantly in the decidua. Transcript expression levels are shown in transcripts per million values (mean±SD) for control samples (GD19+6hrs) and P4-treated samples.

		Control		P4	
Gene symbol	Gene name	TPM	±SD	TPM	±SD
Upregulated genes					
Proc	protein C	279.51	466.82	1140.36	1974.03
Tagln	transgelin	47.17	10.26	397.46	105.16
Alb	albumin	1.74	1.62	115.79	174.01
Eln	elastin	2.07	0.67	60.82	102.71
Rarres1	retinoic acid receptor responder (tazarotene induced) 1	8.86	6.43	56.18	56.98
Plekhd1	pleckstrin homology domain containing, family D (with coiled-coil domains) member 1	11.83	13.23	31.43	52.11
Hmx3	H6 family homeobox 3	0.09	0.13	17.14	29.63
Rgs4	regulator of G-protein signaling 4	2.46	2.79	13.01	15.41
Downregulated genes					
Aqp8	aquaporin 8	15.88	8.58	0.01	0.01
Clrn3	clarin 3	4.33	1.81	0.02	0.04
Il20ra	interleukin 20 receptor, alpha	1.16	1.66	0.03	0.05
Slc34a3	solute carrier family 34 (type II sodium/phosphate contransporter), member 3	5.19	4.41	0.03	0.05
Abcc8	ATP-binding cassette, subfamily C (CFTR/MRP), member 8	5.67	4.81	0.05	0.09
RGD1305807	hypothetical LOC298077	2.14	2.08	0.06	0.07
Mybpc3	myosin binding protein C, cardiac	9.94	2.49	0.07	0.09
Akr7a3	aldo-keto reductase family 7, member A3 (aflatoxin aldehyde reductase)	5.64	3.15	0.08	0.13
Tm4sf20	transmembrane 4 L six family member 20	6.12	3.31	0.14	0.17
Apoa2	apolipoprotein A-II	255.70	230.37	0.22	0.20
Kcnj16	potassium inwardly-rectifying channel, subfamily J, member 16	1.42	0.78	0.22	0.07
Hnf4a	hepatocyte nuclear factor 4, alpha	5.87	1.83	0.22	0.26
Colec10	collectin sub-family member 10 (C-type lectin)	1.00	0.57	0.26	0.21
Slc2a2	solute carrier family 2 (facilitated glucose transporter), member 2	5.37	3.33	0.27	0.38
Cubn	cubilin (intrinsic factor-cobalamin receptor)	34.90	17.01	0.28	0.26
Apom	apolipoprotein M	87.18	33.70	0.32	0.16
Agt	angiotensinogen (serpin peptidase inhibitor, clade A, member 8)	15.52	7.91	0.46	0.28

Continued on next page

Table F.4 – continued from previous page

		Control		P4	
Gene symbol	Gene name	TPM	±SD	TPM	±SD
Fmo1	flavin containing monooxygenase 1	16.56	6.65	0.47	0.55
Aadat	aminoadipate aminotransferase	20.54	12.08	0.54	0.18
Amn	amnion associated transmembrane protein	17.79	3.29	0.56	0.20
Apon	apolipoprotein N	4.06	3.19	0.63	0.38
Fxyd2	FXYD domain-containing ion transport regulator 2	23.85	15.48	0.66	0.60
Sdsl	serine dehydratase-like	4.46	4.03	0.72	1.25
Doxl1	diamine oxidase-like protein 1	62.80	87.77	1.07	1.48
Tst	thiosulfate sulfurtransferase	28.25	10.97	1.17	0.34
Hbe1	hemoglobin, epsilon 1	148.03	215.78	1.65	1.95
Apoc2	apolipoprotein C-II	73.03	57.13	1.83	3.14
F2	coagulation factor II	38.52	19.11	2.49	3.36
Apob	apolipoprotein B	535.64	256.06	2.69	1.59
Spp2	secreted phosphoprotein 2	100.64	96.49	2.85	4.10
Apoa4	apolipoprotein A-IV	213.84	113.78	3.16	3.33
Prf1	perforin 1 (pore forming protein)	6.90	5.57	3.17	2.96
Fgg	fibrinogen gamma chain	42.01	21.19	3.35	2.48
Ctsz	cathepsin Z	63.74	27.75	5.95	3.31
RGD1310507	similar to RIKEN cDNA 1300017J02	25.76	23.50	6.60	5.13
Entpd2	ectonucleoside triphosphate diphosphohydrolase 2	71.15	33.86	7.90	2.34
Fga	fibrinogen alpha chain	78.63	39.83	10.23	13.56
Afp	alpha-fetoprotein	2331.59	1656.67	14.59	14.92
Apoa1	apolipoprotein A-I	651.04	422.62	15.92	25.90
Rbp4	retinol binding protein 4, plasma	126.35	153.08	16.81	26.73
Ttr	transthyretin	660.29	525.55	20.28	32.71

Table F.5: Genes that change significantly in the inner myometrium. Transcript expression levels are shown in transcripts per million (TPM) values (mean±SD) for control (GD19+6hrs) samples and P4-treated samples.

		Control		P4	
Gene symbol	Gene name	TPM	±SD	TPM	±SD
Upregulated genes					
Slc6a12	solute carrier family 6 (neurotransmitter transporter), member 12	11.46	4.59	164.12	248.29
Plce1	phospholipase C, epsilon 1	7.35	2.84	34.70	12.62
Itga8	integrin, alpha 8	4.07	3.06	23.08	13.44
Ibsp	integrin-binding sialoprotein	0.71	0.43	7.68	12.31
Duoxa1	dual oxidase maturation factor 1	0.11	0.01	5.48	3.52
Downregulated genes					
Atg9b	autophagy related 9B	16.12	18.50	0.00	0.00
Cbs	cystathionine beta synthase	3.70	6.07	0.00	0.00
Wfdc16	WAP four-disulfide core domain 16	10.14	11.47	0.00	0.00
Cyp2f4	cytochrome P450, family 2, subfamily f, polypeptide 4	15.32	19.78	0.00	0.01
Tspyl4	TSPY-like 4	4.47	2.67	0.03	0.06
Mchr1	melanin-concentrating hormone receptor 1	17.12	19.70	0.06	0.03
Il17rb	interleukin 17 receptor B	9.03	7.81	0.11	0.15
Atp6v0a4	ATPase, H+ transporting, lysosomal V0 subunit A4	25.42	21.81	0.35	0.10
Fam160a1	family with sequence similarity 160, member A1	12.03	7.82	0.37	0.23
Dio3	deiodinase, iodothyronine, type III	32.23	19.05	0.47	0.43
Doxl1	diamine oxidase-like protein 1	49.84	48.50	1.10	1.02
Lrp2	low density lipoprotein receptor-related protein 2	31.21	28.24	1.13	1.02
Col14a1	collagen, type XIV, alpha 1	13.78	5.92	1.37	0.53
Slc4a11	solute carrier family 4, sodium borate transporter, member 11	125.33	110.33	1.41	1.32
Hmgcs2	3-hydroxy-3-methylglutaryl-CoA synthase 2 (mitochondrial)	78.42	71.42	1.43	1.28
Ctsj	cathepsin J	53.08	59.67	1.47	1.15
Ltbp4	latent transforming growth factor beta binding protein 4	29.47	30.97	1.49	0.37
Abcb1b	ATP-binding cassette, subfamily B (MDR/TAP), member 1B	129.18	118.61	1.81	2.10
Lrat	lecithin-retinol acyltransferase (phosphatidylcholine-retinol-O-acyltransferase)	120.84	118.41	2.91	1.51
Ctsr	cathepsin R	83.06	86.91	3.02	4.60
Ca2	carbonic anhydrase 2	52.53	35.79	3.39	1.73
Mill1	MHC I like leukocyte 1	36.28	8.50	3.99	1.03
Ctsql2	cathepsin Q-like 2	67.21	73.38	4.32	5.98
Bcam	basal cell adhesion molecule (Lutheran blood group)	89.57	73.51	5.34	2.49

Continued on next page

Table F.5 – continued from previous page

		Control		P4	
Gene symbol	Gene name	TPM	±SD	TPM	±SD
Csf1	colony stimulating factor 1 (macrophage)	159.80	202.04	7.74	6.55
Pcsk6	proprotein convertase subtilisin/kexin type 6	49.75	20.09	9.20	3.25
Tns3	tensin 3	43.07	10.26	10.29	0.74
Isyna1	inositol-3-phosphate synthase 1	718.80	625.89	30.47	6.85
Spp1	secreted phosphoprotein 1	607.02	435.91	47.12	22.63
Ezr	ezrin	288.55	57.09	62.12	24.20

Table F.6: Genes that change significantly in the outer myometrium. Transcript expression levels are shown in transcripts per million (TPM) values (mean±SD) for control (GD19+6hrs) samples and P4-treated samples.

		Control		P4	
Gene symbol	Gene name	TPM	±SD	TPM	±SD
Upregulated genes					
Penk	proenkephalin	7.65	3.75	106.51	44.86
Olfml2b	olfactomedin-like 2B	8.62	7.09	84.60	30.65
Csf2rb	colony stimulating factor 2 receptor, beta, low-affinity (granulocyte-macrophage)	8.78	10.10	44.01	24.43
Tnn	tenascin N	0.41	0.33	33.66	21.36
Tpsb2	tryptase beta 2	0.01	0.02	13.13	5.20
Zcchc12	zinc finger, CCHC domain containing 12	0.01	0.01	4.24	3.82
Downregulated genes					
Gucy2c	guanylate cyclase 2C	1.44	1.62	0.31	0.16
LOC171573	spleen protein 1 precursor	1612.19	2779.47	3.33	3.87
Psg29	pregnancy-specific glycoprotein 29	406.70	686.64	4.19	1.97
Itga10	integrin, alpha 10	16.88	29.22	5.99	10.17

Table F.7: Biological functions of genes that were upregulated in the decidua of P4-treated samples. The genes were analysed for GO term enrichment using BiNGO. The overrepresented GO terms are shown with their corresponding adjusted p-values and the number of genes within the test set that are annotated to that function.

Description	Corrected p-value	No. Genes
cholesterol transport	7.64E-08	6
sterol transport	7.64E-08	6
positive regulation of cholesterol esterification	9.61E-08	4
regulation of cholesterol esterification	9.61E-08	4
regulation of lipid metabolic process	9.61E-08	8
cholesterol efflux	9.61E-08	5
positive regulation of lipid metabolic process	2.36E-07	6
lipid homeostasis	4.29E-07	6
reverse cholesterol transport	7.05E-07	4
regulation of biological quality	7.05E-07	17
phospholipid efflux	9.40E-07	4
transport	9.79E-07	20
establishment of localization	1.03E-06	20
lipid transport	1.03E-06	7
positive regulation of fatty acid biosynthetic process	1.03E-06	4
chemical homeostasis	1.49E-06	11
lipid localization	1.49E-06	7
positive regulation of steroid metabolic process	1.49E-06	4
protein-lipid complex remodeling	1.49E-06	4
plasma lipoprotein particle remodeling	1.49E-06	4
macromolecular complex remodeling	1.49E-06	4
regulation of steroid metabolic process	2.49E-06	5
regulation of fatty acid biosynthetic process	6.50E-06	4
localization	7.03E-06	20
regulation of lipid biosynthetic process	1.15E-05	5
positive regulation of fatty acid metabolic process	1.21E-05	4

Continued on next page

Table F.7 – continued from previous page

Description	Corrected p-value	No. Genes
positive regulation of lipid biosynthetic process	1.21E-05	4
cholesterol metabolic process	2.25E-05	5
homeostatic process	2.25E-05	11
phospholipid transport	2.25E-05	4
coagulation	2.25E-05	5
blood coagulation	2.25E-05	5
hemostasis	2.25E-05	5
protein-lipid complex assembly	2.31E-05	3
sterol metabolic process	2.81E-05	5
regulation of lipase activity	3.12E-05	5
lipoprotein metabolic process	3.68E-05	5
sterol homeostasis	4.53E-05	4
cholesterol homeostasis	4.53E-05	4
lipoprotein transport	5.77E-05	3
macromolecular complex subunit organization	7.08E-05	10
regulation of transport	7.20E-05	9
steroid metabolic process	8.86E-05	6
positive regulation of lipid catabolic process	1.15E-04	3
regulation of localization	1.16E-04	10
regulation of body fluid levels	1.16E-04	5
negative regulation of lipoprotein oxidation	1.28E-04	2
regulation of lipoprotein oxidation	1.28E-04	2
lipoprotein particle clearance	1.29E-04	3
regulation of cholesterol transport	1.85E-04	3
regulation of sterol transport	1.85E-04	3
response to wounding	1.86E-04	8
regulation of fatty acid metabolic process	2.31E-04	4
platelet activation	2.43E-04	3
phosphatidylcholine metabolic process	2.43E-04	3
negative regulation of very-low-density lipoprotein particle remodeling	3.28E-04	2
regeneration	3.71E-04	5
amine metabolic process	3.75E-04	7
regulation of very-low-density lipoprotein particle remodeling	5.92E-04	2
negative regulation of cytokine secretion involved in immune response	5.92E-04	2
high-density lipoprotein particle assembly	5.92E-04	2
high-density lipoprotein particle clearance	5.92E-04	2
regulation of cellular ketone metabolic process	6.98E-04	4
cellular amino acid derivative metabolic process	7.14E-04	5
negative regulation of transport	7.45E-04	5
regulation of lipid catabolic process	7.51E-04	3
regulation of secretion	7.51E-04	6
anatomical structure morphogenesis	7.53E-04	10
response to chemical stimulus	8.32E-04	18
negative regulation of lipid metabolic process	8.37E-04	3
regulation of cytokine secretion involved in immune response	8.37E-04	2
negative regulation of lipoprotein metabolic process	8.37E-04	2
low-density lipoprotein particle remodeling	8.37E-04	2
ethanolamine and derivative metabolic process	9.04E-04	3
cellular biogenic amine metabolic process	9.31E-04	4
wound healing	9.41E-04	5
regulation of lipid transport	9.55E-04	3
response to organic substance	1.01E-03	11
positive regulation of triglyceride catabolic process	1.13E-03	2
negative regulation of sterol transport	1.13E-03	2
negative regulation of cholesterol transport	1.13E-03	2
regulation of cellular localization	1.28E-03	6
macromolecular complex assembly	1.32E-03	8
cellular amino acid and derivative metabolic process	1.39E-03	6
regulation of triglyceride catabolic process	1.45E-03	2
regulation of lipoprotein metabolic process	1.45E-03	2
triglyceride-rich lipoprotein particle remodeling	1.45E-03	2
plasma lipoprotein particle assembly	1.45E-03	2
negative regulation of protein transport	1.48E-03	3
response to stimulus	1.49E-03	21
response to inorganic substance	1.55E-03	6
hormone metabolic process	1.66E-03	4
regulation of production of molecular mediator of immune response	1.75E-03	3
positive regulation of lipoprotein lipase activity	1.75E-03	2
negative regulation of lipase activity	1.75E-03	2

Continued on next page

Table F.7 – continued from previous page

Description	Corrected p-value	No. Genes
toxin metabolic process	1.75E-03	2
high-density lipoprotein particle remodeling	1.75E-03	2
response to metal ion	2.02E-03	5
response to carbohydrate stimulus	2.02E-03	4
regulation of protein transport	2.12E-03	4
neutral lipid catabolic process	2.12E-03	2
glycerol ether catabolic process	2.12E-03	2
acylglycerol catabolic process	2.12E-03	2
regulation of establishment of protein localization	2.40E-03	4
lipid metabolic process	2.47E-03	8
negative regulation of cytokine secretion	3.08E-03	2
axon regeneration in the peripheral nervous system	3.08E-03	2
glycerolipid catabolic process	3.08E-03	2
positive regulation of lipase activity	3.47E-03	3
alcohol metabolic process	3.47E-03	6
secondary metabolic process	3.50E-03	3
phosphatidylcholine biosynthetic process	3.50E-03	2
positive regulation of triglyceride metabolic process	3.50E-03	2
ovulation from ovarian follicle	3.50E-03	2
sex differentiation	3.62E-03	4
regulation of protein localization	3.73E-03	4
regulation of protein secretion	3.73E-03	3
positive regulation of catabolic process	3.73E-03	3
cellular amine metabolic process	3.78E-03	5
cellular component organization	4.42E-03	13
glycerolipid metabolic process	4.42E-03	4
cellular component assembly	4.42E-03	8
SMAD protein signal transduction	4.42E-03	2
regulation of triglyceride metabolic process	4.42E-03	2
regulation of hormone levels	4.74E-03	4
regulation of insulin secretion	4.84E-03	3
negative regulation of lipid transport	4.97E-03	2
development of primary female sexual characteristics	4.97E-03	3
positive regulation of hydrolase activity	5.05E-03	4
female sex differentiation	5.98E-03	3
regulation of peptide hormone secretion	5.98E-03	3
ovulation	6.18E-03	2
negative regulation of multicellular organismal process	6.41E-03	4
regulation of peptide transport	6.53E-03	3
regulation of peptide secretion	6.53E-03	3
vitamin transport	6.68E-03	2
negative regulation of protein secretion	6.68E-03	2
small molecule metabolic process	6.74E-03	10
organ morphogenesis	6.77E-03	6
regulation of hydrolase activity	6.95E-03	5
organ regeneration	7.26E-03	3
cellular component biogenesis	7.53E-03	8
macromolecule localization	7.59E-03	8
negative regulation of cellular protein metabolic process	7.76E-03	4
axon regeneration	7.82E-03	2
regulation of lipoprotein lipase activity	8.57E-03	2
negative regulation of secretion	8.87E-03	3
regulation of cytokine production involved in immune response	9.27E-03	2
cell activation	9.27E-03	4
negative regulation of protein metabolic process	9.74E-03	4
aromatic compound catabolic process	9.95E-03	2
neuron projection regeneration	1.08E-02	2
response to glucose stimulus	1.10E-02	3
response to nutrient levels	1.12E-02	5
cellular amino acid derivative catabolic process	1.15E-02	2
response to hexose stimulus	1.21E-02	3
response to monosaccharide stimulus	1.24E-02	3
regulation of hormone secretion	1.34E-02	3
regulation of organ growth	1.35E-02	2
response to extracellular stimulus	1.35E-02	5
cardiac chamber development	1.35E-02	2
cardiac chamber morphogenesis	1.35E-02	2
regulation of immune effector process	1.35E-02	3
gonad development	1.35E-02	3

Continued on next page

Table F.7 – continued from previous page

Description	Corrected p-value	No. Genes
innate immune response in mucosa	1.35E-02	1
response to muscle activity involved in regulation of muscle adaptation	1.35E-02	1
mucosal immune response	1.35E-02	1
negative regulation of cholesterol transporter activity	1.35E-02	1
regulation of cholesterol transporter activity	1.35E-02	1
positive regulation of phospholipid catabolic process	1.35E-02	1
mycotoxin catabolic process	1.35E-02	1
mycotoxin metabolic process	1.35E-02	1
negative regulation of lipoprotein lipid oxidation	1.35E-02	1
regulation of lipoprotein lipid oxidation	1.35E-02	1
negative regulation of interleukin-1 beta secretion	1.35E-02	1
female genitalia morphogenesis	1.35E-02	1
sugar utilization	1.35E-02	1
renal control of peripheral vascular resistance involved in regulation of systemic arterial blood pressure	1.35E-02	1
isoprenoid transport	1.35E-02	1
terpenoid transport	1.35E-02	1
spermatogonial cell division	1.35E-02	1
retinol transport	1.35E-02	1
establishment of blood-nerve barrier	1.35E-02	1
aflatoxin metabolic process	1.35E-02	1
aflatoxin catabolic process	1.35E-02	1
toxin catabolic process	1.35E-02	1
diacylglycerol catabolic process	1.35E-02	1
regulation of blood vessel size by renin-angiotensin angiotensin mediated vasoconstriction involved in regulation of systemic arterial blood pressure	1.35E-02	1
negative regulation of plasma lipoprotein oxidation	1.35E-02	1
regulation of plasma lipoprotein oxidation	1.35E-02	1
response to stress	1.37E-02	10
negative regulation of cellular process	1.39E-02	10
glycerophospholipid metabolic process	1.46E-02	3
regulation of multicellular organismal process	1.56E-02	8
regulation of cytokine secretion	1.58E-02	2
reproductive developmental process	1.58E-02	4
response to drug	1.61E-02	5
development of primary sexual characteristics	1.61E-02	3
cellular protein complex assembly	2.05E-02	3
protein complex assembly	2.15E-02	5
protein complex biogenesis	2.15E-02	5
reproductive structure development	2.15E-02	3
acylglycerol metabolic process	2.18E-02	2
neutral lipid metabolic process	2.18E-02	2
protein polymerization	2.18E-02	2
female gamete generation	2.18E-02	2
response to osmotic stress	2.18E-02	2
carbohydrate homeostasis	2.18E-02	2
regulation of protein stability	2.18E-02	2
glucose homeostasis	2.18E-02	2
positive regulation of cellular metabolic process	2.18E-02	7
organ or tissue specific immune response	2.18E-02	1
cholesterol import	2.18E-02	1
negative regulation of protein import into nucleus, translocation	2.18E-02	1
female genitalia development	2.18E-02	1
maintenance of gastrointestinal epithelium	2.18E-02	1
regulation of phospholipid catabolic process	2.18E-02	1
hemoglobin import	2.18E-02	1
response to lipid hydroperoxide	2.18E-02	1
epithelial structure maintenance	2.18E-02	1
sterol transmembrane transport	2.18E-02	1
sterol import	2.18E-02	1
negative regulation of cholesterol import	2.18E-02	1
regulation of cholesterol import	2.18E-02	1
negative regulation of interleukin-1 secretion	2.18E-02	1
smooth muscle cell proliferation	2.18E-02	1
cellular response to prostaglandin stimulus	2.18E-02	1
embryonic retina morphogenesis in camera-type eye	2.18E-02	1
fructose transport	2.18E-02	1
NADPH oxidation	2.18E-02	1

Continued on next page

Table F.7 – continued from previous page

Description	Corrected p-value	No. Genes
negative regulation of transmembrane transport	2.18E-02	1
germ-line cyst formation	2.18E-02	1
male germ-line cyst formation	2.18E-02	1
multicellular organismal lipid catabolic process	2.18E-02	1
renin-angiotensin regulation of aldosterone production	2.18E-02	1
glycerol ether metabolic process	2.19E-02	2
positive regulation of biosynthetic process	2.20E-02	6
positive regulation of cellular catabolic process	2.37E-02	2
organic ether metabolic process	2.37E-02	2
negative regulation of biological process	2.37E-02	10
regulation of cellular protein metabolic process	2.38E-02	5
response to axon injury	2.44E-02	2
gamete generation	2.49E-02	4
digestion	2.63E-02	2
regulation of growth	2.65E-02	4
lipid catabolic process	2.70E-02	3
positive regulation of metabolic process	2.70E-02	7
positive regulation of phospholipase activity	2.80E-02	2
cellular lipid metabolic process	2.85E-02	5
negative regulation of cellular component organization	2.93E-02	3
negative regulation of metabolic process	2.93E-02	6
regulation of microvillus organization	2.93E-02	1
regulation of microvillus assembly	2.93E-02	1
establishment of tissue polarity	2.93E-02	1
positive regulation of muscle hypertrophy	2.93E-02	1
positive regulation of cardiac muscle hypertrophy	2.93E-02	1
negative regulation of tyrosine phosphorylation of Stat5 protein	2.93E-02	1
urinary bladder development	2.93E-02	1
uterus development	2.93E-02	1
ovarian follicle rupture	2.93E-02	1
phenylpropanoid catabolic process	2.93E-02	1
coumarin catabolic process	2.93E-02	1
response to lipopolysaccharide	3.06E-02	3
rhythmic process	3.10E-02	3
positive regulation of ion transport	3.15E-02	2
regulation of phospholipase activity	3.15E-02	2
cardiac muscle tissue development	3.36E-02	2
anatomical structure development	3.49E-02	11
response to molecule of bacterial origin	3.51E-02	3
sexual reproduction	3.51E-02	4
heart morphogenesis	3.51E-02	2
negative regulation of hydrolase activity	3.51E-02	2
phospholipid metabolic process	3.51E-02	3
negative regulation of very-low-density lipoprotein particle clearance	3.51E-02	1
regulation of very-low-density lipoprotein particle clearance	3.51E-02	1
triglyceride mobilization	3.51E-02	1
genitalia morphogenesis	3.51E-02	1
kynurenine metabolic process	3.51E-02	1
response to stimulus involved in regulation of muscle adaptation	3.51E-02	1
regulation of intestinal cholesterol absorption	3.51E-02	1
Cdc42 protein signal transduction	3.51E-02	1
negative regulation of tyrosine phosphorylation of STAT protein	3.51E-02	1
negative regulation of nerve growth factor receptor signaling pathway	3.51E-02	1
negative regulation of receptor-mediated endocytosis	3.51E-02	1
myosin filament assembly	3.51E-02	1
myosin filament assembly or disassembly	3.51E-02	1
astrocyte activation	3.51E-02	1
brain renin-angiotensin system	3.51E-02	1
regulation of renal output by angiotensin	3.51E-02	1
lipoprotein catabolic process	3.51E-02	1
renal response to blood flow involved in circulatory		
renin-angiotensin regulation of systemic arterial blood pressure	3.51E-02	1
dehydroascorbic acid transport	3.51E-02	1
cell development	3.52E-02	5
regulation of protein metabolic process	3.56E-02	5
regulation of cell growth	3.61E-02	3
metal ion transport	3.64E-02	4
female gonad development	3.66E-02	2
response to external stimulus	3.95E-02	5

Continued on next page

Table F.7 – continued from previous page

Description	Corrected p-value	No. Genes
organophosphate metabolic process	3.99E-02	3
regulation of protein amino acid phosphorylation	3.99E-02	3
muscle structure development	4.02E-02	3
cellular hormone metabolic process	4.02E-02	2
glycerophospholipid biosynthetic process	4.02E-02	2
developmental process	4.02E-02	12
ornithine metabolic process	4.02E-02	1
negative regulation of interleukin-1 beta production	4.02E-02	1
positive regulation of gluconeogenesis	4.02E-02	1
smooth muscle cell differentiation	4.02E-02	1
regulation of gastrulation	4.02E-02	1
positive regulation of immunoglobulin secretion	4.02E-02	1
regulation of nerve growth factor receptor signaling pathway	4.02E-02	1
vagina development	4.02E-02	1
negative regulation of cardiac muscle cell proliferation	4.02E-02	1
canalicular bile acid transport	4.02E-02	1
very-low-density lipoprotein particle remodeling	4.02E-02	1
chylomicron remnant clearance	4.02E-02	1
diacylglycerol metabolic process	4.02E-02	1
lipid digestion	4.02E-02	1
inorganic anion transport	4.17E-02	2
cellular ion homeostasis	4.45E-02	4
system development	4.45E-02	10
cellular chemical homeostasis	4.45E-02	4
ovulation cycle process	4.45E-02	2
response to calcium ion	4.45E-02	2
tryptophan catabolic process	4.45E-02	1
negative regulation of lipoprotein particle clearance	4.45E-02	1
cellular phosphate ion homeostasis	4.45E-02	1
positive regulation of cholesterol storage	4.45E-02	1
negative regulation of interleukin-1 production	4.45E-02	1
cellular di-, tri-valent inorganic anion homeostasis	4.45E-02	1
positive regulation of potassium ion transport	4.45E-02	1
positive regulation of interleukin-8 biosynthetic process	4.45E-02	1
cellular sodium ion homeostasis	4.45E-02	1
cellular response to superoxide	4.45E-02	1
cellular response to oxygen radical	4.45E-02	1
coumarin metabolic process	4.45E-02	1
negative regulation of astrocyte differentiation	4.45E-02	1
fibrinolysis	4.45E-02	1
indolalkylamine catabolic process	4.45E-02	1
progesterone metabolic process	4.45E-02	1
indole derivative catabolic process	4.45E-02	1
negative regulation of JAK-STAT cascade	4.45E-02	1
removal of superoxide radicals	4.45E-02	1
tryptophan catabolic process to kynurenine	4.45E-02	1
phenylpropanoid metabolic process	4.45E-02	1
regulation of peptidyl-tyrosine phosphorylation	4.49E-02	2
cofactor metabolic process	4.49E-02	3
multicellular organismal development	4.49E-02	11
glycerolipid biosynthetic process	4.67E-02	2
response to cAMP	4.67E-02	2
inflammatory response	4.67E-02	3
regulation of immune response	4.72E-02	3
vitamin metabolic process	4.73E-02	2
regulation of muscle system process	4.73E-02	2
cellular lipid catabolic process	4.83E-02	2
regulation of lipoprotein particle clearance	4.86E-02	1
response to hydroperoxide	4.86E-02	1
peristalsis	4.86E-02	1
response to muscle activity	4.86E-02	1
natriuresis	4.86E-02	1
detection of light stimulus involved in sensory perception	4.86E-02	1
detection of light stimulus involved in visual perception	4.86E-02	1
phosphate ion homeostasis	4.86E-02	1
di-, tri-valent inorganic anion homeostasis	4.86E-02	1
heart trabecula formation	4.86E-02	1
cellular response to tumor necrosis factor	4.86E-02	1
endothelial cell development	4.86E-02	1

Continued on next page

Table F.7 – continued from previous page

Description	Corrected p-value	No. Genes
low-density lipoprotein particle clearance	4.86E-02	1
transmembrane receptor protein serine/threonine kinase signaling pathway	4.87E-02	2
ovulation cycle	4.97E-02	2

Table F.8: Biological functions of genes that were downregulated in the decidua of P4-treated samples. The genes were analysed for GO term enrichment using BiNGO. The overrepresented GO terms are shown with their corresponding adjusted p-values and the number of genes within the test set that are annotated to that function.

Description	Corrected p-value	No. Genes
sequestering of actin monomers	2.98E-02	1
regulation of formin-nucleated actin cable assembly	2.98E-02	1
positive regulation of formin-nucleated actin cable assembly	2.98E-02	1
positive regulation of cytoskeleton organization	2.98E-02	1
regulation of actin filament bundle assembly	2.98E-02	1
positive regulation of actin filament bundle assembly	2.98E-02	1
negative regulation of actin filament polymerization	3.13E-02	1
negative regulation of protein polymerization	3.13E-02	1
negative regulation of protein complex assembly	3.18E-02	1
regulation of actin filament length	3.30E-02	1
regulation of actin filament polymerization	3.30E-02	1
regulation of protein polymerization	3.30E-02	1
regulation of actin polymerization or depolymerization	3.30E-02	1
negative regulation of cytoskeleton organization	3.57E-02	1
regulation of actin cytoskeleton organization	4.23E-02	1
regulation of actin filament-based process	4.23E-02	1

Table F.9: Biological functions of genes that were upregulated in the inner myometrium of P4-treated samples. The genes were analysed for GO term enrichment using BiNGO. The overrepresented GO terms are shown with their corresponding adjusted p-values and the number of genes within the test set that are annotated to that function.

Description	Corrected p-value	No. Genes
extracellular matrix organization	1.80E-02	2
cellular water homeostasis	1.80E-02	1
kidney development	1.80E-02	2
renal system development	1.80E-02	2
extracellular structure organization	1.80E-02	2
urogenital system development	1.91E-02	2
cellular hyperosmotic response	3.12E-02	1
cellular response to osmotic stress	4.77E-02	1

Table F.10: Biological functions of genes that were down-regulated in the inner myometrium of P4-treated samples. The genes were analysed for GO term enrichment using BiNGO. The overrepresented GO terms are shown with their corresponding adjusted p-values and the number of genes within the test set that are annotated to that function.

Description	Corrected p-value	No. Genes
positive regulation of bone resorption	8.04E-03	2
positive regulation of bone remodeling	8.04E-03	2
ossification	8.04E-03	4
bone development	9.41E-03	4
positive regulation of tissue remodeling	1.05E-02	2
regulation of biological quality	1.10E-02	10
osteoclast differentiation	1.21E-02	2
regulation of hormone levels	1.29E-02	4
regulation of bone resorption	1.89E-02	2
regulation of bone remodeling	1.96E-02	2
response to nutrient levels	2.16E-02	5
response to extracellular stimulus	2.52E-02	5

Continued on next page

Table F.10 – continued from previous page

Description	Corrected p-value	No. Genes
regulation of tissue remodeling	2.52E-02	2
positive regulation of myeloid leukocyte differentiation	2.52E-02	2
skeletal system development	2.93E-02	4
response to nutrient	2.93E-02	4
hormone metabolic process	2.93E-02	3
secretion	2.93E-02	4
response to vitamin D	2.93E-02	2
myeloid leukocyte differentiation	2.93E-02	2
cation homeostasis	2.93E-02	4
positive regulation of myeloid cell differentiation	2.93E-02	2
small molecule metabolic process	2.93E-02	8
cysteine biosynthetic process from serine	2.93E-02	1
boron transport	2.93E-02	1
response to linoleic acid	2.93E-02	1
negative regulation of collateral sprouting of intact axon in response to injury	2.93E-02	1
regulation of collateral sprouting of intact axon in response to injury	2.93E-02	1
fat cell proliferation	2.93E-02	1
brown fat cell proliferation	2.93E-02	1
naphthalene metabolic process	2.93E-02	1
trichloroethylene metabolic process	2.93E-02	1
homocysteine catabolic process	2.93E-02	1
phosphoenolpyruvate-dependent sugar phosphotransferase system	2.93E-02	1
sphinganine-1-phosphate metabolic process	2.93E-02	1
cysteine biosynthetic process via cystathionine	2.93E-02	1
regulation of pH	2.93E-02	2
response to vitamin	3.24E-02	3
regulation of myeloid leukocyte differentiation	3.41E-02	2
tissue development	3.41E-02	5
response to external stimulus	3.41E-02	5
positive regulation of homeostatic process	3.41E-02	2
monovalent inorganic cation homeostasis	3.41E-02	2
organ development	3.41E-02	8
regulation of collateral sprouting	3.41E-02	1
negative regulation of collateral sprouting	3.41E-02	1
neurotrophin production	3.41E-02	1
nerve growth factor production	3.41E-02	1
response to triglyceride	3.41E-02	1
establishment of endothelial blood-brain barrier	3.41E-02	1
cysteine catabolic process	3.41E-02	1
homoserine metabolic process	3.41E-02	1
hemoglobin import	3.41E-02	1
establishment of blood-brain barrier	3.41E-02	1
response to prostaglandin F stimulus	3.41E-02	1
L-cysteine metabolic process	3.41E-02	1
transsulfuration	3.41E-02	1
cysteine biosynthetic process	3.41E-02	1
L-cysteine catabolic process	3.41E-02	1
chlorinated hydrocarbon metabolic process	3.41E-02	1
halogenated hydrocarbon metabolic process	3.41E-02	1
hydrogen sulfide metabolic process	3.41E-02	1
hydrogen sulfide biosynthetic process	3.41E-02	1
amine metabolic process	3.41E-02	4
multicellular organismal development	3.78E-02	10
odontogenesis	4.16E-02	2
system development	4.27E-02	9
response to steroid hormone stimulus	4.27E-02	4
L-serine catabolic process	4.27E-02	1
homocysteine metabolic process	4.27E-02	1
sulfur amino acid catabolic process	4.27E-02	1
negative regulation of axon regeneration	4.27E-02	1
establishment of endothelial barrier	4.27E-02	1
ketone body biosynthetic process	4.27E-02	1
sphinganine metabolic process	4.27E-02	1
response to acid	4.27E-02	2
response to starvation	4.63E-02	2
ion homeostasis	4.73E-02	4
regulation of myeloid cell differentiation	4.79E-02	2
proton transport	4.91E-02	2
isoprenoid metabolic process	4.91E-02	2

Continued on next page

Table F.10 – continued from previous page

Description	Corrected p-value	No. Genes
hydrogen transport	4.91E-02	2
epithelium development	4.91E-02	3
negative regulation of neuron projection regeneration	4.91E-02	1
positive regulation of cellular pH reduction	4.91E-02	1
nerve growth factor processing	4.91E-02	1
bicarbonate transport	4.91E-02	1
sulfur compound catabolic process	4.91E-02	1
response to abiotic stimulus	4.93E-02	4

F.3 Response to Treatment with Progesterone

Table F.11: Genes that change significantly in the decidua. Transcript expression levels are shown in transcripts per million values (mean±SD) for control samples and P4-treated samples.

		Control		P4	
Gene symbol	Gene name	TPM	±SD	TPM	±SD
Upregulated genes					
Htra4	HtrA serine peptidase 4	211.30	132.10	1074.14	1806.54
Plvap	plasmalemma vesicle associated protein	8.69	4.43	311.06	435.70
Itm2a	integral membrane protein 2A	1.77	0.47	193.05	333.78
Csf1r	colony stimulating factor 1 receptor	14.57	5.08	167.00	242.44
RGD1564534	similar to CHCHD4 protein	4.61	3.56	148.16	249.98
Eps8l2	EPS8-like 2	5.21	2.40	131.61	219.35
Alb	albumin	0.98	0.19	115.79	174.01
Rab11fip1	RAB11 family interacting protein 1 (class I)	6.06	4.10	113.13	97.06
Slco4a1	solute carrier organic anion transporter family, member 4a1	2.74	2.31	109.62	151.91
Cdh1	cadherin 1	2.09	1.21	108.55	173.41
Stard8	StAR-related lipid transfer (START) domain containing 8	4.99	2.29	103.26	146.79
Plagl1	pleiomorphic adenoma gene-like 1	2.10	2.32	98.87	169.04
Tf	transferrin	1.63	0.72	81.91	136.90
Shroom4	shroom family member 4	4.62	0.68	57.82	94.12
Rarres1	retinoic acid receptor responder (tazarotene induced) 1	5.94	2.27	56.18	56.98
Plekhg5	pleckstrin homology domain containing, family G (with RhoGef domain) member 5	5.40	1.24	55.53	89.63
Epn3	epsin 3	2.79	1.98	52.58	84.46
Scel	sciellin	0.98	0.89	46.36	65.98
Kazn	kazrin, periplakin interacting protein	4.02	1.89	35.35	55.38
Shisa6	shisa family member 6	0.00	0.00	34.57	40.62
Rhox12	reproductive homeobox 12	0.06	0.03	33.15	56.85
LOC498662	similar to RIKEN cDNA 2610019F03	0.98	0.37	32.81	51.88
Slc4a1	solute carrier family 4 (anion exchanger), member 1	1.73	0.66	29.76	26.43
Arid3b	AT rich interactive domain 3B (Bright like)	1.95	0.88	23.73	39.85
LOC680590	hypothetical protein LOC680590	0.04	0.08	21.86	37.48
P2ry4	pyrimidinergic receptor P2Y, G-protein coupled, 4	0.00	0.00	19.86	28.34
Hmx3	H6 family homeobox 3	0.01	0.01	17.14	29.63
Fhdc1	FH2 domain containing 1	1.32	0.72	16.92	25.82
Ihh	Indian hedgehog	0.00	0.00	15.32	13.19
Epb41l3	erythrocyte membrane protein band 4.1-like 3	0.66	0.13	12.03	19.83
Capn8	calpain 8	0.02	0.02	11.59	19.95
Dsc2	desmocollin 2	1.96	0.75	10.90	5.23
Fbn2	fibrillin 2	1.02	0.34	8.31	11.22
Mchr1	melanin-concentrating hormone receptor 1	0.00	0.01	7.93	13.74
Hoxc4	homeo box C4	1.38	0.91	7.47	11.16
Sall3	spalt-like transcription factor 3	0.56	0.41	2.67	3.57
Downregulated genes					
Rnase1l1	ribonuclease, RNase A family, 1-like 1 (pancreatic)	11.86	11.55	0.00	0.00
Tac1	tachykinin, precursor 1	9.63	8.51	0.00	0.00
Hey1	hes-related family bHLH transcription factor with YRPW motif 1	3.72	2.78	0.18	0.28
Tnn	tenascin N	38.22	39.91	0.56	0.60

Continued on next page

Table F.11 – continued from previous page

		Control		P4	
Gene symbol	Gene name	TPM	±SD	TPM	±SD
Thbs2	thrombospondin 2	24.72	25.11	1.39	0.92
Figf	c-fos induced growth factor	36.53	38.14	1.82	1.78
Derl3	derlin 3	80.72	56.52	4.30	2.88
G0s2	G0/G1switch 2	8.24	9.15	4.35	3.72
Igfbp5	insulin-like growth factor binding protein 5	125.97	82.39	6.55	4.21
Mmp11	matrix metallopeptidase 11	886.79	608.51	10.30	14.50
Ceacam9	carcinoembryonic antigen-related cell adhesion molecule 9	514.25	886.25	17.75	23.14
Mgp	matrix Gla protein	508.86	346.75	21.76	11.39

Table F.12: Genes that change significantly in the inner myometrium in response to P4-treatment. Transcript expression levels are shown in transcripts per million (TPM) values (mean±SD) for control samples and P4-treated samples.

		Control		P4	
Gene symbol	Gene name	TPM	±SD	TPM	±SD
Upregulated genes					
Gatm	glycine amidinotransferase (L-arginine:glycine amidinotransferase)	23.16	18.54	500.98	382.05
Olr773	olfactory receptor 773	0.00	0.00	192.67	333.72
Vom2r34	vomeronasal 2 receptor, 34	8.51	1.50	165.20	228.69
Pla2g2a	phospholipase A2, group IIA (platelets, synovial fluid)	2.00	1.81	141.15	191.37
Pdlim3	PDZ and LIM domain 3	22.08	11.12	104.52	20.75
Kcnk2	potassium channel, subfamily K, member 2	11.70	3.79	71.42	14.02
Ism1	isthmin 1, angiogenesis inhibitor	2.37	1.23	68.39	50.24
Hspb7	heat shock protein B7	4.71	5.10	62.19	39.29
Cspg4	chondroitin sulfate proteoglycan 4	7.53	3.13	40.30	22.60
Car5b	carbonic anhydrase 5b, mitochondrial	8.54	1.27	39.97	6.35
Fam163b	family with sequence similarity 163, member B	0.05	0.09	8.75	15.15
Col2a1	collagen, type II, alpha 1	0.05	0.05	7.53	12.63
Clec12b	C-type lectin domain family 12, member B	0.00	0.00	3.73	2.36
Ntf3	neurotrophin 3	0.06	0.11	3.40	3.85
Colq	collagen-like tail subunit (single strand of homotrimer) of asymmetric acetylcholinesterase	0.00	0.00	3.27	4.78
Fancd2os	FANCD2 opposite strand	0.07	0.03	2.95	2.70
Cdh16	cadherin 16	0.00	0.00	2.35	4.03
Syt4	synaptotagmin IV	0.05	0.02	1.51	1.18
Nr1i2	nuclear receptor subfamily 1, group I, member 2	0.00	0.00	1.42	1.81
Downregulated genes					
Fam150b	family with sequence similarity 150, member B	21.86	36.95	0.00	0.00
Hs3st6	heparan sulfate (glucosamine) 3-O-sulfotransferase 6	10.02	17.36	0.00	0.00
Il17f	interleukin 17F	6.94	11.96	0.00	0.00
Lypd3	Ly6/Plaur domain containing 3	5.26	5.58	0.00	0.00
Tff3	trefoil factor 3, intestinal	5.48	9.02	0.00	0.00
Tns4	tensin 4	19.81	27.72	0.00	0.00
Tssk6	testis-specific serine kinase 6	42.14	72.99	0.00	0.00
Cd70	Cd70 molecule	16.60	27.92	0.00	0.01
MGC114246	similar to cathepsin R	29.97	51.43	0.01	0.02
Kcnn2	potassium intermediate/small conductance calcium-activated channel, subfamily N, member 2	2.85	4.86	0.02	0.03
Psgb1	pregnancy-specific beta 1-glycoprotein	318.33	547.14	0.02	0.04
Mpp2	membrane protein, palmitoylated 2 (MAGUK p55 subfamily member 2)	11.23	16.61	0.04	0.07
Irx3	iroquois homeobox 3	4.20	5.74	0.05	0.05
Utf1	undifferentiated embryonic cell transcription factor 1	14.24	24.67	0.06	0.10
LOC685544	hypothetical protein LOC685544	106.53	184.51	0.08	0.09
Il22ra1	interleukin 22 receptor, alpha 1	9.54	5.21	0.13	0.18
Hand1	heart and neural crest derivatives expressed 1	54.15	92.96	0.50	0.41
Dlx3	distal-less homeobox 3	26.97	46.14	0.83	0.65
Hmgcs2	3-hydroxy-3-methylglutaryl-CoA synthase 2 (mitochondrial)	27.14	36.72	1.43	1.28
Ctsj	cathepsin J	827.48	1426.78	1.47	1.15
Htr2a	5-hydroxytryptamine (serotonin) receptor 2A, G protein-coupled	86.91	148.90	1.86	1.35
Ebf3	early B-cell factor 3	18.63	21.52	1.91	1.63
Cmbl	carboxymethylenebutenolidase homolog (Pseudomonas)	45.50	38.94	2.04	0.53
Sema4d	sema domain, immunoglobulin domain (Ig),				

Continued on next page

Table F.12 – continued from previous page

		Control		P4	
Gene symbol	Gene name	TPM	±SD	TPM	±SD
	transmembrane domain (TM) and short cytoplasmic domain, (semaphorin) 4D	17.81	15.11	2.20	1.06
Psg29	pregnancy-specific glycoprotein 29	662.38	1056.85	2.22	0.91
Htr1d	5-hydroxytryptamine (serotonin) receptor 1D, G protein-coupled	38.84	54.17	2.58	1.59
Sh2d3c	SH2 domain containing 3C	25.17	15.34	2.71	0.58
Cldn4	claudin 4	248.75	405.09	2.72	2.26
Cldn7	claudin 7	56.65	97.63	2.86	2.88
Ctsr	cathepsin R	602.94	1037.01	3.02	4.60
Acvr1	activin A receptor, type I	36.67	52.66	3.13	1.91
Eps8l2	EPS8-like 2	37.79	61.61	3.14	2.98
Slc38a4	solute carrier family 38, member 4	369.43	607.05	3.32	4.05
Cilp	cartilage intermediate layer protein, nucleotide pyrophosphohydrolase	46.49	28.93	3.56	1.77
Podxl	podocalyxin-like	27.00	26.85	3.88	1.16
Mill1	MHC I like leukocyte 1	37.52	48.49	3.99	1.03
Cgm4	carcinoembryonic antigen gene family 4	785.39	1204.63	4.04	5.66
Rnf128	ring finger protein 128, E3 ubiquitin protein ligase	72.10	105.07	4.13	3.67
Folr1	folate receptor 1 (adult)	41.98	70.89	4.14	0.61
Rhox9	reproductive homeobox 9	59.41	43.55	5.51	4.94
Ctsm	cathepsin M	224.42	353.44	5.54	4.33
Prl3d4	prolactin family 3, subfamily d, member 4	1052.22	1680.08	5.54	7.69
Rsad2	radical S-adenosyl methionine domain containing 2	50.42	21.61	6.03	1.98
Dmkn	dermokine	59.60	64.61	7.19	3.98
Fndc3c1	fibronectin type III domain containing 3C1	169.74	138.42	8.10	4.53
Oasl	2'-5'-oligoadenylate synthetase-like	131.13	159.32	8.26	4.19
Sbsn	suprabasin	238.85	372.54	9.03	5.96
LOC171573	spleen protein 1 precursor	919.26	1472.08	10.12	14.78
Sfmbt2	Scm-like with four mbt domains 2	73.02	34.22	10.94	4.37
Creg1	cellular repressor of E1A-stimulated genes 1	296.56	352.72	13.00	6.01
Gab1	GRB2-associated binding protein 1	74.93	35.56	16.00	4.00
Prl7a3	prolactin family 7, subfamily a, member 3	153.98	51.71	16.85	9.83
Foxo4	forkhead box O4	132.66	49.22	18.85	8.46
Fbln1	fibulin 1	62.05	107.47	31.66	20.91
Ednrb	endothelin receptor type B	346.91	137.08	32.70	22.04
Hmox1	heme oxygenase (decycling) 1	155.63	67.00	34.47	8.49
Cited1	Cbp/p300-interacting transactivator with Glu/Asp-rich carboxy-terminal domain 1	483.54	198.23	80.33	45.66
Cited2	Cbp/p300-interacting transactivator, with Glu/Asp-rich carboxy-terminal domain, 2	675.80	617.52	86.67	40.77
Prl4a1	prolactin family 4, subfamily a, member 1	4709.14	2435.51	949.93	414.88

Table F.13: Genes that change significantly in response to P4-treatment in the outer myometrium. Transcript expression levels are shown in transcripts per million (TPM) values (mean±SD) for control samples and P4-treated samples.

		Control		P4	
Gene symbol	Gene name	TPM	±SD	TPM	±SD
Upregulated genes					
Itm2a	integral membrane protein 2A	9.51	6.30	1111.71	1574.43
C1qtnf3	C1q and tumor necrosis factor related protein 3	0.82	0.67	453.63	771.85
Tnnt3	troponin T type 3 (skeletal, fast)	5.50	5.69	362.45	619.87
Myh8	myosin, heavy chain 8, skeletal muscle, perinatal	0.74	0.24	269.58	458.13
Leprel4	leprecan-like 4	30.21	13.07	255.44	374.95
Mfap2	microfibrillar-associated protein 2	3.94	5.63	248.02	375.19
Cthrc1	collagen triple helix repeat containing 1	5.00	4.47	239.17	293.61
Leprel2	leprecan-like 2	18.33	13.70	233.25	276.65
Smoc2	SPARC related modular calcium binding 2	4.85	2.62	232.65	367.52
Mylpf	myosin light chain, phosphorylatable, fast skeletal muscle	2.99	1.83	226.56	379.60
Capn6	calpain 6	0.42	0.40	225.78	382.74
Fkbp10	FK506 binding protein 10	9.75	7.62	175.52	232.59
Zim1	zinc finger, imprinted 1	3.70	0.75	130.36	183.00
RGD1305645	similar to RIKEN cDNA 1500015O10	5.20	5.17	126.34	191.09
Epyc	epiphycan	0.00	0.00	112.12	194.21
Scrg1	stimulator of chondrogenesis 1	0.01	0.01	100.38	173.87

Continued on next page

Table F.13 – continued from previous page

		Control		P4	
Gene symbol	Gene name	TPM	±SD	TPM	±SD
Car4	carbonic anhydrase 4	2.78	1.02	68.02	86.28
Col27a1	collagen, type XXVII, alpha 1	1.98	0.95	61.86	102.86
Prf1	perforin 1 (pore forming protein)	7.04	1.63	48.15	28.78
Enpp2	ectonucleotide pyrophosphatase/phosphodiesterase 2	3.26	2.18	40.99	34.09
Mmp16	matrix metallopeptidase 16	1.69	1.01	39.48	61.01
Ndn	necdin, melanoma antigen (MAGE) family member	2.66	2.13	37.57	11.48
Sln	sarcolipin	0.35	0.25	37.19	63.13
Myl3	myosin, light chain 3, alkali; ventricular, skeletal, slow	0.01	0.01	33.63	55.40
Efs	embryonal Fyn-associated substrate	2.49	1.06	27.53	16.62
Atp1b4	ATPase, (Na+)/K+ transporting, beta 4 polypeptide	0.50	0.41	25.70	43.63
Aff3	AF4/FMR2 family, member 3	1.19	0.90	20.30	21.21
Sgcd	sarcoglycan, delta (dystrophin-associated glycoprotein)	2.11	2.52	17.89	15.44
Tpsb2	tryptase beta 2	0.10	0.14	13.13	5.20
Fzd9	frizzled class receptor 9	0.02	0.03	11.57	20.03
Sgca	sarcoglycan, alpha (dystrophin-associated glycoprotein)	0.00	0.00	10.01	11.46
Kera	keratocan	0.01	0.01	7.63	13.06
Smtnl1	smoothelin-like 1	0.01	0.02	6.93	11.83
RGD1561795	similar to RIKEN cDNA 1700012B09	0.01	0.02	6.31	8.87
Itga10	integrin, alpha 10	0.02	0.04	5.99	10.17
Tpsab1	tryptase alpha/beta 1	0.00	0.00	5.05	4.12
Trdn	triadin	0.06	0.02	4.19	7.15
Pak3	p21 protein (Cdc42/Rac)-activated kinase 3	0.20	0.26	3.58	5.27
Clstn3	calsyntenin 3	0.05	0.04	3.36	5.25
Asb12	ankyrin repeat and SOCS box-containing 12	0.00	0.00	3.13	2.92
Kcnj12	potassium inwardly-rectifying channel, subfamily J, member 12	0.36	0.16	3.06	0.23
Downregulated genes					
Lpo	lactoperoxidase	99.94	125.95	0.00	0.00
Pax2	paired box 2	36.73	47.52	0.00	0.00
Npbwr1	neuropeptides B/W receptor 1	21.42	27.19	0.00	0.00
Psca	prostate stem cell antigen	18.54	17.82	0.00	0.00
B3gnt3	UDP-GlcNAc:betaGal beta-1,3-N-acetylglucosaminyltransferase 3	18.10	18.09	0.00	0.00
Capsl	calcyphosine-like	17.18	12.89	0.00	0.00
Prl3a1	Prolactin family 3, subfamily a, member 1	16.33	5.06	0.00	0.00
Smlr1	small leucine-rich protein 1	9.12	12.15	0.00	0.00
Aadac	arylacetamide deacetylase	8.90	15.32	0.00	0.00
Sult1b1	sulfotransferase family, cytosolic, 1B, member 1	6.82	9.63	0.00	0.00
Alox15b	arachidonate 15-lipoxygenase, type B	6.34	8.35	0.00	0.00
Slc30a10	solute carrier family 30, member 10	6.05	10.27	0.00	0.00
Pla2g4c	phospholipase A2, group IVC	4.57	4.58	0.00	0.00
Noxo1	NADPH oxidase organizer 1	4.47	3.81	0.00	0.00
Igfals	insulin-like growth factor binding protein, acid labile subunit	4.22	5.21	0.00	0.00
Slc17a1	solute carrier family 17, member 1	3.70	6.08	0.00	0.00
Marco	macrophage receptor with collagenous structure	3.64	6.16	0.00	0.00
Iqcg	IQ motif containing G	3.60	4.26	0.00	0.00
Tmprss11g	transmembrane protease, serine 11G	3.30	3.28	0.00	0.00
Ccdc64b	coiled-coil domain containing 64B	3.01	3.04	0.00	0.00
Entpd8	ectonucleoside triphosphate diphosphohydrolase 8	2.76	2.25	0.00	0.00
Adam28	ADAM metallopeptidase domain 28	2.68	2.07	0.00	0.00
Il24	interleukin 24	2.37	2.59	0.00	0.00
Slc5a1	solute carrier family 5, member 1	2.26	3.41	0.00	0.00
Ttll10	tubulin tyrosine ligase-like family, member 10	1.54	0.44	0.00	0.00
Serpinb11	serpin peptidase inhibitor, clade B (ovalbumin), member 11	1.51	1.20	0.00	0.00
Macc1	metastasis associated in colon cancer 1	4.52	3.27	0.01	0.02
Kap	kidney androgen regulated protein	1514.85	999.61	2.48	3.96
Apoa1	apolipoprotein A-I	1327.79	1142.31	20.91	29.46
Psg16	Psg16	716.10	1237.31	1.57	1.50
Psg29	pregnancy-specific glycoprotein 29	648.04	1117.62	4.19	1.97
Cgm4	carcinoembryonic antigen gene family 4	558.99	961.92	2.84	2.60
Cuzd1	CUB and zona pellucida-like domains 1	492.78	409.84	0.59	1.03
Krt19	keratin 19	396.19	327.46	90.59	59.13
Cldn4	claudin 4	367.31	529.47	9.97	8.21

Continued on next page

Table F.13 – continued from previous page

		Control		P4	
Gene symbol	Gene name	TPM	±SD	TPM	±SD
Ceacam3	carcinoembryonic antigen-related cell adhesion molecule 3	353.04	608.70	4.70	5.23
Apoh	apolipoprotein H (beta-2-glycoprotein I)	324.36	443.23	7.02	11.13
LOC171573	spleen protein 1 precursor	312.83	523.46	3.33	3.87
Slc9a3r1	solute carrier family 9, subfamily A , member 3 regulator 1	311.36	201.25	76.73	16.63
RGD1309676	family with sequence similarity 213, member A	178.41	127.27	35.13	18.42
F2	coagulation factor II	172.70	238.48	6.63	10.91
Gpx2	glutathione peroxidase 2	160.81	81.14	6.87	8.63
Cfb	complement factor B	157.75	97.41	27.78	16.27
Glrx	glutaredoxin (thioltransferase)	135.84	123.07	22.67	11.60
Hmox1	heme oxygenase (decycling) 1	135.48	62.26	27.66	24.25
Cldn2	claudin 2	135.04	114.17	0.83	0.46
RGD1310507	similar to RIKEN cDNA 1300017J02	133.95	103.79	6.49	1.27
Mmp7	matrix metallopeptidase 7	131.36	56.43	0.18	0.15
Lcn2	lipocalin 2	126.31	66.72	25.73	24.45
Gnmt	glycine N-methyltransferase	107.74	186.61	0.23	0.39
RGD1309139	similar to CG5435-PA	106.99	138.26	13.20	5.76
Prom1	prominin 1	105.22	100.68	1.91	0.60
Gstt3	glutathione S-transferase, theta 3	104.84	71.91	5.78	4.25
Tnfaip6	tumor necrosis factor alpha induced protein 6	101.61	108.15	13.50	13.20
Alcam	activated leukocyte cell adhesion molecule	86.39	83.80	9.89	7.56
Cyp4a8	cytochrome P450, family 4, subfamily a, polypeptide 8	85.73	103.28	12.04	4.27
Pllp	plasmolipin	77.98	94.38	4.74	1.35
Elf3	E74-like factor 3	70.44	73.54	3.02	3.86
Slc26a4	solute carrier family 26 (anion exchanger), member 4	69.38	68.87	0.16	0.23
Lpcat4	lysophosphatidylcholine acyltransferase 4	67.64	67.55	8.49	1.53
Tspan1	tetraspanin 1	67.06	39.29	3.44	3.06
Serpinb1a	serine (or cysteine) proteinase inhibitor, clade B, member 1a	63.64	34.31	11.93	9.60
Slc10a1	solute carrier family 10, member 1	61.59	87.32	3.66	3.26
Slc13a3	solute carrier family 13, member 3	55.69	51.79	1.92	1.95
Pigr	polymeric immunoglobulin receptor	55.40	69.41	0.31	0.36
Sh2d4a	SH2 domain containing 4A	53.59	31.99	11.89	2.43
RGD1309313/Tmem180	transmembrane protein 180	53.18	40.76	9.63	4.99
Ptprh	protein tyrosine phosphatase, receptor type, H	49.37	42.47	0.28	0.24
Lamc2	laminin, gamma 2	44.77	46.30	3.40	2.37
Napsa	napsin A aspartic peptidase	42.31	33.89	5.00	2.50
Aadat	aminoadipate aminotransferase	41.93	42.22	2.10	2.65
F5	coagulation factor V (proaccelerin, labile factor)	39.50	32.53	3.67	2.53
Eya2	eyes absent homolog 2 (Drosophila)	37.63	37.38	1.30	1.08
Hnf4a	hepatocyte nuclear factor 4, alpha	36.88	22.69	0.47	0.30
Cndp1	carnosine dipeptidase 1 (metallopeptidase M20 family)	35.15	22.93	3.81	3.11
Mal2	mal, T-cell differentiation protein 2	32.51	32.69	1.41	1.60
Lgals2	lectin, galactoside-binding, soluble, 2	30.51	23.52	0.41	0.39
Ehf	ets homologous factor	29.02	34.55	0.12	0.14
RGD1563547/Smim22	small integral membrane protein 22	28.31	20.33	0.48	0.17
Slc16a14	solute carrier family 16, member 14	28.20	33.75	1.22	0.55
Fermt1	fermitin family member 1	28.01	32.36	1.11	0.60
Pklr	pyruvate kinase, liver and RBC	27.71	27.58	3.11	1.89
Cubn	cubilin (intrinsic factor-cobalamin receptor)	25.73	21.78	0.54	0.09
LOC500797	mitotic spindle positioning	24.58	20.86	0.78	0.69
Chdh	choline dehydrogenase	24.26	22.69	1.30	0.86
Gpa33	glycoprotein A33 (transmembrane)	24.22	28.58	0.64	1.05
Hgfac	HGF activator	23.55	23.19	0.55	0.90
Cftr	cystic fibrosis transmembrane conductance regulator	22.54	29.22	0.07	0.07
Ehhadh	enoyl-CoA, hydratase/3-hydroxyacyl CoA dehydrogenase	21.25	16.87	1.93	1.39
Cldn1	claudin 1	20.50	25.59	2.83	2.01
Fcgbp	Fc fragment of IgG binding protein	20.48	25.88	0.90	0.98
Irf6	interferon regulatory factor 6	20.26	14.60	2.10	0.55
LOC689065	hypothetical protein LOC689065	18.99	14.78	0.84	1.23
Dcdc2	doublecortin domain containing 2	18.15	13.93	1.94	0.55
Rab17	RAB17, member RAS oncogene family	17.60	13.99	0.05	0.08
Unc5cl	unc-5 homolog C (C. elegans)-like	17.36	9.72	0.19	0.33
Trib3	tribbles pseudokinase 3	16.37	18.18	0.05	0.09
Prss22	protease, serine, 22	16.08	13.44	0.30	0.18

Continued on next page

Table F.13 – continued from previous page

		Control		P4	
Gene symbol	Gene name	TPM	±SD	TPM	±SD
Vil1	villin 1	15.99	13.20	0.40	0.53
Abcg2	ATP-binding cassette, subfamily G (WHITE), member 2	15.93	11.24	0.65	0.31
Wfdc10	WAP four-disulfide core domain 10	13.74	14.94	0.05	0.09
RGD1565844	similar to RIKEN cDNA 1700045I19	12.92	14.81	0.08	0.07
Pemt	phosphatidylethanolamine N-methyltransferase	12.90	11.75	0.37	0.11
Cdh16	cadherin 16	12.25	12.69	0.10	0.11
Grpr	gastrin releasing peptide receptor	11.69	6.82	0.23	0.23
Wnt7a	wingless-type MMTV integration site family, member 7A	11.54	9.93	0.09	0.02
Gucy2c	guanylate cyclase 2C	11.04	8.82	0.31	0.16
Usp43_predicted	ubiquitin specific peptidase 43	9.24	9.55	0.05	0.08
Tcerg1l	transcription elongation regulator 1-like	7.00	11.83	0.02	0.03
Kcnj16	potassium inwardly-rectifying channel, subfamily J, member 16	6.87	6.70	0.14	0.04
LOC691352	similar to Robo-1	6.84	5.45	0.59	0.07
Epor	erythropoietin receptor	6.53	11.11	0.04	0.06
Grik2	glutamate receptor, ionotropic, kainate 2	6.42	2.72	0.08	0.07
Glp1r	glucagon-like peptide 1 receptor	6.40	5.13	0.22	0.21
Fut9	fucosyltransferase 9 (alpha (1,3) fucosyltransferase)	5.57	4.91	0.32	0.07
Lgals12	lectin, galactoside-binding, soluble, 12	4.37	4.30	0.12	0.14
Cldn8	claudin 8	4.29	5.87	0.03	0.05
Fam84a	family with sequence similarity 84, member A	3.90	2.47	0.10	0.12
Tmprss4	transmembrane protease, serine 4	3.84	2.88	0.02	0.04
Slco1a1	solute carrier organic anion transporter family, member 1a1	2.91	4.91	0.02	0.04
Acsm5	acyl-CoA synthetase medium-chain family member 5	2.70	4.68	0.02	0.04
Cyp2b3	cytochrome P450, family 2, subfamily b, polypeptide 3	2.68	4.16	0.02	0.04
Gad1	glutamate decarboxylase 1	1.15	0.56	0.02	0.02

Table F.14: Biological functions of genes that were upregulated in the decidua of P4-treated samples. The genes were analysed for GO term enrichment using BiNGO. The overrepresented GO terms are shown with their corresponding adjusted p-values and the number of genes within the test set that are annotated to that function.

Description	Corrected p-value	No. Genes
maternal process involved in female pregnancy	3.54E-02	2
disruption by symbiont of host cells	3.54E-02	1
camera-type eye photoreceptor cell fate commitment	3.54E-02	1
response to platinum ion	3.54E-02	1
regulation of eye pigmentation	3.54E-02	1
negative regulation of eye pigmentation	3.54E-02	1
negative regulation of developmental pigmentation	3.54E-02	1
hemolysis by symbiont of host erythrocytes	3.54E-02	1
hemolysis of cells in other organism involved in symbiotic interaction	3.54E-02	1
modification by organism of cell membrane in other organism involved in symbiotic interaction	3.54E-02	1
retinal pigment epithelium development	3.54E-02	1
modification by symbiont of host cell membrane	3.54E-02	1
modification by symbiont of host cellular component	3.54E-02	1
modification by symbiont of host structure	3.54E-02	1
modification of cellular component in other organism involved in symbiotic interaction	3.54E-02	1
modification of structure of other organism involved in symbiotic interaction	3.54E-02	1
hemolysis of cells in other organism	3.54E-02	1
killing by symbiont of host cells	3.54E-02	1
cytolysis by symbiont of host cells	3.54E-02	1
cytolysis of cells of another organism	3.54E-02	1
cytolysis of cells in other organism involved in symbiotic interaction	3.54E-02	1
tube morphogenesis	3.76E-02	3
chloride transport	3.76E-02	2
intein-mediated protein splicing	4.02E-02	1
camera-type eye photoreceptor cell differentiation	4.02E-02	1
vitelline membrane formation	4.02E-02	1
maintenance of mitochondrion location	4.02E-02	1
maintenance of organelle location	4.02E-02	1
eye photoreceptor cell fate commitment	4.02E-02	1
embryo sac morphogenesis	4.02E-02	1
gametophyte development	4.02E-02	1
megagametogenesis	4.02E-02	1

Continued on next page

Table F.14 – continued from previous page

Description	Corrected p-value	No. Genes
embryo sac development	4.02E-02	1
tube lumen cavitation	4.02E-02	1
protein splicing	4.02E-02	1
photoreceptor cell fate commitment	4.02E-02	1
salivary gland cavitation	4.02E-02	1

Table F.15: Biological functions of genes that were down-regulated in the decidua of P4-treated samples. The genes were analysed for GO term enrichment using BiNGO. The overrepresented GO terms are shown with their corresponding adjusted p-values and the number of genes within the test set that are annotated to that function.

Description	Corrected p-value	No. Genes
regulation of cell migration	3.57E-02	3
regulation of cellular component movement	3.57E-02	3
regulation of locomotion	3.57E-02	3
regulation of developmental process	4.14E-02	4
regulation of ossification	4.14E-02	2
positive regulation of developmental process	4.14E-02	3
positive regulation of response to external stimulus	4.14E-02	2
regulation of angiogenesis	4.14E-02	2
regulation of mast cell chemotaxis	4.14E-02	1
positive regulation of mast cell chemotaxis	4.14E-02	1
signaling	4.82E-02	7
ossification	4.82E-02	2
bone development	4.82E-02	2
positive regulation of action potential	4.82E-02	1
positive regulation of natriuresis	4.82E-02	1
skeletal muscle tissue growth	4.82E-02	1
regulation of multicellular organismal process	4.82E-02	4
positive regulation of cell migration	4.82E-02	2
negative regulation of heart rate	4.82E-02	1
positive regulation of synaptic transmission, cholinergic	4.82E-02	1
regulation of synaptic transmission, cholinergic	4.82E-02	1
positive regulation of cellular component movement	4.82E-02	2
positive regulation of locomotion	4.82E-02	2
tachykinin receptor signaling pathway	4.97E-02	1
negative regulation of insulin-like growth factor receptor signaling pathway	4.97E-02	1

Table F.16: Biological functions of genes that were upregulated in the outer myometrium of P4-treated samples. The genes were analysed for GO term enrichment using BiNGO. The overrepresented GO terms are shown with their corresponding adjusted p-values and the number of genes within the test set that are annotated to that function.

Description	Corrected p-value	No. Genes
ventricular cardiac muscle tissue morphogenesis	7.83E-04	3
ventricular cardiac muscle tissue development	7.83E-04	3
cardiac ventricle morphogenesis	7.83E-04	3
cardiac ventricle development	7.83E-04	3
cardiac muscle tissue morphogenesis	7.83E-04	3
muscle tissue morphogenesis	7.83E-04	3
cardiac chamber development	1.20E-03	3
cardiac chamber morphogenesis	1.20E-03	3
cardiac muscle tissue development	8.20E-03	3
heart morphogenesis	8.20E-03	3
regulation of striated muscle contraction	1.31E-02	2
cardiac muscle contraction	1.37E-02	2
muscle structure development	1.55E-02	4
heart process	1.55E-02	2
heart contraction	1.55E-02	2
muscle contraction	1.89E-02	3
muscle system process	2.68E-02	3
striated muscle contraction	3.18E-02	2
striated muscle tissue development	3.18E-02	3

Continued on next page

Table F.16 – continued from previous page

Description	Corrected p-value	No. Genes
regulation of release of sequestered calcium ion into cytosol by sarcoplasmic reticulum	3.32E-02	1
muscle tissue development	3.32E-02	3

Table F.17: Biological functions of genes that were downregulated in the outer myometrium of P4-treated samples. The genes were analysed for GO term enrichment using BiNGO. The overrepresented GO terms are shown with their corresponding adjusted p-values and the number of genes within the test set that are annotated to that function.

Description	Corrected p-value	No. Genes
chemical homeostasis	2.03E-02	12
response to wounding	2.03E-02	11
lipid metabolic process	2.03E-02	14
homeostatic process	2.03E-02	14
wound healing	2.03E-02	7
organic anion transport	2.03E-02	4
ion homeostasis	2.87E-02	10
regulation of biological quality	3.06E-02	20

F.4 Regulation of Differentially Expressed Genes in Control Tissues

Table F.18: Biological functions of genes that were common to P4 and control, GD20-GD22(NL), differentially expressed gene sets in the decidua. The genes were analysed for GO term enrichment using BiNGO. The overrepresented GO terms are shown with their corresponding adjusted p-values and the number of genes within the test set that are annotated to that function.

Description	Corrected p-value	No. Genes
disruption by symbiont of host cells	3.13E-03	1
modification by symbiont of host cell membrane	3.13E-03	1
modification by symbiont of host cellular component	3.13E-03	1
response to platinum ion	3.13E-03	1
modification by symbiont of host structure	3.13E-03	1
modification of cellular component in other organism involved in symbiotic interaction	3.13E-03	1
modification of structure of other organism involved in symbiotic interaction	3.13E-03	1
hemolysis of cells in other organism	3.13E-03	1
killing by symbiont of host cells	3.13E-03	1
cytolysis by symbiont of host cells	3.13E-03	1
hemolysis by symbiont of host erythrocytes	3.13E-03	1
hemolysis of cells in other organism involved in symbiotic interaction	3.13E-03	1
cytolysis of cells of another organism	3.13E-03	1
modification by organism of cell membrane in other organism involved in symbiotic interaction	3.13E-03	1
cytolysis of cells in other organism involved in symbiotic interaction	3.13E-03	1
tube morphogenesis	4.70E-03	2
maintenance of mitochondrion location	4.70E-03	1
maintenance of organelle location	4.70E-03	1
tube lumen cavitation	4.70E-03	1
salivary gland cavitation	4.70E-03	1
response to metal ion	7.54E-03	2
tube development	8.70E-03	2
disruption of cells of other organism involved in symbiotic interaction	8.70E-03	1
killing of cells in other organism involved in symbiotic interaction	8.70E-03	1
response to indole-3-methanol	8.70E-03	1
cellular response to indole-3-methanol	8.70E-03	1
positive regulation of circadian sleep/wake cycle, non-REM sleep	8.70E-03	1
cellular response to lithium ion	1.01E-02	1
response to inorganic substance	1.21E-02	2
regulation of branching involved in salivary gland morphogenesis	1.21E-02	1
killing of cells of another organism	1.21E-02	1
regulation of circadian sleep/wake cycle, non-REM sleep	1.28E-02	1
positive regulation of circadian sleep/wake cycle, sleep	1.28E-02	1
positive regulation of circadian rhythm	1.38E-02	1
response to mercury ion	1.52E-02	1
mitochondrion localization	1.52E-02	1
trophectodermal cell differentiation	1.52E-02	1
positive regulation of biological process	1.53E-02	3
positive regulation of transcription factor import into nucleus	1.53E-02	1
blastocyst formation	1.53E-02	1
modification by symbiont of host morphology or physiology	1.60E-02	1
positive regulation of protein import into nucleus	1.79E-02	1
salivary gland morphogenesis	1.97E-02	1
regulation of circadian sleep/wake cycle, sleep	1.97E-02	1
cell killing	1.97E-02	1
synapse assembly	1.97E-02	1
regulation of circadian sleep/wake cycle	1.97E-02	1
circadian sleep/wake cycle process	1.97E-02	1
salivary gland development	1.97E-02	1
cellular response to metal ion	1.97E-02	1
positive regulation of nucleocytoplasmic transport	2.02E-02	1
circadian sleep/wake cycle	2.02E-02	1
cellular response to inorganic substance	2.02E-02	1
circadian behavior	2.02E-02	1
response to lithium ion	2.02E-02	1
vasodilation	2.02E-02	1
regulation of transcription factor import into nucleus	2.02E-02	1

Continued on next page

Table F.18 – continued from previous page

Description	Corrected p-value	No. Genes
modification of morphology or physiology of other organism involved in symbiotic interaction	2.02E-02	1
rhythmic behavior	2.07E-02	1
regulation of morphogenesis of a branching structure	2.15E-02	1
exocrine system development	2.15E-02	1
pituitary gland development	2.27E-02	1
positive regulation of intracellular protein transport	2.31E-02	1
positive regulation of intracellular transport	2.38E-02	1
regulation of circadian rhythm	2.38E-02	1
tube formation	2.38E-02	1
blastocyst development	2.38E-02	1
regulation of apoptosis	2.43E-02	2
interaction with host	2.43E-02	1
regulation of programmed cell death	2.43E-02	2
regulation of cell death	2.51E-02	2
cellular response to starvation	2.51E-02	1
diencephalon development	2.51E-02	1
maintenance of location in cell	2.53E-02	1
synapse organization	2.56E-02	1
regulation of protein import into nucleus	2.70E-02	1
regulation of tube size	2.70E-02	1
regulation of blood vessel size	2.70E-02	1
positive regulation of behavior	2.73E-02	1
symbiosis, encompassing mutualism through parasitism	2.99E-02	1
vascular process in circulatory system	3.00E-02	1
cellular response to stimulus	3.00E-02	2
interspecies interaction between organisms	3.10E-02	1
regulation of intracellular protein transport	3.10E-02	1
anatomical structure morphogenesis	3.10E-02	2
gland morphogenesis	3.10E-02	1
regulation of nucleocytoplasmic transport	3.12E-02	1
maintenance of location	3.30E-02	1
response to starvation	3.37E-02	1
positive regulation of protein transport	3.48E-02	1
endocrine system development	3.51E-02	1
regulation of behavior	3.51E-02	1
regulation of intracellular transport	3.52E-02	1
regulation of multicellular organismal process	3.53E-02	2
cellular response to nutrient levels	3.57E-02	1
circadian rhythm	3.57E-02	1
organelle localization	3.57E-02	1
regulation of caspase activity	3.82E-02	1
regulation of endopeptidase activity	4.15E-02	1
response to organic substance	4.31E-02	2
regulation of peptidase activity	4.35E-02	1
cellular response to extracellular stimulus	4.44E-02	1
response to toxin	4.44E-02	1
cellular response to external stimulus	4.44E-02	1
extracellular structure organization	4.89E-02	1

Table F.19: Biological functions of genes that were common to P4 and control, GD22(NL)-GD22(L), differentially expressed gene sets in the decidua. The genes were analysed for GO term enrichment using BiNGO. The overrepresented GO terms are shown with their corresponding adjusted p-values and the number of genes within the test set that are annotated to that function.

Description	Corrected p-value	No. Genes
disruption by symbiont of host cells	0.002	1
hemolysis of cells in other organism	0.002	1
killing by symbiont of host cells	0.002	1
modification by symbiont of host cell membrane	0.002	1
cytolysis by symbiont of host cells	0.002	1
hemolysis by symbiont of host erythrocytes	0.002	1
hemolysis of cells in other organism involved in symbiotic interaction	0.002	1
cytolysis of cells of another organism	0.002	1
modification by organism of cell membrane in other organism involved in symbiotic interaction	0.002	1
cytolysis of cells in other organism involved in symbiotic interaction	0.002	1

Continued on next page

Table F.19 – continued from previous page

Description	Corrected p-value	No. Genes
modification by symbiont of host cellular component	0.002	1
response to platinum ion	0.002	1
modification by symbiont of host structure	0.002	1
modification of cellular component in other organism involved in symbiotic interaction	0.002	1
modification of structure of other organism involved in symbiotic interaction	0.002	1
maintenance of mitochondrion location	0.004	1
maintenance of organelle location	0.004	1
positive regulation of myelination	0.005	1
ferric iron transport	0.005	1
disruption of cells of other organism involved in symbiotic interaction	0.007	1
killing of cells in other organism involved in symbiotic interaction	0.007	1
positive regulation of circadian sleep/wake cycle, non-REM sleep	0.007	1
positive regulation of multicellular organismal process	0.007	2
transepithelial chloride transport	0.008	1
regulation of myelination	0.009	1
killing of cells of another organism	0.009	1
positive regulation of circadian sleep/wake cycle, sleep	0.010	1
regulation of circadian sleep/wake cycle, non-REM sleep	0.010	1
positive regulation of circadian rhythm	0.011	1
transepithelial transport	0.011	1
response to mercury ion	0.012	1
mitochondrion localization	0.012	1
modification by symbiont of host morphology or physiology	0.013	1
transport	0.015	3
establishment of localization	0.015	3
cell killing	0.016	1
regulation of circadian sleep/wake cycle	0.016	1
regulation of circadian sleep/wake cycle, sleep	0.016	1
circadian sleep/wake cycle process	0.017	1
circadian sleep/wake cycle	0.018	1
circadian behavior	0.018	1
vasodilation	0.018	1
modification of morphology or physiology of other organism involved in symbiotic interaction	0.018	1
localization	0.018	3
rhythmic behavior	0.018	1
ion transport	0.021	2
acute-phase response	0.022	1
regulation of circadian rhythm	0.022	1
interaction with host	0.023	1
iron ion transport	0.023	1
cellular response to starvation	0.024	1
maintenance of location in cell	0.024	1
chloride transport	0.024	1
cellular iron ion homeostasis	0.024	1
positive regulation of neurological system process	0.024	1
regulation of blood vessel size	0.024	1
regulation of tube size	0.024	1
positive regulation of behavior	0.024	1
iron ion homeostasis	0.025	1
symbiosis, encompassing mutualism through parasitism	0.026	1
vascular process in circulatory system	0.026	1
interspecies interaction between organisms	0.028	1
maintenance of location	0.030	1
response to starvation	0.031	1
transition metal ion transport	0.032	1
regulation of behavior	0.032	1
inorganic anion transport	0.032	1
regulation of multicellular organismal process	0.032	2
cellular response to nutrient levels	0.032	1
circadian rhythm	0.032	1
organelle localization	0.032	1
acute inflammatory response	0.036	1
response to organic substance	0.039	2
cellular response to extracellular stimulus	0.040	1
cellular response to external stimulus	0.040	1
anion transport	0.045	1
regulation of homeostatic process	0.050	1

Table F.20: Biological functions of genes that were common to P4 and control, GD22(NL)-GD22(L), differentially expressed gene sets in the inner myometrium. The genes were analysed for GO term enrichment using BiNGO. The overrepresented GO terms are shown with their corresponding adjusted p-values and the number of genes within the test set that are annotated to that function.

Description	Corrected p-value	No. Genes
embryonic skeletal joint morphogenesis	0.007	1
collagen fibril organization	0.019	1
embryonic skeletal system morphogenesis	0.019	1
embryonic skeletal system development	0.019	1
sensory perception of sound	0.019	1
cartilage development	0.019	1
extracellular matrix organization	0.019	1
sensory perception of mechanical stimulus	0.019	1
visual perception	0.019	1
sensory perception of light stimulus	0.019	1
skeletal system morphogenesis	0.019	1
embryonic organ morphogenesis	0.021	1
extracellular structure organization	0.021	1
embryonic organ development	0.028	1
skeletal system development	0.036	1
embryonic morphogenesis	0.036	1
chordate embryonic development	0.038	1
embryonic development ending in birth or egg hatching	0.038	1

F.5 Regulation of Differentially Expressed Genes in RU486-treated Tissues

Table F.21: Biological functions of genes that were regulated differently in P4 and RU486 decidua samples. The genes were analysed for GO term enrichment using BiNGO. The overrepresented GO terms are shown with their corresponding adjusted p-values and the genes within the test set that are annotated to that function.

Description	Corrected p-value	Genes in test set
tube lumen cavitation	0.0275	CDH1
salivary gland cavitation	0.0275	CDH1
response to indole-3-methanol	0.0298	CDH1
cellular response to indole-3-methanol	0.0298	CDH1
cellular response to lithium ion	0.0298	CDH1
regulation of branching involved in salivary gland morphogenesis	0.0298	CDH1
trophectodermal cell differentiation	0.0298	CDH1
thyroid hormone metabolic process	0.0298	SLCO4A1
cortical actin cytoskeleton organization	0.0298	EPB41L3
cortical cytoskeleton organization	0.0298	EPB41L3
blastocyst formation	0.0298	CDH1
positive regulation of transcription factor import into nucleus	0.0298	CDH1
positive regulation of protein import into nucleus	0.0327	CDH1
salivary gland morphogenesis	0.0327	CDH1
synapse assembly	0.0327	CDH1
cellular response to metal ion	0.0327	CDH1
salivary gland development	0.0327	CDH1
positive regulation of nucleocytoplasmic transport	0.0327	CDH1
cellular response to inorganic substance	0.0327	CDH1
response to lithium ion	0.0327	CDH1
regulation of transcription factor import into nucleus	0.0327	CDH1
regulation of morphogenesis of a branching structure	0.0333	CDH1
exocrine system development	0.0333	CDH1
pituitary gland development	0.0333	CDH1
positive regulation of intracellular protein transport	0.0333	CDH1
positive regulation of intracellular transport	0.0333	CDH1

Continued on next page

Table F.21 – continued from previous page

Description	Corrected p-value	Genes in test set
blastocyst development	0.0333	CDH1
tube formation	0.0333	CDH1
diencephalon development	0.0369	CDH1
synapse organization	0.0375	CDH1
regulation of protein import into nucleus	0.0389	CDH1
regulation of intracellular protein transport	0.0467	CDH1
gland morphogenesis	0.0467	CDH1
regulation of nucleocytoplasmic transport	0.0467	CDH1

Table F.22: Biological functions of genes that were regulated differently in P4 and RU486 outer myometrium samples. The genes were analysed for GO term enrichment using BiNGO. The overrepresented GO terms are shown with their corresponding adjusted p-values and the genes within the test set that are annotated to that function.

Description	Corrected p-value	Genes in test set
cholesterol transport	0.0073	APOA1, CFTR
sterol transport	0.0073	APOA1, CFTR
response to steroid hormone stimulus	0.0106	APOA1, CLDN4, CFTR
response to organic substance	0.0106	LCN2, APOA1, CLDN4, CFTR
cholesterol metabolic process	0.0106	APOA1, CFTR
response to drug	0.0106	LCN2, APOA1, CFTR
sterol metabolic process	0.0106	APOA1, CFTR
negative regulation of interleukin-1 beta secretion	0.0124	APOA1
multi-organism process	0.0124	LCN2, PSG29, CLDN4
female pregnancy	0.0124	PSG29, CLDN4
lipid transport	0.0124	APOA1, CFTR
cholesterol import	0.0124	APOA1
iodide transport	0.0124	CFTR
sterol transmembrane transport	0.0124	APOA1
sterol import	0.0124	APOA1
negative regulation of interleukin-1 secretion	0.0124	APOA1
lipid localization	0.0137	APOA1, CFTR
response to hormone stimulus	0.0142	APOA1, CLDN4, CFTR
negative regulation of very-low-density lipoprotein particle remodeling	0.0146	APOA1
response to herbicide	0.0146	LCN2
response to cytokine stimulus	0.0146	LCN2, CFTR
response to endogenous stimulus	0.0146	APOA1, CLDN4, CFTR
negative regulation of cytokine secretion involved in immune response	0.0146	APOA1
regulation of very-low-density lipoprotein particle remodeling	0.0146	APOA1
bicarbonate transport	0.0146	CFTR
high-density lipoprotein particle assembly	0.0146	APOA1
Cdc42 protein signal transduction	0.0146	APOA1
steroid metabolic process	0.0146	APOA1, CFTR
response to estrogen stimulus	0.0160	APOA1, CFTR
regulation of cytokine secretion involved in immune response	0.0160	APOA1
negative regulation of interleukin-1 beta production	0.0160	APOA1
positive regulation of cholesterol esterification	0.0165	APOA1
regulation of cholesterol esterification	0.0165	APOA1
negative regulation of interleukin-1 production	0.0165	APOA1
protein homotrimerization	0.0165	LCN2
transepithelial chloride transport	0.0165	CFTR
cellular response to stimulus	0.0165	LCN2, APOA1, CFTR
plasma lipoprotein particle assembly	0.0178	APOA1
cellular response to tumor necrosis factor	0.0178	LCN2
negative regulation of lipase activity	0.0189	APOA1
protein trimerization	0.0189	LCN2
protein-lipid complex assembly	0.0189	APOA1
cellular response to interleukin-1	0.0203	LCN2
regulation of interleukin-1 beta secretion	0.0203	APOA1
reverse cholesterol transport	0.0216	APOA1
regulation of interleukin-1 secretion	0.0216	APOA1
phospholipid efflux	0.0218	APOA1
transepithelial transport	0.0218	CFTR
axon regeneration in the peripheral nervous system	0.0218	APOA1
negative regulation of cytokine secretion	0.0218	APOA1

Continued on next page

Table F.22 – continued from previous page

Description	Corrected p-value	Genes in test set
phosphatidylcholine biosynthetic process	0.0231	APOA1
lipid biosynthetic process	0.0231	APOA1, CFTR
water transport	0.0243	CFTR
cellular response to organic substance	0.0248	LCN2, CFTR
positive regulation of steroid metabolic process	0.0252	APOA1
fluid transport	0.0266	CFTR
response to nutrient levels	0.0288	LCN2, APOA1
regulation of interleukin-1 beta production	0.0288	APOA1
positive regulation of vasodilation	0.0288	CFTR
cholesterol efflux	0.0288	APOA1
cellular response to cytokine stimulus	0.0288	LCN2
negative regulation of protein secretion	0.0288	APOA1
response to extracellular stimulus	0.0294	LCN2, APOA1
phosphatidylcholine metabolic process	0.0294	APOA1
axon regeneration	0.0296	APOA1
body fluid secretion	0.0296	CFTR
regulation of interleukin-1 production	0.0296	APOA1
alcohol metabolic process	0.0304	APOA1, CFTR
response to chemical stimulus	0.0307	LCN2, APOA1, CLDN4, CFTR
regulation of cytokine production involved in immune response	0.0307	APOA1
protein stabilization	0.0307	APOA1
neuron projection regeneration	0.0326	APOA1
regulation of vasodilation	0.0326	CFTR
vasodilation	0.0330	CFTR
cholesterol biosynthetic process	0.0330	CFTR
cellular response to lipopolysaccharide	0.0334	LCN2
Rho protein signal transduction	0.0334	APOA1
cellular response to molecule of bacterial origin	0.0354	LCN2
cellular response to chemical stimulus	0.0354	LCN2, CFTR
response to tumor necrosis factor	0.0354	LCN2
phospholipid transport	0.0354	APOA1
sterol biosynthetic process	0.0358	CFTR
cellular response to hydrogen peroxide	0.0358	LCN2
cellular response to stress	0.0368	LCN2, APOA1
regulation of cellular component organization	0.0368	LCN2, APOA1
ethanolamine and derivative metabolic process	0.0368	APOA1
regulation of cytokine secretion	0.0375	APOA1
cholesterol homeostasis	0.0400	APOA1
sterol homeostasis	0.0400	APOA1
transmembrane transport	0.0413	APOA1, CFTR
cellular response to reactive oxygen species	0.0413	LCN2
negative regulation of protein transport	0.0413	APOA1
response to external stimulus	0.0413	LCN2, APOA1
response to progesterone stimulus	0.0413	CLDN4
cellular response to protein stimulus	0.0413	LCN2
response to interleukin-1	0.0413	LCN2
organic anion transport	0.0413	CFTR
chloride transport	0.0413	CFTR
regulation of protein stability	0.0415	APOA1
regulation of steroid metabolic process	0.0415	APOA1
regulation of production of molecular mediator of immune response	0.0416	APOA1
negative regulation of cytokine production	0.0416	APOA1
regulation of tube size	0.0427	CFTR
regulation of blood vessel size	0.0427	CFTR
response to axon injury	0.0433	APOA1
positive regulation of lipid metabolic process	0.0447	APOA1
macromolecular complex assembly	0.0463	LCN2, APOA1
vascular process in circulatory system	0.0475	CFTR
reproductive process	0.0484	PSG29, CLDN4
lipid homeostasis	0.0484	APOA1
cellular response to biotic stimulus	0.0488	LCN2
reproduction	0.0488	PSG29, CLDN4
macromolecular complex subunit organization	0.0492	LCN2, APOA1
cellular response to oxidative stress	0.0493	LCN2

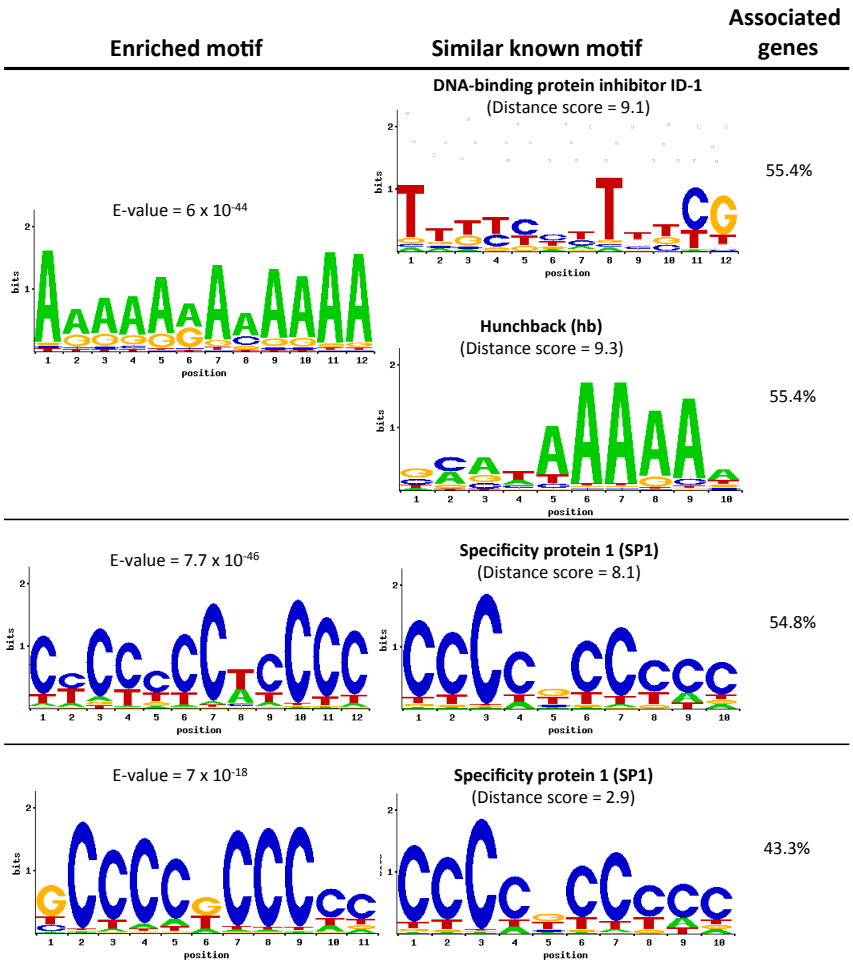

Figure F.1: Motifs identified in 1000 bp-long promoter regions of genes that were responsive to progesterone in the decidua. MEME-LaB was used to identify motifs that were enriched within promoter regions of P4-responsive genes.

F.6 Identification of Common Regulatory Features

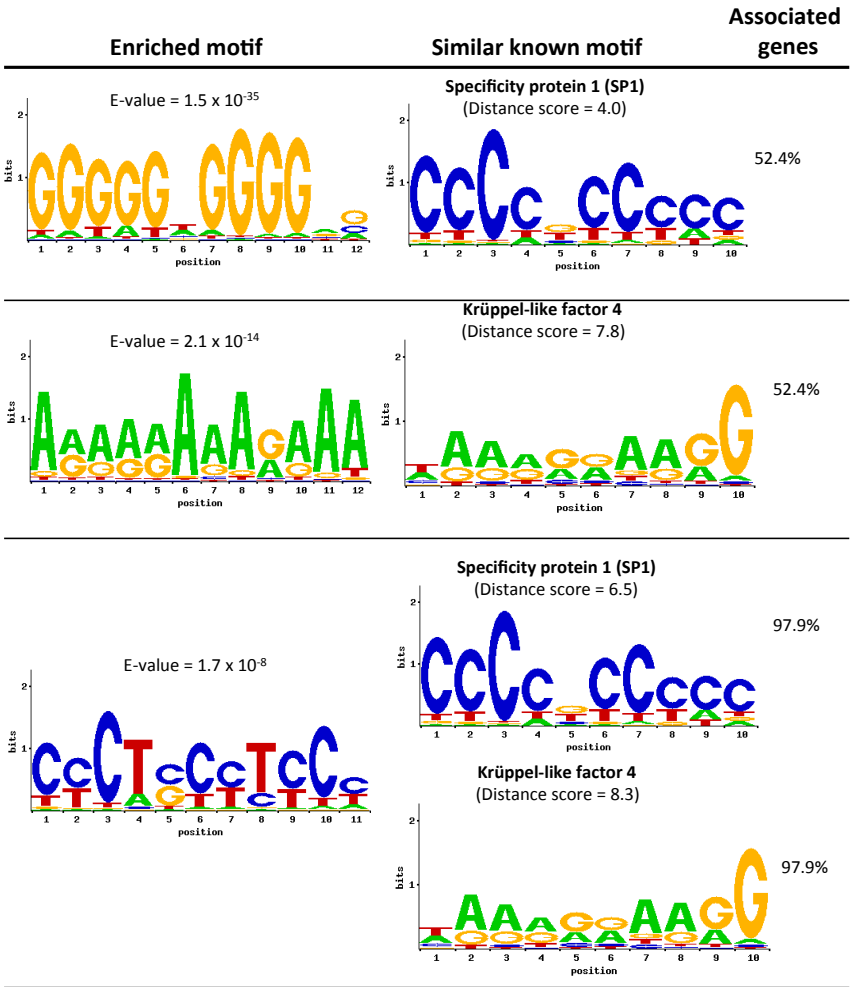

Figure F.2: Motifs identified in 1000 bp-long promoter regions of genes that were responsive to progesterone in the inner myometrium. MEME-LaB was used to identify motifs that were enriched within promoter regions of P4-responsive genes.

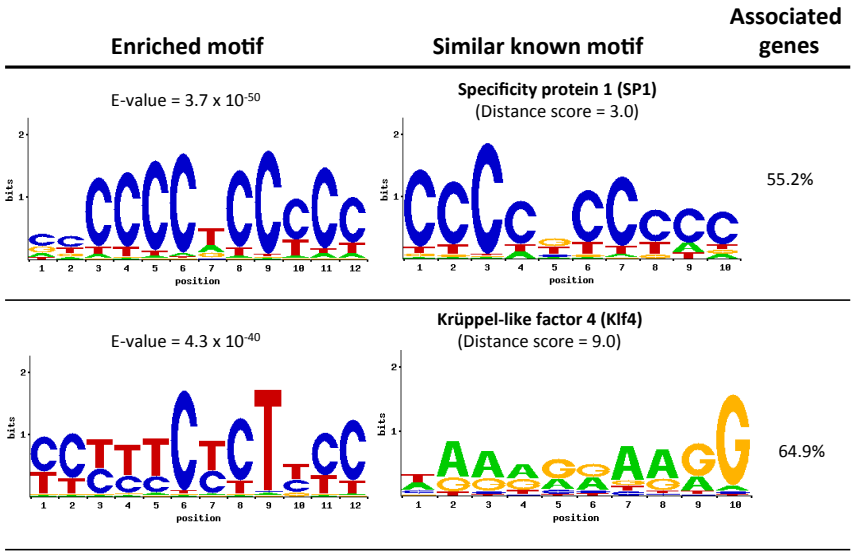

Figure F.3: Motifs identified in 1000 bp-long promoter regions of genes that were responsive to progesterone in the outer myometrium. MEME-LaB was used to identify motifs that were enriched within promoter regions of P4-responsive genes.

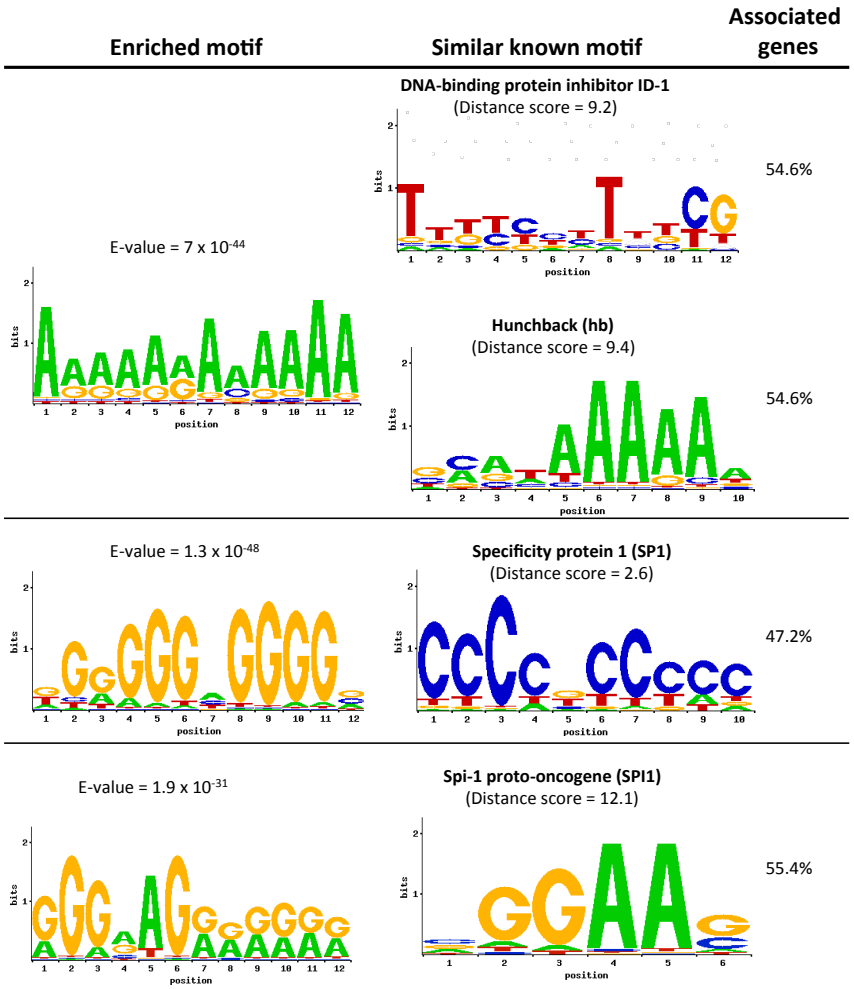

Figure F.4: Motifs identified in 2000 bp-long promoter regions of genes that were responsive to progesterone in the decidua. MEME-LaB was used to identify motifs that were enriched within promoter regions of P4-responsive genes.

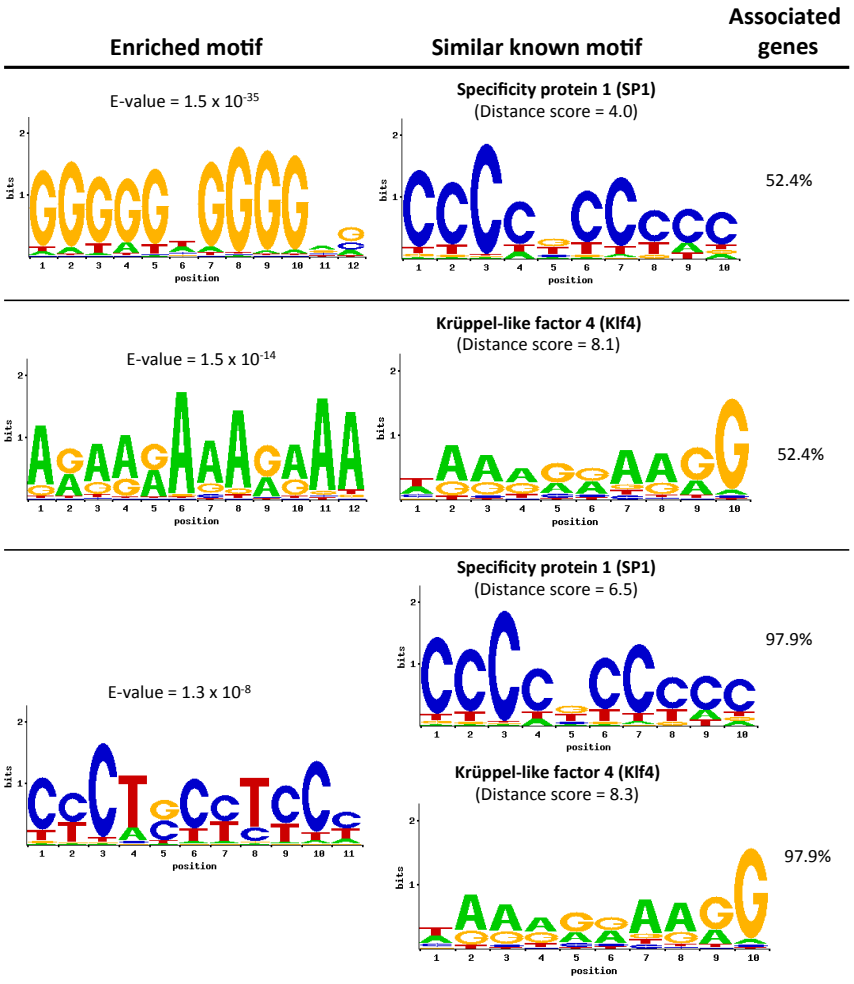

Figure F.5: Motifs identified in 2000 bp-long promoter regions of genes that were responsive to progesterone in the inner myometrium. MEME-LaB was used to identify motifs that were enriched within promoter regions of P4-responsive genes.

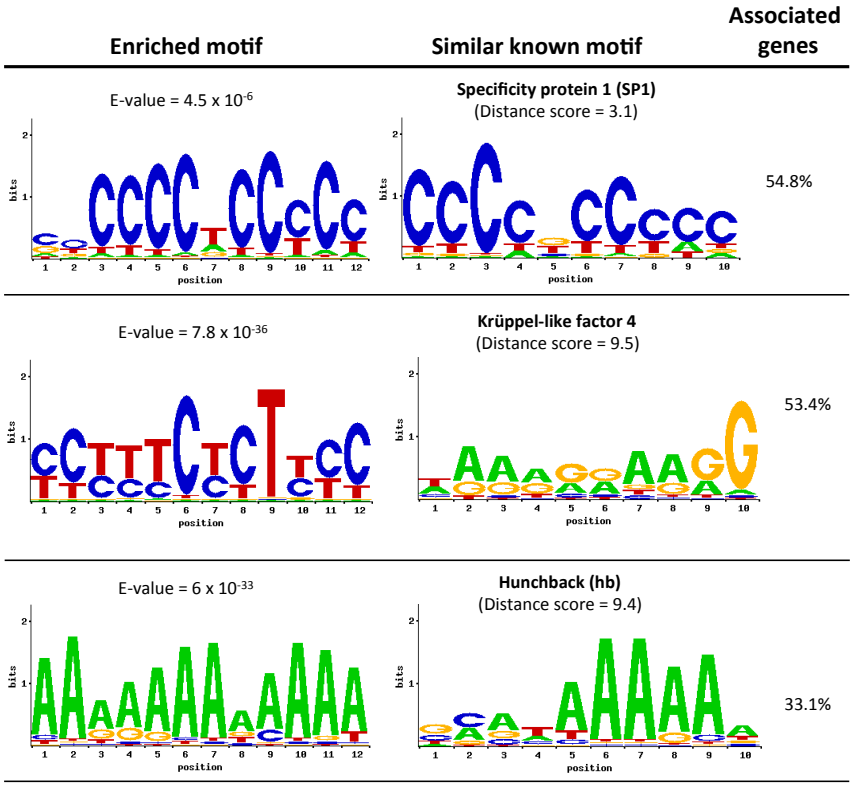

Figure F.6: Motifs identified in 2000 bp-long promoter regions of genes that were responsive to progesterone in the outer myometrium. MEME-LaB was used to identify motifs that were enriched within promoter regions of P4-responsive genes.

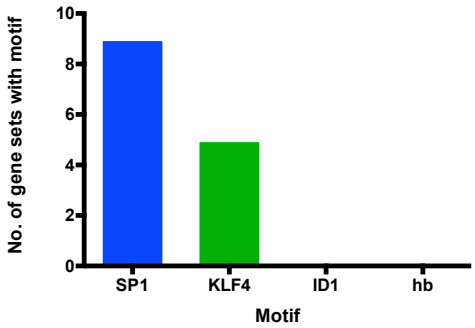

Figure F.7: Occurrence of motifs in random sets of genes. The genes were selected from the expressed uterine transcriptome.